



THE UNIVERSITY
of ADELAIDE

**Analysis of Treatment Efficacy and Molecular and
Cellular Outcomes in Mouse Models of Congenital
Epilepsy and Intellectual Disability.**

Karagh Loring

BSc. (Biomedical Science) Hons.

Intellectual Disability Laboratory

Primary Supervisor: A/Prof Cheryl Shoubridge

External Supervisor: A/Prof Quenten Schwarz

Thesis submitted for the degree of
Doctor of Philosophy

in

Discipline of Paediatrics, Adelaide Medical School

Faculty of Health and Medical Sciences

The University of Adelaide

2020

Contents

List of Tables	6
List of Figures	8
Abstract	11
Thesis Format	13
Thesis Declaration	14
Acknowledgments	15
List of Abbreviations	18
Chapter One: The <i>Aristaless</i> -related homeobox gene: understanding its role in intellectual disability and seizures and the search for effective treatments	20
1.1 Introduction	21
1.2 ARX & neurodevelopmental disorders	22
1.2.1 The <i>Aristaless</i> -related homeobox gene	22
1.2.2 Mutations in <i>ARX</i>	23
1.2.3 Expanded polyalanine tract mutations	24
1.2.4 Current treatments for seizures in <i>ARX</i> patients	30
1.3 ARX & interneurons	31
1.3.1 Interneuron function	31
1.3.2 Interneuron migration	32
1.3.3 Interneuron subtypes	35
1.3.4 ARX & interneuron migration and function	37
1.4 <i>Arx</i> mouse models	45
1.4.1 Expanded polyalanine tract mutations	45
1.4.2 Other <i>Arx</i> mouse models	50
1.4.3 Benefits and limitations of mouse models for research	53
1.5 Exogenous steroids as a treatment for infantile spasms and seizures	55
1.6 Concluding remarks	59
1.7 Project overview	60
Chapter Two: Materials and Methods	62
2.1 General reagents	63
2.2 Animals	63
2.2.1 Animal husbandry	63
2.2.2 Drug preparation and injections	64
2.2.3 Genotyping	66
2.2.4 Behavioural analyses	70
2.2.5 Seizure monitoring and analysis	76
2.2.6 Animal dissections and tissue collection	77
2.2.7 Statistical analysis	77

2.3 Gene expression analysis	78
2.3.1 RNA extraction	78
2.3.2 RNA sequencing	78
2.3.3 RNA sequencing validation	79
2.3.4 Gene enrichment analysis	83
2.4 Immunofluorescence.....	84
2.4.1 Tissue sectioning	84
2.4.2 Immunofluorescence.....	84
2.4.3 Microscopy	85
2.4.4 Interneuron analysis.....	85
2.4.5 Statistical analysis.....	85
Chapter Three: Short-term 17 β -estradiol treatment alleviates the seizure phenotype but not behavioural outcomes in PA1 and PA2 mouse models.	87
3.1 Abstract.....	90
3.2 Introduction.....	91
3.3.1 Optimisation of drug preparation and injections	94
3.4 Results.....	96
3.4.1 Estradiol treatment trial strategy	96
3.4.2 Estradiol treatment reduces seizure frequency and severity in PA mutant mice.....	98
3.4.3 Estradiol treatment does not improve mortality in PA mutant mice	104
3.4.4 Body and tissue weights are unaffected by estradiol in PA mutant mice.....	107
3.4.5 Behavioural deficits are present in PA mutant mice prior to seizure onset, and do not improve with estradiol treatment.	112
3.5 Discussion.....	133
3.5.1 Reproducibility of phenotypic outcomes in different mouse models.....	133
3.5.2 Relating behavioural testing to patient phenotypes	134
3.5.3 No change to the survival of mice with estradiol treatment	136
3.5.4 Behavioural deficits are present prior to seizure onset.....	136
3.5.5 Estradiol and cognition and behaviour	138
3.5.6 Reproducibility of behaviour testing outcomes.....	139
3.5.7 Side effects of estradiol treatment	142
3.6 Study outcomes.....	143
Chapter Four: The deregulated transcriptome in PA1 and PA2 <i>Arx</i> mutant mice is not restored by early postnatal 17 β -estradiol treatment.....	144
4.1 Abstract.....	146
4.2 Introduction.....	147
4.3 Results.....	150
4.3.1 PA1 and PA2 mice have a deregulated cortical transcriptome at postnatal day 10.	150

4.3.2 Estradiol treatment targets genes outside of the deregulated transcriptome of PA1 and PA2 mutant mice.....	160
4.4 Discussion.....	171
4.4.1 Ongoing effects to the transcriptome from a partial loss of <i>Arx</i>	171
4.4.2 Interneuron genes and genes associated with neurodevelopmental disorders are deregulated by disease and estradiol treatment.....	173
4.4.3 Differences between PA1 and PA2 mutant mice.....	175
4.4.4 Estrogen response genes in our analysis.....	176
4.4.5 Environmental effects on transcriptomic results.	177
4.5 Study outcomes.....	178
Chapter Five: Interneuron genes are deregulated with <i>Arx</i> PA mutations, but are not rescued directly with 17 β -estradiol treatment.	179
5.1 Abstract.....	180
5.2 Introduction.....	181
5.3 Results.....	184
5.3.1 Deregulated interneurons in untreated PA1 and PA2 mutant mice at postnatal day 3 and postnatal day 10.	184
5.3.2 Estradiol treatment does not alter interneuron abundance in the PA1 and PA2 mouse prefrontal cortex.	194
5.4 Discussion.....	198
5.4.1 Novel findings from this study	198
5.4.2 Differences in interneuron findings between studies.....	203
5.4.3 Future experiments for interneurons in PA mutant mice.....	205
5.5 Study Outcomes.....	206
Chapter Six: Discussion.....	207
6.1 Novel findings of this project	208
6.2 Reproducibility of pre-clinical trials.....	210
6.3 Separating behaviour and seizures in PA mice.....	212
6.4 Understanding the transcriptome of the developing PA brain in early postnatal life...	214
6.5 Future directions	215
6.6 Concluding remarks.....	218
References.....	220
Appendices.....	230

List of Tables

Table 1.1: Overview of interneuron markers and their respective interneuron subtypes.

Table 1.2: Overview of phenotypic differences between the two different PA1 and PA2 mouse models.

Table 2.1: Mouse weight range brackets with lower and upper weight limits, with correct volume of drug to inject.

Table 2.2: Mouse genotyping PCR primers.

Table 2.3: Parameters measured for each behavioural test using the AnyMaze software.

Table 2.4: Housekeeping primer set.

Table 2.5: TaqMan® assay details.

Table 2.6: Primary antibodies used for immunofluorescence.

Table 2.7: Secondary antibodies used for immunofluorescence.

Table 4.1: Genes deregulated by disease in PA1, PA2 and PA^{pool} mice compared to wild-type littermates.

Table 4.2: Neurodevelopmental disorder and key brain development genes deregulated by disease in PA1, PA2, PA^{pool} and core overlap gene lists.

Table 4.3: Pathways enriched through PANTHER analysis in PA^{pool} (green), PA1 (orange) and PA2 (blue) mice.

Table 4.4: Genes deregulated by estradiol treatment and those containing estrogen response elements (EREs) in PA1, PA2 and PA^{pool} mice compared to wild-type littermates.

Table 4.5: Neurodevelopmental disorder and key brain development genes deregulated by estradiol in PA1, PA2 and PA^{pool}.

Table 4.6: Pathways enriched through PANTHER analysis in PA^{pool}, PA1 and PA2 mice.

Table 5.1: Genes deregulated by disease in untreated PA1, PA2 and PA^{pool} mice compared to untreated wild-type littermates at the same time points.

Table 5.2: Interneuron associated genes enriched in untreated PA1, PA2 and PA^{pool} mice at postnatal day 3 and day 10.

Table 5.3: Interneuron deficits present in the PA1 and PA2 mouse models from different studies at different timepoints.

Table 5.4: Interneuron deficits in PA mutant mice in this study.

List of Figures

Figure 1.1: Pathogenic mutations within the ARX gene and their associated phenotypes.

Figure 1.2: Phenotypic variability associated with expansions of the first and second polyalanine tracts in ARX.

Figure 1.3: Mouse cortical development.

Figure 1.4: Expression and migration of Arx positive cells in the developing brain.

Figure 1.5: Comparison of normal cortical development and impaired development with loss of ARX function.

Figure 1.6: Accumulation of arrested calbindin positive (Cb+) cells in the ventral cortex.

Figure 2.1: Mouse toe tagging numbering system.

Figure 3.1: DMSO toxicity curve for apoptosis of neurons in P7 mice.

Figure 3.2: Estradiol study timeline.

Figure 3.3: Early estradiol treatment diminishes observed seizure severity and frequency in PA mutant mice.

Figure 3.4: Estradiol treatment did not delay the age of first observed seizure in PA mutant mice.

Figure 3.5: Seizure severity and frequency are reduced in PA mutant mice treated with estradiol.

Figure 3.6: Early estradiol does not improve mortality in PA mutant mice.

Figure 3.7: Age of death in PA mutant mice treated with vehicle or estradiol.

Figure 3.8: Body weights of PA mutant mice treated with vehicle or estradiol.

Figure 3.9: Testes and cortex weights of PA mutant mice treated with vehicle or estradiol.

Figure 3.10: Estradiol does not improve anxiety-like behavioural deficits in PA mutant mice.

Figure 3.11: PA mutant mice do not exhibit an anxiety-like deficit in the elevated zero maze.

Figure 3.12: PA mutant mice do not show significant differences in number of explorative head dips in the elevated zero maze.

Figure 3.13: Estradiol does not improve social deficits in PA mutant mice.

Figure 3.14: Estradiol does not improve social preference deficits in PA mutant mice.

Figure 3.15: Estradiol does not improve social deficits in PA^{pool} mutant mice.

Figure 3.16: Estradiol does not improve social preference deficits in PA^{pool} mutant mice.

Figure 3.17: PA mutant do not exhibit a short-term memory deficit in the Y-maze.

Figure 3.18: PA mutant mice do not display learning and memory deficits in the Barnes maze.

Figure 3.19: PA mutant mice display reduced neuromuscular strength.

Figure 4.1: Overlapping genes deregulated in PA1 and PA2 mutant mice with disease.

Figure 4.2: Genes associated with interneurons are downregulated in PA1 and PA2 mutant mice.

Figure 4.3: Enrichment analysis of genes deregulated by disease in PA mutant mice.

Figure 4.4: Overlapping response between the disease deregulated transcriptome and the estradiol deregulated transcriptome of PA mutant mice.

Figure 4.5: Estradiol treatment reverses the expression of genes deregulated by disease in PA mutant mice.

Figure 4.6: Comparison of response size to estradiol treatment in PA mice.

Figure 4.7: Enrichment analysis of genes deregulated with estradiol treatment in PA mutant mice.

Figure 5.1: RNA sequencing outcomes of key interneuron associated genes in untreated PA mutant mice at postnatal day 3 and day 10.

Figure 5.2: Enrichment of different interneuron subtypes in genes deregulated in untreated postnatal day 3 and day 10 PA mutant mice.

Figure 5.3: Region of the cortex used for immunofluorescence analysis.

Figure 5.4: Abundance of calbindin and neuropeptide-Y positive cells counted in the prefrontal cortex.

Abstract

Children with severe intellectual disability have an increased prevalence of refractory seizures. Steroid treatment may improve seizure outcomes, but the mechanism remains unknown. Here we demonstrate that short term, daily delivery of an exogenous steroid 17 β -estradiol (40 ng/g) in early postnatal life significantly reduced the number and severity of seizures, but did not improve behavioural deficits, in mice modelling mutations in the *Aristaless*-related homeobox gene (*ARX*), expanding the first (PA1) or second (PA2) polyalanine tract. *ARX* polyalanine expansion mutations in children cause intellectual disability and developmental delay, frequently presenting with comorbidities such as autism, dystonia, and refractory seizures and infantile spasms. Frequency of observed seizures on handling (n = 14/treatment/genotype) were significantly reduced in PA1 (32% reduction) and more modestly reduced in PA2 mice (14% reduction) with steroid treatment compared to vehicle. Spontaneous seizures were assessed (n = 7/treatment/genotype) at 7 weeks of age coinciding with a peak of seizure activity in untreated mice. PA1 mice treated with steroids no longer present with the most severe category of prolonged myoclonic seizures, while treated PA2 mice had a complete absence of any seizures during this analysis. Despite the reduction in seizures, 17 β -estradiol treated mice showed no improvement in behavioural or cognitive outcomes in adulthood. For the first time we show that these deficits due to mutations in *Arx* are already present before seizure onset and do not worsen with seizures. *ARX* is a transcription factor and *Arx* PA mutant mice have deregulated transcriptome profiles in the developing embryonic brain. At postnatal day 10, treatment completion, RNAseq identified 129 genes significantly deregulated (log₂FC > \pm 0.5, P-value < 0.05) in the frontal cortex of mutant compared to wild-type mice. This list reflects genes deregulated in disease and was particularly enriched for known genes in neurodevelopmental disorders and those involved in signalling and developmental pathways. 17 β -estradiol treatment of mutant mice significantly deregulated 295 genes, with only 23 deregulated genes overlapping between vehicle and steroid treated mutant mice. Furthermore, when we investigated

populations of inhibitory interneurons in the cortex of PA mice immediately following estradiol treatment at P10, we saw no improvement to cell density, despite seeing a marked change in the expression of interneuron associated genes both due to disease, and changing with administration of estradiol at the same developmental timepoint. We conclude that 17 β -estradiol treatment recruits processes and pathways to reduce the frequency and severity of seizures in the *Arx* PA mutant mice but does not precisely correct the deregulated transcriptome, cellular deficits, mortality, or behavioural and cognitive deficits. Our outcomes show that although estradiol may not represent the ideal therapeutic option for PA patients currently, our data provides insights into developing novel drugs by broadening our understanding of the mechanisms of disease caused by *Arx* PA mutations, particularly by uncovering pathways that may overlap with other neurodevelopmental disorders and present convergent targets for future treatment options.

Thesis Format

This thesis is presented in a conventional format, consisting of an introduction covering the background of the research conducted in this thesis and a thorough review of the current literature (Chapter 1), a chapter containing materials and methods (Chapter 2), followed by three results chapters (Chapters 3-5) and a final discussion and conclusions chapter (Chapter 6). Figures and tables are independently numbered within each chapter. While Chapters 3 and 4 provide the basis for my published paper, here they are presented in the conventional format, and include additional data. The publication (submitted to *Neurobiology of Disease*) is included in Appendix 1.

Thesis Declaration

I certify that this work contains no material which has been accepted for the award of any other degree or diploma in my name, in any university or other tertiary institution, and to the best of my knowledge, contains no material previously published or written by another person, except where due reference has been made in the text. In addition, I certify that no part of this work will, in the future, be used in a submission in my name, for any other degree or diploma in any university or other tertiary institution without the prior approval of the University of Adelaide. I give consent to this copy of my thesis when deposited in the University Library, being made available for loan and photocopying, subject to the provisions of the Copyright Act of 1968. I acknowledge that copyright of published works contained within this thesis resides with the copyright holder(s) of those works.

I also give permission for the digital version of my thesis to be made available of the web, via the University's digital research repository, the Library Search and also through web search engines, unless permission has been granted by the University to restrict access for a period of time.

I acknowledge the support I have received for my research through provision of an Australian Government Research Training Program Scholarship.

Karagh Loring
Bachelor of Science (Biomedical Science) Hons.
Student Number: a1606960
DATE: 01/11/2020

Acknowledgments

I wish to thank all the people whose assistance was invaluable in the completion of my PhD project. First and foremost, I wish to express my sincere appreciation to my supervisor, Associate Professor Cheryl Shoubridge, for her guidance, patience, and never-ending knowledge. Without her knowledge of *ARX*, as well as knowing all there is to know about molecular and functional experiments, I would not have been able to survive this PhD. Thank you for being so patient with me when I was hesitant about trying new things, or when I slowly learned how to write manuscripts, and during all of my practice presentations for conferences. Cheryl has provided so much of her time for meetings, valuable advice, reading drafts, helping edit my work, and having tissues on hand in her office when I was stressed about science. I am so grateful for the opportunity to be mentored by her, professionally and personally.

A special thank you to Dr Kristie Lee, who was originally my co-supervisor before going on maternity leave. Kristie taught me so much about animal models and developmental biology in the short time we worked together and set me down the right path for my project. I will forever be grateful for her guidance and wisdom over the phone, email and at coffee dates, even when you were still on leave with a newborn and a toddler. I would also like to thank my external supervisor, Associate Professor Quenten Schwarz, for providing so much knowledge about interneurons and how to quantify them. Thank you for being there with whatever antibody I wanted to try out next, listening to my next experiment idea, reading drafts, and helping edit, as well coming along to all my review meetings.

I would like to say thank you to the members of the Intellectual Disability Research Group, past and present; Kristie Lee, Matilda Jackson, Aneta Zysk, Tessa Mattiske, Laura Redpath, Oliver Dearsley and Monica Thai. I would like to especially thank Matilda, Kristie and Aneta for their assistance with the animal breeding colonies, behavioural studies, and helping with all of my

mouse injections, particularly on Sunday mornings. Additionally, I would like to thank all of the members of the Neurogenetics Laboratory, for offering feedback, lab resources and guidance when required (and an extra special thank you for all the birthday morning teas).

I am very grateful to Laboratory Animal Services at the University of Adelaide for their assistance with caring for our mouse colonies and providing valuable advice for breeding and environmental enrichment for our animals. I would also like to thank Catherine Jawahar and Bernard Baune for the generous use of their behavioural testing equipment and software.

My village extends beyond the confines of academia, however. Thank to you the wonderful scientist friends I have made throughout my time in the lab; Laura, Aneta, Monica, Bec, and Thomas. Without you, lunchtimes would have been incredibly boring, and I appreciate your understanding, love, support, and for always being there to lean on. You've become some of my best friends and I wouldn't have been able to write this thesis without you. Thank you to my parents, Kirrily and Jeff, for always encouraging me to keep going, even when I questioned myself and my studies. You have always supported my education and motivated me at every stage, from primary school to PhD, and for that I will always be grateful. Thank you to my little brother, Dale, my grandparents, Lynette and Geoff, and my parents-in-law, Bruce and Marina, for your support, and pretending to understand what I was researching. Another special acknowledgment to my sister-in-law Nicole, and my beautiful friend, Alanna. You have provided some of the best hugs when the PhD stress became a little bit too much and I needed extra encouragement. My PhD has been a process of self-discovery, and at times has had a dramatic impact on my mental health. Alongside my friends, partner and family, my support network extended to others who had my back and helped me find reprieve from stress and sadness. I want to thank my GP, and my psychologist, for countless hours of support and guidance.

Last but not least, Gregory, my fiancé. Without you supporting me and helping me grow, laugh, and learn, I would not be here, finishing my PhD, and writing this thesis. Thank you encouraging me, for convincing me to keep going when I wanted to give up, for loving me unconditionally, and for all the dinners you cooked and dishes you did when I was too stressed or tired. You have been the ray of sunshine in my life over the last four years. I love you. You have helped me more than you will ever know.

List of Abbreviations

<i>Abbreviation</i>	<i>Full Description</i>
ACTH	Adrenocorticotrophic hormone
ADHD	Attention deficit hyperactivity disorder
AEC	Animal ethics committee
ARX	Aristaless-related homeobox
ASD	Autism spectrum disorder
BSA	Bovine serum albumin
CB	Calbindin
CB	Cannabidiol receptor
CGE	Caudal ganglionic eminence
CR	Calretinin
DAVID	Database for Annotation, Visualisation, and Integrated Discovery
DMSO	Dimethyl sulfoxide
DNA	Deoxyribonucleic acid
DTT	Dithiothreitol
E2	17 β -estradiol
EEG	Electroencephalogram
EIEE	Early infantile epileptic encephalopathy
ER	Estrogen receptor
ERE	Estrogen response element
GABA	Gamma aminobutyric acid
ID	Intellectual disability
IEDE	Intellectual epileptic dyskinetic encephalopathy
IGTP	Interferon gamma induced GTPase
IQ	Intelligence quotient
LGE	Lateral ganglionic eminence
MGE	Medial ganglionic eminence
MRI	Magnetic resonance image
NDD	Neurodevelopmental disorder
NDNF	Neuron derived neurotrophic factor
NMDA	N-methyl-D-aspartic acid
NPY	Neuropeptide-Y
OAR	<i>Opt/Aristaless/Rax</i> domain
OCT	Optimal cutting temperature compound
OS	Ohtahara syndrome
P	Postnatal day
PA	Polyalanine
PANTHER	Protein Analysis Through Evolutionary Relationships
PBS	Phosphate buffered saline
PCR	Polymerase chain reaction

PFA	Paraformaldehyde
PTZ	Pentylentetrazol
PVALB	Parvalbumin
RNA	Ribonucleic acid
RT	Room temperature
SEM	Standard error of the mean
SERM	Selective estrogen receptor modulator
SNCG	γ -synuclein
SST	Somatostatin
SUDEP	Sudden unexpected death in epilepsy
TBE	Tris-borate-EDTA buffer
TBS	Tris buffered saline
TMM	Trimmed mean of M values
VIP	Vasoactive intestinal peptide
WHO	World Health Organisation
WT	Wild-type
XLAG	X-linked lissencephaly with abnormal genitalia

Chapter One:

**The *Aristaless*-related homeobox gene:
understanding its role in intellectual disability
and seizures and the search for effective
treatments**

1.1 Introduction

Intellectual disability (ID) is defined as impaired cognitive function paired with a deficit in adaptive behaviour before the age of 18. ID affects approximately 1 in 50 people worldwide and is estimated to cost Australia \$14 billion per year (WHO, 2019, Australian Institute of Health and Welfare 2008). In first world countries, a genetic cause is responsible for approximately 40% of cases (Willemsen and Kleefstra, 2014, Chiurazzi and Pirozzi, 2016, Ellis *et al.*, 2020). Children with ID often have a range of debilitating comorbidities, including autism spectrum disorder (ASD), attention deficit hyperactivity disorder (ADHD), dystonia, and intractable epilepsy and infantile spasms. It is often not understood whether the causes of these comorbidities have a singular causative mechanism, or whether there are multiple pathways at play. In terms of understanding these disorders in order to treat them, it is vital to investigate the mechanisms behind their pathogenesis.

Epileptic conditions are complex and often have significant long-term implications on ongoing health and cognition. Cognitive function is suspected to be impaired with persistent and severe seizures, particularly early in childhood and infancy. The distribution of IQ scores in children with epilepsy are often skewed to lower values and learning difficulties are frequently reported (Farwell *et al.*, 1985, Neyens *et al.*, 1999, Prasad *et al.*, 2014). Many children also regress in mental development after experiencing severe seizures (Neyens *et al.*, 1999). While cognition is a source of concern for infants with spasms very early in life, it can be difficult to elucidate how much of a child's intellectual disability was pre-existing and the extent that was caused by spasms early in key periods of brain development (Nabbout and Dulac, 2003).

The brain is a highly complex organ, comprised of multiple cell types, acting in synchrony to perform cognitive functions. Neurons in the brain can be classed as excitatory (output of neuronal activity) or inhibitory (inhibiting excitation). The development, migration and function of these cells is dependent on tightly controlled regulation of genes during embryonic

development, and throughout childhood, adolescence, and adulthood. Disruption of these genes can lead to the neurodevelopmental disorders (NDDs), such as intellectual disability, epilepsy and autism (Paciorkowski *et al.*, 2011, Olivetti and Noebels, 2012). There are currently more than 1200 genes implicated in intellectual disability, each with small numbers of cases, making this disorder a collection of rare genetic diseases (Chiurazzi and Pirozzi, 2016). One such gene is the *Aristaless*-related homeobox gene (*ARX*), a highly conserved transcription factor, playing a regulatory role in key events of proliferation and migration of inhibitory neurons in the brain (Kitamura *et al.*, 2002, Stromme *et al.*, 2002, Turner *et al.*, 2002). When *ARX* function is interrupted in humans, phenotypes arising include intellectual disability and developmental delay as key features, as well as varying comorbidities of infantile spasms, epileptic syndromes, dystonia, ADHD and ASD, through to severe brain malformations (Shoubridge *et al.*, 2010). Seizures and spasms associated with *ARX* mutations, like many other genetic NDDs, are often resistant to current anti-epileptic therapies. In addition, intellectual disability and developmental delay can have a serious impact on the quality of life of affected children and their families. We need to better understand the pathogenesis of *ARX* mutations, to enable identification of novel strategies to treat children with these disorders.

1.2 ARX & neurodevelopmental disorders

1.2.1 The *Aristaless*-related homeobox gene

The *Aristaless*-related homeobox gene (*ARX*) is located on the X-chromosome and spans a 12.25 kB genomic region. The *ARX* gene has five coding exons, with a 1686 bp open reading frame and a 562 amino acid length protein (Gécz *et al.*, 2006). *ARX* is a paired-like homeodomain transcription factor, comprised of various domains, including a highly conserved DNA-binding homeodomain, an *Aristaless* or OAR domain, and four polyalanine tracts (Figure 1.1). Consistent with critical roles in development for homeobox transcription factors, *ARX* is a transcriptional regulator consistently implicated in the development and migration of cholinergic and cortical interneurons (Kitamura *et al.*, 2002, Poirier *et al.*, 2004, Colombo *et*

al., 2007). When *ARX* function is interrupted in humans, phenotypes arise that invariably include intellectual disability and developmental delay.

1.2.2 Mutations in *ARX*

The number and profile of mutations in *ARX* has grown since 2002 when this was first identified as an intellectual disability gene (Bienvenu *et al.*, 2002, Stromme *et al.*, 2002). In addition to the variable degrees of intellectual disability, mutations in *ARX* frequently present with a wide spectrum of comorbidities, including autism, dystonia, and childhood-onset epilepsy and malformation phenotypes of the brain and genitalia (Bienvenu *et al.*, 2002, Kitamura *et al.*, 2002, Stromme *et al.*, 2002, Turner *et al.*, 2002). While all patients with *ARX* variants have intellectual disability, the broad spectrum of specific cognitive deficits and behavioural phenotypes of *ARX* patients makes it difficult to determine the aetiologies of their intellectual disability, particularly when the pathophysiological mechanisms of the disease are complex and poorly understood. The varied nature of these mutations, their positions within the domains of the *ARX* protein, and their associated phenotypes is outlined in Figure 1.1.

ARX function is critical to normal brain development and postnatal life. When mutations in *ARX* result in a complete loss of function, patients have a catastrophic malformation phenotype of X-linked lissencephaly with abnormal genitalia (XLAG or now called LIS2, OMIM #257320) and die early in life (Kitamura *et al.*, 2002). This syndrome results in severe brain malformations, like lissencephaly and hydrocephaly, with abnormally developed genitalia such as a small penis and undescended testes. Mutations contributing to these severe phenotypes include nonsense mutations as well as some missense mutations in the conserved homeodomain of *ARX*, shown to interfere with or abolish the normal DNA-binding properties of this region (Shoubridge *et al.*, 2010). Missense mutations that occur across the length of the *ARX* gene lead to milder phenotypes of intellectual disability with and without comorbidities (Stromme *et al.*, 2002, Wallerstein *et al.*, 2008, Shoubridge *et al.*, 2010, Sirisena *et al.*, 2014). While mutations

occur across the entire gene, approximately 60% of all reported mutations result in expansions of the first and second polyalanine tracts of *ARX* (Shoubridge *et al.*, 2010).

1.2.3 Expanded polyalanine tract mutations

There are four polyalanine tracts in *ARX*, and expansion mutations of the first two tracts make up more than half of reported cases of mutations found in patients. Mutations in these tracts cause a wide variety of different phenotypes, with all patients featuring intellectual disability of varying degrees of severity, with some exhibiting severe infantile spasms, epilepsy and dystonia. The length of the expansion generally correlates with the severity of the phenotype (Figure 1.2) (Marques *et al.*, 2015).

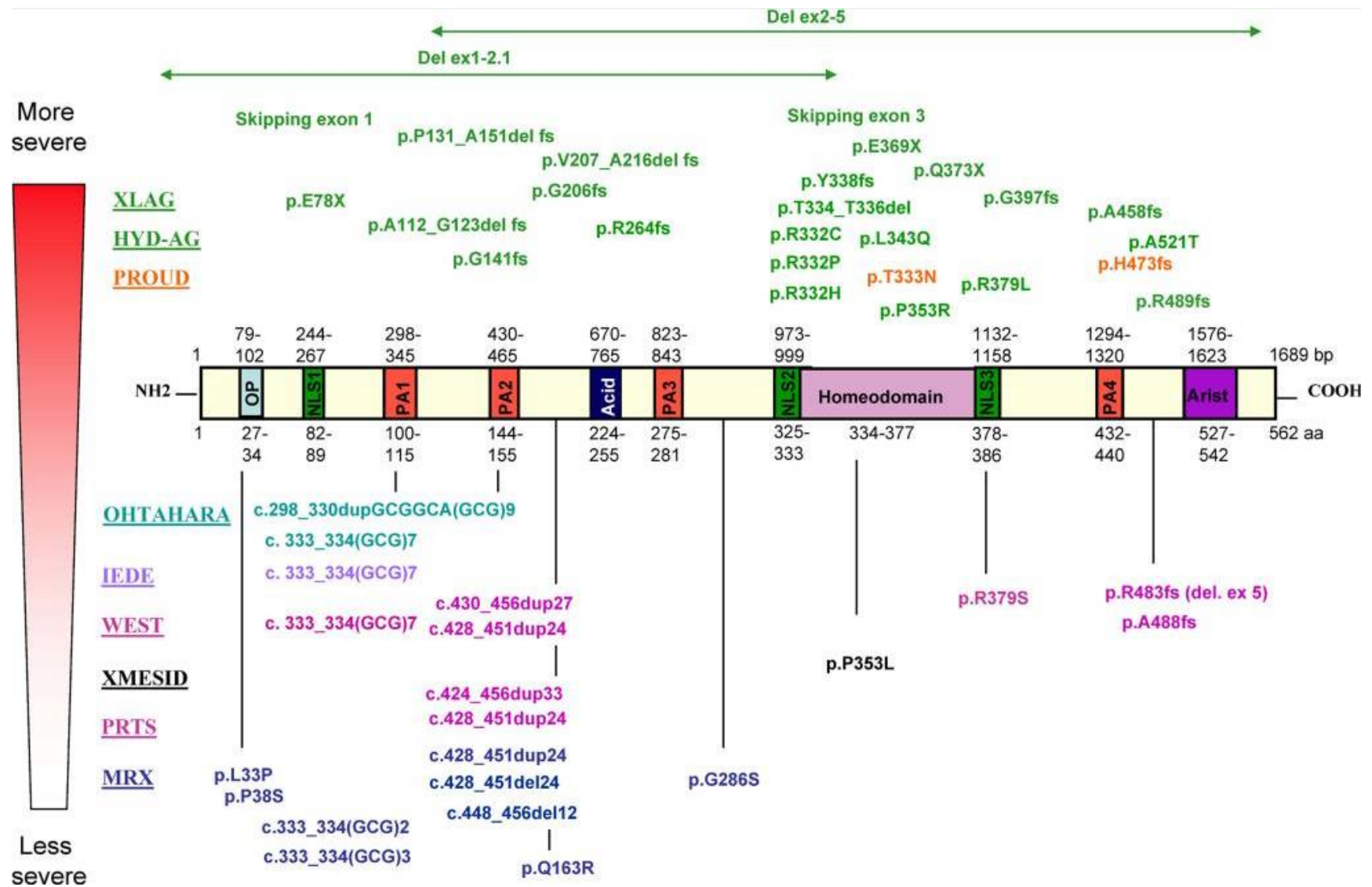


Figure 1.1: Pathogenic mutations within the ARX gene and their associated phenotypes. A schematic of the ARX genes and various functional domains with their respective amino acid positions listed. Mutations are associated with the broad range of phenotypes seen in patients, with phenotypes listed from most severe to least severe. Mutations are listed with position and amino acid change. Functional domains of ARX; OP (octopeptide), NLS (nuclear location sequence), PA (polyalanine tract), acid (acidic), arist (*Aristaless*), and homeodomain. Phenotypes associated with ARX mutations; XLAG (X-linked lissencephaly with abnormal genitalia), HYD-AG (hydrocephaly with abnormal genitalia), PROUD (Proud syndrome), OHTAHARA (Ohtahara syndrome), IEDE (idiopathic epileptic-dyskinetic encephalopathy), WEST (West syndrome), XMESID (X-linked myoclonic seizures, spasticity and intellectual disability), PRTS (Partington syndrome) and MRX (non-specific X-linked mental retardation). Figure from (Friocourt and Parnavelas, 2010).

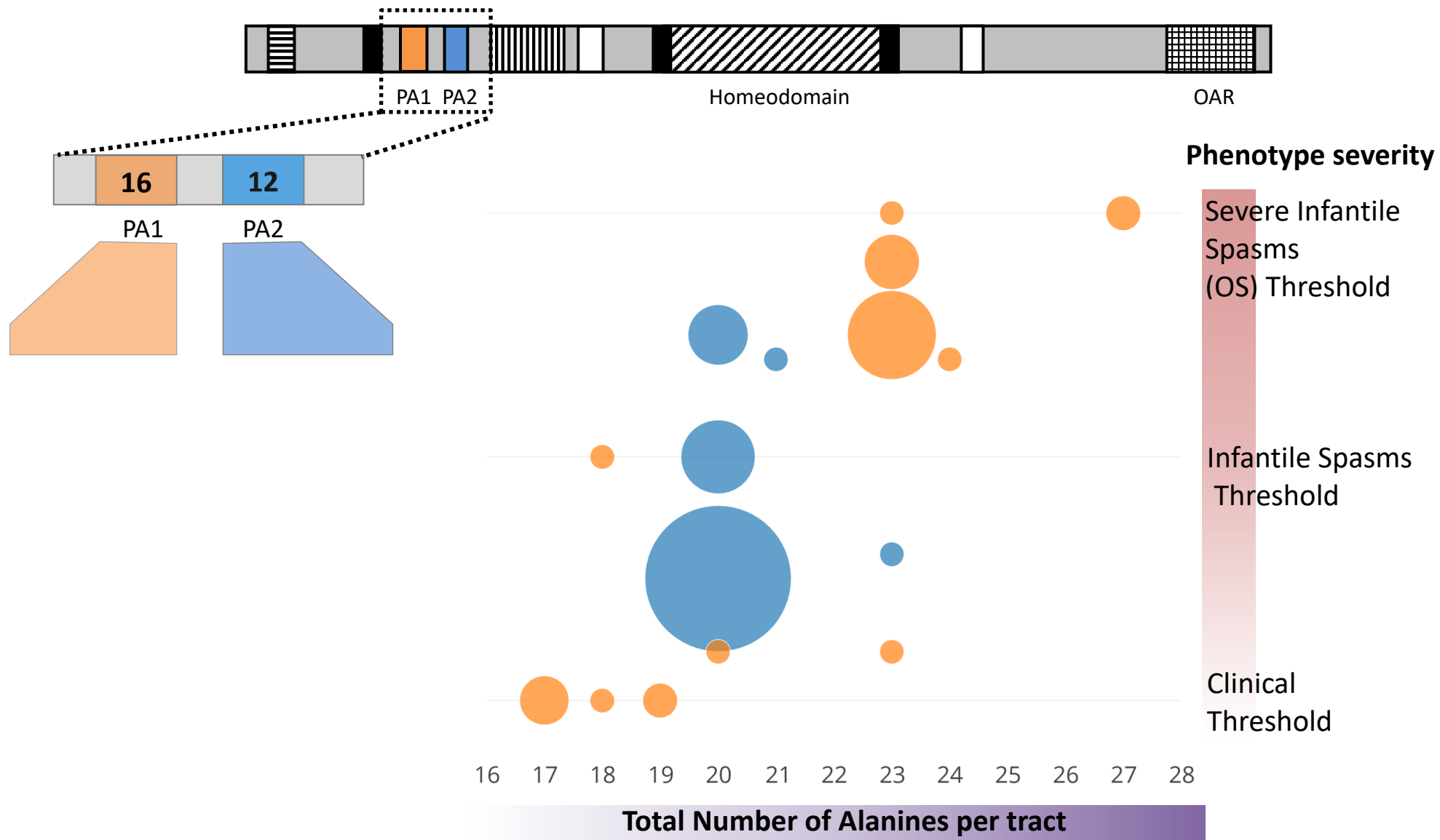


Figure 1.2: Phenotypic variability associated with expansions of the first and second polyalanine tracts in *ARX*. Diagram shows the expansion of the first (orange) and second (blue) polyalanine tracts of the *ARX* gene. Each circle represents the proportion of patients with the number of alanines per tract, and where this number places them on the spectrum of clinical phenotypes (ranging from infantile spasms to severe infantile spasms and Ohtahara syndrome). With increasing numbers of alanines per tract, there is an increase in clinical severity. Other domains of *ARX* include the DNA-binding homeodomain and the *Aristaless* (OAR) domains pictured. Figure adapted from (Marques *et al.*, 2015).

Expansions in the first polyalanine tract result in a variety of clinical presentations. The most common expansion mutation is the c.340ins(GCG)₇ mutation, which leads to the addition of seven alanines, resulting in a total of 23 alanines compared to the normal 16. X-linked infantile spasms with associated comorbidities make up the phenotype of about half of reported families with expansions of the first polyalanine tract expansions. These comorbidities include severe intellectual disability, dystonia, autism spectrum disorder, developmental delay and a hypsarrhythmic EEG patterns, also termed West syndrome (Wohlrab *et al.*, 2005, Guerrini *et al.*, 2007, Poirier *et al.*, 2008, Wallerstein *et al.*, 2008). Several severe and often early onset seizure phenotypes have been reported, including early infantile epileptic encephalopathy (EIEE) and infantile epileptic-dyskinetic encephalopathy (IEDE) (Guerrini *et al.*, 2007) (Shinozaki *et al.*, 2009, Absoud *et al.*, 2010). Interestingly, the same mutation in this tract has resulted in different phenotypes, patients with or without infantile spasms. The mechanisms contributing to this pleiotropy are not yet understood.

Expansions of the second polyalanine tract are overwhelmingly the most common mutation in *ARX*, resulting from the mutation c.429-452dup, expanding the tract from 12 to 20 alanines. The mutation accounts for 40% of all mutations in *ARX*, and of those with expanded polyalanine tract mutations, makes up almost 70% (Shoubbridge *et al.*, 2010). In comparison to patients with mutations of the first polyalanine tract, with quite a severe epileptic phenotype, the majority of patients with mutations of the second tract present with Partington syndrome, a phenotype comprised of non-syndromic intellectual disability, associated with dystonic movement of the hands (Stromme *et al.*, 2002, Partington *et al.*, 2004). A smaller subset of patients present with X-linked infantile spasms/West syndrome (Stromme *et al.*, 2002, Kato *et al.*, 2004, Partington *et al.*, 2004). Furthermore, the behavioural aspects of PA2 patients shine light on the finer details of psychiatric disturbances in these patients. Children with PA2 mutations have been described as having emotional instability, self-aggression, and deficits in social behaviour, with

only 56.3% of patients described to have “adequate personal relationships” (Bienvenu *et al.*, 2002, Stromme *et al.*, 2002, Dubos *et al.*, 2018). Again, the spectrum of phenotypes observed within patients with the same mutation, and indeed even within families, has been noted but not explained (Turner *et al.*, 2002).

While few studies have investigated the effects of these polyalanine expansion mutations in human patients, one study by Curie and colleagues in 2018, performed post-mortem brain examinations, to examine human ARX expression at different foetal stages, and the adult brain, in patients with c.429-452dup mutations. There was strong expression of ARX in the second trimester brain, particularly in neuronal progenitor cells in the cortex, in migratory streams of cells leaving the ganglionic eminences. Interestingly, while there were no major brain malformations in these patients, striatal volume and hippocampal size were decreased, and there was reduced grey matter in the brain, possibly caused by a loss of neurons. The precentral gyrus, part of the primary motor cortex, was also thinner in these patients. This structural malformation may explain the specific motor phenotype of Partington syndrome in c.429-452dup patients (Curie *et al.*, 2018).

1.2.4 Current treatments for seizures in ARX patients

The current intervention for infantile spasms includes adrenocorticotrophic hormone (ACTH) and vigabatrin as first-line treatments (Pellock *et al.*, 2010). ACTH therapy induces the release of adrenal steroids, through which steroid-dependent action on melanocortin receptors, reduces neuronal excitability (Brunson *et al.*, 2002). Vigabatrin serves as a gamma aminobutyric acid (GABA) analogue for the enzyme responsible for GABA catabolism. Thereby, it acts to inhibit GABA being broken down within the brain, increasing inhibition and reducing excitability (Pesaturo *et al.*, 2011). New anti-epileptic drugs as topiramate, and diet regimes such as the ketogenic or Atkins diet have shown promising effectiveness (Song *et al.*, 2017). However, in many ARX patients, spasms and seizures are refractory to these treatments, and in fact, ACTH

can have very severe side effects. These include increased susceptibility to infection due to immunosuppression, hypertension, osteoporosis and metabolic disorders (Riikonen and Donner, 1980, Riikonen, 2004). Among children treated for infantile spasms with ACTH, the most common form of death in childhood was infection (Riikonen, 1996). Furthermore, follow up studies in children receiving ACTH therapy show that only 16% of the patients had normal development following treatment, with 47% continuing to have refractory seizures (Hancock *et al.*, 2013).

West syndrome and infantile spasms are notoriously difficult to treat. Spasms persist in 33-56% of patients treated with ACTH therapy (Song *et al.*, 2017). Further to the lack of effectiveness of ACTH, there have been no new treatments discovered for infantile spasms in the last few years (Specchio *et al.*, 2020). While the lack of reliable animal models for infantile spasms is a contributing factor, the variability in the causes of infantile spasms has made pre-clinical and clinical studies difficult (Specchio *et al.*, 2020). The outlook for patients and their families at this stage is poor, but pre-clinical trials using exogenous steroids have shown promising results for future treatments. Understanding the role that ARX plays in brain development and function is critical to understanding what is happening in the brains of patients, and why current treatments are not effective for treating these disorders.

1.3 ARX & interneurons

1.3.1 Interneuron function

The prefrontal cortex (here after referred to as cortex) of the brain is a highly complex region, comprising approximately 80% of all cells in the brain, and performing intricate functions that are dependent on balanced circuitry. The circuits of the cortex are comprised of two types of cells: excitatory neurons, and inhibitory interneurons. Interneurons comprise approximately 20% of neural cells in this region (Meinecke and Peters, 1987). The diverse cell populations of

the cortex assist in the control of excitatory activity, providing balance of excitation and inhibition. These circuits play an important role in the control of information processing in the cortex. GABA is a neurotransmitter found exclusively in interneurons. GABAergic signalling is required to drive key developmental processes, such as cell migration, axonal and dendritic remodelling, and synapse formation (Sernagor *et al.*, 2010). Hence, interneurons are key regulators of both excitatory and inhibitory outputs of the cortex, as well as modulators of cortical developmental and plasticity.

There are a variety of ways in which interneurons control inhibition in the cortex. Direct inhibition achieves local inhibitory action from a distant interneuron. An example of this is the axons of neocortical interneurons that cross the corpus callosum of the brain to directly innervate their contralateral hemispheric targets (Higo *et al.*, 2007, Tomioka and Rockland, 2007). Feedforward inhibition, on the other hand, reduces the excitatory spike counts of pyramidal (excitatory) neurons by competing with dendritic excitation or reducing spike output. This process involves interneurons receiving excitatory input from an external sources, and in turn inhibiting pyramidal neurons (Buzsáki, 1984). The various dendritic domains of excitatory neurons have dedicated classes of interneurons that target them, and these form the feedforward circuits.

1.3.2 Interneuron migration

Interneurons migrate from the ganglionic eminences, a transitory brain structure in the telencephalon that is present only in early, embryonic brain development. The ganglionic eminences form at approximately embryonic day 11 in the mouse and can be divided into three distinct sub-areas; the lateral ganglionic eminence (LGE), medial ganglionic eminence (MGE) and the caudal ganglionic eminence (CGE). Early in development, most interneurons residing in the cortex are derived from the MGE and CGE, with the LGE aiding in the migration of interneurons during the mid-stage of cortical development (Tan and Breen, 1993, De Carlos *et*

al., 1996, Buchsbaum and Cappello, 2019). GABAergic interneurons migrate tangentially from the MGE primarily, to the cortex, where they can then migrate radially into the cortical layers (described in Figure 1.3). Labelling cells of the MGE with DiI crystals demonstrates that these cells migrate to the developing cortex, where they are dispersed as GABAergic interneurons (Lavdas *et al.*, 1999). Furthermore, MGE and LGE tissue from embryonic mice transplanted into the adult mouse brain, showed that transplanted neuronal precursors from the MGE dispersed and differentiated into multiple adult brain regions, extensively towards the cortex (Wichterle *et al.*, 1999).

Interneuron migration is a tightly regulated process influenced in particular by homeobox transcription factors. The vertebrate distal-less (*Dlx*) genes, encoding the homeobox proteins *Dlx-1* and *Dlx-2*, are expressed in the striatum and pallidum structures of the developing brain. A role for these genes in interneuron migration is demonstrated by a *Dlx-1* and *Dlx-2* double knockout mouse model showing a 70% reduction in the number of cortical interneurons coupled with abnormal migration of interneurons out of the LGE, resulting in the accumulation of only partially differentiated neurons in the LGE, and a loss of normal olfactory bulb interneurons. These double knockout mice do not survive into postnatal life, dying on postnatal day 0 (Anderson *et al.*, 1997). The thyroid transcription factor 1 (*Nkx2.1*) is another homeobox gene expressed in the precursor cells of the pallidum. *Nkx2.1* knock out mice not only die at postnatal day 0, but do not develop a MGE structure at all, due to a loss of cells migrating from the pallidum to the striatum (Sussel *et al.*, 1999). These studies highlight that homeobox genes are vital to the proper development and migration of interneurons in the developing brain.

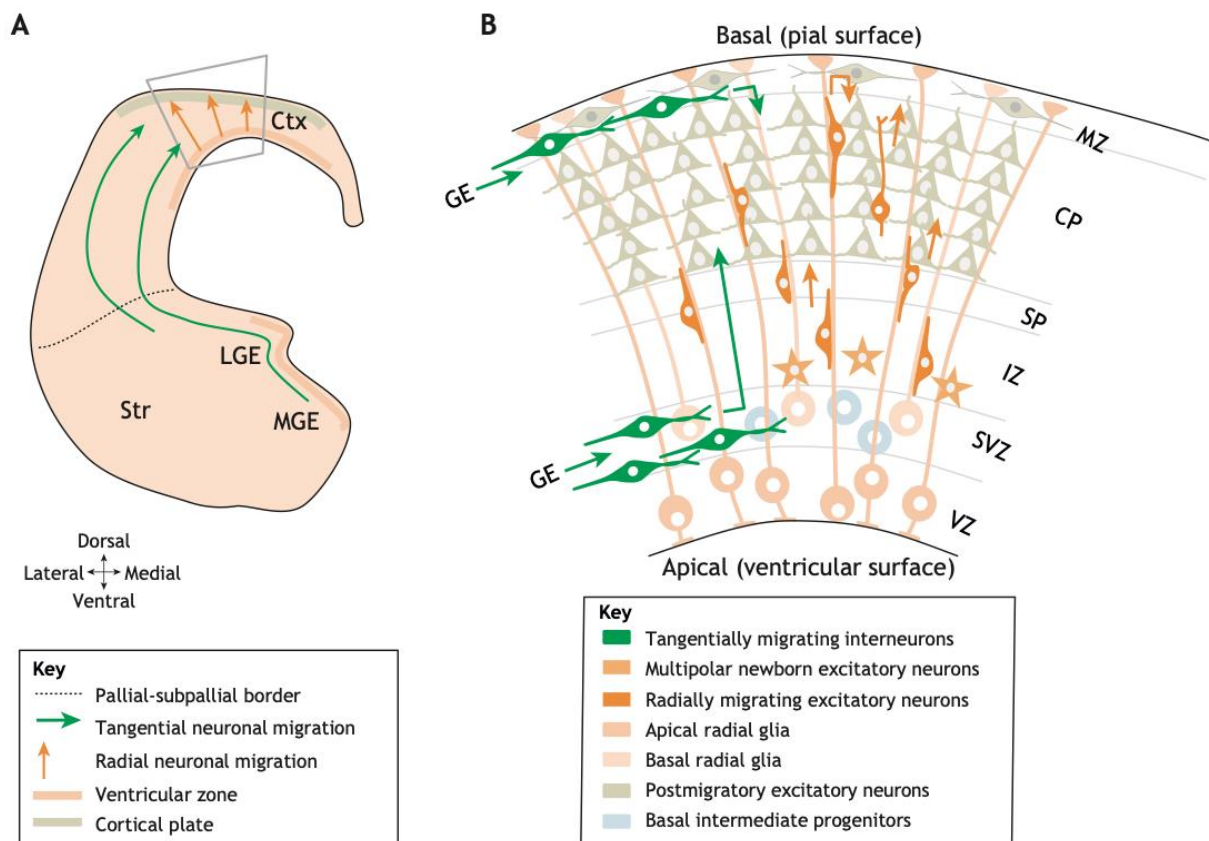


Figure 1.3: Mouse cortical development. (A) Provides a schematic diagram of a coronal section of the developing telencephalon of a mouse at embryonic day 14. The grey box is enlarged in (B). (B) Provides a schematic diagram of the cellular composition of the developing mouse cortex, with radially migrating excitatory pyramidal neurons, and tangentially migrating inhibitory interneurons, which then switch to radial migration in the dorsal cortex. Key: Ctx: cerebral cortex; CP: cortical plate; GE: ganglionic eminences; IZ: intermediate zone; LGE: lateral ganglionic eminence; MGE: medial ganglionic eminence; MZ: marginal zone; SP: subplate; Str: striatum; SVZ: sub ventricular zone; VZ: ventricular zone. Figure taken from (Buchsbbaum and Cappello, 2019)

1.3.3 Interneuron subtypes

When considering the cells in the brain, interneurons have the largest diversity in terms of their morphology, connectivity, and physiology. Interneurons can be categorised based on their morphology, the markers they possess on their surface, and their subsequent function. Interneuron progenitor cells undergo complex migration. Both the site of origin and the migratory path influence the differentiation into the eventual subtype of the mature interneuron. For example, during migration to the cortex interneurons from the MGE gives rise to parvalbumin-positive and somatostatin-positive (STT) interneurons, while the CGE gives rise to less common interneuron subtypes, such as neurogliaform, bipolar and vasoactive intestinal polypeptide (VIP) positive interneurons (Wichterle *et al.*, 2001, Fogarty *et al.*, 2007). This indicates that there are dedicated progenitor populations designated to differentiate into specific subtypes, defined by the gene expression within different regions. From the population of Nkx2.1 expressing progenitors, expression of *Lhx6*, a known target of Nkx2.1, is required for the differentiation of parvalbumin and somatostatin-positive interneurons (Sussel *et al.*, 1999, Fogarty *et al.*, 2007). The most prevalent interneuron subtypes are parvalbumin and somatostatin-positive interneurons (Jinno and Kosaka, 2003). Parvalbumin is present on the surface of basket or chandelier interneurons. These subtypes specifically target the soma of excitatory neurons. Somatostatin is present on the membranes of Martinotti cells, which target the dendrites of excitatory neurons. Approximately 10-12% of GABAergic interneurons are calbindin-positive, and other smaller subsets include VIP, calretinin and neuropeptide-Y-positive interneurons (Gulyás *et al.*, 1991). The functional diversity of the most common interneuron markers and subtypes is outlined in Table 1.1.

Table 1.1: Overview of interneuron markers and their respective interneuron subtypes.

	Developmental origin	Cell types	Targets
Parvalbumin (PV+)	MGE	Basket interneurons Chandelier interneurons	Excitatory cell dendrites and axons
Somatostatin (STT+)	MGE	Martinotti cells	Excitatory cell dendrites
Vasoactive intestinal peptide (VIP+)	CGE	Bipolar interneurons Multipolar interneurons	Interneurons
Non-VIP+	CGE	Single bouquet cells Neurogliaform	Synapses

1.3.4 ARX & interneuron migration and function

ARX expression peaks between embryonic days 12.5 and 15.5, continuing to be expressed throughout embryogenesis, before being downregulated in postnatal life (Figure 1.4 A) (Miura *et al.*, 1997, Kitamura *et al.*, 2002). ARX is highly expressed in the embryonic brain, ovaries, and testes and to a lesser degree in other tissues including skeletal muscle and pancreas (Figure 1.4 A) (Miura *et al.*, 1997, Kitamura *et al.*, 2002, Heller *et al.*, 2005, Biressi *et al.*, 2007). Within the embryonic brain ARX is expressed in neural progenitor cells and immature neurons through the subpallium, a region which includes the LGE and MGE (Figure 1.4 B) (Lee *et al.*, 2014). These cells further develop into various regions of the brain; the striatum, globus pallidus and cholinergic nuclei, as well as differentiating into the interneurons that migrate tangentially to the cortex, olfactory bulb and hippocampus (Miura *et al.*, 1997, Poirier *et al.*, 2004). In human patients with loss of function mutations in *ARX*, a classical lissencephaly phenotype can arise, seen in MRIs of patients (Figure 1.5). This is the result of disorganised neuronal migration. The abnormal neuronal migration leads to a smooth and thickened cortex without gyri, with an accumulation of cells in the sub cortical layers, and a wider, extra layer resulting below the normal cortical plate (Figure 1.5) (Romero *et al.*, 2018). This phenotype is a result of the loss of ARX's function in migration of both inhibitory and excitatory neural progenitor cells (Kitamura *et al.*, 2002, Romero *et al.*, 2018).

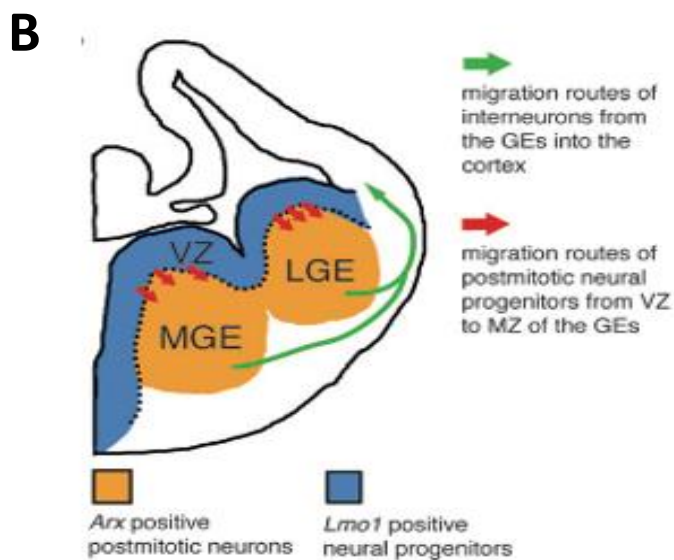
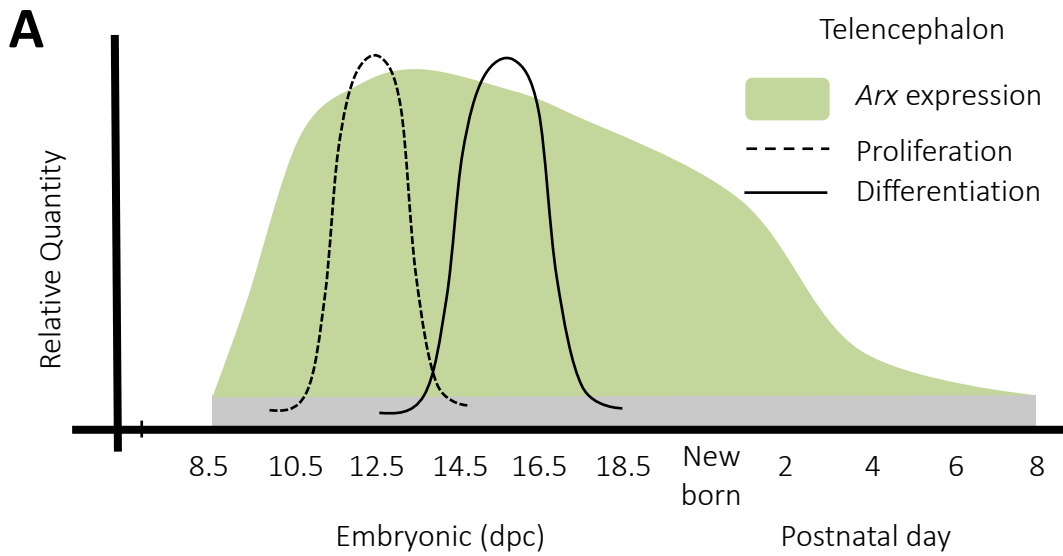


Figure 1.4: Expression and migration of Arx positive cells in the developing brain. (A) Expression of *Arx* in the mouse telencephalon from embryonic day 8.5 to postnatal day 8. Expression of *Arx* peaks with proliferation and differentiation of developing neuronal cells. (B) Migration patterns of interneurons from the ganglionic eminences to the cortex, with *Arx* expression highlighted in orange. Arrows indicate direction of migration of neuronal progenitor cells. Figure (B) adapted from (Lee *et al.*, 2014).

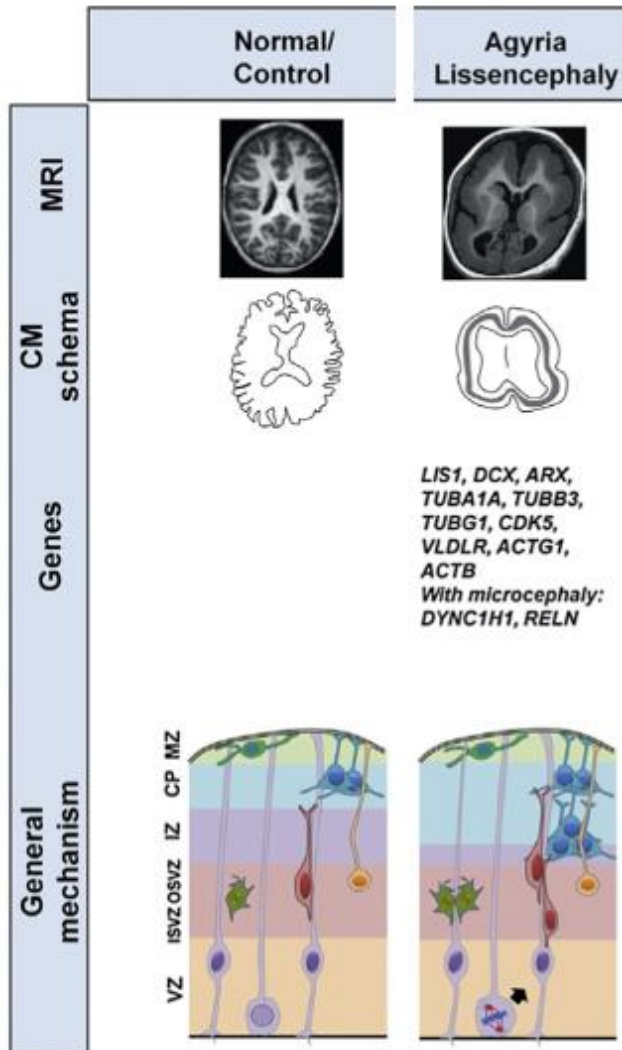


Figure 1.5: Comparison of normal cortical development and impaired development with loss of ARX function. MRI images from patients describe normal imaging of the brain compared to the agyria/classical lissencephaly phenotype seen in patients with loss of function mutations in *ARX*. Schematic diagrams show mechanism leading to lissencephaly. Key: mature neurons (blue), immature neurons (red), radial glial cells (purple), intermediate progenitors (green), ventricular zone (VZ), intermediate zone (IZ), cortical plate (CP), marginal zone (MZ) and inner and outer sub ventricular zones (ISVC & OSVC). Figure adapted from (Romero *et al.*, 2018).

Some of the most compelling studies on ARX function come from knocking out the *Arx* gene in mice. A study by Kitamura and colleagues showed that when *Arx* was knocked out in male mice by disrupting exon 2, the mice had severe brain malformations and died early in postnatal life, generally around postnatal day 2. Compared to wild-type mice, the brains were smaller, the cortical plate was thinner, and there was a deficit in tangential migration of GABAergic interneurons from the MGE to the cortex, and a complete failure of radial migration from the LGE. The mice also showed a reduction in the proliferation and migration of excitatory neurons (Kitamura *et al.*, 2002). Focusing on interneuron migration, a study by Colombo and colleagues in 2007 used these *Arx* deficient mice to show that not only was tangential migration towards the cortex reduced, radial migration of cells towards the cortex was also reduced, and these deficits lead to abnormal accumulation of neuropeptide-Y and calretinin-positive interneurons in the MGE. These mice had reduced expression of *Map2* in the brain, a marker of differentiated neurons. Together, this data highlights the critical function of *Arx* in promoting interneuron migration in the brain, but also in differentiating cells to allow proper targeting to their correct position in the layers of the cortex (Colombo *et al.*, 2007).

Using a different approach, Friocourt and colleagues in 2008 used *in utero* electroporation to either knock down or overexpress *Arx* in the progeny of pregnant female mice. Here, inhibition of *Arx* caused cortical progenitor cells to exit the cell cycle prematurely and impaired their migration towards the cortex. Conversely, overexpression of *Arx* lengthened the cell cycle. Interestingly, both inhibition and overexpression of *Arx* impaired the migration of GABAergic interneurons from the ganglionic eminences to the cortex. Inhibition of *Arx* also decreased neuronal motility, while overexpression of *Arx* affected the radial migration of pyramidal neurons. This study demonstrates the importance of *Arx* regulation and strict control of cellular migration for proper brain development (Friocourt *et al.*, 2008).

ARX is thought to regulate neuronal migration through transcriptional activity. A study by Colasante and colleagues in 2009 used microarrays, quantitative PCR and RNA *in situ* hybridisation techniques with the *Arx* deficient mouse model, to investigate the role of *Arx* regulating gene expression in the telencephalon. They found that when *Arx* was lost, many critical developmental genes were upregulated or downregulated. *Ebf1*, a neuronal transcription factor, with roles in the radial migration of neurons, had increased expression with the loss of *Arx*, indicating a strong interaction between the two proteins. *Cxcr4* and *Cxcr7*, genes found to be repressed with loss of *Arx*, also have critical roles in neuronal migration, and are present in developing interneurons. Interestingly, it was found that genes *Lmo1*, *Lmo3* and *Lmo4*, were more strongly upregulated in the MGE compared to the LGE, indicating differing impacts of the repressive role of *Arx* in different regions of the brain (Figure 1.4 B) (Colasante *et al.*, 2009, Lee *et al.*, 2014). A subsequent study focusing specifically on the cortical interneurons between embryonic days 13.5 and 15.5, highlight 14 known *Arx* target genes enriched and five downregulated in migrating interneurons (Friocourt and Parnavelas, 2011).

An indirect way of studying *Arx* and its transcriptional activity, is by studying knock out mouse models of *Npas1* and *Npas3*. These genes are expressed in the progenitor neurons of the basal ganglia, and have opposing effects on the brain when their function is lost. *Npas1* knock out mice exhibit increased inhibition in the cortex, with excess STT and VIP interneurons. There was also increased expression of *Arx* in the MGE and CGE. Contrary, *Npas3* knock out mice featured a loss of cortical inhibition, with a reduction of STT and VIP interneurons, and decreased expression of *Arx* in the ganglionic eminences (Stanco *et al.*, 2014). Importantly, this study shows that *Npas1* is a key regulator of *Arx* enhancer activity, and overexpression of *Arx* leads to an increase of progenitor cells in the CGE, leading to this excess inhibition and increased interneuron density in the cortex (Stanco *et al.*, 2014).

When partial loss of *Arx* is modelled by expansion mutations of the first and second polyalanine tracts of the gene, disruptions to gene regulation are observed. A transcriptome wide RNA sequencing study performed within our laboratory, analysed the developing telencephalon of these mouse models at embryonic day 12.5 found a large number of deregulated genes in mice with mutations of the first and second polyalanine tracts of *Arx*. This allowed a thorough transcriptomic profile of “*Arx* responsive genes” to be compiled. These genes were enriched in pathways involved in key neurodevelopmental processes, such as cell to cell adhesion, neuronal development and neuronal membrane properties, or were strongly associated with neurodevelopmental disorders like intellectual disability and epilepsy (Mattiske *et al.*, 2016). Furthermore, another mouse model with an expansion of the second polyalanine tract features deregulated interneuron development genes in the forebrain of pups at embryonic day 15.5. Genes involved in processes involving synaptic transmission, central nervous system development and DNA interaction (Dubos *et al.*, 2018). These gene expression studies are particularly interesting, as these partial loss of function models of *Arx* still have a significant impact on the transcriptome of these mice and can help to investigate pathophysiology and pathways associated with neurodevelopmental disorders in which *Arx* is implicated.

In terms of specific interneuron deficits in these mice, there are prominent features in two mouse models with expansion mutations of the first polyalanine tract (PA1). In one of these mouse models, there was an overall reduction in calbindin and neuropeptide-Y positive interneurons in the cortex and striatum of six week old mice (Price *et al.*, 2009). Furthermore, there is a wave of elevated apoptosis in the cortex in the first postnatal week of life in these mice (Siehr *et al.*, 2020). Interestingly, in an alternate PA1 mouse model, the model used in our laboratory, while there is a scarcity of neuropeptide-Y, somatostatin, and GABA positive cells in the cortex, there is no overall loss of calbindin positive interneurons, but instead a deficit in normal migration of these cells (Kitamura *et al.*, 2009, Lee *et al.*, 2017). Lee *et al.* found that there was a specific spatial loss of approximately 50% of calbindin positive cells in the cortex of these mice at

postnatal day 0 compared to wild-type mice. When looking at specific regions of the brain, this was shown to be due to a lag in migration of these cells. Calbindin positive cells were found to be arrested in the ventral subpallium of the cortex, while migrating to the cortex through the process of tangential migration, which Arx is known to play a pivotal role in (Figure 1.6). This suggested that the halt in migration of the calbindin positive cells was in fact due to slowed migration rather than changes to cell proliferation or the cells exiting the mitotic cycle (Lee *et al.*, 2017). Tangential migration of somatostatin positive interneurons is also suppressed in this PA1 mouse model (Kitamura *et al.*, 2009). Importantly, this research indicates that even a partial loss of Arx function can have drastic effects on correct interneuron positioning and abundance in the developing cortex of mice.

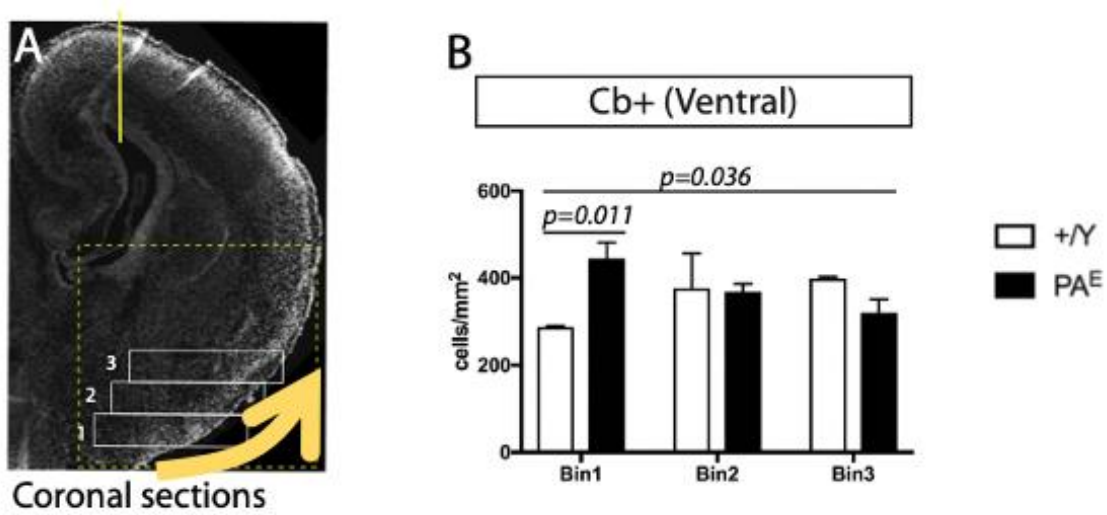


Figure 1.6: Accumulation of arrested calbindin positive (Cb+) cells in the ventral cortex.

Coronal sections were used to investigate the density of Cb+ cells in the ventral telencephalon of PA1 and PA2 mice at postnatal day 0. The region screened is seen in (A) in the yellow box. Yellow arrow indicates direction of normal migration of Cb+ positive cells. Cells were counted within bins 1, 2 and 3, identified in (A). Quantification of Cb+ cells was conducted within these boxes, demonstrating the distribution of Cb+ cells was increased in Bin 1 in PA mutant mice (B). Scale bar in (A): 500 μ M. Figure taken from (Lee *et al.*, 2017).

1.4 *Arx* mouse models

1.4.1 Expanded polyalanine tract mutations

There have been several mouse models created with the mutations expanding the polyalanine tracts of *Arx*, representative of those present in patients. At present, there are two PA1 mouse models. Kitamura and colleagues developed a mouse modelling the expansion of the first polyalanine tract (PA1), an $Arx^{(GCG)7/Y}$ mouse model. This mouse presents with a phenotype of X-linked infantile spasms, or West syndrome, recapitulating the phenotype seen in PA1 patients. This mouse has 40-60% less *Arx* protein when compared to the wild-type mice. Most of the mice with this mutation died before three months of age, with some living to 5-6 months, with deaths presumably caused by the seizures observed in 70% of mutant mice. The mice also presented with impaired learning and cognitive function, with deficits in spatial learning and procedural learning. $Arx^{(GCG)7/Y}$ mice also had increased locomotor activity and high anxiety when compared to the wild-type mice (Kitamura *et al.*, 2009). This is the PA1 mouse model we have used in our study.

Price and colleagues developed an independent PA1 model in 2009, the $Arx^{(GCG)10+7}$ mouse (Price *et al.*, 2009). The seizure phenotype of the $Arx^{(GCG)10+7}$ mouse is similar to the $Arx^{(GCG)7/Y}$ mouse model, with 75% of adult mice having abnormal EEG results (reminiscent of a seizure), compared to 70% in the $Arx^{(GCG)7/Y}$ mouse model. The $Arx^{(GCG)10+7}$ mouse also presented with infantile spasms quite early in development. The $Arx^{(GCG)10+7}$ mouse display subnormal anxiety levels, presenting as a less fearful model than their wild-type counterparts. Similar to the Kitamura PA1 model these mice showed a lack of learned fear responses and autistic-like behaviour (Price *et al.*, 2009). We refer to this model as the alternate PA1 mouse.

Although both PA1 models show similar phenotypes, there are some distinct differences reported (Table 1.2). While it is unknown why exactly the two models differ, it is interesting to note the differences in the expansion of the PA1 tract in each model. The Kitamura mouse

model ($Arx^{(GCG)7/Y}$) mimics the length of the expansion of the tract seen in mice, with the addition of seven GCG repeats (the human codon usage) (Kitamura *et al.*, 2009). The Price *et al.* mouse model, the $Arx^{(GCG)10+7}$ mouse, utilised the mixed codon usage seen in mice (GCG, GCC and GCT), and added eight repeats to expand the tract to 23 alanines, the length seen in human patients (Price *et al.*, 2009). While both models present with seizures and behavioural deficits, the interneuron subtypes determined to be affected in these models differ, which may contribute to differences in the phenotype of each model.

Kitamura and colleagues also generated a mouse model of the most commonly mutated polyalanine tract 2, but the $Arx^{432-455dup/Y}$ mice were not as extensively studied in the initial report (Kitamura *et al.*, 2009). The Shoubridge laboratory has been investigating the $Arx^{(GCG)7/Y}$ or PA1 and $Arx^{432-455dup/Y}$ or PA2 models derived from the Kitamura laboratory in a comparative manner. Overwhelmingly, they have shown that the PA2 model presents with a very similar phenotype to the PA1 model in terms of seizures and behavioural deficits (Jackson *et al.*, 2017). This is the second of the two mouse models utilised in my study.

In terms of seizures, video-EEG analysis, all PA2 mutant males showed abnormal epileptic activity, with bursts of high frequency spikes, and low amplitude oscillatory discharges. These episodes of abnormal epileptic activity lasted up to 90 seconds in duration. This was visually correlated to physical movement capture by video monitoring, varying from mouth movement, head movement, tail extension, and mild myoclonic seizures or rearing and falling with clonus of the forelimbs. Seizures were categorised (in conjunction with the Video-EEG data) into four categories, providing a powerful tool to assess the severity and frequency of the types of seizure in these mouse models using non-invasive video seizure monitoring. Category 1 was movement phenotypes, such as head and tail movements; category 2 was mild myoclonic seizures; category 3 was severe myoclonic seizures, lasting longer than 10 seconds; with category 4 where mice were found dead presumably from a lack of recovery after a seizure. There was a

wide variability in seizure severity and frequency between individual mice, similar to that seen in patients with these mutations. However, the first myoclonic seizures were observed at postnatal days 18 and 19 in the PA1 and PA2 mice, with most seizures observed after one month of age. By weaning (postnatal day 21), myoclonic seizures had been witnessed in 18% of PA1 mice and 42% of PA2 mice. By postnatal day 70, as many as 73% of PA1 and 97% of PA2 mice had an observed seizure. Both PA1 and PA2 mice likely died from their seizures, with 45% of the PA1 cohort dying and only 15% of PA2 mice surviving to postnatal day 70.

Behavioural testing in these two strains also demonstrated similar phenotypic presentations between the PA1 and PA2 mice generated by Kitamura. Prior to this study, no behavioural phenotyping data had been published on the PA2 mouse. There was increased anxiety in both mice coupled to decreased exploratory behaviour in the open field apparatus. Increased exploratory behaviour with a decreased fear response was demonstrated in both strains using an elevated zero maze. Despite these seemingly conflicting data, these tests assess different types of anxiety, in relation to open spaces and height respectively. Further testing of cognitive function indicated a decreased capacity in both mouse models (Y-maze test) with autistic-like traits (sociability testing) demonstrated in these mice, both characteristic features of human patients with these mutations (Jackson *et al.*, 2017). The similarities between these two mouse models was thought to be driven by overlapping deregulated transcriptomes of these two mutations, as described by Mattiske and colleagues, in early embryogenesis at embryonic day 12.5 (Mattiske *et al.*, 2016).

An independent PA2 mouse model has more recently been developed by Dubos and colleagues (Dubos *et al.*, 2018). These mice are a partially humanised model, with the c.428_451 dup24 mutation duplication, creating the *Arx*^{dup24/0} mouse. Interneuron migration was altered in these mice, with a deficit in cells expressing *Arx*, calretinin, calbindin, somatostatin and *Chat* (expressed by cholinergic cells), in the embryonic brain and at postnatal day 0. Interestingly,

only 8% of mutant pups had infantile spasms, and at the adult stage, mutant mice had no spontaneous seizures. When injected with a pro-epileptic drug, pentylenetetrazol (PTZ), mutant mice had no difference to seizure susceptibility. The mice exhibited hyperactivity in the open field test and displayed altered anxiety and contextual fear learning in the fear conditioning test. The mice also had significant deficits to fine motor skills such as grasping and reaching, comparative to patients with expansions of the second polyalanine tract (Dubos *et al.*, 2018). These mice recapitulate the milder PA2 phenotype of patients, thus providing a useful future model to compare alongside the Kitamura *et al.* mice, to examine the convergent cell and molecular contributors to the phenotype in PA2 patients.

While the phenotypes reported do vary slightly between the two PA1 and the two PA2 mouse models, the spectrum of phenotypes between the different models, and within individual mice, recapitulates the spectrum of phenotypes reported in human patients. Differences align between the varied interneuron subtype deficits we see between the two PA1 mouse models, indicating a possible difference in pathogenesis at the cellular model of these mice, though both show a very similar seizure phenotype. The Kitamura *et al.* PA2 mouse model represents the more severe end of the seizure phenotype that is reported in a small number of PA2 patients. Although PA2 patients show a variety of seizure phenotypes, generally PA1 patients all have severe epileptic phenotypes. The interneuron deficits between the Kitamura PA2 mouse and the Kitamura PA1 are also quite similar, shown in Lee *et al.* (Lee *et al.*, 2017). The Dubos *Arx*^{dup24/0} mice show the milder phenotype seen in the majority of PA2 patients. Meanwhile, both PA1 mouse models closely align to the spectrum of phenotype seen in patients.

Table 1.2: Overview of phenotypic differences between the two different PA1 and PA2 mouse models.

	PA1		PA2	
	Kitamura <i>et al.</i> 2009 model	Price <i>et al.</i> 2009 model	Kitamura <i>et al.</i> 2009 model	Dubos <i>et al.</i> 2018 model
Seizures	70% mice had abnormal EEG patterns 70% mice with observed seizures	75% mice had abnormal EEG patterns Pups had infantile spasms	100% mice had abnormal EEG patterns 97% mice with observed seizures	8% of pups had infantile spasms No seizures in adult mice No increase to induced seizure susceptibility
Fear/anxiety	↓ Fear response ↑ Anxiety	↓ Fear response Subnormal anxiety	↑ Anxiety ↓ Fear response	Hyperactivity Altered anxiety
Locomotion/exploration	↑ Locomotor activity ↓ Exploratory behaviour		↑ Locomotor activity ↓ Exploratory behaviour	↓ Fine motor skills
Cognition	↓ Cognitive function		↓ Cognitive function	↓ Contextual fear learning
Autistic-like behaviour	Yes	Yes	Yes	No
Mortality	45% mice died before two months of age		85% mice died before two months of age	

1.4.2 Other *Arx* mouse models

Looking at conditional loss of *Arx* can have advantages to studying the function of *Arx* without other severe sides of a phenotype interfering with studying brain development. Two main conditional knock-out models will be discussed. One such model is the *Arx*^{-Y}; *Dlx5/6*^{CIG} (hemizygous males) and *Arx*^{-/+}; *Dlx5/6*^{CIG} (heterozygous females) mice. These mice have a near complete loss of *Arx* from the ventral forebrain from embryonic day 14.5 onwards. All hemizygous males exhibit abnormal EEG activity and spontaneous seizures, with similar features to the epileptic spasms seen in infantile spasms patients and the PA1 and PA2 *Arx* mouse models described, such as whole body flexion and extension, forelimb clonus and rearing. Interestingly, heterozygous females also showed a seizure phenotype, not seen in the other *Arx* mouse models, with about 50% presenting with seizures, similar to those seen in the hemizygous male mice (Marsh *et al.*, 2009).

No major anatomical differences were seen in the brains of the hemizygous or heterozygous mice, nor were there any differences to body or brain weights. However, specific interneuron deficits were observed at P14, P17 and in the adult brain. Similar to the Price *et al.* PA1 mouse, the most severe loss was seen in calbindin positive interneurons. Smaller reductions were observed in calretinin positive cells, and no change was observed in parvalbumin positive cells. This shows that when *Arx* is knocked out in the interneurons of the brain, interneuron subtype specific development is suppressed (Marsh *et al.*, 2009).

More extensive studies of specific interneuron development have since gone on to be studied in this mouse model, involving crossing the mouse with a fluorescent marker to study migration and development of the affected cell types. There was a great deal of variability in the number of *Arx* positive cells in the brain at embryonic day 18.5, P14 and in the adult brain, but an almost complete loss of *Arx* was still seen. At P14, there was a reduction of *Arx* positive neurons in the upper layers of the cortex, but with some preservation of these cells in the

deeper layers. This study also found that the calbindin positive cells were actually increased in the ventral regions of the cortex, including the striatum, at embryonic day 14.5, but decreased in the dorsal telencephalon (Marsh *et al.*, 2009). This indicates that Arx is pivotal for migration of these cells, and without this migratory guidance, these cells are halted, shown in the expanded polyalanine tract mutation models as well (Lee *et al.*, 2017).

Further, no differences were observed at embryonic day 18.5 or postnatal day 14 in the cortex, but there was a loss in the hippocampus at this later time point. While there was a trend towards loss of calretinin positive cells in the cortex, this did not reach significance. However, the study did show a loss of neuropeptide-Y positive cells in the ventral region of the forebrain, which persisted to postnatal day 14. No differences in somatostatin positive cells were observed. Parvalbumin, not expressed until postnatal day 14, was shown to be reduced in the hippocampus but increased in the cortex (Marsh *et al.*, 2016).

Another mouse model, a conditional knock-out $Arx^{-/Y}; Emx1^{Cre}$ mouse, selectively removes Arx from the dorsal telencephalon. Interestingly, this mouse model did not show any difference to the number of interneurons compared to the brains of their wild-type litter mates. Predictably, these mice did not present with the seizure phenotype we see in most of the other Arx mouse models. When a large battery of behaviour tests was performed on these mice, spatial learning and memory was found to be comparable to wild-type mice, but fear-based memory was impaired, something seen in other Arx models. These mice were less anxious however, and more exploratory, and, comparable to the PA1 and PA2 mice, were more hyperactive than wild-type mice. These mice also presented with autistic-like behaviour, with social deficits shown through sociability testing (Simonet *et al.*, 2015).

Anatomically, the $Arx^{-/Y}; Emx1^{Cre}$ mouse had smaller cortices, amygdalas and white matter tracts compared to wild-type, hypothesised to be the cause of the decreased anxiety phenotype

seen in this model. This study, while surprising compared to the usual phenotype seen in patients with *ARX* mutations, with no seizures or spatial learning deficits, sheds light on the function of *Arx* in different regions of the brain. The loss of *Arx* in the progenitor cells in the mouse led to structural, function and behavioural deficits, through a loss of cortical connections and reduced cortical and amygdala volumes, but showed a longer lifespan due to the lack of a seizure phenotype (Simonet *et al.*, 2015). The lack of interneuron deficits coupled with a no seizures or grip strength deficiency, provides further evidence to the importance of interneurons on these particular aspects of *Arx/ARX* mutant phenotypes. This mouse also further shows that cognitive dysfunction is not simply due to the epilepsy phenotype of these patients, and that some behaviours are due to the *Arx* mutation itself, further shown in that some patients present without seizures but with intellectual disability, particularly PA2 patients (Turner *et al.*, 2002).

A mouse model with selective *Arx* loss in the cerebral cortex has proven useful to understanding the spatial importance of the gene in the brain. The developing brains of this model had a specific loss of cortical progenitor cells, particularly in the intermediate zone. Furthermore, later in brain development, there was a loss of neurons in the upper layers of the cortex, but not within the deeper layers (Colasante *et al.*, 2015). Transcriptional profiling in embryonic life at E14.5, interestingly showed that with this loss of *Arx*, there was overexpression of *Cdkn1c*, a key inhibitor of cell cycle progression. This data provides evidence that *Arx* is a direct regulator of *Cdkn1c* transcription, and inhibition of this process contributes to the loss of neurons and progenitor cells in the brains of these mice (Colasante *et al.*, 2015).

1.4.3 Benefits and limitations of mouse models for research

Animal models remain vital to understanding mechanisms of disease and to find methods and drugs to treat diseases. When using mouse models for research however, it is important to consider the benefits and limitations. The mouse is closely related to humans, being a mammal, can produce multiple progeny reasonably quickly, and strains are inbred, meaning they will be highly conserved and similar between individuals. The mouse is genetically and physiologically like humans, making it a useful model for pre-clinical screening of potential therapies for disorders. Furthermore, mice being inbred means they do not capture the genetic variation existing in the human population, something that could be key to the phenotypic variation seen in patients with *Arx* mutations. In general, however, mice are not human, and using mouse models to test novel therapeutic strategies is only part of pre-clinical investigation.

Embryonic development differs in the mouse, with gestation being 18 days compared to 270 days in humans. This means that the timing of key developmental milestones between mouse and human do not readily match up, and much of what occurs while still *in utero* in human development occurs postnatally in the mouse, particularly in the brain. For instance, neurogenesis occurs up to postnatal day 0 in the mouse, with neuronal pruning occurring up to day 21 postnatal, while this all occurs *in utero* in humans. Telencephalic neuronal migration occurs before 20 weeks gestation in humans, while this occurs up to embryonic day 16 in mouse, with cortical positioning occurring to postnatal day 10 (Pressler and Auvin, 2013, Semple *et al.*, 2013, Olivetti *et al.*, 2014). The mouse does recapitulate many aspects of human brain development however, with the basic steps of neurogenesis remaining conserved between both models, as well as the general migratory patterns of inhibitory and excitatory neurons (Buchsbbaum and Cappello, 2019). However, there are differences in the numbers of neuronal progenitors, their expansion and division capacity, as well as the complexity of the human

cortex compared to that of the mouse. This unsurprisingly results in the higher cognitive functions a human can perform (Buchsbaum and Cappello, 2019).

Cognitive testing batteries are thorough and allow research into intellectual disability in mouse models. These behavioural tests investigate both exploratory behaviours through open field test for example, as well as learned behaviour like Y-maze and Barnes maze, which test more complex memory, both working and long-term (Wahlsten, 2011). However, these tests have their limitations. Many memory-based tests work from hippocampal or spatial memory. If the hippocampus is not the most weakened region of the brain in a disease of interest, these tests may not show the full extent of impaired learning, compared to a test that works from cortical learning (Wahlsten, 2011). High mortality rates of mouse models can also impair the ability to perform cognitive testing, as it can be difficult to reach the required sample sizes for large scale studies.

Additionally, there can be discrepancies between clinical trials and treatment studies between mice and humans, often having quite different outcomes (Lee *et al.*, 2012). An increased understanding of the molecular mechanisms behind neurodevelopmental disorders has since lead to the production of more physiologically or genetically relevant mouse models which recapitulate the human phenotypes, providing a platform to enhance the capacity for translatable outcomes arising from pre-clinical trials (Gross *et al.*, 2015, Berry-Kravis *et al.*, 2018). Although limitations do need to be considered when using these models, particularly differences in brain structure and development, overall, genetically modified mice provide a clinically relevant model for assessing cognitive function and investigating the neuropathological basis of diseases and testing drugs. Mouse models provide important information on the mechanisms of disease and subsequent treatments, allowing for more robust and reproducible results when moving to human clinical trials. One relevant example for ARX

and my project, is the recent work investigating the role of exogenous steroids to alleviate the severity of otherwise intractable seizures.

1.5 Exogenous steroids as a treatment for infantile spasms and seizures

While conventional therapies aren't effective for the refractory seizures we see in some patients with *ARX* mutations, a study performed by our collaborators, Olivetti and colleagues, found that short-term β -estradiol (E2) given to the *Arx*^{(GCG)¹⁰⁺⁷} PA1 mouse model between postnatal days 3 and 10 improved the seizure outcomes of these mice (Olivetti *et al.*, 2014). In the developing male mouse brain, there is a surge of E2 due to the conversion of testicular testosterone to E2, and heightened estrogen receptor expression in the brain (Wonders and Anderson, 2006, McCarthy, 2008, Sugiyama *et al.*, 2008). This period overlaps with interneuron migration and the positioning of interneurons in the cortical layers, occurring between embryonic day 11 and postnatal day 10. E2 is a short-acting exogenous steroid and has roles in modulating neuronal excitability and neurotransmitter release. E2 induces changes to gene expression via the estrogen receptor, inducing effects on developing neurons, to produce long-term transcriptional changes. These pathways have been shown to play roles in the proliferation of progenitor cells, neuronal migration, synaptogenesis and dendritic spine formation, all key developmental milestones in the brain (McCarthy, 2008, Boulware and Mermelstein, 2009). These processes are part of the normal maturation process of neuronal cells, and it was hypothesised that by improving these processes in the brains of PA1 mice, their phenotype would be improved.

To determine the appropriate timing of treatment, E2 was given both at an early postnatal age and again later in life, between postnatal days 33 and 40. The late-treated group of mice showed no difference to seizure frequency as determined through EEG, while the early-treated group, given E2 between postnatal days 3 and 10, showed a 64% reduction in seizures. This mouse

model shows spasms between postnatal days 7 and 11, and when treated with E2 no mice displayed spontaneous spasms compared to about one third of mice treated with a vehicle (Olivetti *et al.*, 2014).

To investigate a potential mechanism of action for E2, the interneurons of mice treated with E2 or a vehicle were investigated. With E2 treatment, mice had 30% more neuropeptide-Y interneurons in the somatosensory cortex compared to wild-type mice, where vehicle treated mutants had a 36% decrease in this subtype of interneuron, meaning E2 rescued the phenotype to above the wild-type level. This was shown for calbindin-positive interneurons as well, however no deficit in this subtype was seen in the vehicle treated mutants, indicating that estradiol increased the calbindin-positive cell number in the brain to 42% above wild-type mice treated with vehicle. Interestingly, E2 also increased calbindin-positive interneurons in wild-type mice, who do not show a deficit in these cells in the normal brain. E2 rescued the reduced numbers of cholinergic interneurons to wild-type levels (Olivetti *et al.*, 2014). These results show that E2 promotes migration and recovery of neurons in the brain, even independent of the impact of a mutation in *Arx*.

Furthermore, E2 also changed the expression of genes normally regulated by *Arx*. Normally *Arx* represses *Ebf3*, *Lmo1* and *Shox2* and activates *Lhx7*, *Cxcr4*, *Cxcr7* and *Lgi1* in interneurons (Friocourt and Parnavelas, 2010, Mattiske *et al.*, 2016). Quantitative real-time PCR was performed on the brains of mutant mice treated with E2. *Shox2* expression was decreased, *Lgi1* expression was upregulated, and *Ebf3* expression was repressed (Olivetti *et al.*, 2014). These results show that not only does E2 improve the interneuron deficits in PA1 mutant mice, it also acts upon downstream targets of *Arx*. The findings of this study provide promising research for exploring exogenous steroids as potential treatment options for infantile spasms and epilepsy.

Further to this initial study on the Price *et al.* PA1 mouse model, investigations on apoptosis in the brain of these mice, found that E2 treatment did not diminish this wave of cell death. The treatment however did still rescue the populations of *Arx* positive cells in the cortex. This indicates the apoptosis in the brain is not solely responsible for the seizure phenotype in this PA1 mouse model, as the treatment was still effective at improving seizure outcomes in the mice (Siehr *et al.*, 2020). This study shows the importance of using treatment trials to help understand the pathophysiological mechanisms of disease.

Following the Olivetti study, other research groups have attempted to reproduce the effect of E2 on alleviating infantile spasms in different models of the disorder. One such study used a betamethasone-NMDA model of infantile spasms in rats, where betamethasone is given *in utero* around embryonic day 15. The rats were then treated with the same dosage of E2 used in the Olivetti study, between postnatal days 3 and 10. At postnatal days 12, 13 and 15, the rats were subject to NMDA triggered spasms. ACTH was used as a positive control, as this treatment is known to alleviate these induced spasms in this animal model. It was shown that E2 treatment had no effect on the spasms in this model (Chachua *et al.*, 2016).

Interneuron populations were investigated in these rats, the number of GAD67 positive cells, a marker for interneurons, was 23% higher in the brains of E2 treated rats compared to those treated with vehicle. A battery of behavioural tests was also performed, showing no difference to anxiety traits but instead altered the exploration pattern in the novel objection recognition test. The behavioural results found in this study showed a trend towards E2 treated male rats shifting to a more female style of exploratory behaviour. Weight gain was also noted in E2 treated rats, not noted in the Olivetti study (Chachua *et al.*, 2016).

While this study provided behavioural data for animals treated with E2, an investigation not performed in the Olivetti study was to show any difference in cognition in the mice. There are

limitations to this study when looking at E2 for a model other than one with an *Arx* mutation. Given that the primary deficit in the PA1 mouse brain is an interneuron deficiency, which E2 rescued to treat seizures in the mouse, it is reasonable to say that E2 may not have worked in this model as it did not show a deficit in interneurons in the first place, therefore not providing any additional benefits to rescue spasms. It is likely that given ACTH is used as a positive control in this study, the pathophysiology of the spasms is different to those seen in the *Arx* mouse models, and hence E2 may not rescue the phenotype in this induced spasm rat model. Another study performed in a different induced spasm rat model also attempted to validate whether E2 could alleviate infantile spasms. This model was induced at postnatal day 3 and presents with multiple clusters of spasms between postnatal days 4 and 13, with other seizure types also occurring after postnatal day 9. This model also presents with cognitive deficits to learning, memory and sociability behaviour, so has a phenotype more similar to the PA1 *Arx* mouse model. However, when treated with the same dosage of E2 as the Olivetti study between postnatal days 3 and 10, no difference was seen in spasm or seizure frequency, and there were no differences to mortality, or behavioural deficits. There was also no difference in weight between vehicle and E2 treated rats, different again to the Chachua study (Galanopoulou *et al.*, 2017).

This induced spasm model does present with a deficit in interneurons, however these are predominantly in parvalbumin-positive cells, and this subtype was not affected by E2 in the Olivetti study. Again, it was concluded that different types of interneuron deficits can cause spasms, and that E2 may not act upon all the cellular causes of these spasms. It is also interesting to note that mice and rats, though genetically close, have different neurodevelopment milestones at different times. It is possible that the postnatal day 3 to 10 timing of the E2 treatment is not when this cortical positioning occurs in rats.

While not an infantile spasms model, a study into the effects of E2 on prematurely born rabbits has also been performed. Premature birth can lead to disrupted interneuron migration and development, due to neurological complications and a drop in estrogen levels. Estrogen can drop 100-fold in premature newborns, due to the termination of the *in utero* environment. This change in estrogen can interrupt neurogenesis and the maturation of interneurons. This study found that parvalbumin and somatostatin-positive interneurons were significantly deficient in the brains of prematurely born rabbits, and an overall loss of GAD67 positive cells. Estradiol treatment not only restored parvalbumin-positive interneurons in the cortex of prematurely born rabbit pups, but also increased the number of Arx expressing interneuron progenitor cells (Panda *et al.*, 2018).

1.6 Concluding remarks

The seizures and intellectual disability associated with mutations in *ARX* can be devastating for children and their families. However, these pre-clinical studies show promise for exogenous steroids like estradiol as a potential therapy to alleviate the burden of comorbidities that are strongly associated with intellectual disability that may lead to damage to cognitive functioning, impaired quality of life due to the side effects of current anti-epileptic therapies, seizures interfering with day to day activities, or even early death. The mouse models developed for the expanded polyalanine tract mutations mirror the spectrum of patient phenotypes and provide an excellent resource for investigating E2 and other potential treatments. Understanding the molecular and cellular effects of these mutations will not only help us find potential pathways to be targeted by therapeutic interventions, but also to help us further understand the pathophysiology of disorders associated with *ARX*.

1.7 Project overview

By understanding how treatment affects these mice and the mechanisms behind the improvement to the clinical phenotype, we may be able to understand the relatively unknown pathophysiological mechanisms of mutations in *ARX*, and their involvement in intellectual disability and its associated comorbidities. The experimental aims of my PhD project addressed the following questions.

1. Does estradiol treatment alleviate seizure frequency and severity in a different model of PA1 mice, as well as in PA2 mice, modelling the most common human mutation of *ARX*?
2. Does the reduction of seizures driven by estradiol treatment, change the behavioural and cognitive outcomes in PA1 and PA2 mice? Or does estradiol treatment directly change these behavioural deficits?
3. What are the molecular and cellular effects underpinning the mechanisms of pathogenesis in PA1 and PA2 mice? What are the improvements to these when PA1 and PA2 mice are treated with estradiol?

To dissect our research questions, I undertook the following aims.

Aim 1: To study the effects of short-term, daily estradiol treatment between postnatal days 3 and 10, in PA1 and PA2 mice, on seizure severity and frequency.

Aim 2: To investigate if estradiol treatment can improve behavioural and cognitive outcomes in PA1 and PA2 mice. We will examine if improvements are due to a direct effect of estradiol treatment or due to improving seizure outcomes.

Aim 3: To perform unbiased transcriptomic analysis using RNA sequencing on the brains of PA1 and PA2 mice compared to wild-type mice at postnatal day 10, to determine the impact of *ARX* mutations on the postnatal cortex and assess the changes to gene expression being driven by estradiol treatment.

I hypothesised that estradiol treatment given early in postnatal life, would improve seizure outcomes in PA1 mice, as well as PA2 mice, given the overlapping phenotype of these two mouse models. Further, I predicted that the improvement in seizure severity and frequency early in brain development, due to estradiol treatment, would improve the cognitive deficits in both PA1 and PA2 mice. I hypothesised that these treatment effects would be due to estradiol's strong action on gene expression in the brain, by impacting pathways and genes targeted or associated with *Arx*, and those involved with brain development and cellular migration, particularly of interneurons.

Chapter Two:

Materials and Methods

2.1 General reagents

PBS: Phosphate Buffered Saline; 10X: 1.37M NaCl, 27mM KCl, 100mM Na₂HPO₄, 20mM KH₂PO₄, adjusted to pH 7.4

TBS: Tris Buffered Saline; 10X: 50mM Tris-Cl, 150mM NaCl, adjusted to pH 7.4

TBE: Tris/Borate/EDTA; 10X: 89mM Tris, 89mM boric acid, 2mM EDTA, pH 7.6

4% PFA: Paraformaldehyde; 0.1M NaOP, 4M NaOH, 4M NaCl, 4% PFA powder, pH 7.4

2.2 Animals

2.2.1 Animal husbandry

All animal procedures were approved by the Animal Ethics Committee (AEC) of The University of Adelaide, Adelaide. *Arx*^{GCG7/+} (RBRC03654) and *Arx*^{432-455dup/+} (RBRC03653) heterozygous females, called PA1 and PA2 mice respectively throughout this thesis, were imported from RIKEN Bioresource Centre, Japan (Kitamura *et al.*, 2009), and were maintained on the C57BL/6N-Hsd background.

Breeding animals were housed in individually ventilated cages under constant temperature and humidity with a 12-hour light/dark cycle, with standard chow and sterile water available *ad libitum*. PA1 and PA2 heterozygous females were bred as trios with wild-type C57BL/6N-Hsd stud males to produce wild-type and hemizygous males for this study. There were no abnormal parenting behaviours in our heterozygous female mothers to report. Multiple breeding trios were set up concurrently to ensure an adequate number of litters (and hemizygous male pups) would be born within the same time frame. Females were separated and single housed once visibly pregnant (approximately two weeks post-conception) with access to autoclaved sunflower seeds and crushed standard chow soaked in sterile water, refreshed daily.

Litters of male mice were weaned from their mothers at approximately postnatal day 21 to day 23 (P21-P23) upon the smallest pup reaching 8 grams of body weight as a minimum. Mice

were co-weaned with male pups from other litters of the same mutant strain and treatment group where possible. Hemizygous males were weighed, monitored and scored daily from P3 on a Clinical Record Sheet for general health and welfare, appearance and any observed seizure activity. Experimental male mice were housed in individually ventilated cages under constant temperature and humidity with a 12-hour light/dark cycle. Mice were given environmental enrichment in the form of red plastic dome houses, crinkled nesting paper, and a cardboard toilet roll or small cardboard box. Experimental mice were given a diet of 10% fat chow, autoclaved sunflower seeds and sterile water available *ad libitum*, as well as standard chow soaked in sterile water in an accessible feeding dish, refreshed daily.

2.2.2 Drug preparation and injections

A 5mg/mL stock of 17 β -estradiol (E2) (Sigma) was dissolved in sterile-filtered 100% dimethyl sulfoxide (DMSO) (Sigma). This was stored in a glass bottle away from light for up to four months at 4°C. For injection, 4ng/ μ L of E2 in 0.75% DMSO was prepared in sterile sesame oil (Sigma). The vehicle injection control was similarly prepared, minus the E2. Aliquots of E2 and vehicle injection stocks were given batch numbers, and stored away from light in 2mL amber glass vials (Sigma) at 4°C. Each batch was re-labelled with a colour code by a ‘non-involved’ member of the lab, with the information stored in a secure location until the end of the study. Drugs were referred to by their codes throughout the experimental trials until data analysis was complete, ensuring the investigators were blinded to treatment identity.

For these studies, only male pups were injected. Expansions of the first and second polyalanine tracts of *Arx* result in an X-linked disorder, meaning only male mice are affected by the disease. We treated hemizygous male mice, as well as wild-type male control mice. Daily injections were performed for seven days, between P3 and P10 inclusive, at the same time of day between 8:00 am and 10:00 am. Drugs were taken out of 4°C storage 15 minutes prior to injection and warmed to 37°C. Pups were gently removed from their home cage and placed in a plastic tub

with tissue and used bedding from their home cage and placed on a 37°C slide warmer. Mice were visually sexed at P3. Pups were weighed before injection, with the dose of E2 achieving 40ng/g. For example, mice weighing 1.5g received 50ng of E2. Table 2.1 shows the upper and lower weight limits for each weight range, and the subsequent dose of E2 given if the mouse weighed within that bracket. A sterile BD Ultra-Fine II short needle insulin syringe (0.3mL, 0.25mm 31G x 8mm) (Becton-Dickinson) was used for injections. Pups were injected subcutaneously with the drug, alternating injecting site daily between the neck and left and right hips of the pup. Pups were toe tagged for identification and genotyping purposes on P4. Once injected, pups were returned to dam in home cage and monitored post-injection, to ensure the mother did not reject injected pups. All male mice in each litter were treated with the same drug (blinded to the investigator by colour code). To reduce the cannibalisation/rejection rates of litters during the treatment phase, the female littermates (within an experimental litter) were injected with vehicle, ensuring all pups in the litter smelt the same to the mother.

At the end of the injection phase, male mice were humanely killed by decapitation for tissue collection for RNA sequencing analysis at P10 in the afternoon following their last injection, no less than six hours after injection, between 14:00 and 16:00. Otherwise, animals for behavioural/seizure monitoring analysis were carried through to weaning as described in 2.2.1 above.

2.2.3 Genotyping

A small piece of toe tissue was removed with sterile technique at postnatal day 4 or 5 for genotyping and to provide an individual identification mark (Figure 2.1). Tissue was stored at -20°C until analysed. Genomic DNA was extracted as per manufacturer's instructions for the High Pure PCR Template Preparation Kit (Roche) or the Maxwell® RSC Tissue DNA kit (Promega).

Genotyping polymerase chain reaction (PCR) of all pups was performed using Taq polymerase (cloned in house) and FailSafe™ PCR 2X PreMix J (Epicentre) for 35 cycles of 30 seconds denaturation at 94°C, 20 seconds annealing at 60°C and 40 seconds elongation at 72°C. Primers to amplify the *Arx* knock-in region were described previously (Kitamura *et al.*, 2009). We also included an *Sry* sexing PCR as part of our genotyping protocol as described previously (Lee *et al.*, 2014). All genotyping primers are listed in Table 2.2. PCR products were separated by electrophoresis at 110V for 25 minutes on a 2% agarose (w/v) in 1X TBE gel, and the correct PCR product was confirmed by comparison to the migration measured against a 1kB+ molecular weight ladder, viewed under UV light using GeneSnap software (SynGene).

In addition to the genotyping described above, all heterozygous female breeders and experimental male pups were genotyped to confirm either the PA1 or PA2 genotype. This specific genotyping PCR was performed using Long Template Expand Taq polymerase (Roche) and FailSafe™ PCR 2X PreMix J (Epicentre) for 35 cycles of 30 seconds denaturation at 94C, 40 seconds annealing at 60C and 40 seconds elongation at 68C. Primers used to amplify the PA1 and PA2 regions are listed in Table 2.2. PCR products were separated by gel electrophoresis at 80V for 45 minutes on a 2% agarose (w/v) in 1X TBE gel, and the correct PCR product was confirmed by comparison to the migration measured against a 1kB+ molecular weight ladder, viewed using GeneSnap software (SynGene).

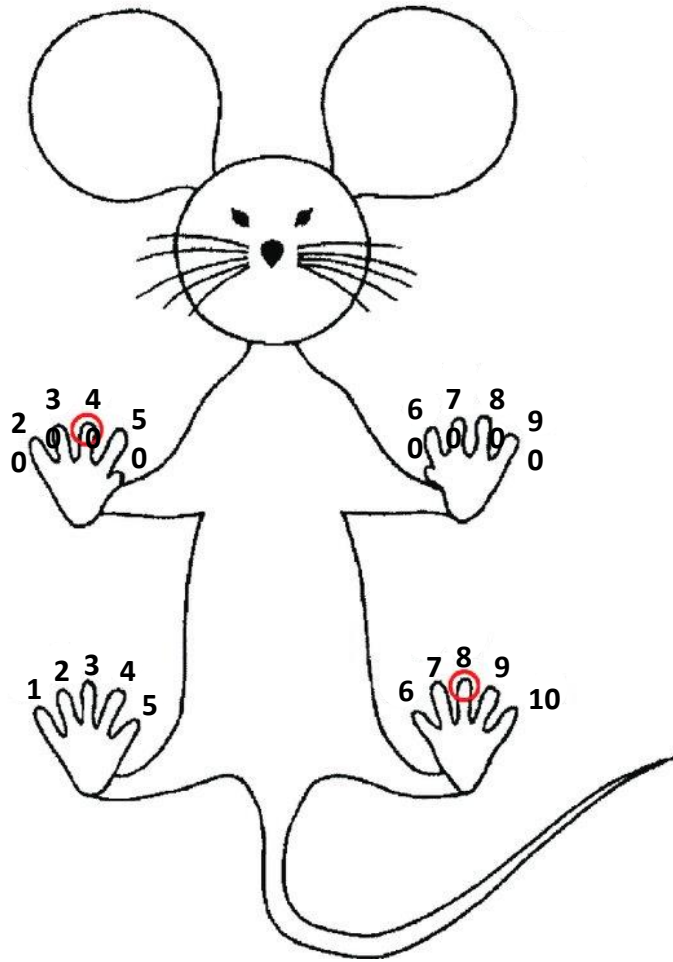


Figure 2.1: Mouse toe tagging numbering system. Diagram showing numbering system for toe tagging identification (mouse viewed from below). In this example, the third toe of the paw on the right fore limb, and of the paw on the left hind limb (circled in red) would be cut, giving a mouse identification number of 48. Diagram adapted from (Paluch *et al.*, 2014).

Table 2.1: Mouse weight range brackets with lower and upper weight limits, with correct volume of drug to inject.

Lower weight (g)	1.375	1.625	1.875	2.125	2.375	2.625	2.875	3.125	3.375
Higher weight (g)	1.624	1.874	2.124	2.374	2.624	2.874	3.124	3.374	3.624
Volume injected (µL)	15	17.5	20	22.5	25	27.5	30	32.5	35
Lower weight (g)	3.625	3.875	4.125	4.375	4.625	4.875	5.125	5.375	5.625
Higher weight (g)	3.874	4.124	4.374	4.624	4.874	5.124	5.374	5.624	5.874
Volume injected (µL)	37.5	40	42.5	45	47.5	50	52.5	55	57.5
Lower weight (g)	5.875	6.125	6.375	6.625	6.875	7.125	7.375	7.625	7.875
Higher weight (g)	6.124	6.374	6.624	6.874	7.124	7.374	7.624	7.874	8.124
Volume injected (µL)	60	62.5	65	67.5	70	72.5	75	77.5	80
Lower weight (g)	8.125	8.375	8.625	8.875	9.125	9.375	9.625	9.875	
Higher weight (g)	8.374	8.624	8.874	9.124	9.374	9.624	9.874	10.124	
Volume injected (µL)	82.5	85	87.5	90	92.5	95	97.5	100	

Table 2.2: Mouse genotyping PCR primers.

Detection	Primer Name	Direction	Primer Sequence	Length (bp)	PCR annealing Tm (°C)	PCR product (bp)
Sex	Sry-F	Forward	CACTGGCCTTTTCTCCTACC	20	60	349
	Sry-R	Reverse	CATGGCATGCTGTATTGACC	20		
Knock-In	pMC1neo ATGr	Reverse	TGTTCAATGGCCGATCCCAT	20	60	
	mArx jjr	Reverse	CTTTAGCTCCCCTTCCCTGGCACAC	24		
	mArx kkf	Forward	AAAGGCGAAAAGGACGAGGAAAGG	24		
PA1 mutation	mARX-GCG	Forward	GCGCTGACCACTTTTCCTT	19	60	208
	mARX-GCG v2	Reverse	ACCTCTCCACGGGGACCT	18		
PA2 mutation	mARX-Dp24	Forward	AGGGGAGCGTCAGGACAG	18	60	282
	mARX-Dp24	Reverse	AACAGCTCCTCCTCGTCGT	19		

2.2.4 Behavioural analyses

Behavioural testing was performed at approximately one and two months of age. Tests were conducted in the light cycle, always beginning at 9:00 and ending by 13:00. Tests at one month of age ran for one week and were performed in a conventional order for behaviour testing, running from the least stressful to the most stressful test (Wahlsten, 2011): open field and inverted grid (day 1), elevated zero maze (day 2), Y-maze (day 3) and sociability and social novelty (day 4). Tests at two months of age ran for two weeks and were performed in the same order in the first week, followed by Barnes maze for five days in the second week of testing. All testing was conducted using ANYmaze video tracking software (Stoelting). Behavioural apparatuses were thoroughly cleaned with F10 Veterinary Detergent between mice to remove olfactory traces. Environment (room appearance, lighting, background noise, temperature, humidity, and clothing of tester) was kept consistent for each round of behavioural testing. For all behaviour tests performed, several parameters could be measured using the AnyMaze software. While we have only reported those of interest or with significant differences, we have included a table with these parameters listed (Table 2.3).

Table 2.3: Parameters measured for each behavioural test using the AnyMaze software.

Behavioural test	Parameters measured
Open field	Time spent in zones Distance spent in zones* Total distance travelled* Average speed of mouse Speed of mice in zones Time spent stationery in zones Total time spent stationery
Elevated zero maze	Time spent in zones* Distance spent in zones Total distance travelled* Average speed of mouse Speed of mice in zones Time spent stationery in zones Total time spent stationery Number of head dips*
Y-maze	Time spent in zones* Distance spent in zones Total distance travelled* Average speed of mouse
Sociability & social novelty	Time spent interacting with stranger/familiar mice* Time spent in stranger/familiar mouse zone Total distance travelled Average speed of mouse
Barnes maze	Latency to find escape hole* Distance travelled to find escape hole Number of false entries

*indicates parameter reported in this thesis (Chapter 3)

2.2.4.1 Inverted grid

Mice were placed on a wire grid (bar diameter of 1mm, 1cm apart) with an area of 10cm by 18cm taped off around the edge to prevent mice from climbing on to the top of the wire grid. The mouse's tail was pulled gently so that it gripped on to the grid, and the grid was quickly flipped to suspend the mouse upside down. The grid was suspended approximately 50cm above a plastic-coated pillow surface. Mice were timed for the duration they remained suspended from the wire grid for a maximum time of 120 seconds, which was considered a successful trial. If the mouse fell in the first 10 seconds it was trialled for a second time, and if it fell again it was counted as a fail. Time the mice held on to the grid was measured as 'latency to fall'. Numbers of successful and failed attempts were also recorded.

2.2.4.2 Open field

Baseline locomotor activity and anxiety-like behaviour was quantified in the open-field, under stress-inducing conditions. Mice were placed in a 40cm by 40cm, well-lit (overhead light) plexiglass box, lined with black contact, in the south-west corner. Wild-type mice will typically spend time exploring the entire box, while mice with an abnormal fear and anxiety response will spend more time in the outer, darker areas of the open field apparatus (periphery), and won't spend as much time in the central zone of the apparatus. Wild-type mice will typically spend time exploring the entire box, while mice with an abnormal fear and anxiety response will spend more time in the outer, darker areas of the open field apparatus (Wahlsten, 2011). Time and distance spent in the periphery or centre zone of the open field was recorded over a 5-minute period.

2.2.4.3 Elevated zero maze

Anxiety-like and exploratory behaviours were investigated using the elevated zero maze. The elevated zero maze is comprised of a circular elevated platform, 40cm above the floor (a diameter of 50cm, and a platform 5cm wide). The maze is split into four quadrants; two closed quadrants with 27cm high walls and two open quadrants with no walls. Mice were alternately placed in the centre of the northern or southern open quadrant and allowed to explore. Wild-type mice typically explore the open quadrants of the elevated zero maze more than mice with an abnormal fear response, who tend to spend more time in the closed, darker quadrants (Wahlsten, 2011). Mice were recorded for a 5-minute period, measuring distance and time spent in open or closed quadrants. Head dipping behaviour was manually recorded (exploratory behaviour where a mouse looks over the side of the maze platform).

2.2.4.4 Y-maze

Hippocampal dependent spatial memory and exploratory behaviour was measured using the Y-maze. The Y-maze is comprised of three arms shaped as a 'Y', each 35cm long and 5cm wide with 10cm walls. The arms are at a 120° angle to each other. Each of the test walls had a different marking in black tape to allow mice to spatially differentiate between the left and right arms. There are two stages of the Y-maze test; training and testing.

2.2.4.4.1 Stage 1: Training

During Stage 1, mice were placed in the southern arm of the Y-maze. The mice explored the maze for a ten-minute period, with one of the lateral arms closed and the other open (alternated to the left and right arms between animals).

2.2.4.4.2 Stage 2: Testing

Thirty minutes after Stage 1, mice were placed in the southern arm of the Y-maze for Stage 2 of this test. All three arms were open for exploration for a duration of five minutes. Mice with intact hippocampal learning and memory will display a preference for the novel environment of a previously unexplored arm, and mice with a memory impairment will not recognise the novel arm, resulting in a greater or equal amount of time spent in the familiar, previously explored arm of the maze (Wahlsten, 2011).

2.2.4.5 Sociability

Sociability testing was carried out to investigate social behaviour and autistic-like traits. The test is comprised of a rectangular, plexiglass box with three separate chambers divided by walls. Each chamber is 20cm by 40.5cm with 22cm high walls connected by closable doors. The sociability test is conducted in three stages. Each stage is five minutes long, and all stages are performed in a row for each mouse, before moving on to the next mouse.

2.2.4.5.1 Stage 1: Habituation

The mouse was placed in the middle chamber with doors to the left and right chambers left open, for a duration of five minutes.

2.2.4.5.2 Stage 2: Sociability

A wild-type, age-matched male stranger mouse (Stranger 1; no previous interaction with the testing mice) was placed in a round wire cage, with bars wide enough to allow nose contact. The stranger cage was placed in the left or right chamber (alternating between each test mouse). An empty cage was placed in the opposite chamber. The test mouse was placed in the middle chamber and allowed to access all chambers for a period of five minutes. The time the test mouse spent interacting with Stranger 1 was recorded as an index of social behaviour.

Interaction was measured manually and defined as the time the test mouse spent sniffing, interacting with, or climbing on the cage of Stranger 1.

2.2.4.5.3 Stage 3: Preference for social novelty

A second wild-type, age-matched male stranger mouse (Stranger 2) was placed in the previously empty cage in the previously empty chamber. The test mouse was allowed to access all chambers for a five-minute period. The time the test mouse spent interacting with Stranger 1 and Stranger 2 was measured as an index of preference for social novelty.

Mice usually have a preference for social novelty, and those with normal social behaviour will typically spend more time interacting with Stranger 2 (novel mouse) than the Stranger 1 mouse (familiar mouse) in Stage 3, and a preference for social interaction by spending time with Stranger 1 in Stage 2. Mice displaying autistic-like behaviour will have altered social behaviour and will not interact with stranger mice as preferentially as wild-type mice do in sociability or preference for social novelty tests (Wahlsten, 2011).

2.2.4.6 Barnes maze

The Barnes maze was used to investigate spatial learning and memory as well as cognitive flexibility. The Barnes maze is comprised of a round table 91cm in diameter, with an overhead light above the table. The maze has 20 equally spaced holes around the outside edge. However only one leads to a real escape box underneath the table. All other holes are blocked and have no escape box. The Barnes maze was conducted over four training days.

2.2.4.6.1 Days 1-4: Training

A four-day training period was used to measure spatial learning. Each day, the test mouse was placed in the centre of the Barnes maze table under an opaque plastic container. Once the container was lifted, the test mouse was given three minutes to find the escape box and learn its location. If the mouse failed to find the escape box, it was guided to the box and had the

plastic container kept over it for one minute in order to learn its location. Mice were tested three times on each testing day, with the score averaged. Outcomes were recorded as latency to locate the escape box over the training period.

2.2.5 Seizure monitoring and analysis

Mice received daily injections between day 3 and day 10 and remained with their mothers until weaning. From the start of treatment (postnatal day 3) until postnatal day 70, all mice for behavioural testing and seizure monitoring were handled and weighed daily. Any observed seizures occurring during this daily handling were recorded. Spontaneous seizures were assessed during non-invasive video monitoring (with offline analysis) across the peak period of seizures (previously determined in untreated mice to occur between postnatal days 35 and 60) (Jackson *et al.*, 2017). Video monitoring for seizure activity was conducted three times a week in four hour blocks from 11:00 until 15:00 during light cycle, on PA1 and PA2 hemizygous males and age matched control wild-type littermates, between the ages of P38 and P56. Cage mates were placed in a Perspex covered 17.5cm by 31cm cage, with a small piece of Nectragel (Able Scientific) and food available *ad libitum* during the filming period. Natural behaviour was captured and automatically saved in 50-minute video files by a Sony FDR-AXP35 4K Handycam or a Panasonic HC-VX980M 4K Video Camera. Activity levels and seizure activity were viewed offline using VLC Media Player (version 2.1.3). Videos were analysed by observers blinded to genotype and treatment. Seizure activity was scored using a defined scoring system based on categorisation of seizures compared directly to video-electroencephalography in untreated mutant mice from a previous study (Jackson *et al.*, 2017). In brief, seizures in mutant mice were characterised into four categories: (1) rapid and jerky movements around the cage and stationary seizures, (2) mild repetitive myoclonic jerks (duration less than 10 secs), (3) prolonged myoclonic seizures lasting longer than 10 seconds and (4) found dead. Myoclonic seizures were recorded for length of seizure in seconds.

2.2.6 Animal dissections and tissue collection

Animals for RNA sequencing analysis were humanely killed by decapitation at postnatal day 10, and behavioural/seizure monitoring animals were humanely killed at approximately postnatal day 70 by CO₂ asphyxiation, if not euthanised for humane reasons prior to end point. The brain was dissected, and the cortex was separated from the cerebellum and cut in half sagittally along the cerebral fissure. The left half of the cortex was minced and snap frozen in liquid nitrogen and stored at -80°C. The right half of the cortex was fixed in either 4% PFA or 10% formalin (Sigma).

Samples fixed in 4% PFA were washed three times in high-volume, cold 1X PBS for five minutes per wash on a rocker, before being transferred to 30% sucrose in PBS to equilibrate. Samples were then embedded in OCT medium (TissueTek, ProSciTech) and stored at -80°C. Samples fixed in 10% formalin were washed three times in high-volume, cold 1X PBS for five minutes per wash on a rocker, and stored in 70% ethanol at 4°C.

Other tissue was also dissected from the animals; testes, pancreas, and forelimb muscle. The left testis, left forelimb muscle and pancreas were snap frozen in liquid nitrogen and stored at -80°C. The right testis and right forelimb muscle were fixed in either 4% PFA or 10% formalin. Fixed samples were washed and embedded as per procedures described above.

2.2.7 Statistical analysis

All data analysis was performed using GraphPad Prism version 7.0 (GraphPad Software Inc.). Data normality was confirmed using a D'Agostino and Pearson normality test. Statistical significance of the difference between means of each genotype (PA1 and PA2), treatment groups, and wild-type littermates was determined using either a one-way or two-way analysis of variance (ANOVA) followed by a Tukey's HSD post-hoc test. Where comparisons were

made between two treatment groups of the same genotype (PA1 or PA2), without wild-type littermates included, a two-tailed unpaired t-test was performed to determine significance.

2.3 Gene expression analysis

2.3.1 RNA extraction

RNA was extracted from the cortex of hemizygous male mice and age-matched male wild-type littermates using Trizol (ThermoFisher). Frozen cortex samples were thoroughly homogenised in 1mL of Trizol, and the sample passed through a P1000 pipette tip until completely homogenised. Samples were left at room temperature (RT) for five minutes. 200µL of chloroform was then added to the tube, and shaken vigorously for one minute, then left for two minutes at RT for layers to separate. The tube was then centrifuged at 10,000 x g for 15 minutes at 4°C. The RNA was then extracted and purified as per manufacturer's instructions for the RNeasy Mini Kit (Qiagen) and RNase-Free DNase kit (Qiagen). RNA was eluted in 50µL of RNase-Free H₂O. RNA concentration was determined using a UV spectrophotometer (Nanodrop). RNA quality was also determined using gel electrophoresis. 3µL of RNA was combined with 5µL of 2X loading dye, with RNA then separated by electrophoresis at 80V for 60 minutes on a 1% agarose (w/v) in 1X TBE gel. The correct products were confirmed by comparison to the migration measured against a 1kB+ molecular weight ladder, viewed under UV light using GeneSnap software (SynGene).

2.3.2 RNA sequencing

Illumina's TruSeq stranded RNA sample preparation protocol was used to process samples prior to sequencing. 56 mouse RNA samples were sequenced on an Illumina NextSeq Platform. The primary sequence data was generated using the Illumina bc12fastq.2.19.1.403 pipeline. The per base sequence quality was >95% bases above Q30 across all samples. The reads were also screened for the presence of any Illumina adapter/overrepresented sequences and cross-species contamination. The cleaned sequence reads were then aligned against the *Mus musculus*

genome (build version nm10). The TopHat aligner (v2.1.1) was used to map reads to the genomic sequences. The counts of reads mapping to each known gene were summarised and used for computing differential gene expression with 'edgeR'. edgeR version 3.12.1 was used to perform differential expression analysis. Low counts were filtered out ($\text{cpm} < 1$) and the default TMM normalisation method of edgeR was used to normalise the counts between samples. A generalised linear model was then used to quantify the differential expression between the groups (treatment and genotype). Transcripts that were significantly different within genotype and treatment group comparison, were then selected by applying a p-value cut off of < 0.05 and a \log_2 fold-change of ± 0.5 .

2.3.3 RNA sequencing validation

2.3.3.1 Reverse transcription cDNA synthesis

cDNA was prepared as described in SuperScriptIII reverse transcriptase (ThermoFisher) manual, with $1\mu\text{g}$ of RNA primed by random hexanucleotides. Template negative and reverse transcriptase negative controls (where template or SuperScriptIII was replaced with H_2O) were included to determine product specificity. Synthesised cDNA was diluted by adding $20\mu\text{L}$ of H_2O . Samples were stored at -20°C .

2.3.3.2 Polymerase chain reaction (PCR)

The efficiency of reverse transcription was determined using PCR. The primers used were specific to the ubiquitously expressed housekeeping gene, *Beta-Actin*. Primers used are listed in Table 2.4. For this reaction, cDNA was amplified with $1\mu\text{L}$ of Taq DNA polymerase (Roche), 1x PCR buffer with MgCl_2 (Roche), single stranded DNA primers (Table 2.4) and H_2O to make the reaction up to $50\mu\text{L}$. The PCR cycle conditions were as follows: initial denaturation at 94°C for 5 minutes, 35 cycles of denaturation at 94°C for 30 seconds, annealing for 30 seconds at 60°C , extension at 72°C for 30 seconds, and a final extension at 72°C for 10 minutes. PCR products were visualised on a 1% agarose (w/v) gel in 1X TBE buffer with ethidium bromide

added (0.2 μ g/mL) for 45 minutes at 100V, with 1kB+ molecular weight ladder, and viewed under UV light using GeneSnap software (SynGene).

Table 2.4: Housekeeping primer set.

Name	Species	Primer Sequence (5'-3')	Length	PCR annealing Tm (°C)	PCR product (bp)
<i>Beta-Actin</i> Forward	Mouse	GATATCGCTGCGCTGGTCGTC	21	60	177
<i>Beta-Actin</i> Reverse	Mouse	TCTCTTGCTCTGGGCCTCGTCAC	23		

2.3.3.3 Quantitative real-time PCR (RT-PCR)

Genes selected for validation studies were assayed as described in the TaqMan® PreAmp Master Mix Kit user guide (Applied Biosystems). Pre-designed TaqMan® Gene Expression Assays were selected from ThermoFisher. Reactions were set up in a 96-well plate, with each well containing 2µL of cDNA template (of a 1ng/µL to 50ng/µL stock), 1µL of the 20X TaqMan® Gene Expression Assay (FAMTM dye-labelled MGB probe) and 1µL of the 20x TaqMan® Endogenous Control Assay (VIC® dye-labelled MGB probe), 10µL of the 2x TaqMan® Gene Expression Master Mix and RNase-free H₂O. Each validation gene was quantified using a FAM labelled TaqMan® probe, with the expression values normalised to the reference gene, *Beta-Actin*, labelled with VIC.

Reactions were run on the Applied Biosystems StepOnePlusTM Real-Time PCR System using a standard run with the following conditions: activation at 50°C for 2 minutes, 95°C incubation for 10 minutes, 40 cycles of denaturation at 95°C for 15 seconds and extension at 60°C for 1 minute. The signal emitted from the dye was recorded at the end of each cycle. All samples were analysed in triplicate. The efficiency of the assay was determined by amplification of the standard curve of a diluted control cDNA sample (in this case, an untreated wild-type cortical sample from an age-matched control). Expression values were calculated using the StepOnePlusTM software (v2.3), using the standard curve method. Table 2.5 refers to all TaqMan® probes used in this thesis.

Table 2.5: TaqMan® assay details.

Gene name	Oligo name	Probe label	Species	Amplicon length
<i>Arc</i>	Mm01204954_g1	FAM	Mouse	145
<i>Arx</i>	Mm00545903_m1	FAM	Mouse	104
<i>Beta-Actin</i>	ACTB Control Mix, pre-developed Taqman assay reagent	VIC	Mouse	
<i>Calb2</i>	Mm00801461_m1	FAM	Mouse	80
<i>Chrna2</i>	Mm00460630_m1	FAM	Mouse	63
<i>Egr1</i>	Mm00656724_m1	FAM	Mouse	182
<i>Fos</i>	Mm00487425_m1	FAM	Mouse	59
<i>Gbp3</i>	Mm00497606_m1	FAM	Mouse	79
<i>Inhba</i>	Mm00434339_m1	FAM	Mouse	65
<i>Lgi3</i>	Mm00507490_m1	FAM	Mouse	95
<i>Lhx1</i>	Mm01297482_m1	FAM	Mouse	60
<i>Lmo1</i>	Mm01168131_m1	FAM	Mouse	70
<i>Ncald</i>	Mm01137205_m1	FAM	Mouse	64
<i>Ndnf</i>	Mm00549567_m1	FAM	Mouse	74
<i>Nkx2-1</i>	Mm00447558_m1	FAM	Mouse	95
<i>Npy</i>	Mm01410146_m1	FAM	Mouse	130
<i>Npy2r</i>	Mm01218209_m1	FAM	Mouse	86
<i>Nt5e</i>	Mm00501910_m1	FAM	Mouse	77
<i>Nxph2</i>	Mm00801892_m1	FAM	Mouse	91
<i>Pcp4l1</i>	Mm01295270_m1	FAM	Mouse	63
<i>Spp1</i>	Mm00436767_m1	FAM	Mouse	114
<i>Th</i>	Mm00447557_m1	FAM	Mouse	61
<i>Wnt10a</i>	Mm00437325_m1	FAM	Mouse	69

2.3.4 Gene enrichment analysis

Venn diagrams for gene expression data analyses were created using <http://bioinformatics.psb.ugent.be/webtools/Venn>. Statistical analysis of the enrichment of gene expression data was performed using Database for Annotation, Visualisation and Integrated Discovery (DAVID) Functional Annotation Bioinformatics Microarray Analysis (Huang da *et al.*, 2009, Huang da *et al.*, 2009). DAVID uses multiple databases to create annotation clusters. These clusters are then given overarching theme names and ranked. Annotation clusters were ranked by enrichment score calculated by DAVID. PANTHER (Protein Analysis Through Evolutionary Relationships) was used for pathway enrichment analysis (Thomas *et al.*, 2003, Mi *et al.*, 2013).

Our lists of deregulated genes were compared with a number of reference lists of genes associated with autism and intellectual disability, epilepsy, inhibitory neurons, and estrogen response element containing genes. The statistical significance of the overlap of genes between two groups was calculated using hypergeometric probability (http://nemates.org/MA/progs/overlap_stats.html).

2.4 Immunofluorescence

2.4.1 Tissue sectioning

Cortex from mice was coronally embedded in OCT and stored at -80°C until sectioning. The samples were sectioned by the University of Adelaide Histology Department. Coronal sections of 10µm thickness (~2-3 cells thick) at 100µM apart were taken serially using a Leica Cryostat (Leica Biosystems) at -24°C. Sections were fixed to Superfrost™ Plus microscope slides (ThermoFisher). Frozen cortical sections were stored at -20°C until analysis. At least four sections across the right hemisphere were used for immunofluorescence analysis. Sections analysed align to sections 100-124 of the Nissl stained postnatal day 7 coronal brain of the Allan Brain Atlas reference guide.

2.4.2 Immunofluorescence

Frozen cortical sections were first air-dried for one hour at room temperature prior to immunofluorescence staining. The following procedure was performed in a humidified chamber (a dark box lined with damp paper towel) to prevent tissue from drying. Rinses and washes were performed in Coplin jars.

Tissue sections were permeabilised in 1X PBS + 0.5% Triton-X for 5 minutes. Slides were then rinsed in 1X PBS, before being incubated with blocking solution (10% horse serum and 10% BSA in 1X PBS + 0.1% Triton) at room temperature, for 30 minutes. Slides were incubated with primary antibodies overnight at 4°C, followed by incubation with secondary antibodies at room temperature for 2 hours. Between each antibody staining, slides were washed three times with 1X PBS + 0.01% Tween 20. Following secondary staining and washing, slides were mounted with ProLong Gold Antifade Reagent with DAPI (Life Technologies) to stain the cell nuclei and mount coverslips. All antibodies used and antibody dilutions are listed in Table 2.6 and Table 2.7.

2.4.3 Microscopy

All immunofluorescence images were captured using a Zeiss Axio Imager.M2 microscope equipped with Axio Vision software (version 5.1). Immunofluorescence images were acquired by Zeiss AxioCam mRM camera. All comparative images within the same batch were captured with the same exposure times.

Captured images were processed by Image J for quantification analysis. To ensure comparable signals were obtained across all genotypes within an independent experiment for quantification, all images within the same batch were captured with the same microscope settings within one session.

2.4.4 Interneuron analysis

Images from a section were first stitched together using Microsoft Image Compositor (Microsoft), and imported into Image J (FIJI) for processing and analysis. Manual cell counts were performed using the Cell Counter plugin for Image J. The counting method used was derived from Lee *et al.* 2017. Cells that were considered for analysis had a circular-like cell body (calbindin) or cytoplasmic and/or nuclear staining (neuropeptide-Y) with clear boundaries of the structure, with a clear nucleus from DAPI staining. Counts were exported into Excel and a cell density of number of cells/mm² were derived as an outcome (positive cells counted/area of section counted in mm²).

2.4.5 Statistical analysis

For statistical analysis of interneuron cell counts, PA1 and PA2 mice were pooled. A one-way ANOVA was performed to determine statistical significance between PA^{pool} mice treated with vehicle or estradiol, followed by a Tukey's post-hoc test to determine individual differences

Table 2.6: Primary antibodies used for immunofluorescence.

Protein	Species	Affinity	Cat #	Company	Dilution
Calbindin	Rabbit	Polyclonal	PC253L	Merck	1:1000
Neuropeptide-Y	Sheep	Polyclonal	AB1583	Merck	1:1000

Table 2.7: Secondary antibodies used for immunofluorescence.

Host	Target	Conjugate	Clonality	Cat #	Company	Dilution
Goat	α Rabbit	Alexa 555	Polyclonal	A27039	ThermoFisher	1:400
Donkey	α Sheep	Alexa 488	Polyclonal	A11015	ThermoFisher	1:400

Chapter Three:

Short-term 17β -estradiol treatment alleviates the seizure phenotype but not behavioural outcomes in PA1 and PA2 mouse models.

Publications and presentations from this work:

Publications

Loring, K.E., Lee, K., Mattiske, T., Zysk, A., Jackson, M.R., Noebels, J.L. and Shoubridge, C. (2020) “17- β estradiol reduces seizures but does not improve abnormal behaviour in mice with expanded polyalanine tracts in the *Aristaless*-related homeobox gene (*ARX*).”

Manuscript is Appendix 1. Submitted to *Neurobiology of Disease*.

In addition to this publication, I assisted with the animal husbandry, seizure monitoring and behavioural analysis for another study in a similar mouse model, as part of the work I performed for this chapter. While this work will not be contributing to the examination of this thesis, this work resulted in the following publication, with my inclusion as a co-author.

Jackson, M.R., Loring, K.E., Homan, C.C., Thai, M.H.N., Määttänen, L., Arvio, M., Jarvela, I., Shaw, M., Gardner, A., Gecz, J. and Shoubridge, C. (2019) “Heterozygous loss of function of *IQSEC2/Iqsec2* leads to increased activated Arf6 and severe neurocognitive seizure phenotype in females.” *Life Science Alliance*, 2 (4). (DOI: 10.26508/lsa.201900386)

Manuscript is Appendix 2.

Conferences

Loring, K.E., Lee, K., Mattiske, T., Zysk, A., Jackson, M.R. and Shoubridge, C. “Can estradiol improve phenotypic outcomes in mice with mutations in *Arx*?”

Presented as an oral presentation at the following conferences:

Japanese Neuroscience Society Annual Meeting (2019), Niigata, Japan.

Australian Neuroscience Society Annual Meeting (2018), Adelaide, SA.

Australian Society of Medical Research SA Meeting (2018), Adelaide, SA.

Australian Society of Medical Research SA Meeting (2017), Adelaide, SA.

Presented as a poster at the following conferences:

Australian Neuroscience Society Annual Meeting (2018), Adelaide, SA.

Florey Conference at the University of Adelaide (2018), Adelaide, SA.

Florey Conference at the University of Adelaide, (2017), Adelaide, SA.

3.1 Abstract

Children with severe intellectual disability have an increased prevalence of refractory seizures. Exogenous steroid treatment may improve seizure outcomes, but the mechanism responsible for these improvements remains unknown. Further, it is unclear whether these treatments can improve cognition and behavioural deficits, either through direct action, or by improving seizure outcomes. Here we demonstrate that short term, daily delivery of the exogenous steroid, 17 β -estradiol (40 ng/g) in early postnatal life significantly reduced the number and severity of seizures, but did not improve behavioural deficits, in mice modelling mutations in the Aristaless-related homeobox gene (*ARX*), expanding the first (PA1) or second (PA2) polyalanine tract. Frequency of observed seizures on handling (n = 14/treatment/genotype) were significantly reduced in PA1 (32% reduction) and more modestly reduced in PA2 mice (14% reduction) with treatment compared to vehicle. Spontaneous seizures were assessed (n = 7/treatment/genotype) at 7 weeks of age coinciding with a peak of seizure activity in untreated mice. PA1 mice treated with estradiol no longer present with the most severe category of prolonged myoclonic seizures, while treated PA2 mice had a complete absence of any seizures during this analysis. Despite the reduction in seizures, 17 β -estradiol treated mice showed no improvement in behavioural or cognitive outcomes after peak seizure onset. For the first time we show that these deficits due to mutations in *Arx* are already present prior to seizure onset and do not worsen with seizures. This comprehensive seizure and behavioural analysis provides a basis for further investigations into the molecular mechanism of estradiol treatment, and an understanding of the pathways that are impacted to achieve a reduction in the frequency and severity of seizures in the *Arx* PA mutant mice, and why the behavioural outcomes are not improved with early estradiol intervention.

3.2 Introduction

Epilepsy is a devastating neurodevelopmental disorder that affects approximately 50 million people worldwide with recent estimates of active epilepsy as high as 1.2% in developed Western countries (Zack and Kobau, 2017). This disorder is characterised by involuntary seizures, due to an imbalance of excitatory and inhibitory neuronal activity in the brain (WHO, 2019). One form of epilepsy in early infancy is infantile spasms, including X-linked infantile spasms syndrome (ISSX; MIM# 308350). This disorder has a prognosis of severe epilepsy coupled with intellectual disability persisting throughout childhood and adolescence (Olivetti and Noebels, 2012, Hrachovy and Frost, 2013). Children with neurodevelopmental disorders often have complex overlapping phenotypes. For example, patients with severe intellectual disability have a 15-20% greater incidence than the general population of co-morbid features including recurrent seizures and autism spectrum disorder (ASD). As many as half of intellectual disability cases and epileptic syndromes are believed to be caused by genetic mutations (Willemsen and Kleefstra, 2014, Chiurazzi and Pirozzi, 2016, Ellis *et al.*, 2020). The increasing list of genes responsible are involved in various pathways including development and maintenance of neuronal and brain function and cortical architecture (Paciorkowski *et al.*, 2011, Olivetti and Noebels, 2012).

The *Aristaless*-related homeobox gene (*ARX*) [NM_139058.2] (MIM#300382) is known to play a pivotal role in the development of the brain, specifically the migration and differentiation of interneurons (Miura *et al.*, 1997, Kitamura *et al.*, 2002, Kitamura *et al.*, 2009, Lee *et al.*, 2014). Interneurons are small, locally projecting neurons that use the neurotransmitters γ -aminobutyric acid (GABA), acetylcholine and other neuropeptides, to modulate excitation within neural networks. Due to the importance of excitatory and inhibitory balance, it is not surprising that dysfunction of GABA interneurons in the cerebral cortex is involved in neuropathology including epilepsy, schizophrenia, autism and intellectual disability syndromes (Le Magueresse and Monyer, 2013, Smith-Hicks, 2013). Mutations in *ARX* invariably lead to intellectual

disability, with a wide spectrum of other neurological comorbidities, including autism, dystonia, and epilepsy (Kitamura *et al.*, 2002, Shoubridge *et al.*, 2010). Over half of all mutations in *ARX* patients are expansions of the first or second polyalanine tracts. Clinical presentation of families with expansion mutations in the first tract (PA1) generally present with phenotypes of infantile spasms and seizures (81%) (Shoubridge *et al.*, 2010, Marques *et al.*, 2015), while patients with mutations in the second tract (PA2) present with non-syndromic intellectual disability (68%), with dysarthria, dystonic hand movements (20%) and infantile spasms (26%) (Partington *et al.*, 2004, Shoubridge *et al.*, 2010, Marques *et al.*, 2015, Jackson *et al.*, 2017). The mechanisms underpinning this clinical variability remain unclear.

Children with infantile spasms associated with severe intellectual disabilities respond poorly to anti-convulsant medication. Adrenocorticotrophic hormone (ACTH) therapy is known to stimulate production and release of corticosteroids, as a frontline treatment for these disorders but often has low efficacy, high relapse rates and severe side effects that alongside early-onset seizures, are thought to further exacerbate the behavioural and cognitive deficits in affected children (Hrachovy and Frost, 2013). Second to the effects of anti-convulsant therapy, persistent and severe seizures can have dramatic effects on the regression of cognition of children with epilepsy (Farwell *et al.*, 1985, Neyens *et al.*, 1999, Prasad *et al.*, 2014). A preclinical trial in a different *Arx* PA1 mouse model (Price *et al.*, 2009) found that short-term 17 β -estradiol (E2) given daily in the first postnatal week alleviated the severe seizure phenotype in adult male mice (Price *et al.*, 2009, Olivetti *et al.*, 2014). Estradiol being an exogenous steroid, plays important roles in the developing brain in synaptogenesis and morphology of neurons and glial cells, and can induce long-term changes in gene expression in the brain via activation of estrogen receptor and non-receptor pathways. 17 β -estradiol treatment of PA1 mice partially restored the interneuron migration deficits in the neocortex, increased populations of neuropeptide-Y and calbindin positive interneurons, and changed the expression of several genes normally regulated by *Arx* (Olivetti *et al.*, 2014).

The migration of these inhibitory cells along with other stages of cortical laminar positioning occur in mice from embryonic day 9 until postnatal day (P) 10. In the developing male mouse brain, there is a surge of intrinsic estradiol and conversion of testicular testosterone into estradiol during this period of brain development (McCarthy, 2008). While much research into estradiol's effects on the epileptic brain has been focused on the pro-epileptic activity of the hormone in the adult brain, its neuroprotective effects in the developing nervous system are still being explored. Estradiol has long-lasting transcriptional actions via estrogen receptors α and β , with genes regulated by estradiol being involved in cell proliferation, neuronal migration, synaptogenesis and cell survival. Estradiol also regulates GABAergic neuronal populations and increases the numbers of inhibitory neurons in the pyramidal layers of the cortex (Nakamura and McEwen, 2005, Velíšková, 2006).

Here we investigate the role of early estradiol treatment in mice modelling the PA1 and the more frequent PA2 *ARX* mutations (originally reported by Kitamura *et al.* 2009). Our study explores the effect of estradiol on the seizure phenotype in *Arx* mutant mice and extends the investigation to the impact of this treatment on cognitive outcomes before and after the peak onset of seizures. We hypothesised that estradiol would reduce the severity and frequency of seizures in both PA1 and PA2 mice, given their overlapping phenotypes. We predicted that by improving the epilepsy phenotype, the impact of seizures on cognitive and behavioural deficits in these mice might be improved.

3.3 Materials and Methods

3.3.1 Optimisation of drug preparation and injections

We performed a pilot study to optimise the drug preparation and injections. The original protocol was to dissolve 17 β -estradiol in vegetable oil. As vegetable oil can contain high levels of phytoestrogens, we chose sterile sesame oil (Sigma) for the vehicle (Kuhnle *et al.*, 2008). 17 β -estradiol was first dissolved in 100% dimethyl sulfoxide (DMSO) (Sigma). The LD₅₀ of DMSO is 6.2mL/kg. Doses of DMSO above 10% can cause increased apoptosis in the brain as well as Tau protein phosphorylation (Hanslick *et al.*, 2009). The concentration of DMSO required to dissolve our dose of 17 β -estradiol was 0.075mL/kg in the final solution of sesame oil, estradiol and DMSO, or 0.075%. The concentration we used is in a non-toxic range of the DMSO toxicity curve (Figure 3.1).

The DMSO, 17 β -estradiol and sesame oil solution needed to be warmed in a water bath or incubator at 37°C to form a homogenous solution before pipetting into glass vials ready for injection. Injection of the drug was optimised in an injection pilot study prior to the experimental study performed for this chapter. As the sesame oil solution for injections was viscous, a larger volume than needed for each pup was drawn up into the syringe, and then adjusted to the volume required based on the weight of the pup. This procedure was also made easier with warming, by leaving syringes on a microscope slide warmer before injecting pups.

When injecting the pups, we first used the back of the neck as the subcutaneous injection site. This process left pockets of sesame oil when the mice were euthanised on P10, after seven days of injections. For the next litter, we trialled swapping the injection site from the neck, to the left hip and the right hip, for the seven days of injection. This protocol resolved the issues with oil pockets upon euthanasia on P10. During the pilot study, we found above average rates of cannibalisation and neglect of injected pups by the mother, compared to their uninjected, female littermates. We hypothesised this was due to the smell of the estradiol/vehicle solution

remaining on the skin following injections. To overcome this, we trialled injecting the non-experimental, female pups of the litter with vehicle, to ensure all pups smelt the same. This protocol reduced rates of cannibalisation. These injection protocols were adopted for the larger experimental study described in this chapter.

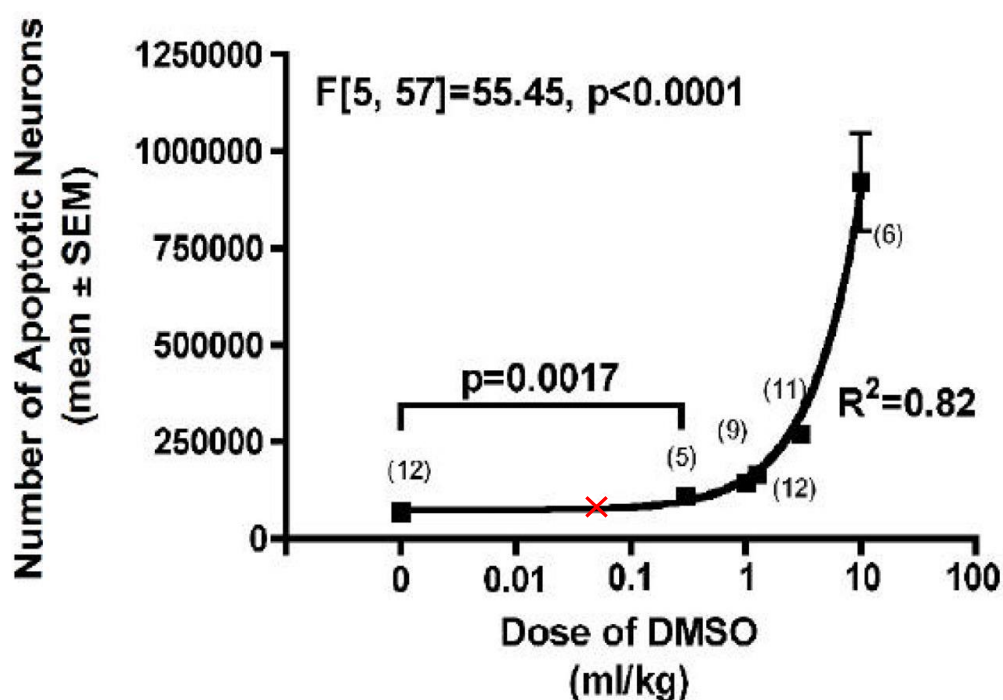


Figure 3.1: DMSO toxicity curve for apoptosis of neurons in P7 mice. Number of apoptotic neurons recorded for mice at P7 treated with different doses of DMSO. Mice did not have significantly greater apoptosis than mice treated with 9 mL/kg until the dose was greater than 0.1 mL/kg. The dose of DMSO used for estradiol preparation in our study is marked with a red cross. Figure from Hanslick *et al.* 2009.

3.4 Results

3.4.1 Estradiol treatment trial strategy

Four staggered rounds of breeding were conducted for this study. A variety of dams from different lineages within the two mouse colonies were chosen for breeding purposes. This ensured adequate genetic diversity within our experimental cohort. A list of the mice used for estradiol treatment trial is in Appendix 3.

PA1 and PA2 mutant male mice and their wild-type male littermates were treated with daily subcutaneous injection of 17β -estradiol (40ng/g) for seven days between P3 and P10, as described in Chapter 2 (2.2.2). Following treatment, mice remained with their mothers until weaned at P21. We then performed behaviour testing before and after the peak period of seizures, where we performed video seizure monitoring. Mice were euthanised at the end of the study, at P70 (Figure 3.2).

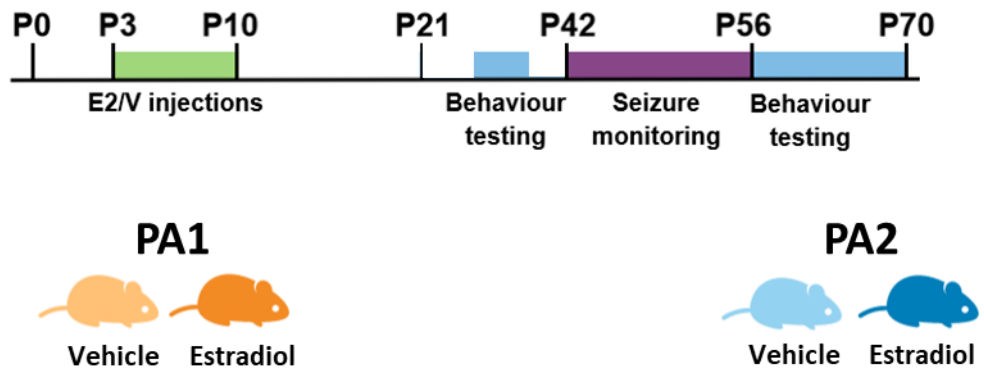


Figure 3.2: Estradiol study timeline. Timeline showing the experimental course of the mouse treatment study. Estradiol or vehicle was administered between P3 and P10 (green). Behaviour testing (blue) was performed before and after the peak of seizures, and video seizure monitoring (purple) was performed between P42 and P56. Spontaneous seizures upon handling were recorded across the entire lifespan of the mice (P0 – P70). PA1 mice are consistently represented in light orange (vehicle treated) and dark orange (estradiol treated), while PA2 mice are represented in light blue (vehicle treated) and dark blue (estradiol treated).

3.4.2 Estradiol treatment reduces seizure frequency and severity in PA mutant mice.

To address the hypothesis that 17 β -estradiol would reduce seizure severity in *Arx* PA1 and PA2 mutant mice, we chose to measure seizure outcomes using two methods; observed seizures occurring on handling and recorded across the lifespan of the mice (until P70), and spontaneous seizures occurring during non-invasive video monitoring during the peak period of seizures in untreated mice (between P35 and P60). An established scoring system was used throughout the evaluation of seizures, with a score of 1 applied to rapid, jerky movement around the cage, a score of 2 given to myoclonic seizures less than 10 seconds in duration, and a score of 3 given to prolonged myoclonic seizures, lasting longer than 10 seconds (Jackson *et al.*, 2017).

Estradiol treatment significantly reduced the overall proportion of adult PA1 mutant mice experiencing seizures on handling, with a 32% reduction compared to vehicle treated mice. Within the PA2 cohort, a 14% reduction was noted with estradiol treatment (44% versus 58%, respectively) but this did not reach significance ($p = 0.4243$) (Figure 3.3 A). In PA1 mice, both the total number of observed seizure events and the number of severe seizures (scores of 3 or 4) were significantly reduced in estradiol treated animals compared to vehicle treated mutant mice. However, this was not significant in the PA2 cohort. (Figure 3.3 B).

Despite these dramatic reductions to the number and severity of observed seizures recorded on daily handling of the mice, the age of seizure onset remained unchanged between PA1 mice treated with either vehicle or estradiol. The average age of seizure onset in mice treated with vehicle was postnatal day 40.78 ± 6.71 (mean \pm SEM), compared to postnatal day 44.50 ± 1.50 in the estradiol treated cohort (Figure 3.4). However, the effect of estradiol on the age of seizure onset differed between the two *Arx* mutations. Estradiol actually accelerated the onset of seizures in the PA2 mice, with estradiol treated mice having their first seizure at postnatal day 26 ± 2.5 (mean \pm SEM) (Figure 3.4). These data demonstrate that observed seizures on handling the *Arx* mutant mice are reduced in both severity and frequency with estradiol treatment,

however, the specific intragenic mutation produced a differential response to estradiol, with accelerated epileptogenesis in PA2 mice compared to PA1. Mice observed having a seizure upon daily handling that subsequently went on to die from a presumed seizure (found dead in their cage) within 2-4 days of having seizure are shown as stars on Figure 3.4. Interestingly, two of the three PA2 mice treated with estradiol in this category died during this early time point, whilst the third mouse died after a subsequent seizure at a later time point (P56). Within the PA2 vehicle cohort, five mice were found dead between P12 and P25 but none of these mice were recorded as having an observed seizure on handling during this period. However, we cannot rule out that seizures may have occurred outside of the times we were handling and observing the animals as part of daily health checks (P3 to P70) or outside the times captured by video seizure monitoring during P35 to P60.

In untreated mutant mice the peak of observed seizures clustered between P35 and P60 (Jackson *et al.*, 2017). To exclude any influence of induced stress due to handling of the mice, we investigated seizures in a spontaneous setting via non-invasive video monitoring (12 hours per mouse over a period of four days) during this peak period. At P45 to P48, 36% (4/11) of PA1 mice treated with vehicle displayed a large number of clusters of individual seizure events ranging from rapid, jerky movement around the cage (score 1) through to severe myoclonic seizures of increasing duration (score 2 and 3) (Figure 3.5). Although 30% (3/10) of the estradiol treated PA1 mice displayed seizures across this same period of time, both the number and severity of seizure events were significantly reduced (Figure 3.5). This trend is even more striking in the PA2 cohort; 33% (4/12) of vehicle treated mice displaying a total of 28 seizure events across all scoring categories, compared to seizures being completely absent in the estradiol treated mice (0/7) during this same monitoring period (Figure 3.5). Further, when looking at the observed seizures on handling that PA2 mice experienced, only one mutant mouse treated with estradiol experienced seizures during this same period of time. We observed

that there were no seizures in vehicle or estradiol treated wild-type mice by either the observed seizures on handling or non-invasive video seizure monitoring analysis.

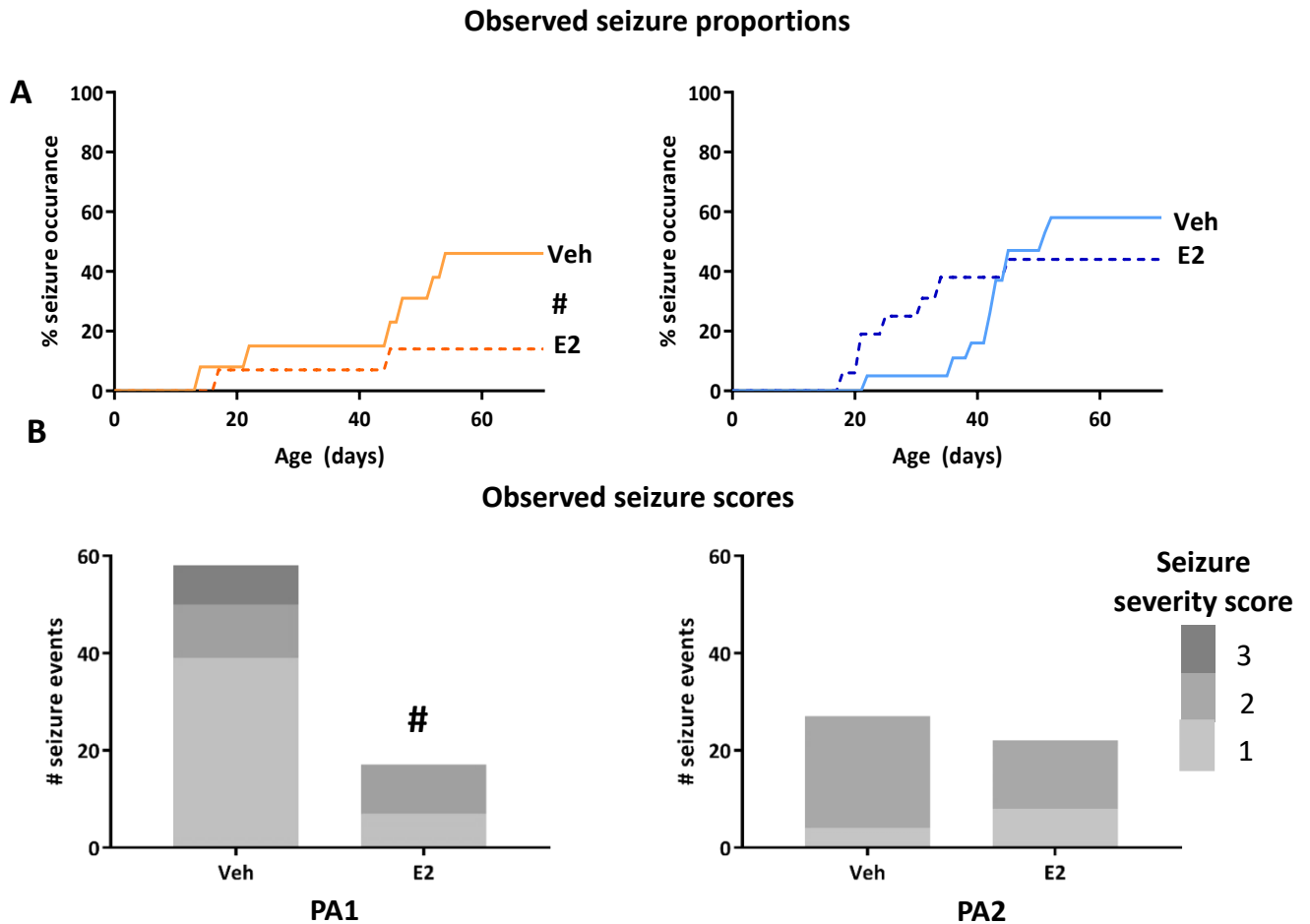


Figure 3.3: Early estradiol treatment diminishes observed seizure severity and frequency in PA mutant mice. PA1 and PA2 mutant mice exhibit reduced seizure frequency (A) and seizure severity (B) when treated with estradiol compared to their vehicle treated counterparts (percentage seizure occurrence – percentages do not include repeated seizures from the same mouse). (B) Shows increasing seizure severity with darker shade of grey (key). (PA1: (A) two-tailed t-test, $p < 0.0001$, $df = 70$; (B) Chi square test, $p = 0.0036$, $df = 11.26, 2$). Analysis across five separate breeding rounds each for PA1 mice (estradiol; $n = 14$; dark orange (dashed line); vehicle; $n = 13$ light orange (solid line)) and PA2 mice (estradiol; $n = 16$; dark blue (dashed line) vs vehicle; $n = 19$; light blue (solid line)). # $p < 0.05$ indicates significant difference between estradiol and vehicle treated animals across the duration of the study.

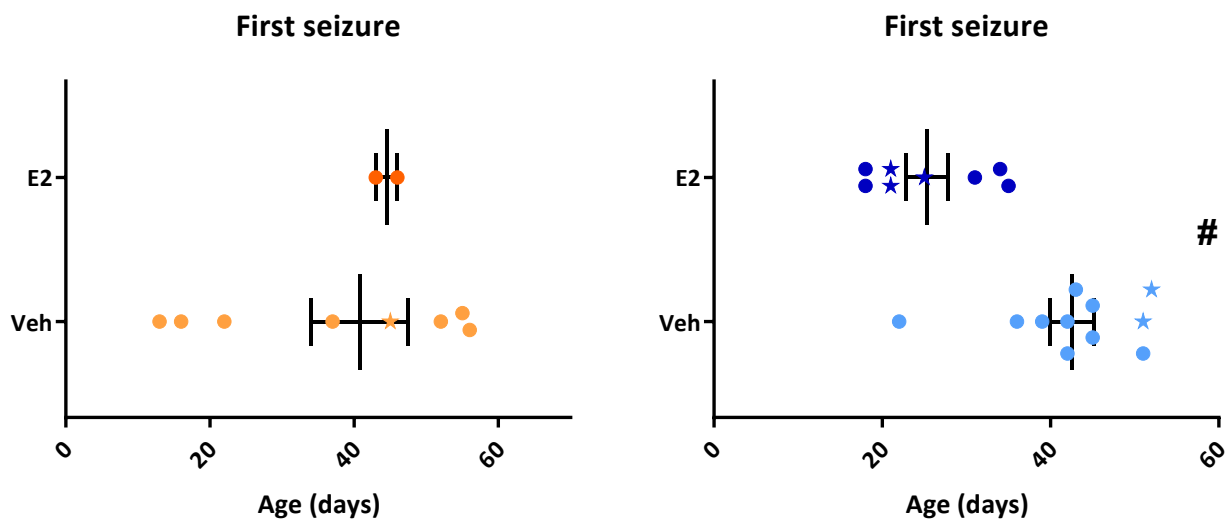


Figure 3.4: Estradiol treatment did not delay the age of first observed seizure in PA mutant mice. Estradiol treatment did not delay the age of first seizure in either mutant strain (PA2: two-tailed t-test, $p = 0.0002$, $F = 1.463$ (10,7), $df = 17$). Mice marked with a star died of a seizure (found dead in cage) within 2-4 days of having an observed seizure on handling. Median \pm min/max is presented for PA1 and PA2 mice from vehicle and estradiol treatment groups. Each dot represents an individual animal at the age of their first seizure. Analysis across five separate breeding rounds each for PA1 mice (estradiol; $n = 14$; dark orange; vehicle; $n = 13$ light orange and PA2 mice (estradiol; $n = 16$; dark blue; vehicle; $n = 19$; light blue. # $p < 0.05$ indicates significant difference between estradiol and vehicle treated animals across the duration of the study.

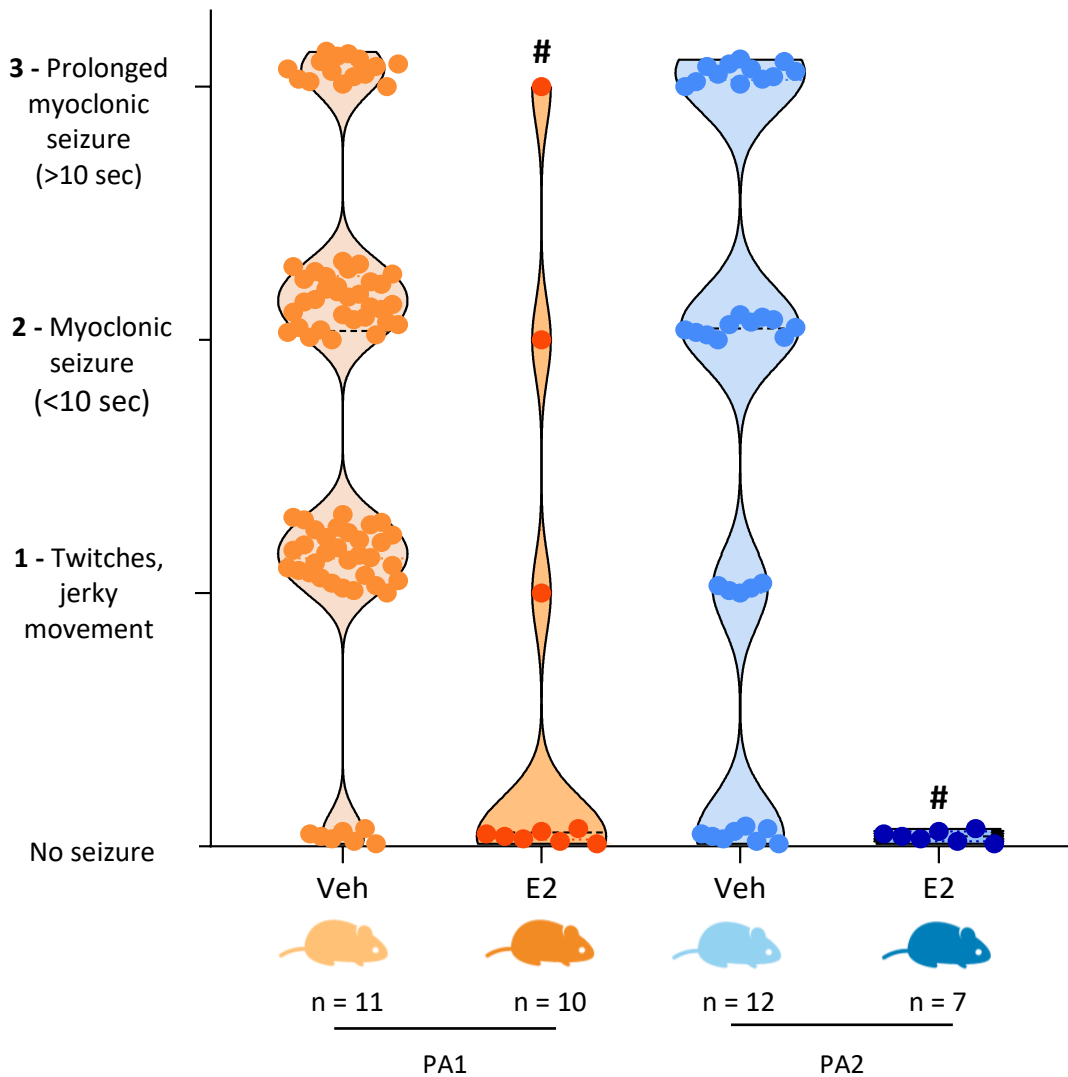


Figure 3.5: Seizure severity and frequency are reduced in PA mutant mice treated with estradiol. PA1 and PA2 mice exhibit reduced seizure frequency and severity when treated with estradiol (PA1; n = 10; dark orange) (PA2; n = 7; dark blue) compared to their vehicle treated counterparts (PA1; n = 11 light orange) and (PA2; n = 12; light blue). Each dot represents an individual seizure event measured during 12 hours of video footage per mouse. Increased seizure scores increase with severity from “no seizure” (0) to “prolonged myoclonic seizure” (3) on the Y-axis. # indicates significant difference between estradiol and vehicle treated PA mice (one-way ANOVA, Tukey’s HSD post hoc analysis, $F(3, 135) = 11.28, p < 0.0001$).

3.4.3 Estradiol treatment does not improve mortality in PA mutant mice

Despite the significant improvements in frequency and severity of seizures in both the PA1 and PA2 mutant mice treated with estradiol, the median survival rates of these animals were not significantly extended compared to vehicle treated animals (Figure 3.6). Survival was recorded from P0 to P70. These data excluded mice that were cannibalised by their mother prior to P10 as this occurred in both WT and mutant mice and was not considered to be due to the mutant phenotype. Mice still alive at the completion of the experimental period were culled at P70. Considering the animals that died before the experimental end point at P70, 62% of PA1 mice treated with vehicle died compared to 64% treated with estradiol (Figure 3.6). Similarly, 37% of PA2 mice treated with vehicle died before the experimental end point at P70, compared to 31% treated with estradiol (Figure 3.6). The mean age of death (excluding survival to end point cull) in vehicle treated compared to estradiol treated mutant mice was not significantly different for either PA1 or PA2 mice; PA1 vehicle treated mice 53 ± 5.1 (mean \pm SEM) compared to 52 ± 5.5 in PA1 estradiol treated mice, with PA2 vehicle treated mice was 45 ± 4.6 , compared to 37 ± 5.2 in PA2 estradiol treated mice (Figure 3.7). While it appeared that PA2 mice treated with estradiol may exhibit a faster rate of death compared to their vehicle treated counterparts, this was not significant.

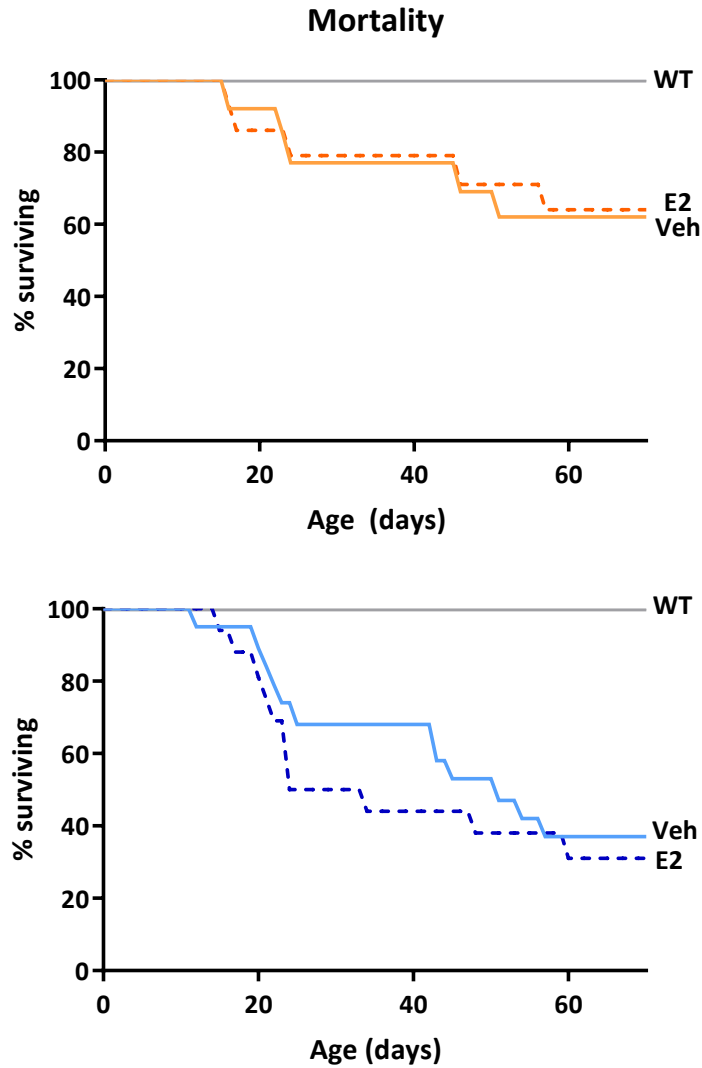


Figure 3.6: Early estradiol does not improve mortality in PA mutant mice. Estradiol did not improve mortality in either PA1 or PA2 mice. Analysis across five separate breeding rounds each for PA1 mice (estradiol; n = 14; dark orange (dashed line) vs vehicle; n = 13 light orange (solid line)) and PA2 mice (estradiol; n = 16; dark blue (dashed line) vs vehicle; n = 19; light blue (solid line)). There were no WT mice treated with vehicle and estradiol that died during the trial with data pooled into one group (grey line).

Age of Death

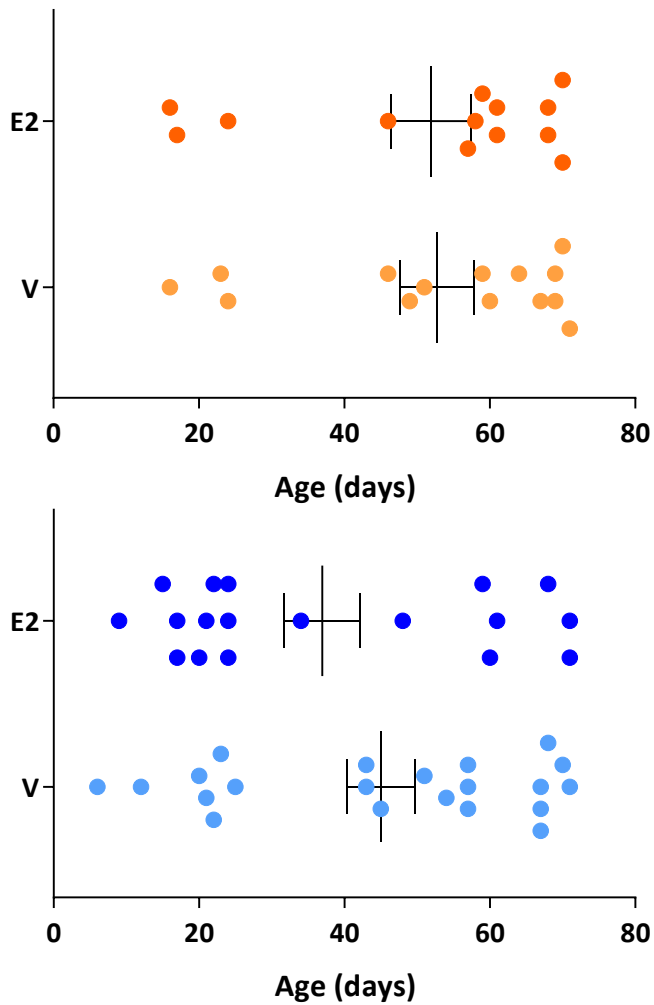


Figure 3.7: Age of death in PA mutant mice treated with vehicle or estradiol. PA1 and PA2 mice treated with estradiol (PA1; n = 13; dark orange) (PA2; n = 18; dark blue) do not exhibit any improvement to age of death when compared to their vehicle treated counterparts (PA1; n = 14; light orange) (PA2; n = 21; light blue). Individual dots represent individual mice throughout the duration of the study (up to P70). Data is shown as mean age \pm SEM.

3.4.4 Body and tissue weights are unaffected by estradiol in PA mutant mice

Further to our seizure and mortality findings, we confirm in this study that compared to WT littermates, the PA mutant mice have reduced testes weight and reduced body weight, consistent with previous reports (Kitamura *et al.*, 2009, Jackson *et al.*, 2017). Here we demonstrate that there were no improvements to the reduced body weight of mutant mice compared to WT littermates with estradiol treatment (significance tested and shown at four different stages of their lifespan) (Figure 3.8).

Cortex and testes were collected from PA1, PA2 and WT mice treated with estradiol or vehicle upon euthanasia at P70. These tissues were weighed for analysis. Similarly, there was no change to the weight of the testes or brain in WT, PA1 or PA2 mice following estradiol treatment (Figure 3.9). However, we demonstrated that PA1 and PA2 mutant mice have significantly reduced testes weight compared to their WT littermates (Figure 3.9).

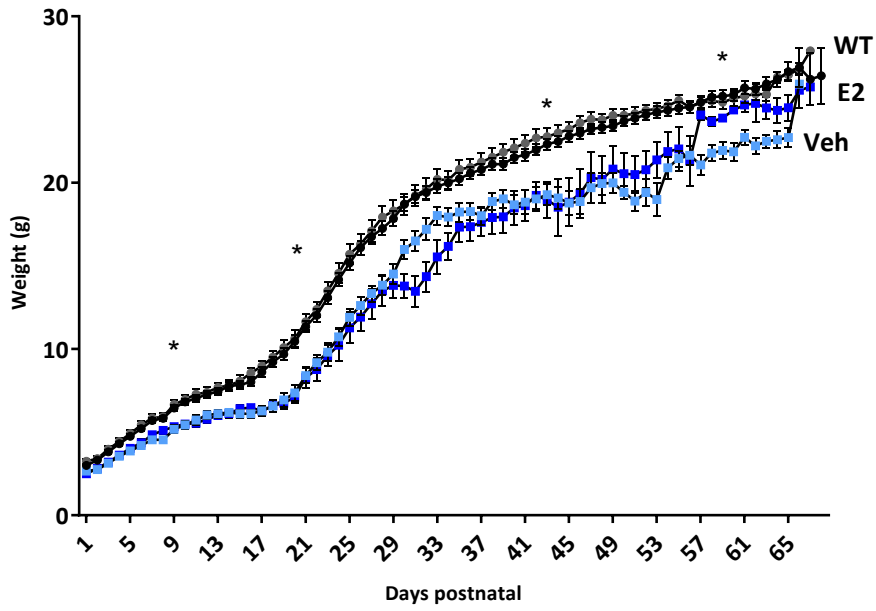
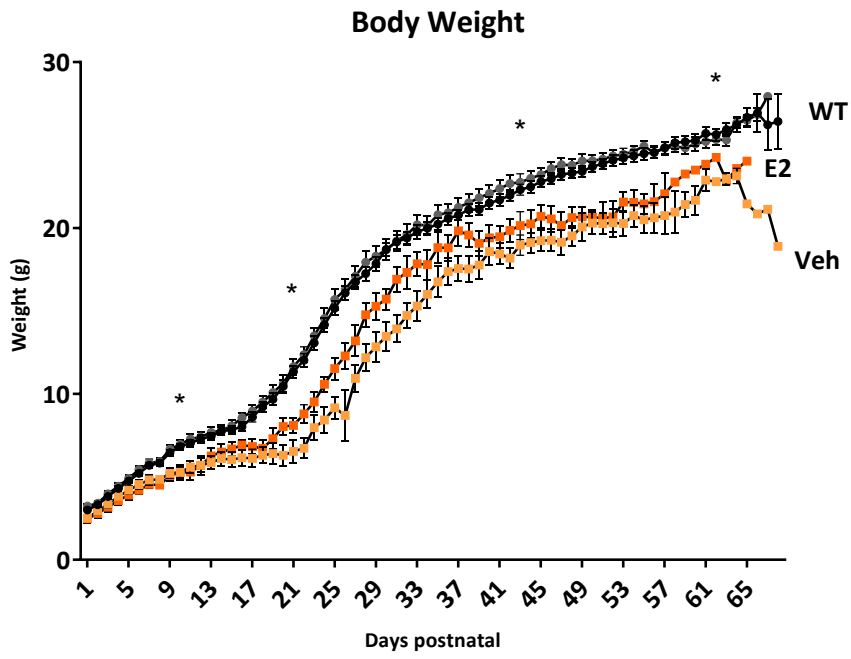
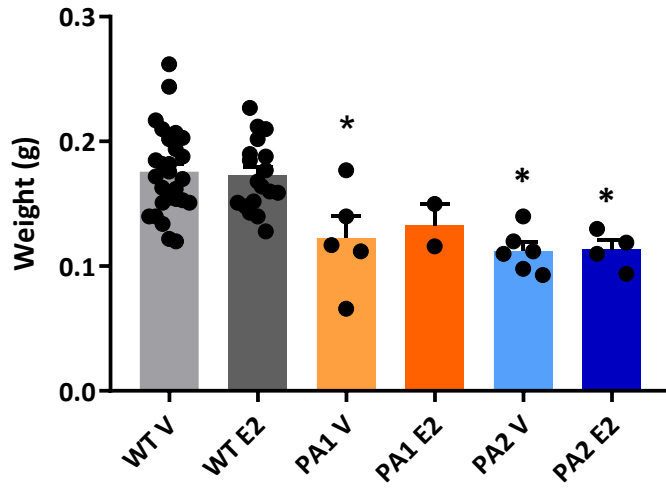


Figure 3.8: Body weights of PA mutant mice treated with vehicle or estradiol. PA1 and PA2 mice treated with estradiol (PA1; n = 13; dark orange) (PA2; n = 18; dark blue) or vehicle (PA1; n = 14; light orange) (PA2; n = 21; light blue) do not exhibit any improvement to body weight through the duration of the study (postnatal day 0 to postnatal day 70), compared to their WT littermates, treated with either estradiol (n = 30; dark grey) or vehicle (n = 23; light grey). Data is shown at mean weight on each day of the study \pm SEM. Data analysed across all groups in one-way ANOVA, Tukey's HSD post hoc analysis at each time point. * $p < 0.05$ significance compared to WT littermates at postnatal P10 ($F(5, 91) = 7.668, p < 0.0001$), P21 ($F(5, 81) = 14.31, p < 0.0001$), P45 ($F(5, 65) = 7.979, p < 0.0001$), and P60 ($F(5, 44) = 8.797, p < 0.0001$) shown on graphs.

Testes



Cortex

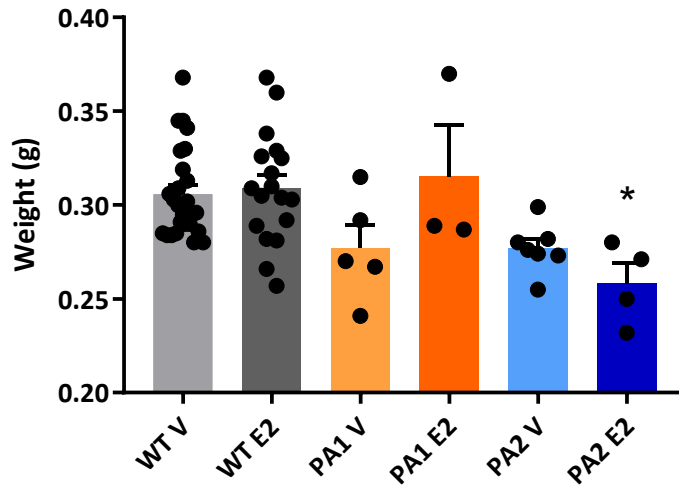


Figure 3.9: Testes and cortex weights of PA mutant mice treated with vehicle or estradiol.

Testes (left and right combined) and cortex (left and right combined) were weighed following euthanasia and tissue collection of mice at postnatal day 70. From WT mice, 27 vehicle-treated testes were weighed (light grey) and 18 estradiol-treated testes were weighed (dark grey), and 26 vehicle-treated cortices were weighed (light grey) and 18 estradiol-treated cortices were weighed (dark grey). From PA1 mice, 5 vehicle-treated testes and 5 vehicle-treated cortices were weighed (light orange), and 2 estradiol-treated testes and 3 estradiol treated cortices were weighed (dark orange). From PA2 mice, 6 vehicle-treated testes were weighed (light blue) and 4 estradiol-treated testes were weighed (dark blue), along with 7 vehicle-treated cortices (light blue) and 4 estradiol-treated cortices (dark blue). * $p < 0.05$ significance compared to WT littermates (one-way ANOVA, Tukey's HSD post hoc analysis; testes data: $F(5, 56) = 8.337$, $p < 0.0001$); cortex data: $F(5, 57) = 4.747$, $p = 0.0011$).

3.4.5 Behavioural deficits are present in PA mutant mice prior to seizure onset, and do not improve with estradiol treatment.

Both PA1 and PA2 mice have been shown to exhibit increased locomotor activity, abnormal anxiety-like behaviour and reduced sociability and autistic-like behaviour at two months of age (Kitamura *et al.*, 2009, Jackson *et al.*, 2017). Here we undertook a battery of behavioural tests between P30 and P37 (one month of age – prior to peak seizure onset), and again at P56 and P70 (two months of age – after peak seizure onset), with and without estradiol treatment. Open field, elevated zero maze, Y-maze, three-chambered sociability tests, inverted grid and the Barnes maze (two months only), were performed to determine the locomotor, anxiety-like and autistic-like behaviour, neuromuscular strength, and memory of PA mutant mice, at one and two months of age, to investigate their cognitive function over disease progression, and in response to estradiol treatment.

3.4.5.1 Anxiety-like behaviour

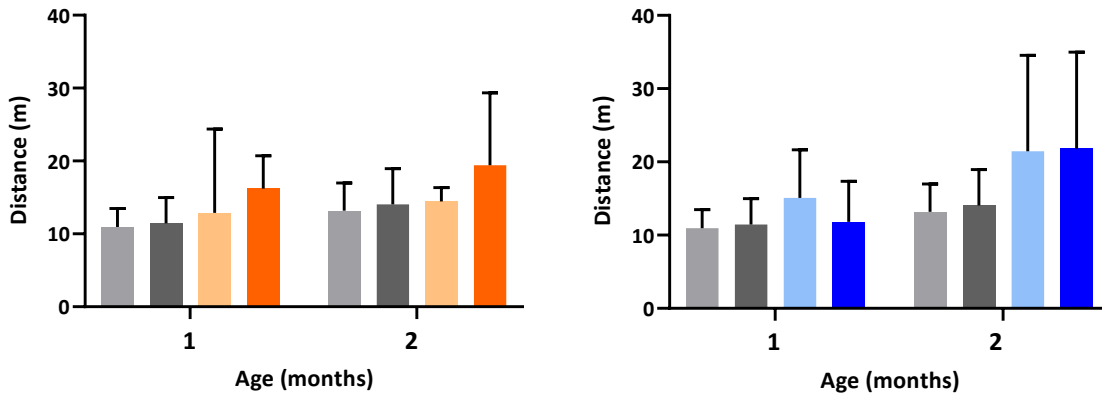
We demonstrated that the anxiety-response in the open field test in PA mutant mice was different compared to WT littermates. There was no significant difference in the total distance the mice travelled during the five minute duration of the open field test in PA mutant mice compared to their wild-type littermates (Figure 3.10 A). We demonstrated that the anxiety-response in PA mutant mice was different compared to WT littermates and did not regress over the duration of the study. At two months of age, WT littermates displayed normal exploratory behaviour with an average of 84% (vehicle) and 80% (estradiol) of the total distance travelled in the open field periphery. Contrary to this, PA1 mutant mice spent significantly more time in the periphery versus the central field of the open field apparatus, with an average of 91% (vehicle) and 96% (estradiol) (Figure 3.10 B). This was also observed in the PA2 cohort, in both treatment groups with an average of 95% (vehicle) and 93% (estradiol) (Figure 3.10 B). These results are indicative of decreased exploratory behaviour in both PA mutant mice compared to WT littermates, with increased anxiety-like behaviour (increased fear of venturing

into the central field, choosing to stay in the safety of the periphery). These differences are shown in the tracking maps from the respective genotypes in the open field test (Figure 3.10 C). We also analysed the time PA mutant mice spent immobile during the test, to determine if this was the cause of decreased distance in the periphery. There was no significant difference in the time immobile versus mobile in PA mutant mice compared to their WT littermates, with or without treatment. There were no significant differences observed between the two ages sampled in either PA mutant cohort, indicating there was little change due to disease progression or age of the mice in either genotype. This data indicates that early estradiol treatment did not improve anxiety or fear behaviour in adult PA mutant mice.

The elevated zero maze was also used to investigate anxiety-like behaviour in PA mutant mice. As with the open field test, there was no significant difference observed in the total distance PA mutant mice travelled during the five minute duration of the test, indicating no deficits in total activity during the testing period compared to WT mice (Figure 3.11 A). We showed no significant differences in the outcomes of this test, even having previously shown a deficit to fear response and anxiety-like behaviour in untreated PA1 and PA2 mice using this apparatus. Mice with an altered anxiety or fear response tend to spend more time in the closed arms of the test, fearing the open spaces. We observed no significant differences in the time PA mutant mice spent in the open versus the closed arms of the test at either one or two months of age with no difference due to estradiol treatment (Figure 3.11 B). There appeared to be a trend towards less head dips in PA1 mice treated with vehicle compared to WT mice, indicative of reduced exploratory behaviour (Figure 3.12). However, this was not significant, possibly due to the broad range in the number of head dips recorded in mice during this test, indicated by the large SEM in this data set.

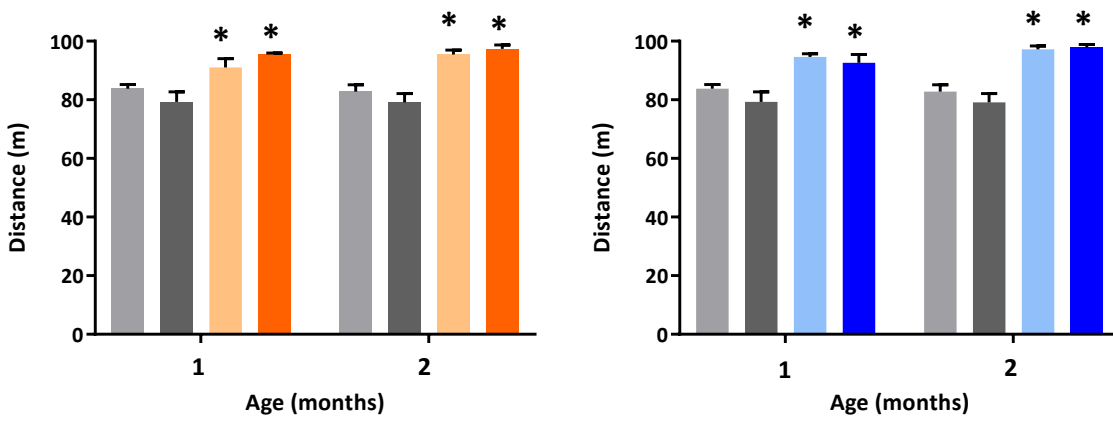
Total Distance

A



% distance in periphery

B



C

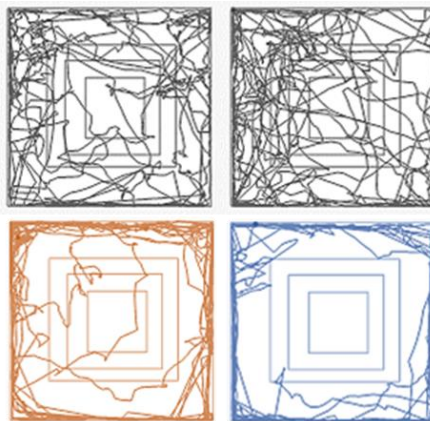
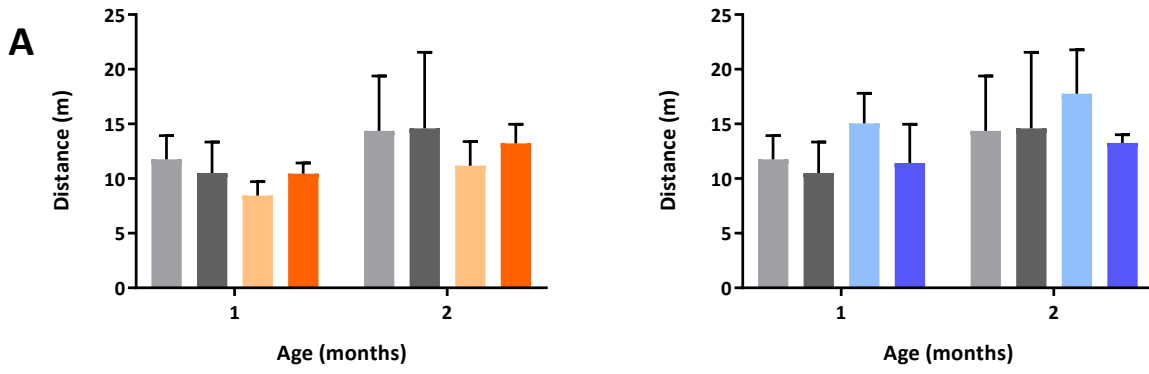


Figure 3.10: Estradiol does not improve anxiety-like behavioural deficits in PA mutant mice. Anxiety-like and fear response behaviour was measured using the open field test. (A) The total distance the mice travelled in the open field apparatus during the duration of the test at one month and two months of age. (B) The percentage of the total distance travelled that the mice spend in the periphery of the open field test measured in distance (m) is shown at one month and two months of age. WT mice treated with vehicle (n = 17/12; light grey) and estradiol (n = 8/8; dark grey); PA1 mice treated with vehicle (n = 6/5; light orange) and estradiol (n = 4/3; dark orange); PA2 mice treated with vehicle (n = 11/6; light blue) and estradiol (n = 5/5; dark blue). * $p < 0.05$ (two-way ANOVA with Tukey's HSD post hoc analysis; PA1: $F(3, 55) = 14.801, p < 0.0001$); PA2: $F(3, 64) = 24.91, p < 0.0001$). (C) Representative tracking maps of mice travelling in the open field apparatus from wild-type (n = 2; grey), PA1 (n = 1; orange) and PA2 (n = 1; blue) mice.

Total Distance



B % time in open and closed arms

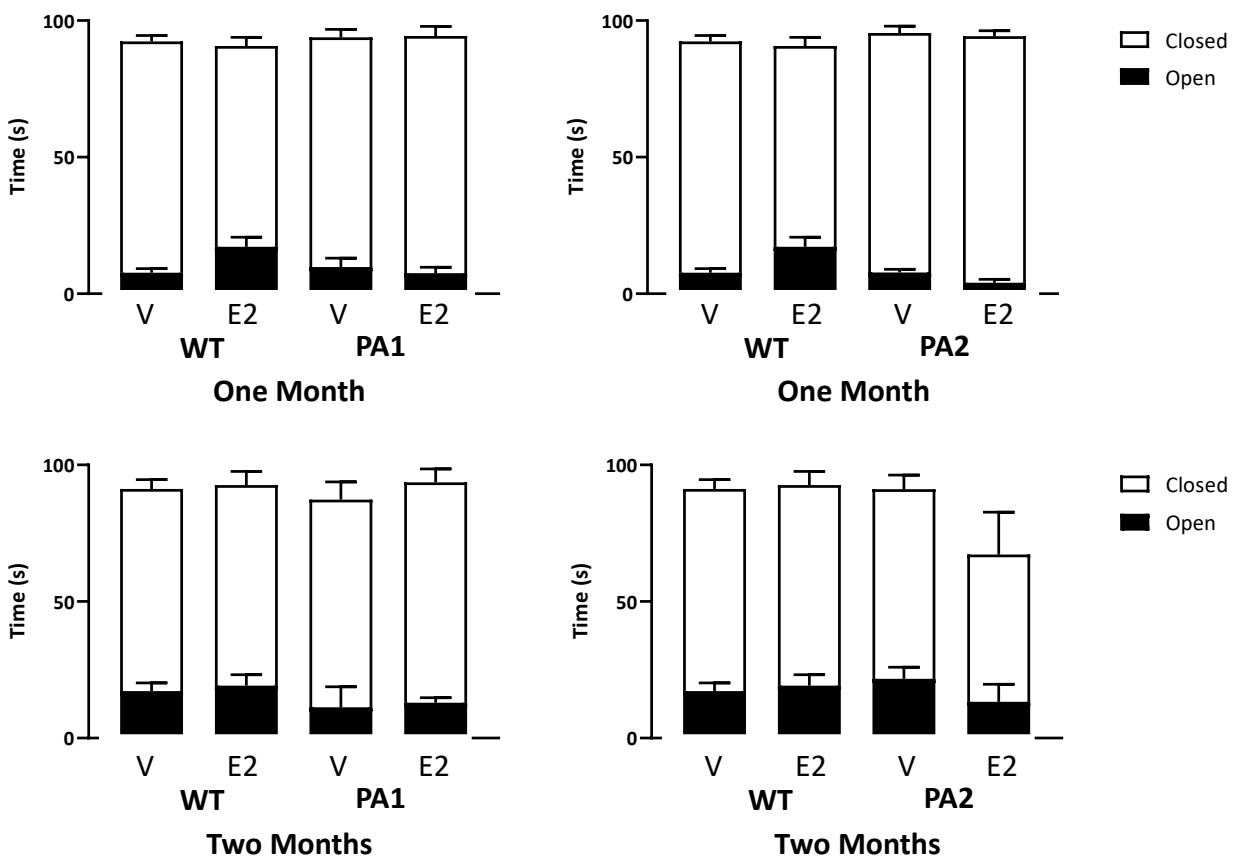


Figure 3.11: PA mutant mice do not exhibit an anxiety-like deficit in the elevated zero maze. Anxiety-like and fear response behaviour was measured using the elevated zero maze. (A) The total distance the mice travelled in the elevated zero maze apparatus during the duration of the test at one month and two months of age. (B) The percentage of the total time that mice travelled in the open arms or closed arms of the elevated zero maze, measured in seconds (s) is shown at one month and two months of age. WT mice treated with vehicle (n = 17/12; light grey) and estradiol (n = 8/8; dark grey); PA1 mice treated with vehicle (n = 6/5; light orange) and estradiol (n = 4/3; dark orange); PA2 mice treated with vehicle (n = 11/6; light blue) and estradiol (n = 5/5; dark blue).

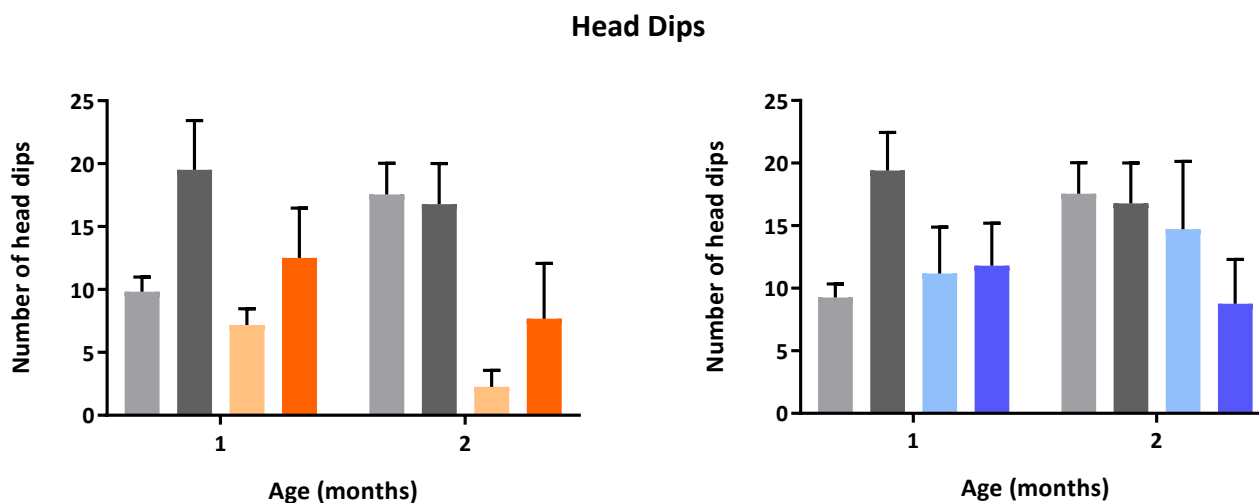


Figure 3.12: PA mutant mice do not show significant differences in number of explorative head dips in the elevated zero maze. Anxiety-like and fear response behaviour was measured using the elevated zero maze. The number of head dips recorded manually during the duration of the elevated zero maze at one and two months of age. WT mice treated with vehicle (n = 17/12; light grey) and estradiol (n = 8/8; dark grey); PA1 mice treated with vehicle (n = 6/5; light orange) and estradiol (n = 4/3; dark orange); PA2 mice treated with vehicle (n = 11/6; light blue) and estradiol (n = 5/5; dark blue).

3.4.5.2 Autistic-like behaviour

Sociability testing measures several behavioural traits seen in mouse autism models. The mouse being tested is placed in a central chamber, with an empty chamber on one side and a chamber containing another mouse in the other. The time spent interacting with the other mouse is measured (sociability). The next phase of the test includes placing a novel mouse in third (previously empty) chamber. The time the test mouse then spends interacting with this new and novel mouse (social novelty: novel) is compared to the time spent interacting with the existing or familiar mouse (social novelty: familiar). As expected, WT littermates chose to interact with another mouse over an inanimate object (empty chamber) (sociability phase: Figure 3.13), and then chose to interact with novel (or stranger) animal over the familiar (or known) animal (social novelty phase: Figure 3.14). This pattern of behaviour is indicative of normal social interaction and memory recall. In contrast, the PA1 mutant mice of both vehicle and estradiol treatment groups showed significantly reduced sociability (Figure 3.13) and social novelty (Figure 3.14) compared to WT mice. The interaction times with other mice in the test chambers were reduced, regardless of whether the mouse occupant was novel or familiar. This behavioural deficit was the same for PA2 mutant mice. There was no significant difference between the two age points in either PA cohort, indicating reduced sociability was already present at one month of age and did not change with disease progression or age.

Interestingly, in PA1 estradiol treated mice there was a significant difference between the time spent interacting with both stranger and familiar mice in the social novelty phase compared to vehicle treated mice, but only at one month of age. Similarly, PA2 mice treated with estradiol spent an increased amount of time interacting with stranger and familiar mice compared to their vehicle treated counterparts, but this was only significant at two months of age. This may indicate small improvements to social cognitive behaviour in PA mice treated with estradiol, however, the sample sizes for these groups were small, and given the similarities in phenotype between PA1 and PA2 mice in this test, we combined PA1 and PA2 mice to create a PA^{pool}

group (green) for these measures to strengthen our findings. We demonstrated that PA^{pool} mutant mice of both vehicle and estradiol treatment groups showed significantly reduced sociability (Figure 3.15) and social novelty (Figure 3.16) compared to WT mice. Again, the overall time interacting was reduced in mutant mice, regardless of whether it was with the stranger or familiar mouse. There was no significant difference between the two time points in the PA^{pool} cohort.

Sociability

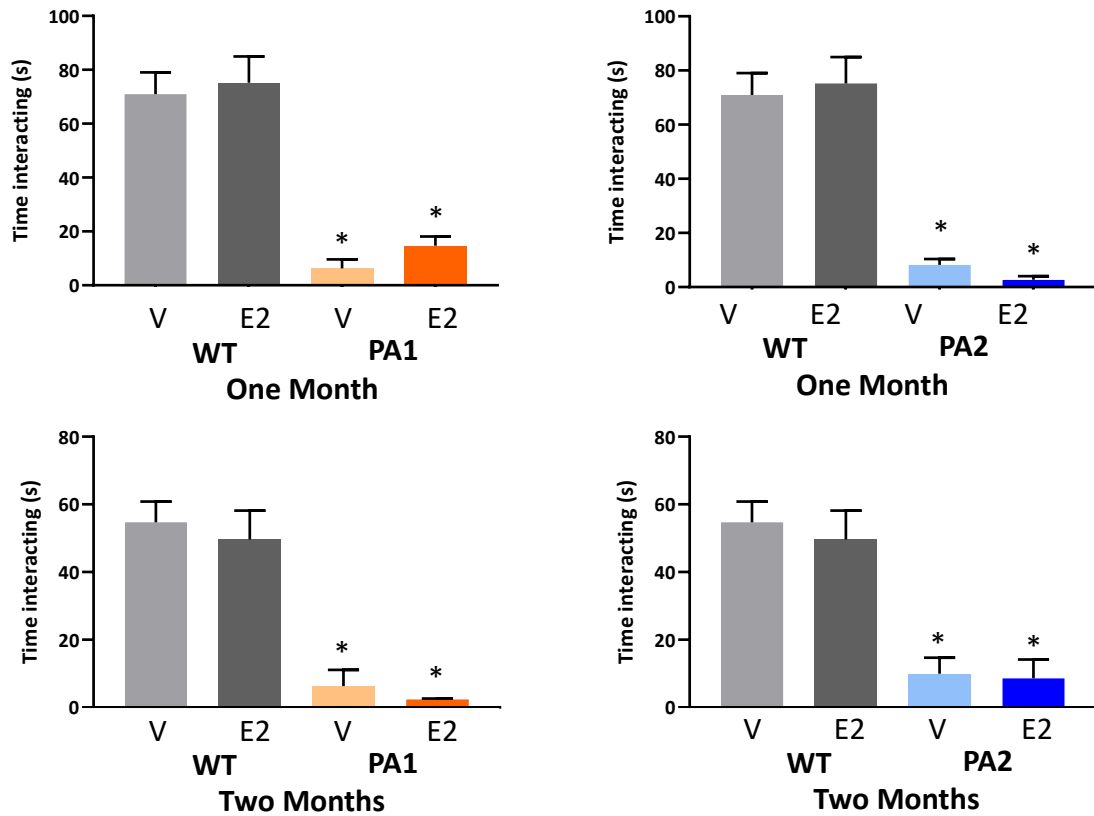


Figure 3.13: Estradiol does not improve social deficits in PA mutant mice. Autistic-like behaviour was measured using the sociability test. Social interaction of PA mutant mice at one and two months of age was measured by the time in seconds (s) the mice spent interacting with a stranger mouse. WT mice treated with vehicle (n = 15/9; light grey) and estradiol (n = 8/6; dark grey); PA1 mice treated with vehicle (n = 6/4; light orange) and estradiol (n = 3/2; dark orange); PA2 mice treated with vehicle (n = 9/5; light blue) and estradiol (n = 5/4; dark blue). * $p < 0.05$ (two months; one-way ANOVA, $F(5, 24) = 12.34$, $P < 0.0001$).

Social Novelty

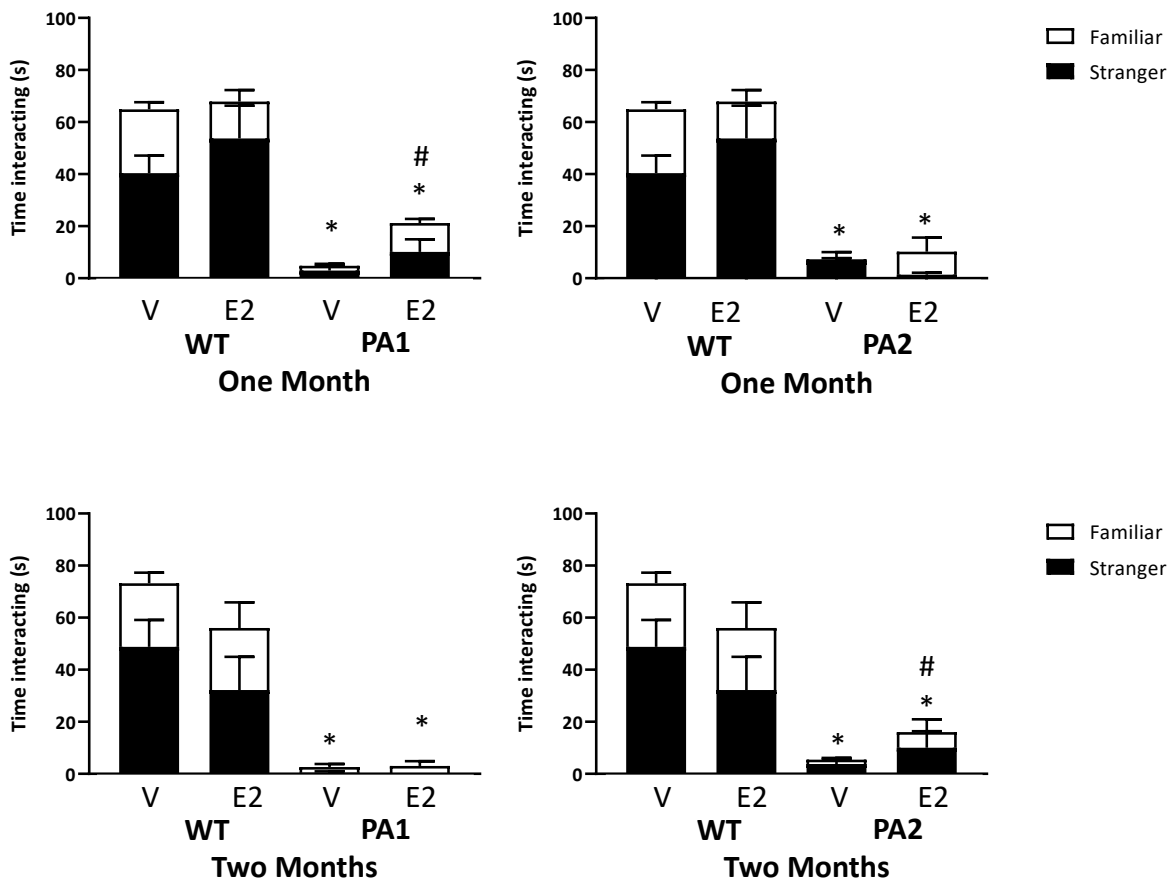


Figure 3.14: Estradiol does not improve social preference deficits in PA mutant mice.

Autistic-like behaviour was measured using the social novelty test. Social interaction of PA mutant mice at one and two months of age was measured by the time in seconds (s) the mice spent interacting with either a stranger or familiar mouse. WT mice treated with vehicle ($n = 15/9$; light grey) and estradiol ($n = 8/6$; dark grey); PA1 mice treated with vehicle ($n = 6/4$; light orange) and estradiol ($n = 3/2$; dark orange); PA2 mice treated with vehicle ($n = 9/5$; light blue) and estradiol ($n = 5/4$; dark blue). * $p < 0.05$ (one-way ANOVA with Tukey's HSD post-hoc analysis of PA mutant mice compared to WT). # indicates significant difference between PA mutant mice treated with either vehicle or estradiol. * $p < 0.05$ (PA1; two-way ANOVA, $F(3, 45) = 19.37$, $P < 0.0001$).

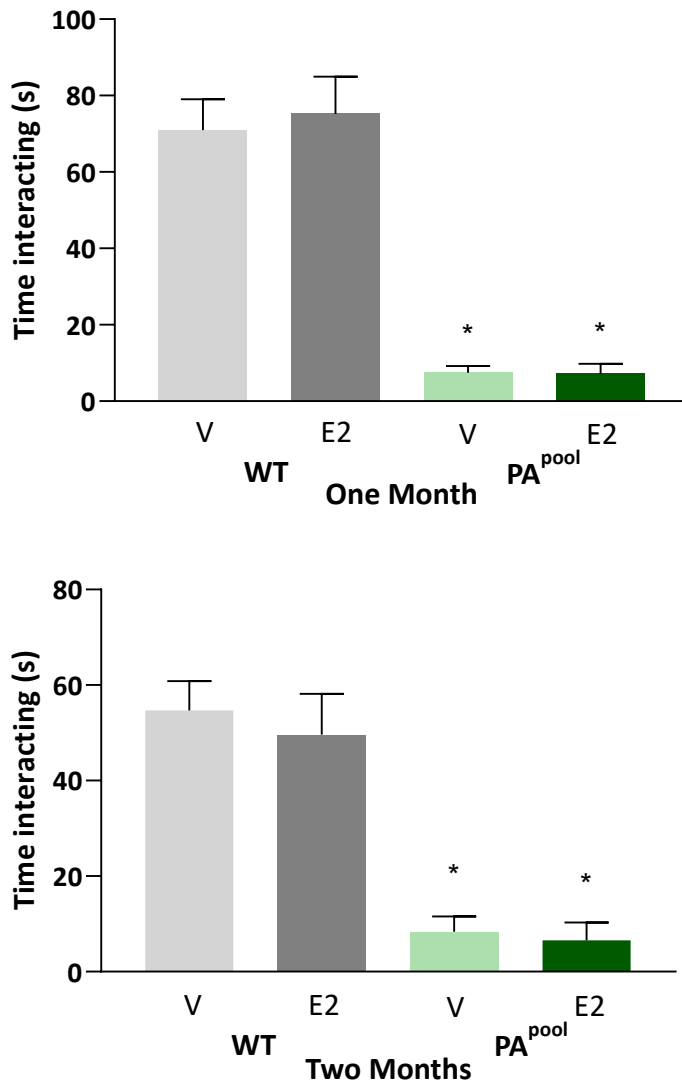


Figure 3.15: Estradiol does not improve social deficits in PA^{pool} mutant mice. Autistic-like behaviour was measured at one and two months of age by the time in seconds (s) the mice spent interacting with a new mouse in the sociability test. WT mice treated with vehicle ($n = 15/9$; light grey) and estradiol ($n = 8/6$; dark grey); PA^{pool} mice treated with vehicle ($n = 15/9$; light green) and estradiol ($n = 8/6$; dark green). * $p < 0.05$ (two months; one-way ANOVA, $F(3, 26) = 21.85$, $P < 0.0001$).

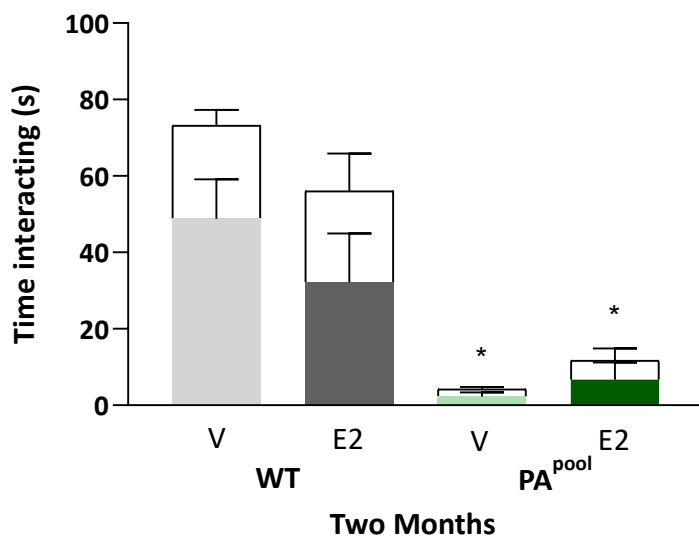
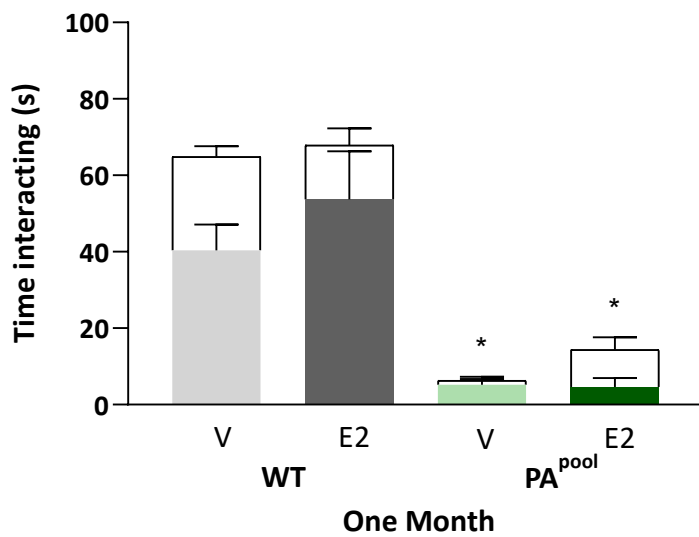


Figure 3.16: Estradiol does not improve social preference deficits in PA^{pool} mutant mice.

Autistic-like behaviour was measured at one and two months of age by the time in seconds (s) the mice spent interacting with a familiar mouse (white bars) or stranger mouse (coloured bars) in the social novelty test. WT mice treated with vehicle ($n = 15/9$; light grey) and estradiol ($n = 8/6$; dark grey); PA^{pool} mice treated with vehicle ($n = 15/9$; light green) and estradiol ($n = 8/6$; dark green). * $p < 0.05$ (two months; two-way ANOVA, $F(3, 52) = 13.44$, $P < 0.0001$).

3.4.5.3 Learning and memory

Spatial learning and memory were assessed in PA mutant mice using two different behavioural tests; Y-maze and Barnes maze. Y-maze assesses short-term memory while the Barnes maze assesses the learning and memory of mice over a one week duration. In the Y-maze, mice were exposed to one arm of a Y-shaped apparatus, which became the familiar arm to the mice. After 30 minutes, mice were re-exposed to the Y-maze, with both arms open for them to explore. The time that the mouse spends in the familiar or novel arm is then assessed, with WT mice usually preferring to spend more time exploring the novel arm. The arms of the Y-maze have shapes on them to assist the mice in remembering which the familiar and novel arms are.

Interestingly, when looking at the total distance mice travelled during the duration of the final exploration of testing in the Y-maze, there were groups of PA mutant mice that travelled significantly more distance than WT mice, possibly indicative of hyperactivity in the PA cohorts (Figure 3.17 A). A memory deficit in the Y-maze in untreated PA1 and PA2 mutant mice has been reported previously (Jackson *et al.*, 2017). In this study however, we did not see a significant difference between the time the mutant mice spent in the familiar arm versus the novel arm compared to their WT littermates, at either one or two months of age (Figure 3.17 B). There was also no significant difference in the time spent in each arm between mice treated with either vehicle or estradiol (Figure 3.17 B). These results indicated no deficits in short-term memory in PA mutant mice either before or after the peak of seizure onset.

To assess the impact of treatment on cognition and learning, the Barnes maze tested the amount of time each mouse required to locate an escape hole (in relation to false holes) in the testing apparatus, with improving or shorter times gained during subsequent testing. This test is conducted at two months of age. All groups tested showed normal adaptive function and memory, demonstrating shorter times to find the escape hole over a progressive four-day testing period (Figure 3.18). This was shown through a multi-way ANOVA using mixed effects for

multiple comparisons. We found that when analysing four groups together (WT and PA^{po01} from each treatment), there was a significant difference in latency to find the escape hole between days 1 and 4 of testing ($p = 0.0003$). However, while this tells us that the mice are learning in this test, we are not seeing any difference due to genotype or treatment. Although we have previously demonstrated a memory deficit when testing via the Barnes maze in untreated PA mutant mice (Jackson *et al.*, 2017), in the current trial we did not detect a significant difference between the PA mutant mice of either treatment group and their WT littermates. This difference is likely due to the limited numbers of animals achieving the age required to perform this test. Of note, there was no difference in the performance of WT or mutant animals when vehicle treated animals were compared to estradiol treated animals.

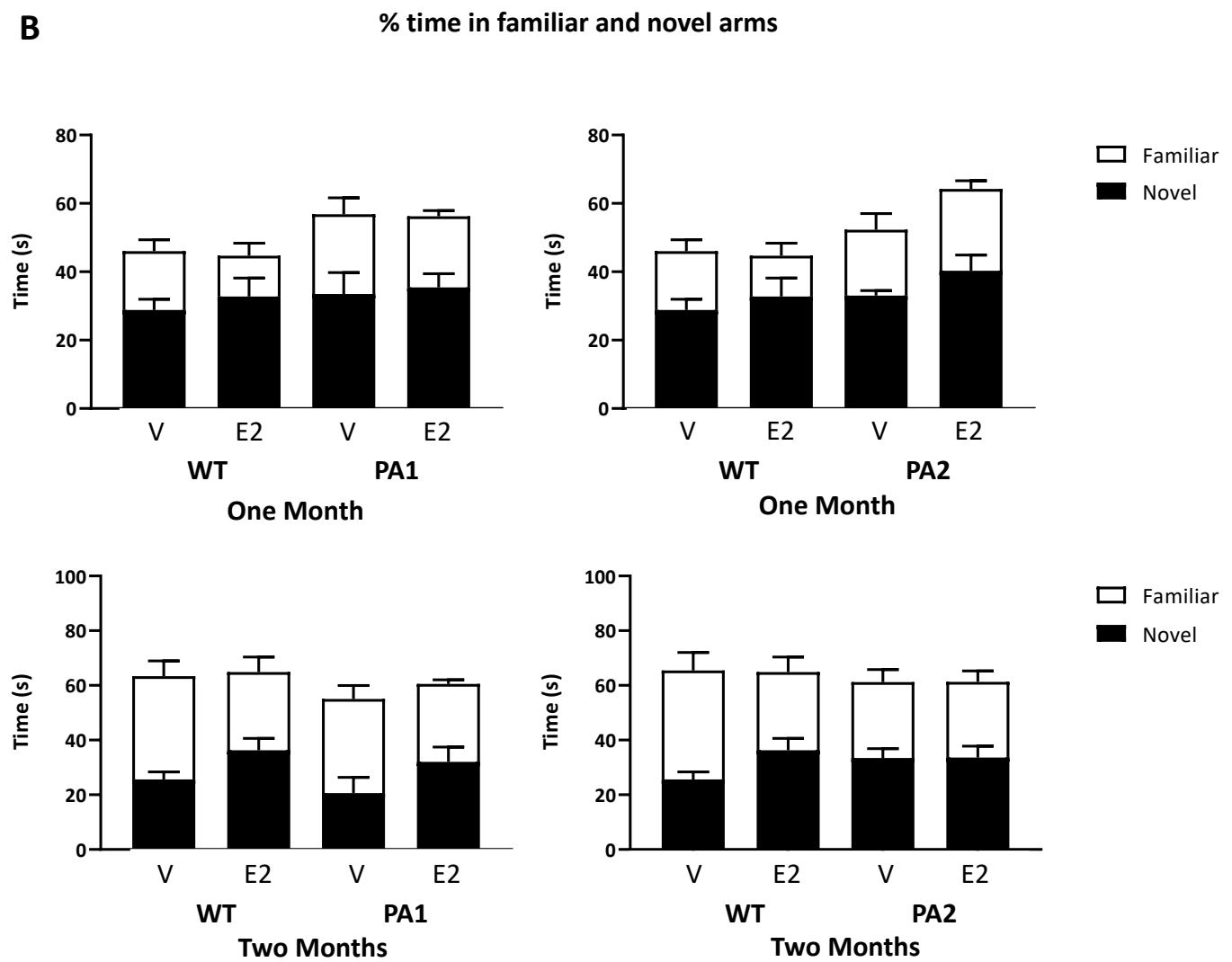
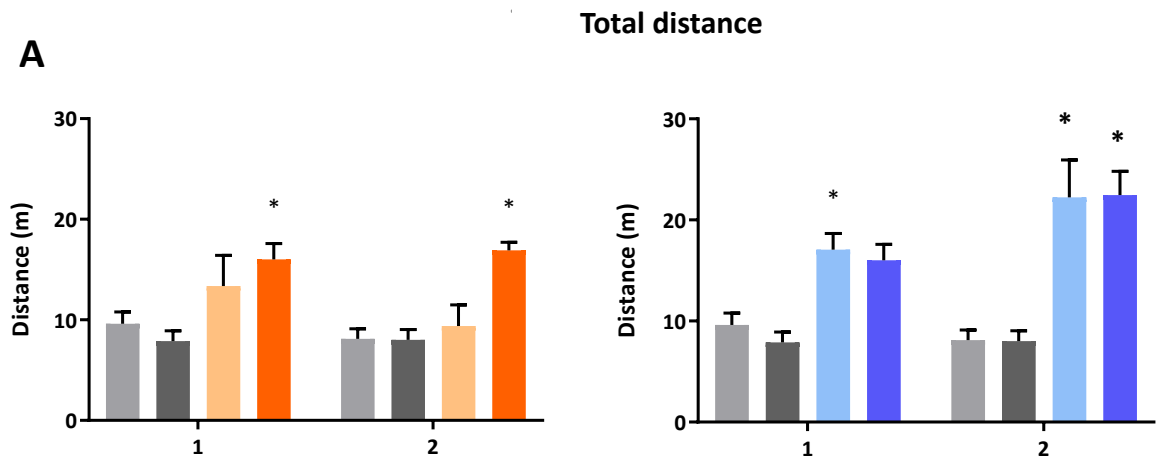


Figure 3.17: PA mutant do not exhibit a short-term memory deficit in the Y-maze. Short-term memory and exploratory behaviour were measured using the Y-maze. (A) The total distance the mice travelled in the Y-maze during the duration of the test at one month and two months of age. (B) The percentage of total time travelled that the mice spent in either the familiar or novel arms of the Y-maze, measured in seconds (s) is shown at one and two months of age. (C) WT mice treated with vehicle (n = 17/12; light grey) and estradiol (n = 8/8; dark grey); PA1 mice treated with vehicle (n = 6/5; light orange) and estradiol (n = 4/3; dark orange); PA2 mice treated with vehicle (n = 11/6; light blue) and estradiol (n = 5/5; dark blue). * $p < 0.05$ (two-way ANOVA with Tukey's HSD post hoc analysis; PA1: $F(3, 56) = 8.303$ $p = 0.0001$); PA2: $F(3, 62) = 25.81$, $p < 0.0001$).

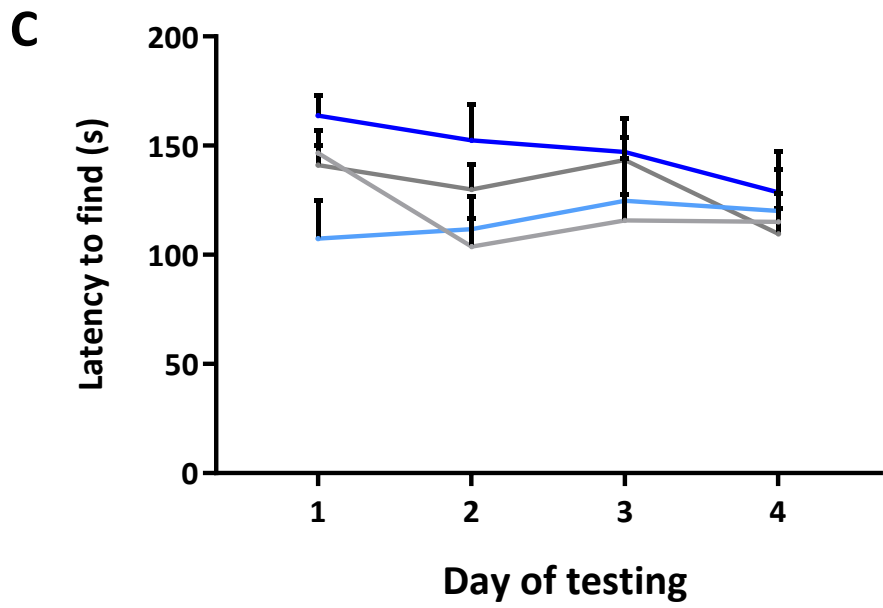
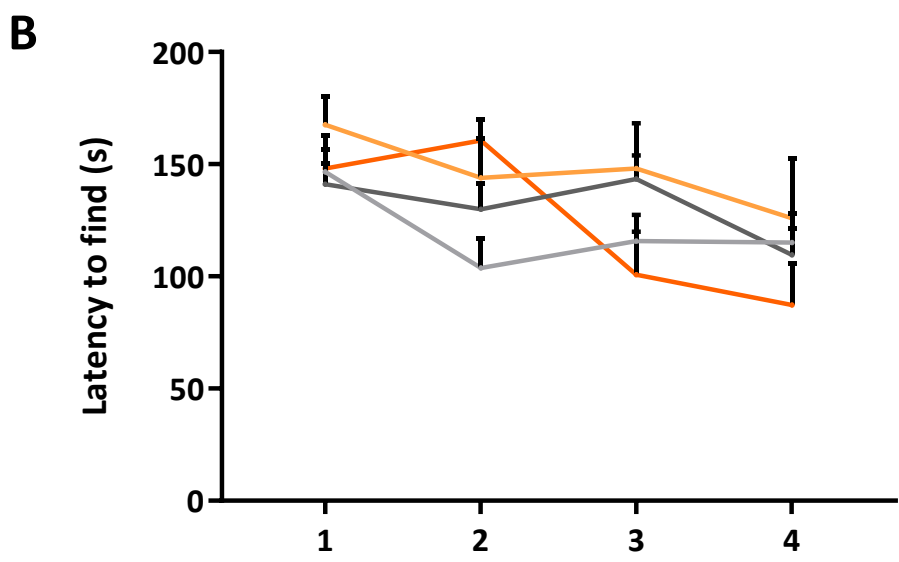
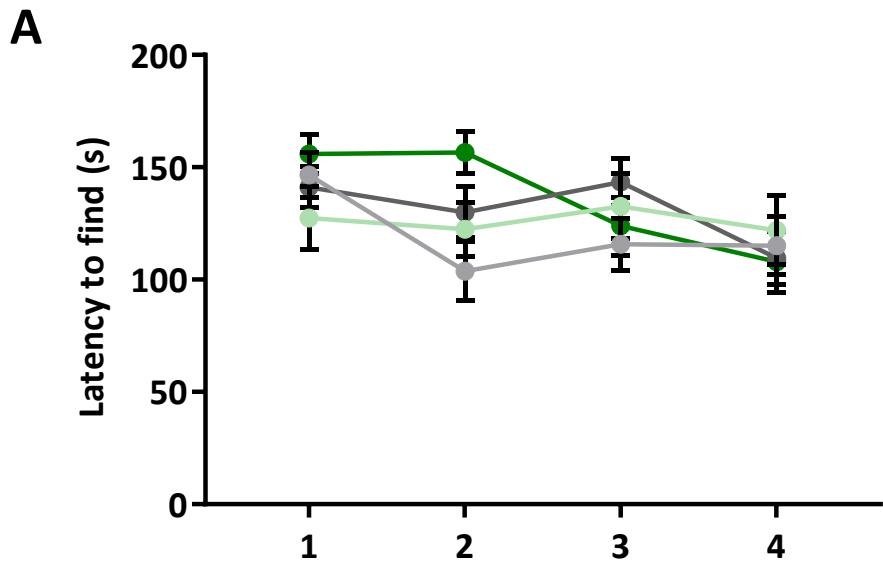


Figure 3.18: PA mutant mice do not display learning and memory deficits in the Barnes maze. Learning and memory was measured using the Barnes maze at two months of age only. The latency to find the escape hole was measured in seconds (s) across a four-day testing period. Mice were measured from WT treated with estradiol ($n = 10$; dark grey) or vehicle ($n = 8$; light grey) with A) PA1 and PA2 mice were combined as a PA^{pool} group. PA^{pool} treated with estradiol ($n = 6$; dark green) or vehicle ($n = 6$; light green). B) PA1 mice treated with estradiol ($n = 4$; dark orange) and vehicle ($n = 2$; light orange). C) PA2 mice treated with estradiol ($n = 4$; dark blue) and vehicle ($n = 4$; light blue). Latency to find (mean \pm SEM).

3.4.5.4 Neuromuscular strength

We chose to test neuromuscular strength due to the prominent phenotype of dystonia, particularly in the hands, of PA2 patients. The impact of *Arx* genotype and 17 β -estradiol treatment on the neuromuscular strength in PA mutant mice was determined using the inverted grid test, at two months of age. WT littermates decreased latency to fall from the grid averaged 76 seconds (vehicle) and 90 seconds (estradiol) compared to PA1 mice with 25 seconds (vehicle) and PA2 mice for 23 seconds (estradiol) (Figure 3.19 A). Pooling the data for the mutant mice (PA^{pool} group) to increase the sample size, both vehicle and estradiol had significantly decreased latency to fall from the grid compared to their respective WT groups (Figure 3.19 B).

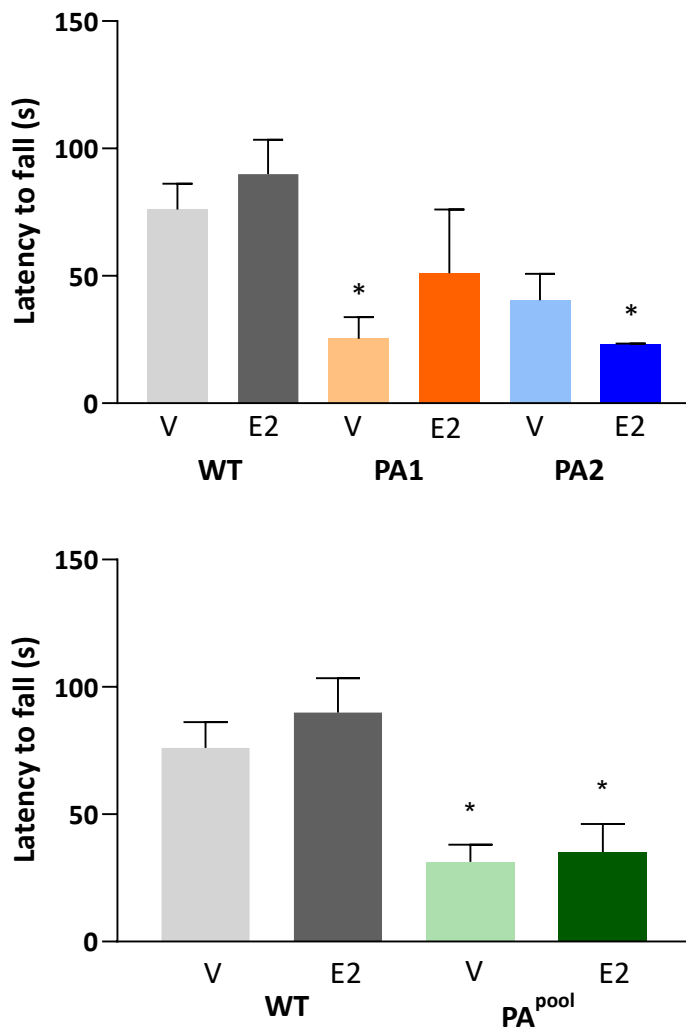


Figure 3.19: PA mutant mice display reduced neuromuscular strength. Neuromuscular strength measured using the inverted grid test at two months of age (one-way ANOVA, $F(3,31) = 7.920$, $P=0.0005$). The latency for mice to fall from the inverted grid was measured in seconds (s). WT mice treated with vehicle ($n = 11$; light grey) and estradiol ($n = 7$; dark grey); PA1 mice treated with vehicle ($n = 6$; light orange) and estradiol ($n = 3$; dark orange); PA2 mice treated with vehicle ($n = 4$; light blue) and estradiol ($n = 4$; dark blue). In the second graph, PA1 and PA2 mice were combined as a PA^{pool} group. WT mice treated with vehicle ($n = 11$; light grey) and estradiol ($n = 7$; dark grey); PA^{pool} mice treated with vehicle ($n = 10$; light green) and estradiol ($n = 7$; dark green). * $p < 0.05$ (PA^{pool}; one-way ANOVA, $F(3,31) = 7.920$, $P=0.0005$).

3.5 Discussion

3.5.1 Reproducibility of phenotypic outcomes in different mouse models

Here we present a comprehensive seizure and behavioural assessment of the impact of early postnatal estradiol treatment on the development of seizures in mice modelling the two most common *ARX* polyalanine expansion mutations. Our data demonstrates that despite the sustained benefit of short term 17 β - estradiol treatment early in postnatal life on the frequency and severity of seizures in both PA1 and PA2 mutant mouse models, there were no significant improvements to survival, anxiety, sociability, cognitive or neuromuscular deficits in treated mice in adult life.

Importantly, our data provides support for reproducible anti-epileptogenic outcomes previously reported in a comparable *Arx* PA1 mutant mouse, studied on a different genetic background (Olivetti *et al.*, 2014). We have characterised the reduction in seizure frequency and severity in both PA mutant mice using a scoring matrix via video monitoring correlated to video-EEG (Jackson *et al.*, 2017). Here we expand these findings to indicate that short term, early 17 β -estradiol administration also reduced seizures in the PA2 mutant mouse that models the most frequently reported polyalanine tract expansion mutation in *ARX* patients. The findings from our study also demonstrates that behavioural deficits in these models are present prior to seizure onset, and that seizure onset does not appreciably exacerbate deficits to intellectual and adaptive functioning or autistic-like behaviour, at least in these genetic mice modelling *Arx* mutations.

There were some interesting outcomes from our seizure analysis approach that require addressing. Unsurprisingly, there was a stark difference in the outcomes of seizures recorded on handling of the mice, compared to seizures recorded during video seizure monitoring. Seizures recorded on handling are likely to be higher due to the impact of stress on the mice. While measures are taken to make weighing and observing have minimal impact on the mice, it is still time away from their home environment in the hands of a human observer. Video

seizure monitoring on the other hand allows the mice to remain in a home cage environment with their littermates for a portion of time, a much less stressful situation. This allows a more “natural” occurrence of seizures, so that we may determine a truer incidence of frequency.

There was also a surprising increase in the occurrence of observed seizures in estradiol treated PA2 early in postnatal life compared to their vehicle treated counterparts, whereas treated PA1 mice had no difference in the onset of observed seizures. It is possible that estradiol treatment can induce seizures in specific situations and studies, however these differences are usually observed in females (Hom *et al.*, 1993, Velišková, 2006, Younus and Reddy, 2016, Azcoitia *et al.*, 2019). There was no increase in seizure occurrence in PA2 mice with estradiol treatment in our seizure monitoring results, however this is performed at approximately 1.5 months of age. It is difficult to determine the reason for this increase in seizure onset PA2 mice, but this result may be limited by the caveats of recording seizures on handling as described above.

3.5.2 Relating behavioural testing to patient phenotypes

The battery of behavioural tests performed in my study builds on our extensive phenotyping of these mice (Jackson *et al.*, 2017) and assesses a variety of different behavioural domains. The open field and elevated zero maze measure anxiety-like behaviour, the Y-maze measures exploration, the sociability test measures aspects of social cognition, the Barnes maze measures spatial learning, and the inverted grid measure motor deficits and neuromuscular strength (Wahlsten, 2011). These behavioural domains align closely with behavioural deficits reported in patients with expansion mutations in *ARX*. For example, in a cohort of French patients carrying the dup24 mutation in PA2 deeply phenotyped hyperactivity was detected in 47.6% of patients (Dubos *et al.*, 2018). In the Y-maze, we found that both PA1 and PA2 mice spent significantly more time moving during the test than their wild-type littermates, leading to a higher total distance travelled, a measure of hyperactivity. Dubos *et al.* also demonstrated that

only 14.3% of PA2 patients were assessed as “calm”, with 19% having a diagnosis of severe anxiety (Dubos *et al.*, 2018). In our mice we show that PA2, and PA1 mice, display anxiety-like behaviour in the open field test, with mice spending more time in the periphery, indicative of increased fear. We also found strong evidence for reduced social cognition in PA mutant mice. In agreement, only 56.3% of PA2 patients displayed what is described as adequate interpersonal relationships, defined by the Vineland Adaptive Behavioural Scale (Dubos *et al.*, 2018). Other studies on PA2 patients have reported deficits in social behaviour, autism spectrum disorder, severe developmental delay and mental retardation, emotional instability, self-aggression and language delays (Bienvenu *et al.*, 2002, Stromme *et al.*, 2002, Partington *et al.*, 2004, Gestinari-Duarte Rde *et al.*, 2006, Reish *et al.*, 2009). Hence, anxiety-like and hyperactivity behaviour and social behaviour in the PA mouse models closely mimics phenotypes in the ARX PA2 patients. We contend that the PA mutant mice provide a useful tool to examine the effectiveness of treatments on behaviour. Interestingly, many studies into the clinical phenotypes of PA1 patients lack the detailed reports of behavioural phenotypes, likely due to a combination of severe intellectual disability phenotypes and limited affected patient numbers. This lack of deep phenotyping of PA1 patients makes it difficult to compare the profile of human behaviour to the outcomes we measure in our mouse model.

3.5.3 No change to the survival of mice with estradiol treatment

Despite a striking reduction in the frequency and severity of seizures there was no improvement to mortality of either PA1 or PA2 mice with estradiol treatment. We report that there was no statistical difference in the numbers of estradiol and vehicle treated PA1 or PA2 hemizygous male mice that were found dead. This was a novel finding. The cause of death could not be confirmed by post-mortem examination due to the timing of death occurring overnight. However, death due to a seizure can be hypothesised when deceased mice show extension of the hind legs, a marker of death according to a modified Racine scale (Butler *et al.*, 1995). On examination in the mornings, we could not contribute death to any obvious cause. While the immediate cause of death in PA mutant mice is unclear, the lack of progressive deterioration and presence of convulsive seizures suggests that sudden unexpected death in epilepsy (SUDEP), or prolonged status epilepticus, is a possible diagnosis. Although 17 β -estradiol treatment decreased the frequency and severity seizures in mutant PA *Arx* mouse models, the residual amount of seizures still present particularly evident upon handling, could account for the premature mortality in these mice.

3.5.4 Behavioural deficits are present prior to seizure onset

The distribution of IQ scores in children with epilepsy and infantile spasms are often skewed to lower values, and patients experience difficulties learning in school, or regress in mental development (Farwell *et al.*, 1985, Neyens *et al.*, 1999, Prasad *et al.*, 2014). However, it can often be difficult to elucidate how much of a child's intellectual disability was pre-existing and how much was caused by epilepsy in key periods of brain development (Nabbout and Dulac, 2003). In the case of genetic conditions in which intellectual disability is an invariable feature, such as *ARX* mutations, determining the impact of persistent and severe seizures, particularly early in childhood and infancy, upon cognitive function remains challenging. A cardinal finding of our study is the relative differential response of seizure severity compared to behavioural and cognitive deficits following estradiol treatment. We predicted that seizure onset would lead to

a worsening of cognitive and behavioural impairments in the PA1 and PA2 mutant mice. An extension of this prediction would be that 17 β -estradiol treatment alleviating seizures might improve cognitive and behavioural deficits. In contrast to our predictions, we demonstrate that behaviour did not improve with alleviation of seizures and that the deficits were already present before and did not decline further after the point of seizure onset. This provides important evidence separating the impact of seizures upon behavioural deficits in PA1 and PA2 mice.

An epileptic encephalopathy is defined as a condition where seizures or frequent interictal discharges exacerbate neurocognitive dysfunction beyond what would be expected on the basis of underlying aetiology (Nickels and Wirrell, 2017). This occurs in intractable epileptic disorders that start early in life, such as Ohtahara syndrome (OS), also known as Early Infantile Epileptic Encephalopathy (EIEE). Infants with these severe epileptic encephalopathies generally present with poor cognitive outcomes, with profound intellectual disability in 50% of patients if they survive severe spasms and seizures in infancy. These disorders have many different genetic aetiologies. Both of these conditions are reported in patients with expanded polyalanine tract mutations in *ARX* (Shoubridge *et al.*, 2010, Marques *et al.*, 2015). Closer examination of the clinical spectrum in patients with *ARX* mutations in the first polyalanine tract (100% of who had seizures), indicates that developmental delay is reported in 25% of cases. The onset of seizures spanning from 0 to 18 months of age (median 4 months). Furthermore, only 26% of individuals with expansions of the second polyalanine tract exhibit seizures, despite 100% of these patients having intellectual disability (Jackson *et al.*, 2017). Our findings on the broader behavioural phenotypes of PA1 and PA2 mice support the idea that the mechanisms underlying the cognitive deficits in PA patients are complex.

3.5.5 Estradiol and cognition and behaviour

In this study we demonstrated that estradiol did not improve behavioural and cognitive outcomes in PA1 or PA2 mice. Studies predict that estradiol exerts pro-cognitive effects through two mechanisms; by enhancing synaptic plasticity, and inducing long-term potentiation of NMDA receptors (Gould *et al.*, 1990, Woolley and McEwen, 1992, Woolley and McEwen, 1994, Smith *et al.*, 2016). However, to this date, no studies have shown an effect on intellectual disability with estrogen. In fact, many studies on the cognitive effects of estradiol are focused on the complete abolition of estrogens by ovariectomy in female mice. When menopause is induced in female mice, spatial memory performance in the Y-maze is impaired. Long-term estradiol treatment then recovered this cognitive deficit (Schroeder *et al.*, 2017). In a surgical menopause rat model, seven months of estradiol treatment also had benefits to spatial memory (Koebele *et al.*, 2020). These studies however are difficult to compare to our experiments, as they show that a baseline level of estrogen in female rodents is key to normal cognition, rather than supplementing the existing estrogens in the brain with a lower dose such as the 40ng/g given to our PA mutant mice.

In general, few studies have been conducted on the effects of estradiol treatment in non-ovarectomised, female rodent models. Estradiol treatment has been explored in an induced Alzheimer's disease model, where estradiol given in the early stages of pathogenesis ameliorated memory impairment (tested using the Morris water maze) and restored numbers of depleted hippocampal neurons (Zheng *et al.*, 2017). This treatment was given over a 60 day period in a continuous release pellet. A further study investigated the effects of knocking out estrogen receptor β (ER β) in the nervous system, on behaviour in male mice. ER β abolition resulted in decreased social interaction and aggressive behaviour, as well as increased locomotor activity (Dombret *et al.*, 2020).

Estradiol, 17 β -estradiol in particular, has been shown to have strong anti-inflammatory action in the brain, by stimulating a non-genomic, signalling cascade that inhibits the translocation of the nuclear factor kappa (NF- κ B) transcription factor, which activates inflammatory genes (Ghisletti *et al.*, 2005). This might indicate that any effects estradiol is having on cognition in inflammatory diseases such as Alzheimer's disease, is possibly due to its anti-inflammatory properties. Estradiol has been shown to have positive influences in other inflammatory neurological diseases, such as Parkinson's disease, schizophrenia and multiple sclerosis (Pozzi *et al.*, 2006). We did not see any effects of estradiol treatment on social, memory or locomotor outcomes in our cohort. The phenotype of *Arx* mutations are not associated with an increase of inflammation in the brain. This could be the reason for estradiol not eliciting positive effects on behavioural deficits in our models. When considering these studies, it is also possible that in our study, estradiol was not given for a long enough duration of time for behavioural effects to become apparent, or at a high enough dose to improve behavioural deficits. The behavioural deficits in PA mutant mice, particularly in social interaction, may also be too severe to expect an improvement with short term estradiol treatment. The mechanisms behind estradiol and cognition in male mice, remain unclear, and requires further investigation.

3.5.6 Reproducibility of behaviour testing outcomes

We have previously demonstrated a memory deficit in the Barnes maze and the Y-maze in untreated PA mutant mice (Jackson *et al.*, 2017). However, in this study, we did not detect any differences between PA1 and PA2 mice and their WT counterparts in either of these behavioural tests. This could be due to a number of reasons for each test.

The limited sample size of mice reaching the age required to perform the Barnes maze (two months of age), due to the mortality of more severely affected animals meant that many were dead prior to the two month time point. This may have resulted in a less robust result from this study compared to Jackson *et al.* (2017). Untreated PA mutant mice also have a severe

phenotype and many die before reaching behaviour testing milestones. In the current work, due to the intensive injection protocol in early postnatal life, this limited the number of mice able to be tested across different time points. However, numerous studies have examined the reproducibility and replicability of behaviour tests in rodents, and despite these two studies being performed on the same colonies of mice within the same laboratory, variations between studies from the same research groups have been documented before. In our case, it appeared that neither WT nor mutant mice seemed to exhibit “learning” in the Barnes maze. This is a potential caveat of this test as a measure of cognition in this model, and makes it difficult to determine any differences between genotypes in this instance.

Variability in the experimenter has been shown to have an effect on the outcomes of behavioural testing. This can include the experimenter’s stress levels or mood, and even body odour (Hånell and Marklund, 2014). Increased handling of animals over time, such as over the progression of a study, has also been shown to alter behavioural outcomes, as the mice become more accustomed to human handling (Hånell and Marklund, 2014). Nevertheless, for this study we performed testing across four separate cohorts at different times throughout the study to decrease any effects of situational factors such as stress and mood, and variability in the experimenter was kept to a minimum, ensuring the same colour clothing was worn, perfumes were not used, and handling was kept the same across all rounds of testing.

In a study by Crabbe *et al.*, identical mouse strains and a mutant mouse strain were tested simultaneously in three different laboratories (Crabbe *et al.*, 1999). They showed that despite their best efforts to keep laboratory environments the same, they found large effects at each site on behavioural variables. Six of eight behavioural measures had differing effects based on the site of the experiments (Crabbe *et al.*, 1999). Locomotor tests show robust replicability between different studies (Wahlsten *et al.*, 2006). Short-term anxiety tests on the other hand have been reported to be particularly susceptible to environmental factors, giving different outcomes in

behavioural phenotypes of mice (Hurst & West 2010). This may explain the different outcomes we observed between tests measuring anxiety-like behaviour in our study, with significant results seen in the open field test, but not the elevated zero maze for example. Tests of spontaneous behaviour, such as the three-chambered sociability tests, can be considered more robust than tests that use hunger or fear as a motivator however, as these tests reduce the stress on the animal. All tests used in our study use spontaneous behaviour, with the exception of an overhead light which causes the animals to want to “hide” during the open field and elevated zero maze.

Despite the variation we observe between the current study and the previous study on untreated mice by Jackson and colleagues (2017), all variables were maintained as constant as possible in these experiments, shown by reduced variability between individual rounds of behavioural testing, indicating that differences between these studies may be due to laboratory factors, or potential small genetic differences in the inbred mouse strain, including short DNA repeat sequences or copy number variations, which can impact gene expression and hence mouse behaviour (Lathé, 2004). It can be argued that having some level of variation between behavioural studies is important for improving the validity of behaviour research, as this mimics the “real” world more than an extremely controlled behavioural testing environment.

3.5.7 Side effects of estradiol treatment

During this study, the systemic effects of estradiol on infant male mice, even though given at a relatively low dose for a short period of time, were considered. Testes were weighed at postnatal day 70 upon euthanasia, and we observed no difference in weight in WT or PA mutant mice when treated with estradiol. There was also no impact to testes descent (physically observed) in treated mice. We observed no difference in body weight, including no “rescue” of the small body weight of PA mutants compared to their WT littermates. This was considered interesting given the weight gain and arrested testes descent in the Chachua *et al.* study in 2016, where the same dose of estradiol was given to an induced infantile spasms rat model. It is likely that our *Arx* mutant mouse models and the induced seizure model have different underlying pathogenesis and hence a different response to estradiol treatment. The weight difference between PA1 and PA2 mutant mice is significant and has been reported previously and may be too large to be rescued to WT baseline weight with a short dose of estradiol treatment. Long-term seizures over the duration of the PA mouse’s lifetime may also be impacting their decreased body weight.

3.6 Study outcomes

In this study we provide evidence to begin understanding the relationship between seizures and cognitive and behavioural deficits in a genetic model of a neurodevelopmental disorder. We demonstrated that behavioural and cognitive outcomes did not improve in the *Arx* PA mutant mice, despite significant alleviation of the frequency and severity of seizures achieved with early, postnatal estradiol intervention. Behavioural deficits were already present prior to the peak onset of seizures in these mice, and did not appear to regress with seizures, providing evidence for separating the impact of seizures upon behavioural deficits in *Arx* expanded polyalanine tract mutant mice. Furthermore, we provide reproducible outcomes of seizure alleviation in a different PA1 mouse model, as well as the more frequent mutation seen in human patients, PA2. Reproducible outcomes are key for finding novel therapies for disorders, particularly those with a lack of effective treatments for intellectual disability, behavioural impairments and early onset seizures, which remain a therapeutic challenge. This study highlights the need to elucidate molecular mechanisms of the intellectual disability phenotype, as necessary first steps towards a treatment for neurodevelopmental disorders, as the multiple comorbidities often present in these patients, remain a significant clinical challenge.

Chapter Four:

The deregulated transcriptome in PA1 and PA2

***Arx* mutant mice is not restored by early
postnatal 17 β -estradiol treatment.**

Publications and presentations from this work:

Publications

Loring, K.E., Lee, K., Mattiske, T., Zysk, A., Jackson, M.R., Noebels, J.L. and Shoubridge, C. (2020) “17- β estradiol reduces seizures but does not improve abnormal behaviour in mice with expanded polyalanine tracts in the *Aristaless*-related homeobox gene (*ARX*).”

Manuscript is Appendix 1. Submitted to Neurobiology of Disease.

Conferences

Loring, K.E., Lee, K., Mattiske, T., Zysk, A., Jackson, M.R. and Shoubridge, C. “Can estradiol improve phenotypic outcomes in mice with mutations in *Arx*?”

Presented as an oral presentation at the following conferences:

Japanese Neuroscience Society Annual Meeting (2019), Niigata, Japan.

Australian Neuroscience Society Annual Meeting (2018), Adelaide, SA.

Presented as a poster at the following conferences:

Australian Neuroscience Society Annual Meeting (2018), Adelaide, SA.

Florey Conference at the University of Adelaide (2018), Adelaide, SA.

4.1 Abstract

ARX is a transcription factor, which is key to the development and migration of neurons in the developing brain. *Arx* PA mutant mice have deregulated transcriptome profiles in embryonic development. It remains unclear to what extent the transcriptome at postnatal day 10 would remain deregulated from the downstream effects of a partial loss of *Arx* expression early in development. Further, the impact of early postnatal treatment with estradiol would have on the transcriptome of PA1 and PA2 mutant mice remains to be elucidated. At postnatal day 10, following completion of seven days of daily delivery of 17 β -estradiol or vehicle treatment, RNAseq identified 129 genes significantly deregulated (Log₂FC $>\pm 0.5$, P-value <0.05) in the frontal cortex of mutant compared to wild-type mice. When comparing genes deregulated in PA mutant mice to wild-type littermates, these were particularly enriched for known genes in neurodevelopmental disorders and those involved in signalling and developmental pathways. Following completion of seven days of daily delivery of 17 β -estradiol, mutant mice had 295 significantly deregulated genes, with only 23 deregulated genes overlapping between vehicle and estradiol treated mutant mice. Estradiol treatment did not “restore” deficits due to the loss of function of *Arx*, but instead acted through a different mechanism to reduce seizure frequency and severity in PA1 and PA2 mice. Many of the genes estradiol treatment deregulated were *Arx* responsive genes, and neurodevelopmental disorder associated genes. We conclude that 17 β -estradiol treatment recruits processes and pathways to reduce the frequency and severity of seizures in the *Arx* PA mutant mice but does not precisely correct the deregulated transcriptome nor improve mortality or behavioural and cognitive deficits.

4.2 Introduction

The *Aristaless*-related homeobox gene (*ARX*) [NM_139058.2] (MIM#300382) is known to play an important role in the migration and differentiation of inhibitory and excitatory neurons, particularly interneurons (Miura *et al.*, 1997, Kitamura *et al.*, 2002, Kitamura *et al.*, 2009, Lee *et al.*, 2014). *ARX* encodes a transcription factor, and regulates the migration of interneurons through regulation of gene expression during neurodevelopment. *Arx* is highly expressed in the developing (embryonic) brain during cellular proliferation and the first wave of neuron migration from the ganglionic eminence to the developing cortex (Colombo *et al.*, 2007, Friocourt *et al.*, 2008, Colasante *et al.*, 2009, Lee *et al.*, 2014). Although few studies have investigated *ARX* expression in human patients, one study of *ARX* in patients with expansion mutations of the second polyalanine tracts found that there was very strong expression of *ARX* in neuronal progenitor cells of the cortex in the second trimester brain during foetal development (Curie *et al.*, 2018).

Given the embryonic expression pattern of *Arx*, previous investigations focused on disruption of the transcriptome in forebrain of PA mutant mice at embryonic day 12.5 (Mattiske *et al.*, 2016). Mattiske *et al.* (2016) found 852 genes deregulated in PA1 mice, and 78 in PA2 mice, in the developing telencephalon. These genes were enriched in pathways involved in key neurodevelopmental processes, such as neuron development, cell adhesion, and neuronal membranes. Deregulated genes were also found to be strongly associated with causative genes for neurodevelopmental disorders, including intellectual disability, autism and epilepsy, such as *Twist1* and *Hdac4*. Other *Arx* deficient mouse models demonstrate an impact on many critical neurodevelopment genes in the key brain regions involved in neuron migration, including other neuronal transcription factors such as *Ebf1* (Colasante *et al.*, 2009). Our laboratory has also demonstrated that there was a delayed migration of calbindin-positive interneurons in the cortex of newborn PA mice (Lee *et al.*, 2017). These studies in *Arx* mouse models show that disruption of *Arx*'s transcriptional regulation activity disrupts critical stages of brain development,

particularly in inhibitory interneurons, leading to an imbalance of excitation in the cortex, and the subsequent phenotypes of patients and mice.

The preclinical trial in the Price *et al.* *Arx* PA1 mouse model, utilising short-term 17 β -estradiol (E2) given daily in the first postnatal week, alleviated the severe seizure phenotype for an extended period, through to adulthood in male mice (Price *et al.*, 2009, Olivetti *et al.*, 2014). Estradiol can induce long-term changes in gene expression in the brain via activation of estrogen receptors and non-receptor pathways. 17 β -estradiol treatment of PA1 mice partially restored the interneuron migration deficits in the neocortex, increased populations of neuropeptide-Y and calbindin positive interneurons, and impacted the expression of several genes normally regulated by *Arx* (Olivetti *et al.*, 2014). Interestingly, 17 β -estradiol also changed the expression of genes normally regulated by *Arx*. *Arx* represses *Ebf3*, *Lmo1* and *Shox2* and activates *Lhx7*, *Cxcr4*, *Cxcr7* and *Lgil* in interneurons (Colasante *et al.*, 2008, Mattiske *et al.*, 2016). Gene expression analysis (quantitative real-time PCR) in the brains of mutant mice treated with E2, showed that *Shox2* expression was decreased, *Lgil* expression was up regulated, and *Ebf3* expression was repressed (Olivetti *et al.*, 2014). E2 is known to have strong transcriptional behaviour in the central nervous system, with signalling mediated by classical estrogen receptors, ER α and ER β , in the nucleus, cell membrane and cytoplasm, as well as ER-independent signalling mechanisms (Azcoitia *et al.*, 2019). These signalling pathways regulate transcriptional activity in neurons and glial cells (McCarthy, 2008, Azcoitia *et al.*, 2019). The findings of this study provide evidence to support the notion of exogenous steroids such as estradiol as potential treatment options for infantile spasms and epilepsy. However, potential mechanisms of action need to be determined. Exploring how estradiol acts in the brain to alleviate seizures may also illuminate the pathogenesis of *Arx* mutations in the mouse brain.

The aim of the current study was to generate an unbiased map of mRNA expression changes in the cortical transcriptome at P10 due to *Arx* PA mutations. We first analysed genome wide transcriptomic changes using RNA sequencing in the neocortex of PA1 and PA2 mutant mice compared to their wild-type littermates. This was to establish the impact of these *Arx* mutations on gene expression in the brain at postnatal day 10. Building on this, we investigated the effects of seven days of E2 treatment (postnatal days 3-10) on the transcriptome of the neocortex of PA mutant mice at postnatal day 10. Here our comparison was between mutant mice treated with either E2 or a vehicle. This strategy was adopted to elucidate the molecular mechanisms driving the seizures and intellectual disability due to *Arx* PA mutations, persisting in early postnatal life, and to address if E2 would “repair” the dysregulated transcriptome, or recruit new pathways, diminish the frequency of seizures in these mice.

4.3 Results

4.3.1 PA1 and PA2 mice have a deregulated cortical transcriptome at postnatal day 10.

To capture the molecular disruptions that persist in early postnatal life contributing to *Arx* associated clinical phenotypes, we undertook transcriptome wide RNA sequencing from brains of mice at postnatal day 10. The first consideration was what I will term “genes changed by disease”, with mutant mice being compared to wild-type (WT) littermates. Compared to age-matched, vehicle treated WT mice (n = 6), analysis of PA1 mice (n = 4) revealed 63 genes deregulated by Log₂ fold change greater than ± 0.5 with a *p*-value of less than 0.05. The majority (65%) of these genes were found at a decreased level of expression compared to WT (Table 4.1). PA2 mice (n = 4) demonstrated 80 genes deregulated using the same fold cut-off, with 46% of genes having decreased expression when compared to WT mice (Table 4.1). These gene lists are outlined in Appendix 4.

Given the highly similar neurological phenotypes between the PA1 and PA2 mice coupled with similar reductions in *Arx* protein abundance (Jackson *et al.*, 2017) and the similar responses to estradiol treatment observed in our current study we chose to also analyse the gene expression data combining the four males from each of the PA1 and PA2 mice as a single mutant group (PA^{pool}). This analysis indicates 58 genes are deregulated using the same fold cut-off, with 62% demonstrating a decreased level of expression compared to the pooled WT controls (Table 4.1). Prior to gene enrichment analysis, we chose twelve genes for biological validation of our RNA sequencing approach by gold standard quantitative real-time PCR (qRT-PCR), on a different set of mouse cortical samples to those used for RNA sequencing analysis. Of these genes, 100% (12/12) validated in PA1 mice, and 60% (7/12) validated in PA2 mice (Appendix 5).

Table 4.1: Number of genes deregulated by disease in PA1, PA2 and PA^{pool} mice compared to wild-type littermates.

Genes deregulated by disease			
	PA1	PA2	PA^{pool}
vs WT	63	80	58
↑	22 (35%)	43 (54%)	22 (38%)
↓	41 (65%)	37 (46%)	36 (62%)

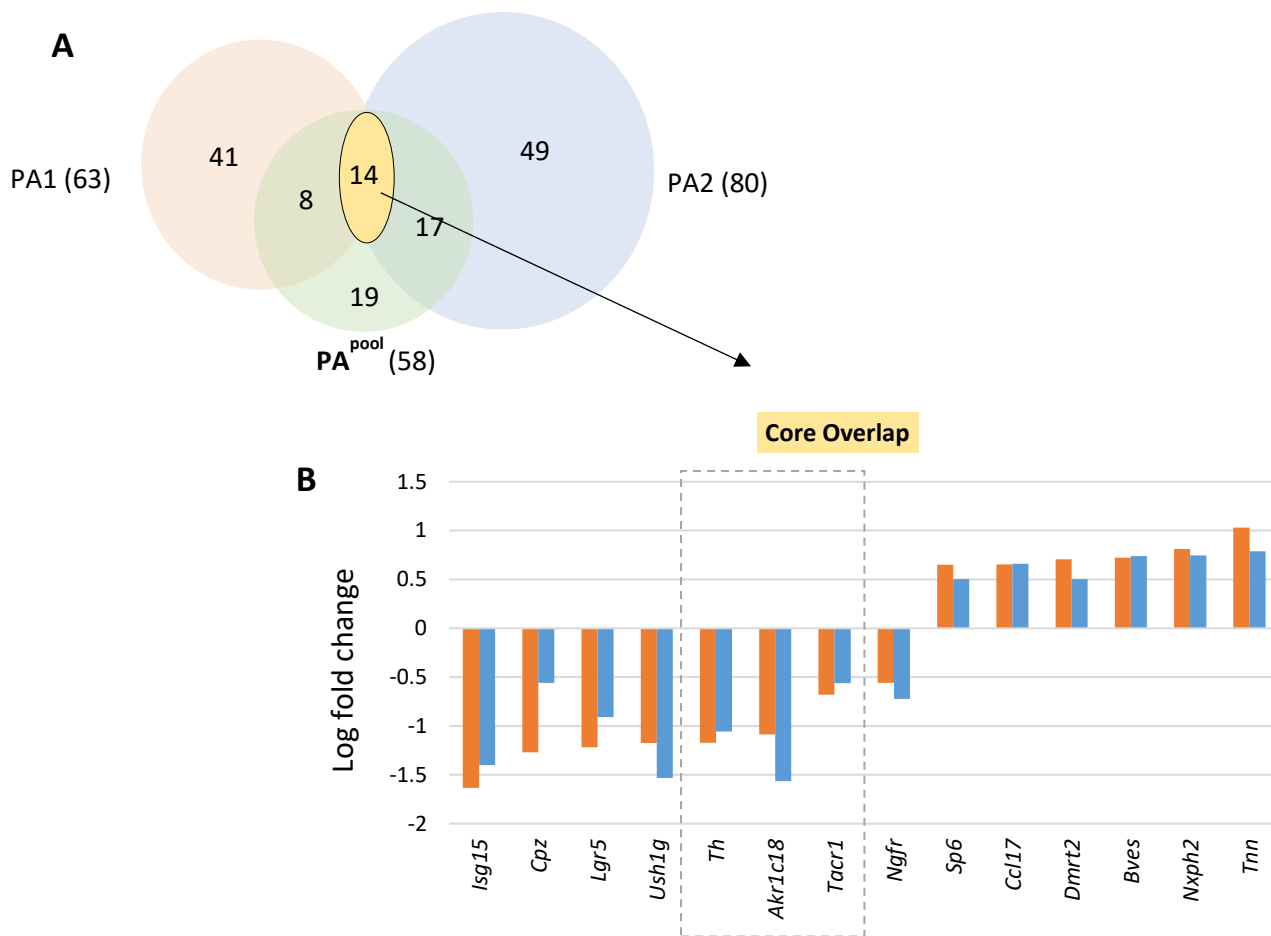


Figure 4.1: Overlapping genes deregulated in PA1 and PA2 mutant mice with disease. (A) Venn diagram displaying overlap of deregulated genes in PA1 (orange), PA2 (blue) and PA^{pool} (green) groups, as well as core overlapping genes (yellow). (B) Graph showing log fold change values of genes from the core overlap lists in (A). Key interneuron genes are highlighted in the dashed box in (B).

There were only fourteen genes deregulated that overlapped in both mutant mice. This equated to 22% and 18% of genes deregulated in PA1 and PA2 mice respectively (Figure 4.1 A). Of this core overlap group, 57% (8/14) of genes were decreased in expression (Figure 4.1 B). On examination, three of the downregulated genes in this core overlap group, *Th*, *Tacr1* and *Akr1c18*, are highly associated with interneuron development and function (Figure 4.1 B). Interestingly, the genes in the core overlap group repressed due to disease have a larger change in expression (log fold change) than genes with increased expression in this group.

To better understand the profile of genes deregulated by disease at P10, we identified enriched genes by comparing deregulated genes in PA1, PA2 and PA^{pool} to relevant gene lists (Appendix 6). To do this, we sought to determine the number of known neurodevelopmental disease associated genes, Arx responsive genes and interneuron associated genes enriched in our data set, to investigate the functions of the gene expression that was deregulated with PA mutations.

Arx target and responsive genes (that were identified in Mattiske *et al.* 2016), were significantly enriched in the list of deregulated genes in the PA^{pool} group (10/58, 17% $p < 1.288e^{-5}$), and in each of the PA1 (13/63, 21%, $p < 7.366e^{-8}$) and PA2 groups (9/80, 11%, $p < 9.641e^{-4}$) (Table 4.2). Genes known to be associated with autism and intellectual disability (Gene Dx Xpanded Panel (GeneDx, 2020)) were significantly enriched in the PA^{pool} group (5/58, 12%, $p < 0.001$), as well as in the PA2 group (7/80, 11%, $p < 0.0004067$) (Table 4.2). Known epilepsy genes (from colleagues in the Neurogenetics Research Program/Professor Jozef Gecz) were not significantly enriched in any group of genes deregulated by disease (PA1; 2/63, 3%, $p < 0.100$; PA2; 2/80, 2%, $p < 0.343$; PA^{pool}; 3/58, 5%, $p < 0.058$) (Table 4.2). Furthermore, we found that genes containing high-affinity estrogen response elements (EREs) were significantly enriched in the PA1 group (13/63, 21%, $p < 0.013$) and the PA^{pool} group (11/58, 19%, $p < 0.038$).

Genes associated with inhibitory neuron regulation or development (in house curated reference list) were also significantly enriched in the PA^{pool} group (10/58, 17%, $p < 6.957e-16$), as well as in the PA1 (5/63, 8%, $p < 8.197e-7$) and PA2 groups (8/80, 10%, $p < 5.649e-8$) (Table 4.2). Interestingly, the majority of these enriched interneuron genes were downregulated in their expression for all three genotypes (PA1, PA2 and PA^{pool}) (11/13, 84.6%) (Figure 4.2). These included *Th* and *Tacr1*, associated with somatostatin positive interneurons, *Akr1c18*, associated with the function and development of parvalbumin interneurons, and *Chat*, which plays a key role in cholinergic interneurons. We contend that reduced expression of these inhibitory neuron genes, as well as the genes associated with autism and intellectual disability, are likely contributing to the seizure and cognitive phenotype of the PA mice.

Table 4.2: Neurodevelopmental disorder and key brain development genes deregulated by disease in PA1, PA2, PA^{pool} and core overlap gene lists.

Neurodevelopmental disorder genes deregulated by disease				
	Core Overlap	PA1	PA2	PA ^{pool}
Autism/ ID	<i>Cpz, Th</i>	6% <i>Dnah11, Enpp1</i>	11%* <i>Chat, Chrna2, Lrp2, Ntrk1, Prima1, Slc5a7, Sp7</i>	12%* <i>Chat, Chrna2, Msx1, Ntrk1, Sp7</i>
Epilepsy		3% <i>Col3a1, Npy</i>	2% <i>Chrna2, Lrp2</i>	5% <i>Chrna2, Cyp27a1, Msx2</i>
ARX target genes	<i>Isg15, Th</i>	21%* <i>4932411E22Rik, Ankfh1, Fam124b, Fau, Gprin2, Isg15, Lmo1, Npy, Pde3a, Rsg1, Syt15, Th, Thbs4</i>	11%* <i>1700007G11Rik, Ccdc60, Crabp1, Fam183b, Isg15, Lrp2, Meis1, Myh8, Th</i>	17%* <i>Crabp1, Fosb, Frmd7, Gpnmb, Isg15, Mafa, Myh8, Th, Thbs4</i>
Interneuron genes	<i>Akr1c18, Tacr1, Th</i>	8%* <i>Akr1c18, Npy, Pdlim3, Tacr1, Th</i>	10%* <i>Akr1c18, Chat, Chrna2, Col14a1, Myh8, Slc18a3, Tacr1, Th</i>	17%* <i>Akr1c18, Chat, Chrna2, Fosb, Frmd7, Myh8, Pdlim3, Spp1, Tacr1, Th</i>

* indicates significant enrichment of genes

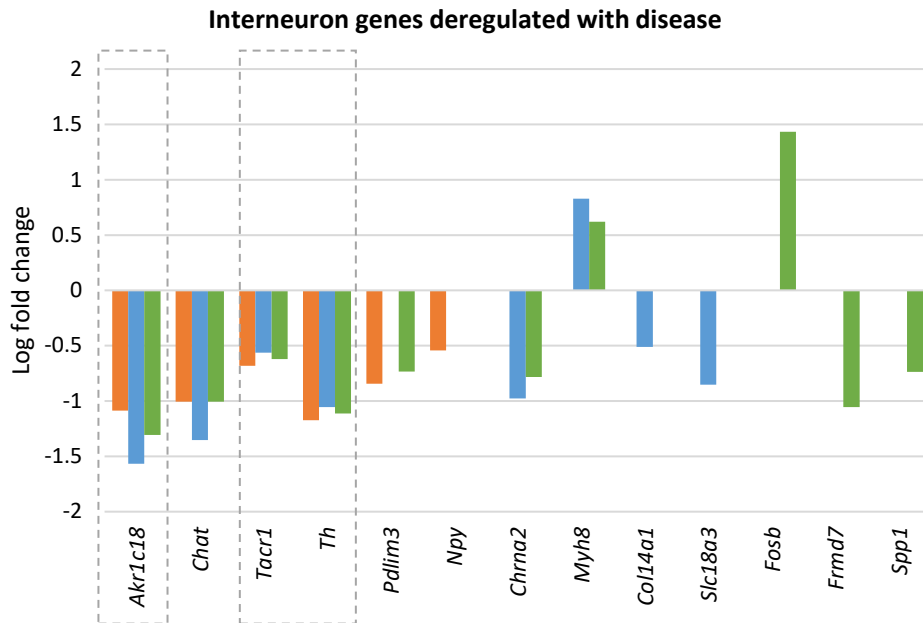


Figure 4.2: Genes associated with interneurons are downregulated in PA1 and PA2 mutant mice. Graph showing log fold change values of genes from enriched interneuron genes. Genes from core overlap group are in the dashed box.

To extend our consideration of the profile of genes deregulated by PA mutants in early postnatal life, we used the Database for Annotation, Visualisation and Integrated Discovery (DAVID) to analyse pathways and ontology terms enriched within disease-deregulated transcriptomes. Enrichment clusters were ranked by enrichment score, with two clusters overlapping between PA1 and PA2 mice: glycoproteins and glycoprotein receptors (Figure 4.3). Other enriched functions of note were PI3K-Akt signalling, neurotransmitter biosynthesis, and synaptic processes (Figure 4.3). Many of the clusters are associated with brain and neuron development or signalling that when disrupted may be predicted to contribute to the phenotypic features of the PA mutant mice.

To identify specifically enriched pathways populated by genes deregulated by disease, we used the PANTHER (Protein Analysis Through Evolutionary Relationships) Classification System. This database allowed us to rank pathways using the p-value calculated by PANTHER following the input of lists of deregulated genes. Outcomes were reported as the overlap of genes in our data, out of the total number of genes involved in that process (Table 4.3). In the PA^{pool} group, six pathways were found to be significant using this tool. Of interest were the nicotinic acetylcholine receptor signalling pathway (neuroprotective), the JAK/STAT signalling pathway (regulation of cell division and apoptosis), and the 5HT receptor mediated pathway (mediating excitatory and inhibitory neurotransmission) (Table 4.3). The JAK/STAT pathway was also enriched in genes deregulated in the PA1 mice, and the nicotinic acetylcholine receptor signalling pathway was enriched in genes deregulated in PA2 mice (Table 4.3).

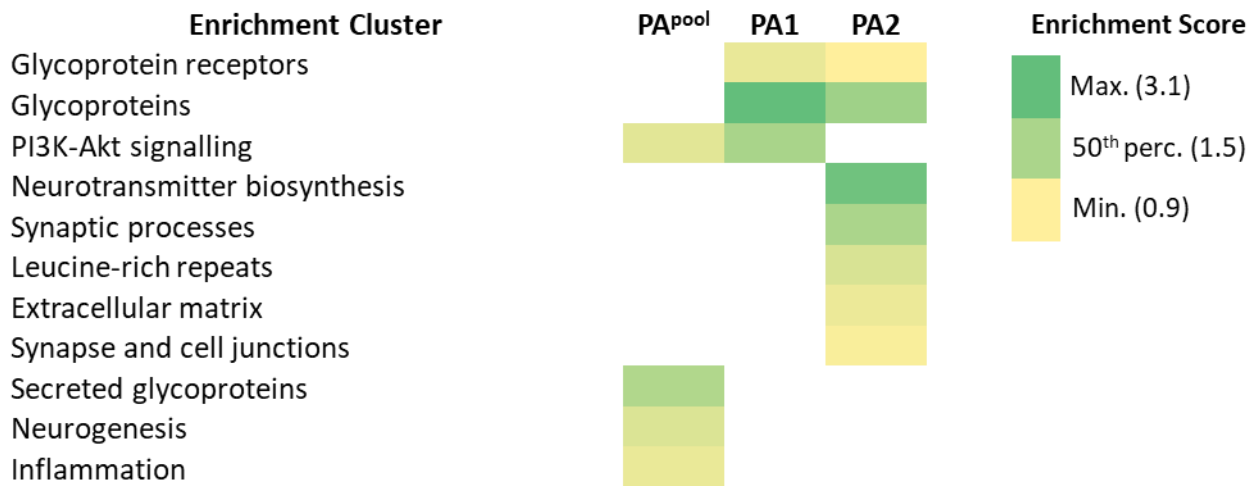


Figure 4.3: Enrichment analysis of genes deregulated by disease in PA mutant mice. Heat map showing significant gene enrichment terms in deregulated genes in PA1, PA2 and PApool groups from DAVID cluster annotation analysis. Clusters with enrichment scores of <0.9 are not shown. Heat map is based on maximum, minimum and 50th percentile score in data set (legend in figure).

Table 4.3: Pathways enriched through PANTHER analysis in PA^{pool} (green), PA1 (orange) and PA2 (blue) mice.

Term	Overlap	P-value	Genes
Nicotinic acetylcholine receptor signalling pathway	3/68	0.00101467	<i>Chrna2, Chat, Myh8</i>
Vitamin D metabolism and pathway	1/8	0.0229697	<i>Cyp27a1</i>
JAK/STAT signalling pathway	1/14	0.03985599	<i>Socs1</i>
Plasminogen activating cascade	1/15	0.04264235	<i>Plaur</i>
5HT3 type receptor mediated signalling pathway	1/16	0.04542077	<i>Slc6a4</i>
5HT4 type receptor mediated signalling pathway	1/16	0.04542077	<i>Slc6a4</i>
Blood coagulation	2/38	0.006381749	<i>Procr, Plaur</i>
Apoptosis signalling pathway	2/102	0.041129164	<i>Tnfsf10, Atf3</i>
JAK/STAT signalling pathway	1/14	0.043221871	<i>Stat5a</i>
Plasminogen activating cascade	1/15	0.046237826	<i>Plaur</i>
Nicotinic acetylcholine receptor signalling pathway	5/68	7.72E-06	<i>Slc5a7, Chrna2, Chat, Myh8, Slc18a3</i>
Muscarinic acetylcholine receptor 2 and 4 signalling pathway	3/39	5.08E-04	<i>Slc5a7, Chat, Slc18a3</i>
Muscarinic acetylcholine receptor 1 and 3 signalling pathway	3/42	6.32E-04	<i>Slc5a7, Chat, Slc18a3</i>

4.3.2 Estradiol treatment targets genes outside of the deregulated transcriptome of PA1 and PA2 mutant mice.

To investigate the impact of estradiol treatment at the transcriptome level, we first analysed WT mice treated with vehicle compared to WT mice treated with estradiol. There were 56 genes deregulated by Log₂ fold change greater than ± 0.5 with a p-value of less than 0.05 in the WT cohort when treated with estradiol (Table 4.4). Genes deregulated in the WT mice estradiol treatment group that overlapped with the PA mutant groups were removed from subsequent analysis of PA1, PA2 and PA^{pool} groups (Appendix 7). This included only four genes in PA1 and two genes in each of PA2 and PA^{pool} that overlapped with WT mice.

The aim of this experiment was to determine the impact of estradiol treatment on PA mutant mice, by comparing them to their vehicle treated PA mutant counterparts. Analysis of PA1 mice with estradiol treatment compared to PA1 mice treated with vehicle resulted in 124 genes deregulated by Log₂ fold change greater than ± 0.5 with a p-value of less than 0.05 (Table 4.6). The majority (75%) of genes were found to have increased levels of expression compared to vehicle treated PA1 mice (Table 4.4). This was in contrast to the smaller response of genes with increased expression due to genotype alone (PA1 mice compared to WT (35% upregulated)). PA2 mice treated with estradiol treatment compared to PA2 mice treated with vehicle, resulted in 158 genes deregulated at the same cut off values (Table 4.4). Estradiol treated PA2 mice, in contrast to PA1 mice, showed a larger proportion of genes with decreased levels of expression (77%). Again, this differed to the response of gene expression of disease changed genes (PA2 versus WT mice) having increased or decreased expression (54% versus 46%, respectively). In the estradiol treated PA^{pool} mice there were 55 genes deregulated by the same cut off, with 64% having increased expression (Table 4.4). Genes changed with estradiol treatment are listed in Appendix 8.

We randomly chose nine genes for the validation of our RNA sequencing data, using gold standard quantitative real-time PCR. For this biological validation, we used a different set of mouse cortical samples than those used for RNAseq analysis, with 44% (4/9), 22% (2/9) and 56% (5/9) validating in PA1, PA2 and PA^{pool} mice respectively (Appendix 9).

Table 4.4: Number of genes deregulated by estradiol treatment and those containing estrogen response elements (EREs) in PA1, PA2 and PA^{pool} mice compared to wild-type littermates.

Genes deregulated by E2 treatment				
	WT	PA1	PA2	PA^{pool}
vs VEH	56	124	158	53
↑	27 (48%)	93 (75%)	36 (23%)	33 (62%)
↓	29 (52%)	31 (25%)	122 (77%)	20 (38%)
ERE	12 (21%)*	22 (18%)*	22 (15%)	8 (15%)

*** indicates significant enrichment of genes containing estrogen response elements (ERE)**

We next determined if the profile of genes deregulated by estradiol treatment were enriched for genes containing estrogen response elements (EREs). To achieve this, I compared genes changed with treatment to a list of mouse genes containing high-affinity mouse EREs (Bourdeau *et al.*, 2004). ERE-containing genes were significantly enriched in the WT gene list (12/56, 21%, $p < 0.012$) and in PA1 mice treated with estradiol (22/124, 18%, $p < 0.010$) but not in PA^{pool} (8/53, 15%, $p < 0.190$) or PA2 mice (22/158, 15%, $p < 0.106$) (Table 4.4).

The number of genes with altered expression in response to estradiol treatment in PA1 and PA2 mice was much larger in comparison to genes deregulated by the *Arx* mutations alone. Moreover, there was very little overlap (Figure 4.4). Genes deregulated by estradiol treatment were quite different between genotypes, with only small numbers of overlapping genes (8 genes in PA1 mice, 12 genes in PA2 mice and 3 in PA^{pool}) (Figure 4.4). Interestingly, all of the genes deregulated by disease that were also changed with estradiol treatment were deregulated in the opposite direction with treatment (Figure 4.5). When we analysed the proportion of genes deregulated by estradiol in all three mutant groups (PA1, PA2 and PA^{pool}), the response to estradiol treatment between these three groups was strikingly different. Only 11 genes overlapped between the PA1 and PA2 estradiol response (Figure 4.6).

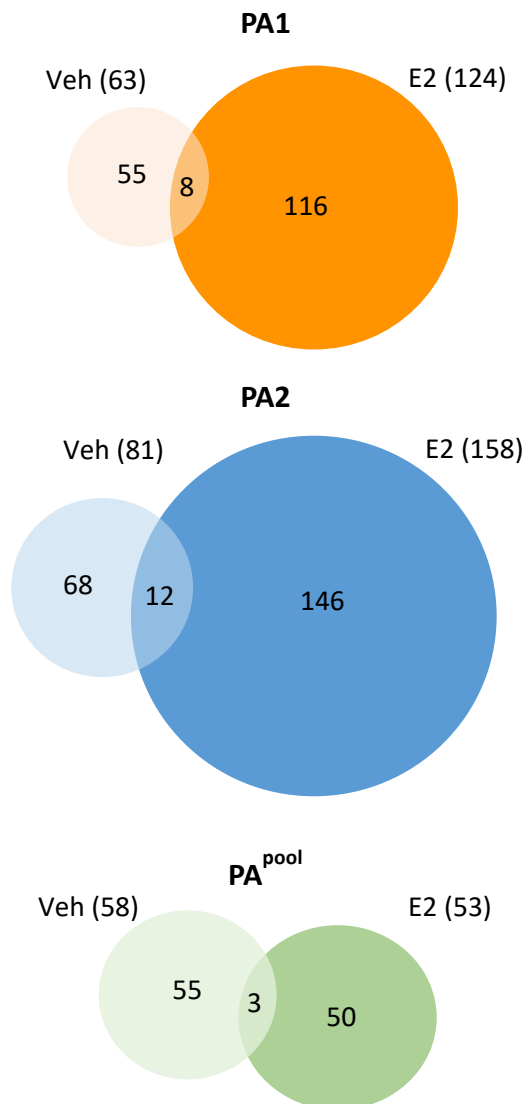


Figure 4.4: Overlapping response between the disease deregulated transcriptome and the estradiol deregulated transcriptome of PA mutant mice. Venn diagram showing genes overlapping between the disease-deregulated transcriptome and the estradiol-treated transcriptome of PA1, PA2 and PA^{pool} mice.

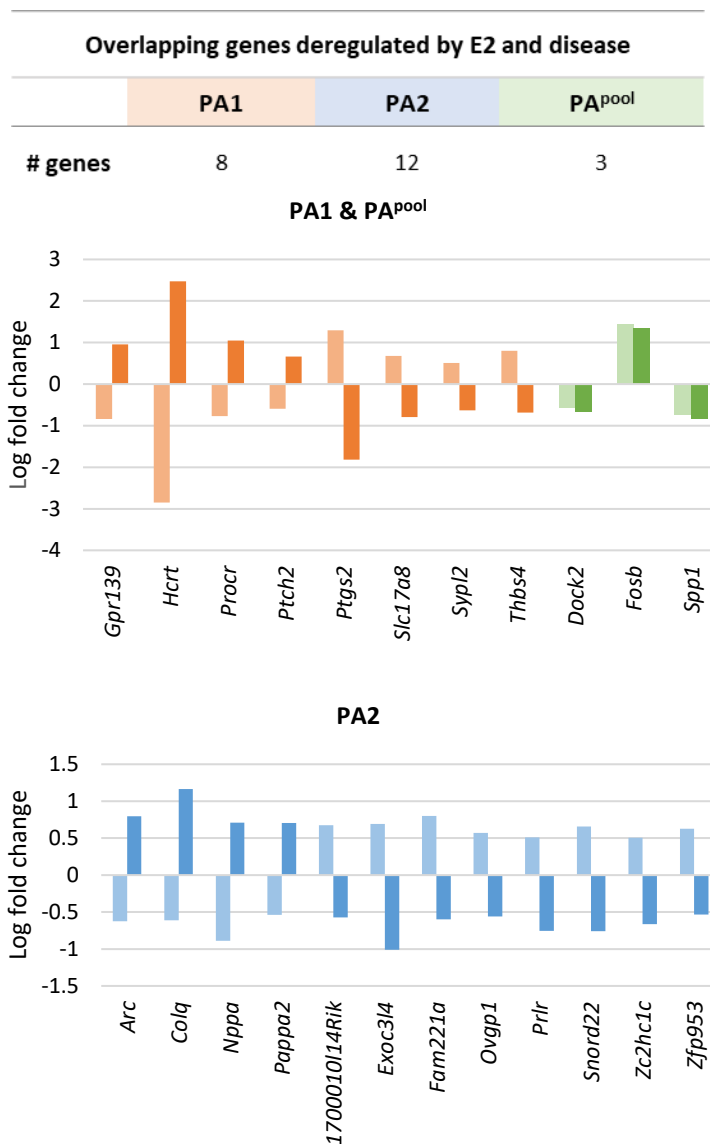


Figure 4.5: Estradiol treatment reverses the expression of genes deregulated by disease in PA mutant mice. Table gives numbers of overlapping genes between disease and estradiol deregulated transcriptomes of PA mutant mice. Graphs showing the direction of deregulation between genes overlapping between disease (light bars) and estradiol (dark bars) changed genes in PA1, PA2 and PA^{pool}, shown by log fold change values of genes.

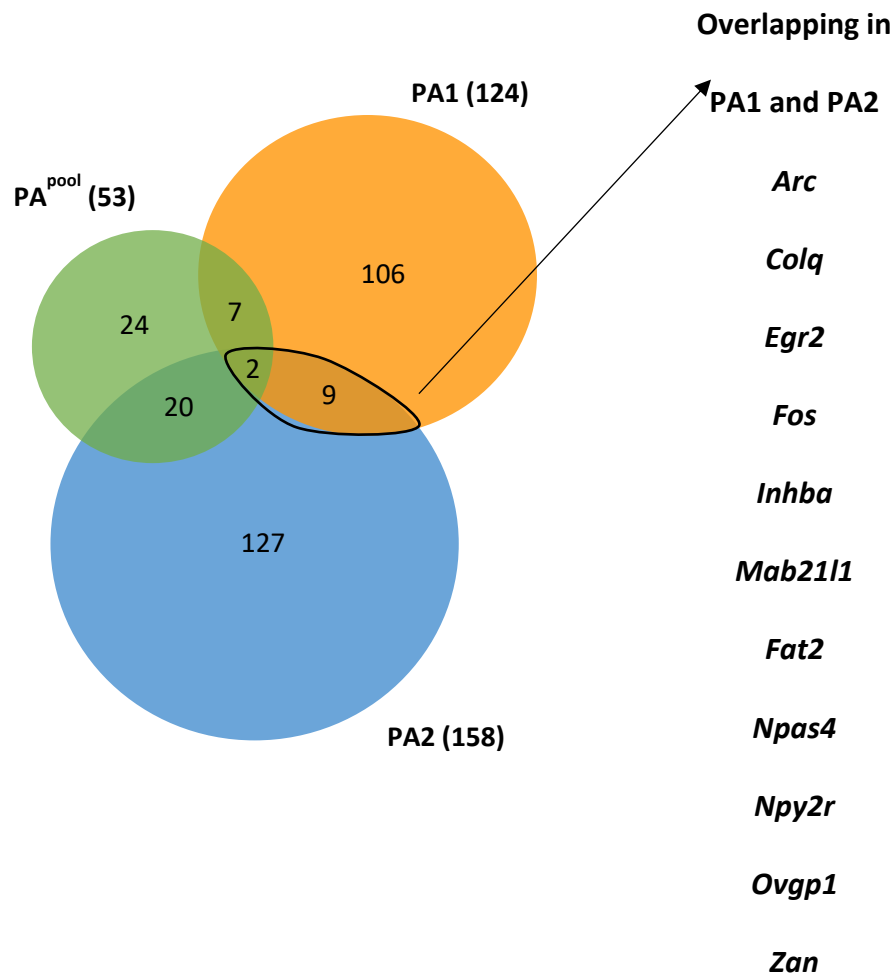


Figure 4.6: Comparison of response size to estradiol treatment in PA mice. Venn diagram displaying overlapping genes between the estradiol treated transcriptomes of PA1 (orange), PA2 (blue) and PA^{pool} (green) mice. List of 11 genes overlapping between the PA1 and PA2 mutant mouse response to estradiol treatment.

Extending the data from genes deregulated by *Arx* mutations, both neurodevelopmental disorder and inhibitory neuron associated genes were enriched in the genes deregulated in estradiol treated mice. Genes associated with inhibitory neurons were significantly enriched in the list of genes deregulated with estradiol treatment (PA^{pool}; 6/55, 11%, $p < 8.962e^{-9}$; PA1; 7/128, 6%, $p < 6.424e^{-8}$; PA2; 9/161, 6%, $p < 6.609e^{-10}$) (Table 4.5). In contrast to the consistent downregulation of interneuron associated genes due to genotype alone, these genes were not trending in a particular direction with estradiol, with approximately equal proportions being increased or decreased in expression with treatment in PA mutant mice. Genes associated with autism and intellectual disability were significantly enriched in all groups treated with estradiol (PA^{pool}: 9/53, 13%, $p < 2.083e^{-5}$; PA1; 15/124, 10%, $p < 0.000003$; PA2; 10/158, 6%, $p < 0.016$) (Table 4.5). Epilepsy associated genes were enriched to a very low level, and variably depending upon the mutant group considered (PA1; 6/124, 5%, $P < 0.014$; PA^{pool}; 1/53, 2%, $p < 0.431$; PA2; 3/158, 2%, $P < 0.442$) (Table 4.5).

Analysis of deregulated genes that overlap with known *Arx* target and responsive genes (Mattiske *et al.*, 2016) showed these were also significantly enriched in genes deregulated by E2 treatment in all three genotype; PA^{pool} (12/53, 22%, $p < 1.215e^{-7}$), PA1 (15/124, 12%, $p < 1.404e^{-5}$) and PA2 (20/158, 12%, $p < 2.166e^{-7}$) (Table 4.5). Interestingly, there were no *Arx* responsive genes deregulated due to disease that were altered by estradiol treatment. This suggests that while estradiol treatment is impacting genes that are *Arx* targets, they are different to those that were initially affected by disease. Of note, *Twist1* was identified as being downregulated in estradiol changed genes in the PA^{pool} group. *Twist1* has also been identified as a key gene deregulated in the forebrain of PA1 and PA2 mutant mice at embryonic day 12.5. Dysregulation of the *Arx-Hdac4-Twist1* pathway was predicted to contribute to phenotypic outcomes, with *Twist1* thought to be a facilitator for a portion of genes deregulated in PA mutant mice (Mattiske *et al.*, 2016).

Table 4.5: Neurodevelopmental disorder and key brain development genes deregulated by estradiol in PA1, PA2 and PA^{pool}.

Neurodevelopmental disorder genes deregulated by E2			
	PA1	PA2	PA ^{pool}
	10%*	6%*	13%*
Autism/ID	<i>Bdnf, Cacna1h, Col1a1, Cpz, Dbh, Eln, Flna, Fos, Iyd, Med12, Nlrp3, Npas4, Pabpc4l, Traip, Unc13d</i>	<i>Clrn1, Ebf3, Fos, Gabrq, Hap1, Lhx1, Nkx2-1, Npas4, Sim1, Trhr</i>	<i>Col1a1, Cpz, Dbh, Ebf3, Lhx1, Nlrp3, Nr4a2, Shox2, Twist1</i>
	5%*	2%	2%
Epilepsy	<i>Bdnf, Cacna1h, Eln, Flna, Med12, Rbp4</i>	<i>Gata3, Magel2, Nod2</i>	<i>Gata3</i>
	12%*	12%*	22%*
Arx target genes	<i>Cckbr, Dcdc2b, Egr3, Fhod1, Fos, Fosb, Ggnbp1, Nox4, Nr3c2, Pdgfrl, Prox1, Slc2a9, Thbs4, Zfp69, Zkscan2</i>	<i>Calcr, Cox7a1, Crb1, Ebf3, Egfl6, Egr1, Fos, Gabrq, Gata3, Hap1, Hspb3, Lars2, Lhx5, Magel2, Meig1, Rn45s, Serpinb1b, Slc47a1, Tbx15, Ttc32</i>	<i>Ebf3, Fosb, Gata3, Ido1, Lhx5, Nr4a2, Serpinb1b, Shox2, Siglece, Twist1, Uncx, Upp2</i>
	6%*	6%*	11%*
Interneuron genes	<i>Bdnf, Cox6a2, Fosb, Mab211l, Npy2r, Nt5e, Spp1</i>	<i>Calca, Cbln4, Chodl, Hspb3, Irs4, Mab211l, Npy2r, Nr2f2, Tacr3</i>	<i>Calca, Cbln4, Fosb, Mab211l, Nr4a2, Spp1</i>

* indicates significant enrichment of genes

When we consider the functionality or pathways responding to estradiol (via DAVID analysis), there are four enrichment clusters that overlap between two or three of the mutant groups, including transcription regulation and glycoproteins. Many of the enriched clusters identified by DAVID analysis are known to be direct responses to the estrogen receptor pathway according to KEGG (Kanehisa and Goto, 2000, Kanehisa, 2019, Kanehisa *et al.*, 2019), and include transcription regulation, glycoproteins, synaptic function, and G-coupled protein receptors (Figure 4.7). Of note, genes involved in transcription regulation included *Shox2* and *Ebf3*. In the Olivetti *et al.* estradiol study in a different PA1 mouse model, both of these genes were significantly downregulated with treatment (Olivetti *et al.*, 2014). We see this same downregulation in *Shox2* and *Ebf3* in PA2 mice in our study, however not in the PA1 mice, possibly due to the variation between samples.

To extend our functional analysis, we used the PANTHER database to analyse specific pathways enriched the deregulated genes with estradiol treatment. The nicotinic acetylcholine receptor signalling pathway was significantly enriched in both the PA^{pool} and PA2 groups (Table 4.6). Of further interest in the PA^{pool} list was the Wnt signalling pathway (key signalling pathway in neurodevelopment) (Table 4.6). This was quite interesting, as ARX has been shown to interact with components of the Wnt signalling pathway in a proteomics study (Cho *et al.*, 2017). Furthermore, the dopamine receptor mediated signalling pathway was enriched in PA1 mice (regulation of motor behaviour, memory, and reward) (Table 4.6). Interestingly, the only pathway overlapping between the PANTHER analysis of disease deregulated genes and estradiol changed genes was the nicotinic acetylcholine receptor signalling pathway.

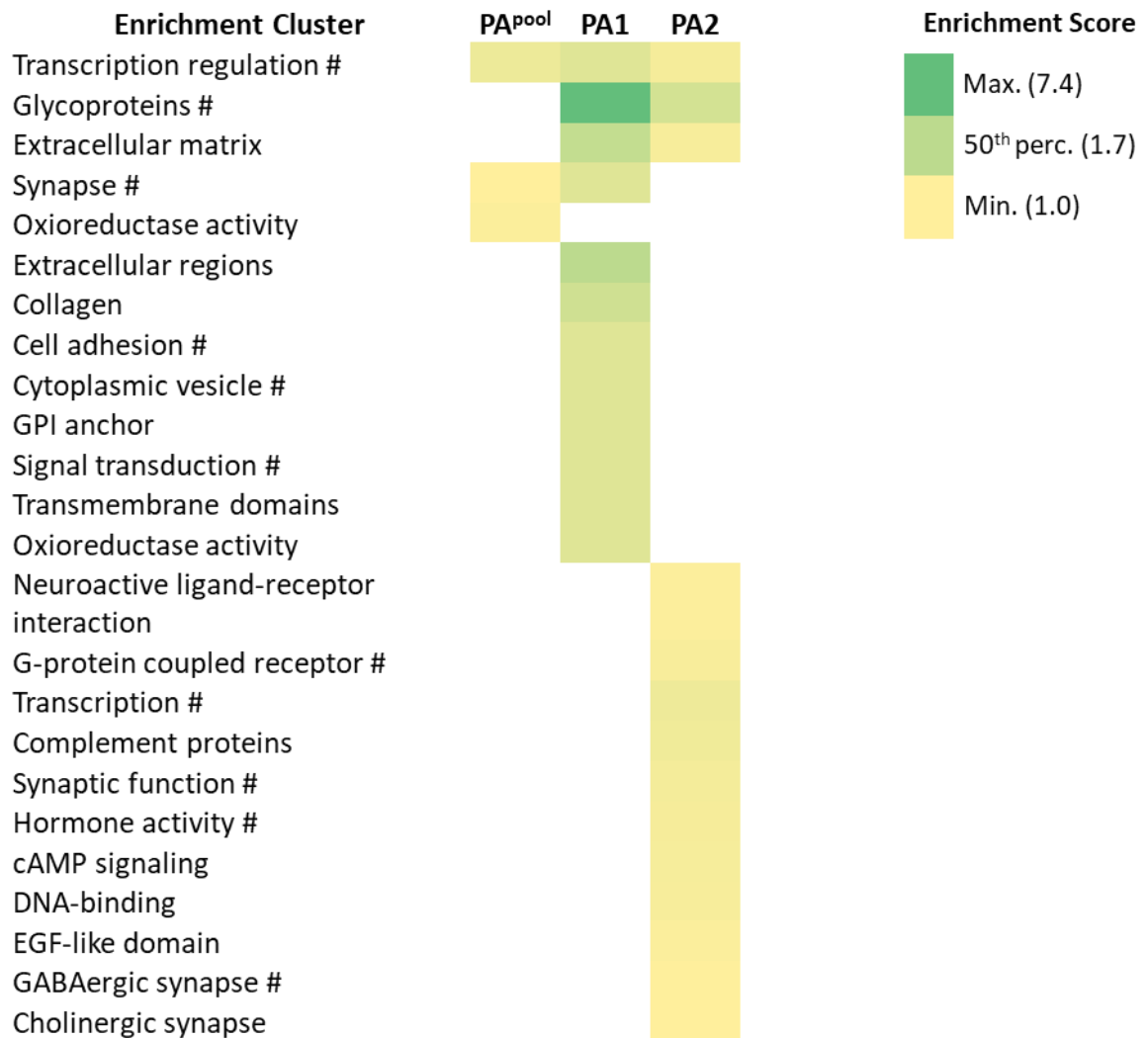


Figure 4.7: Enrichment analysis of genes deregulated with estradiol treatment in PA mutant mice. Heat map showing significant gene enrichment terms in deregulated genes in PA1, PA2 and PA^{pool} groups from DAVID cluster annotation analysis. Clusters with enrichment scores of <1.0 are not shown. Heat map is based on maximum, minimum and 50th percentile score in data set (legend in figure). Clusters with # are pathways and functions known to be regulated by the estrogen receptor pathway.

Table 4.6: Pathways enriched through PANTHER analysis in PA^{pool}, PA1 and PA2 mice.

Term	Overlap	P-value	Genes
Nicotinic acetylcholine receptor signalling pathway	3/68	8.69E-04	<i>Myh2, Myo3b, Chrna6</i>
5-Hydroxytryptamine degradation	1/5	0.01367582	<i>Aldh3a1</i>
Inflammation mediated by chemokine and cytokine signalling pathway	3/188	0.014993079	<i>Myh2, Myo3b, C5ar1</i>
Cytoskeletal regulation by Rho GTPase	2/70	0.015912295	<i>Myh2, Myo3b</i>
Salvage pyrimidine ribonucleotides	1/10	0.027168031	<i>Upp2</i>
Wnt signalling pathway	3/278	0.041044604	<i>Myh2, En2, Fat2</i>
Integrin signalling pathway	5/156	0.003318563	<i>Col1a1, Col16a1, Col1a2, Itgbl1, Flna</i>
Dopamine receptor mediated signalling pathway	2/52	0.043775525	<i>Flna, Dbh</i>
Nicotinic acetylcholine receptor signalling pathway	4/68	0.002207847	<i>Acta2, Myh2, Myo3b, Chrna6</i>
Cytoskeletal regulation by Rho GTPase	3/70	0.018914596	<i>Acta2, Myh2, Myo3b</i>
Insulin/IGF pathway-mitogen activated protein kinase kinase/MAP kinase cascade	2/29	0.022679173	<i>Irs4, Fos</i>

4.4 Discussion

4.4.1 Ongoing effects to the transcriptome from a partial loss of *Arx*.

My study found that the postnatal brain transcriptome remains deregulated in early postnatal life, with genes deregulated in PA1 and PA2 mutant mice at P10, compared to their WT littermates. These genes were involved with key neurodevelopmental processes and inhibitory interneurons, as well as including known *Arx* target and responsive genes. *Arx* is highly expressed during embryonic brain development in mice and humans, with expression detected as early as 8 days post conception (dpc) in the mouse brain (Bienvenu *et al.*, 2002). *Arx* expression decreases throughout development, with lower levels of expression detected in newborn mouse brains, and throughout postnatal life and adulthood (Bienvenu *et al.*, 2002, Mattiske *et al.*, 2016). While it has also been shown that *Arx* remains expressed in the adult brain at low levels, it is likely that this is within a small population of neural precursor cells (Poirier *et al.*, 2004). As such, the majority of studies into the effects of a partial loss of *Arx* on gene expression have been focused in the embryonic brain.

In gene expression studies on the developing brain in mice, from embryonic day 12.5, 14.5, 15.5 and 18.5, with a loss of *Arx* or due to expanded PA mutations, *Arx* has consistently been shown to repress *Ebf3*, *Lmo1*, *Lmo3*, *Lmo4* and *Shox2* (Fulp *et al.*, 2008, Colasante *et al.*, 2009, Quillé *et al.*, 2011, Mattiske *et al.*, 2016). This repressive function has also been identified in neuroblastoma cells transfected with *Arx* (Quillé *et al.*, 2011). However, at P3, in the brains of the Price *et al.* PA1 mouse model, there was no difference noted to *Ebf3* and *Lmo1* due to *Arx* mutations, while *Shox2* expression was increased (Olivetti *et al.*, 2014). From these studies, a comprehensive list of *Arx* target genes, or genes impacted by *Arx* dosage, was devised in our laboratory and was used to determine the numbers of known *Arx* target or responsive genes in our data sets at P10. *Arx* target genes were significantly increased in our disease changed gene analysis, in PA1, PA2 and PA^{pool} mice (21%, 11% and 17% of genes respectively). These genes included *Lmo1* which showed increased expression in PA1 mice. This was fascinating, as even

though *Arx* expression is low at P10, may still elicit some repressive function on *Lmo1*, which when lost leads to increased expression of the gene. These high proportions of *Arx* responsive genes expressed at postnatal day 10 in PA mutant mice may indicate “ripple effects” in gene expression caused by the early partial loss of *Arx* due to the expanded polyalanine tract mutations, even when *Arx*’s expression is minimal.

The gene enrichment clusters found in our study are similar to those reported in these studies into embryonic gene expression with loss of *Arx*. In genes with expression changed by disease, we found neurogenesis, cell signalling, and processes associated with cell migration were deregulated. Cell cycle processes and neurogenesis were both found to be deregulated by *Arx* mutations in the embryonic, developing brain, indicating that these functions appear to remain deregulated in postnatal life (Fulp *et al.*, 2008, Dubos *et al.*, 2018). It has also been shown that in the Price *et al.* PA1 mouse model, there was elevated apoptosis in the cortex of mice in the first postnatal week of life (Siehr *et al.*, 2020). Our PANTHER analysis showed that the apoptotic pathway was deregulated by the PA1 mutation, however not in PA2 mice. This was an interesting finding and may warrant further investigation in the future. Furthermore, genes involved in autism, epilepsy and intellectual disability were deregulated in embryonic studies of gene expression with *Arx* mutations, again, similar to our study in postnatal life. From our analysis, the disturbed transcriptomic profiles of mice with *Arx* mutations closely aligned from embryonic development to early postnatal life, and despite the lower levels of *Arx* expression, indicate these “ripple effects” from early, embryonic loss of *Arx* may cause sustained perturbation of these processes throughout brain development.

Interestingly, with estradiol treatment, the expression of *Shox2* and *Ebf3* was decreased in this PA1 model (Olivetti *et al.*, 2014). In PA2 mice in our study, estradiol treatment also decreased the expression of both *Shox2* and *Ebf3*, however, these were both unchanged in PA1 mice, largely due the variation between samples in both of these genes. Further to these genes, *Twist1*,

a key *Arx* target gene and validated to be part of a core pathway of transcriptional regulators controlled by *Arx* function at embryonic day 12.5, was decreased with estradiol treatment in our PA^{pool} group (Mattiske *et al.*, 2016). It is attractive to speculate that the expression of these key *Arx* target genes being decreased with estradiol treatment may be contributing to the improvements to severity and frequency of seizures we observed in this study (Chapter 3 of this thesis).

4.4.2 Interneuron genes and genes associated with neurodevelopmental disorders are deregulated by disease and estradiol treatment.

Arx is strongly expressed in the developing brain during the key events of proliferation and migration of interneurons to the cortex but has very limited expression in postnatal life (Colombo *et al.*, 2007, Friocourt *et al.*, 2008, Colasante *et al.*, 2009, Lee *et al.*, 2014). Given this expression pattern, our laboratory's previous investigations focused on understanding the disruption of the transcriptome in the forebrain of PA mutant mice at embryonic day 12.5 (Mattiske *et al.*, 2016). Further, it was also demonstrated that there was a delayed migration of calbindin-positive interneurons in the cortex of newborn PA mice (Lee *et al.*, 2017). Interneuron associated genes were also downregulated in the forebrain of PA2 mice at embryonic day 15.5 (Dubos *et al.*, 2018). From these studies we contend that the initial disruption to the transcriptome and subsequent impaired interneuron migrations caused by these mutations in *Arx* drive the seizures and behavioural deficits measured in the PA mutant mice. Later in postnatal life (genes deregulated due to altered functionality of mutant *Arx*) in particular, interneuron associated genes were enriched for, with overwhelmingly decreased expression. Interestingly, of the interneuron genes overlapping between PA1 and PA2 mutant mice, *Th* and *Tacr1* are associated with somatostatin positive interneurons, while *Akr1c18* is associated with parvalbumin positive interneurons. Neither of these subtypes have been previously shown to be disturbed in our PA1 and PA2 models at P10, so this is a novel finding.

Despite the significantly enriched number of inhibitory neuron genes deregulated by disease and with estradiol treatment, we did not see changes in genes coding for *Calb1* and *Calb2*, involved in calbindin positive interneurons. Previously, this interneuron subtype was shown to have delayed migration in our PA mutant mouse models. However, from this data, we cannot speculate on potential migratory deficits in these cells due in part to the bulk RNA sequencing approach taken within this study. Many subsets of interneurons are lowly expressed in the brain. Given their importance to the PA mutant phenotype and in *Arx* function more broadly, single-cell RNA sequencing could be a useful future strategy to determine the impact of disease and treatment on these specific subtypes of inhibitory neurons.

In the current study we demonstrate a modest number of deregulated genes from the cortex at P10. This is in comparison to the larger number of deregulated genes detected at embryonic day 12.5 in wildtype compared to *Arx* PA mutant mice (vehicle treated mice only) (Mattiske et al., 2016). Genes included *Tnn* and *Ngfr*, regulators of differentiation, growth, and migration of neuronal populations (Degen et al., 2007, Lin et al., 2015), while *Tacr1* is part of the family of G coupled-protein receptors, highly concentrated in the central nervous system (UniProt, 2020). Consistent with clinical phenotypes known to present in patients with *ARX* expansion mutations, *Cpz* is associated with autism spectrum disorders and/or intellectual disability (Loch et al., 2018). Despite reduced *Arx* expression within the brain at P10, the genes with deregulated expression in mutant mice were enriched for *Arx* responsive genes and genes known to be associated with autism and intellectual disability. The genes overlapping in mutant animals at P10 are important in brain development, including metal ion binding, known to be involved in cognitive decline in Down syndrome (Malakooti et al., 2014) and Alzheimer's disease (Cristóvão et al., 2016), as well as signal transduction and glycoproteins, both heavily involved in neurotransmitter release and modifying neuronal functioning (as shown in KEGG pathway analysis) (Kanehisa and Goto, 2000, Kanehisa, 2019, Kanehisa et al., 2019). Although epilepsy associated genes were not significantly enriched in the mutant mice at P10, genes associated

with inhibitory neurons were. *Th* is a gene of particular interest. Downregulation of *Th* was validated in both PA1 and PA2 vehicle-treated mice compared to WT and is an enzyme that assists in the formation of dopamine, a neurotransmitter, as well as having an association with interneurons (Mao *et al.*, 2019, Yang *et al.*, 2020, Zhang *et al.*, 2020). *Th* was unaltered with estradiol treatment, as well as other interneuron genes downregulated with disease. This supports the notion that disturbed function of these inhibitory cells are likely to play a critical role in the seizure phenotype due to mutations in *Arx*, and that the lack of “rescuing” of these genes might be associated with the remaining seizures we see with treatment in mutant mice, as well as the unaltered cognitive and behavioural phenotype.

Of note, we did not find that epilepsy associated genes were significantly enriched in genes deregulated by disease in PA mutant mice. This was perhaps not surprising, as many known epilepsy causative genes are overwhelmingly associated with excitatory neurons. While mutations in *Arx* can cause seizures and epilepsy in patients, these are due to a disruption to inhibition in the brain, with dysregulation of interneuron migration and function. *Arx* mutations therefore do not cause channelopathies as many epilepsy disorders are, and rather, cause “interneuronopathies”, a smaller subset of epilepsy-associated disorders.

4.4.3 Differences between PA1 and PA2 mutant mice.

Given the striking similarity in behavioural and seizure phenotypes, we were somewhat surprised by the difference in gene expression in PA1 and PA2 mice. This difference related to both genes changed by disease and in response to estradiol treatment. This difference in the number of genes changed in each of the two genotypes was also observed at embryonic day 12.5 (Mattiske *et al.*, 2016). We were also uncertain if 17 β -estradiol treatment would “rescue” the deregulated transcriptome of the PA mutant mice at P10, or if this treatment would target alternative pathways to reduce seizure frequency and severity. In the previous study in an alternate PA1 mutant mouse model, the same strategy of 17 β -estradiol treatment altered

expression of three downstream targets of *Arx*, namely *Shox2*, *Ebf3* and *Lgi1* (Olivetti *et al.*, 2014). In the current study, we demonstrated only minimal overlap in the genes deregulated by disease (PA mutant mice compared to WT mice – vehicle treated only) compared to genes deregulated by 17 β -estradiol treatment (vehicle treated mice compared to estradiol treated mice – PA mutant mice only). Despite these small numbers of genes that overlapped between these two comparisons, the genes that did overlap in PA1 and PA2, were deregulated in the opposite direction when treated with estradiol. In the PA1 gene list, there were some key genes of note, including *Ptgs2* (involved in schizophrenia, another neurodevelopmental disorder) and *Slc17a8* (highly involved in synaptic vesicle function in excitatory neurons) (Wei and Hemmings, 2004, UniProt, 2020). In PA2, these genes included *Arc* (a master regulator of synaptic plasticity, and associated with epilepsy and schizophrenia), and *Nppa* (a regulator of neuropeptide hormone activity) (Haug *et al.*, 2000, Huentelman *et al.*, 2015). Though these genes may play a role in the alleviation of the seizure phenotype of PA mutant mice, these modest number of disease genes deregulated when treated with estradiol indicates that treatment in early postnatal life is less likely to be “repairing” the gene expression pathways deregulated by the PA mutant genotype and more likely recruiting new pathways to affect the reduction in seizures.

4.4.4 Estrogen response genes in our analysis.

Genes containing known conserved estrogen response elements (ERE) were only enriched to very low levels in PA mutant mice with estrogen treatment compared to vehicle treatment. Estradiol signalling can occur by direct genomic signalling where there is estrogen receptor dimerization and binding to EREs, as well as via indirect signalling, where estradiol can influence the expression of genes without EREs. As many as one third of estrogen responsive genes lack ERE-like elements (Vrtačnik *et al.*, 2014). Hence, using DAVID, we analysed pathways and ontology terms enriched within the data that were known effects of 17 β -estradiol signalling. Many of our enriched clusters were known to be direct or indirect effects of the estradiol pathway (Kanehisa and Goto, 2000, Kanehisa, 2019, Kanehisa *et al.*, 2019). Our data

demonstrates that 17 β -estradiol treatment in early postnatal life recruits pathways impacting synaptic function, signal transduction, transcriptional regulation, and hormone activity responsible in reducing the frequency and severity of seizures in PA mutant mice.

4.4.5 Environmental effects on transcriptomic results.

An obviously surprising outcome in our transcriptomic findings is the striking difference between PA1 and PA2 mice, despite their similar phenotype. There are some limitations in the RNAseq approach taken that may partially contribute to this result. Cortex samples used for this RNAseq analysis were only taken at P10, one time point. This means that environmental overlay may have impacted the transcriptomic results of individual samples, and without a larger group of mice at multiple time points, these effects may lead to differences that were not averaged out. These environmental effects may include stress, seizure activity (though no seizures were observed in our mice this early), or maternal parenting differences. However, we attempted to keep the study as robust as possible, by treating all cohorts of mice the same from birth to collection point at P10, and collecting samples at the same time of day.

4.5 Study outcomes

This investigation provides an unbiased study into the transcriptomic profile of PA1 and PA2 mice at postnatal day 10 (without estradiol treatment) to determine the impact of partial loss of *Arx* early in development. In addition, the impact of estradiol treatment on these mice was investigated to understand how estrogen might be improving the seizure frequency and severity in adolescence. We have shown that significant numbers of genes associated with neurodevelopmental disorders and interneuron genes, and known *Arx* target and responsive genes had deregulated expression in both PA mice. Given the dramatic reduction to seizure occurrence, we were somewhat surprised to find that estradiol treatment did not appear to “rescue” the deregulated transcriptome of PA mutant mice at postnatal day 10. Instead, estradiol treatment recruited molecular and cellular pathways to reduce the frequency and severity of seizures rather than restoring pathways initially deregulated in *Arx* PA mutant mice driving pathogenesis. Investigating gene expression and pathways disrupted due to mutations in *Arx* and the subsequent response to treatment is vital for looking for therapeutic targets, even those that could potentially be delivered prenatally to the foetus *in utero*. We conclude that 17 β -estradiol treatment recruits processes and pathways to reduce the frequency and severity of seizures in the *Arx* PA mutant mice but does not precisely correct the deregulated transcriptome nor improve mortality or behavioural and cognitive deficits. We chose to focus our investigations on the effects of these expanded polyalanine tract mutations on the interneurons in the brain, with and without treatment.

Chapter Five:

Interneuron genes are deregulated with *Arx* PA mutations, but are not rescued directly with 17 β -estradiol treatment.

5.1 Abstract

The lack of effective treatments for intellectual disability and neuropsychiatric disturbances remains a significant challenge and highlights the continued need to elucidate the molecular and cellular drivers of the intellectual disability phenotype as the first necessary steps toward a treatment. Many NDD genes have been linked to the function, development and migration of interneurons, an inhibitory cell type in the brain. Interneurons balance excitation and inhibition in the cortex, providing a balance to the overall network. The *Aristaless*-related homeobox gene, *ARX*, is a transcription factor strongly expressed in immature neurons and interneurons in the embryonic brain. When *ARX* function is compromised, intellectual disability with associated comorbidities like severe epilepsy and infantile spasms can be the result. The transcriptomic profile of interneuron genes at postnatal days 3 and 10 in untreated PA mutant mice was analysed, demonstrating that many interneuron deficits were already present at this early stage of postnatal brain development, particularly somatostatin and parvalbumin positive interneurons. We contend that early disruption of *Arx* function results in deregulation of interneuron associated genes early in postnatal life, contributing to the disease phenotype. Further, to determine the effect of estradiol on the abundance of calbindin and neuropeptide-Y interneurons, we used immunofluorescent microscopy at postnatal day 10, immediately following treatment. These two interneuron subtypes have been previously shown to be deficient in PA mutant mice, and rescued with estradiol. Despite differences in the expression of multiple interneuron genes at postnatal day 10 following estradiol treatment, we did not determine any significant differences in the number of calbindin and neuropeptide-Y interneurons in PA mutant mice. Despite changes to gene expression of specific interneurons, our data suggests that rescue of interneuron deficits/cell density, is unlikely to be the sole cause of estradiol's effect on seizure alleviation in PA mice.

5.2 Introduction

The cortex of the brain is highly diverse, made up of a number of cell types which perform a variety of functions, dependent on balanced neural circuits. GABAergic inhibitory interneurons are vital to controlling neuronal excitability and balancing the synchrony of neural networks in the brain. If there is a dysfunction in interneurons in the brain, this can lead to aberrant firing of excitatory cells, due to a lack of inhibition and an imbalance of these networks. These networks play a pivotal role in the control of memory and information processing functions of the cortex, and if disrupted, can be associated with a wide spectrum of neurodevelopmental disorders such as intellectual disability, epilepsy, schizophrenia and autism (Benes and Berretta, 2001, Lewis *et al.*, 2005, Rubenstein, 2010, Olivetti and Noebels, 2012).

Many neurodevelopmental disorders, particularly intellectual disability and epilepsy, share similar developmental origins, with causative genes for these disorders overlapping. Of these disease associated genes, some have been linked to the function, development, and migration of cortical interneurons. The *Aristaless*-related homeobox gene, *ARX*, is a transcriptional repressor, strongly expressed in neural progenitor cells and immature neurons in the developing, embryonic brain, peaking between embryonic days 12.5 and 15.5 in the mouse cortex in particular (Miura *et al.*, 1997, Kitamura *et al.*, 2002, Poirier *et al.*, 2004, Colombo *et al.*, 2007). When *Arx* is completely knocked out in a mouse model, the male mice have severe brain malformations, with a thinner cortical plate, a deficit in tangential migration of interneurons to the cortex, and a complete lack of radial migration of interneurons. These mice also had significantly reduced numbers of excitatory neurons (Kitamura *et al.*, 2002). *In utero* knock down of *Arx* causes progenitor cells to prematurely exit the cell cycle and impaired the migration of interneurons into the cortex, as well as the radial migration of excitatory neurons (Friocourt *et al.*, 2008). This demonstrates the dramatic effects of a loss of *Arx* on interneuron migration, and is reflected in the severe phenotypes in human patients due to complete loss of function mutations.

In mice with mutations expanding the first and second polyalanine tracts of *Arx*, there is a deficit in the number of interneurons, as well as their migration. In 2017 Lee *et al.* showed an overall reduction in GABAergic interneurons in the postnatal day 0 brain of both PA1 and PA2 mice. When looking at specific interneuron subtypes, there was a 40-50% loss of calbindin positive cells in the cortex. These cells were found to be arrested in the ventral subpallium of the cortex, where migration of these cells had been halted or delayed (Lee *et al.*, 2017). This same PA1 mouse has also been shown to have reduced numbers of neuropeptide-Y positive interneurons in the brain at one month of age (Kitamura *et al.*, 2009). Furthermore, transcriptomic studies of the embryonic brain of PA mutant mice have shown deregulation of key interneuron functional and developmental genes, however we have not yet performed RNA sequencing of the brain in postnatal life (Mattiske *et al.*, 2016, Dubos *et al.*, 2018). These mouse models have demonstrated that even a partial loss of *Arx* due to these expanded tracts can impact the normal functioning and migration of these key inhibitory cells of the brain.

Arx is mostly expressed embryonically. To understand the ongoing effects of these mutations throughout postnatal life, there have been few studies in the postnatal brain of these PA1 and PA2 mouse model. A recent study involving an alternate PA1 mouse model found that early postnatal treatment with 17 β -estradiol restored some of the interneuron deficits at approximately one month of age, particularly in neuropeptide-Y and cholinergic cells (Olivetti *et al.*, 2014). Furthermore, in rats, treatment with estradiol increased the number of inhibitory cells in an induced seizure rat model, and in a premature birth model in rabbits (Chachua *et al.*, 2016, Panda *et al.*, 2018). Taken together, these studies suggest that estradiol may be able to improve interneuron populations in the brain, even in the presence of a functional deficit in *Arx*.

To investigate the effects of these mutations in early postnatal life, we established the status of the expression of interneuron associated genes aligned with the commencement of estradiol treatment at P3, and immediately following treatment at P10, using RNA sequencing. We

suspected that genes involved with the development, migration and function of interneurons would be deregulated in PA mutant mice. RNA sequencing was used to determine the changes to gene expression in the prefrontal cortices of PA1 and PA2 mutant mice and their wild-type littermates. We then investigated the effects of early estradiol treatment on the cell density of interneuron subtypes within the cortex. Previous studies in PA1 and PA2 mice, with and without estradiol treatment, have shown deficits to calbindin and neuropeptide-Y positive interneurons in the cortex, early and later in development (Kitamura *et al.*, 2009, Olivetti and Noebels, 2012, Olivetti *et al.*, 2014, Lee *et al.*, 2017). Hence, I chose to focus on these two interneuron subtypes, investigating with immunofluorescent analysis of a specified region of the prefrontal cortex at postnatal day 10. We hypothesised that treatment with estradiol would improve the numbers of neuropeptide-Y and calbindin positive interneurons in the postnatal day 10 cortex of PA1 and PA2 mice, restoring deficits in migration observed at birth.

5.3 Results

5.3.1 Deregulated interneurons in untreated PA1 and PA2 mutant mice at postnatal day 3 and postnatal day 10.

Further to our RNA sequencing analysis comparing vehicle and estradiol treated PA mutant and WT mice at postnatal day 10, discussed extensively in Chapter Four of this thesis, we also performed RNA sequencing of postnatal day 3 (P3) and day 10 (P10) cortex samples from completely untreated PA mutant and their WT littermates. Here we complete a characterisation of the impact of disrupted Arx function on the expression of interneuron associated genes at these two early postnatal time points.

We demonstrate that the transcriptomes of mutant mice at P3 and P10 were disrupted due to expanded polyalanine tract mutations, compared to their WT counterparts. Compared to age-matched, untreated WT mice ($n = 6$), analysis of PA1 at P3 ($n = 4$) found 497 genes deregulated with a Log2 fold change greater than ± 0.5 and a p -value of less than 0.05. PA2 mice had 110 genes deregulated with the same cut-off value, and when combining these two groups to create a PA^{pool} group, we found 130 genes deregulated. At P10, compared to age-matched, untreated WT mice ($n = 6$), PA1 mice ($n = 4$) had 179 genes deregulated with a Log2 fold change greater than ± 0.5 and a p -value of less than 0.05. PA2 mice had 135 genes deregulated, and PA^{pool} mice had 134 genes deregulated (Table 5.1).

Table 5.1: Genes deregulated by disease in untreated PA1, PA2 and PA^{pool} mice compared to untreated wild-type littermates at the same time points.

	Untreated	PA1	PA2	PA ^{pool}
P3	vs. P3 WT	497	110	130
P10	vs. P10 WT	179	135	134

To understand the interneuron genes disrupted by the disease genotype in PA mutant mice, we investigated enriched genes within these lists. Utilising the in house curated reference list of inhibitory neuron associated genes. At P3, there were 15, five and seven interneuron associated genes disrupted in PA1, PA2 and PA^{pool} groups, respectively (Table 5.2). Interestingly, these genes were significantly enriched in all three groups; PA1 (15/497, 3%, $p < 9.212e^{-13}$), PA2 (5/110, 5%, $p < 6.271e^{-6}$) and PA^{pool} (7/130, 5%, $p < 2.573e^{-8}$) (Table 5.2).

At P10, there were 13 interneuron associated genes disrupted in PA1 mice, six disrupted in PA2, followed by eleven genes disrupted in the PA^{pool} group (Table 5.2). As we also saw at P3, there was significant enrichment of interneuron genes in PA1 mice (13/179, 7%, $p < 4.491e^{-16}$), PA2 mice (6/135, 4%, $p < 8.183e^{-7}$) and PA^{pool} mice (11/134, 8%, $p < 2.233e^{-14}$) (Table 5.2). Perhaps not surprisingly, these percentages are similar to those in vehicle treated mutant mice at P10, with 8%, 10% and 17% of deregulated genes being interneuron genes, including *Akr1c18*, *Chat*, *Th* and *Tacr1*.

Table 5.2: Interneuron associated genes enriched in untreated PA1, PA2 and PA^{pool} mice at postnatal day 3 and day 10.

	PA1	PA2	PA ^{pool}
P3	<i>Col25a1, Cryab, Fign, Frem1, Hspb3, Itih5, Ndst4, Npy, Pvalb, Slc18a3, Sncg, Spp1, Tac2, Th, Tll1</i>	<i>Cartpt, Crh, Fosb, Npy, Tac2</i>	<i>Cryab, Hspb3, Npy, Slc18a3, Spp1, Tac2, Tll1</i>
Significant enrichment of interneuron genes	*	*	*
P-value	$p = 9.212e^{-13}$	$p = 6.271e^{-6}$	$p = 2.573e^{-8}$
P10	<i>Akr1c18, Chat, Chrna2, Fosb, Frmd7, Has2, Mybpc1, Pde11a, Pvalb, Sla18a3, Spp1, Tacr1, Th</i>	<i>Akr1c18, Fosb, Frmd7, Mybpc1, Myh8, Spp1</i>	<i>Akrc1c18, Chat, Chrna2, Fosb, Frmd7, Has2, Mybpc1, Pvalb, Spp1, Tacr1, Th</i>
Significant enrichment of interneuron genes	*	*	*
P-value	$p = 4.491e^{-16}$	$p = 8.183e^{-7}$	$p = 2.233e^{-14}$

Focusing our investigation of the disruptions to key interneuron genes and the pattern of deregulation between the two time points of P3 or P10, the *Calb1* gene, responsible for the calbindin protein expressed by calbindin positive interneurons, was not significantly different between WT or PA mutant mice at either time point (Figure 5.1). This was interesting given the migration impediment in these interneuron subtypes exhibited at P0 in PA1 and PA2 mice, previously established by Lee *et al.* 2017. Disruption to the *Pvalb* gene, responsible for the parvalbumin protein on parvalbumin positive interneurons, was observed at both timepoints in PA1 group, and at P10 in the PA^{pool} group (Figure 5.1). The disruption to *Pvalb* persisted from P3 and was still present at P10. There was no deficit to parvalbumin abundance reported in Lee *et al.* 2017, however this gene is not strongly expressed until approximately postnatal day 14 (Allen Brain Atlas).

Disruption to expression of the *Chat* gene at P10 in PA1, PA2 and PA^{pool} groups was also found from our RNAseq analysis (Figure 5.1). This gene plays key roles in cholinergic interneurons, a subtype previously shown to be deficient in the alternate PA1 mutant mouse model (Olivetti *et al.*, 2014). We also detected disruption to the *Th* gene in all three mutant groups, at both P3 and at P10 (Figure 5.1). *Th* is also a key player in cholinergic interneurons. This is the first time deregulated expression of these genes in PA1 and PA2 mice has been reported. We demonstrated significant deregulation of the *Npy* gene at P3 in all three mutant groups (Figure 5.1). At postnatal day 3 this deregulation was significant in meeting our cut off values for our RNA sequencing data, being a *p*-value >0.05 paired with a log2 fold change of ± 0.5 , however at P10, *Npy* was deregulated with a *p*-value >0.05, but did not meet the log2 fold change criteria. Fascinatingly, all interneuron gene deficits in PA1 and PA2 mice, apart from *Chat* which was not detected at P3, persisted from P3 to P10.

Three additional interneuron associated genes were also disrupted in these mutant groups. These genes did not overlap completely with each mutant group. *Spp1* was downregulated in

PA1 and PA^{pool} at both P3 and P10, and *Slc18a3* downregulated in PA1 only. *Fosb* was an interesting finding, being significantly upregulated in PA2 mice at P3, but significantly downregulated compared to WT littermates at P10 (data not shown).

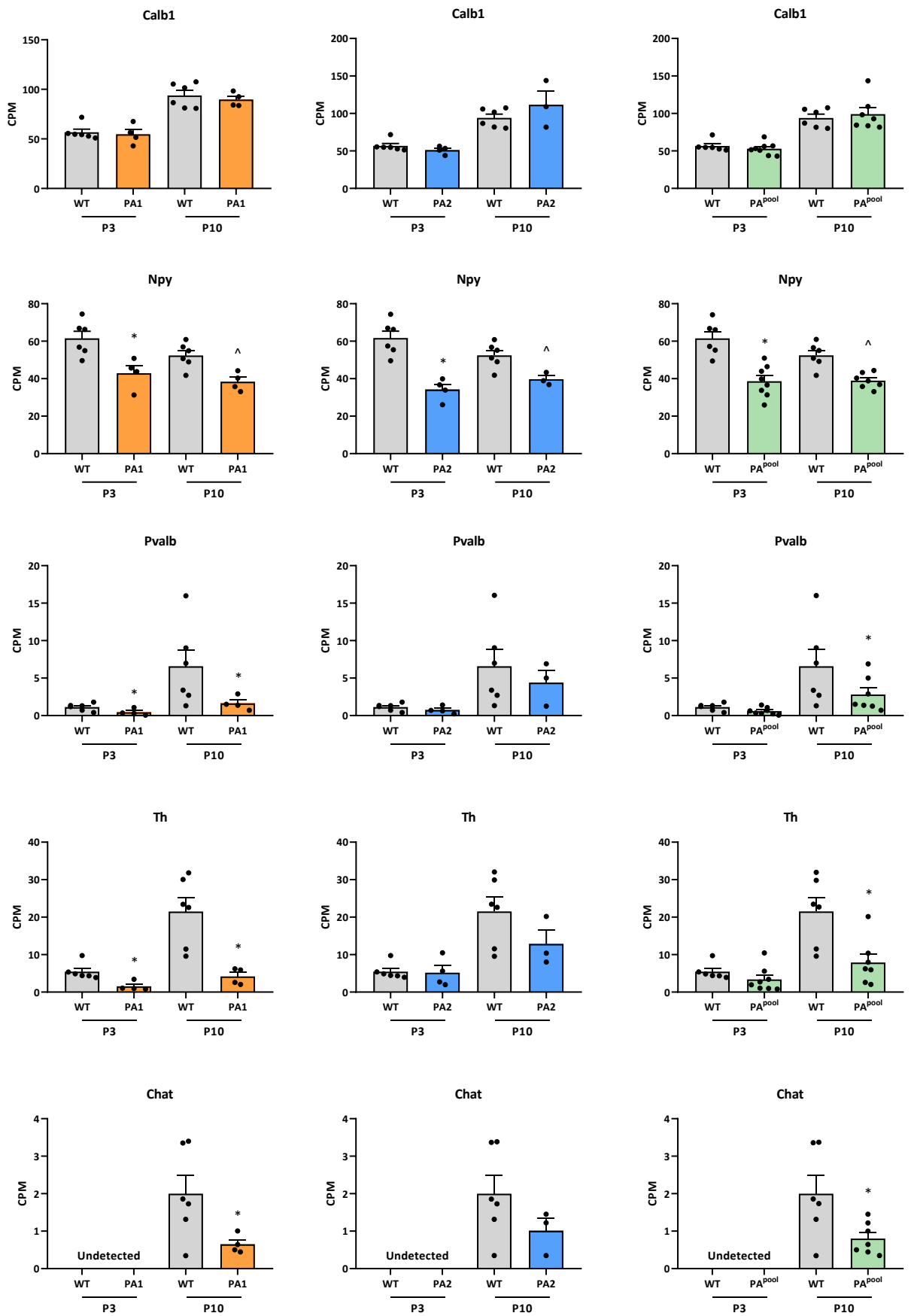
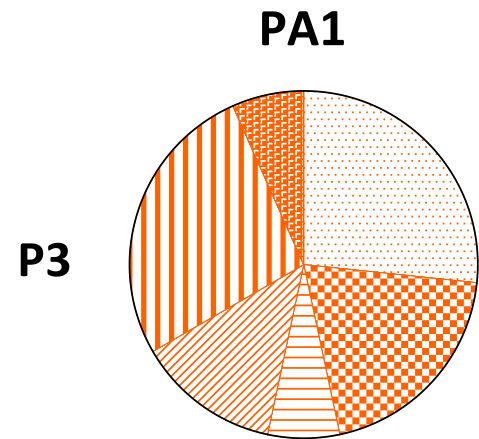
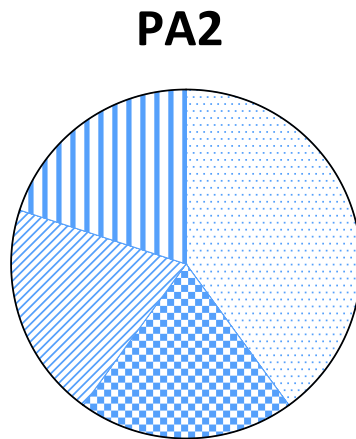


Figure 5.1: RNA sequencing outcomes of key interneuron associated genes in untreated PA mutant mice at postnatal day 3 and day 10. Gene expression as counts per million (CPM) for selected interneuron associated genes enriched in untreated PA mutant mice compared to untreated WT littermates. Dots represent values for individual animals. PA1 mice at P3 (n = 4; blue) and P10 (n = 4; blue); PA2 mice at P3 (n = 4; blue) and P10 (n = 3; blue); PA^{pool} mice at P3 (n = 8; green) and P10 (n = 7; green); WT mice at P3 (n = 6; grey) and P10 (n = 6; grey). * p<0.05 and log fold change ± 0.5 . ^ p<0.05 but did not meet log fold change cut off.

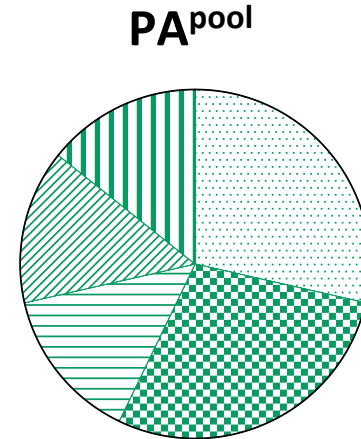
To identify which genes corresponded to specific interneuron subtypes, we analysed expression data using Gemma to assign cell populations to the gene most abundantly expressed (Zoubarov *et al.*, 2012). A table of these interneuron subtypes with the genetic markers identified in our analysis is listed in Appendix 10. From this investigation, we found that these interneuron genes enriched in PA1, PA2 and PA^{pool} mice were primarily associated with vasoactive intestinal polypeptide (VIP), somatostatin (SST), neuron-derived neurotrophic factor (NDNF), parvalbumin (PVALB), interferon gamma-induced GTPase (IGTP) and synuclein- γ (SNCG) interneuron subtypes. The types of interneurons most enriched for genes deregulated in PA mutant mice at both P3 and P10 included VIP, SST and PVALB (Figure 5.2). In the case of PA2 mice, there was a change from P3 (VIP and SST) to also include PVALB at P10 (Figure 5.2). In the pooled data, we see a change in the enrichment of genes expressed in interneuron subtypes, with VIP at P3 disrupted, to SST and PVALB at P10 (Figure 5.2). This investigation identified SST, VIP and PVALB as the most common interneuron subtypes with deregulated gene expression in *Arx* mutant groups.



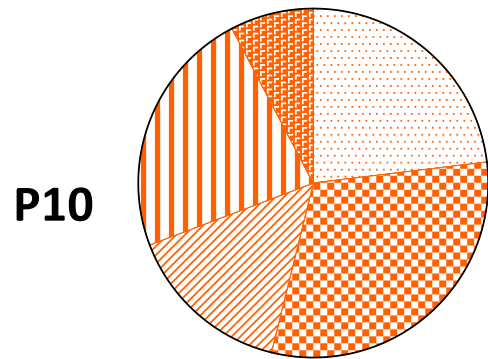
- VIP
- SST
- IGTP
- NDNF
- PVALB
- SCNG



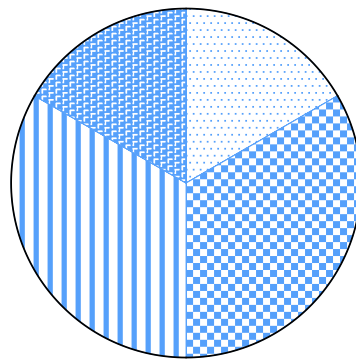
- VIP
- SST
- NDNF
- PVALB



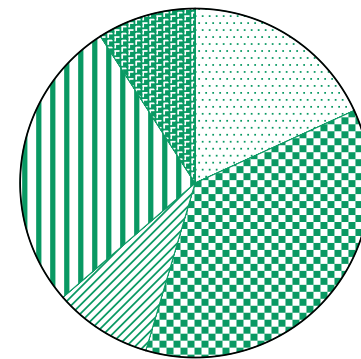
- VIP
- SST
- IGTP
- NDNF
- PVALB



- VIP
- SST
- NDNF
- PVALB
- SCNG



- VIP
- SST
- PVALB
- SCNG



- VIP
- SST
- NDNF
- PVALB
- SCNG

Figure 5.2: Enrichment of different interneuron subtypes with genes deregulated in untreated postnatal day 3 and day 10 PA mice. Pie charts display subtypes of interneurons based on deregulated interneuron gene expression in untreated PA mutant mice at P3 and P10 (PA1 = orange, PA2 = blue, PA^{pool} = green). Patterns represent each interneuron subtype, as described in figure. Proportions of each subtype is based on deregulated interneuron associated genes in Table 5.2. Key for interneuron subtypes is as follows; VIP: vasoactive intestinal polypeptide; SST: somatostatin; NDNF: neuron-derived neurotrophic factor; PVALB: parvalbumin; IGTP: interferon gamma-induced GTPase; SNCG: synuclein- γ .

5.3.2 Estradiol treatment does not alter interneuron abundance in the PA1 and PA2 mouse prefrontal cortex.

Immunofluorescence microscopy of the prefrontal cortex at P10 was performed in a specific region of the cortex for all animals studied (Figure 5.3). Representative examples of calbindin and neuropeptide-Y positive cells were observed (Figure 5.4 A&B). The cell density analysis first separated WT mice treated with either estradiol or vehicle. For this experiment we chose to combine these into a WT combined treatment group, to look for any changes in interneuron populations compared to mutant mice. We did not observe any deficits to calbindin-positive cell density in vehicle treated PA^{pool} mice compared to their WT littermates (Figure 5.4 C). Again, with neuropeptide-Y, we did not observe any decrease or difference in cell density due to disease, when comparing mutant mice to their WT littermates (Figure 5.4 D). We did not see any differences to cell density in either of these interneuron subtypes in mutant mice immediately following cessation of estradiol treatment (Figure 5.4 C&D).

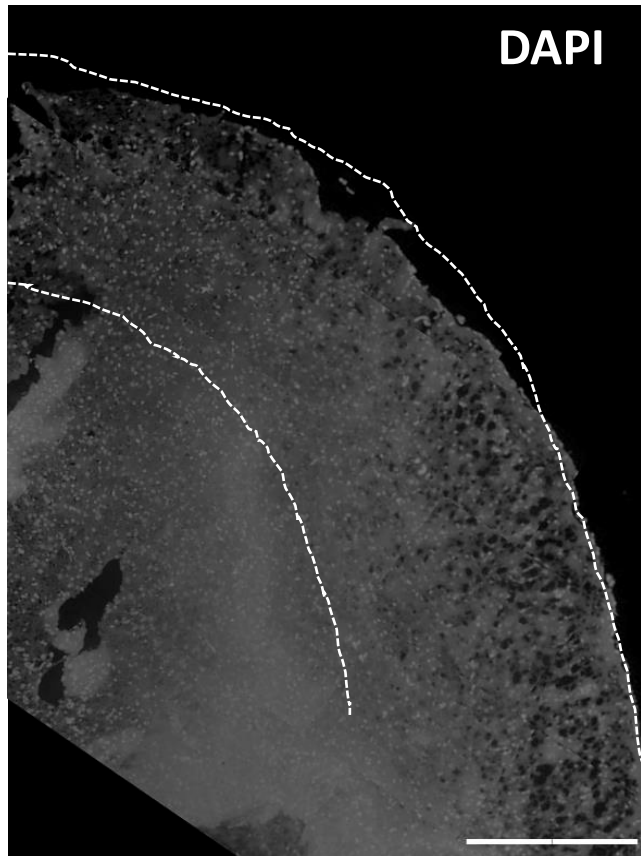


Figure 5.3: Region of the cortex used for immunofluorescence analysis. Representative DAPI stained image of the brain in a WT mouse illustrating the region of the brain analysed (within dashed lines). Scale bar 200 μ M.

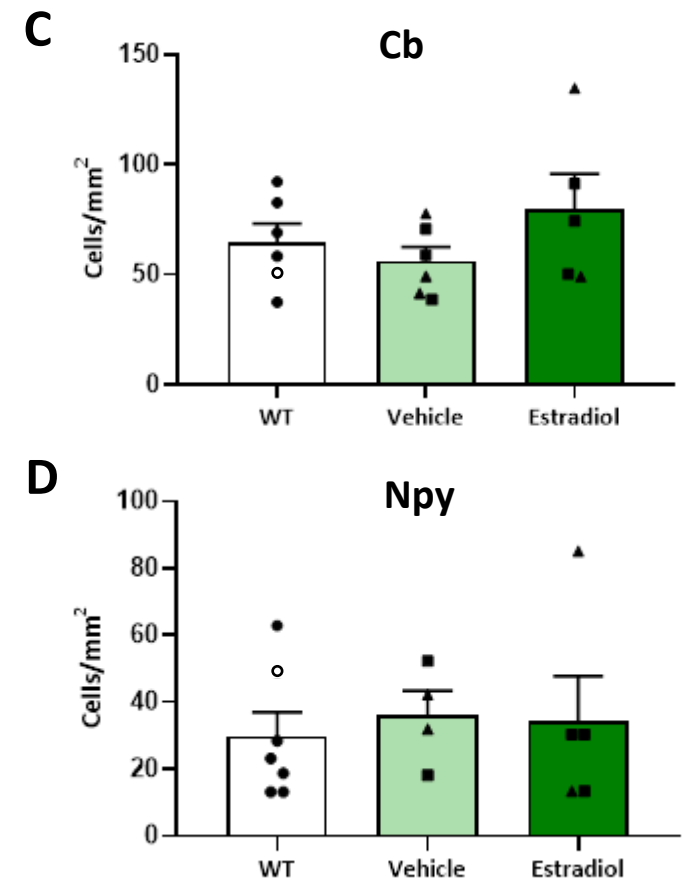
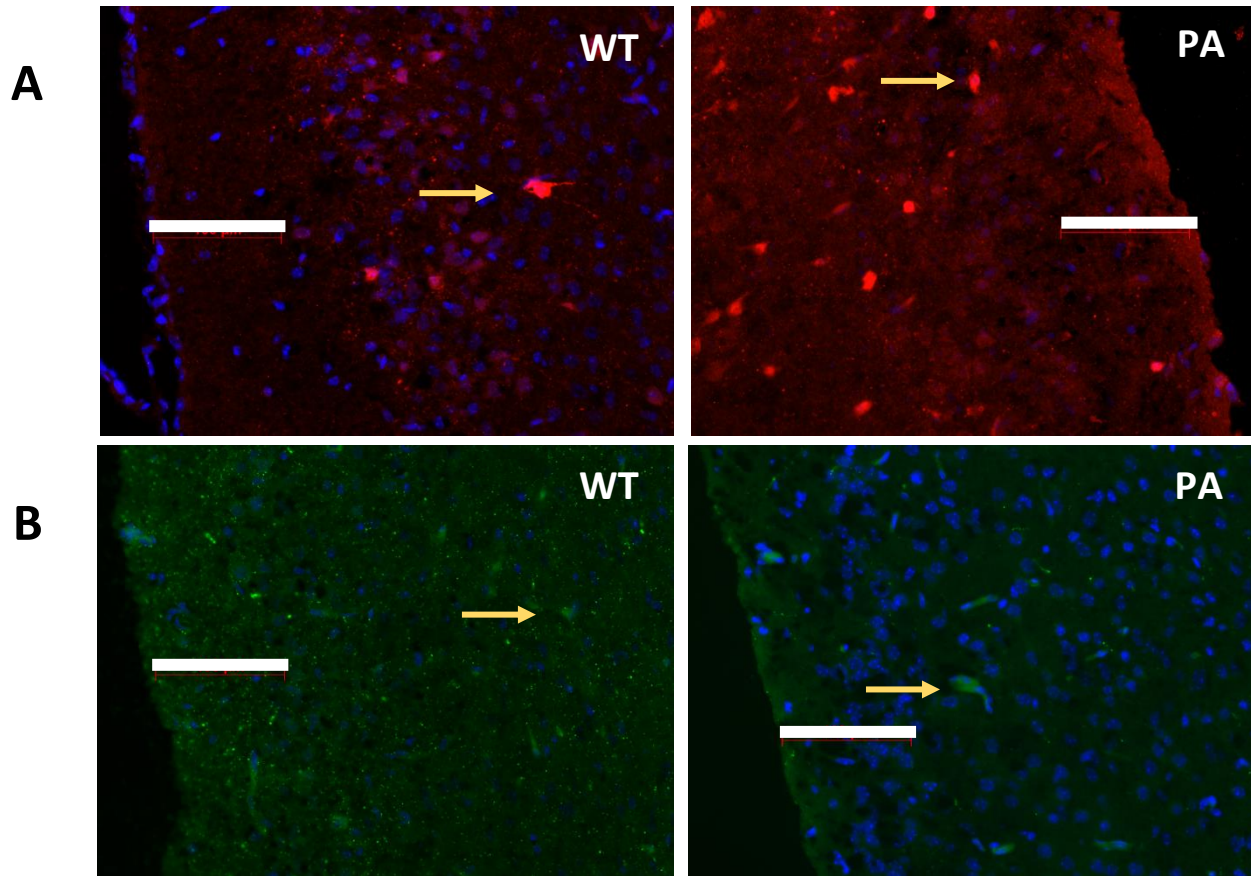


Figure 5.4: Abundance of calbindin and neuropeptide-Y positive interneurons in the prefrontal cortex. (A) Immunofluorescence analysis of calbindin (Cb) interneurons in coronal brain sections of PA mutant mice at P10 and was superimposed with DAPI staining and imaged with 20x objective. Arrows depict representative examples of Cb positive cells in a WT and a PA mouse. Scale bar 100 μ m. (B) Immunofluorescence analysis of neuropeptide-Y (Npy) interneurons in coronal brain sections of PA mutant mice at P10 and was superimposed with DAPI staining and imaged with 20x objective. Arrows depict representative examples of Npy positive cells in a WT and a PA mouse. Scale bar 100 μ m. (C) Density of Cb positive cells in WT mice (n = 6; white; vehicle = solid dots; estradiol = circles) and PA^{pool} mice (PA1 = squares; PA2 = triangles) treated with vehicle (n = 6; light green) or estradiol (n = 5; dark green). (D) Density of Npy positive cells in WT mice (n = 6; white; vehicle = solid dots; estradiol = circles) and PA^{pool} mice (PA1 = squares; PA2 = triangles) treated with vehicle (n = 4; light green) or estradiol (n = 5; dark green).

5.4 Discussion

5.4.1 Novel findings from this study

As part of our investigation into the effects of short-term 17β -estradiol treatment on PA1 and PA2 mutant mice, we performed microscopy analysis of the cortex at postnatal day 10, immediately following treatment. Interestingly, at the cessation of treatment, we reported no significant difference in the cell density of calbindin and neuropeptide-Y interneurons with estradiol. However, we also did not observe any significant deficit in these cells in mutant mice compared to WT. Previously our laboratory reported a lag in the migration of calbindin positive interneurons at P0 in both PA1 and PA2 mice, with an accumulation of cells being arrested when they should have migrated into the cortical layers (Lee *et al.*, 2017). This outcomes was supported by our analysis, demonstrating no difference to *Calb1* (encoding calbindin) in our gene expression data at P10 either with or without treatment. This could indicate that this deficit of calbindin positive cells in the cortex is in fact caused by slow migration, as opposed to a complete loss of this interneuron subtype. As we did not carry out detailed microdissection of the cortical tissue, our results are based on the entire cortical region studied. This is a limitation in determining any lag in the migration of these cells at P10, manifested by changes to the density of calbindin cells in different layers.

Furthermore, our collaborators showed reduced density of neuropeptide-Y cells in the adult brain, and an increase with estradiol treatment (Olivetti *et al.*, 2014). In agreement, we determined a modest reduction in the expression of the *Npy* gene expression in PA1 mutant mice compared to WT animals at the earlier time point of P10. However, we did not find any significant differences to density of *Npy* positive interneurons. The expression of *Npy* is known to increase in the brain from approximately P14, meaning we cannot rule out that changes to the density of *Npy* positive interneurons at later stages of development may occur and contribute to the sustained reduction in seizures observed in estradiol treated mice (Lein *et al.*,

2007). Although we detect differences in gene expression of multiple interneuron associated genes at P10 of development, our data indicates to us that the many other genes (and pathways) regulated by estradiol treatment are likely to be participating in the alleviation of seizures, as opposed to increased inhibition in the brain as the sole mechanism.

We also completed a comprehensive investigation of key genes involved in interneuron function, migration and development, in untreated PA1 and PA2 mutant mice at P3 and P10. This is the first time the transcriptomic profile of these mice has been investigated at these time points. We demonstrated a substantial and significant deregulation of interneuron associated genes at both time points in PA1, PA2 and PA^{pool} mice. Most of these interneuron deficits were sustained from P3 through to P10, indicating no improvement throughout brain development during this period. *Parv* and *Th* both increased in expression from P3 to P10, remaining decreased compared to WT still, however *Npy* maintained around the same expression. This decrease in *Npy* expression in PA mutant mice compared to WT was not reflected in our immunofluorescence data. Interestingly, key interneuron subtypes that were deregulated were somatostatin and parvalbumin positive interneurons. At postnatal day 0, Lee *et al.* did not observe any differences to these two interneuron subtypes in the cortex of mutant mice (Lee *et al.*, 2017). However, both of these cells increase in population throughout postnatal life. The differences in interneuron deficits between studies in each of the two mouse models for the PA1 and PA2 mutations are outlined in Table 5.3, with results from this study summarised in Table 5.4. These will be discussed further in 5.4.2.

An interesting outcome of our gene expression data was the reduction in *Chat* and *Th* at P10 in both PA1 and PA2 mice. *Chat* and *Th* are expressed by cholinergic neurons, which use acetylcholine (ACh) as their primary neurotransmitter (Ahmed *et al.*, 2019). Changes to the function of cholinergic neurons can lead to disruptions in motor control, which provides a possible explanation for the reduced neuromuscular strength we observed in PA mutant mice

in Chapter 3 (Bordia *et al.*, 2016, Ahmed *et al.*, 2019). Disruptions of these neurons can also reduce the capacity of behavioural flexibility, memory and social behaviour in mice. As such, our findings are consistent with these deficits not being rescued with estradiol treatment, and are likely to contribute to the sustained intellectual disability phenotype, despite the reduction in seizures we observed (Albert-Gascó *et al.*, 2017, Martos *et al.*, 2017, Okada *et al.*, 2018, Ahmed *et al.*, 2019).

Table 5.3: Interneuron deficits present in the PA1 and PA2 mouse models from different studies at different timepoints.

	Embryonic	Postnatal day 0	Approx. 1 month	Adult	Publication
PA1 Kitamura model		↓ Npy, Sst, GABA	↓ Chat		Kitamura <i>et al.</i> 2009
		↓ Cb, GABA			Lee <i>et al.</i> 2017
PA1 Price model			↓ Npy, Cb		Price <i>et al.</i> 2009
				↓ Npy, Cb Npy, Cb ↑with E2	Olivetti <i>et al.</i> 2014
PA2 Kitamura model			↓ Chat		Kitamura <i>et al.</i> 2009
		↓ Cb, GABA			Lee <i>et al.</i> 2017
PA2 Dubos model	↓ Cb, Cr, Chat	↓ Cb, Sst		↓ Cb, Chat	Dubos <i>et al.</i> 2018

Legend: Neuropeptide-Y (Npy), calbindin (Cb), calretinin (Cr), somatostatin (Sst), cholinergic (Chat), parvalbumin (Parv), gamma aminobutyric acid (GABA).

Table 5.4: Interneuron deficits in PA mutant mice in this study.

		P3	P10		
		Untreated	Untreated	Vehicle	E2
PA1	Gene expression	↓ Npy, Sst, Parv	↓ Npy, Sst, Parv, Chat	↓ Sst, Parv, Chat	
	Cell density			No change - Npy, Cb	No change - Npy, Cb
PA2	Gene expression	↓ Npy, Sst	↓ Npy, Sst, Chat	↓ Sst, Parv, Chat	
	Cell density			No change - Npy, Cb	No change - Npy, Cb

Legend: Neuropeptide-Y (Npy), calbindin (Cb), somatostatin (Sst), cholinergic (Chat), parvalbumin (Parv).

5.4.2 Differences in interneuron findings between studies

The discrepancies in interneuron findings between our findings and published studies, are described in Tables 5.3 and 5.4. A major contributor in differences reported may be due to the time period studied. Most interneuron investigations in the Kitamura *et al.* mouse models have been performed early in development, while many of the Price *et al.* PA1 mouse studies have been performed in adulthood. The expression of interneuron populations changes across different stages of brain development. For example somatostatin and parvalbumin subtypes primarily disturbed in our gene expression data, are expressed highly from P14-P28 compared to embryonic and early postnatal life (Lein *et al.*, 2007). This highlights that a systematic evaluation of changes to interneuron subtype expression and changes to cell density of interneuron populations within different cortical layers, with and without treatment, is warranted.

We also observed some differences in the interneuron subtypes improved with estradiol treatment, when compared to the study in the Price *et al.* PA1 mouse model. Olivetti and colleagues showed an improvement in neuropeptide-Y and calbindin interneuron density in response to treatment. Again, this was reported in the adult brain in specific brain regions. It is possible that the effects of estradiol on this subset of interneurons requires additional time to manifest in a significant change to cellular density in the brain, as opposed to our study, where we examined the brain immediately following treatment. This may contribute to the increase in interneuron associated genes we observed at P10, immediately following treatment cessation, but not with limited effect at the cellular level.

From our studies, we contend that the effect of estradiol on interneurons is only part of the impact of estradiol treatment leading to alleviation of seizures in PA mutant mice. A number of pathways and genes are deregulated with estradiol treatment. As such, the direct effects of treatment may not be easily detected at the cellular level in the brains of these mice. The exciting

aspect of this conclusion is that the additional pathways estradiol is targeting may provide potential targets for the treatment for other epileptic disorders, not just those caused by interneuron deficits.

5.4.3 Future experiments for interneurons in PA mutant mice

There are multiple ways interneurons are able to be investigated in the brains of PA mutant mice, and with advances in transcriptomic techniques we believe a single-cell RNA sequencing approach would be beneficial. This would allow a comprehensive investigation of the gene expression profiles of individual cell types impacted by mutations in *Arx*, including progenitor inhibitory and excitatory neurons. Given the small number of cells of the brain that are affected by the mutations in *Arx*, this approach would have the ability to determine small and direct effects in different subsets of specific neural cell types (Aevermann *et al.*, 2018, Chen *et al.*, 2019). This type of deep investigation could potentially determine specific and novel treatment targets to treat multiple aspects of the disease phenotype, including cognition and mortality, not just seizures.

By investigating treatments that target interneurons more directly, we could potentially treat the intellectual disability side of the PA mutant phenotype. Despite improving seizure frequency and severity with estradiol, cognitive effects remained unchanged, with deficits to anxiety, social cognition, and hyperactivity. Interneuron dysfunction is responsible for a number of neurodevelopmental disorders, such as autism, epileptic syndromes, and even schizophrenia, and hence treatments targeting these specific cells may help alleviate phenotypes for patients with these other disorders. Hence, investigating these important cells is key for not just patients with *ARX* mutations, but those with a broad umbrella of disorders termed “interneuronopathies”.

5.5 Study Outcomes

Through a comprehensive study of interneuron associated genes in untreated mutant mice at P3 and P10, we showed disruptions to *Npy*, as well as deregulation of somatostatin, parvalbumin and vasoactive intestinal protein positive interneurons. This disruption to interneurons was sustained throughout this early period of development. We conclude that this early disruption to genes involved in the function and development of interneurons, caused by these partial loss of function mutations in *Arx*, is at least partially responsible for the intellectual disability and seizure phenotype we see in PA mutant mice. However, despite estradiol improving seizure frequency and severity in both PA1 and PA2 mice, we did not detect any increase to the cell density of calbindin and neuropeptide-Y positive interneurons at P10, immediately following the last dose of treatment. We believe that further analysis on the interneuron deficits in PA mutant mice would be beneficial for finding novel treatment targets for children with these mutation, but also for patients with other interneuronopathies, such as epilepsy, autism and schizophrenia.

Chapter Six:

Discussion

6.1 Novel findings of this project

My PhD project provides novel insights into the behavioural and molecular phenotype of the *Arx* PA1 and PA2 mouse models, and contributes to the understanding of how 17 β -estradiol treatment works to reduce the frequency and severity of seizures in these mice. For the first time, I have shown that there are abnormal behavioural traits present early in postnatal life prior to the peak of seizure onset in PA mutant mice, and that there is no regression of behavioural deficits or cognition between one and two months of age. PA1 and PA2 mutant mice have been shown to have deficits to social cognition, anxiety and fear response, and learning and memory at two months of age (Jackson *et al.*, 2017). However, determining the impact of severe and recurring seizures on the behavioural profile of these mice had not yet been examined. The behavioural deficits I established allowed me to determine whether or not improving seizures in PA mice via 17 β -estradiol treatment would subsequently improve these behaviour deficits. Unfortunately, despite my hypothesis, a cardinal finding of my project was that 17 β -estradiol treatment had no effect on behaviour in these mice, nor did the reduction in seizures reduce behavioural deficits later in development. Despite 17 β -estradiol treatment not improving the behavioural and cognitive phenotype of PA mutant mice, I showed efficacy in its use as anti-epileptic treatment when given in early postnatal life, at least in mice. This is the first time that 17 β -estradiol treatment has been shown to reduce seizure frequency and severity in the Kitamura *et al.* PA1 mouse model, as well as the PA2 mouse model, with the second model mirroring the most frequent *ARX* mutation seen in humans. This provides much needed reproducibility of results in two independent models of *Arx* mutations, with our collaborators demonstrating a reduction in seizures in a different PA1 mouse model (Price *et al.* model). Despite our work demonstrating the effectiveness of 17 β -estradiol as a treatment for seizures, we unfortunately cannot report that the improvement by reduction in seizure frequency and severity increased the survival of PA mutant mice.

To better understand the role of *Arx* in early postnatal life and the effects of estradiol treatment, we performed unbiased RNA sequencing on postnatal day 10 brains of PA1 and PA2 mice following treatment with 17 β -estradiol. This provided novel results on the ongoing effect of a partial loss of *Arx* early in brain development on the transcriptome of PA mutant mice in early postnatal life. We established the deregulated transcriptomic profile in PA1 and PA2 mutant mice (untreated) compared to wild-type littermates, and found that despite low *Arx* expression in the brain, genes associated with neurodevelopmental processes were deregulated. We determined that 17 β -estradiol treatment did not repair the deregulated transcriptome but instead recruited alternative gene pathways that we conclude contribute to the reduced seizure frequency and severity.

Another important finding of our study was the comprehensive analysis we performed of interneuron associated genes at P3 and P10 in untreated PA1 and PA2 mice. This analysis of interneuron genes across developmental time points has not been performed in these mutant mice, and we determined that many genes with deregulated expression persist from P3 to P10. Despite our immunofluorescence analysis at P10 showing no deficits in calbindin or neuropeptide-Y positive interneuron populations, we provided evidence for somatostatin, parvalbumin, neuropeptide-Y and cholinergic interneurons being deregulated in PA mutant mice early in postnatal day life. This analysis provides insight into specific subtypes of inhibitory cells that might be affected by the expanded polyalanine tract mutations in *Arx*, and provide evidence for mechanisms of disease.

We demonstrate neuromuscular deficits are present in both PA mutant mice for the first time. Patients with expansion mutations, particularly of the second polyalanine tract, feature dystonia of the hands as a significant part of their phenotype (Stromme *et al.*, 2002, Shoubridge *et al.*, 2010). This phenotype is referred to as Partington Syndrome with 63% of patients with expansions of PA2 having dystonic movements of the hands (Partington *et al.*, 2004). This

aspect of the phenotype was further characterised by Dubos *et al.* with impaired grasping movements of the hands in PA2 patients (Partington *et al.*, 2004, Dubos *et al.*, 2018). Generalised dystonia has been reported in patients with expansions of the first polyalanine tract. A report by Guerrini *et al.* reported six male patients with generalised dystonia that worsened to severe quadriplegic dyskinesia by two years of age (Guerrini *et al.*, 2007). My study found that PA2 mice had decreased grip strength in the inverted grid test compared to their wild-type littermates, perhaps not surprising as this is such a prominent feature in PA2 patients. Interestingly, PA1 mice also had reduced grip strength at two months of age (trending at one month but non-significant). The Price *et al.* PA1 mouse model presents with better performance in the rotarod test than their wild-type littermates, indicative of increased locomotor coordination (Price *et al.*, 2009). A different PA2 mouse model that has since been developed since the beginning of my project, has been reported to have a deficit in reaching and grasping (Dubos *et al.*, 2018). However, these two studies are the only reported information of neuromuscular strength deficits in any PA mouse models. My study provides novel findings for a neuromuscular strength deficit in the Kitamura *et al.* PA1 and PA2 mouse models. Unfortunately, estradiol treatment at the current dosage and timing of treatment did not improve this phenotypic outcome.

6.2 Reproducibility of pre-clinical trials

Reproducibility between preclinical trials is vital to the process of eventually getting novel therapies to human clinical trials. The rate of translation from preclinical trials to human clinical application is approximately 8% (Mak *et al.*, 2014). This low translation level is partially due to treatment and clinical studies from mice and humans often having quite different outcomes. However, increased understanding of molecular mechanisms behind inherited disorders has led to more relevant mouse models for treatment trials being established (Berry-Kravis *et al.*, 2018). The Kitamura and Price PA1 mouse models differ slightly in their seizure, behavioural and

cellular phenotypes, but both mice strongly recapitulate many aspects of the human phenotype in patients with PA1 expansion mutations in *ARX*.

Estradiol treatment early in postnatal life modelled in our study, based on the previous study by our collaborators (Olivetti *et al.*, 2014), shows vast effectiveness in reducing aspects of the seizure burden in PA1 mice, as well as PA2 mice. Moreover, treatment given very early in postnatal life provided lasting impact on reductions in seizures for up to 2 months of age (study end point) which spans the normal peak of seizures in these models. However, this regime of estradiol treatment failed to improve cognitive and behavioural outcomes in either mouse model. Reproducibility of behavioural testing can be difficult to measure in mice, using the *Fmr1*-KO mouse model of Fragile X Syndrome as an example, we can begin to understand why preclinical trials in intellectual disability models are challenging. Fragile X Syndrome is the most common genetic form of intellectual disability and autism in humans (Berry-Kravis *et al.*, 2018). The *Fmr1*-KO mouse model shows variability and small effect size in cognitive deficits, displaying differing results in standard behaviour tests in different laboratories and on different genetic backgrounds (Kazdoba *et al.*, 2014, Gross *et al.*, 2015, Leach *et al.*, 2016).

The effects of this early intervention with estradiol treatment on seizure outcomes in PA1 and PA2 mice is striking. This is the first study reporting the effects (or lack thereof) of estradiol on behaviour in the PA1 and PA2 mouse models. While intellectual disability is a cardinal feature of *ARX* mutations, inconsistent or small deficits in cognition and behaviour in a mouse model have the potential to limit the value of these particular mouse models for evaluating the effects of early estradiol treatment on behaviour. Future studies investigating the effects of a treatment outcome on intellectual disability models may benefit from using a touchscreen platform to investigate subtle changes to cognitive outcomes, with high translation of the behavioural phenotype to human cognitive outcomes (Horner *et al.*, 2013). Touchscreen testing in rodents

requires several months of training prior to testing. As such, the high and early mortality rate in the *Arx* mutant mice means this platform was not a viable option for us to consider.

6.3 Separating behaviour and seizures in PA mice

Separating behaviour from seizures is notoriously difficult, particularly when many neurodevelopmental disorders feature seizures as a co-morbidity, and many patients with epilepsy are known to have cognitive disabilities. As many as 30% of autistic children have epilepsy (Chow *et al.* 2019). There is a high number of genes that when mutated lead to not only intellectual disability but also present with autism and epilepsy. This suggests that convergent molecular processes are being impacted by a variety of genetic insults early in development. Epileptic encephalopathies are defined as disorders in which early, severe seizures contribute to cognitive and behavioural impairments (Nickels and Wirrell, 2017). While the exact mechanisms are yet to be determined, seizures early in development are thought to impair neurogenesis, synaptic reorganisation, and spinal loss in hippocampal neurons (Nickels and Wirrell, 2017). Individuals predisposed to epileptic syndromes are highly correlated with intellectual disability, even in the absence of seizures (Nickels and Wirrell, 2017). All patients with mutations in *ARX* have intellectual disability, but the extent to which seizures contribute to the cognitive impairment is not clear.

Analysing the behavioural comorbidities in children with severe epilepsy can be challenging. In humans, it can be difficult to interpret whether behavioural abnormalities and cognitive regression are primary or secondary conditions, occurring before or after the onset of seizures, and if these phenotypic aspects worsen with seizures. This can be further complicated by the effects that anti-epileptic drugs may have on cognition and behaviour (Thompson *et al.*, 2000, Mazarati, 2019). Animal models like the PA mutant mice provide the capacity to test if the primary cognitive deficits are present (and at what level) before the onset of seizures. For the first time in an *Arx* mutant mouse model, we have demonstrated that behavioural deficits in

sociability, anxiety, neuromuscular strength and hyperactivity, are all present prior to the major peak of seizure onset compared to wild-type littermates. Furthermore, we have shown that these traits do not change between one and two months of age despite the frequency and severity of seizures that PA1 and PA2 mice present with (with or without estradiol treatment). This leads us to suggest that expanded PA mutations in *ARX* may not cause traditional epileptic encephalopathies in humans. This is supported by the lack of cognitive regression observed in the mouse models, and limited evidence of regression of cognitive or behavioural deficits in patients. This is a cardinal finding for novel therapeutic development for these disorders, as a drug that targets seizures may not necessarily be effective for the intellectual disability in these patients, as observed in our study. Hence, treating intellectual disability in *ARX* patients remains problematic to address, particularly with such an early onset of phenotype, and the embryonic expression of the gene.

The timing of treatment remains one of the most significant challenges in treating children with genetic mutations that cause neurodevelopmental disorders, such as *ARX*. The timing of key neurodevelopmental events, particularly interneuron development, takes part in mostly prenatal period in humans. In contrast, this process is still being completed in early postnatal life in mice. Hence, this time is available to target in the *Arx* mutant mice used in my PhD project with the period of estradiol treatment from postnatal days 3 to 10 but is equivalent to prenatal development of the brain in humans. In addition, the initial genetic insult we are modelling reflects *ARX* expression that is largely restricted to embryonic life. This undoubtedly presents a limitation of my study. However, given estradiol treatment during early postnatal period is effective at treating seizure frequency and severity in the PA mouse models, it provides important results for how exogenous steroids may impact the transcriptome of the brain, and enable identification of the potential pathways activated.

6.4 Understanding the transcriptome of the developing PA brain in early postnatal life

Despite low levels of *Arx* expression in the postnatal brain we wanted to establish the impact of PA mutations in *Arx* on the transcriptome in PA1 and PA2 mutant mice during early postnatal development. The genes that were deregulated in the PA1 and PA2 mutant mice at P10 were enriched for those involved with neurodevelopment, especially interneuron function. It is attractive to speculate that these deregulated interneuron genes contribute to the sustained seizures and behavioural phenotype reported in these PA mouse models. *Arx* is a transcriptional regulator and activator in embryonic brain development, so it was fascinating to see how the effects of a partial loss of function of this gene early in embryonic life impacts the brains of these mice, still at postnatal day 10. Many *Arx* target and responsive genes remain deregulated in our P10 data. This is interesting given that *Arx* expression is normally very low in the postnatal brain. Hence, I hypothesise that the loss of *Arx* during early development causes a “ripple” effect, with these genes and downstream targets being dysregulated even when *Arx* expression (and function) would normally be minimal.

My original hypothesis was that estradiol treatment would improve seizure frequency and severity by rescuing the interneuron deficits present in the brain of PA mutant mice. This is the mechanism of action proposed by our collaborators when estradiol proved effective in the alternate Price *et al.* PA1 mouse model (Olivetti *et al.*, 2014). However, while interneuron associated genes were deregulated without estradiol treatment, the majority of the deregulated transcriptome was unchanged by estradiol treatment. There was only a small overlap in genes deregulated by disease alone and the subsequent response to estradiol treatment. Furthermore, our immunofluorescence analysis of the brain did not indicate any increase to interneurons positive for calbindin or neuropeptide-Y with estradiol treatment. My analysis of the transcriptome following estradiol treatment indicates different pathways and processes are impacted compared to those initially disrupted. This is a potentially exciting finding as the beneficial effect of estradiol treatment may be useful for diminishing the severity of seizures

across a number of genetic causes of neurodevelopmental disorders where interneuron deficiency is not the mechanism of pathogenesis, such as epilepsies caused by disturbed excitatory neuron output. Instead our data leads us to propose that estradiol treatment acts via direct and non-direct estrogen signalling to change gene expression in pathways involved in transcriptional regulation, synaptic activity, neuronal development and other key brain related processes, to activate and repress genes outside of the disturbed PA transcriptome. The fact that estradiol did not act upon the same inhibitory neuron processes disrupted by the PA mutations may provide some explanation as to why treatment did not improve the cognitive phenotype in these mice.

6.5 Future directions

We have shown a reproducible effect of estradiol on the seizure phenotype of the PA1 and PA2 mice in my study compared to an independent PA mouse model. However, my findings are in contrast when compared to induced models of seizures in mice. In an induced rat model of infantile spasms, the same dose (40ng/g) of estradiol did not reduce spasms, even while increasing the number of GABAergic cells in the neocortex (Chachua *et al.*, 2016). The investigators concluded that estradiol treatment may only be effective in genetic models of interneuronopathies, and not in artificially induced seizure models, in this case, by using betamethasone and N-methyl-D-aspartic acid (NMDA). Genetic models of epilepsy and seizures have an advantage in regards to induced seizures models of implementing treatments early in development, prior to seizure onset. This is the case with the Olivetti *et al.* (2014) study, where early postnatal (P3-10) but not late (P33-40) estradiol treatment produced prolonged activation of estrogen receptors and gave an extended anti-epileptogenic effect. These anti-epileptogenic effects of estradiol remain relatively unexplored. Much of the field has focused on the pro-epileptogenic effects of estradiol in female rodents, with oral contraceptives facilitating increased seizure activity and accelerating the rate of seizure onset in female mice (Younus and Reddy, 2016). Further investigation into the effects of estradiol in

neurodevelopmental models exhibiting seizures, even if not associated with interneuron deficits, would be particularly useful to further understand the anti-epileptogenic effects of low dose estradiol treatment.

Fortunately, we found no adverse effects of 40ng/g 17 β -estradiol for the seven-day period mice were treated in our study. Selective estrogen receptor modulators (SERMs) may be a potential treatment for epilepsy, without side effects that may come with higher doses of estradiol. While the research is still in early stages, raloxifene, a SERM currently authorised for treatment of osteoporosis, has shown promising results for treating epilepsy in post-menopausal women, for whom estradiol treatment is inadvisable (Pottoo *et al.*, 2014). However, these preliminary studies have been in post-menopausal women (as with many studies into estradiol and epilepsy). In contrast, my project provides insight into low dose estradiol treatment in young, male mice. Interestingly, adjunct treatment of raloxifene may improve cognitive functioning, something we did not find estradiol treatment improved. A pilot study in schizophrenia patients using raloxifene with a calcium channel blocker, found that cognitive tests assessing memory were significantly improved with treatment (Pottoo *et al.*, 2020). SERMs may provide a potential therapeutic target for neurodevelopmental disorders with both epilepsy and intellectual disability as key components of the clinical phenotype.

My project utilised a bulk RNA sequencing technique to investigate the broad effects of *Arx* PA expansion mutations on the cortex of the brain. This approach has several limitations, including that gene expression levels are impacted by the proportion of individual cell types within the tissue, and the relative abundance of these cells, which in this case include excitatory and inhibitory neurons, as well as other cell lineages of the brain, such as abundant astrocytes (Sutton and Voineagu, 2020). With the advances in the techniques (including availability and cost) future experiments in these PA mice would benefit from using single cell RNA sequencing approaches to study the gene expression profiles deregulated by *Arx* mutations. The increased

resolution would have the capacity to determine the small but direct effects of a partial loss of *Arx* in subsets of cells and cell types. This approach could potentially determine the impact of these mutations and subsequent treatment on interneurons within the cortex specifically. Whilst potentially very powerful, this technology still has limitations. Due to the lower input of single cell RNA sequencing, there is often higher levels of “noise” within the sample which requires additional analysis power. This method provides a sparse data set, with only a small subset of genes detected per cell (Sutton and Voineagu, 2020). To overcome these challenges a process of deconvolution could be utilised to enhance the usefulness of the pre-existing bulk RNA sequencing data obtained in my study. Deconvolution estimates the cellular composition of a tissue sample from its gene expression profile. This then allows approximate separation of gene expression patterns of each individual cell type within the tissue (Sutton and Voineagu, 2020). This method could allow separation of inhibitory interneuron gene expression from our data set of the postnatal day 10 cortex. Colleagues within my collaborator’s laboratory (Prof. Jozef Gecz, University of Adelaide, Australia) are currently building upon the limited methods for deconvolution of bulk RNA sequencing brain data, developing expertise in this growing field. Application of this analysis to gene expression studies in neurodevelopmental mouse models, including the *Arx* PA1 and PA2 mice would be of great interest to discovery and translational scientists alike.

Currently there are only 34 clinical trials underway for infantile spasms in North America (www.clinicaltrials.gov). The discovery of new anti-epileptic drugs has been limited in recent times, and newer drugs have not yet shown increased efficacy over traditional therapies to date (Rho and White, 2018). The traditional anti-epileptic drugs are often of limited use against the refractory seizures in infantile spasms patients, including those with PA expansion mutations. While estradiol may provide a unique therapeutic approach to treating infantile spasms, the research is currently still limited, and treating male patients with high doses may prove problematic. Cannabidiol is currently being used in five clinical trials in North America

(www.clinicaltrials.gov). Cannabidiol is the non-hallucinogenic component of cannabis, and while its direct anti-epileptic mechanism of action is unknown, there are promising studies emerging. The endocannabinoid system is being increasingly associated with seizure activity, and uses endocannabinoid receptors CB₁ and CB₂ (Gaston and Szaflarski, 2018). Cannabidiol may have antagonist activity for these receptors, as well as blocking amandamide uptake, increasing its availability to activate CB₁ and CB₂ (Wallace *et al.*, 2001, Thomas *et al.*, 2007). Interestingly in terms of my study, there are now overlapping molecular pathways associated with CB₁ and CB₂ and estrogens (Dobovišek *et al.*, 2016). 17 β -estradiol has been shown to regulate the expression of CB₁ in the brain in particular, and can increase the expression of both CB₁ and CB₂ in osteoblasts (Riebe *et al.*, 2010, Rossi *et al.*, 2013). Estrogen and cannabinoid receptors both activate the protein kinase A, cAMP, MAPK and PI3K pathways, and selective estrogen receptor modulating drugs have been shown to also act as agonists to CB₁ and CB₂ (Dobovišek *et al.*, 2016, Dobovišek *et al.*, 2020). Cannabidiol has recently been shown to be effective in treating refractory seizures (with sustained results) in Dravet syndrome patients, providing promising results for neurodevelopmental disorders with refractory epilepsy as a comorbidity (Moore and Robinson, 2018, Devinsky *et al.*, 2019). With the interactions between estradiol and Cannabidiol becoming increasingly known, it is possible that the two drugs could act as adjunct therapies in treating these refractory seizures in neurodevelopmental patients.

6.6 Concluding remarks

Throughout my PhD project, I have investigated the effects of daily, short-term estradiol treatment given for 7 days in early postnatal life, to mice with expansion mutations in the first and second polyalanine tracts of *Arx*. I have documented the impact of estradiol treatment on seizures, cognition and behaviour, and investigated the transcriptomic profile of the brain in these mice. Estradiol treatment significantly reduced both the frequency and severity of seizures in the PA1 mouse model, and a model of the most common *ARX* mutation, PA2, in agreement with previous studies in an alternate PA1 mouse model. This provides reproducibility in pre-

clinical animal studies, an important outcome of my project. Animal studies involving therapeutic targets for neurodevelopmental disorders are notoriously difficult to reproduce, but with the remarkable recapitulation of the patient phenotype in both of these PA mouse model, this reproducibility is promising in a field where new therapies for spasms and seizures have been lacking. However, the challenge remains in treating a disorder which impacts the brain in embryonic life, and we have still yet to show improvement to the debilitating intellectual disability aspect of *ARX* PA mutations. Importantly, we continue to uncover novel insights into the pathogenesis of PA mutations, showing the ongoing effects of a partial loss of *Arx* to the transcriptome at postnatal day 10, even with limited expression of *Arx* at this age. The association of interneurons of the cortex uncovered in my studies provides new insights into the cortex of these mice, and how different gene pathways contribute to the dramatic seizure phenotype of these mice, as well as the persistent anxiety and autistic-like behaviour. Although estradiol may not represent a clinical therapy for PA patients currently, by bettering our understanding of the mechanisms of disease and the impacts of estradiol treatment and outcomes on phenotype may provide critical insights to develop this as a potential adjunct therapy with other novel anti-epileptic drugs. Taken together, my data indicates strongly that estradiol treatment recruits processes and pathways reducing the frequency and severity of seizures in the *Arx* PA mutant mice, without precisely correcting the deregulated transcriptome, nor improving mortality or cognitive deficits. It is my firm belief that future studies will find my investigation into estradiol treatment for PA mutant mice valuable. It is my sincere hope that my studies may contribute to development of an effective therapy for infantile spasms and seizures with associated intellectual disability for patients and their families in the near future.

References

Absoud M, Parr JR, Halliday D, Pretorius P, Zaiwalla Z, Jayawant S. A novel ARX phenotype: rapid neurodegeneration with Ohtahara syndrome and a dyskinetic movement disorder. *Developmental Medicine & Child Neurology*. 2010;52(3):305-7.

Aevermann BD, Novotny M, Bakken T, Miller JA, Diehl AD, Osumi-Sutherland D, et al. Cell type discovery using single-cell transcriptomics: implications for ontological representation. *Human Molecular Genetics*. 2018;27(R1):R40-R7.

Ahmed NY, Knowles R, Dehorter N. New Insights Into Cholinergic Neuron Diversity. *Frontiers in Molecular Neuroscience*. 2019;12(204).

Albert-Gascó H, García-Avilés Á, Moustafa S, Sánchez-Sarasua S, Gundlach AL, Olucha-Bordonau FE, et al. Central relaxin-3 receptor (RXFP3) activation increases ERK phosphorylation in septal cholinergic neurons and impairs spatial working memory. *Brain Struct Funct*. 2017;222(1):449-63.

Anderson SA, Eisenstat DD, Shi L, Rubenstein JLR. Interneuron Migration from Basal Forebrain to Neocortex: Dependence on *Dlx* Genes. *Science*. 1997;278(5337):474.

Azcoitia I, Barreto GE, Garcia-Segura LM. Molecular mechanisms and cellular events involved in the neuroprotective actions of estradiol. Analysis of sex differences. *Frontiers in Neuroendocrinology*. 2019;55:100787.

Benes FM, Berretta S. GABAergic Interneurons: Implications for Understanding Schizophrenia and Bipolar Disorder. *Neuropsychopharmacology*. 2001;25:1.

Berry-Kravis EM, Lindemann L, Jønch AE, Apostol G, Bear MF, Carpenter RL, et al. Drug development for neurodevelopmental disorders: lessons learned from fragile X syndrome. *Nat Rev Drug Discov*. 2018;17(4):280-99.

Bienvenu T, Poirier K, Friocourt G, Bahi N, Beaumont D, Fauchereau F, et al. ARX, a novel Prd-class-homeobox gene highly expressed in the telencephalon, is mutated in X-linked mental retardation. *Human Molecular Genetics*. 2002;11(8):981-91.

Bienvenu T, Poirier K, Friocourt G, Bahi N, Beaumont D, Fauchereau F, et al. ARX, a novel Prd-class-homeobox gene highly expressed in the telencephalon, is mutated in X-linked mental retardation. *Hum Mol Genet*. 2002;11(8):981-91.

Biressi S, Messina G, Collombat P, Tagliafico E, Monteverde S, Benedetti L, et al. The homeobox gene *Arx* is a novel positive regulator of embryonic myogenesis. *Cell Death Differ*. 2007;15(1):94-104.

Bordia T, Zhang D, Perez XA, Quik M. Striatal cholinergic interneurons and D2 receptor-expressing GABAergic medium spiny neurons regulate tardive dyskinesia. *Exp Neurol*. 2016;286:32-9.

Boulware MI, Mermelstein PG. Membrane estrogen receptors activate metabotropic glutamate receptors to influence nervous system physiology. *Steroids*. 2009;74(7):608-13.

Bourdeau V, Deschênes J, Métivier R, Nagai Y, Nguyen D, Bretschneider N, et al. Genome-wide identification of high-affinity estrogen response elements in human and mouse. *Mol Endocrinol*. 2004;18(6):1411-27.

Brunson KL, Avishai-Eliner S, Baram TZ. ACTH TREATMENT OF INFANTILE SPASMS: MECHANISMS OF ITS EFFECTS IN MODULATION OF NEURONAL EXCITABILITY. *International review of neurobiology*. 2002;49:185-97.

Buchsbaum IY, Cappello S. Neuronal migration in the CNS during development and disease: insights from *in vivo* and *in vitro* models. *Development*. 2019;146(1):dev163766.

Butler LS, Silva AJ, Abeliovich A, Watanabe Y, Tonegawa S, McNamara JO. Limbic epilepsy in transgenic mice carrying a Ca^{2+} /calmodulin-dependent kinase II alpha-subunit mutation. *Proceedings of the National Academy of Sciences*. 1995;92(15):6852.

Buzsáki G. Feed-forward inhibition in the hippocampal formation. *Progress in Neurobiology*. 1984;22(2):131-53.

Chachua T, Di Grazia P, Chern C-R, Johnkutty M, Hellman B, Lau HA, et al. Estradiol does not affect spasms in the betamethasone-NMDA rat model of infantile spasms. *Epilepsia*. 2016;57(8):1326-36.

Chen G, Ning B, Shi T. Single-Cell RNA-Seq Technologies and Related Computational Data Analysis. *Front Genet*. 2019;10:317-.

Chiurazzi P, Pirozzi F. Advances in understanding - genetic basis of intellectual disability. *F1000Res*. 2016;5.

Cho IT, Lim Y, Golden JA, Cho G. Aristaless Related Homeobox (ARX) Interacts with β -Catenin, BCL9, and P300 to Regulate Canonical Wnt Signaling. *PLoS One*. 2017;12(1):e0170282.

Colasante G, Collombat P, Raimondi V, Bonanomi D, Ferrai C, Maira M, et al. Arx Is a Direct Target of Dlx2 and Thereby Contributes to the Tangential Migration of GABAergic Interneurons. *The Journal of Neuroscience*. 2008;28(42):10674-86.

Colasante G, Sessa A, Crispi S, Calogero R, Mansouri A, Collombat P, et al. Arx acts as a regional key selector gene in the ventral telencephalon mainly through its transcriptional repression activity. *Developmental Biology*. 2009;334(1):59-71.

Colasante G, Simonet JC, Calogero R, Crispi S, Sessa A, Cho G, et al. ARX regulates cortical intermediate progenitor cell expansion and upper layer neuron formation through repression of Cdkn1c. *Cereb Cortex*. 2015;25(2):322-35.

Colombo E, Collombat P, Colasante G, Bianchi M, Long J, Mansouri A, et al. Inactivation of Arx, the Murine Ortholog of the X-Linked Lissencephaly with Ambiguous Genitalia Gene, Leads to Severe Disorganization of the Ventral Telencephalon with Impaired Neuronal Migration and Differentiation. *The Journal of neuroscience : the official journal of the Society for Neuroscience*. 2007;27(17):4786-98.

Crabbe JC, Wahlsten D, Dudek BC. Genetics of mouse behavior: Interactions with laboratory environment. *Science*. 1999;284(5420):1670-2.

Cristóvão JS, Santos R, Gomes CM. Metals and Neuronal Metal Binding Proteins Implicated in Alzheimer's Disease. *Oxid Med Cell Longev*. 2016;2016:9812178-.

Curie A, Friocourt G, des Portes V, Roy A, Nazir T, Brun A, et al. Basal ganglia involvement in ARX patients: The reason for ARX patients very specific grasping? *NeuroImage : Clinical*. 2018;19:454-65.

De Carlos JA, López-Mascaraque L, Valverde F. Dynamics of Cell Migration from the Lateral Ganglionic Eminence in the Rat. *The Journal of Neuroscience*. 1996;16(19):6146.

Degen M, Brellier F, Kain R, Ruiz C, Terracciano L, Orend G, et al. Tenascin-W is a novel marker for activated tumor stroma in low-grade human breast cancer and influences cell behavior. *Cancer Res*. 2007;67(19):9169-79.

Devinsky O, Nabbout R, Miller I, Laux L, Zolnowska M, Wright S, et al. Long-term cannabidiol treatment in patients with Dravet syndrome: An open-label extension trial. *Epilepsia*. 2019;60(2):294-302.

Dobovišek L, Hojnik M, Ferik P. Overlapping molecular pathways between cannabinoid receptors type 1 and 2 and estrogens/androgens on the periphery and their involvement in the pathogenesis of common diseases (Review). *Int J Mol Med*. 2016;38(6):1642-51.

Dobovišek L, Krstanović F, Borštnar S, Debeljak N. Cannabinoids and Hormone Receptor-Positive Breast Cancer Treatment. *Cancers (Basel)*. 2020;12(3):525.

Dombret C, Naulé L, Trouillet A-C, Parmentier C, Hardin-Pouzet H, Mhaouty-Kodja S. Effects of neural estrogen receptor beta deletion on social and mood-related behaviors and underlying mechanisms in male mice. *Scientific Reports*. 2020;10(1):6242.

Dubos A, Meziane H, Iacono G, Curie A, Riet F, Martin C, et al. A new mouse model of ARX dup24 recapitulates the patients' behavioral and fine motor alterations. *Hum Mol Genet*. 2018;27(12):2138-53.

Ellis CA, Petrovski S, Berkovic SF. Epilepsy genetics: clinical impacts and biological insights. *Lancet Neurol*. 2020;19(1):93-100.

Farwell JR, Dodrill CB, Batzel LW. Neuropsychological Abilities of Children with Epilepsy. *Epilepsia*. 1985;26(5):395-400.

Fogarty M, Grist M, Gelman D, Marín O, Pachnis V, Kessar N. Spatial Genetic Patterning of the Embryonic Neuroepithelium Generates GABAergic Interneuron Diversity in the Adult Cortex. *The Journal of Neuroscience*. 2007;27(41):10935.

Friocourt G, Kanatani S, Tabata H, Yozu M, Takahashi T, Antypa M, et al. Cell-Autonomous Roles of ARX in Cell Proliferation and Neuronal Migration during Corticogenesis. *The Journal of Neuroscience*. 2008;28(22):5794.

Friocourt G, Parnavelas JG. Mutations in ARX Result in Several Defects Involving GABAergic Neurons. *Frontiers in Cellular Neuroscience*. 2010;4:4.

Friocourt G, Parnavelas JG. Identification of Arx targets unveils new candidates for controlling cortical interneuron migration and differentiation. *Frontiers in Cellular Neuroscience*. 2011;5:28.

Fulp CT, Cho G, Marsh ED, Nasrallah IM, Labosky PA, Golden JA. Identification of Arx transcriptional targets in the developing basal forebrain. *Hum Mol Genet*. 2008;17(23):3740-60.

Galanopoulou AS, Mowrey WB, Liu W, Li Q, Shandra O, Moshé SL. Preclinical Screening for Treatments for Infantile Spasms in the Multiple Hit Rat Model of Infantile Spasms: An Update. *Neurochemical Research*. 2017;42(7):1949-61.

Gaston TE, Szaflarski JP. Cannabis for the Treatment of Epilepsy: an Update. *Curr Neurol Neurosci Rep*. 2018;18(11):73.

Géczy J, Cloosterman D, Partington M. ARX: a gene for all seasons. *Current Opinion in Genetics & Development*. 2006;16(3):308-16.

Gestinari-Duarte Rde S, Santos-Rebouças CB, Boy RT, Pimentel MM. ARX mutation c.428-451dup (24bp) in a Brazilian family with X-linked mental retardation. *Eur J Med Genet*. 2006;49(3):269-75.

Ghisletti S, Meda C, Maggi A, Vegeto E. 17beta-estradiol inhibits inflammatory gene expression by controlling NF-kappaB intracellular localization. *Mol Cell Biol*. 2005;25(8):2957-68.

Gould E, Woolley CS, Frankfurt M, McEwen BS. Gonadal steroids regulate dendritic spine density in hippocampal pyramidal cells in adulthood. *Journal of Neuroscience*. 1990;10(4):1286-91.

Gross C, Hoffmann A, Bassell GJ, Berry-Kravis EM. Therapeutic Strategies in Fragile X Syndrome: From Bench to Bedside and Back. *Neurotherapeutics*. 2015;12(3):584-608.

Guerrini R, Moro F, Kato M, Barkovich AJ, Shiihara T, McShane MA, et al. Expansion of the first PolyA tract of ARX causes infantile spasms and status dystonicus. *Neurology*. 2007;69(5):427-33.

Gulyás AI, Tóth K, Dános P, Freund TF. Subpopulations of GABAergic neurons containing parvalbumin, calbindin D28k, and cholecystokinin in the rat hippocampus. *The Journal of Comparative Neurology*. 1991;312(3):371-8.

Hancock EC, Osborne JP, Edwards SW. Treatment of infantile spasms. *Cochrane Database of Systematic Reviews*. 2013(6).

Hånell A, Marklund N. Structured evaluation of rodent behavioral tests used in drug discovery research. *Frontiers in Behavioral Neuroscience*. 2014;8(252).

Hanslick JL, Lau K, Noguchi KK, Olney JW, Zorumski CF, Mennerick S, et al. Dimethyl sulfoxide (DMSO) produces widespread apoptosis in the developing central nervous system. *Neurobiol Dis*. 2009;34(1):1-10.

Haug K, Kremerskothen J, Hallmann K, Sander T, Dullinger J, Rau B, et al. Mutation screening of the chromosome 8q24.3-human activity-regulated cytoskeleton-associated gene (ARC) in idiopathic generalized epilepsy. *Mol Cell Probes*. 2000;14(4):255-60.

Heller RS, Jenny M, Collombat P, Mansouri A, Tomasetto C, Madsen OD, et al. Genetic determinants of pancreatic ϵ -cell development. *Developmental Biology*. 2005;286(1):217-24.

Higo S, Udaka N, Tamamaki N. Long-range GABAergic projection neurons in the cat neocortex. *The Journal of Comparative Neurology*. 2007;503(3):421-31.

Hom AC, Leppik IE, Rask CA. Effects of estradiol and progesterone on seizure sensitivity in oophorectomized DBA/2J mice and C57/EL hybrid mice. *Neurology*. 1993;43(1):198-204.

Horner AE, Heath CJ, Hvoslef-Eide M, Kent BA, Kim CH, Nilsson SRO, et al. The touchscreen operant platform for testing learning and memory in rats and mice. *Nature protocols*. 2013;8(10):1961-84.

Hrachovy RA, Frost JD. Chapter 63 - Infantile spasms. In: Dulac O, Lassonde M, Sarnat HB, editors. *Handbook of Clinical Neurology*: Elsevier; 2013. p. 611-8.

Huang da W, Sherman BT, Lempicki RA. Bioinformatics enrichment tools: paths toward the comprehensive functional analysis of large gene lists. *Nucleic Acids Res*. 2009;37(1):1-13.

Huang da W, Sherman BT, Lempicki RA. Systematic and integrative analysis of large gene lists using DAVID bioinformatics resources. *Nat Protoc*. 2009;4(1):44-57.

Huentelman MJ, Muppala L, Corneveaux JJ, Dinu V, Pruzin JJ, Reiman R, et al. Association of SNPs in EGR3 and ARC with Schizophrenia Supports a Biological Pathway for Schizophrenia Risk. *PLoS One*. 2015;10(10):e0135076.

Jackson MR, Lee K, Mattiske T, Jaehne EJ, Ozturk E, Baune BT, et al. Extensive phenotyping of two ARX polyalanine expansion mutation mouse models that span clinical spectrum of intellectual disability and epilepsy. *Neurobiology of Disease*. 2017;105:245-56.

Jinno S, Kosaka T. Patterns of expression of neuropeptides in GABAergic nonprincipal neurons in the mouse hippocampus: Quantitative analysis with optical disector. *The Journal of Comparative Neurology*. 2003;461(3):333-49.

Kanehisa M. Toward understanding the origin and evolution of cellular organisms. *Protein Sci*. 2019;28(11):1947-51.

Kanehisa M, Goto S. KEGG: kyoto encyclopedia of genes and genomes. *Nucleic Acids Res*. 2000;28(1):27-30.

Kanehisa M, Sato Y, Furumichi M, Morishima K, Tanabe M. New approach for understanding genome variations in KEGG. *Nucleic Acids Res*. 2019;47(D1):D590-D5.

Kato M, Das S, Petras K, Kitamura K, Morohashi K-i, Abuelo DN, et al. Mutations of ARX are associated with striking pleiotropy and consistent genotype–phenotype correlation. *Human Mutation*. 2004;23(2):147-59.

Kazdoba TM, Leach PT, Silverman JL, Crawley JN. Modeling fragile X syndrome in the Fmr1 knockout mouse. *Intractable Rare Dis Res*. 2014;3(4):118-33.

Kitamura K, Itou Y, Yanazawa M, Ohsawa M, Suzuki-Migishima R, Umeki Y, et al. Three human ARX mutations cause the lissencephaly-like and mental retardation with epilepsy-like pleiotropic phenotypes in mice. *Human Molecular Genetics*. 2009;18(19):3708-24.

Kitamura K, Yanazawa M, Sugiyama N, Miura H, Iizuka-Kogo A, Kusaka M, et al. Mutation of ARX causes abnormal development of forebrain and testes in mice and X-linked lissencephaly with abnormal genitalia in humans. *Nat Genet*. 2002;32(3):359-69.

Koebele SV, Nishimura KJ, Bimonte-Nelson HA, Kemmou S, Ortiz JB, Judd JM, et al. A long-term cyclic plus tonic regimen of 17 β -estradiol improves the ability to handle a high spatial working memory load in ovariectomized middle-aged female rats. *Hormones and Behavior*. 2020;118:104656.

Kuhnle GGC, Dell'Aquila C, Aspinall SM, Runswick SA, Mulligan AA, Bingham SA. Phytoestrogen Content of Beverages, Nuts, Seeds, and Oils. *Journal of Agricultural and Food Chemistry*. 2008;56(16):7311-5.

Lathe R. The individuality of mice. *Genes, Brain and Behavior*. 2004;3(6):317-27.

Lavdas AA, Grigoriou M, Pachnis V, Parnavelas JG. The Medial Ganglionic Eminence Gives Rise to a Population of Early Neurons in the Developing Cerebral Cortex. *The Journal of Neuroscience*. 1999;19(18):7881.

Le Magueresse C, Monyer H. GABAergic interneurons shape the functional maturation of the cortex. *Neuron*. 2013;77(3):388-405.

Leach PT, Hayes J, Pride M, Silverman JL, Crawley JN. Normal Performance of *Fmr1* Mice on a Touchscreen Delayed Nonmatching to Position Working Memory Task. *eneuro*. 2016;3(1):ENEURO.0143-15.2016.

Lee K, Ireland K, Bleeze M, Shoubridge C. ARX polyalanine expansion mutations lead to migration impediment in the rostral cortex coupled with a developmental deficit of calbindin-positive cortical GABAergic interneurons. *Neuroscience*. 2017;357:220-31.

Lee K, Mattiske T, Kitamura K, Gecz J, Shoubridge C. Reduced polyalanine-expanded Arx mutant protein in developing mouse subpallium alters Lmo1 transcriptional regulation. *Human Molecular Genetics*. 2014;23(4):1084-94.

Lee MJ, Hatton BA, Villavicencio EH, Khanna PC, Friedman SD, Ditzler S, et al. Hedgehog pathway inhibitor saridegib (IPI-926) increases lifespan in a mouse medulloblastoma model. *Proc Natl Acad Sci U S A*. 2012;109(20):7859-64.

Lein ES, Hawrylycz MJ, Ao N, Ayres M, Bensinger A, Bernard A, et al. Genome-wide atlas of gene expression in the adult mouse brain. *Nature*. 2007;445(7124):168-76.

Lewis DA, Hashimoto T, Volk DW. Cortical inhibitory neurons and schizophrenia. *Nature Reviews Neuroscience*. 2005;6:312.

Lin Z, Tann JY, Goh ET, Kelly C, Lim KB, Gao JF, et al. Structural basis of death domain signaling in the p75 neurotrophin receptor. *Elife*. 2015;4:e11692.

Loch JJ, Bonarek P, Tworzydło M, Łazińska I, Szydłowska J, Lipowska J, et al. The engineered β -lactoglobulin with complementarity to the chlorpromazine chiral conformers. *Int J Biol Macromol*. 2018;114:85-96.

Mak IW, Evaniew N, Ghert M. Lost in translation: animal models and clinical trials in cancer treatment. *Am J Transl Res*. 2014;6(2):114-8.

Malakooti N, Pritchard MA, Adlard PA, Finkelstein DI. Role of metal ions in the cognitive decline of Down syndrome. *Front Aging Neurosci*. 2014;6:136-.

Mao M, Nair A, Augustine GJ. A Novel Type of Neuron Within the Dorsal Striatum. *Front Neural Circuits*. 2019;13:32.

Marques I, Sá MJ, Soares G, Mota MdC, Pinheiro C, Aguiar L, et al. Unraveling the pathogenesis of ARX polyalanine tract variants using a clinical and molecular interfacing approach. *Molecular Genetics & Genomic Medicine*. 2015;3(3):203-14.

Marsh E, Fulp C, Gomez E, Nasrallah I, Minarcik J, Sudi J, et al. Targeted loss of Arx results in a developmental epilepsy mouse model and recapitulates the human phenotype in heterozygous females. *Brain*. 2009;132(6):1563-76.

Marsh ED, Nasrallah MP, Walsh C, Murray KA, Nicole Sunnen C, McCoy A, et al. Developmental interneuron subtype deficits after targeted loss of Arx. *BMC Neuroscience*. 2016;17:35.

Martos YV, Braz BY, Beccaria JP, Murer MG, Belforte JE. Compulsive Social Behavior Emerges after Selective Ablation of Striatal Cholinergic Interneurons. *J Neurosci*. 2017;37(11):2849-58.

Mattiske T, Lee K, Gecz J, Friocourt G, Shoubridge C. Embryonic forebrain transcriptome of mice with polyalanine expansion mutations in the ARX homeobox gene. *Human Molecular Genetics*. 2016;25(24):5433-43.

Mazarati A. Can we and should we use animal models to study neurobehavioral comorbidities of epilepsy? *Epilepsy Behav*. 2019;101(Pt A):106566.

McCarthy MM. Estradiol and the Developing Brain. *Physiological reviews*. 2008;88(1):91-124.

Meinecke DL, Peters A. GABA immunoreactive neurons in rat visual cortex. *The Journal of Comparative Neurology*. 1987;261(3):388-404.

Mi H, Muruganujan A, Thomas PD. PANTHER in 2013: modeling the evolution of gene function, and other gene attributes, in the context of phylogenetic trees. *Nucleic Acids Res*. 2013;41(Database issue):D377-86.

Miura H, Yanazawa M, Kato K, Kitamura K. Expression of a novel aristaless related homeobox gene 'Arx' in the vertebrate telencephalon, diencephalon and floor plate. *Mechanisms of Development*. 1997;65(1–2):99-109.

Moore Y, Robinson R. Cannabidiol reduced frequency of convulsive seizures in drug resistant Dravet syndrome. *Arch Dis Child Educ Pract Ed*. 2018;103(5):278-9.

Nabbout R, Dulac O. Epileptic Encephalopathies: A Brief Overview. *Journal of Clinical Neurophysiology* November/December. 2003;20(6):393-7.

Nakamura NH, McEwen BS. Changes in interneuronal phenotypes regulated by estradiol in the adult rat hippocampus: a potential role for neuropeptide Y. *Neuroscience*. 2005;136(1):357-69.

Neyens LGJ, Aldenkamp AP, Meinardi HM. Prospective follow-up of intellectual development in children with a recent onset of epilepsy. *Epilepsy Research*. 1999;34(2):85-90.

Nickels KC, Wirrell EC. Cognitive and Social Outcomes of Epileptic Encephalopathies. *Seminars in Pediatric Neurology*. 2017;24(4):264-75.

Okada K, Nishizawa K, Setogawa S, Hashimoto K, Kobayashi K. Task-dependent function of striatal cholinergic interneurons in behavioural flexibility. *Eur J Neurosci*. 2018;47(10):1174-83.

Olivetti PR, Maheshwari A, Noebels JL. Neonatal Estradiol Stimulation Prevents Epilepsy in Arx Model of X-Linked Infantile Spasms Syndrome. *Science Translational Medicine*. 2014;6(220):220ra12.

Olivetti PR, Noebels JL. Interneuron, interrupted: molecular pathogenesis of ARX mutations and X-linked infantile spasms. *Curr Opin Neurobiol*. 2012;22(5):859-65.

Paciorkowski AR, Thio LL, Dobyns WB. Genetic and biologic classification of infantile spasms. *Pediatr Neurol*. 2011;45(6):355-67.

Paluch LR, Lieggi CC, Dumont M, Monette S, Riedel ER, Lipman NS. Developmental and behavioral effects of toe clipping on neonatal and preweanling mice with and without vapocoolant anesthesia. *J Am Assoc Lab Anim Sci*. 2014;53(2):132-40.

Panda S, Dohare P, Jain S, Parikh N, Singla P, Mehdizadeh R, et al. Estrogen Treatment Reverses Prematurity-Induced Disruption in Cortical Interneuron Population. *J Neurosci*. 2018;38(34):7378-91.

Partington MW, Turner G, Boyle J, Géczy J. Three new families with X-linked mental retardation caused by the 428–451dup(24bp) mutation in ARX. *Clinical Genetics*. 2004;66(1):39-45.

Pellock JM, Hrachovy R, Shinnar S, Baram TZ, Bettis D, Dlugos DJ, et al. Infantile spasms: A U.S. consensus report. *Epilepsia*. 2010;51(10):2175-89.

Pesaturo KA, Spooner LM, Belliveau P. Vigabatrin for Infantile Spasms. *Pharmacotherapy: The Journal of Human Pharmacology and Drug Therapy*. 2011;31(3):298-311.

Poirier K, Eisermann M, Caubel I, Kaminska A, Peudonnier S, Boddaert N, et al. Combination of infantile spasms, non-epileptic seizures and complex movement disorder: A new case of ARX-related epilepsy. *Epilepsy Research*. 2008;80(2):224-8.

Poirier K, Van Esch H, Friocourt G, Saillour Y, Bahi N, Backer S, et al. Neuroanatomical distribution of ARX in brain and its localisation in GABAergic neurons. *Molecular Brain Research*. 2004;122(1):35-46.

Pottoo FH, Bhowmik M, Vohora D. Raloxifene protects against seizures and neurodegeneration in a mouse model mimicking epilepsy in postmenopausal woman. *Eur J Pharm Sci*. 2014;65:167-73.

Pottoo FH, Tabassum N, Javed MN, Nigar S, Sharma S, Barkat MA, et al. Raloxifene potentiates the effect of fluoxetine against maximal electroshock induced seizures in mice. *Eur J Pharm Sci*. 2020;146:105261.

Pozzi S, Benedusi V, Maggi A, Vegeto E. Estrogen Action in Neuroprotection and Brain Inflammation. *Annals of the New York Academy of Sciences*. 2006;1089(1):302-23.

Prasad AN, Burneo JG, Corbett B. Epilepsy, comorbid conditions in Canadian children: Analysis of cross-sectional data from Cycle 3 of the National Longitudinal Study of Children and Youth. *Seizure*. 2014;23(10):869-73.

Pressler R, Auvin S. Comparison of Brain Maturation among Species: An Example in Translational Research Suggesting the Possible Use of Bumetanide in Newborn. *Frontiers in Neurology*. 2013;4:36.

Price MG, Yoo JW, Burgess DL, Deng F, Hrachovy RA, Frost JD, et al. A Triplet Repeat Expansion Genetic Mouse Model of Infantile Spasms Syndrome, Arx((GCG)₁₀₊₇), with Interneuronopathy, Spasms in Infancy, Persistent Seizures, and Adult Cognitive and Behavioral Impairment. *The Journal of neuroscience : the official journal of the Society for Neuroscience*. 2009;29(27):8752-63.

Quillé ML, Carat S, Quéméner-Redon S, Hirchaud E, Baron D, Benech C, et al. High-throughput analysis of promoter occupancy reveals new targets for Arx, a gene mutated in mental retardation and interneuronopathies. *PLoS One*. 2011;6(9):e25181.

Reish O, Fullston T, Regev M, Heyman E, Gecz J. A novel de novo 27 bp duplication of the ARX gene, resulting from postzygotic mosaicism and leading to three severely affected males in two generations. *Am J Med Genet A*. 2009;149A(8):1655-60.

Rho JM, White HS. Brief history of anti-seizure drug development. *Epilepsia open*. 2018;3(Suppl Suppl 2):114-9.

Riebe CJN, Hill MN, Lee TTY, Hillard CJ, Gorzalka BB. Estrogenic regulation of limbic cannabinoid receptor binding. *Psychoneuroendocrinology*. 2010;35(8):1265-9.

Riikonen R. Long-Term Outcome of West Syndrome: A Study of Adults with a History of Infantile Spasms. *Epilepsia*. 1996;37(4):367-72.

Riikonen R. Topical Review: Infantile Spasms: Therapy and Outcome. *Journal of Child Neurology*. 2004;19(6):401-4.

Riikonen R, Donner M. ACTH therapy in infantile spasms: side effects. *Archives of Disease in Childhood*. 1980;55(9):664-72.

Romero DM, Bahi-Buisson N, Francis F. Genetics and mechanisms leading to human cortical malformations. *Seminars in Cell & Developmental Biology*. 2018;76:33-75.

Rossi F, Bellini G, Luongo L, Mancusi S, Torella M, Tortora C, et al. The 17- β -oestradiol inhibits osteoclast activity by increasing the cannabinoid CB2 receptor expression. *Pharmacological Research*. 2013;68(1):7-15.

Rubenstein JLR. Three hypotheses for developmental defects that may underlie some forms of autism spectrum disorder. *Current Opinion in Neurology*. 2010;23(2):118-23.

Schroeder A, Hudson M, Du X, Wu YWC, Nakamura J, van den Buuse M, et al. Estradiol and raloxifene modulate hippocampal gamma oscillations during a spatial memory task. *Psychoneuroendocrinology*. 2017;78:85-92.

Semple BD, Blomgren K, Gimlin K, Ferriero DM, Noble-Haeusslein LJ. Brain development in rodents and humans: Identifying benchmarks of maturation and vulnerability to injury across species. *Progress in neurobiology*. 2013;0:1-16.

Sernagor E, Chabrol F, Bony G, Cancedda L. GABAergic control of neurite outgrowth and remodeling during development and adult neurogenesis: general rules and differences in diverse systems. *Frontiers in Cellular Neuroscience*. 2010;4(11).

Shinozaki Y, Osawa M, Sakuma H, Komaki H, Nakagawa E, Sugai K, et al. Expansion of the first polyalanine tract of the ARX gene in a boy presenting with generalized dystonia in the absence of infantile spasms. *Brain and Development*. 2009;31(6):469-72.

Shoubridge C, Fullston T, Gecz J. ARX spectrum disorders: making inroads into the molecular pathology. *Human Mutation*. 2010;31(8):889-900.

Siehr MS, Massey CA, Noebels JL. Arx expansion mutation perturbs cortical development by augmenting apoptosis without activating innate immunity in a mouse model of X-linked infantile spasms syndrome. *Dis Model Mech*. 2020;13(3).

Simonet JC, Sunnen CN, Wu J, Golden JA, Marsh ED. Conditional Loss of Arx From the Developing Dorsal Telencephalon Results in Behavioral Phenotypes Resembling Mild Human ARX Mutations. *Cerebral Cortex (New York, NY)*. 2015;25(9):2939-50.

Sirisena ND, McElreavey K, Bashamboo A, de Silva KSH, Jayasekara RW, Dissanayake VHW. A Child with a Novel de novo Mutation in the Aristaless Domain of the Aristaless-Related Homeobox *(ARX)* Gene Presenting with Ambiguous Genitalia and Psychomotor Delay. *Sexual Development*. 2014;8(4):156-9.

Smith-Hicks CL. GABAergic dysfunction in pediatric neuro-developmental disorders. *Front Cell Neurosci*. 2013;7:269.

Smith CC, Smith LA, Bredemann TM, McMahon LL. 17 β estradiol recruits GluN2B-containing NMDARs and ERK during induction of long-term potentiation at temporoammonic-CA1 synapses. *Hippocampus*. 2016;26(1):110-7.

Song JM, Hahn J, Kim SH, Chang MJ. Efficacy of Treatments for Infantile Spasms: A Systematic Review. *Clin Neuropharmacol*. 2017;40(2):63-84.

Specchio N, Pietrafusa N, Ferretti A, De Palma L, Santarone ME, Pepi C, et al. Treatment of infantile spasms: why do we know so little? *Expert Rev Neurother*. 2020;20(6):551-66.

Stanco A, Pla R, Vogt D, Chen Y, Mandal S, Walker J, et al. NPAS1 represses the generation of specific subtypes of cortical interneurons. *Neuron*. 2014;84(5):940-53.

Stromme P, Mangelsdorf ME, Shaw MA, Lower KM, Lewis SME, Bruyere H, et al. Mutations in the human ortholog of Aristaless cause X-linked mental retardation and epilepsy. *Nat Genet*. 2002;30(4):441-5.

Sugiyama N, Andersson S, Lathe R, Fan X, Alonso-Magdalena P, Schwend T, et al. Spatiotemporal dynamics of the expression of estrogen receptors in the postnatal mouse brain. *Molecular Psychiatry*. 2008;14:223.

Sussel L, Marin O, Kimura S, Rubenstein JL. Loss of Nkx2.1 homeobox gene function results in a ventral to dorsal molecular respecification within the basal telencephalon: evidence for a transformation of the pallidum into the striatum. *Development*. 1999;126(15):3359.

Sutton GJ, Voineagu I. Comprehensive evaluation of human brain gene expression deconvolution methods. *bioRxiv*. 2020:2020.06.01.126839.

Tan S-S, Breen S. Radial mosaicism and tangential cell dispersion both contribute to mouse neocortical development. *Nature*. 1993;362:638.

Thomas A, Baillie GL, Phillips AM, Razdan RK, Ross RA, Pertwee RG. Cannabidiol displays unexpectedly high potency as an antagonist of CB1 and CB2 receptor agonists in vitro. *Br J Pharmacol*. 2007;150(5):613-23.

Thomas PD, Campbell MJ, Kejariwal A, Mi H, Karlak B, Daverman R, et al. PANTHER: a library of protein families and subfamilies indexed by function. *Genome Res*. 2003;13(9):2129-41.

Thompson PJ, Baxendale SA, Duncan JS, Sander JW. Effects of topiramate on cognitive function. *J Neurol Neurosurg Psychiatry*. 2000;69(5):636-41.

Tomioka R, Rockland KS. Long-distance corticocortical GABAergic neurons in the adult monkey white and gray matter. *The Journal of Comparative Neurology*. 2007;505(5):526-38.

Turner G, Partington M, Kerr B, Mangelsdorf M, Gecz J. Variable expression of mental retardation, autism, seizures, and dystonic hand movements in two families with an identical ARX gene mutation. *American Journal of Medical Genetics*. 2002;112(4):405-11.

UniProt. SLC17A8 - Vesicular glutamate transporter 3. 2020 [cited 2020; Available from: <https://www.uniprot.org/uniprot/Q8NDX2#function>

UniProt. TACR1 - Substance-P receptor. 2020 [cited 2020; Available from: <https://www.uniprot.org/uniprot/P25103>

Velíšková J. The role of estrogens in seizures and epilepsy: The bad guys or the good guys? *Neuroscience*. 2006;138(3):837-44.

Vrtačnik P, Ostanek B, Mencej-Bedrač S, Marc J. The many faces of estrogen signaling. *Biochem Med (Zagreb)*. 2014;24(3):329-42.

Wahlsten D. Chapter 3 - Tests of Mouse Behavior. *Mouse Behavioral Testing*. London: Academic Press; 2011. p. 39-51.

Wahlsten D, Bachmanov A, Finn DA, Crabbe JC. Stability of inbred mouse strain differences in behavior and brain size between laboratories and across decades. *Proceedings of the National Academy of Sciences of the United States of America*. 2006;103(44):16364-9.

Wallace MJ, Wiley JL, Martin BR, DeLorenzo RJ. Assessment of the role of CB1 receptors in cannabinoid anticonvulsant effects. *Eur J Pharmacol*. 2001;428(1):51-7.

Wallerstein R, Sugalski R, Cohn L, Jawetz R, Friez M. Expansion of the ARX spectrum. *Clinical Neurology and Neurosurgery*. 2008;110(6):631-4.

Wei J, Hemmings GP. A study of a genetic association between the PTGS2/PLA2G4A locus and schizophrenia. *Prostaglandins Leukot Essent Fatty Acids*. 2004;70(4):413-5.

WHO. Epilepsy. 2019 [cited 2019; Available from: <https://www.who.int/news-room/fact-sheets/detail/epilepsy>

Wichterle H, Garcia-Verdugo JM, Herrera DG, Alvarez-Buylla A. Young neurons from medial ganglionic eminence disperse in adult and embryonic brain. 1999;2:461.

Wichterle H, Turnbull DH, Nery S, Fishell G, Alvarez-Buylla A. In utero fate mapping reveals distinct migratory pathways and fates of neurons born in the mammalian basal forebrain. *Development*. 2001;128(19):3759.

Willemsen MH, Kleefstra T. Making headway with genetic diagnostics of intellectual disabilities. *Clin Genet*. 2014;85(2):101-10.

Wohlrab G, Uyanik G, Gross C, Hehr U, Winkler J, Schmitt B, et al. Familial West syndrome and dystonia caused by an Aristaless related homeobox gene mutation. *European Journal of Pediatrics*. 2005;164(5):326-8.

Wonders CP, Anderson SA. The origin and specification of cortical interneurons. *Nature Reviews Neuroscience*. 2006;7:687.

Woolley CS, McEwen BS. Estradiol mediates fluctuation in hippocampal synapse density during the estrous cycle in the adult rat. *Journal of Neuroscience*. 1992;12(7):2549-54.

Woolley CS, McEwen BS. Estradiol regulates hippocampal dendritic spine density via an N-methyl- D-aspartate receptor-dependent mechanism. *Journal of Neuroscience*. 1994;14(12):7680-7.

Yang X, Li Y, Chen L, Xu M, Wu J, Zhang P, et al. Protective effect of hydroxysafflor yellow A on dopaminergic neurons against 6-hydroxydopamine, activating anti-apoptotic and anti-neuroinflammatory pathways. *Pharm Biol*. 2020;58(1):686-94.

Younus I, Reddy DS. Seizure facilitating activity of the oral contraceptive ethinyl estradiol. *Epilepsy Res*. 2016;121:29-32.

Zack MM, Kobau R. National and State Estimates of the Numbers of Adults and Children with Active Epilepsy - United States, 2015. *MMWR Morb Mortal Wkly Rep*. 2017;66(31):821-5.

Zhang W, Zhou M, Lu W, Gong J, Gao F, Li Y, et al. CNTNAP4 deficiency in dopaminergic neurons initiates parkinsonian phenotypes. *Theranostics*. 2020;10(7):3000-21.

Zheng J-y, Liang K-s, Wang X-j, Zhou X-y, Sun J, Zhou S-n. Chronic Estradiol Administration During the Early Stage of Alzheimer's Disease Pathology Rescues Adult Hippocampal Neurogenesis and Ameliorates Cognitive Deficits in A β 1-42 Mice. *Molecular Neurobiology*. 2017;54(10):7656-69.

Zoubarev A, Hamer KM, Keshav KD, McCarthy EL, Santos JRC, Van Rossum T, et al. Gemma: a resource for the reuse, sharing and meta-analysis of expression profiling data. *Bioinformatics*. 2012;28(17):2272-3.

Appendices

Appendix 1

Statement of Authorship

Title of Paper	Early 17 β -estradiol treatment reduces seizures but not abnormal behaviour in mice with expanded polyalanine tracts in the Anirax ⁺ -related homeobox gene (Arx).
Publication Status	<input type="checkbox"/> Published <input type="checkbox"/> Accepted for Publication <input checked="" type="checkbox"/> Submitted for Publication <input type="checkbox"/> Unpublished and Unsubmitted work written in manuscript style
Publication Details	manuscript submitted to Neurobiology of Disease.


Principal Author

Name of Principal Author (Candidate)	Karagh Loring	
Contribution to the Paper	methodology, validation, formal analysis, investigation, writing - original draft, review and editing, data visualisation.	
Overall percentage (%)	80%	
Certification:	This paper reports on original research I conducted during the period of my Higher Degree by Research candidature and is not subject to any obligations or contractual agreements with a third party that would constrain its inclusion in this thesis. I am the primary author of this paper.	
Signature		Date 28/10/2020

Co-Author Contributions

By signing the Statement of Authorship, each author certifies that:

- i. the candidate's stated contribution to the publication is accurate (as detailed above);
- ii. permission is granted for the candidate to include the publication in the thesis; and
- iii. the sum of all co-author contributions is equal to 100% less the candidate's stated contribution.

Name of Co-Author	Cheryl Shoubridge	
Contribution to the Paper	conceptualisation, methodology, writing - original draft, review and editing, visualisation, supervision, project administration, funding acquisition.	
Signature		Date 28-10-20

Name of Co-Author	Tessa Matiske	
Contribution to the Paper	validation, formal analysis, investigation, review and editing.	
Signature		Date 04/11/20

Please cut and paste additional co-author panels here as required.

Statement of Authorship

Title of Paper	
Publication Status	<input type="checkbox"/> Published <input type="checkbox"/> Accepted for Publication <input type="checkbox"/> Submitted for Publication <input type="checkbox"/> Unpublished and Unsubmitted work written in manuscript style
Publication Details	

Principal Author

Name of Principal Author (Candidate)	
Contribution to the Paper	
Overall percentage (%)	
Certification:	This paper reports on original research I conducted during the period of my Higher Degree by Research candidature and is not subject to any obligations or contractual agreements with a third party that would constrain its inclusion in this thesis. I am the primary author of this paper.
Signature	Date

Co-Author Contributions

By signing the Statement of Authorship, each author certifies that:

- i. the candidate's stated contribution to the publication is accurate (as detailed above);
- ii. permission is granted for the candidate to include the publication in the thesis; and
- iii. the sum of all co-author contributions is equal to 100% less the candidate's stated contribution.

Name of Co-Author	Krisie Lee		
Contribution to the Paper	conceptualisation, methodology, investigation, review and editing, supervision,		
Signature		Date	30/10/2020

N	Name of Co-Author	Aneta Zysk	
C	Contribution to the Paper	Investigation, review and editing.	
S	Signature		Date 30/10/2020

Please cut and paste additional co-author panels here as required.

F

Statement of Authorship

Title of Paper	
Publication Status	<input type="checkbox"/> Published <input type="checkbox"/> Accepted for Publication <input type="checkbox"/> Submitted for Publication <input type="checkbox"/> Unpublished and Unsubmitted work written in manuscript style
Publication Details	

Principal Author

Name of Principal Author (Candidate)	
Contribution to the Paper	
Overall percentage (%)	
Certification:	This paper reports on original research I conducted during the period of my Higher Degree by Research candidature and is not subject to any obligations or contractual agreements with a third party that would constrain its inclusion in this thesis. I am the primary author of this paper.
Signature	Date

Co-Author Contributions

By signing the Statement of Authorship, each author certifies that:

- i. the candidate's stated contribution to the publication is accurate (as detailed above);
- ii. permission is granted for the candidate to include the publication in the thesis; and
- iii. the sum of all co-author contributions is equal to 100% less the candidate's stated contribution.

Name of Co-Author	Marilda Jackson		
Contribution to the Paper	methodology, review and editing, supervision.		
Signature		Date	02/11/2020

Name of Co-Author	Jeffrey Noebels		
Contribution to the Paper	Review and editing, funding acquisition.		
Signature		Date	10/28/2020

Please cut and paste additional co-author panels here as required.

Full title:

Early 17 β -estradiol treatment reduces seizures but not abnormal behaviour in mice with expanded polyalanine tracts in the *Aristaless* related homeobox gene (*ARX*).

Short title:

Estradiol reduces seizures in mice with *Arx* mutations.

Karagh E. Loring^{1,2}, Tessa Mattiske^{1,2}, Kristie Lee^{1,2}, Aneta Zysk^{1,2}, Matilda R. Jackson^{1,2}, Jeffrey L. Noebels³ and Cheryl Shoubridge^{*1,2}.

¹ *Intellectual Disability Research, Adelaide Medical School, The University of Adelaide, Adelaide, SA, Australia*

² *Robinson Research Institute, The University of Adelaide, Adelaide, SA, Australia*

³ *Department of Neurology, Baylor College of Medicine, Houston, USA*

* Correspondence should be addressed to Associate Professor Cheryl Shoubridge, Robinson Research Institute, Adelaide Medical School, Faculty of Health Sciences, Adelaide Health and Medical Sciences Building, University of Adelaide, Adelaide, South Australia, Australia. Postal Address: Level 8, Adelaide Health and Medical Sciences Building, University of Adelaide, Adelaide, 5005, Australia.

Phone: Intl 61-8-8313-2355

E-mail: cheryl.shoubridge@adelaide.edu.au

Abstract

Children with severe intellectual disability have an increased prevalence of refractory seizures. Steroid treatment may improve seizure outcomes, but the mechanism remains unknown. Here we demonstrate that short term, daily delivery of an exogenous steroid 17β -estradiol (40 ng/g) in early postnatal life significantly reduced the number and severity of seizures, but did not improve behavioural deficits, in mice modelling mutations in the *Aristaless*-related homeobox gene (*ARX*), expanding the first (PA1) or second (PA2) polyalanine tract. Frequency of observed seizures on handling (n=14/treatment/genotype) were significantly reduced in PA1 (32% reduction) and more modestly reduced in PA2 mice (14% reduction) with steroid treatment compared to vehicle. Spontaneous seizures were assessed (n=7/treatment/genotype) at 7 weeks of age coinciding with a peak of seizure activity in untreated mice. PA1 mice treated with steroids no longer present with the most severe category of prolonged myoclonic seizures, while treated PA2 mice had a complete absence of any seizures during this analysis. Despite the reduction in seizures, 17β -estradiol treated mice showed no improvement in behavioural or cognitive outcomes in adulthood. For the first time we show that these deficits due to mutations in *Arx* are already present before seizure onset and do not worsen with seizures. *ARX* is a transcription factor and *Arx* PA mutant mice have deregulated transcriptome profiles in the developing embryonic brain. At postnatal day 10, treatment completion, RNAseq identified 129 genes significantly deregulated ($\text{Log}_2\text{FC} > \pm 0.5$, $P\text{-value} < 0.05$) in the frontal cortex of mutant compared to wild-type mice. This list reflects genes deregulated in disease and was particularly enriched for known genes in neurodevelopmental disorders and those involved in signalling and developmental pathways. 17β -estradiol treatment of mutant mice significantly deregulated 295 genes, with only 23 deregulated genes overlapping between vehicle and steroid treated mutant mice. We conclude that 17β -estradiol treatment recruits processes and pathways to reduce the frequency and severity of seizures in the *Arx* PA mutant mice but does not precisely correct the deregulated transcriptome nor improve mortality or behavioural and cognitive deficits.

Highlights

- Mice with PA expansions in *Arx* present with severe seizures and behavioural deficits.
- 17 β -estradiol treatment in early postnatal life reduced seizure frequency and severity.
- Treatment with 17 β -estradiol did not improve abnormal behaviour or mortality.
- Behavioural deficits were present prior to and did not worsen with seizures.
- 17 β -estradiol treatment activated alternate gene pathways to those disturbed due to mutant genotype to improve seizure outcomes.

Key Words

Childhood epilepsy

Genetics: epilepsy

Genetics: learning disability

Epilepsy: co-morbidity

Molecular genetics

Transcriptomics

List of abbreviations

ACTH: adrenocorticotrophic hormone

DAVID: Database for Annotation, Visualisation and Integrated Discovery

DMSO: dimethyl sulfoxide

E2: 17 β -estradiol

EIEE: early infantile epileptic encephalopathy

ERE: estrogen response element

ID: intellectual disability

OS: Ohtahara syndrome

PA: polyalanine

SUDEP: sudden unexpected death in epilepsy

WT: wild-type

Introduction

Epilepsy is a devastating disorder that affects more than 50 million people worldwide (WHO, 2019), with recent estimates of active epilepsy as high as 1.2% in developed western countries (Zack and Kobau, 2015). This disorder is characterised by involuntary seizures, due to an imbalance of excitatory and inhibitory neuronal activity in the brain. One form of epilepsy in infancy is epileptic spasms, including X-linked infantile spasms syndrome (ISSX; MIM# 308350). This disorder has a prognosis of severe epilepsy coupled with intellectual disability persisting throughout childhood and adolescence (Olivetti and Noebels, 2012, Hrachovy and Frost, 2013). Children with neurodevelopmental disorders often have complex overlapping phenotypes. For example, patients with severe intellectual disability have a 15-20% incidence higher than the general population of co-morbid features including recurrent seizures and autism spectrum disorder (ASD). As many as half of intellectual disability cases and epileptic syndromes are believed to be caused by genetic mutations, with an increasing list of genes responsible (Willemsen and Kleefstra, 2014, Chiurazzi and Pirozzi, 2016, Ellis *et al.*, 2020), with genes involved in various pathways including development and maintenance of the brain function and architecture, and neuronal functioning often mutated (Paciorkowski *et al.*, 2011, Olivetti and Noebels, 2012).

The Aristaless-related homeobox gene (*ARX*) [NM_139058.2] (MIM#300382) is known to play a pivotal role in the development of the brain, specifically the migration and differentiation of interneurons (Miura *et al.*, 1997, Kitamura *et al.*, 2002, Kitamura *et al.*, 2009, Lee *et al.*, 2014). Interneurons are small, locally projecting neurons that use the neurotransmitters γ -aminobutyric acid (GABA), acetylcholine and neuropeptides, to modulate excitation within neural networks. It is not surprising that dysfunction of GABA interneurons in the cerebral cortex is involved in neuropathology including epilepsy, schizophrenia, autism and intellectual disability syndromes (Le Magueresse and Monyer, 2013, Smith-Hicks, 2013). Mutations in *ARX* invariably lead to intellectual disability, with a wide spectrum of other neurological

comorbidities, including autism, dystonia, and epilepsy (Kitamura *et al.*, 2002, Shoubridge *et al.*, 2010). Over half of all inherited mutations in *ARX* patients leads to expansion of the first or second polyalanine tracts. Clinical presentation of families with expansion mutations in the first tract (PA1) generally present with phenotypes of infantile spasms and seizures (81%) (Shoubridge *et al.*, 2010, Marques *et al.*, 2015), while patients with mutations in the second tract (PA2) present with non-syndromic intellectual disability (68%), with dysarthria, dystonic hand movements (20%) and infantile spasms (26%) (Partington *et al.*, 2004, Shoubridge *et al.*, 2010, Marques *et al.*, 2015, Jackson *et al.*, 2017). The mechanisms underpinning this clinical variability remain unclear.

Children with infantile spasms associated with severe intellectual disabilities respond poorly to anti-convulsant medication. Adrenocorticotrophic hormone (ACTH) therapy known to stimulate production and release of corticosteroids is a frontline treatment for these disorders but often has low efficacy, high relapse rates and severe side effects that alongside early-onset seizures, are thought to further exacerbate the behavioural and cognitive deficits in affected children (Hrachovy and Frost, 2013). A preclinical trial in the *Arx* PA1 mouse (Price *et al.*, 2009) model found that short-term 17β -estradiol (E2) given daily in the first postnatal week alleviated the severe seizure phenotype in adult male mice (Price *et al.*, 2009, Olivetti *et al.*, 2014). Estradiol is a neurosteroid produced in the nervous system which plays important roles in the developing brain in synaptogenesis and morphometry of neurons and glial cells and can induce long-term changes in gene expression in the brain via activation of estrogen receptors and non-receptor pathways. 17β -estradiol treatment of PA1 mice partially restored the interneuron migration deficits in the neocortex, increased populations of neuropeptide-Y and calbindin positive interneurons, and changed the expression of several genes normally regulated by *Arx* (Olivetti *et al.*, 2014).

The migration of these inhibitory cells and other stages of cortical laminar positioning occurs in mice from embryonic day 9 until postnatal day (P) 10. In the developing male mouse brain,

there is a surge of intrinsic estradiol and conversion of testicular testosterone into estradiol during this period of brain development (McCarthy, 2008). While much research into estradiol's effects on the epileptic brain has been focused on the pro-epileptic activity of the hormone in the adult brain, its neuroprotective effects in the developing nervous system are still being explored. Estradiol has long-lasting transcriptional actions via estrogen receptors α and β , with genes regulated by estradiol being involved in cell proliferation, neuronal migration, synaptogenesis and cell survival. Estradiol also regulates of GABAergic neuronal populations and increases the numbers of inhibitory neurons in the pyramidal layers of the cortex (Nakamura and McEwen, 2005, Velíšková, 2006).

Here we investigate the role of early estradiol treatment in mice modelling both the common PA1 and the more frequent PA2 *ARX* mutations (originally reported by Kitamura *et al.* 2009). Our study explores the effect of estradiol on the seizure phenotype in *Arx* mutant mice and extends the investigation to the impact of this treatment on cognitive outcomes before and after the peak onset of seizures. We also analysed genome wide transcriptomic changes in the postnatal neocortex in PA1 and PA2 mutant mice with and without estradiol treatment to elucidate molecular mechanisms driving infantile spasms, seizures and intellectual disability due to *ARX* mutations.

Materials and Methods

Animals. All animal procedures were approved by the Animal Ethics Committee of The University of Adelaide, Adelaide. *Arx*^{GCG7/+} (RBRC03654) and *Arx*^{432-455dup/+} (RBRC03653) heterozygous females, called PA1 and PA2 mice respectively, originally imported from RIKEN Bioresource Centre, Japan were maintained on the C57BL/6N-Hsd background (Kitamura *et al.*, 2009). Animals were housed in individually ventilated cages under constant temperature and humidity with an 8:00 to 20:00 light/dark cycle. Animals were given a diet of 10% fat food and water available *ad libitum*, as well as crushed standard chow soaked in sterile water in an accessible feeding dish, refreshed daily. PA1 and PA2 heterozygous females were bred as trios with wild-type C57BL/6N-Hsd stud males to produce wild-type and hemizygous mutant males. There were no abnormal parenting behaviours in our heterozygous female mothers to report. Five rounds of staggered breeding were performed to generate experimental cohorts. Litters of male mice were weaned from their mothers at approximately postnatal day 21 to day 23 (P21-P23) upon the smallest pup reaching 8 grams of body weight as a minimum. All pups were weighed from P3 and monitored and scored daily for general health and welfare, appearance, and any observed seizure activity.

Genotyping. A small piece of toe tissue was removed by sterile technique at postnatal day 5 or 6 for genotyping and to provide an individual identification mark. Genomic DNA was extracted as per manufacturers' instructions for the High Pure PCR Template Preparation Kit (Roche) or the Maxwell® RSC Tissue DNA kit (Promega). Genotyping PCR was performed as described in (Lee *et al.*, 2014).

Drug preparation and injections. In all cases, male mice were studied. 17 β -estradiol (E2) (Sigma) was diluted in sterile sesame oil (Sigma) containing 0.75% (v/v) dimethyl sulfoxide (DMSO) (Sigma). Vehicle comprised sesame oil with 0.75% (v/v) DMSO. Estradiol and vehicle were stored in amber glass bottles at 4°C until required. Mice were visually sexed on

P3 and all males from one litter were injected subcutaneously with either estradiol or vehicle daily from P3 until P10 inclusive, alternating injection site daily between the neck and left and right hips of the pup. The estradiol dose used was 40ng/g, therefore mice weighing 1.5g received 60ng of estradiol (Olivetti *et al.*, 2014).

Treatment groups. All male mice in each litter were injected with either estradiol or vehicle treatment (Drug 1 or Drug 2 as these were blinded for the duration of the study). Genotypes and drugs were unblinded at the end of the study. This resulted in six different treatment groups for subsequent analysis: wild-type mice treated with either vehicle or estradiol, PA1 mice treated with either vehicle or estradiol, and PA2 mice treated with either vehicle or estradiol.

Behavioural analyses. Repeat behavioural testing was performed at approximately one and two months of age. Tests were conducted in the light phase of the cycle, always beginning by 9:00 and ending by 13:00. Testing at one month of age ran for one week and were performed in the following order: open field and inverted grid; sociability and social novelty. Testing at two months of age ran for two weeks and were performed in the same order in the first week, followed by Barnes maze in the second week. All testing was analysed using ANYmaze video tracking software (Stoelting). Behavioural apparatuses were thoroughly cleaned with F10 Veterinary Detergent between mice to remove olfactory traces. The behavioural testing protocols were previously described (Jackson *et al.*, 2017). A more detailed description of the behaviour testing protocols used for this study is outlined in Supplementary File 1.

Seizure monitoring and analysis. Mice received daily injections between day 3 and day 10 and remained with their mothers until weaning. From the start of treatment (postnatal day 3) until postnatal day 70, all mice for behavioural testing and seizure monitoring were handled and weighed daily. Any observed seizures occurring during this daily handling were recorded. Spontaneous seizures were assessed during non-invasive video monitoring (with offline analysis) across the peak period of seizures (previously determined in untreated mice to occur between postnatal days 35 and 60) (Jackson *et al.*, 2017). Video monitoring for seizure activity

was conducted three times a week in four hour blocks from 11:00 until 15:00 during light cycle, on PA1 and PA2 hemizygous males and age matched control wild-type littermates, between the ages of P38 and P56. Cage mates were placed in a Perspex covered 17.5cm by 31cm cage, with a small piece of Nectragel (Able Scientific) and food available *ad libitum* during the filming period. Natural behaviour was captured and automatically saved in 50-minute video files by a Sony FDR-AXP35 4K Handycam or a Panasonic HC-VX980M 4K Video Camera. Activity levels and seizure activity were viewed offline using VLC Media Player (version 2.1.3). Videos were analysed by observers blinded to genotype and treatment. Seizure activity was scored using a defined scoring system based on categorisation of seizures compared directly to video-electroencephalography in untreated mutant mice from a previous study (Jackson *et al.*, 2017). In brief, seizures in mutant mice were characterised into four categories: (1) rapid and jerky movements around the cage and stationary seizures, (2) mild repetitive myoclonic jerks (duration less than 10 secs), (3) prolonged myoclonic seizures lasting longer than 10 seconds and (4) found dead. Myoclonic seizures were recorded for length of seizure in seconds.

Tissue collection. Animals for RNA sequencing analysis were humanely killed by decapitation at P10, and behavioural/seizure monitoring animals were humanely killed at approximately P70 by CO₂ asphyxiation, if not euthanised for humane reasons prior to endpoint. The brain was dissected, and the forebrain separated from the cerebellum and cut in half sagittally along the cerebral fissure. The left hemisphere of the brain was minced and snap frozen in liquid nitrogen and stored at -80°C.

RNA isolation and sequencing. RNA was extracted from the cortex of hemizygous male mice from each of the two strains, PA1 and PA2, and matched wild-type littermates, using Trizol (Sigma) and RNAeasy Mini Kit (Qiagen). RNA was prepared using Illumina's TruSeq stranded RNA sample preparation protocol and sequenced on an Illumina NextSeq Platform ($n = 6$ wild-type samples and $n = 4$ PA1 and PA2 samples for each treatment group). The primary sequence

data was generated using the Illumina bcl2fastq 2.19.1.403 pipeline. The per base sequence quality was >95% bases above Q30 across all samples. The reads were also screened for the presence of any Illumina adaptor/overrepresented sequences and cross-species contamination. The cleaned sequence reads were then aligned against the *Mus musculus* genome (Build version mm10). The Tophat aligner (v2.1.1) was used to map read to the genomic sequences. The counts of reads mapping to each known gene were summarised and used for computing differential gene expression with 'edgeR' version 3.12.1 to assess differential expression. Low counts were filtered out (cpm<1) and the default TMM normalisation method of edgeR was used to normalise the counts between samples. A generalised linear model was then used to quantify the differential expression between the groups. Transcripts that were significantly different within genotype and treatment group comparisons were selected by applying a p-value cut off <0.05 and a log2 fold-change of ± 0.5 .

RT-qPCR for RNAseq validation. RNAseq results were validated using Taqman RT-qPCR on two groups of RNA; a technical validation cohort on the samples used for RNAseq, and a biological validation cohort, using RNA from mouse samples ($n = 6$ wild-type samples and $n = 4$ PA1 and PA2 samples for each treatment group). RNA was extracted as described above. cDNA was prepared and RT-qPCR was performed as previously described (Mattiske *et al.*, 2016). Expression of genes was determined using Taqman probes labelled with FAM with expression normalised to the reference gene, *Beta-Actin* assayed within the same sample using a Taqman probe labelled with VIC. Taqman probes used in this study are listed in Supplementary Table 1.

Gene enrichment analysis. Venn diagrams for gene expression data analysis were created using <http://bioinformatics.psb.ugent.be/webtools/Venn>. Statistical analysis of the enrichment of gene expression data was performed using Database for Annotation, Visualization and Integrated Discovery (DAVID) Functional Annotation Bioinformatics Microarray Analysis. DAVID uses multiple databases to create annotation clusters (Huang da *et al.*, 2009, Huang da

et al., 2009). These clusters were given overarching theme names and ranked. To rank the enrichment results we used enrichment scores calculated by DAVID.

Interneuron quantification - Tissue sectioning. Cortex from mice was coronally embedded in OCT and stored at -80°C until sectioning. Coronal sections of 10µm thickness (~2-3 cells thick) at 100µM apart were taken serially using a Leica Cryostat (Leica Biosystems) at -24°C. Sections were fixed to Superfrost™ Plus microscope slides (ThermoFisher). Frozen cortical sections were stored at -20°C until analysis. Sections analysed align to sections 100-124 of the Nissl stained postnatal day 7 coronal brain of the Allan Brain Atlas reference guide.

Staining and microscopy. Immunofluorescence staining was performed as described in Lee *et al.* 2017. Primary antibodies: rabbit anti-calbindin (1:1000, Merck PC252L) and sheep anti-neuropeptide Y (1:1000, Sigma T2200). Secondary antibodies: goat anti-rabbit (1:500, Alexa 555, Thermo Fisher A27039) and donkey anti-sheep (1:500, Alexa 488, Thermo Fisher A11015). Immunofluorescent images were captured using a Zeiss AxioCam mRM camera attached to a Zeiss Axio Imager.M2 microscope equipped with Axio Vision software (version 5.1). All comparative images were captured with the same exposure times.

Interneuron analysis. At least four sections across the right hemisphere were analysed. Images were stitched together using Microsoft Image Compositor (Microsoft, version X) and imported into Image J (FIJI, version X) for processing and analysis. Manual cell counts were performed using the Cell Counter plugin for Image J, using method described in Lee *et al.* 2017. Calbindin positive cells had a circular-like cell body with neuropeptide-Y cells displaying cytoplasmic and/or nuclear staining with clear boundaries of the structure, correlating to a clear nucleus DAPI stained. Counts were exported into Excel and a cell density of number of cells/mm² were derived as an outcome (positive cells counted/area of section counted in mm²).

Statistical analysis. Data analysis was performed using GraphPad Prism version 7.0 (GraphPad Software Inc.). Data normality was confirmed using a D'Agostino and Pearson normality test. Statistical significance of the difference between means of each genotype (PA1 or PA2), treatment groups (estradiol or vehicle) and wild-type littermates was determined using a one-way analysis of variance (ANOVA) followed by a Tukey's HSD post-hoc test. When comparisons were made between two treatment groups of the same genotype (PA1 or PA2), without wild-type littermates included in the comparisons (seizure data), a two-tailed, unpaired t-test was performed to determine statistical significance. The statistical significance of the overlap of genes between two groups was calculated using exact hypergeometric probability (http://nemates.org/MA/progs/overlap_stats.html; date last accessed April 19, 2020). For statistical analysis of interneuron cell counts, PA1 and PA2 mice were pooled. A one-way ANOVA was performed to determine statistical significance between PA^{pool} mice treated with vehicle or estradiol, followed by a Tukey's post-hoc test.

Results

Estradiol treatment reduces seizure frequency and severity but does not improve mortality in PA mutant mice.

PA1 and PA2 mutant males and wild-type (WT) male littermates were treated with daily subcutaneous injections of estradiol (40ng/g) for seven days between P3 and P10 (Figure 1A). Estradiol treatment significantly reduced the overall proportion of adult PA1 mutant mice experiencing seizures on daily handling, with a 32% reduction compared to vehicle treated mice (14% and 46% respectively, Figure 1B). Within the PA2 cohort, a 14% reduction was noted with estradiol treatment (44% versus 58%, respectively) but this did not reach significance ($p = 0.4243$). In PA1 mice, both the total number of observed seizure events and the number of severe seizures (scores of 2 or 3) were significantly reduced in estradiol treated animals compared to vehicle treated mutant mice (Figure 1C).

However, the effect of estradiol on the age of seizure onset differed between the two mutations. Estradiol actually accelerated the onset of seizures in PA2 mice, with estradiol-treated mice having their first seizure at postnatal day 26 ± 2.5 (mean \pm SEM) (Figure 1D), while treatment had no effect on PA1 mutants (45 ± 1.5) and vehicle treatment (43 ± 2.6) (Figure 1D). These data demonstrate that observed seizures on handling the *Arx* mutant mice are reduced in both severity and frequency with estradiol treatment, however, the specific intragenic mutation produced a differential response with estradiol, with accelerated epileptogenesis in PA2 mice compared to PA1. Mice observed having a seizure upon daily handling that subsequently went on to die from a presumed seizure (found dead in their cage) within 2-4 days of having seizure are shown as stars on Figure 1D. Interestingly, 2 of the 3 PA2 mice treated with estradiol in this category died during this early time point (Supplementary Figure 1), whilst the third mouse died after a subsequent seizure at a later time point (postnatal day 56). Within the PA2 vehicle cohort, five mice were found dead between days 12 and 25 but none of these mice were

recorded as having an observed seizure on handling during this period. However, we cannot rule out that seizures may have occurred outside of the times we were handling and observing the animals as part of daily health checks (P3 to P70) or outside the times captured by video seizure monitoring during P35 to P60.

In untreated mutant mice the peak of observed seizures was clustered between P35 and P60 (Jackson *et al.*, 2017). To exclude any influence of induced stress due to handling of the mice, we investigated seizures in a spontaneous setting via non-invasive video monitoring (12 hours per mouse over a period of four days) during this peak period. At P45 to P48, 36% (4/11) of PA1 mice treated with vehicle displayed a large number of clusters of individual seizure events ranging from rapid, jerky movement around the cage (score 1) through to increasingly severe myoclonic seizures (score 2 and 3) (Figure 2). Video clips of seizures in these mice are available (Jackson *et al.*, 2017). Although 30% (3/10) of the estradiol treated PA1 mice displayed seizures across this same period of time, both the number and severity of seizure events were significantly reduced (Figure 2). This trend is even more striking in the PA2 cohort; 33% (4/12) of vehicle treated mice displaying a total of 28 seizure events across all scoring categories, compared to seizures being completely absent in the estradiol treated mice (0/7) during this same monitoring period (Figure 2). Further, when looking at the observed seizures on handling that PA2 mice experienced during this time, only one mutant mouse treated with estradiol experienced seizures during this same period of time. We observed that there were no seizures in vehicle or estradiol treated wild-type mice by either the observed seizures on handling or non-invasive video seizure monitoring analysis.

Despite the significant improvements in frequency and severity of seizures in both the PA1 and PA2 mutant mice treated with estradiol, the median survival rates of these animals were not significantly extended compared to vehicle treated animals (Figure 3). Survival was recorded from P0 to P70. These data excluded mice that were cannibalised by their mother prior to P10 as this occurred in both WT and mutant mice and was not considered to be due to the mutant

phenotype. Mice still alive at the completion of the experimental period were culled at P70. Considering the animals that died before the experimental end point at P70, 62% of PA1 mice treated with vehicle died compared to 64% treated with estradiol (Figure 3). Similarly, 37% of PA2 mice treated with vehicle died before the experimental end point at P70, compared to 31% treated with estradiol (Figure 3). The mean age of death (excluding survival to end point cull) in vehicle treated compared to estradiol treated mutant mice was not significantly different for either PA1 or PA2 mice; PA1 vehicle treated mice 53 ± 5.1 (mean \pm SEM) compared to 52 ± 5.5 in PA1 estradiol treated mice, with PA2 vehicle treated mice was 45 ± 4.6 , compared to 37 ± 5.2 in PA2 estradiol treated mice (Supplementary Figure 1). There were no deaths among the WT group (vehicle or estradiol) other than animals culled to provide age matched littermate samples for mutant mice where required.

Further to our seizure and mortality findings, we confirm in this study that compared to WT littermates the PA mutant mice have reduced testes weight and reduced body weight, consistent with previous reports (Kitamura *et al.*, 2009, Jackson *et al.*, 2017). Here we demonstrate that there was no change to the weight of the testes or brain in WT, PA1 or PA2 mice following estradiol treatment (Supplementary Figure 2). Similarly, there were no improvements to the reduced body weight of mutant mice compared to WT littermates with estradiol treatment (Supplementary Figure 3).

Behavioural deficits are present in PA mice prior to seizure onset, and do not improve with estradiol treatment.

Both PA1 and PA2 mutant mice exhibit increased locomotor activity, abnormal anxiety traits and reduced sociability and autistic-like behaviour at two months of age (Kitamura *et al.*, 2009, Jackson *et al.*, 2017). To examine disease progression in relation to seizure onset, we tested these behavioural traits between P30 and P37 (one month of age – prior to peak seizure onset),

and again at P56 to P70 (two months of age – after peak seizure onset) with and without estradiol treatment. We did not observe any significant difference in the total distance travelled, nor time spent immobile by PA mutant mice compared to wild-type littermates (Supplementary Figure 4). In contrast, we demonstrated that the anxiety-response in PA mutant mice was different compared to WT littermates and did not regress over the duration of the study. At 2 months of age, WT littermates displayed normal exploratory behaviour with an average of 84% (vehicle) and 80% (estradiol) of the total distance travelled in the open field periphery. Contrary to this, PA1 mutant mice spent significantly more time in the periphery versus the central field of the open field apparatus, with an average of 91% (vehicle) and 96% (estradiol) (Figure 4A). This was also observed in the PA2 cohort, in both treatment groups with an average of 95% (vehicle) and 93% (estradiol) (Figure 4A). These results are indicative of decreased exploratory behaviour in both PA mutant mice compared to WT littermates, with increased anxiety-like behaviour (increased fear of venturing into the central field, choosing to stay in the safety of the periphery). These differences are shown in the tracking maps from the respective genotypes in the open field test (Figure 4B). There were no significant differences observed between the two ages sampled in either PA mutant cohort, indicating there was little change due to disease progression or age of the mice in either genotype. This data indicates that early estradiol treatment did not improve anxiety or fear behaviour in adult PA mutant mice.

Sociability testing measures several behavioural traits seen in mouse autism models. As expected, WT littermates chose to interact with another mouse over an inanimate object (empty chamber) (sociability phase: Figure 4C), and then chose to interact with novel (or stranger) animal over the familiar (or known) animal (social novelty phase: Figure 4D). This pattern of behaviour is indicative of normal social interaction and memory recall. Combining the mutant PA1 and PA2 data to create a PA^{pool} group compared to wild-type littermates, we demonstrate the PA^{pool} mutant mice of both vehicle and estradiol treatment groups showed significantly reduced sociability (Figure 4C) and social novelty (Figure 4D) compared to WT mice

(individual PA graphs are supplied in Supplementary Figure 5). The interaction times with other mice in the test chambers were reduced, regardless of whether the mouse occupant was novel or familiar. There was no significant difference between the two time points in the PA^{pool} cohort, indicating reduced sociability was already present at one month of age and did not change with disease progression or age.

Next we determined the impact of genotype and treatment on the neuromuscular strength in PA mice at two months of age using the inverted grid test. WT littermates decreased latency to fall from the grid averaged 76 seconds (vehicle) and 90 seconds (estradiol) compared to PA1 mice with 25 seconds (vehicle) and PA2 mice for 23 seconds (estradiol) (Figure 4E). Pooling the data for the mutant mice (PA^{pool} group) to increase the sample size, both vehicle and estradiol had significantly decreased latency to fall from the grid compared to their respective WT groups (Figure 4E).

To assess the impact of treatment on cognition and learning, the Barnes maze tested the amount of time each mouse required to locate an escape hole (in relation to false holes) in the testing apparatus, with improving or shorter times gained during subsequent testing. This test is conducted at two months of age. All groups tested showed normal adaptive function and memory, demonstrating shorter times to find the escape hole over a progressive four-day testing period (Supplementary Figure 6). Although we have previously demonstrated a memory deficit when testing via the Barnes maze in untreated PA mutant mice (Jackson *et al.*, 2017), in the current trial we did not detect a significant difference between the PA mutant mice of either treatment group and their WT littermates. This difference is likely due to the limited numbers of animals achieving the age required to perform this test. Of note, there was no difference in the performance of WT or mutant animals when vehicle treated animals were compared to estradiol treated animals.

PA1 and PA2 mutant mice have a deregulated cortical transcriptome at postnatal day 10.

Since *Arx* is a transcription factor, our next aim was to generate an unbiased map of RNAseq mRNA copy number changes in the cortical transcriptome at P10 due to *Arx* PA mutations. Compared to age-matched, vehicle treated WT mice analysis of PA1 mice revealed 63 genes deregulated by Log₂ fold change greater than ± 0.5 with a *P*-value of less than 0.05 (Supplementary Table 2). The majority (65%) of genes were found at a decreased level of expression compared to WT (Figure 5A). PA2 mice demonstrated 80 genes deregulated using the same fold cut-off (Supplementary Table 2), with 46% of genes having decreased expression when compared to WT mice (Figure 5A). Of the twelve genes chosen for biological validation by quantitative PCR, 100% (12/12) validated in PA1 mice and 60% (7/12) validated in PA2 mice (Supplementary Figure 7). There were fourteen genes deregulated in both PA1 (22%) and PA2 (18%) mice (Figure 5B). Of this core overlap group, 57% (8/14) of genes were downregulated in their expression and included genes important in neuronal development and associated with neurodevelopmental disorders (Figure 5C). Given the highly similar neurological phenotypes between the PA1 and PA2 mice coupled with similar responses to estradiol treatment observed in this study we chose to combine the data of the four males from each of the PA1 and PA2 mice as a single mutant group (PA^{pool}). This analysis showed 58 genes deregulated using the same fold cut-off, with 62% demonstrating a decreased level of expression compared to the pooled WT controls (Figure 5A).

Arx target genes (identified in Mattiske *et al.* 2016) were significantly enriched in the list of deregulated genes in the PA^{pool} group (10/58, 17%, $p < 1.288e^{-5}$) and in each of the PA1 (13/63, 21%, $p < 7.366e^{-8}$) and PA2 groups (9/80, 11%, $p < 9.641e^{-4}$). Known epilepsy genes (in house curated reference list) were not significantly enriched in any group of genes deregulated by disease (PA1; 2/63, 3%, $p < 0.100$; PA2; 2/80, 2%, $p < 0.343$; PA^{pool}; 3/58, 5%, $p < 0.058$). Genes associated with autism and ID (Gene Dx Xpanded Panel, (GeneDx, 2020)) were significantly enriched in the PA^{pool} group (5/58, 12%, $p < 0.001$), as were genes associated with inhibitory

neuron regulation or development (in house curated reference list) (10/58, 17%, $p < 6.957e^{-16}$) compared to WT mice (Figure 5D). Interestingly, the majority of these enriched interneuron genes were downregulated in their expression for all three genotypes (PA1, PA2 and PA^{pool}) (11/13, 84.6%) (Figure 5E).

Using the Database for Annotation, Visualization and Integrated Discovery (DAVID) we analysed pathways and ontology terms enriched within the disease-deregulated transcriptomes of PA mutant mice (Supplementary Figure 8). These clusters were ranked by enrichment score, with two clusters overlapping between PA1 and PA2; glycoproteins and glycoprotein receptors. Other enriched functions of note were PI3K-Akt signalling, neurotransmitter biosynthesis, and synaptic processes (Supplementary Figure 8). Many of the clusters are associated with brain and neuron development or signalling that when disrupted may be predicted to contribute to the phenotypic features of the PA mutant mice.

Estradiol targets genes outside of the deregulated transcriptome of PA mutant mice.

To investigate the impact of estradiol treatment at the transcriptome level, we first analysed WT mice treated with vehicle compared to estradiol. There were 56 genes deregulated by Log2 fold change greater than ± 0.5 with a *P*-value of less than 0.05 in the WT cohort when treated with estradiol. Genes deregulated in the WT mice estradiol treatment group that overlapped with the PA mutant groups were removed from subsequent analysis of PA1, PA2 and PA^{pool} (Supplementary Table 3).

Analysis of PA1 mice with estradiol treatment compared to vehicle resulted in 124 genes deregulated by Log2 fold change greater than ± 0.5 with a *p*-value of less than 0.05 (Supplementary Table 4). The majority (75%) of genes were found with an increased level of expression compared to vehicle treated PA1 mice. This was in contrast to the smaller response of disease changed genes in PA1 mice compared to WT (35% upregulated) (Figure 5A). PA2

mice with estradiol treatment compared to vehicle resulted in 158 genes deregulated at the same cut-off (Figure 6A).

In contrast to the PA1 mice, in the estradiol treated PA2 mice had 77% of genes with a decreased level of expression (Figure 6A). This is compared to the similar numbers of disease changed genes (PA2 vs WT) having increased or decreased expression (54% vs 46%, respectively). In the estradiol treated PA^{pool} mice there were 55 genes deregulated by the same cut-off, with 62% having increased expression (Figure 6A). We randomly chose nine genes for biological validation by quantitative PCR, with 44% (4/9), 22% (2/9) and 56% (5/9) validating in PA1, PA2 and PA^{pool} mice respectively (Supplementary Figure 9).

We next determined if genes deregulated by estradiol were enriched for genes containing estrogen response elements by comparing to a list of mouse genes containing high-affinity estrogen response elements (EREs) (Bourdeau *et al.*, 2004). ERE-containing genes were significantly enriched in WT (12/56, 21%, $p < 0.012$) and in PA1 mice treated with estradiol (22/124, 18%, $p < 0.010$) but not in PA^{pool} (8/53, 15%, $p < 0.190$) or PA2 mice (22/158, 15%, $p < 0.106$) (Figure 6A).

The size of the gene expression response to estradiol treatment in PA1 and PA2 mice was larger in comparison to genes deregulated by the *Arx* mutation alone and with little overlap (Figure 6B). Genes deregulated by estradiol treatment were quite different between genotypes, with only small numbers of overlapping genes (8 genes in PA1 mice, 12 genes in PA2 mice and 3 in PA^{pool}) (Figure 6C). Interestingly, all of the genes deregulated by disease that were also changed with estradiol treatment were deregulated in the opposite direction with treatment (Figure 6C). When we analysed the proportion of genes deregulated by estradiol in all three mutant groups (PA1, PA2 and PA^{pool}) the response to estradiol treatment between these three groups is strikingly different (Figure 6D). Only 11 genes overlapped between the PA1 and PA2 estradiol response (Figure 6D). When we consider the functionality or pathways responding to estradiol (via DAVID analysis), there are four enrichment clusters that overlap between two or

three of the mutant groups, including transcription regulation and glycoproteins (Supplementary Figure 10). Of note, genes involved in transcription regulation included *Shox2* and *Ebf3*. Both of these genes were significantly downregulated with treatment (Olivetti *et al.*, 2014). We see this in PA2 mice in our study, however not in the PA1 mice, largely due to the variation between samples.

Extending the data from genes deregulated by *Arx* mutation (Figure 5D), both neurodevelopmental disorder and inhibitory neuron associated genes were enriched in estradiol-treated mice (Figure 6E). However, in comparison to disease changed genes, interneuron associated genes were not trending in a particular direction with estradiol, with approximately equal proportions being increased or decreased in expression with treatment in the PA mutant mice (data not shown). Genes associated with autism and intellectual disability were significantly enriched in all groups treated with estradiol (PA^{pool}: 9/53, 13%, $p < 2.083e^{-5}$; PA1; 15/124, 10%, $p < 0.000003$; PA2; 10/158, 6%, $p < 0.016$). Epilepsy associated genes were enriched to a very low level, and variably depending upon the mutant group considered (PA1; 6/124, 5%, $P < 0.014$; PA^{pool}; 1/53, 2%, $p < 0.431$; PA2; 3/158, 2%, $P < 0.442$) (Figure 6E). Genes associated with inhibitory neurons were significantly enriched in the list of genes deregulated with estradiol treatment (PA^{pool}; 6/55, 11%, $p < 8.962e^{-9}$; PA1; 7/128, 6%, $p < 6.424e^{-8}$; PA2; 9/161, 6%, $p < 6.609e^{-10}$) (Figure 6E).

Next we performed immunofluorescent microscopy to determine the abundance of calbindin (Cb) and neuropeptide-Y (Npy) positive interneurons in the prefrontal cortex of mutant and WT mice at postnatal day 10. There were no significant deficits in the density of Cb or Npy positive interneurons in PA^{pool} mice compared to WT at postnatal day 10 across all layer of the cortex (Figure 7A-B). Nor did we see any difference to cell density of either of these interneurons in the mutant mice immediately following cessation of estradiol treatment (Figure 7C).

Discussion

Here we present a comprehensive behavioural and transcriptomic assessment of the impact of early postnatal steroid treatment on the development of seizures in mice modelling the two most common *ARX* polyalanine expansion mutations. Our data demonstrates that despite the sustained benefit of short term 17β - estradiol treatment early in postnatal life on the frequency and severity of seizures in both PA1 and PA2 mutant mouse models, there were no significant improvements to survival, anxiety, sociability, cognitive or neuromuscular deficits in treated mice in adult life. Importantly, our data provides support for reproducible anti-epileptogenic outcomes previously reported in a comparable *Arx* PA1 mutant mouse, studied on a different genetic background (Olivetti *et al.*, 2014). We have characterised the reduction in seizure frequency and severity in both PA mutant mice using a scoring matrix via video monitoring correlated to video-EEG (Jackson *et al.*, 2017). Here we expand these findings to indicate that short term, early 17β -estradiol administration also reduced seizures in the PA2 mutant mouse that models the most frequently reported polyalanine tract expansion mutation in *ARX* patients.

In contrast to the reproducible effect of estradiol on the seizure phenotype of the PA1 and PA2 mice, the same dose (40ng/g) of estradiol in an induced rat model of infantile spasms (via betamethasone and N-methyl-D-aspartic acid) did not improve spasms, even while increasing the number of GABAergic cells in the neocortex (Chachua *et al.*, 2016). Similarly, estradiol treatment was demonstrated to have no effect in an induced infantile spasms rat model (Galanopoulou and Moshé, 2015). The anti-epileptogenic effects of estradiol remain relatively unexplored with much of the field focused on the pro-epileptogenic effects of estradiol in female rodents (Younus and Reddy, 2016). Investigation into the effects of estradiol in other neurodevelopmental models exhibiting seizures, with and without associated interneuron deficits, would be particularly useful to better understand the anti-epileptogenic effects of estradiol treatment.

Despite the reduction in the frequency and severity of seizures there was no reduction in mortality of either PA1 or PA2 mice with steroid treatment. This was a novel finding. The cause of death could not be confirmed by post-mortem due to the timing of death occurring overnight. On examination in the mornings, we could not contribute death to any obvious cause. While the immediate cause of death in PA mutant mice is unclear, the lack of progressive deterioration and presence of convulsive seizures suggests that sudden unexpected death in epilepsy (SUDEP), or prolonged status epilepticus, as a possible diagnosis. Although 17β -estradiol treatment decreased the frequency and severity seizures in mutant PA *Arx* mouse models, the residual amount of seizures still present particularly evident upon handling, could account for the premature mortality in these mice.

An epileptic encephalopathy is defined as a condition where seizures or frequent interictal discharges exacerbate neurocognitive dysfunction beyond what would be expected on the basis of underlying aetiology (Nickels and Wirrell, 2017). This occurs in intractable epileptic disorders that start early in life, such as Ohtahara syndrome (OS), or Early Infantile Epileptic Encephalopathy (EIEE). Infants with these severe epileptic encephalopathies generally present with poor cognitive outcomes, with profound intellectual disability in 50% of patients if they survive severe spasms and seizures in infancy. Although these disorders have many different genetic aetiologies, both of these conditions are reported in patients with expanded polyalanine tract mutations in *ARX* (Shoubridge *et al.*, 2010, Marques *et al.*, 2015). Closer examination of the clinical spectrum in patients with *ARX* mutations in the first polyalanine tract (100% of who had seizures), indicates that developmental delay is reported in 25% of cases. The onset of seizures spanning from 0 to 18 months of age (median 4 months). Furthermore, only 26% of individuals with expansions of the second polyalanine tract exhibit seizures, despite 100% of these patients having intellectual disability (Jackson *et al.*, 2017).

The distribution of IQ scores in children with epilepsy and infantile spasms are often skewed to lower values, and patients experience difficulties learning in school, or regress in mental

development (Farwell *et al.*, 1985, Neyens *et al.*, 1999, Prasad *et al.*, 2014). However, it can often be difficult to elucidate how much of a child's intellectual disability was pre-existing and how much was caused by epilepsy early in key points of brain development (Nabbout and Dulac, 2003). A cardinal finding of our study is the relative differential response of seizure severity compared to behavioural and cognitive deficits following estradiol treatment. We predicted that seizure onset would lead to a worsening of cognitive and behavioural impairments in the PA1 and PA2 mutant mice. An extension of this prediction would be that 17 β -estradiol treatment alleviating seizures might improve cognitive and behavioural deficits. In contrast to our predictions, we demonstrate that behaviour did not improve with alleviation of seizures and that the deficits were already present before and did not decline further after the point of seizure onset. This provides important evidence separating the impact of seizures upon behavioural deficits in PA1 and PA2 mice.

Arx is highly expressed in the developing (embryonic) brain during cellular proliferation and the first wave of neuron migration from the ganglionic eminence to the developing cortex (Colombo *et al.*, 2007, Friocourt *et al.*, 2008, Colasante *et al.*, 2009, Lee *et al.*, 2014). The transcriptome in forebrain of PA mutant mice at embryonic day 12.5 demonstrated that interneuron associated genes were enriched in this data, with the majority having decreased expression (Mattiske *et al.*, 2016). In the newborn period, there is a delayed migration of calbindin-positive interneurons in the cortex of PA mutant mice (Lee *et al.*, 2017). From these studies we contend that the initial disruption to the transcriptome and subsequent impaired interneuron migration caused by these mutations in *Arx* drive the seizures and behavioural deficits measured in the PA mutant mice. In the current study we demonstrate a modest number of deregulated genes from the cortex at P10. This is in comparison to the larger number of deregulated genes detected at embryonic day 12.5 in wildtype compared to *Arx* PA mutant mice (vehicle treated mice only) (Mattiske *et al.*, 2016). Genes included *Tnn* and *Ngfr*, regulators of differentiation, growth, and migration of neuronal populations (Degen *et al.*,

2007, Lin *et al.*, 2015), while *Tacr1* is part of the family of G coupled-protein receptors, highly concentrated in the central nervous system (UniProt, 2020). Consistent with clinical phenotypes known to present in patients with *ARX* expansion mutations, *Cpz* is associated with autism spectrum disorders and/or intellectual disability (Loch *et al.*, 2018). Despite the reduced expression of *Arx* within the brain at P10, the genes deregulated in mutant mice were enriched for *Arx* target genes and genes known to be associated with autism and intellectual disability. The genes overlapping in mutant animals at P10 are important in brain development, including metal ion binding, known to be involved in cognitive decline in Down syndrome (Malakooti *et al.*, 2014) and Alzheimer's disease (Cristóvão *et al.*, 2016), as well as signal transduction and glycoproteins, both heavily involved in neurotransmitter release and modifying neuronal functioning (as shown in KEGG pathway analysis) (Kanehisa and Goto, 2000, Kanehisa, 2019, Kanehisa *et al.*, 2019). Although epilepsy associated genes were not significantly enriched in the mutant mice at P10, genes associated with inhibitory neurons were enriched.

Of the interneuron genes overlapping between PA1 and PA2 mutant mice, *Th* and *Tacr1* are associated with somatostatin positive interneurons, *Akr1c18* is associated with parvalbumin positive interneurons and *Chat* is known to play key roles in cholinergic interneurons. Neither of these subtypes have been previously shown to be disturbed in the PA1 and PA2 models at P10. *Th* is a gene of particular interest. Downregulation of *Th* was validated in both PA1 and PA2 vehicle-treated mice compared to WT and is an enzyme that assists in the formation of dopamine, a neurotransmitter, as well as having an association with interneurons. *Th* was unaltered with estradiol treatment, as well as other interneuron genes downregulated with disease. This supports the notion that disturbed function of these inhibitory cells are likely to play a critical role in the seizure phenotype due to mutations in *Arx*, and that the lack of “rescuing” of these genes might be associated with the remaining seizures we see with treatment in mutant mice, as well as the unaltered cognitive and behavioural phenotype. Many subsets of interneurons are lowly expressed in the brain. Given their importance to the PA

mutant phenotype and in Arx function more generally, single cell RNA sequencing would be a useful future strategy to determine the impact of disease and treatment on specific subtypes of inhibitory neurons.

We were somewhat surprised by the difference in gene expression in PA1 and PA2 mice, given their strikingly similar behavioural and seizure phenotypes, both in disease changed genes, and in their response to estradiol treatment. In terms of log₂ fold change and counts per million (gene expression level) we saw that PA2 had a greater number of genes with reduced expression compared to PA1 (Supplementary Figure 11). It was also unclear if 17 β -estradiol treatment would “rescue” the deregulated transcriptome of the PA mutant mice at P10, or if this treatment would target alternative pathways to reduce seizure frequency and severity. In the previous study in an alternate PA1 mutant mouse model the same strategy of 17 β -estradiol treatment altered expression of three downstream targets of Arx, namely *Shox2*, *Ebf3* and *Lgi1* (Olivetti *et al.*, 2014). In the current study, we demonstrated only minimal overlap in the genes deregulated by disease (PA mutant mice compared to WT mice – vehicle treated only) compared to genes deregulated by 17 β -estradiol treatment (vehicle treated mice compared to estradiol treated mice – PA mutant mice only). Despite these small numbers of genes that overlapped between these two comparisons, the genes that did overlap in PA1 and PA2, were deregulated in the opposite direction when treated with estradiol. In the PA1 gene list, there were some key genes of note, including *Ptgs2* (involved in schizophrenia, another neurodevelopmental disorder) and *Slc17a8* (highly involved in synaptic vesicle function in excitatory neurons) (Wei and Hemmings, 2004, UniProt, 2020). In PA2, these genes included *Arc* (a master regulator of synaptic plasticity, and associated with epilepsy and schizophrenia), and *Nppa* (a regulator of neuropeptide hormone activity) (Haug *et al.*, 2000, Huentelman *et al.*, 2015). Though these genes may play a role in the alleviation of the seizure phenotype of PA mutant mice, these modest number of disease genes deregulated when treated with estradiol indicates that treatment in early postnatal life is less likely to be “repairing” the gene expression

pathways deregulated by the PA mutant genotype and more likely recruiting new pathways to affect the reduction in seizures.

Genes containing known conserved estrogen response elements (ERE) were only enriched to very low levels in PA mutant mice with estrogen treatment (Figure 6A, Supplementary Figure 5). Estradiol signalling can occur by direct genomic signalling where there is estrogen receptor dimerization and binding to EREs, as well as via indirect signalling, where estradiol can influence the expression of genes without EREs. As many as one third of estrogen responsive genes lack ERE-like elements (Vrtačnik *et al.*, 2014). Hence, using DAVID, we analysed pathways and ontology terms enriched within the data that were known effects of 17 β -estradiol signalling. Many of our enriched clusters were known to be direct responses to the estrogen receptor pathway according to KEGG or indirect effects of the estradiol pathway (Kanehisa and Goto, 2000, Kanehisa, 2019, Kanehisa *et al.*, 2019). Our data demonstrates that 17 β -estradiol treatment in early postnatal life recruits pathways impacting synaptic function, signal transduction, transcriptional regulation, and hormone activity responsible in reducing the frequency and severity of seizures in PA mutant mice.

We have previously reported specific spatial differences in the density of Cb interneurons at postnatal day 0 in PA1 and PA2 mutant mice, suggestive of a lag in migration at this developmental period compared to WT mice (Lee *et al.* 2017). At the cessation of estradiol treatment at postnatal day 10, we did not detect any significant differences between WT and mutant animals, with or without treatment, in the gene expression of markers for Cb interneurons, nor in the density of these neurons within the cortical layers of the brain. In the case of Npy positive interneurons, the alternative PA1 mouse displayed a reduced density of these cells in adult brain, which was ameliorated with early postnatal E2 treatment (Olivetti *et al.*, 2014). In agreement, we determined a modest reduction in the expression of the *Npy* gene expression in PA1 mutant mice compared to WT animals at the earlier time point of P10. However, we did not find any significant differences to density of Npy interneurons within the

cortex at this time point, with or without estradiol treatment. The expression of *Npy2r* is known to increase in the brain from approximately P14 (Allen brain atlas), meaning we cannot rule out that changes to the density of Npy positive interneurons at later stages of development may occur and contribute to the sustained reduction in seizures observed in estradiol treated mice. Although we detect differences in gene expression of multiple interneuron associated genes at P10 of development, our data indicates to us that the many other genes (and pathways) regulated by estradiol treatment are likely to be participating in the alleviation of seizures, as opposed to increased inhibition in the brain as the sole mechanism.

Conclusion

Here we provide evidence to begin separating the relationship between seizures and cognitive and behavioural deficits in a genetic model of a neurodevelopmental disorder. We demonstrate that behaviour and cognitive outcomes did not improve in the *Arx* PA mutant mice despite significant reductions to the frequency and severity of seizures achieved with early postnatal steroid treatment. Indeed, behavioural deficits were already present prior to peak of seizure onset and do not decline with seizures. Our findings on the broader behavioural phenotypes of PA1 and PA2 mice support the idea that the mechanisms underlying the cognitive deficits in PA patients are complex. The 17- β estradiol treatment early in postnatal life recruited molecular and cellular pathways to reduce the frequency and severity of seizures rather than restoring pathways initially deregulated in *Arx* PA mutant mice driving pathogenesis. Taken together, our data strongly indicates that reduced expression of the inhibitory neuron genes, as well as the genes associated with autism/ID contribute to the seizure and cognitive phenotype of the PA mice. The lack of effective treatments for intellectual disability and neuropsychiatric disturbances, let alone associated early onset seizures, remains a significant challenge and highlights the continued need to elucidate the molecular and cellular drivers of the intellectual disability phenotype as the first necessary steps toward a treatment.

Acknowledgements

We are grateful to Monica Thai and Laboratory Animal Services at The University of Adelaide for their kind assistance with the mice. We wish to acknowledge the guidance and use of behavioural testing equipment and software from Dr Catherine Jawahar and Professor Bernhard Baune.

Data Availability

The data that support the findings of this study are available from the corresponding author, upon reasonable request.

Funding

This research, undertaken by the Intellectual Disability Research program in the Adelaide Medical School, University of Adelaide, Australia, was funded by the Australian National Health and Medical Research Council (Grant No. 1099538). CS was supported by the Australian Research Council (Future Fellowship FT120100086). KL was supported by an Australian Research Training Program Stipend (RTPS).

Competing Interests

The authors have no competing interests to declare.

References

- Bourdeau V, Deschênes J, Métivier R, Nagai Y, Nguyen D, Bretschneider N, et al. Genome-wide identification of high-affinity estrogen response elements in human and mouse. *Mol Endocrinol*. 2004;18(6):1411-27.
- Chachua T, Di Grazia P, Chern C-R, Johnkuty M, Hellman B, Lau HA, et al. Estradiol does not affect spasms in the betamethasone-NMDA rat model of infantile spasms. *Epilepsia*. 2016;57(8):1326-36.
- Chiurazzi P, Pirozzi F. Advances in understanding - genetic basis of intellectual disability. *F1000Res*. 2016;5.
- Colasante G, Sessa A, Crispi S, Calogero R, Mansouri A, Collombat P, et al. Arx acts as a regional key selector gene in the ventral telencephalon mainly through its transcriptional repression activity. *Developmental Biology*. 2009;334(1):59-71.
- Colombo E, Collombat P, Colasante G, Bianchi M, Long J, Mansouri A, et al. Inactivation of Arx, the Murine Ortholog of the X-Linked Lissencephaly with Ambiguous Genitalia Gene, Leads to Severe Disorganization of the Ventral Telencephalon with Impaired Neuronal Migration and Differentiation. *Journal of neuroscience*, 2007;27(17):4786-98.
- Cristóvão JS, Santos R, Gomes CM. Metals and Neuronal Metal Binding Proteins Implicated in Alzheimer's Disease. *Oxid Med Cell Longev*. 2016;2016:9812178-.
- Degen M, Brellier F, Kain R, Ruiz C, Terracciano L, Orend G, et al. Tenascin-W is a novel marker for activated tumor stroma in low-grade human breast cancer and influences cell behavior. *Cancer Res*. 2007;67(19):9169-79.
- Ellis CA, Petrovski S, Berkovic SF. Epilepsy genetics: clinical impacts and biological insights. *Lancet Neurol*. 2020;19(1):93-100.
- Farwell JR, Dodrill CB, Batzel LW. Neuropsychological Abilities of Children with Epilepsy. *Epilepsia*. 1985;26(5):395-400.
- Friocourt G, Kanatani S, Tabata H, Yozu M, Takahashi T, Antypa M, et al. Cell-Autonomous Roles of ARX in Cell Proliferation and Neuronal Migration during Corticogenesis. *The Journal of Neuroscience*. 2008;28(22):5794.
- Galanopoulou AS, Moshé SL. Pathogenesis and new candidate treatments for infantile spasms and early life epileptic encephalopathies: A view from preclinical studies. *Neurobiology of Disease*. 2015;79:135-49.
- GeneDx. Autism/ID Xpanded Panel. 2020 [cited 2020; Available from: <https://www.genedx.com/test-catalog/available-tests/autismid-xpanded-panel/>]

Haug K, Kremerskothen J, Hallmann K, Sander T, Dullinger J, Rau B, et al. Mutation screening of the chromosome 8q24.3-human activity-regulated cytoskeleton-associated gene (ARC) in idiopathic generalized epilepsy. *Mol Cell Probes*. 2000;14(4):255-60.

Hrachovy RA, Frost JD. Chapter 63 - Infantile spasms. In: Dulac O, Lassonde M, Sarnat HB, editors. *Handbook of Clinical Neurology*; Elsevier; 2013. p. 611-8.

Huang da W, Sherman BT, Lempicki RA. Bioinformatics enrichment tools: paths toward the comprehensive functional analysis of large gene lists. *Nucleic Acids Res*. 2009;37:1-13.

Huang da W, Sherman BT, Lempicki RA. Systematic and integrative analysis of large gene lists using DAVID bioinformatics resources. *Nat Protoc*. 2009;4(1):44-57.

Huentelman MJ, Muppana L, Corneveaux JJ, Dinu V, Pruzin JJ, Reiman R, et al. Association of SNPs in EGR3 and ARC with Schizophrenia Supports a Biological Pathway for Schizophrenia Risk. *PLoS One*. 2015;10(10):e0135076.

Jackson MR, Lee K, Mattiske T, Jaehne EJ, Ozturk E, Baune BT, et al. Extensive phenotyping of two ARX polyalanine expansion mutation mouse models that span clinical spectrum of intellectual disability and epilepsy. *Neurobiology of Disease*. 2017;105:245-56.

Kanehisa M. Toward understanding the origin and evolution of cellular organisms. *Protein Sci*. 2019;28(11):1947-51.

Kanehisa M, Goto S. KEGG: kyoto encyclopedia of genes and genomes. *Nucleic Acids Res*. 2000;28(1):27-30.

Kanehisa M, Sato Y, Furumichi M, Morishima K, Tanabe M. New approach for understanding genome variations in KEGG. *Nucleic Acids Res*. 2019;47(D1):D590-D5.

Kitamura K, Ito Y, Yanazawa M, Ohsawa M, Suzuki-Migishima R, Umeki Y, et al. Three human ARX mutations cause the lissencephaly-like and mental retardation with epilepsy-like pleiotropic phenotypes in mice. *Human Molecular Genetics*. 2009;18(19):3708-24.

Kitamura K, Yanazawa M, Sugiyama N, Miura H, Iizuka-Kogo A, Kusaka M, et al. Mutation of ARX causes abnormal development of forebrain and testes in mice and X-linked lissencephaly with abnormal genitalia in humans. *Nat Genet*. 2002;32(3):359-69.

Le Magueresse C, Monyer H. GABAergic interneurons shape the functional maturation of the cortex. *Neuron*. 2013;77(3):388-405.

Lee K, Ireland K, Bleeze M, Shoubridge C. ARX polyalanine expansion mutations lead to migration impediment in the rostral cortex coupled with a developmental deficit of calbindin-positive cortical GABAergic interneurons. *Neuroscience*. 2017;357:220-31.

- Lee K, Mattiske T, Kitamura K, Gecz J, Shoubridge C. Reduced polyalanine-expanded Arx mutant protein in developing mouse subpallium alters Lmo1 transcriptional regulation. *Human Molecular Genetics*. 2014;23(4):1084-94.
- Lin Z, Tann JY, Goh ET, Kelly C, Lim KB, Gao JF, et al. Structural basis of death domain signaling in the p75 neurotrophin receptor. *Elife*. 2015;4:e11692.
- Loch JI, Bonarek P, Tworzydło M, Łazińska I, Szydłowska J, Lipowska J, et al. The engineered β -lactoglobulin with complementarity to the chlorpromazine chiral conformers. *Int J Biol Macromol*. 2018;114:85-96.
- Malakooti N, Pritchard MA, Adlard PA, Finkelstein DI. Role of metal ions in the cognitive decline of Down syndrome. *Front Aging Neurosci*. 2014;6:136-.
- Marques I, Sá MJ, Soares G, Mota MdC, Pinheiro C, Aguiar L, et al. Unraveling the pathogenesis of ARX polyalanine tract variants using a clinical and molecular interfacing approach. *Molecular Genetics & Genomic Medicine*. 2015;3(3):203-14.
- Mattiske T, Lee K, Gecz J, Friocourt G, Shoubridge C. Embryonic forebrain transcriptome of mice with polyalanine expansion mutations in the ARX homeobox gene. *Human Molecular Genetics*. 2016;25(24):5433-43.
- McCarthy MM. Estradiol and the Developing Brain. *Physiological reviews*. 2008;88(1):91-124.
- Miura H, Yanazawa M, Kato K, Kitamura K. Expression of a novel aristaless related homeobox gene 'Arx' in the vertebrate telencephalon, diencephalon and floor plate. *Mechanisms of Development*. 1997;65(1-2):99-109.
- Nabbout R, Dulac O. Epileptic Encephalopathies: A Brief Overview. *Journal of Clinical Neurophysiology* November/December. 2003;20(6):393-7.
- Nakamura NH, McEwen BS. Changes in interneuronal phenotypes regulated by estradiol in the adult rat hippocampus: a potential role for neuropeptide Y. *Neuroscience*. 2005;136(1):357-69.
- Neyens LGJ, Aldenkamp AP, Meinardi HM. Prospective follow-up of intellectual development in children with a recent onset of epilepsy. *Epilepsy Research*. 1999;34(2):85-90.
- Nickels KC, Wirrell EC. Cognitive and Social Outcomes of Epileptic Encephalopathies. *Seminars in Pediatric Neurology*. 2017;24(4):264-75.
- Olivetti PR, Maheshwari A, Noebels JL. Neonatal Estradiol Stimulation Prevents Epilepsy in Arx Model of X-Linked Infantile Spasms Syndrome. *Science Translational Medicine*. 2014;6(220):220ra12.

- Olivetti PR, Noebels JL. Interneuron, interrupted: molecular pathogenesis of ARX mutations and X-linked infantile spasms. *Curr Opin Neurobiol.* 2012;22(5):859-65.
- Paciorkowski AR, Thio LL, Dobyns WB. Genetic and biologic classification of infantile spasms. *Pediatr Neurol.* 2011;45(6):355-67.
- Partington MW, Turner G, Boyle J, Gécz J. Three new families with X-linked mental retardation caused by the 428–451dup(24bp) mutation in ARX. *Clinical Genetics.* 2004;66(1):39-45.
- Prasad AN, Burneo JG, Corbett B. Epilepsy, comorbid conditions in Canadian children: Analysis of cross-sectional data from Cycle 3 of the National Longitudinal Study of Children and Youth. *Seizure.* 2014;23(10):869-73.
- Price MG, Yoo JW, Burgess DL, Deng F, Hrachovy RA, Frost JD, et al. A Triplet Repeat Expansion Genetic Mouse Model of Infantile Spasms Syndrome, Arx((GCG)₁₀₊₇), with Interneuronopathy, Spasms in Infancy, Persistent Seizures, and Adult Cognitive and Behavioral Impairment. *Journal of Neuroscience,* 2009;29(27):8752-63.
- Shoubridge C, Fullston T, Gécz J. ARX spectrum disorders: making inroads into the molecular pathology. *Human Mutation.* 2010;31(8):889-900.
- Smith-Hicks CL. GABAergic dysfunction in pediatric neuro-developmental disorders. *Front Cell Neurosci.* 2013;7:269.
- UniProt. SLC17A8 - Vesicular glutamate transporter 3. 2020 [cited 2020; Available from: <https://www.uniprot.org/uniprot/Q8NDX2#function>
- UniProt. TACR1 - Substance-P receptor. 2020 [cited 2020; Available from: <https://www.uniprot.org/uniprot/P25103>
- Velíšková J. The role of estrogens in seizures and epilepsy: The bad guys or the good guys? *Neuroscience.* 2006;138(3):837-44.
- Vrtačnik P, Ostanek B, Mencej-Bedrač S, Marc J. The many faces of estrogen signaling. *Biochem Med (Zagreb).* 2014;24(3):329-42.
- Wei J, Hemmings GP. A study of a genetic association between the PTGS2/PLA2G4A locus and schizophrenia. *Prostaglandins Leukot Essent Fatty Acids.* 2004;70(4):413-5.
- WHO. Epilepsy. 2019 [cited 2019; Available from: <https://www.who.int/news-room/fact-sheets/detail/epilepsy>
- Willemsen MH, Kleefstra T. Making headway with genetic diagnostics of intellectual disabilities. *Clin Genet.* 2014;85(2):101-10.
- Younus, I. and D. S. Reddy (2016). "Seizure facilitating activity of the oral contraceptive ethinyl estradiol." *Epilepsy Res* **121**: 29-32.

Zack, M. M. and R. Kobau (2017). "National and State Estimates of the Numbers of Adults and Children with Active Epilepsy - United States, 2015." MMWR Morb Mortal Wkly Rep **66**(31): 821-825.

Figure Legends

Figure 1: Early estradiol treatment diminishes observed seizure severity and frequency in PA mutant mice. Timeline showing the experimental course of the mouse treatment study (A). PA1 and PA2 mutant mice exhibit reduced seizure frequency (B) and seizure severity (C) when treated with estradiol compared to their vehicle treated counterparts (percentage seizure occurrence – percentages do not include repeated seizures from the same mouse). (PA1: (B) two-tailed t-test, $p < 0.0001$, $df = 70$; (C) Chi square test, $p = 0.0036$, $df = 11.26, 2$). Estradiol treatment did not delay the age of first seizure (D) in either mutant strain (PA2: two-tailed t-test, $p = 0.0002$, $F = 1.463 (10,7)$, $df = 17$). Mice marked with a star died of a seizure (found dead in cage) within 2-4 days of having an observed seizure on handling. Median \pm min/max is presented for PA1 and PA2 mice from vehicle and estradiol treatment groups. Each dot represents an individual animal at the age of their first seizure. Analysis across five separate breeding rounds each for PA1 mice (Estradiol; $n = 14$; dark orange (dashed line/square dots) vs vehicle; $n = 13$ light orange (solid line/circles)) and PA2 mice (Estradiol; $n = 16$; dark blue (dashed line/square dots) vs vehicle; $n = 19$; light blue (solid line/circles)). # $p < 0.05$ indicates significant difference between estradiol and vehicle treated animals across the duration of the study.

Figure 2: Seizure severity and frequency during video seizure monitoring are reduced in PA mutant mice treated with estradiol. PA1 and PA2 mice exhibit reduced seizure frequency and severity when treated with estradiol (PA1; $n = 10$; dark orange) (PA2; $n = 7$; dark blue) compared to their vehicle treated counterparts (PA1; $n = 11$ light orange) and (PA2; $n = 12$; light blue). Each dot represents an individual seizure event measured during 12 hours of video footage per mouse across multiple days. Seizure scores increase with severity from “no seizure” to “prolonged myoclonic seizure” on the Y-axis. # indicates significant difference

between estradiol and vehicle treated PA mice (one-way ANOVA, Tukey's HSD post hoc analysis, $F(3, 135) = 11.28, p < 0.0001$).

Figure 3: Early estradiol does not improve survival in PA mutant mice. Estradiol did not improve mortality in either PA1 or PA2 mice. Analysis across five separate breeding rounds each for PA1 mice (Estradiol; $n = 14$; dark orange (dashed line) vs vehicle; $n = 13$ light orange (solid line)) and PA2 mice (Estradiol; $n = 16$; dark blue (dashed line) vs vehicle; $n = 19$; light blue (solid line)). There were no WT mice treated with vehicle and estradiol that died during the trial with data pooled into one group (grey line).

Figure 4: Early estradiol does not improve behavioural deficits in PA mutant mice. Anxiety-like behaviour was measured using the open field test. (A) The distance the mice travelled in the periphery versus the central field of the open field was measured in metres (m) is shown at one month and two months of age. WT mice treated with vehicle ($n = 17/12$; light grey) and estradiol ($n = 8/8$; dark grey); PA1 mice treated with vehicle ($n = 6/5$; light orange) and estradiol ($n = 4/3$; dark orange); PA2 mice treated with vehicle ($n = 11/6$; light blue) and estradiol ($n = 5/5$; dark blue) (Two months ~one-way ANOVA, $F(5,33) = 12.25, P < 0.0001$). (B) Representative tracking maps from WT ($n = 2$; grey), PA1 ($n = 1$; orange) and PA2 ($n = 1$; blue). (C) Autistic-like behaviour was measured at one and two months of age by the time in seconds (s) the mice spent interacting with a new mouse in the sociability test (Two months ~one-way ANOVA, $F(3,26) = 21.85, P < 0.0001$), (D) or the familiar (white bars) or stranger (coloured bars) mouse in the social novelty test. WT mice treated with vehicle ($n = 15/9$; light grey) and estradiol ($n = 8/6$; dark grey); PA^{pool} mice treated with vehicle ($n = 15/9$; light green) and estradiol ($n = 8/6$; dark green); (E) Neuromuscular strength measured using the inverted

grid test at two months of age (one-way ANOVA, $F(3,31) = 7.920$, $P=0.0005$). The latency for mice to fall from the inverted grid was measured in seconds (s). WT mice treated with vehicle ($n = 11$; light grey) and estradiol ($n = 7$; dark grey); PA1 mice treated with vehicle ($n = 6$; light orange) and estradiol ($n = 3$; dark orange); PA2 mice treated with vehicle ($n = 4$; light blue) and estradiol ($n = 4$; dark blue). In the second graph, PA1 and PA2 mice were combined as a PA^{pool} group. WT mice treated with vehicle ($n = 11$; light grey) and estradiol ($n = 7$; dark grey); PA^{pool} mice treated with vehicle ($n = 10$; light green) and estradiol ($n = 7$; dark green). * indicates significant difference between PA mutant mice and WT control littermates across the duration of the study, $p < 0.05$, Tukey's HSD post hoc analysis.

Figure 5: Transcriptome is deregulated by disease in PA mutant mice. Transcriptomic analysis of postnatal day (P) 10 brains of PA mutant mice. Differential expression of genes from P10 mice was determined using EdgeR and selected based on a Log₂ fold change greater than ± 0.5 with a p-value < 0.05 . (A) Total number of deregulated genes and the percentage of either upregulated or downregulated genes from our analysis of vehicle treated PA1, PA2 and PA^{pool} mice compared to vehicle treated WT littermates. (B) Venn diagram displaying overlap of deregulated genes in PA1 (orange), PA2 (blue) and PA^{pool} (dotted circle) groups, as well as core overlapping genes (green with list of genes). (C) Graph showing log fold change values of genes from the core overlap lists in (B). Interneuron genes are highlighted in the grey dashed box. (D) Table showing overlap of deregulated genes from vehicle treated PA1, PA2 and PA^{pool} mice with known neurodevelopmental disorder (NDD), inhibitory cell and ARX target genes. (E) Graph showing log fold change values of genes from enriched interneuron genes in (D). Genes from core overlap are in the grey dashed box. * indicates significant overlap with reference gene lists ($p < 0.05$).

Figure 6: Estradiol alters the transcriptome of PA mutant mice. Transcriptomic analysis of postnatal day (P) 10 brains of PA mutant mice. Differential expression of genes from P10 mice was determined using EdgeR and selected based on a Log₂ fold change greater than ± 0.5 with a p-value < 0.05 . (A) Total number of deregulated genes and the percentage of either upregulated or downregulated genes from our analysis of estradiol treated PA1, PA2 and PA^{pool} mice compared to vehicle treated PA mutant mice. Table also shows number and percentage of genes known to contain a high-affinity mouse estrogen-response element (ERE). * indicates significant overlap between genes deregulated by estradiol and ERE-containing mouse genes ($p < 0.05$). (B) Venn diagram showing overlapping between the disease-deregulated transcriptome and the estradiol-treated transcriptome of PA1, PA2 and PA^{pool} mice. (C) Graphs showing the opposite deregulation direction between genes overlapping between disease and estradiol changed genes in PA1 and PA2. (D) Venn diagram displaying overlapping genes between the estradiol-treated transcriptomes of PA1 (orange), PA2 (blue) and PA^{pool} (green) mice. (E) Overlap of deregulated genes from estradiol treated PA1, PA2 and PA^{pool} mice with known neurodevelopmental disorder (NDD) and inhibitory cell genes. * indicates significant overlap with reference gene lists ($p < 0.05$).

Figure 7: Abundance of calbindin (Cb) and neuropeptide-Y (Npy) positive cells in the prefrontal cortex. (A) Representative DAPI stained image of the brain in a WT mouse illustrating the region of the brain analysed (within dashed lines). Scale bar 200 μ M. (B) Pictomicrographs of brain sections with arrows indicating positive cells corresponding to Cb and Npy interneurons. Scale bar 50 μ M. (C) Density of Cb and Npy positive cells/mm² in WT (Veh and E2 combined) (circles) and PA^{pool} mice (PA1; squares and PA2; triangles). treated with vehicle or estradiol. Cb: WT mice ($n = 5$; white), PA^{pool} mice treated with vehicle ($n = 6$; light grey) and estradiol ($n = 5$; dark grey). Npy: WT mice ($n = 7$; white); PA^{pool} mice treated with vehicle ($n = 4$; light grey) and estradiol ($n = 5$; dark grey).

Supplementary Figure Legends

Supplementary File 1: Detailed behaviour testing protocols.

Supplementary Table 1: Taqman assay details. RNA sequencing validation experiments were prepared as described in the Taqman PreAmp Master Mix Kit user guide (Applied Biosystems). Expression values were normalised to reference gene *β -Actin*.

Supplementary Figure 1: Ages of death in PA mutant mice treated with vehicle or estradiol. PA1 and PA2 mice treated with estradiol (PA1; $n = 13$; dark orange) (PA2; $n = 18$; dark blue) do not exhibit improved survival when compared to their vehicle treated counterparts (PA1; $n = 14$; light orange) (PA2; $n = 21$; light blue). Individual circles represent individual mice throughout the duration of the study (up to 70 days postnatal). Data is shown as mean age \pm SEM.

Supplementary Figure 2: Testes and brain weights of PA mutant mice treated with vehicle or estradiol. Testes (left and right combined) and cerebral hemispheres (left and right combined) were weighed at postnatal day 70. WT mice, vehicle-treated (light grey) testes (n=27) and brain (n=26) and estradiol-treated (dark grey) testes and brain (n=18). PA1 mice, vehicle-treated (light orange) testes and brain (n=5) and estradiol treated (dark orange) testes (n=2) and brain (n=3). PA2 mice, vehicle-treated (light blue) testes (n=6) brain (n=7) estradiol-treated (dark blue) testes and brain (n=4). * indicates significant difference between PA mutant mice and WT littermates, $p < 0.05$, one-way ANOVA with Tukey's HSD.

Supplementary Figure 3: Body weights of PA mutant mice treated with vehicle or estradiol. PA1 and PA2 mice treated with estradiol (PA1; $n = 13$; dark orange) (PA2; $n = 18$; dark blue) or vehicle (PA1; $n = 14$; light orange) (PA2; $n = 21$; light blue) do not exhibit any improvement to body weight through the duration of the study (postnatal day 0 to postnatal day 70), compared to their WT littermates, treated with either estradiol (WT; $n = 30$; dark grey) or vehicle (WT; $n = 23$; light grey). Data is shown at mean weight on each day of the study \pm SEM. * indicates significant difference at postnatal days 10, 21, 45 and 60 between PA mutant mice and WT littermates, $p < 0.05$, one-way ANOVA with Tukey's HSD.

Supplementary Figure 4: PA mutant mice do not display hyperactivity as measured by total distance in the open field test. Anxiety-like and fear response behaviour was measured using the open field test. (A) The total distance the mice travelled in the open field apparatus during the duration of the test at one month and two months of age. Wild-type mice treated with vehicle ($n = 17/12$; light grey) and estradiol ($n = 8/8$; dark grey); PA1 mice treated with vehicle ($n = 6/5$; light orange) and estradiol ($n = 4/3$; dark orange); PA2 mice treated with vehicle ($n = 11/6$; light blue) and estradiol ($n = 5/5$; dark blue).

Supplementary Figure 5: PA1 and PA2 mutant mice display autistic-like behaviour as measured by sociability and social novelty tests. (A) Autistic-like behaviour was measured at one and two months of age by the time in seconds (s) the mice spent interacting with a new mouse in the sociability test, (B) or the familiar (white) or stranger (black) mouse in the social novelty test. WT mice treated with vehicle ($n = 15/9$; light grey) and estradiol ($n = 8/6$; dark grey); PA1 mice treated with vehicle ($n = 6/4$; light orange) and estradiol ($n = 3/2$; dark orange); PA2 mice treated with vehicle ($n = 9/5$; light blue) and estradiol ($n = 5/4$; dark blue). * indicates significant difference between PA mutant mice and WT control littermates across the duration of the study, $p < 0.05$, one-way ANOVA with Tukey's HSD. # indicates significant difference between estradiol and vehicle treated mutant animals across the duration of the study, $p < 0.05$, one-way ANOVA with Tukey's HSD.

Supplementary Figure 6: PA mutant mice do not display learning and memory deficits in the Barnes maze. Learning and memory was measured using the Barnes maze at two months of age only. The latency to find the escape hole was measured in seconds (s) across a four-day testing period. Mice were measured from WT treated with estradiol ($n = 10$; dark grey) or vehicle ($n = 8$; light grey) with A) PA1 and PA2 mice were combined as a PA^{pool} group and PA^{pool} treated with estradiol ($n = 6$; dark green) or vehicle ($n = 6$; light green). B) PA1 mice treated with estradiol ($n = 4$; dark orange) and vehicle ($n = 2$; light orange). C) PA2 mice treated with estradiol ($n = 4$; dark blue) and vehicle ($n = 4$; light blue).

Supplementary Figure 7: Biological validation of genes deregulated by disease in PA mutant mice by quantitative PCR (qPCR) analysis. Samples tested were RNA samples prepared from the cortex of vehicle-treated mice at postnatal day 10 across each genotype (WT; $n = 6$; PA1; $n = 4$; PA2; $n = 4$; PA^{pool}; $n = 4$ PA1 + 4 PA2 samples combined). Expression values were normalised to the reference gene, *β -Actin*. (A) Represents genes of mostly higher

counts per million from our RNAseq data, where qPCR results agreed with RNAseq results.

(B) Represents control genes that were non-significant in both RNAseq and qPCR analysis.

(C) Represents genes where the breadth of signal was variable across the three genotype groups between the RNAseq and qPCR analysis. Summary tables show results of these genes in RNAseq and qPCR data, with final column showing whether the qPCR results agreed with the RNAseq data. Grayscale colours in significance tables represent significance of result (lightest grey $p < 0.05$, medium grey $p < 0.005$ and darkest grey $p < 0.0001$). Individual graphs show relative quantity for each gene for WT (grey), PA1 (orange), PA2 (blue) and PA^{pool} (green). * $p < 0.05$, ** $p < 0.005$, *** $p < 0.0001$ (one-tailed t-test of PA1, PA2 or PA^{pool} compared to WT).

Supplementary Figure 8: Enrichment analysis of genes deregulated by disease in PA mutant mice. Table showing significant gene enrichment terms in deregulated genes in PA1, PA2 and PA^{pool} groups from DAVID cluster annotation analysis. Clusters with enrichment scores of < 0.9 are not shown. Heat map is based on maximum, minimum and 50th percentile score in data set (legend in figure).

Supplementary Figure 9: Biological validation of genes deregulated by estradiol in PA mutant mice by quantitative PCR analysis. Samples tested were pooled RNA samples prepared from the cortex of vehicle and estradiol treated mice at postnatal day 10 across each genotype. WT pooled samples contained RNA from $n = 6$ cortex samples for each treatment group. PA1 and PA2 pooled samples contained RNA from $n = 4$ cortex samples for each treatment group. Expression values were normalised to the reference gene, *β -Actin*. (A) Summary table shows results of these genes in RNAseq and qPCR data, with final column showing whether the qPCR results agreed with the RNAseq data. Grayscale colours in significance tables represent significance of result (lightest grey $p < 0.05$, medium grey $p < 0.005$

and darkest grey $p < 0.0001$). (B) Individual graphs of relative quantity for each gene for WT (vehicle = light grey; estradiol = dark grey), PA1 (vehicle = light orange; estradiol = dark orange), and PA2 (vehicle = light blue; estradiol = dark blue). Significance indicated by * $p < 0.05$, ** $p < 0.005$, *** $p < 0.0001$, one-tailed t-test of vehicle treated WT, PA1 and PA2 compared to estradiol treated WT, PA1 and PA2).

Supplementary Figure 10: Enrichment analysis of genes deregulated by estradiol in PA mutant mice. Significant gene enrichment terms in genes deregulated by estradiol in PA1, PA2 and PA^{pool} groups from DAVID cluster annotation analysis. Heat map is based on maximum, minimum and 50th percentile score in data set (legend in figure). No clusters with enrichment scores of < 1.0 are shown. Clusters with # are pathways and functions known to be regulated by the estrogen receptor pathway.

Supplementary Figure 11: Technical validation of genes deregulated by disease in PA mutant mice by quantitative PCR analysis. Scatter plots showing relationship between log₂fold change and average log count per million (CPM) of genes changed with estradiol treatment in PA1 (A) and PA2 (B) mice. Orange lines show log₂fold change ± 1 and black lines show log₂fold change ± 0.5 . (C) shows individual quantitative PCR results, from untreated pooled samples of those used for RNAseq analysis (WT; $n = 6$; PA1; $n = 4$; PA2; $n = 4$). Expression values were normalised to the reference gene, β -Actin. *Frmd7* was significantly decreased in PA1 in our RNAseq analysis and this was validated by qPCR. *Shox2* was significantly decreased compared to their WT littermates in PA2 in our RNAseq analysis, however, this was not validated by qPCR. *Th* was significantly decreased in PA1 and PA2 in our RNAseq analysis and this was validated in PA1 but not PA2 by qPCR.

Figure 1

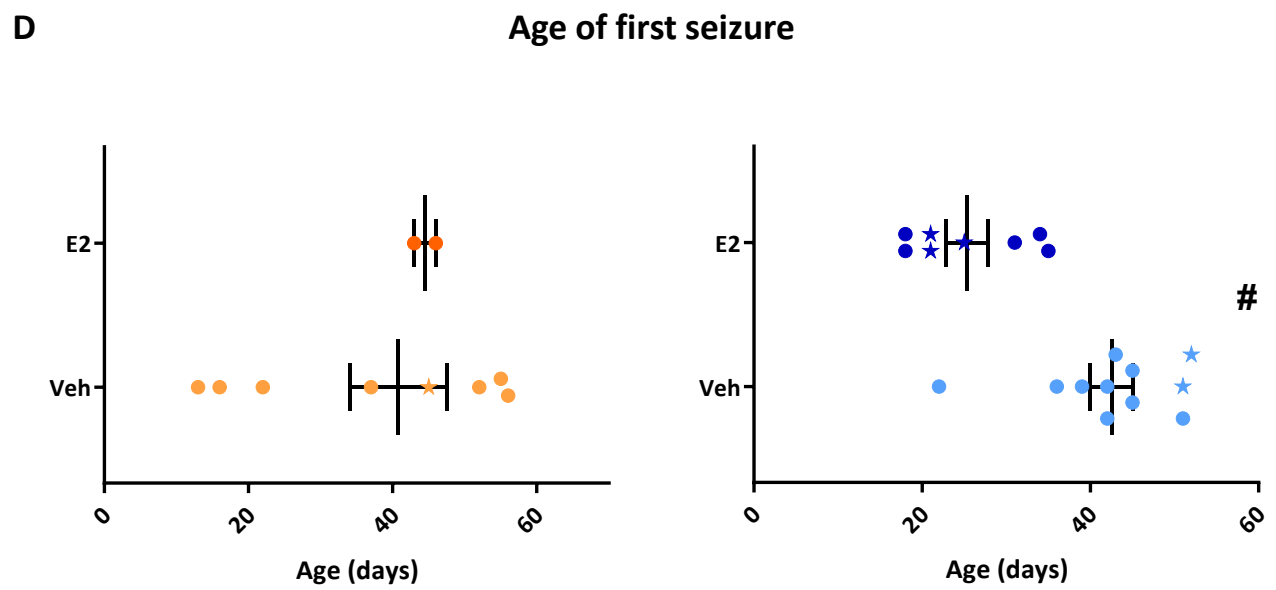
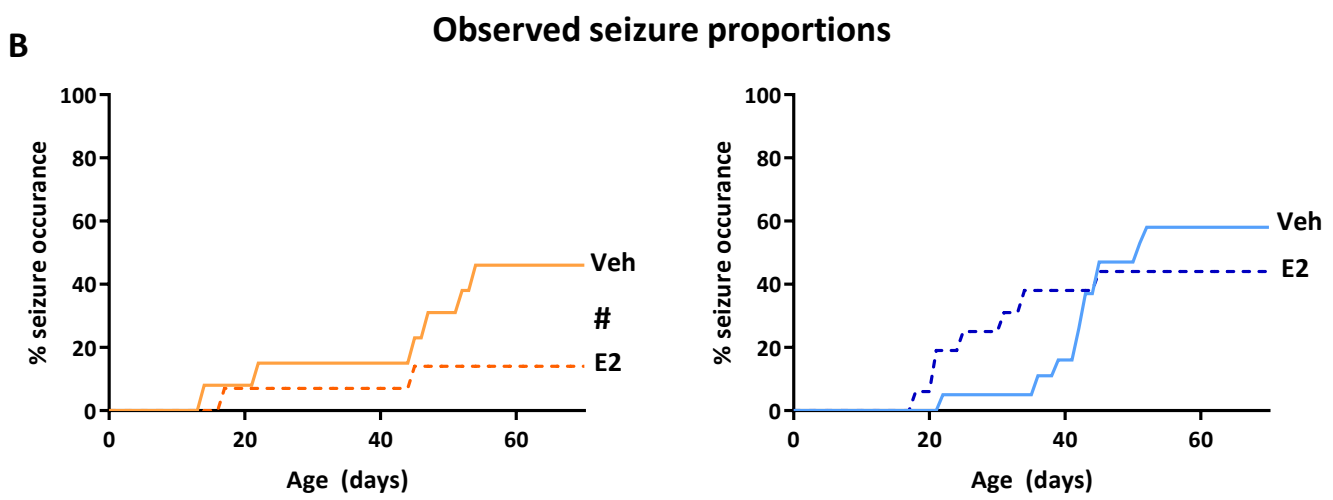
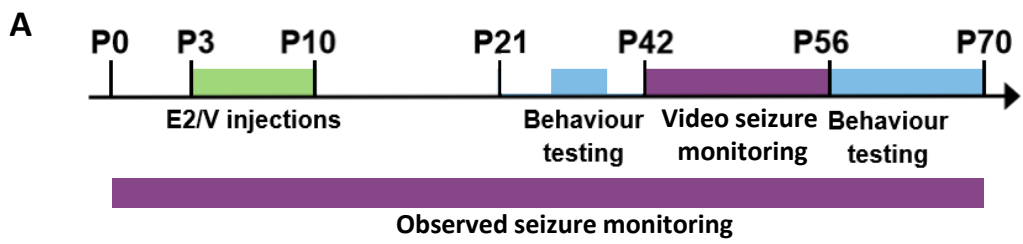


Figure 2

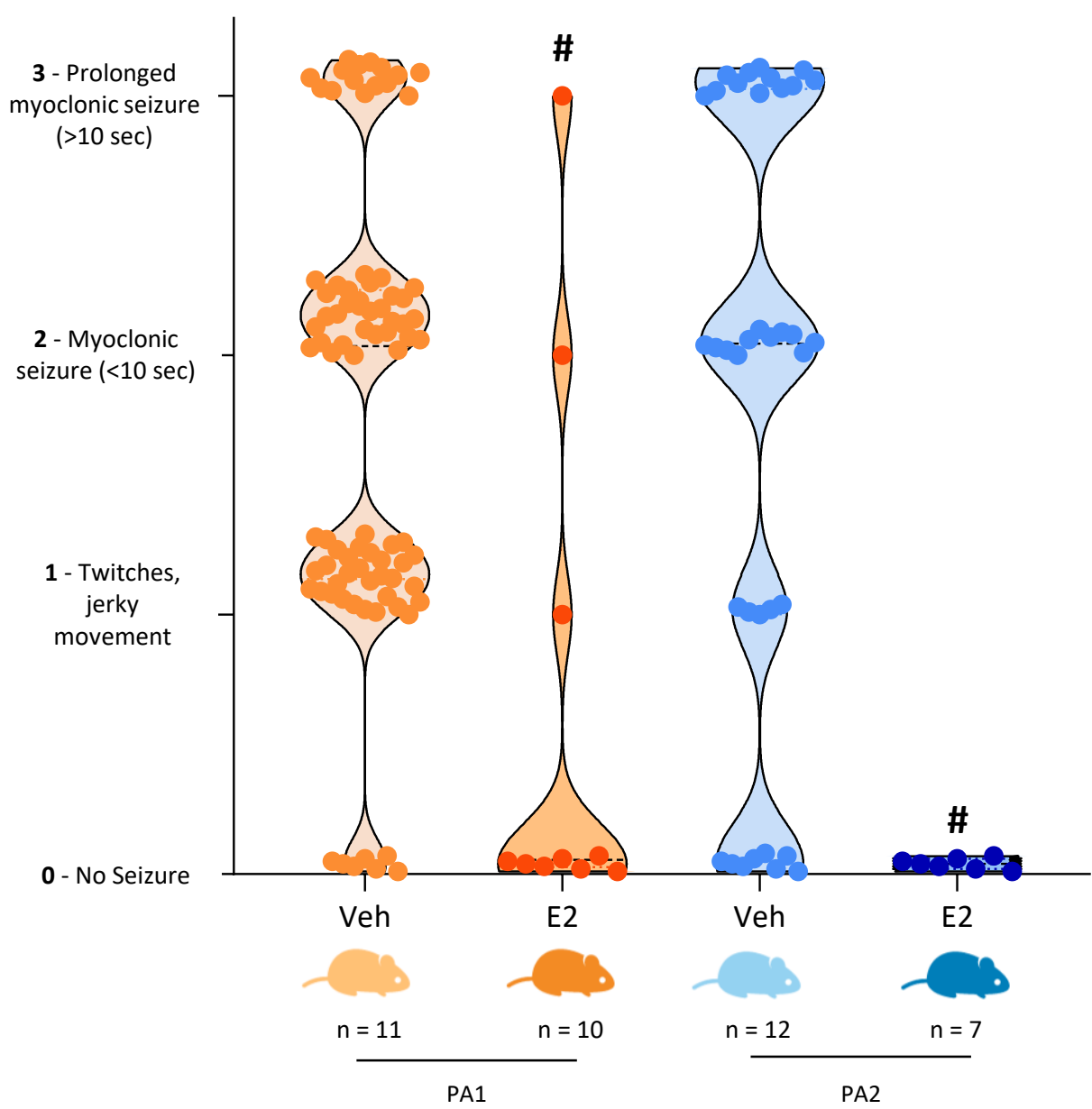


Figure 3

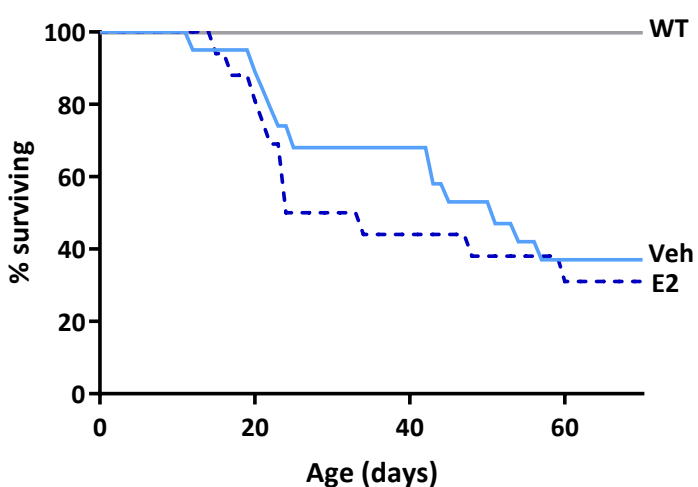
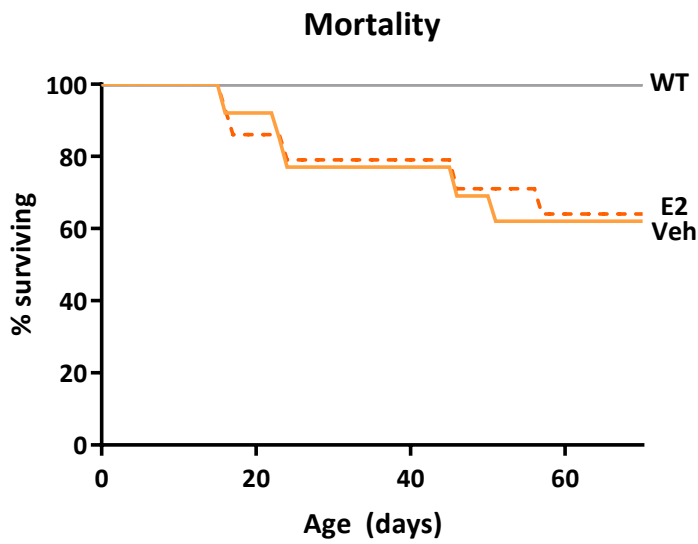


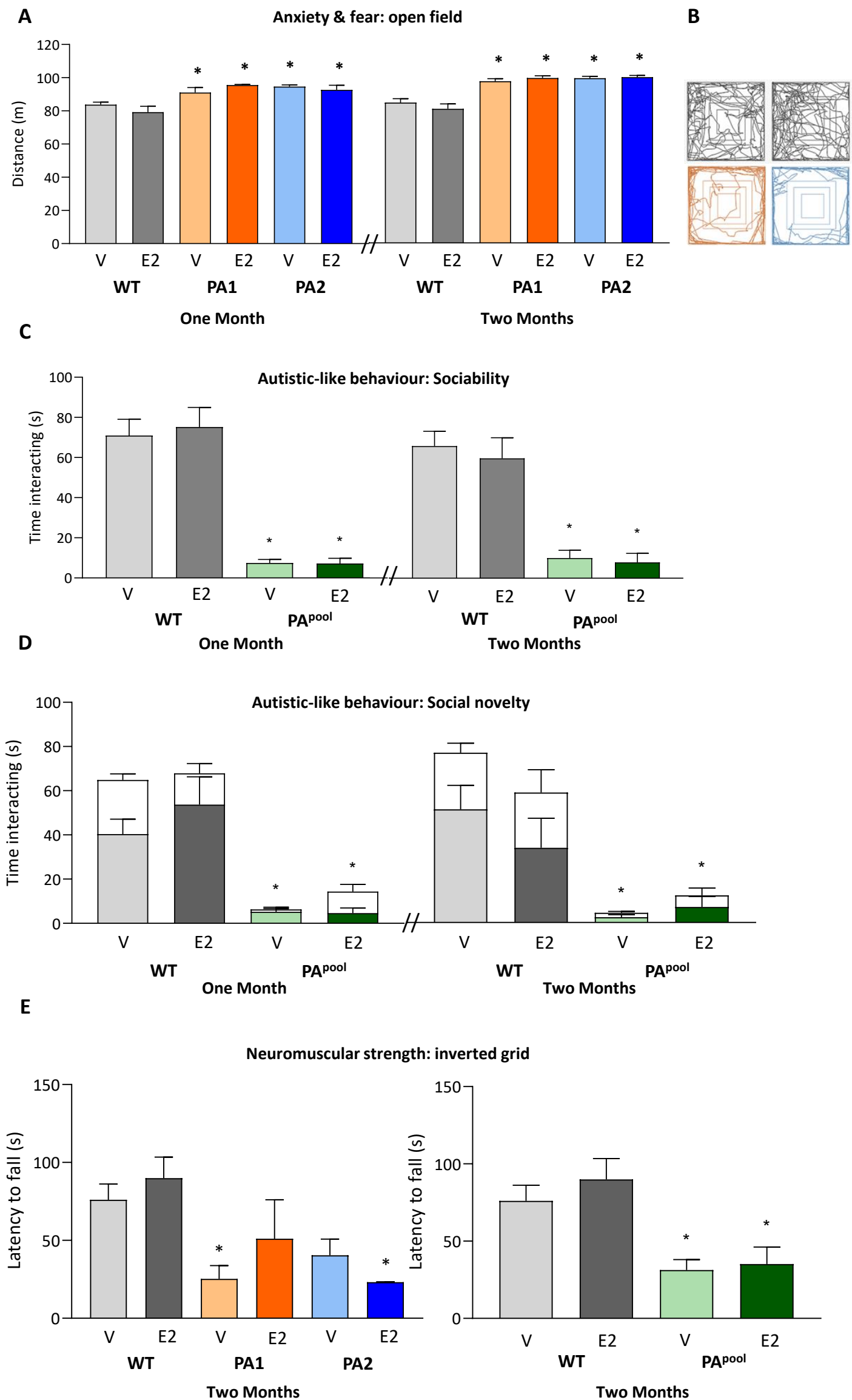
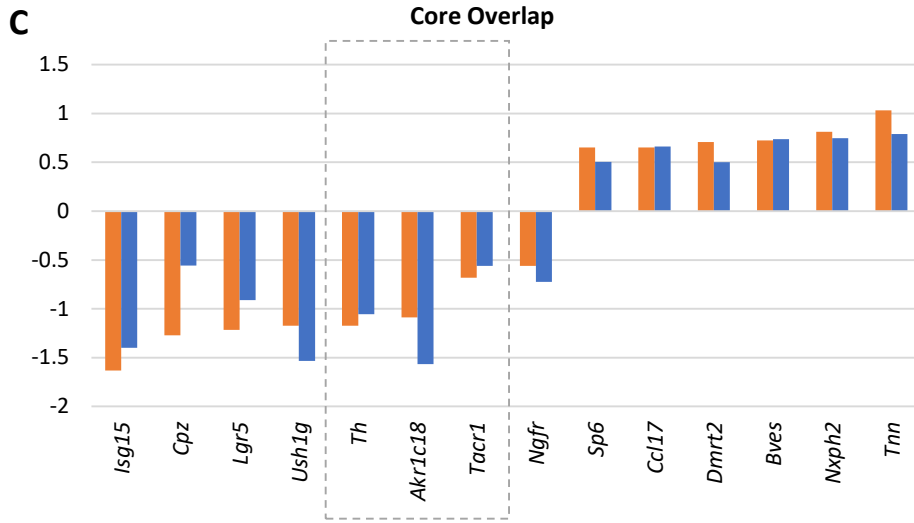
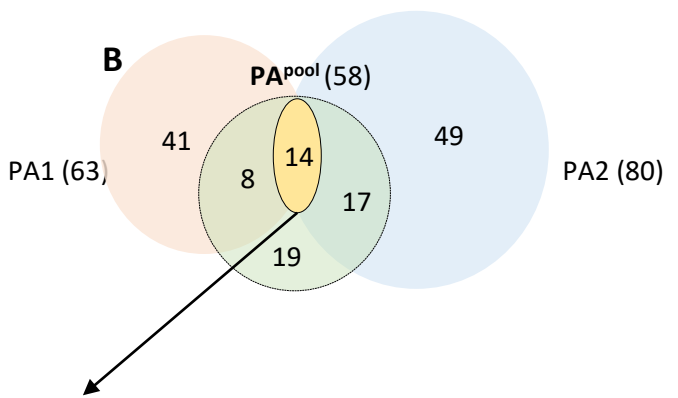
Figure 4

Figure 5

A Genes deregulated by disease

	PA1	PA2	PA ^{pool}
vs WT	63	80	58
↑	22 (35%)	43 (54%)	22 (38%)
↓	41 (65%)	37 (46%)	36 (62%)
ERE	13 (21%)	11 (14%)	11 (19%)



D Neurodevelopmental disorder genes deregulated by disease

	Core Overlap	PA1	PA2	PA ^{pool}
Autism/ID	<i>Cpz</i> , <i>Th</i>	6% <i>Dnah11</i> , <i>Enpp1</i>	11%* <i>Chat</i> , <i>Chrna2</i> , <i>Lrp2</i> , <i>Ntrk1</i> <i>Prima1</i> , <i>Slc5a7</i> , <i>Sp7</i>	12%* <i>Chat</i> , <i>Chrna2</i> , <i>Msx1</i> , <i>Ntrk1</i> <i>Sp7</i>
Epilepsy		3% <i>Col3a1</i> , <i>Npy</i>	2% <i>Chrna2</i> , <i>Lrp2</i>	5% <i>Chrna2</i> , <i>Cyp27a1</i> , <i>Msx2</i>
ARX target genes	<i>Isg15</i> , <i>Th</i>	21%* <i>4932411E22Rik</i> , <i>Ankfh1</i> , <i>Fam124b</i> , <i>Fau</i> , <i>Gprin2</i> , <i>Isg15</i> , <i>Lmo1</i> , <i>Npy</i> , <i>Pde3a</i> , <i>Rsg1</i> , <i>Syt15</i> , <i>Th</i> , <i>Thbs4</i>	11%* <i>1700007G11Rik</i> , <i>Ccdc60</i> , <i>Crabp1</i> , <i>Fam183b</i> , <i>Isg15</i> , <i>Lrp2</i> , <i>Meis1</i> , <i>Myh8</i> , <i>Th</i>	17%* <i>Crabp1</i> , <i>Fosb</i> , <i>Frmd7</i> , <i>Gpnmb</i> , <i>Isg15</i> , <i>Mafa</i> , <i>Myh8</i> , <i>Th</i> , <i>Thbs4</i>
Interneuron genes	<i>Akric18</i> , <i>Tacr1</i> , <i>Th</i>	8%* <i>Akric18</i> , <i>Npy</i> , <i>Pdlim3</i> , <i>Tacr1</i> , <i>Th</i>	10%* <i>Akric18</i> , <i>Chat</i> , <i>Chrna2</i> , <i>Col14a1</i> , <i>Myh8</i> , <i>Slc18a3</i> , <i>Tacr1</i> , <i>Th</i>	17%* <i>Akric18</i> , <i>Chat</i> , <i>Chrna2</i> , <i>Fosb</i> , <i>Frmd7</i> , <i>Myh8</i> , <i>Pdlim3</i> , <i>Spp1</i> , <i>Tacr1</i> , <i>Th</i>

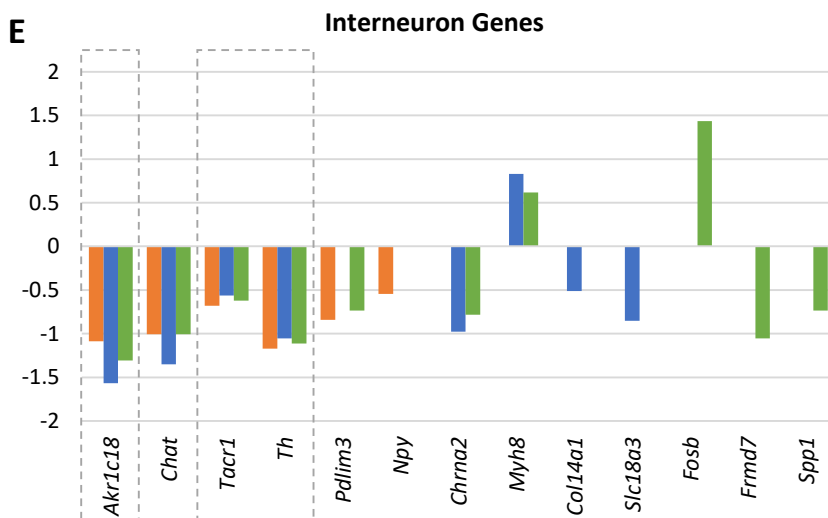


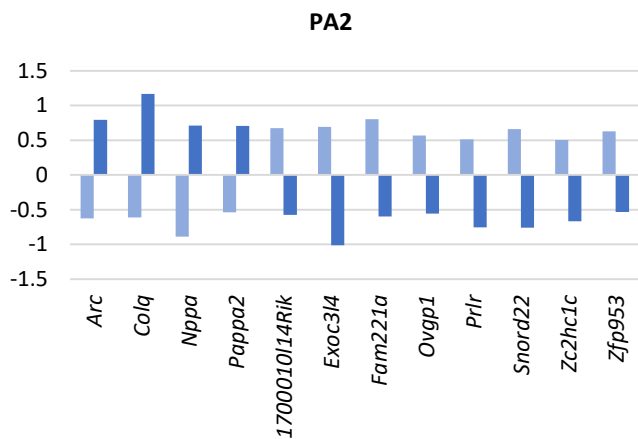
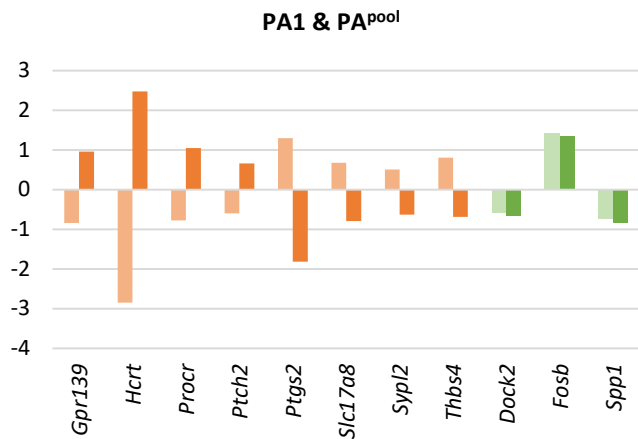
Figure 6

A

Genes deregulated by E2 treatment				
	WT	PA1	PA2	PA ^{pool}
vs VEH	56	124	158	53
↑	27 (48%)	93 (75%)	36 (23%)	33 (62%)
↓	29 (52%)	31 (25%)	122 (77%)	20 (38%)
ERE	12 (21%)*	22 (18%)*	22 (15%)	8 (15%)

C

Overlapping genes deregulated by E2 and disease			
	PA1	PA2	PA ^{pool}
# genes	8	12	3



E

Neurodevelopmental disorder genes deregulated by E2			
	PA1	PA2	PA ^{pool}
	10%*	6%*	13%*
Autism/ID	<i>Bdnf, Cacna1h, Col1a1, Cpz, Dbh, Eln, Flna, Fos, Iyd, Med12, Nlrp3, Npas4, Pabpc4l, Traip, Unc13d</i>	<i>Clrn1, Ebf3, Fos, Gabrq, Hap1, Lhx1, Nkx2-1, Npas4, Sim1, Trhr</i>	<i>Col1a1, Cpz, Dbh, Ebf3, Lhx1, Nlrp3, Nr4a2, Shox2, Twist1</i>
	5%*	2%	2%
Epilepsy	<i>Bdnf, Cacna1h, Eln, Flna, Med12, Rbp4</i>	<i>Gata3, Magel2, Nod2</i>	<i>Gata3</i>
	6%*	6%*	11%*
Interneuron genes	<i>Bdnf, Cox6a2, Fosb, Mab211l, Npy2r, Nt5e, Spp1</i>	<i>Calca, Cbln4, Chodl, Hspb3, Irs4, Mab211l, Npy2r, Nr2f2, Tacr3</i>	<i>Calca, Cbln4, Fosb, Mab211l, Nr4a2, Spp1</i>

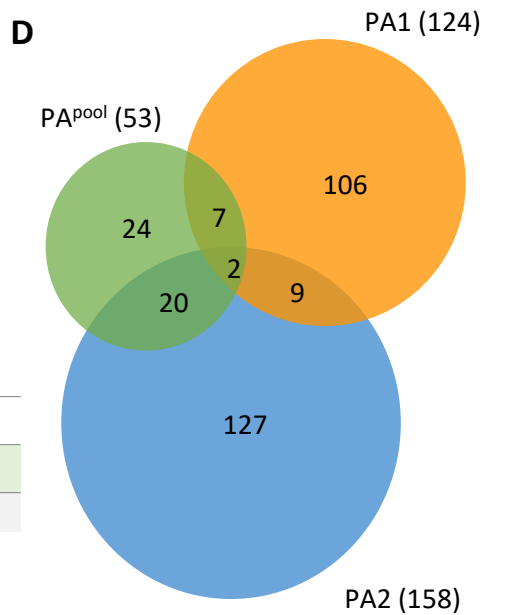
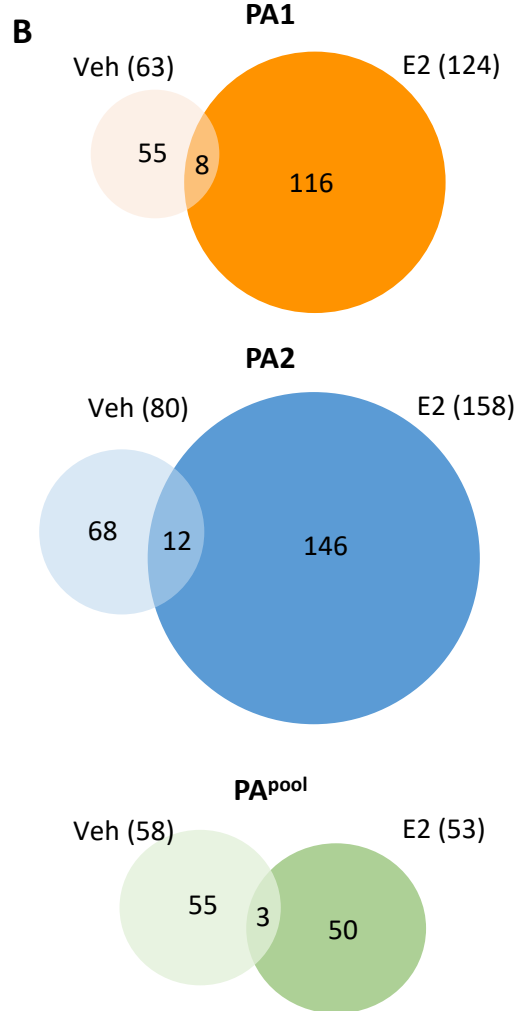
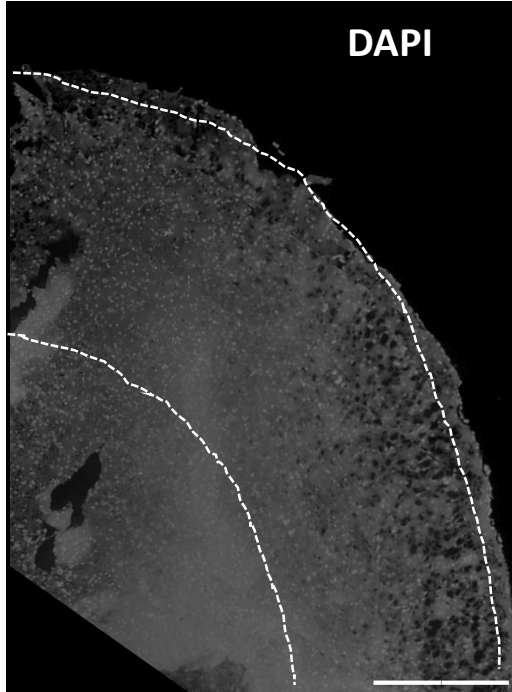
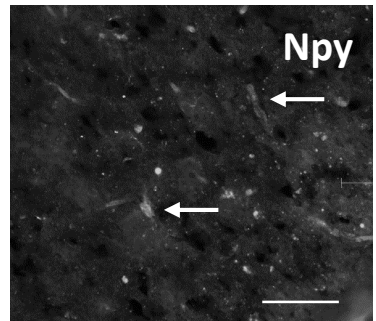
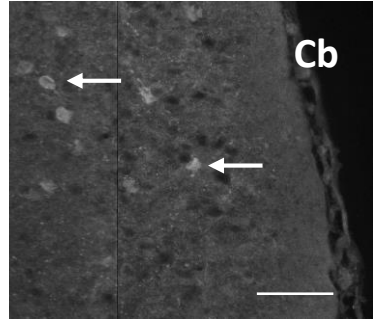


Figure 7

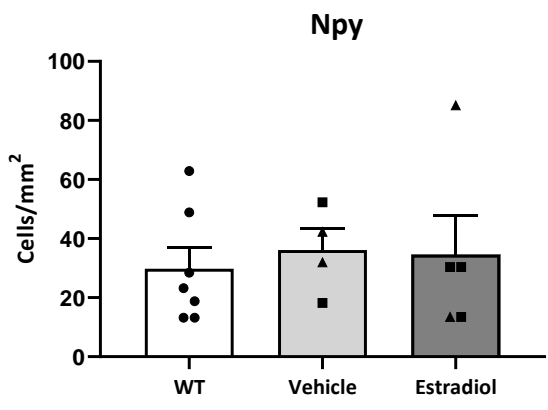
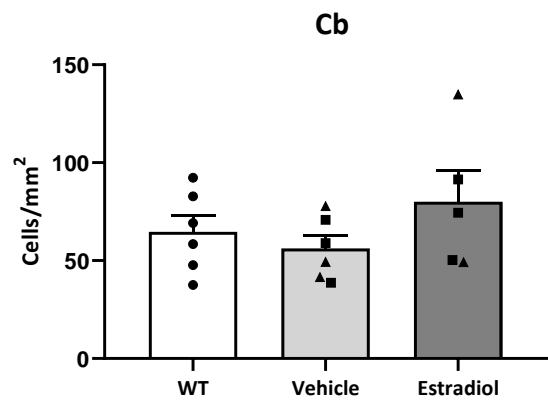
A



B



C



Appendix 2



Heterozygous loss of function of *IQSEC2/Iqsec2* leads to increased activated Arf6 and severe neurocognitive seizure phenotype in females

Matilda R Jackson^{1,2}, Karagh E Loring^{1,2}, Claire C Homan², Monica HN Thai¹, Laura Määttä³, Maria Arvio^{3,4,5} , Irma Jarvela⁶, Marie Shaw², Alison Gardner², Jozef Gecz^{2,7} , Cheryl Shoubridge^{1,2}

Clinical presentations of mutations in the *IQSEC2* gene on the X-chromosome initially implicated to cause non-syndromic intellectual disability (ID) in males have expanded to include early onset seizures in males as well as in females. The molecular pathogenesis is not well understood, nor the mechanisms driving disease expression in heterozygous females. Using a CRISPR/Cas9-edited *Iqsec2* KO mouse model, we confirm the loss of *Iqsec2* mRNA expression and lack of *Iqsec2* protein within the brain of both founder and progeny mice. Both male (52%) and female (46%) *Iqsec2* KO mice present with frequent and recurrent seizures. Focusing on *Iqsec2* KO heterozygous female mice, we demonstrate increased hyperactivity, altered anxiety and fear responses, decreased social interactions, delayed learning capacity and decreased memory retention/novel recognition, recapitulating psychiatric issues, autistic-like features, and cognitive deficits present in female patients with loss-of-function *IQSEC2* variants. Despite *Iqsec2* normally acting to activate Arf6 substrate, we demonstrate that mice modelling the loss of *Iqsec2* function present with increased levels of activated Arf6. We contend that loss of *Iqsec2* function leads to altered regulation of activated Arf6-mediated responses to synaptic signalling and immature synaptic networks. We highlight the importance of *IQSEC2* function for females by reporting a novel nonsense variant c.566C > A, p.(S189*) in an elderly female patient with profound intellectual disability, generalised seizures, and behavioural disturbances. Our human and mouse data reaffirm *IQSEC2* as another disease gene with an unexpected X-chromosome heterozygous female phenotype. Our *Iqsec2* mouse model recapitulates the phenotypes observed in human patients despite the differences in the *IQSEC2/Iqsec2* gene X-chromosome inactivation between the species.

Introduction

X-linked intellectual disability is a common, clinically complex disease arising from mutations in more than 140 genes on the X-chromosome (1), affecting between 1/600 and 1/1,000 males and a substantial number of females (2). X-linked inheritance is more complex than simply X-linked recessive or dominant (3) with both X-inactivation (including associated tissue specific selection) and the impact of individual mutations contributing to this complexity. In mammals, the sex determination system used is XX/XY, with dosage compensation in females as a result of random inactivation of one of the two X chromosomes in every cell. As a consequence, heterozygous females typically have a milder disease phenotype or are not affected. Despite this, there is a growing list of X-chromosome genes which are subject to X-inactivation or escape X-inactivation, including, for example, *PHF6*, *CLCN4*, *ALG13*, *ARX*, or *USP9X*, *DDX3X*, which display distinct phenotypes in males and females depending on the functional severity of the variant, as well as manifesting in a more severe female phenotype than the heterozygous state would predict (4, 5, 6, 7, 8, 9, 10). We contend that the IQ motif and Sec7 domain 2 protein (*IQSEC2*) (NM_001111125) (MIM 300522) is another X-chromosome disease gene in which we see a severe female phenotype because of heterozygous loss-of-function mutation.

We previously implicated *IQSEC2* as an X-linked intellectual disability (XLID) gene through identification of variants in affected males in four separate families (11). These missense variants were clustered around the Sec7 and IQ-like domains and resulted in reduced enzymatic activity (11). Clinical features within these non-syndromic XLID families included moderate to severe intellectual disability (ID) in all affected males, with variable seizures, autistic traits, and psychiatric problems (11). Since then, unbiased, high-throughput sequencing in ID and epilepsy cohorts have identified familial and increasingly de novo loss-of-function *IQSEC2* variants,

DOI [10.26508/lsa.201900386](https://doi.org/10.26508/lsa.201900386) | Received 20 March 2019 | Revised 25 July 2019 | Accepted 15 August 2019 | Published online 22 August 2019

¹Intellectual Disability Research, Adelaide Medical School, The University of Adelaide, Adelaide, Australia ²Department of Paediatrics, Robinson Research Institute, University of Adelaide, Adelaide, Australia ³Department of Child Neurology, Turku University Hospital, Turku, Finland ⁴Joint Authority for Päijät-Häme Social and Health Care, Lahti, Finland ⁵PEDEGO, Oulu University Hospital, Oulu, Finland ⁶Department of Medical Genetics, University of Helsinki, Helsinki, Finland ⁷South Australian Health and Medical Research Institute, Adelaide, Australia

Correspondence: Cheryl.shoubridge@adelaide.edu.au

typically leading to phenotypic outcomes, including severe ID with epileptic encephalopathy, and a high prevalence of speech development deficits and psychiatric features, including autistic spectrum disorder. Interestingly, these severe phenotypes are noted not only in affected males but also in affected, heterozygous females (12). The mechanisms contributing to the disease severity, particularly in heterozygous females is unknown and perplexing.

IQSEC2 is a guanine nucleotide exchange factor, which catalyzes exchange of GDP for GTP in a number of ARF superfamily of proteins. IQSEC2 is highly expressed in the forebrain, specifically localized to excitatory synapses as part of the *N*-methyl-D-aspartate receptor (NMDAR) complex (13, 14). The exact role IQSEC2 plays at excitatory synapses remains unclear. Limited studies indicate a role in the activity-dependent removal of α -amino-3-hydroxy-5-methyl-4-isoxazolepropionic acid receptors (AMPA) and activity-dependent synaptic plasticity (15, 16). Our own studies have shown that IQSEC2 also has a fundamental role in controlling neuronal morphology (17). However, there is currently no published research investigating the impact of loss or altered *Iqsec2* function on the development and resulting cognitive outcomes in any animal model. It is not certain if severe loss-of-function mutations in IQSEC2 can be transmitted in the human setting, with only missense variants giving rise to milder non-syndromic features being maternally inherited. Hence, it was unclear if the loss of *Iqsec2* function modelled in mice would survive into postnatal life, be reproductively viable or useful to model disease pathogenicity observed in humans. Here, we show that mice with the complete loss of function of *Iqsec2* by successfully targeting exon 3 using CRISPR/Cas9 technology survive into postnatal life and are viable. In this study, we investigate the effect of severe loss-of-function mutations driving the phenotype in patients, including the emerging female-specific phenotype using a mouse modelling the KO of *Iqsec2*.

We present an elderly female patient with profound ID and generalised seizures with a novel loss-of-function IQSEC2 variant, providing important life span information for other patients diagnosed with this typically early onset neurodevelopmental disorder. We review the present literature of the growing number of females with loss-of-function variants in IQSEC2, who have a more severe phenotype than the heterozygous state would predict. In humans, the prevailing evidence suggests that IQSEC2 escapes X-inactivation (18, 19); however, in mice, *Iqsec2* is subject to X-inactivation (20). Hence, the mouse modelling heterozygous KO of *Iqsec2* provides an opportunity to assess the impact of X-inactivation and altered *Iqsec2* gene dosage in females. Here, we show that the loss of *Iqsec2* function in mice recapitulates key aspects of the human phenotype, irrespective of the X-inactivation status of the gene in the two species, highlighting that our understanding of the traditional X-chromosome inheritance with heterozygous female sparing needs to be revisited.

Materials and Methods

Animal generation

All animal procedures were approved by the Animal Ethics Committee of The University of Adelaide, Adelaide, Australia, and undertaken in accordance with their regulatory guidelines. Founding *Iqsec2* KO mice

were generated by CRISPR/Cas9 by the South Australian Genome Editing facility (SAGE), University of Adelaide, Adelaide; details given below. Mice were maintained in the C57Bl/6N-Hsd background. Animals were of same sex and housed in individually ventilated cages, with sterile food and water available ad libitum. *Iqsec2* KO hemizygous male founder A was bred with a wild-type female to generate *Iqsec2* KO heterozygous progeny, which were subsequently bred with a wild-type stud male to generate *Iqsec2* KO hemizygous, *Iqsec2* KO heterozygous, and wild-type littermates. *Iqsec2* KO hemizygous males ($n = 46$) and *Iqsec2* KO heterozygous females ($n = 153$) were monitored and scored daily (from postnatal day [P] 14) for general health and welfare, appearance, weight, and the presence of seizure activity. In addition to standard food available ad libitum, crushed chow was soaked in sterile water and placed in an easily accessible feeding dish, which was refreshed daily.

CRISPR/Cas9 guide design

Guides were designed by the SAGE facility, University of Adelaide, under the guidance of Professor Paul Q Thomas as part of a fee for service for the generation of CRISPR/Cas9 *Iqsec2* KO mice. The online tool (<http://crispr.mit.edu/>) was used to search for appropriate CRISPR guide sites targeting the removal of *Iqsec2* exon 3. The most appropriate guide was determined by total score, cut site in target gene, and number of off-target mismatches. Guides' sequences determined most suitable were upstream CRISPR guide 5'-TCTAGTGTACTCACTCAGTT-3' and downstream CRISPR guide 5'-AGGCTGGAAGTGGCGAAAAC-3'. The CRISPR/Cas9 complex will cause double strand breaks in intron 2–3 of *Iqsec2* and intron 3–4, causing exon 3 to be deleted by a process of non-homologous end joining. CRISPR gRNA generation, microinjections of zygotes, and transfer to pseudopregnant recipients were performed by the SAGE facility as previously described (21, 22, 23).

Genotyping

A small segment of toe tissue was removed by sterile technique at P5 from all pups for genotyping and identification purposes. Genomic DNA was extracted as per the manufacturer's instructions for Phire Hot Start II DNA polymerase (Thermo Fisher Scientific). Genotyping PCR was performed using 10 μ M forward and reverse primer pairs (Table S1), 2x Phire Tissue Direct PCR Master Mix, and made up to 20 μ l with MilliQ water. Reactions were placed in a thermocycler for one cycle at 98°C for 5 min, 32 cycles at 98°C for 30 s, 62°C for 30 s, 72°C for 1 min, and one cycle at 72°C for 1 min. PCR products were held at 4°C before visualising on a 1.5% (wt/vol) agarose gel with 0.2 μ g/ml ethidium bromide in TBE buffer (1.1 M Tris, 900 mM borate, and 25 mM EDTA, pH 8.3) alongside 1 kb+ molecular weight marker. Images were captured on a SynGene UV dock at 400 ms exposure on GeneSnap v7.05 for SynGene. DNA sequencing analysis was performed using SeqMan Pro version 10.1.2 (DNASTAR, Inc) against *Iqsec2* cDNA reference sequence [NM_001114664](https://www.ncbi.nlm.nih.gov/nuccore/NM_001114664).

Analysis of *Iqsec2* mRNA and *Iqsec2* protein

Animals were humanely killed by cervical dislocation. Brain was dissected from the skull and cut into two halves sagittally along the

cerebral fissure. The right-hand side brain was separated and minced into cortex ($n = 2$, one each for protein and RNA) and cerebellum, snap-frozen in liquid nitrogen, and stored at -80°C pending analysis. RNA was extracted from 40 mg homogenised brain cortical tissue in TRIzol reagent and converted to cDNA using SuperScript RT (Thermo Fisher Scientific) as described previously (24). *Iqsec2* gene expression was performed using both RT-PCR and qPCR. RT-PCR was performed using 50 pmol forward and reverse primer pairs (Table S1), 20U Roche Taq DNA polymerase, FailSafe PCR 2X PreMix J (Epicentre), and made up to 50 μl with MilliQ water. Reactions were placed in a thermocycler for one cycle at 94°C for 2 min, 35 cycles at 94°C for 30 s, $57\text{--}60^{\circ}\text{C}$ for 30 s, 72°C for 30 s, and one cycle at 72°C for 5 min. Images were captured as described above. qPCR was performed using TaqMan gene expression assay probes (Thermo Fisher Scientific) spanning exon 3–4 boundary (Mm02344188_m1), exon 11–12 boundary (Mm02344183_m1), and exon 13–14 boundary (Mm02344185_m1) with *gapdh* used as a housekeeper (Mm99999915_g1). Wild types were pooled and averaged based on sex ($n = 4$ female wild type, $n = 5$ male wild type). Each individual *Iqsec2* KO hemizygous male or heterozygous female sample was normalised to the averaged wild-type data for their respective sex, with resulting data displayed as relative *Iqsec2* expression to their respective sexed wild-type controls. Protein extraction, SDS–PAGE, and Western blot analysis of protein levels were performed as described previously (17). The primary antibodies were rabbit anti-IQSEC2 (1:2,000) as previously described (17), rabbit anti-IQSEC1 and rabbit anti-IQSEC3, both used at 1:1,000 (Invitrogen), and mouse β -actin (AC-74; 1:20,000; Sigma-Aldrich A2228). Secondary antibodies from DAKO (Santa Clara) were goat antimouse HRP (1:2,000 P0447) and goat antirabbit HRP (1:2,000 P0448). Images were imported into Image Studio (Li-Cor Biosciences), and band intensities of *Iqsec* proteins were normalised to their respective β -actin loading control, and where required were harmonized across multiple immunoblots using a consistent control sample. Each individual *Iqsec2* KO hemizygous or heterozygous sample was normalised to the averaged pooled wild-type data for their respective sex, with relative intensities presented (n for each as described in figure legends).

Behavioural assessment

Iqsec2 KO heterozygous and wild-type females underwent monthly behavioural testing from one to 6 mo of age ($n = 4$ *Iqsec2* KO heterozygous and $n = 3$ wild-type controls at 1 mo, $n = 8$ *Iqsec2* KO heterozygous, and $n = 6$ wild-type controls at all other time points) as previously described (25).

Neuroanatomy

The left-hand side brain, separated along the cerebral fissure, was fixed at 4 degrees in 10% neutral buffered formalin overnight, before being washed three times in cold PBS, and stored in 70% ethanol at 4 degrees. The samples were processed and paraffin-embedded by the Adelaide University Histology Department. Semi-serial sections, measuring 10 μm thick, were collected using a strategy of mounting every fifth serial section across five slides (series 1–5) with up to five replicates of this strategy per sample

(A–E) to span the breadth of the mouse brain in sagittal or coronal orientation. The sections were stained by haematoxylin and eosin or Nissl and scanned using a Hamamatsu NanoZoomer 2.0-HT whole slide imager (Meyer Instruments). Images were imported into ImageJ (Fiji; version 2.0.0-rc-59/1.51k, build fab6e1a004) for processing and measurement.

Multielectrode array

Cortical neuronal were isolated from embryonic day (E) 17.5 *Iqsec2* KO heterozygous female ($n = 12$) and wild-type littermates ($n = 7$ female) as per Hinze *et al* (17). Neuronal suspensions were plated at 2.97×10^5 cells/well on 0.1% polyethyleneimine/20 $\mu\text{g}/\text{ml}$ laminin-coated 24-well glass bottomed multielectrode array (MEA) plate (product: 24W300/30G-288; MultiChannel Systems). After 21 d in culture, 15-min recordings were captured using MultiScreen (version 1.5.9.0; MultiChannel Systems) at a sampling rate of 20,000 Hz and 1,000 ms baseline duration. Spike binning was performed at 100-ms intervals, with minimum burst duration set at 50 ms, with a minimum spike count in burst set at four spikes. Captured data were uploaded and exported using MultiAnalyser (version 1.2.90; MultiChannel Systems). Data obtained from each individual *Iqsec2* heterozygous female embryo was normalised to the averaged wild-type data.

G-LISA Arf6 activation assay

Protein was extracted from snap-frozen cortical tissue of wild-type male mice ($n = 4$), KO male mice ($n = 6$), wild-type female mice ($n = 5$) and HetKO female mice ($n = 9$) following the manufacturer's instructions for use in a G-LISA Arf6 Activation assay Biochem Kit (absorbance based) (Cytoskeleton). The levels of activated Arf6 measured in the cortical tissue were from mice ranging in age from 2 to 9 mo. Each sample was measured with an $n = 4$ replicates. Within each assay, the levels of activated Arf6 measured in the wild-type animals for each sex was set to 1, and values for each of the KO or HetKO samples were determined relative to these age and sex-matched wild-type controls. The relative levels of activated Arf6 for all WT animals measured in a single assay were used to normalise activated Arf6 levels across multiple assays. An aliquot of protein from each cortical sample analysed in the GLISA assays was also prepared for SDS–PAGE and Western blot analysis and probed for *Iqsec2* as described (17) and Arf6 protein abundance using polyclonal Arf6 antibody (PA1-093; Thermo Fisher Scientific) and quantitated as indicated above for *Iqsec2* protein abundance.

Molecular analysis of IQSEC2 variant

The screening protocols were approved by the Women's and Children's Health Network Human Research Ethics Committee and the Human Ethics Committee of The University of Adelaide, Adelaide, Australia (approval number REC2361/03/2020) and conforms with the principles set out in the WMA Declaration of Helsinki and Australian National Statement on Ethical Conduct in Human Research (2018). Informed consent was obtained from carers of the patient, including consent to publish images. DNA from the affected female was whole-exome sequenced on an Illumina HiSeq2500 by the Australian Genome Research Facility. Reads were mapped to

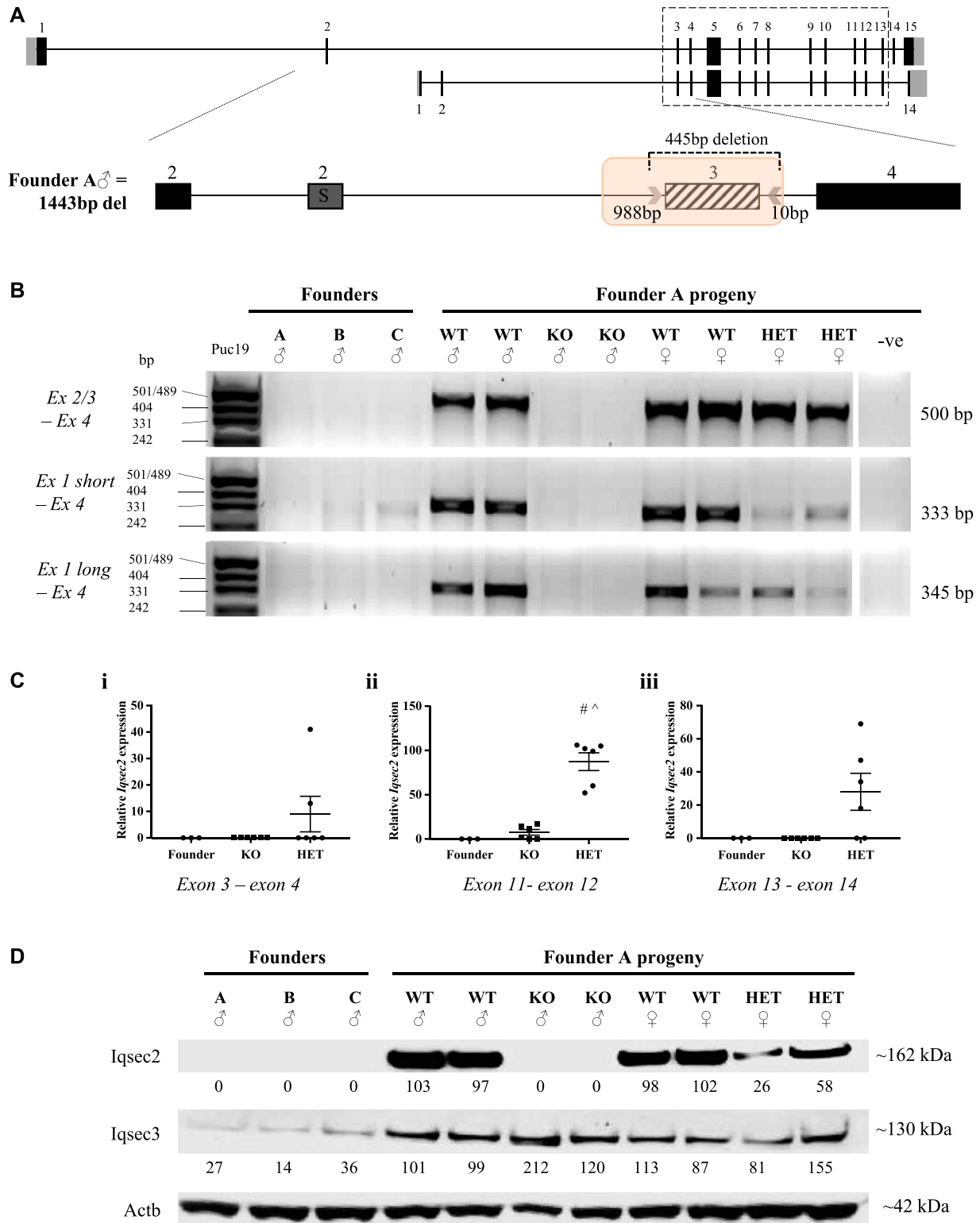


Figure 1. CRISPR/Cas9 targeting of *Iqsec2* resulted in absent (KO males) or reduced (KO HET females) *Iqsec2*/*Iqsec2* expression. (A) Schematic of the exon-intron structure of *Iqsec2* long (NM_001114664) and short (NM_001005475) isoforms, with the dashed box indicating consensus sequence. Zoomed-in schematic of *Iqsec2* exon 2-4 (exon 2 long = 2L and exon 2 short = 2S) with CRISPR guides (arrows) flanking exon 3 (diagonal line fill), resulting in a predicted 445-bp deletion. Actual deletion size (highlighted by an orange box) shown flanking CRISPR guide putative cut sites in Founder A, with sex and total deletion size shown on left-hand side. (B) RT-PCR amplification of exon 2/3 boundary, exon 1 (short isoform), and exon 1 (long isoform) to exon 4 of 3 male founders, and subsequent progeny from founder A. (C) qPCR of three founder males (grouped) and subsequent progeny from founder A. Results are expressed as mean relative expression (\pm SEM; n = 3

the human genome (hg19) using BWA-MEM (26) and mapping refined using Genome Analysis Toolkit version 3.5 (27). Mapping achieved a minimum median target coverage depth of 49 reads/sample and covered 87.67% of intended targets with at least 20 reads. Single-nucleotide variants and small insertions and deletions were called by the genome analysis toolkit haplotype caller version 3.5 (27). Whole-exome sequencing data are available upon request.

All variants were annotated for allele frequency, clinical significance, locus identity, and likely pathogenicity using ANNOVAR (28).

Statistical analysis

The statistical significance ($P < 0.05$) of the difference between means of each strain, namely, *Iqsec2* KO hemizygous males, *Iqsec2* KO heterozygous females, and their respective age-matched control littermates, was determined using multiple statistical means. A one-way ANOVA followed by Tukey's HSD post hoc test was used for qPCR and MEA analysis, whereas a two-way ANOVA followed by Tukey's HSD was used to assess behavioural differences across time. A two-tailed, unpaired t test was used to compute statistical significance of the difference between means for the GLISA analysis, and when wild-type littermates were omitted from statistical analysis (seizure propensity). All data analyses were performed using GraphPad Prism version 7 (GraphPad Software Inc.).

Results

Generation of loss-of-function *Iqsec2* KO mice by CRISPR/Cas9 deletion of exon 3

Generation of a knockout (KO) mouse line to model the loss of *Iqsec2* function was achieved by targeting exon 3 of *Iqsec2* for deletion by CRISPR/Cas9 editing (17). The sequence and targeting of CRISPR guides to remove exon 3 in both isoforms are detailed in Fig S1. Exon 3 is invariable between the two main isoforms of *Iqsec2*, with exons 3–13 comprising consensus sequence (Fig 1A). Injection of the CRISPR/Cas9 guides was performed as a fee for service (South Australian Genome Editing facility, University of Adelaide, Adelaide) (21). PCR amplification of genomic DNA (Fig S2A) and subsequent breakpoint mapping and sequencing of amplicons demonstrate that Founder A (male) had exon 3 removed with neighbouring exon 2 (short and long isoforms), exon 4, and exon 5 unaffected by the deletion, demonstrating successful targeted deletion of exon 3 (Fig 1A). Although exon 3 did not amplify in any of the four founders generated (Fig S2B), founders B and C (males) had larger deletions than expected (Fig S2A), both impacting exon 4, and

founder D (female) had a homozygous deletion of exon 3 (Fig S2C). The homozygous loss of *IQSEC2* has not been reported in the human population. Given the increasing incidence of mutations in girls (heterozygous) with early-onset seizure phenotypes, it was not unexpected that this female homozygous KO mouse was found dead early in postnatal life, negating the opportunity to collect samples for expression analysis, or attempt breeding. This animal was not included in any further analysis. Overall, the editing of all founders extended past the recognised CRISPR/Cas9 guide cut sites in both directions by nonstandard amounts, with larger deletion sizes of this X-chromosome region noted in males. This finding demonstrates that CRISPR/Cas9, although an effective genome editing tool, requires careful validation.

To confirm that deletion of exon 3 by CRISPR/Cas9 editing resulted in loss of *Iqsec2*/*Iqsec2*, we analysed the gene expression and protein level from cortical brain tissue in which *Iqsec2* is highly expressed during postnatal life. We demonstrate in the three founder males and progeny of founder A that *Iqsec2* expression was reduced or absent when detected by RT-PCR (Fig 1B) and significantly reduced compared with sex-matched wild-type progeny when analysed by qPCR (Fig 1C). Founder A and founder B had no detectable *Iqsec2* expression by either analysis. The negligible expression levels of *Iqsec2* short isoform detected for founder C in the RT-PCR analysis was not replicated by qPCR. *Iqsec2* KO hemizygous male progeny from founder A also had no detectable *Iqsec2* expression by RT-PCR (Fig 1B) but demonstrated minimal *Iqsec2* expression by qPCR with the probe spanning across the exon 11–12 boundary Fig 1C. (ii) This result is consistent with very low levels of transcript (~5% of normal) being present before nonsense-mediated mRNA decay. *Iqsec2* KO heterozygous female progeny showed that *Iqsec2* expression by RT-PCR for both the short and long isoforms were reduced to less than half the levels of wild-type female controls (Fig 1B). Similarly, reduced *Iqsec2* expression in these females was also noted by qPCR, with expression levels dependent on the probe used (range 0–79%, mean 35%), but were still significantly elevated above both founder males and *Iqsec2* KO hemizygous male progeny (Fig 1C). We note that expression levels were quite varied between individual heterozygous females and cannot discount differences due to levels of X-inactivation in these animals. The three male founders had no discernible *Iqsec2* protein in the cortex (Fig 1D). Similarly, there was no discernible *Iqsec2* protein in KO hemizygous male progeny and reduced levels of *Iqsec2* protein (~half of the wild-type control levels) in KO heterozygous female progeny (Fig 1D). Off-target analysis of CRISPR/Cas9 editing using computational tools (CRISPR design tool by MIT: <http://crispr.mit.edu/> and COSMID: <https://crispr.bme.gatech.edu>) identified that the majority (92%) of predicted off-targets were located in regions that did not harbour genes or impacted intronic regions within genes and were unlikely to effect the coding region

founders, $n = 6$ *Iqsec2* KO hemizygous males (KO), $n = 6$ *Iqsec2* KO heterozygous females [HET]) normalised to wild types, which were pooled and averaged dependent on sex ($n = 4$ female wild type, $n = 5$ male wild type). (C) TaqMan gene expression assay probes spanning (i) exon 3–4 boundary, (ii) exon 11–12 boundary, and (iii) exon 13–14 boundary with *gapdh* used as a housekeeper. (D) Western blot analysis of *Iqsec2* and *Iqsec3* expression in three founder males and subsequent progeny from founder A. Blots were imported into Image Studio (Li-Cor Biosciences) and band intensities normalised to their respective beta-actin (Actb) loading control. Wild types were pooled and averaged dependent on sex ($n = 2$ female wild type, $n = 2$ male wild type). White spaces indicate a cropped image. # indicates significant difference between HET and founder, $P < 0.0001$ one-way ANOVA, Tukey's HSD, ^ indicates significant difference between HET and KO, $P < 0.0001$; one-way ANOVA, Tukey's HSD.

of the genome (Table S2). For the 31 genes identified to potentially be impacted by off-target effects, 28 were reported with high numbers of mismatch ($n = 4$). In contrast, *Iqsec3* was the only gene predicted to be impacted by either CRISPR guide that was identified by both computational tools (Table S2). *IQSEC3* is highly expressed within multiple regions of the brain, including the cortex. Our analysis of the three founder males demonstrates that *Iqsec3* protein levels in the cortex were reduced (27%, 14%, and 36% of wild-type, respectively) but were normalised to wild-type levels in subsequent founder A progeny (Fig 1D). Taken together, these data suggest successful outbreeding of the potential off-target effects.

To investigate if the loss (or partial loss) of *Iqsec2* protein in the *Iqsec2* KO mice elicited a compensatory effect by other members of the *Iqsec* protein family, we measured the protein abundance of *Iqsec1* and *Iqsec3* in cortical samples of the wild-type and *Iqsec2* KO mice by immunoblot. The levels of *Iqsec1* protein were very low compared with the ready detection of *Iqsec3* protein in the same samples and were not robust enough for semiquantitative analysis. Despite this, we did not see any empirical evidence of a consistent or stronger signal in the *Iqsec2* KO animals. In the case of *Iqsec3*, there was no significant increase in protein abundance in the

brains of *Iqsec2* KO hemizygous male or KO heterozygous female mice compared with wild-type sex-matched mice (Fig S3). Hence, we demonstrate that *Iqsec* protein family members are unlikely to provide a compensatory role to ameliorate the loss or partial loss of *Iqsec2*.

Iqsec2 KO male and female mice present with spontaneous seizures

We observed severe spontaneous seizures in both *Iqsec2* KO hemizygous male and heterozygous female mice modelling loss of *Iqsec2* function. We saw a combination of four seizure subtypes that although distinctive in appearance, were often observed in a single seizure episode in both sexes. The seizures included (i) sudden onset of irregular generalised clonic jerks, where the mouse demonstrated involuntary, uncontrolled, unilateral head movements (Video 1); (ii) repetitive forelimb clonus that commenced with intermittent clonic jerking of the head and forelimbs, which then became rhythmic, associated with tonic posturing of the forelimbs, evolving to rearing and generalised tonic-clonic activity lasting ~60 s (Video 2); (iii) uncontrolled convulsions with bilateral forelimb

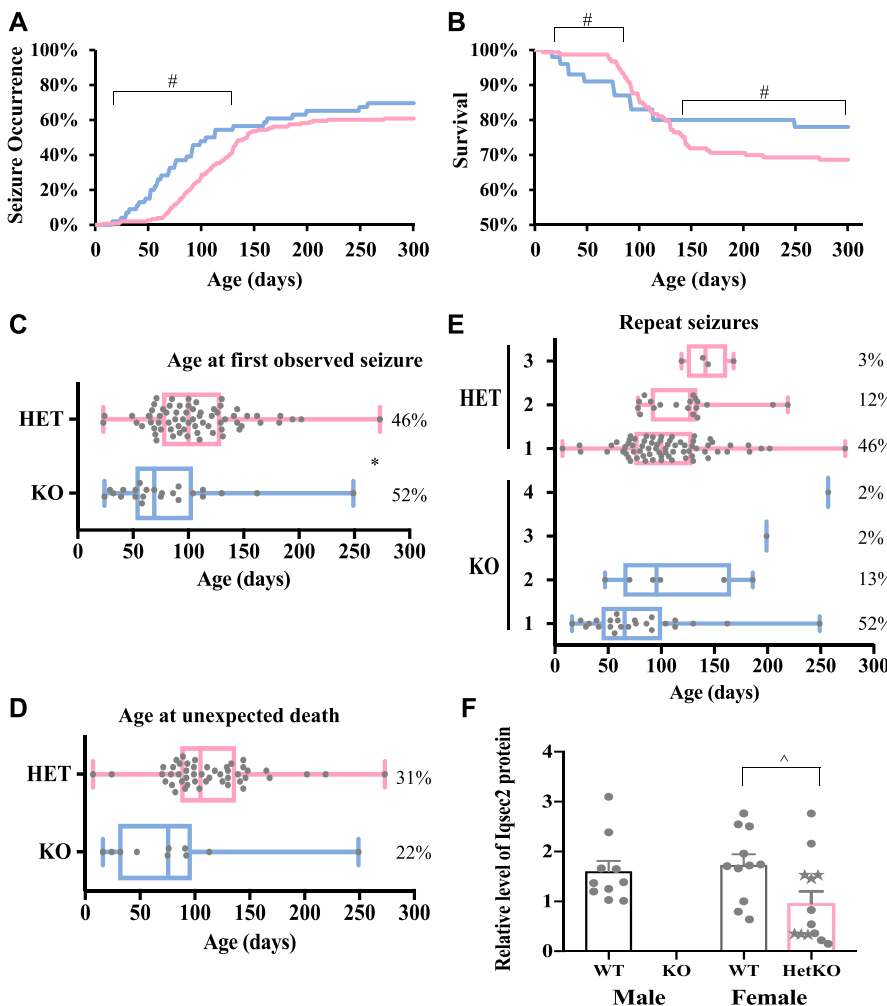


Figure 2. *Iqsec2* KO hemizygous males and heterozygous females exhibit spontaneous seizures and reduced survival, which was not observed in their wild-type control littermates.

The total number of animals phenotyped include KO; $n = 46$ (blue) and HET; $n = 153$ (pink). (A, B, C, D, E) Percentage seizure occurrence and (B) survival presented at daily intervals from birth, with both further subclassified as (C) age at observed first seizure, (D) age at unexpected death, and (E) occurrence of repeat seizures presented as median (\pm min/max), where each dot represents an individual animal. Unexpected death was classified as humane euthanasia or found dead presumed because of seizure or status epilepticus and does not include those individuals taken for experimental end point. These data do not include any movement phenotypes observed. (F) *Iqsec2* heterozygous females (Het/pink; $n = 13$) have reduced levels of *Iqsec2* protein compared with female wild-type animals (WT/grey; $n = 11$). Mean (\pm SEM) data presented. The animals with observed seizures are denoted as stars. There were no significant differences in *Iqsec2* protein abundance between male (WT/Black; $n = 10$) and female wild-type animals (WT/grey; $n = 11$). * indicates significant difference between KO males and HET females, $P < 0.05$, two-tailed, unpaired t test, # indicates $P < 0.0001$, two-tailed, paired t test, ^ indicates $P < 0.05$ between HET/KO and female WT controls, two-tailed, unpaired t test.

outward stretching were also noted which commenced with the sudden onset of irregular generalised clonic jerks followed by hypermotor activity, which lasted ~5 s before ceasing (and often reinitiating; Video 3); and (iv) and full body tonic-clonic seizures that started with symmetrical tonic extension of both forelimbs and hindlimbs, which develop into rhythmic generalised clonic activity after ~15 s, continuing for an additional 30 s before ceasing (Video 4). Seizure episodes were frequently accompanied by twitching ears, a straight tail, and an increase in facial grooming/washing pre- and post-seizure occurrence. *lqsec2* KO mice that were found dead in their cage were classified as having died because of either a seizure or status epilepticus, as no wild-type control littermates were found dead in this study.

In concordance with the clinical variability noted in both male and female human patients with loss-of-function mutations, we measured large variations in age of onset, seizure severity, and progression amongst individual *lqsec2* KO mice. The proportion of *lqsec2* KO hemizygous males exhibiting seizures (all sub-types combined) from birth to 4 mo of age (7–54%, respectively) was

significantly increased when compared with heterozygous females (2–37%, respectively; Fig 2A). However, after 5 mo of age, the proportion of *lqsec2* KO mice exhibiting seizures plateaued, with males ranging from 57 up to 65% at the study end point (~300 d of postnatal life) and females ranging from 54 to 60% across the same time period. The survival from birth to 3 mo of age in *lqsec2* KO hemizygous males (87%) was significantly decreased compared with heterozygous females (91%; Fig 2B). From 4 mo of age, *lqsec2* KO males reached a plateau (80%), whereas survival of heterozygous females continued to significantly decline until 8 mo of age (69%). The first observed seizure occurred with similar timing in both *lqsec2* KO male and female mice, at postnatal day (P) 29 and P23, respectively (Fig 2C), with the first unexplained death occurring at P16 and P7, respectively (Fig 2D). The majority of male (52%) and female (46%) *lqsec2* KO mice were observed to have only one seizure. The proportion of mice observed to have two or more seizures spanning their postnatal life were similar between male and female KO mice (13% and 2% versus 12% and 3%, respectively; Fig 2E). The levels of *lqsec2* protein abundance in cortical tissue

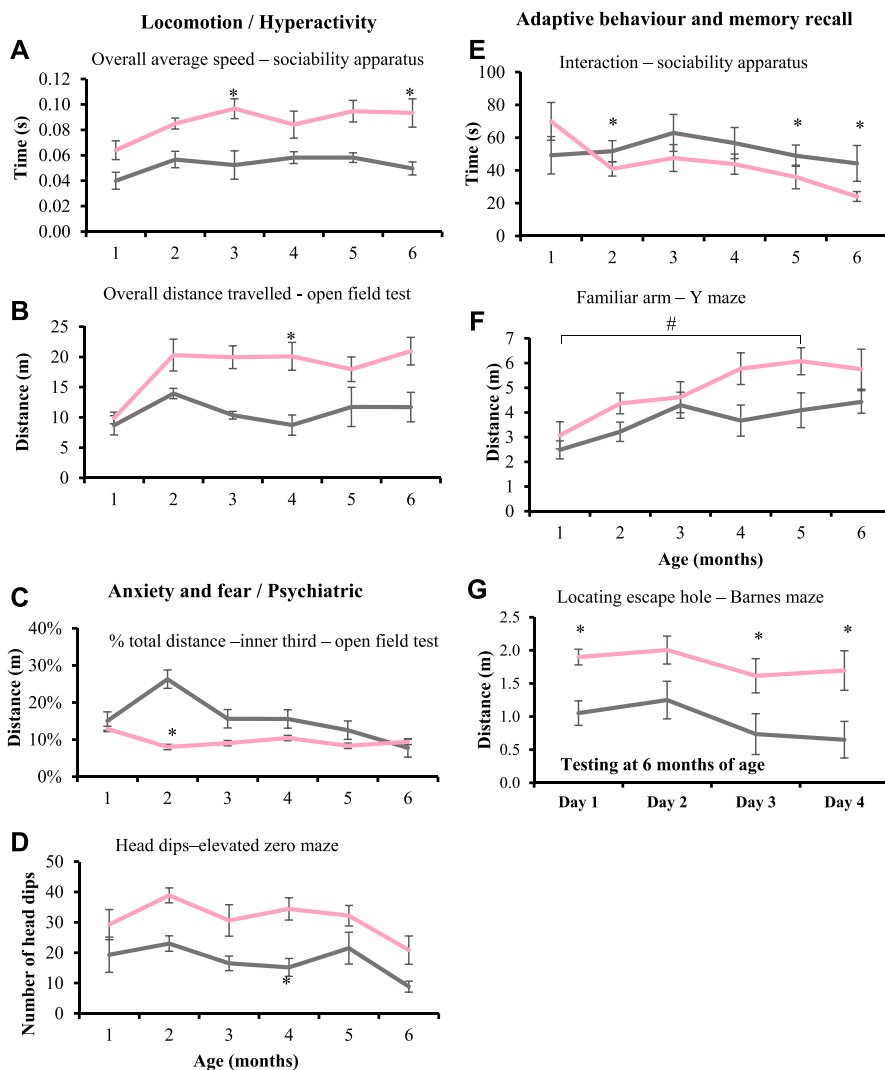


Figure 3. *lqsec2* KO heterozygous females display altered anxiety, increased locomotor activity and reduced spatial learning and memory. (A, B, C, D, E, F, G) Behavioural tests undertaken at monthly intervals between 1 and 6 mo of age show that *lqsec2* KO heterozygous females (HET/pink) (n = 4 at 1 mo; n = 8 at 2–3 mo, n = 7 at 4–6 mo) compared with their wild-type female controls (WT/grey) (n = 3 at 1 mo; n = 6 at 2–6 mo) demonstrate (A) increased speed across multiple apparatus (sociability apparatus shown), (B) increased exploratory behaviour in the open field test, (C) increased anxiety in open field test, (D) decreased fear response in the elevated zero maze, (E) reduced total interaction time in the sociability apparatus regardless of familiar or novel cage occupant, (F) decreased novel recognition in the Y-maze, (G) and reduced spatial learning in the Barnes maze (conducted at 6 mo of age). Mean (±SEM) data presented, where * indicates significance between HET/KO and WT controls, # indicates significant between HET time points, two-way ANOVA with Tukey's HSD.

were reduced in heterozygous female mice compared with wild-type female littermates (1.8 fold, $P = 0.0264$) as measured by semiquantitative immunoblot (Fig 2F). *Iqsec2* protein abundance was not impacted by the presence of an observed seizure (indicated by stars instead of circles).

Iqsec2 KO heterozygous female mice demonstrate altered behavioural phenotyping

Given the striking similarity in the seizure phenotype displayed by the *Iqsec2* KO hemizygous male and heterozygous female mice, coupled with the marked overlap in phenotypic outcomes in loss-of-function male and females patients in the human setting, we contend that the *Iqsec2* KO heterozygous females provide a representative model for this disorder. Interestingly, the male KO progeny were able to breed and transmit the loss-of-function *Iqsec2* mutation with minimal difficulty. In contrast, the *Iqsec2* KO heterozygous females displayed reduced breeding success (Fig S4). However limited, this indicates that a loss-of-function mutation

in *Iqsec2* is able to be transmitted, at least in mice. Due largely to the limited breeding success of our *Iqsec2* KO heterozygous females, generating the required number of age appropriate KO males for behavioural testing was challenging and precluded testing in hemizygous males. Hence, we undertook a battery of behavioural tests at monthly intervals up to 6 mo of age in the *Iqsec2* KO heterozygous females compared with female wild-type controls.

Iqsec2 KO heterozygous females demonstrate an increased locomotor activity and exploratory behaviour. *Iqsec2* KO heterozygous females exhibit reduced neuromuscular strength at 3, 5, and 6 mo of age using the inverted grid test (Fig S5A). Although the difference in overall performance by each genotype on the apparatus was significant ($P = 0.0031$), the variability amongst individuals meant that significance was not reached at any individual time point. Hyperactivity was indicated by a significant ($P < 0.0001$) increase in the overall average speed (Fig 3A; sociability apparatus shown), and overall total distance travelled (Fig 3B; open field test shown) compared with wild-type littermates on multiple apparatus.

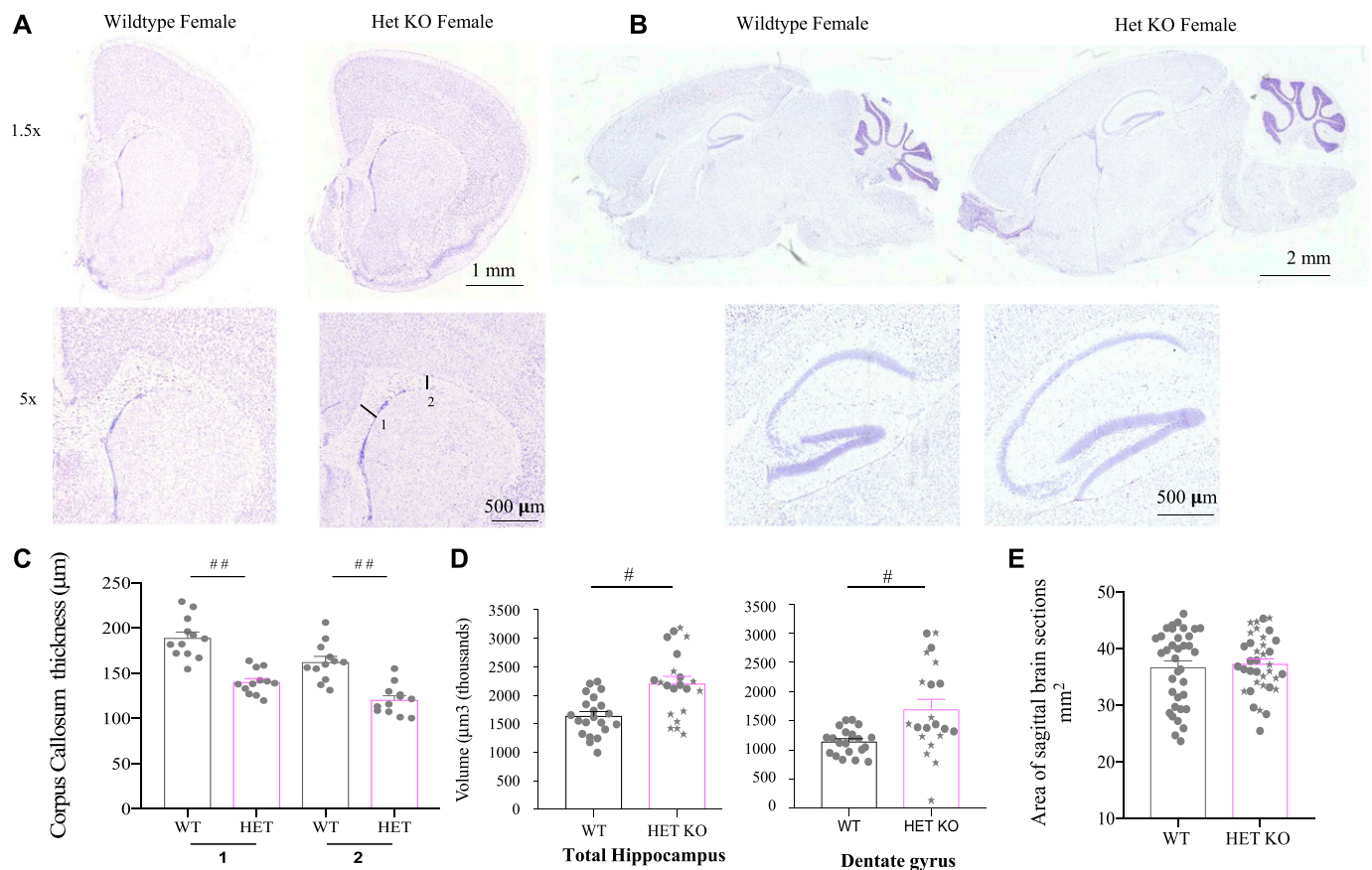


Figure 4. Neuroanatomy changes in *Iqsec2* KO mouse brains.

(A, B) Nissl staining of brain sections in both (A) coronal and (B) sagittal orientations from adult wild-type and heterozygous KO females demonstrate there is no gross disturbance to brain morphology. Scale bars shown for each set of pictomicrographs. (C) The thickness of the corpus callosum (CC) measured where the (1) start and (2) end of the cingulum intercepts the CC in three coronal sections for each of $n = 4$ animals per genotype is significantly thinner in heterozygous female (HET/pink) mice compared with wild-type female (WT/Grey) mice. (D) Heterozygous females have increased total hippocampal and dentate gyrus volume compared with wild-type littermates ($n = 4$ each). (E) The area of the brain was measured in animals from 60 to 155 d postnatal age in sagittal sections in HET/pink and WT/grey females (a total 36 sections measured per genotype: nine sections each for $n = 4$ animals). The *Iqsec2* HetKO animals with observed seizures are denoted by stars. Mean (\pm SEM) data presented where # indicates $P < 0.001$, and ## indicates $P < 0.0001$, two-tailed, unpaired t test between wild-type and heterozygous females.

Altered anxiety and fear response was also noted in *Iqsec2* KO female mice, with a significant increase in percentage total distance travelled in the inner third of the open-field apparatus (Fig 3C and $P = 0.0006$), increased number of head dips on the elevated zero maze (Fig 3D and $P < 0.0001$), and an initial increase in percentage total distance travelled in the open arms of the elevated zero maze (Fig S5B and $P = 0.0007$). This is in comparison with wild-type females, which from 4 mo of age travelled a greater percentage of total distance on the open arms of the elevated zero maze, suggesting habituation (Fig S5B).

Normal social interaction and memory recall is demonstrated by mice choosing to interact with a mouse rather than an empty cage and a preference to interact with a novel mouse over a familiar mouse when tested in a three-chamber sociability apparatus. The *Iqsec2* KO heterozygous females displayed autistic-like behaviour evident by a significant decrease in the total overall time of interaction, regardless of the other cage occupant (Fig 3E and $P < 0.03$). In addition, the behaviour of the *Iqsec2* KO heterozygous females suggests reduced learning capacity and spatial memory retention in contrast to wild-type females. *Iqsec2* KO heterozygous

females had a significant preference toward exploring the familiar arm of the Y-maze increasing over time (Fig 3F and $P = 0.0261$) and took significantly longer and travelled further distance to find the escape hole in the Barnes maze (Fig 3G and $P < 0.0265$).

Altered neuroanatomy in *Iqsec2* KO heterozygous female mice

Nissl stain of both the coronal (Fig 4A) and sagittal (Fig 4B) orientations demonstrate there is no gross disturbance to the overall anatomical structure of the brain in heterozygous female compared with wild-type mice. Emerging evidence suggests that severely affected patients with *IQSEC2* loss-of-function mutations display a phenotype that includes thinning of the corpus callosum. We examined the thickness of the corpus callosum at two distinct points, each in three semi-serial coronal sections from an $n = 4$ animals per genotype (sections relative to the reference Allen Brain Atlas, Mouse, P56, and coronal images 44–46 of 132). Using this approach, we demonstrate that the thickness of these regions was significantly diminished in the heterozygous female mice compared with the wild-type female mice (Fig 4C). In line with the increase in

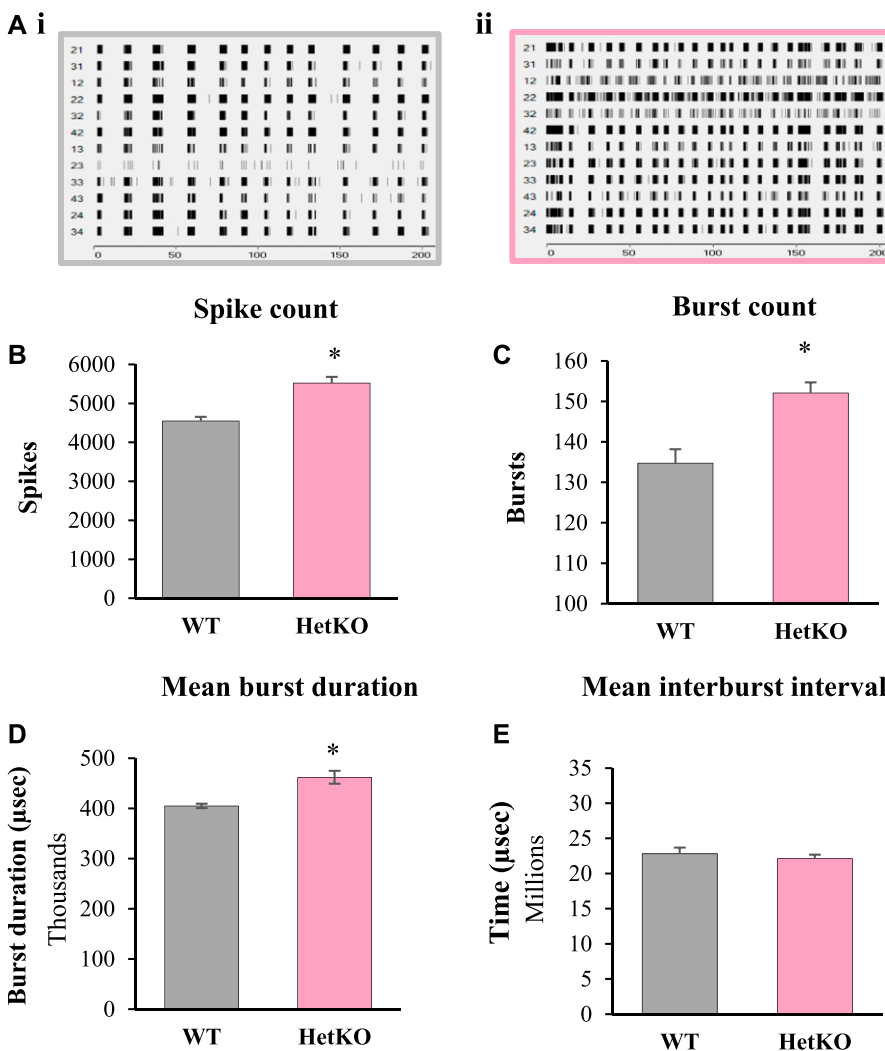


Figure 5. Embryonic (E)17.5 cultured cortical neurons from *Iqsec2* heterozygous females (HET/pink; $n = 449$ electrodes from $n = 12$ embryos) exhibit hallmarks of immature synaptic networks when compared with their respective wild-type (WT) control littermates (WT female/grey $n = 256$ electrodes from $n = 7$ embryos).

(A, B, C, D) Representative raster plots for (A.i) WT female and (A.ii) HET female after 21 d in culture. Quantitatively, HET cultures showed an increased (B) spike count, (C) burst count, and (D) mean burst duration compared with wild-type control littermates. Mean (\pm SEM) data presented, where * indicates significance between HET and WT control, two-tailed, unpaired t test, where $P < 0.05$.

hyperactivity and anxiety noted in our *Iqsec2* KO heterozygous females, we observed an increase in total hippocampal volume in heterozygous KO female mice (34%, $P = 0.0008$ HET versus WT females) and an increase in the volume of the dentate gyrus (48%, $P = 0.0006$ for HET females) shown in Fig 4D (sections relative to the reference Allen Brain Atlas, Mouse, P56, sagittal images 9–10 of 21). Despite these discreet changes to specific neuroanatomical regions of the brain, our analysis indicates there were no significant differences in the area of the brain sections measured between wild-type females and the heterozygous KO females (Fig 4E) (sections relative to the reference Allen Brain Atlas, Mouse, P56, sagittal images 11–12 of 21).

Iqsec2 female mice display hallmarks of immature synaptic networks ex vivo

To investigate the impact of *Iqsec2* on the activity of synaptic networks, we analysed cultured cortical neurons using a multi-electrode array. Neurons isolated from individual *Iqsec2* KO heterozygous female embryos grown for 21 d in culture display hallmarks of immature synaptic networks when compared with neurons from wild-type littermates (Fig 5). Burst activity and bursting behaviour is considered one of the most important properties for analysing synaptic plasticity and information processing within the central nervous system. Wild-type cultures demonstrated consistent, evenly spaced bursts of closely clustered action potentials, suggestive of a highly synchronised culture (Fig 5A.i). In contrast, *Iqsec2* KO heterozygous cultures showed aberrant synchronicity; with action potentials not consistently clustered in large bursts, but included smaller, randomly spaced events (Fig 5A.ii). In line with this observation, cultures from heterozygous females exhibited significantly elevated spike count (121%; Fig 5B and $P < 0.0001$), burst count (113%; Fig 5C and $P = 0.0002$), and mean burst duration (114%; Fig 5D and $P = 0.003$), but no difference in mean burst interval (Fig 5E) when compared with sex-matched wild-type controls. It must be noted that large variations existed in *Iqsec2* KO heterozygous cultures, with some embryos demonstrating burst patterning similar to that of their wild-type counterparts.

Loss of *Iqsec2* function leads to an increased level of activated Arf6 in cortical tissues

There are multiple ArfGEFs, each with a conserved Sec7 domain responsible for catalysing nucleotide exchange and activating members of the small G protein Arfs. Hence, it was not clear what impact the loss-of-function of a single ArfGEF would have on regulating activated Arf-mediated responses to synaptic signalling in vivo. As *Iqsec2* is an ArfGEF particularly for the small GTPase Arf6, we analysed the levels of activated (or GTP bound) Arf6 in cortical tissues from individual mice of each genotype. There was no change in the level of Arf6 activation with increasing postnatal age (range 2–9 mo), and although the levels of activated Arf6 were higher in wild-type females relative to wild-type males, this difference was not significant (1.5 fold; Fig 6A). In contrast, cortical tissues from heterozygous females exhibited significantly elevated levels of activated Arf6 (2.6 fold; $P = 0.0186$) when compared with sex-

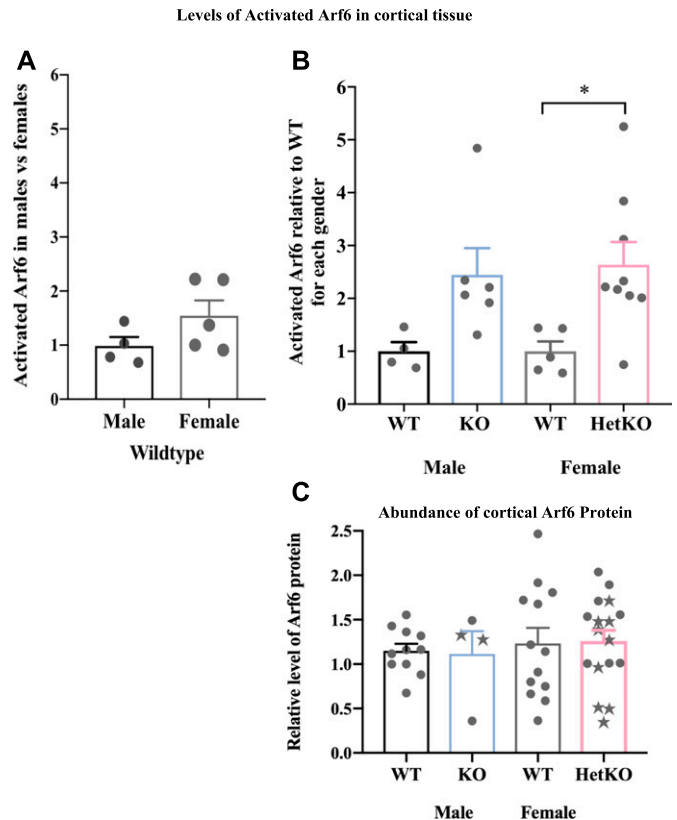


Figure 6. The levels of activated Arf6 in cortical tissue are elevated because of *Iqsec2* KO.

(A) Biochemical assays to measure the levels of activated Arf6 (G-LISA) undertaken in cortical tissues of animals across postnatal development between 2 and 9 mo of age show that (A) the levels of activated Arf6 in wild-type male mice (WT/black) ($n = 4$) are elevated in age-matched wild-type female mice (WT/grey) ($n = 5$). (B) *Iqsec2* KO hemizygous males (KO/blue, $n = 6$) and heterozygous KO females (Het/pink; $n = 9$) both display increased levels of activated Arf6 compared with the sex-matched wild-type controls listed above. (C) The abundance of Arf6 protein measured by immunoblot was not significantly different between any genotype groups. The *Iqsec2* KO animals with observed seizures are denoted by stars. Mean (\pm SEM) data presented, where * indicates significance between WT female control and HET/KO, $P < 0.05$, 2-tailed, unpaired t test.

matched and age-matched wild-type controls (Fig 6B). A similar outcome was observed in cortical tissues from hemizygous males with an elevated, although not statistically significant, level of activated Arf6 (2.45 fold; $P = 0.0536$) (Fig 6B). The increases in activated Arf6 levels in *Iqsec2* KO hemizygous and heterozygous mice were not reflected by a significant increase in Arf6 protein abundance relative to wild-type for either sex (detected in the same [and additional] cortical tissue) (Fig 6C). Nor was Arf6 protein abundance impacted by the presence of an observed seizure (indicated by stars instead of circles; $P = 0.1009$).

Heterozygous loss-of-function variant in *IQSEC2* in a female with a neurocognitive seizure phenotype

Here, we report an elderly, 68-yr-old female (II-2) (Fig 7A) with severe-to-profound ID, early onset of seizures who is nonverbal,

and communicates primarily using sounds and gestures. She has a history of normal early development, learning to sit at 8–10 mo and walk at age 18 mo. After seizure onset at 17 mo, she developed repeated, generalised seizures during the daytime and regression was observed. She later developed additional atypical absence and atonic seizure types. Since the age of 11, she has been living in residential care. Her daily functioning skills are poor, and she needs assistance in every-day life. Facial features include low-set, large ears, and asymmetric facial features with prominent angle of the jaw, thick upper lip with mild hypertrichosis over the upper lip and deep-set eyes (Fig 7B). No brain MRI has been performed because of the requirement of general anaesthesia. A detailed clinical description of the proband is described in Supplemental Data 1. Whole-exome analysis of four Finnish families identified a novel, heterozygous single-nucleotide polymorphism at genomic position ChrX:g.53,349,756 (GRCh37/19) in the female proband of one family. The variant has been submitted to the gene variant database at <https://databases.lovd.nl/shared/genes/IQSEC2> (patient ID 00174867; DB-ID #0000398628). Sanger sequencing confirmed the presence of this variant in the proband (Fig 7C). Samples were not available for the twin brother or parents of the affected female proband to confirm the inheritance status of this variant. This variant in exon 1 of the *NM_00111125.2* long isoform substitutes a single nucleotide at c.566C>A, generating a predicted premature stop codon, p.(S189*)

(*NP_001104595*) in *IQSEC2* (Fig 7D). This variant was not found in ExAC, GnomAD, or dbSNP150 project databases. This predicted premature stop codon is located 141 nucleotides from the exon 1–2 junction, with the transcript predicted to be degraded via the nonsense-mediated mRNA decay pathway, resulting in loss of the *IQSEC2* protein.

Review of the literature shows that the affected female proband adds to the growing number of affected females with loss-of-function variants in *IQSEC2* gene presenting with severe ID and early-onset seizures (Table 1) (29–42) recently reviewed (12). Table 1 details 31 different variants in *IQSEC2* in 38 separate cases of affected female(s) predicted to cause pathogenic loss of *IQSEC2* function. Of these 31 variants, 28 are known to have arisen de novo, one case of gonadal mosaicism in a family of four affected girls, and one case of monozygotic twins, with discordant phenotypes. The inheritance in the proband of the current report was unable to be determined. Although not all cases were accompanied by complete clinical descriptions, 33 of the 38 cases report developmental delay or ID ranging from mild-to-severe or profound and present with a range of comorbid behavioural and psychiatric features (Table 1). Interestingly, 28 of the 38 cases reported a range of seizure types in the affected females, including epileptic encephalopathies (Table 1). In a recent review of the phenotypic spectrum of epileptic encephalopathies in male and female patients with pathogenic *IQSEC2* variants, it was noted that there was no specific electroclinical syndrome that could

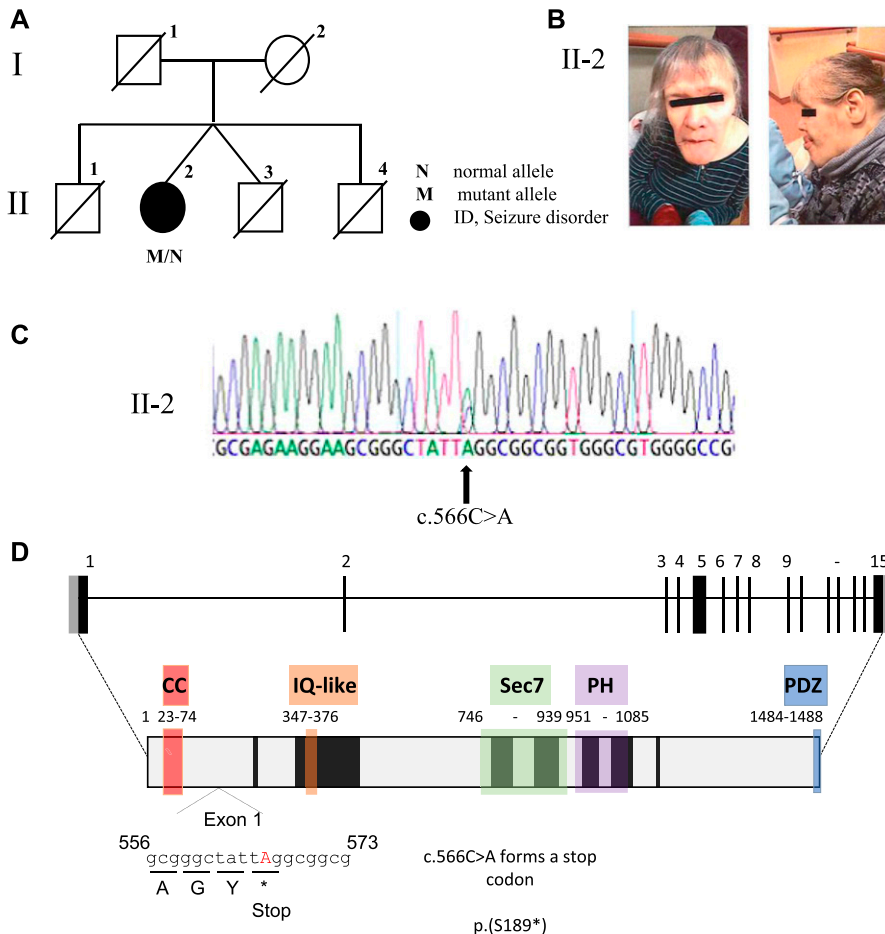


Figure 7. Identification of a c.556C > A (*NM_00111125.2*) variant resulting in a premature stop codon at p.(S189*) (*NP_001104595*) in *IQSEC2*. (A) Pedigree of family. Open symbols represent unaffected individuals and filled black circle represents female with profound-to-severe intellectual disability and epilepsy. Normal (N) and mutant (M) alleles shown for proband. (B) Asymmetrical facial features, prominent angle of the jaw and low-set, large ears of II-2 (front and side). (C) DNA sequence electropherograms for the chrX:g.53349756 (GRCh37/hg19 assembly); c.556C>A mutation in exon 1 of 15 of *IQSEC2* in II-2 affected female. (D) Predicted impact of novel variant in *IQSEC2*. The exon–intron structure of the longest isoform of the *IQSEC2* gene (*NM_00111125.2*) with 15 exons, the ATG and open reading frame and stop codon position in black and 5' and -3' untranslated regions in light grey. The predicted protein structures (*NP_001104595*) with known functional domains highlighted; coiled–coiled (CC–red), IQ-like (orange) Sec7 enzyme domain (Green), PH domain (purple), and PDZ-binding motif (Blue), corresponding amino acids listed below each domain. The variant c.556C>A replaces the codon for Serine (p.189) for a stop codon and is predicted to result in nonsense-mediated mRNA decay and loss of the protein from the mutant allele.

Table 1. Pathogenic loss-of-function variants in IQSEC2 in females with intellectual disability and other comorbidities.

cDNA	Ex	Protein	Dom	Family	DD/ID	Seizures	Behavioural/Psychiatric/ Physical features	Ref
c.55_151delinsAT	1	p.Ala191Ilefs*32	—	P1	Mild ID	None	Speech deficits—pronunciation, syntax issues at 6.5 years. Tantrums, anxiety	(29)
c.83_85del	1	p.Asp28del	CC	108286	Rett like	None	Loss of language. Regression stabilization, gait abnormalities	(30)
c.273_282del	1	p.Asp91Lysfs*112	—	P7	Rett like		Regression stabilization, gait abnormalities, stereotypic hand movements, inappropriate laughing/ screaming spells. Partial or loss of spoken language.	(31)
c.566C>A	1	p.(S189*)	—	Fin2	Severe-profound ID	Generalised seizures (18 mo)	Limited speech, low-set large ears, asymmetric facial features, mild hypertrichosis, mild ASD.	This report
c.804delC	3	p.Tyr269Thrfs*3	—	48		Seizures	Limited phenotype reported.	(32)
c.854del	3	p.Pro285Leufs*21	—	P11	Severe ID	Seizures (12 mo) tonic-clonic	Says words at 16 years. Limb rigidity, walking instability.	(29)
c.928G>T	3	p.Glu310*	—	P16	Mild-mod DD	FE	No ASD or other features. Nonverbal at 3 years.	(33)
c.1556_1599delACCT	5	p.Tyr519Trpfs*87	—	P10	DD, Severe to profound ID	None	Hypotonia, first word at 2 years, stereotypies, and dysmorphic features.	(34)
c.1591C>T	5	p.Arg531*	—	P3	DD, Severe to profound ID	Tonic-clonic, absence	Autism, first words at 11 mo, hypotonia, stereotypies, ataxic gait	(34)
c.1744_1763del	5	p.Arg582Cysfs*9	—	P16	Mild DD	Focal epilepsy (17 mo)	50–60 words at 3 years. Autistic behaviour, hypertonia.	(29)
c.1983_1999del	5	p.Leu662Glnfs*25	—	P17	Global DD	Focal epilepsy (11 mo)	Babbling at 16 mo Hypertonia.	(29)
c.2052_2053delCG	5	p.Cys684*	—	47		Seizures	Limited phenotype reported.	(32)
c.2078delG	5	p.Gly693Valfs*29		P18	Mod global DD	None	Nonverbal at 2.8 years. Self-injurious behaviour, hypotonia	(29)
c.2203C>T	5	p.Gln735*	—	T17563	Mild ID	SGE (5 years)—regression with nonconvulsive SE. Absence to tonic-clonic and myoclonic seizures, drop attacks. Offset at 38 years.	(35)	
c.2272C>T	5	p.Arg758*	—	P19	Severe ID	Multifocal epilepsy (23 mo)	3 words at 11.3 years. Self-injurious behaviours.	(29)
				P20	Mod ID	Seizures (9 years 4 mo) GTCS, focal, atypical absences	Speaks sentences, reasoning difficulties	
c.2317C>T	6	p.Gln773*	Sec7	P6	Global DD	Seizures (18 mo)	Hypotonic, strabismus, dysmorphic face	(36)
				P23	Mod ID	Seizures (14 years), GTCS, absences	Few words at 43 years. ASD (13 years) aggressive.	(29)
c.2317_2332del	6	p.Gln773Glyfs*25	Sec7	P24		Seizures (6 years)	Sentences at 11.3 years	(29)

(Continued on following page)

Table 1. Continued

cDNA	Ex	Protein	Dom	Family	DD/ID	Seizures	Behavioural/Psychiatric/ Physical features	Ref
c.2679_2680insA	8	p.Asp894fs*10	Sec7	K2	DD, Mod-severe ID	Epilepsy	4 affected sisters, nonverbal (2), language delay (1), aggressive when young and ASD traits (2)	(37)
c.2776C>T	9	p.Arg926*	Sec7	P3	Severe ID Rett like	EE	ASD (balance & hand stereotypies), pain sensitivity & aggressive. Speech delay, regression at 2 years. Now nonverbal	(38)
				P26	Profound ID	LGS (23 mo)	Nonverbal at 11.3 years. Autistic behaviour, truncal hypotonia, strabismus.	(29)
	9	p.Tyr933*	Sec7	M2189	Global DD Mod ID		ASD, sleep disturbances, behavioural aspects, oral motor dyspraxia, strabismus. Marked speech delay, nonverbal at 14 years.	(39)
c.2854C>T	9	p.Gln952*	PH	P27	Severe ID	EE (12 years), absences, GTCS	Nonverbal at 16 years. Autistic behaviour, dystonia, tremor, ataxia.	(29)
c.2911C>T	10	p.Arg971*	PH	P8	DD, Severe to profound ID	Seizures	No ASD. Stereotypies and dysmorphic features.	(34)
				P11	DD, Severe to profound ID	Seizures	Autism, first word at 2.3–3 years, stereotypies and dysmorphic features, ataxic gait	(34)
c.3079delC	11	p.Leu1027Serfs*75	PH	P29	Mod-severe ID	None	10 words at 8 years	(29)
c.3163C>T	12	p.Arg1055*	PH	Pat19	Severe ID	Epilepsy	Borderline macrocephaly, skewed X-inactivation (97:3)	(40)
				P31	Mod-severe ID	Seizures (5 years 8 mo) GTCS, focal dyscognitive	3 word sentences, and 20 words at 8 years. Autistic behaviour, Global hypotonia, aggression, hyperactivity.	(29)
c.3278C>A	13	p.Ser1093*	—	P36	Severe ID	None	Few words, rare sentences at 13 years.	(29)
c.3322C>T	13	p.Gln1108*	—	KO		EE		(41)
c.3433C>T	13	p.Arg1145*	—	P39	Severe ID	Focal epilepsy (11 mo) focal, tonic, tonic-clonic	Nonverbal at 11 years. Autistic behaviour.	(29)
c.3457del	14	p.Arg1153Glyfs*244	—	P40	Severe ID	IS (7 mo) spasms, focal, absence, tonic, myoclonic jerks	Nonverbal at 20 years. Autistic behaviour, truncal hypotonia. MRI mild atrophy and cerebral white matter hyperintensities.	(29)
c.4039dupG	15	p.Ala1347Glyfs*40	—	1098 M		EE (19 mo)	ASD, macrocephaly	(42)
				P41	Mild-mod ID	Seizures (3 years) absence and falls	Speaks sentences, writes first name, counts to 15 at 11 years. Mild autistic behaviour.	(29)
c.4401del	15	p.Gly1468Alafs*27	—	P42	Mod-severe ID	None	Short sentences at 11 years. Attention deficit/hyperactivity	(29)

(Continued on following page)

Table 1. Continued

cDNA	Ex	Protein	Dom	Family	DD/ID	Seizures	Behavioural/Psychiatric/ Physical features	Ref
c.4419_4420insC	15	p.Ser1474Glnfs*	—	P6	DD, Severe to profound ID	Absence, complex	Autism, hypotonia. First words at 7 years. Ataxic gait, stereotypies, bouts of laughter, self-injurious behaviour.	(34)
		Twin sister of P6		P7	DD, Mild ID	No	Autism, first words 11.5 mo. Ataxic gait	

ASD, autistic spectrum disorder; DD, developmental delay; EE, epileptic encephalopathy; GTCS, generalised tonic-clonic seizures; IS, infantile spasms; SGE, symptomatic generalised epilepsy.

Del, deletion; dup, duplication. Numbers (alone) in brackets indicate number of affected individuals.

Nucleotide numbering reflects cDNA numbering with +1 corresponding to the A of the ATG translation initiation codon in the reference sequence for *IQSEC2* (GenBank: [NM_00111125.2](https://www.ncbi.nlm.nih.gov/nuccore/NM_00111125.2)).

be defined, with all patients displaying multiple seizure types consisting mainly of atonic, myoclonic, or epileptic spasms. The seizure phenotypes were accompanied with a variety of electroencephalogram (EEG) patterning, including hypsarrhythmia, polyspikes and waves, generalised spikes and waves, slow spikes and waves, as well as background slowing (33). The advanced age of the female proband (68 yr old) we identify and present as part of this study underscores the importance of considering *IQSEC2* as an explanation of ID and, particularly, seizures in females across their life span. Furthermore, this finding reinforces the fact that a female *IQSEC2* phenotype may still be under-ascertained.

Discussion

The cellular and molecular pathogenesis of *IQSEC2* mutations is not well understood. To address this, we used CRISPR/Cas9-targeted editing to generate an *Iqsec2* KO mouse model with no (*Iqsec2* KO hemizygous males) or reduced (*Iqsec2* KO heterozygous females) *Iqsec2* mRNA and protein. We validated both successful genome editing and germline transmission. To date, there have been no reports of transmission of loss-of-function mutations in *IQSEC2* in the human setting, with the exception of gonadal mosaicism in a family of four affected female siblings (37). We demonstrate that hemizygous KO males were viable and able to breed and generate healthy female heterozygous KO offspring. This suggests a potential difference in mouse to human phenotypic outcomes related to brain and sexual development (43, 44). Despite some difficulties, the successful breeding of the *Iqsec2* KO heterozygous female mice shows that a loss-of-function mutation in *Iqsec2* can be transmitted, at least in mice.

In agreement with the expanding phenotypic spectrum and the 67% penetrance of seizures in patients with de novo pathogenic variants in *IQSEC2* (33), we demonstrate that severe spontaneous seizures are observed in approximately half of all the *Iqsec2* KO mice. In these mice, we observed four distinct seizure types: (i) involuntary, uncontrolled, unilateral head movements, (ii) repetitive forelimb clonus, (iii) uncontrolled convulsions with bilateral forelimb outward stretching, and (iv) full body tonic-clonic seizures. Using the (human) International League Against Epilepsy classification system, these seizures can be considered equivalent to (i) generalised clonic seizure, (ii) focal seizure evolving to

bilateral tonic-clonic seizure, (iii) focal motor seizure (likely frontal lobe onset), and (iv) generalised tonic-clonic seizure (Personal communication: A/Prof Nigel C Jones, Department of Neuroscience, Central Clinical School, Monash University, Melbourne, Victoria, Australia). Although EEG analysis was not undertaken in this study, aberrant firing and abnormal burst activity was noted in neuronal cultures of *Iqsec2* KO affected embryos. This abnormal activity is consistent with immature synaptic networks, previously associated with neurodevelopmental disorders (45, 46, 47).

Ionotropic glutamate receptors are ligand-gated cation channels that mediate most of the excitatory neurotransmission in the brain and are classified based on pharmacological selectivity to AMPA, kainic acid, and N-methyl-D-aspartic acid (NMDA). Activation of these receptors couples the electrical signal at the synapse to downstream biochemical signalling pathways. Selected NMDAR subunit genes have been implicated in the pathogenesis of ID (48, 49, 50). Synaptic plasticity associated with changes to spine morphology has been shown to be dependent on activation of these receptors (51, 52, 53, 54). *IQSEC2* is localized to excitatory synapses as part of the protein scaffold downstream of the NMDA receptor complex. Through enzyme activity, *IQSEC2* activates ARF6, a member of the Ras superfamily (55) to facilitate downstream remodelling of actin cytoskeleton, a site of convergence with other ID and autism genes. In the present study, we demonstrate that neurons in culture isolated from individual heterozygous female embryos display hallmarks of immature synaptic networks. Investigating which critical components of synaptic signalling are altered in response to *Iqsec2* dosage, we show surprisingly the loss of *Iqsec2* leads to an increase in the levels of activated Arf6 in cortical tissue during postnatal life. The increase in the active form of Arf6 is independent of changes to the overall abundance of Arf6 protein. Taken together, these data indicate that increased levels of activated Arf6 in the presence of *Iqsec2* loss of function are likely to be at the local, dendritic environment in response to neuron signalling. Using the novel and powerful *Iqsec2* KO hemizygous male and heterozygous female mouse models will enable further investigations into the critical components altered in response to reduced *Iqsec2* dosage and the downstream events contributing to disease outcomes.

Review of the female patients with complete loss-of-function mutations in *IQSEC2* shows that comorbid behavioural and

Table 2. Correlation of behavioural findings in *Iqsec2* KO mice and patients with loss-of-function mutations.

Test	Measure	Finding	Patient trait
Inverted Grid	Neuromuscular strength	Reduced	Dystonia/stereotypic hand movements
Open Field	Exploration	Increased	Hyperactivity and psychiatric issues
	Anxiety (open spaces)	Increased	
Elevated zero maze	Fear response (height)	Reduced	Psychiatric issues
Y-maze	Short term memory	Reduced	Intellectual disability
Sociability	Social traits	Reduced	Autistic-like features
Barnes Maze	Cognition	Reduced	Intellectual disability

psychiatric features are frequently present in addition to ID (Table 1). Hence, it was not surprising that mice modelling *Iqsec2* KO in the heterozygous female state displayed a range of phenotypic traits across a series of behavioural tests corresponding to these additional features (Table 2). Notably, the *Iqsec2* KO heterozygous females recapitulated a reduction in intellectual functioning and autistic-like behaviours, demonstrated through a loss of novel recognition on the Y-maze, a reduction in learning and memory during the Barnes maze trial, and an overall reduction in interaction time during the sociability test. Altered anxiety-like/fear responses and hyperactivity in the *Iqsec2* KO heterozygous female mice on multiple apparatus correlate with an increase in hippocampal volume, which has been associated with mental retardation and psychiatric issues such as autism, attention-deficit disorder, and schizophrenia (56, 57). We also observe a thinning of the corpus callosum in the *Iqsec2* KO heterozygous female mice, a phenotype emerging in several cases (29). Taken together, these findings highlight that our *Iqsec2* KO mouse model recapitulates the complex phenotypic spectrum observed in female patients with loss-of-function *IQSEC2* variants (31, 32, 33, 35, 36, 37, 38, 39, 40, 41). Interestingly, the emergence of a speech phenotype is noted in the proband reported in this study and 26 of the 38 published female cases with loss-of-function variants (Table 1). Although we have not yet addressed this clinical feature in mice, it would be interesting to investigate it, particularly in view of the observations of reduced mothering skills of the breeding heterozygous females.

Female patients with de novo loss-of-function mutations in *IQSEC2* often have a more severe phenotype than the heterozygous state would traditionally predict, particularly if *IQSEC2* is thought to escape X-inactivation. The capacity of genes on the X-chromosome to be silenced, or to escape to some degree X-inactivation is not fully understood. Escape from X-inactivation for *IQSEC2* in humans has long been the prevailing view, as demonstrated by evidence measuring DNA methylation as a predictor of inactivation status across a panel of 27 tissues from 1,875 females (58). In contrast, recent large-scale expression studies from the GTEx consortium demonstrate that the expression of *IQSEC2* is similar in males and females across a broad range of tissues, including regions of the brain (19). This would suggest either dosage compensation in males (up-regulation) or females (down-regulation) or X-chromosome inactivation (XCI) in females. The degree by which incomplete XCI manifests as detectable sex differences in gene expression and phenotypic traits remains poorly understood (58, 59). The *Iqsec2* KO

mouse model studied here shows severe phenotypic presentation in the heterozygous state. This fact would suggest that the severity of the phenotype in heterozygous females with loss-of-function *IQSEC2*/*Iqsec2* allele is generally independent of X-chromosome inactivation. Given that X-inactivation leads to cellular mosaicism in heterozygous females one may speculate that the function and impact of *IQSEC2*/*Iqsec2* is cell nonautonomous, that is, loss of *IQSEC2*/*Iqsec2* impacts wild-type (i.e., where the mutant X is inactivated) as well as mutant (i.e., cells where the wild-type X is inactivated) cells. As such, this genetic KO model will provide an excellent tool to investigate the molecular mechanisms of X-linked inheritance underpinning the male and female phenotypes, providing valuable information not only for *Iqsec2*, but other X-linked genes with an emerging female phenotype (4, 5, 6, 37).

Supplementary Information

Supplementary Information is available at <https://doi.org/10.26508/lsa.201900386>.

Acknowledgements

We would like to thank the members of the South Australian Genome Editing facility, Melissa White and Sandy Piltz, University of Adelaide, under the guidance of Professor Paul Q Thomas, for the expertise generating the *Iqsec2* KO mouse model. We would also like to thank the Laboratory Animal Services, Medical School South (Adelaide), and Aneta Zysk and Laura Redpath (Intellectual Disability Research Group) for their kind assistance with the mice, and Susan Hinze for her initial assistance with the CRISPR guide design, and Carl Campugan and Joel Chan for assistance in histology analysis and breakpoint mapping, respectively. Use of a laptop and behavioural tracking software, Anymaze (Wood Dale, United States of America), were kindly donated by Professor Bernhard Baune and Dr Catharine Jawahar, University of Adelaide. This research undertaken by the Intellectual Disability Research program in the Adelaide Medical School, University of Adelaide, Australia, was funded by the Australian National Health and Medical Research Council (Grant No 1063025) and Channel 7 Children's Research Foundation (Grant 161263). C Shoubridge was supported by the Australian Research Council (Future Fellowship FT120100086).

Author Contributions

MR Jackson: investigation, formal analysis and writing—original draft. KE Loring: investigation and writing—review and editing.

CC Homan: investigation, formal analysis.
 MHN Thai: investigation.
 L Määttänen: investigation.
 M Arvio: investigation.
 I Jarvela: investigation and writing—review and editing.
 M Shaw: data curation.
 A Gardner: investigation.
 J Gecz: investigation, review and editing.
 C Shoubridge: conceptualization, formal analysis, funding acquisition, investigation, and writing—original draft, review, and editing.

Conflict of Interest Statement

The authors declare that they have no conflict of interest.

References

- Neri G, Schwartz CE, Lubs HA, Stevenson RE (2018) X-linked intellectual disability update 2017. *Am J Med Genet A* 176: 1375–1388. doi:[10.1002/ajmg.a.38710](https://doi.org/10.1002/ajmg.a.38710)
- Gecz J, Shoubridge C, Corbett M (2009) The genetic landscape of intellectual disability arising from chromosome X. *Trends Genet* 25: 308–316. doi:[10.1016/j.tig.2009.05.002](https://doi.org/10.1016/j.tig.2009.05.002)
- Dobyns WB (2006) The pattern of inheritance of X-linked traits is not dominant or recessive, just X-linked. *Acta Paediatr Suppl* 95: 11–15. doi:[10.1080/08035320600618759](https://doi.org/10.1080/08035320600618759)
- Reijnders MR, Zachariadis V, Latour B, Jolly L, Mancini GM, Pfundt R, Wu KM, van Ravenswaaij-Arts CM, Veenstra-Knol HE, Anderlid BM, et al (2016) De novo loss-of-function mutations in USP9X cause a female-specific recognizable syndrome with developmental delay and congenital malformations. *Am J Hum Genet* 98: 373–381. doi:[10.1016/j.ajhg.2015.12.015](https://doi.org/10.1016/j.ajhg.2015.12.015)
- Zweier C, Kraus C, Brueton L, Cole T, Degenhardt F, Engels H, Gillissen-Kaesbach G, Graul-Neumann L, Horn D, Hoyer J, et al (2013) A new face of Borjeson-Forssman-Lehmann syndrome? De novo mutations in PHF6 in seven females with a distinct phenotype. *J Med Genet* 50: 838–847. doi:[10.1136/jmedgenet-2013-101918](https://doi.org/10.1136/jmedgenet-2013-101918)
- Snijders Blok L, Madsen E, Juusola J, Gilissen C, Baralle D, Reijnders MR, Venselaar H, Helmsmoortel C, Cho MT, Hoischen A, et al (2015) Mutations in DDX3X are a common cause of unexplained intellectual disability with gender-specific effects on Wnt signaling. *Am J Hum Genet* 97: 343–352. doi:[10.1016/j.ajhg.2015.07.004](https://doi.org/10.1016/j.ajhg.2015.07.004)
- Mattiske T, Moey C, Vissers LE, Thorne N, Georgeson P, Bakshi M, Shoubridge C (2017) An emerging female phenotype with loss-of-function mutations in the Aristaless-related homeodomain transcription factor ARX. *Hum Mutat* 38: 548–555. doi:[10.1002/humu.23190](https://doi.org/10.1002/humu.23190)
- Marsh E, Fulp C, Gomez E, Nasrallah I, Minarcik J, Sudi J, Christian SL, Mancini G, Labosky P, Dobyns W, et al (2009) Targeted loss of Arx results in a developmental epilepsy mouse model and recapitulates the human phenotype in heterozygous females. *Brain* 132: 1563–1576. doi:[10.1093/brain/awp107](https://doi.org/10.1093/brain/awp107)
- Palmer EE, Stuhlmann T, Weinert S, Haan E, Van Esch H, Holvoet M, Boyle J, Leffler M, Raynaud M, Moraine C, et al (2018) De novo and inherited mutations in the X-linked gene CLCN4 are associated with syndromic intellectual disability and behavior and seizure disorders in males and females. *Mol Psychiatry* 23: 222–230. doi:[10.1038/mp.2016.135](https://doi.org/10.1038/mp.2016.135)
- Hamici S, Bastaki F, Khalifa M (2017) Exome sequence identified a c.320A > G ALG13 variant in a female with infantile epileptic encephalopathy with normal glycosylation and random X inactivation: Review of the literature. *Eur J Med Genet* 60: 541–547. doi:[10.1016/j.ejmg.2017.07.014](https://doi.org/10.1016/j.ejmg.2017.07.014)
- Shoubridge C, Tarpey PS, Abidi F, Ramsden SL, Rujirabanjerd S, Murphy JA, Boyle J, Shaw M, Gardner A, Proos A, et al (2010) Mutations in the guanine nucleotide exchange factor gene IQSEC2 cause nonsyndromic intellectual disability. *Nat Genet* 42: 486–488. doi:[10.1038/ng.588](https://doi.org/10.1038/ng.588)
- Shoubridge C, Harvey RJ, Dudding-Byth T (2019) IQSEC2 mutation update and review of the female-specific phenotype spectrum including intellectual disability and epilepsy. *Hum Mutat* 40: 5–24. doi:[10.1002/humu.23670](https://doi.org/10.1002/humu.23670)
- Murphy JA, Jensen ON, Walikonis RS (2006) BRAG1, a Sec7 domain-containing protein, is a component of the postsynaptic density of excitatory synapses. *Brain Res* 1120: 35–45. doi:[10.1016/j.brainres.2006.08.096](https://doi.org/10.1016/j.brainres.2006.08.096)
- Sakagami H, Sanda M, Fukaya M, Miyazaki T, Sukegawa J, Yanagisawa T, Suzuki T, Fukunaga K, Watanabe M, Kondo H (2008) IQ-ArfGEF/BRAG1 is a guanine nucleotide exchange factor for Arf6 that interacts with PSD-95 at postsynaptic density of excitatory synapses. *Neurosci Res* 60: 199–212. doi:[10.1016/j.neures.2007.10.013](https://doi.org/10.1016/j.neures.2007.10.013)
- Myers KR, Wang G, Sheng Y, Conger KK, Casanova JE, Zhu JJ (2012) Arf6-GEF BRAG1 regulates JNK-mediated synaptic removal of GluA1-containing AMPA receptors: A new mechanism for nonsyndromic X-linked mental disorder. *J Neurosci* 32: 11716–11726. doi:[10.1523/jneurosci.1942-12.2012](https://doi.org/10.1523/jneurosci.1942-12.2012)
- Brown JC, Petersen A, Zhong L, Himelright ML, Murphy JA, Walikonis RS, Gerges NZ (2016) Bidirectional regulation of synaptic transmission by BRAG1/IQSEC2 and its requirement in long-term depression. *Nat Commun* 7: 11080. doi:[10.1038/ncomms11080](https://doi.org/10.1038/ncomms11080)
- Hinze SJ, Jackson MR, Lie S, Jolly L, Field M, Barry SC, Harvey RJ, Shoubridge C (2017) Incorrect dosage of IQSEC2, a known intellectual disability and epilepsy gene, disrupts dendritic spine morphogenesis. *Transl Psychiatry* 7: e1110. doi:[10.1038/tp.2017.81](https://doi.org/10.1038/tp.2017.81)
- Balaton BP, Cotton AM, Brown CJ (2015) Derivation of consensus inactivation status for X-linked genes from genome-wide studies. *Biol Sex Differ* 6: 35. doi:[10.1186/s13293-015-0053-7](https://doi.org/10.1186/s13293-015-0053-7)
- Tukiainen T, Villani AC, Yen A, Rivas MA, Marshall JL, Satija R, Aguirre M, Gauthier L, Fleharty M, Kirby A, et al (2018) Landscape of X chromosome inactivation across human tissues. *Nature* 555: 274. doi:[10.1038/nature25999](https://doi.org/10.1038/nature25999)
- Tsuchiya KD, Grealley JM, Yi Y, Noel KP, Truong JP, Disteche CM (2004) Comparative sequence and x-inactivation analyses of a domain of escape in human xp11.2 and the conserved segment in mouse. *Genome Res* 14: 1275–1284. doi:[10.1101/gr.2575904](https://doi.org/10.1101/gr.2575904)
- Van der Hoek KH, Eyre NS, Shue B, Khantisitthiporn O, Glab-Ampi K, Carr JM, Gartner MJ, Jolly LA, Thomas PQ, Adikusuma F, et al (2017) Viperin is an important host restriction factor in control of Zika virus infection. *Sci Rep* 7: 4475. doi:[10.1038/s41598-017-04138-1](https://doi.org/10.1038/s41598-017-04138-1)
- Cong L, Ran FA, Cox D, Lin S, Barretto R, Habib N, Hsu PD, Wu X, Jiang W, Marraffini LA, et al (2013) Multiplex genome engineering using CRISPR/Cas systems. *Science* 339: 819–823. doi:[10.1126/science.1231143](https://doi.org/10.1126/science.1231143)
- Yang H, Wang H, Shivalila CS, Cheng AW, Shi L, Jaenisch R (2013) One-step generation of mice carrying reporter and conditional alleles by CRISPR/Cas-mediated genome engineering. *Cell* 154: 1370–1379. doi:[10.1016/j.cell.2013.08.022](https://doi.org/10.1016/j.cell.2013.08.022)
- Mattiske T, Lee K, Gecz J, Friocourt G, Shoubridge C (2016) Embryonic forebrain transcriptome of mice with polyalanine expansion mutations in the ARX homeobox gene. *Hum Mol Genet* 25: 5433–5443. doi:[10.1093/hmg/ddw360](https://doi.org/10.1093/hmg/ddw360)
- Jackson MR, Lee K, Mattiske T, Jaehne EJ, Ozturk E, Baune BT, O'Brien TJ, Jones N, Shoubridge C (2017) Extensive phenotyping of two ARX polyalanine expansion mutation mouse models that span clinical

- spectrum of intellectual disability and epilepsy. *Neurobiol Dis* 105: 245–256. doi:[10.1016/j.nbd.2017.05.012](https://doi.org/10.1016/j.nbd.2017.05.012)
26. Li H, Durbin R (2009) Fast and accurate short read alignment with Burrows-Wheeler transform. *Bioinformatics* 25: 1754–1760. doi:[10.1093/bioinformatics/btp324](https://doi.org/10.1093/bioinformatics/btp324)
 27. DePristo MA, Banks E, Poplin R, Garimella KV, Maguire JR, Hartl C, Philippakis AA, del Angel G, Rivas MA, Hanna M, et al (2011) A framework for variation discovery and genotyping using next-generation DNA sequencing data. *Nat Genet* 43: 491. doi:[10.1038/ng.806](https://doi.org/10.1038/ng.806)
 28. Wang K, Li MY, Hakonarson H (2010) ANNOVAR: Functional annotation of genetic variants from high-throughput sequencing data. *Nucleic Acids Res* 38: e164. doi:[10.1093/nar/gkq603](https://doi.org/10.1093/nar/gkq603)
 29. Mignot C, McMahon AC, Bar C, Campeau PM, Davidson C, Buratti J, Nava C, Jacquemont ML, Tallot M, Milh M, et al (2018) IQSEC2-related encephalopathy in males and females: A comparative study including 37 novel patients. *Genet Med* 21: 837–849. doi:[10.1038/s41436-018-0268-1](https://doi.org/10.1038/s41436-018-0268-1)
 30. Sajan SA, Jhangjani SN, Muzny DM, Gibbs RA, Lupski JR, Glaze DG, Kaufmann WE, Skinner SA, Annese F, Friez MJ, et al (2017) Enrichment of mutations in chromatin regulators in people with Rett syndrome lacking mutations in MECP2. *Genet Med* 19: 13–19. doi:[10.1038/gim.2016.42](https://doi.org/10.1038/gim.2016.42)
 31. Olson HE, Tambunan D, LaCoursiere C, Goldenberg M, Pinsky R, Martin E, Ho E, Khwaja O, Kaufmann WE, Poduri A (2015) Mutations in epilepsy and intellectual disability genes in patients with features of Rett syndrome. *Am J Med Genet A* 167A: 2017–2025. doi:[10.1002/ajmg.a.37132](https://doi.org/10.1002/ajmg.a.37132)
 32. Helbig KL, Farwell Hagman KD, Shinde DN, Mroske C, Powis Z, Li S, Tang S, Helbig I (2016) Diagnostic exome sequencing provides a molecular diagnosis for a significant proportion of patients with epilepsy. *Genet Med* 18: 898–905. doi:[10.1038/gim.2015.186](https://doi.org/10.1038/gim.2015.186)
 33. Zerem A, Haginoya K, Lev D, Blumkin L, Kivity S, Linder I, Shoubridge C, Palmer EE, Field M, Boyle J, et al (2016) The molecular and phenotypic spectrum of IQSEC2-related epilepsy. *Epilepsia* 57: 1858–1869. doi:[10.1111/epi.13560](https://doi.org/10.1111/epi.13560)
 34. Radley JA, O'Sullivan RBG, Turton SE, Cox H, Vogt J, Morton J, Jones E, Smithson S, Lachlan K, Rankin J, et al (2019) Deep phenotyping of fourteen new patients with IQSEC2 variants, including monozygotic twins of discordant phenotype. *Clin Genet* 95: 496–506. doi:[10.1111/cge.13507](https://doi.org/10.1111/cge.13507)
 35. Epi4K Consortium (2016) De novo mutations in SLC1A2 and CACNA1A are important causes of epileptic encephalopathies. *Am J Hum Genet* 99: 287–298. doi:[10.1016/j.ajhg.2016.06.003](https://doi.org/10.1016/j.ajhg.2016.06.003)
 36. Helm BM, Powis Z, Prada CE, Casasbuenas-Alarcon OL, Balmakund T, Schaefer GB, Kahler SG, Kaylor J, Winter S, Zarate YA, et al (2017) The role of IQSEC2 in syndromic intellectual disability: Narrowing the diagnostic odyssey. *Am J Med Genet A* 173: 2814–2820. doi:[10.1002/ajmg.a.38404](https://doi.org/10.1002/ajmg.a.38404)
 37. Ewans LJ, Field M, Zhu Y, Turner G, Leffler M, Dinger ME, Cowley MJ, Buckley MF, Scheffer IE, Jackson MR, et al (2017) Gonadal mosaicism of a novel IQSEC2 variant causing female limited intellectual disability and epilepsy. *Eur J Hum Genet* 25: 763–767. doi:[10.1038/ejhg.2017.29](https://doi.org/10.1038/ejhg.2017.29)
 38. Allou L, Julia S, Amsallem D, El Chehadeh S, Lambert L, Thevenon J, Duffourd Y, Saunier A, Bouquet P, Pere S, et al (2017) Rett-like phenotypes: Expanding the genetic heterogeneity to the KCNA2 gene and first familial case of CDKL5-related disease. *Clin Genet* 91: 431–440. doi:[10.1111/cge.12784](https://doi.org/10.1111/cge.12784)
 39. Berger SI, Ciccone C, Simon KL, Malicdan MC, Vilboux T, Billington C, Fischer R, Introne WJ, Gropman A, Blancato JK, et al (2017) Exome analysis of Smith-Magenis-like syndrome cohort identifies de novo likely pathogenic variants. *Hum Genet* 136: 409–420. doi:[10.1007/s00439-017-1767-x](https://doi.org/10.1007/s00439-017-1767-x)
 40. Tzschach A, Grasshoff U, Beck-Woedl S, Dufke C, Bauer C, Kehrer M, Evers C, Moog U, Oehl-Jaschkowitz B, Di Donato N, et al (2015) Next-generation sequencing in X-linked intellectual disability. *Eur J Hum Genet* 23: 1513–1518. doi:[10.1038/ejhg.2015.5](https://doi.org/10.1038/ejhg.2015.5)
 41. Epi 4K, Allen AS, Berkovic SF, Cossette P, Delanty N, Dlugos D, Eichler EE, Epstein MP, Glauser T, et al;Epilepsy Phenome/Genome Project, (2013) De novo mutations in epileptic encephalopathies. *Nature* 501: 217–221. doi:[10.1038/nature12439](https://doi.org/10.1038/nature12439)
 42. Parrini E, Marini C, Mei D, Galuppi A, Cellini E, Pucatti D, Chiti L, Rutigliano D, Bianchini C, Virdo S, et al (2017) Diagnostic targeted resequencing in 349 patients with drug-resistant pediatric epilepsies identifies causative mutations in 30 different genes. *Hum Mutat* 38: 216–225. doi:[10.1002/humu.23149](https://doi.org/10.1002/humu.23149)
 43. Clancy B, Darlington RB, Finlay BL (2001) Translating developmental time across mammalian species. *Neuroscience* 105: 7–17. doi:[10.1016/s0306-4522\(01\)00171-3](https://doi.org/10.1016/s0306-4522(01)00171-3)
 44. Semple BD, Blomgren K, Gimlin K, Ferriero DM, Noble-Haeusslein LJ (2013) Brain development in rodents and humans: Identifying benchmarks of maturation and vulnerability to injury across species. *Prog Neurobiol* 106–107: 1–16. doi:[10.1016/j.pneurobio.2013.04.001](https://doi.org/10.1016/j.pneurobio.2013.04.001)
 45. Liu MG, Chen XF, He T, Li Z, Chen J (2012) Use of multi-electrode array recordings in studies of network synaptic plasticity in both time and space. *Neurosci Bull* 28: 409–422. doi:[10.1007/s12264-012-1251-5](https://doi.org/10.1007/s12264-012-1251-5)
 46. Lisman JE (1997) Bursts as a unit of neural information: Making unreliable synapses reliable. *Trends Neurosci* 20: 38–43. doi:[10.1016/s0166-2236\(96\)10070-9](https://doi.org/10.1016/s0166-2236(96)10070-9)
 47. Izhikevich EM, Desai NS, Walcott EC, Hoppensteadt FC (2003) Bursts as a unit of neural information: Selective communication via resonance. *Trends Neurosci* 26: 161–167. doi:[10.1016/s0166-2236\(03\)00034-1](https://doi.org/10.1016/s0166-2236(03)00034-1)
 48. Ende S, Rosenberger G, Geider K, Popp B, Tamer C, Stefanova I, Milh M, Kortum F, Fritsch A, Pientka FK, et al (2010) Mutations in GRIN2A and GRIN2B encoding regulatory subunits of NMDA receptors cause variable neurodevelopmental phenotypes. *Nat Genet* 42: 1021–1026. doi:[10.1038/ng.677](https://doi.org/10.1038/ng.677)
 49. Lemke JR, Hendrickx R, Geider K, Laube B, Schwake M, Harvey RJ, James VM, Pepler A, Steiner I, Hortnagel K, et al (2014) GRIN2B mutations in West syndrome and intellectual disability with focal epilepsy. *Ann Neurol* 75: 147–154. doi:[10.1002/ana.24073](https://doi.org/10.1002/ana.24073)
 50. Hamdan FF, Srour M, Capo-Chichi JM, Daoud H, Nassif C, Patry L, Massicotte C, Ambalavanan A, Spiegelman D, Diallo O, et al (2014) De novo mutations in moderate or severe intellectual disability. *PLoS Genet* 10: e1004772. doi:[10.1371/journal.pgen.1004772](https://doi.org/10.1371/journal.pgen.1004772)
 51. Chen BS, Thomas EV, Sanz-Clemente A, Roche KW (2011) NMDA receptor-dependent regulation of dendritic spine morphology by SAP102 splice variants. *J Neurosci* 31: 89–96. doi:[10.1523/jneurosci.1034-10.2011](https://doi.org/10.1523/jneurosci.1034-10.2011)
 52. Hill TC, Zito K (2013) LTP-induced long-term stabilization of individual nascent dendritic spines. *J Neurosci* 33: 678–686. doi:[10.1523/jneurosci.1404-12.2013](https://doi.org/10.1523/jneurosci.1404-12.2013)
 53. Tada T, Sheng M (2006) Molecular mechanisms of dendritic spine morphogenesis. *Curr Opin Neurobiol* 16: 95–101. doi:[10.1016/j.conb.2005.12.001](https://doi.org/10.1016/j.conb.2005.12.001)
 54. Tian L, Stefanidakis M, Ning L, Van Lint P, Nyman-Huttunen H, Libert C, Itoharu S, Mishina M, Rauvala H, Gahmberg CG (2007) Activation of NMDA receptors promotes dendritic spine development through MMP-mediated ICAM-5 cleavage. *J Cell Biol* 178: 687–700. doi:[10.1083/jcb.200612097](https://doi.org/10.1083/jcb.200612097)
 55. Casanova JE (2007) Regulation of Arf activation: The Sec7 family of guanine nucleotide exchange factors. *Traffic* 8: 1476–1485. doi:[10.1111/j.1600-0854.2007.00634.x](https://doi.org/10.1111/j.1600-0854.2007.00634.x)
 56. Plessen KJ, Bansal R, Zhu H, Whiteman R, Amat J, Quackenbush GA, Martin L, Durkin K, Blair C, Royal J, et al (2006) Hippocampus and amygdala morphology in attention-deficit/hyperactivity disorder. *Arch Gen Psychiatry* 63: 795–807. doi:[10.1001/archpsyc.63.7.795](https://doi.org/10.1001/archpsyc.63.7.795)
 57. Schumann CM, Hamstra J, Goodlin-Jones BL, Lotspeich LJ, Kwon H, Buonocore MH, Lammers CR, Reiss AL, Amaral DG (2004) The amygdala is enlarged in children but not adolescents with autism; the hippocampus

- is enlarged at all ages. *J Neurosci* 24: 6392–6401. doi:[10.1523/jneurosci.1297-04.2004](https://doi.org/10.1523/jneurosci.1297-04.2004)
58. Cotton AM, Price EM, Jones MJ, Balaton BP, Kobor MS, Brown CJ (2015) Landscape of DNA methylation on the X chromosome reflects CpG density, functional chromatin state and X-chromosome inactivation. *Hum Mol Genet* 24: 1528–1539. doi:[10.1093/hmg/ddu564](https://doi.org/10.1093/hmg/ddu564)
59. Schultz MD, He YP, Whitaker JW, Hariharan M, Mukamel EA, Leung D, Rajagopal N, Nery JR, Urich MA, Chen HM, et al (2015) Human body

epigenome maps reveal noncanonical DNA methylation variation. *Nature* 523: 212–U189. doi:[10.1038/nature14465](https://doi.org/10.1038/nature14465)



License: This article is available under a Creative Commons License (Attribution 4.0 International, as described at <https://creativecommons.org/licenses/by/4.0/>).

Appendix 3

Colony	ID	Genotype	DOB	Drug	Breeding Round	Date of death	Reason for death
PA1	2208G	PA1 hemizygous male	17/07/2017	Vehicle	2	26/09/2017	End point
PA1	2209G	PA1 hemizygous male	17/07/2017	Vehicle	2	1/09/2017	Found dead in cage
PA1	2258G	PA1 hemizygous male	21/07/2017	Vehicle	2	26/09/2017	End point
PA1	2302G	PA1 hemizygous male	3/08/2017	Vehicle	3	6/10/2017	End point
PA1	2327G	PA1 hemizygous male	8/09/2017	Vehicle	4	1/10/2017	Found dead in cage
PA1	2330G	PA1 hemizygous male	8/09/2017	Vehicle	4	6/11/2017	End point
PA1	2352G	PA1 hemizygous male	9/09/2017	Vehicle	4	8/11/2017	End point
PA1	2205G	Wild-type male	17/07/2017	Vehicle	2	26/09/2017	End point
PA1	2206G	Wild-type male	17/07/2017	Vehicle	2	26/09/2017	End point
PA1	2207G	Wild-type male	17/07/2017	Vehicle	2	26/09/2017	End point
PA1	2259G	Wild-type male	21/07/2017	Vehicle	2	26/09/2017	End point
PA1	2260G	Wild-type male	21/07/2017	Vehicle	2	26/09/2017	End point
PA1	2300G	Wild-type male	3/08/2017	Vehicle	3	6/10/2017	End point
PA1	2301G	Wild-type male	3/08/2017	Vehicle	3	6/10/2017	End point
PA1	2303G	Wild-type male	3/08/2017	Vehicle	3	6/10/2017	End point
PA1	2304G	Wild-type male	3/08/2017	Vehicle	3	6/10/2017	End point
PA1	2305G	Wild-type male	3/08/2017	Vehicle	3	6/10/2017	End point
PA1	2328G	Wild-type male	8/09/2017	Vehicle	4	8/11/2017	End point
PA1	2329G	Wild-type male	8/09/2017	Vehicle	4	6/11/2017	End point
PA1	2351G	Wild-type male	9/09/2017	Vehicle	4	8/11/2017	End point
PA1	2353G	Wild-type male	9/09/2017	Vehicle	4	8/11/2017	End point
PA1	2354G	Wild-type male	9/09/2017	Vehicle	4	8/11/2017	End point
PA1	2188G	PA1 hemizygous male	29/06/2017	E2	1	7/09/2017	End point
PA1	2217G	PA1 hemizygous male	18/07/2017	E2	2	11/08/2017	Found dead in cage
PA1	2219G	PA1 hemizygous male	18/07/2017	E2	2	3/08/2017	Cannibalised
PA1	2220G	PA1 hemizygous male	18/07/2017	E2	2	4/08/2017	Cannibalised
PA1	2332G	PA1 hemizygous male	8/09/2017	E2	4	8/11/2017	End point
PA1	2337G	PA1 hemizygous male	8/09/2017	E2	4	6/11/2017	End point
PA1	2340G	PA1 hemizygous male	8/09/2017	E2	4	8/11/2017	End point
PA1	2185G	Wild-type male	29/06/2017	E2	1	7/09/2017	End point
PA1	2186G	Wild-type male	29/06/2017	E2	1	7/09/2017	End point
PA1	2187G	Wild-type male	29/06/2017	E2	1	7/09/2017	End point
PA1	2218G	Wild-type male	18/07/2017	E2	2	11/08/2017	Wild-type control
PA1	2333G	Wild-type male	8/09/2017	E2	4	8/11/2017	End point
PA1	2334G	Wild-type male	8/09/2017	E2	4	6/11/2017	End point
PA1	2338G	Wild-type male	8/09/2017	E2	4	27/09/2017	Humane - runt
PA1	2339G	Wild-type male	8/09/2017	E2	4	8/11/2017	End point
Colony	ID	Genotype	DOB	Drug	Breeding Round	Date of death	Reason for death
PA2	2149D	PA2 hemizygous male	28/06/2017	Vehicle	1	7/09/2017	End point
PA2	2151D	PA2 hemizygous male	28/06/2017	Vehicle	1	24/08/2017	Found dead in cage
PA2	2152D	PA2 hemizygous male	28/06/2017	Vehicle	1	18/07/2017	Found dead in cage
PA2	2170D	PA2 hemizygous male	29/06/2017	Vehicle	1	7/09/2017	End point
PA2	2178D	PA2 hemizygous male	29/06/2017	Vehicle	1	11/08/2017	Humane - seizures
PA2	2180D	PA2 hemizygous male	29/06/2017	Vehicle	1	11/08/2017	Humane - seizures
PA2	2181D	PA2 hemizygous male	29/06/2017	Vehicle	1	20/07/2017	Humane - runt
PA2	2232D	PA2 hemizygous male	21/07/2017	Vehicle	2	26/09/2017	End point
PA2	2234D	PA2 hemizygous male	21/07/2017	Vehicle	2	27/07/2017	Cannibalised
PA2	2235D	PA2 hemizygous male	21/07/2017	Vehicle	2	26/09/2017	End point

PA2	2238D	PA2 hemizygous male	21/07/2017	Vehicle	2	26/09/2017	End point
PA2	2280D	PA2 hemizygous male	30/07/2017	Vehicle	3	21/08/2017	Found dead in cage
PA2	2281D	PA2 hemizygous male	30/07/2017	Vehicle	3	24/08/2017	Found dead in cage
PA2	2282D	PA2 hemizygous male	30/07/2017	Vehicle	3	22/08/2017	Found dead in cage
PA2	2283D	PA2 hemizygous male	30/07/2017	Vehicle	3	11/08/2017	Found dead in cage
PA2	2361D	PA2 hemizygous male	10/09/2017	Vehicle	4	6/11/2017	End point
PA2	2362D	PA2 hemizygous male	10/09/2017	Vehicle	4	6/11/2017	End point
PA2	2364D	PA2 hemizygous male	10/09/2017	Vehicle	4	31/10/2017	Found dead in cage
PA2	2150D	Wild-type male	28/06/2017	Vehicle	1	7/09/2017	End point
PA2	2169D	Wild-type male	29/06/2017	Vehicle	1	7/09/2017	End point
PA2	2171D	Wild-type male	29/06/2017	Vehicle	1	7/09/2017	End point
PA2	2177D	Wild-type male	29/06/2017	Vehicle	1	7/09/2017	End point
PA2	2179D	Wild-type male	29/06/2017	Vehicle	1	7/09/2017	End point
PA2	2231D	Wild-type male	21/07/2017	Vehicle	2	26/09/2017	End point
PA2	2233D	Wild-type male	21/07/2017	Vehicle	2	26/09/2017	End point
PA2	2236D	Wild-type male	21/07/2017	Vehicle	2	26/07/2017	Cannibalised
PA2	2237D	Wild-type male	21/07/2017	Vehicle	2	26/09/2017	End point
PA2	2273D	Wild-type male	30/07/2017	Vehicle	3	6/10/2017	End point
PA2	2274D	Wild-type male	30/07/2017	Vehicle	3	6/10/2017	End point
PA2	2275D	Wild-type male	30/07/2017	Vehicle	3	6/10/2017	End point
PA2	2359D	Wild-type male	10/09/2017	Vehicle	4	6/11/2017	End point
PA2	2360D	Wild-type male	10/09/2017	Vehicle	4	6/11/2017	End point
PA2	2363D	Wild-type male	10/09/2017	Vehicle	4	6/11/2017	End point
PA2	2157D	PA2 hemizygous male	28/06/2017	E2	1	15/07/2017	Humane - runt
PA2	2158D	PA2 hemizygous male	28/06/2017	E2	1	7/09/2017	End point
PA2	2159D	PA2 hemizygous male	28/06/2017	E2	1	20/07/2017	Found dead in cage
PA2	2160D	PA2 hemizygous male	28/06/2017	E2	1	13/07/2017	Found dead in cage
PA2	2161D	PA2 hemizygous male	28/06/2017	E2	1	7/07/2017	Humane - runt
PA2	2162D	PA2 hemizygous male	28/06/2017	E2	1	18/07/2017	Found dead in cage
PA2	2210D	PA2 hemizygous male	17/07/2017	E2	2	10/08/2017	Found dead in cage
PA2	2213D	PA2 hemizygous male	17/07/2017	E2	2	26/09/2017	End point
PA2	2223D	PA2 hemizygous male	19/07/2017	E2	2	12/08/2017	Found dead in cage
PA2	2294D	PA2 hemizygous male	1/08/2017	E2	3	30/09/2017	Found dead in cage
PA2	2309D	PA2 hemizygous male	5/08/2017	E2	3	8/09/2017	Humane - seizures
PA2	2311D	PA2 hemizygous male	5/08/2017	E2	3	26/08/2017	Found dead in cage
PA2	2343D	PA2 hemizygous male	8/09/2017	E2	4	8/11/2017	End point
PA2	2345D	PA2 hemizygous male	8/09/2017	E2	4	2/10/2017	Found dead in cage
PA2	2367D	PA2 hemizygous male	10/09/2017	E2	4	8/11/2017	End point
PA2	2155D	Wild-type male	28/06/2017	E2	1	7/09/2017	End point
PA2	2156D	Wild-type male	28/06/2017	E2	1	7/09/2017	End point
PA2	2211D	Wild-type male	17/07/2017	E2	2	26/09/2017	End point
PA2	2212D	Wild-type male	17/07/2017	E2	2	26/09/2017	End point
PA2	2224D	Wild-type male	19/07/2017	E2	2	26/09/2017	End point
PA2	2225D	Wild-type male	19/07/2017	E2	2	26/09/2017	End point
PA2	2286D	Wild-type male	1/08/2017	E2	3	6/10/2017	End point
PA2	2287D	Wild-type male	1/08/2017	E2	3	6/10/2017	End point
PA2	2288D	Wild-type male	1/08/2017	E2	3	6/10/2017	End point
PA2	2293D	Wild-type male	1/08/2017	E2	3	6/10/2017	End point
PA2	2310D	Wild-type male	5/08/2017	E2	3	8/09/2017	Wild-type control
PA2	2312D	Wild-type male	5/08/2017	E2	3	8/09/2017	Wild-type control

PA2	2344D	Wild-type male	8/09/2017	E2	4	8/11/2017	End point
PA2	2365D	Wild-type male	10/09/2017	E2	4	8/11/2017	End point
PA2	2366D	Wild-type male	10/09/2017	E2	4	8/11/2017	End point

Appendix 4

GeneID	logFC	logCPM	LR	PValue	FDR
1700007G11Rik	0.593699697	0.101188128	4.517789545	0.033544144	0.999830311
1700010I14Rik	0.675700367	0.60179567	7.661481133	0.005641217	0.999830311
4930481A15Rik	0.549233248	0.224790427	4.292578945	0.03827906	0.999830311
4933408B17Rik	0.82816721	0.091874136	7.109956592	0.007665697	0.999830311
9430083A17Rik	0.629609892	1.574897233	10.52467324	0.001177912	0.999830311
Acad12	0.527730136	0.560155887	4.57762345	0.032392111	0.999830311
Akr1c18	-1.565972532	0.365068516	7.048213896	0.007934433	0.999830311
Arc	-0.622817614	5.388169925	10.09935598	0.001483211	0.999830311
Armc3	0.520583145	0.874715913	5.340100357	0.020840273	0.999830311
B3gnt4	-0.680465861	0.239804633	4.34478577	0.037122437	0.999830311
BC006965	-0.574952206	0.807649024	4.887206363	0.027056432	0.999830311
Bves	0.738581978	0.665178896	8.844287959	0.002940076	0.999830311
Catip	0.514483972	1.150724217	6.117209697	0.013387195	0.999830311
Ccdc60	0.728797038	0.53253956	8.96313191	0.002754822	0.999830311
Ccl17	0.660450468	0.483802352	4.51569288	0.03358528	0.999830311
Cfap52	0.531688623	1.531096669	5.804853128	0.015982003	0.999830311
Chat	-1.352475754	0.495423795	8.049329446	0.00455205	0.999830311
Chrna2	-0.977895842	0.397850957	6.413861415	0.011323291	0.999830311
Clca3a1	0.502468008	1.121170823	5.340103599	0.020840235	0.999830311
Col14a1	-0.510081924	1.48612544	4.884867163	0.027093119	0.999830311
Colq	-0.610360067	1.022193381	4.31220005	0.037839994	0.999830311
Cpz	-0.558674617	0.814003639	5.130996181	0.023502235	0.999830311
Crabp1	-0.705827664	2.84839265	8.218560723	0.004146407	0.999830311
Dmrt2	0.502511095	1.694868683	3.913056025	0.047912397	0.999830311
Ercc6l	-0.643148248	0.634568213	6.251646067	0.012407795	0.999830311
Exoc3l4	0.693532137	0.334401455	5.817781335	0.015864945	0.999830311
Fam183b	0.532865749	1.225288501	7.192648545	0.007320285	0.999830311
Fam221a	0.800498427	0.310502229	9.605207641	0.001940263	0.999830311
Fgf16	-0.813595344	0.485286679	9.19519943	0.002426507	0.999830311
Flnc	0.52665066	2.35741235	7.322328686	0.006810311	0.999830311
Gm11992	0.625126263	1.012205227	6.781842578	0.009208978	0.999830311
H2-Q4	0.640163253	1.845653462	4.146921308	0.041710295	0.999830311
Hmga2-ps1	-0.56990098	0.48193279	4.353702546	0.036928579	0.999830311
Hrc	-0.548340431	0.296751047	4.169869844	0.041148961	0.999830311
Isg15	-1.39988018	1.002738235	4.26796578	0.038837398	0.999830311
Lgr5	-0.909630825	2.992426639	4.659321254	0.030885398	0.999830311
Lrguk	0.646383874	0.681334626	7.563287537	0.005956923	0.999830311
Lrp2	0.5267983	0.746314771	5.106913395	0.023830681	0.999830311
Lrrc36	0.888871994	0.485750388	12.08455705	0.000508412	0.999830311
Lrrc74b	0.814932142	1.035340038	13.09750257	0.00029569	0.999830311
Mc5r	0.650483735	0.744673761	6.809573715	0.009067041	0.999830311
Meis1	-0.516355843	3.352135448	6.262989208	0.012328601	0.999830311
Mir17hg	-0.71102073	0.793262421	4.636487075	0.031299008	0.999830311
Mme	-0.54302654	3.66271461	4.364221385	0.036701252	0.999830311
Mybl2	0.669436309	0.777960791	8.84346731	0.002941398	0.999830311
Myh8	0.829062204	1.488904463	14.8318672	0.000117533	0.999830311
Ngfr	-0.724033455	2.450204564	5.187995979	0.022743428	0.999830311
Nppa	-0.88782949	1.002833453	4.425983199	0.035395715	0.999830311
Ntrk1	-1.683517417	0.166494995	11.15227791	0.000839286	0.999830311

Nxph2	0.747031405	2.524576563	10.95326832	0.000934387	0.999830311
Omp	-1.463505316	1.147093552	4.374600031	0.036478391	0.999830311
Ovgp1	0.569559485	2.365067256	4.838094441	0.027837639	0.999830311
Pappa2	-0.537589652	2.478917336	6.015116362	0.014183843	0.999830311
Pcp4l1	-0.571950362	6.909373509	4.082339897	0.043333611	0.999830311
Prima1	-0.858012921	0.76991666	7.049692721	0.007927885	0.999830311
Prlr	0.512276845	2.263934458	5.223087009	0.02228895	0.999830311
Rgs22	0.660191102	0.802873638	5.557171784	0.018405125	0.999830311
Rxfp3	0.549120607	2.596764152	11.15223931	0.000839303	0.999830311
S100a4	0.541616536	2.285095409	4.424180296	0.035433129	0.999830311
Serpina3n	0.544280102	4.211210994	8.467382642	0.003615713	0.999830311
Serpib1a	0.536163649	0.667529972	5.386037733	0.020298512	0.999830311
Slc18a3	-0.853818879	1.242835005	9.365482772	0.002211098	0.999830311
Slc5a7	-0.58622272	2.648774517	4.089652276	0.043146518	0.999830311
Slc6a4	-1.356413819	1.303224165	4.350837972	0.036990741	0.999830311
Snord22	0.658422054	0.175634165	4.324815012	0.037560497	0.999830311
Socs1	-0.874431233	0.972939037	10.63966541	0.001106877	0.999830311
Sp6	0.504067161	0.63286386	4.649511124	0.031062393	0.999830311
Sp7	-1.460781938	1.499571632	6.532105991	0.010594445	0.999830311
Spata1	-0.597826355	0.919980252	5.988433399	0.014399986	0.999830311
Spata18	0.563877026	0.374753	4.175078205	0.041022669	0.999830311
Spon2	-0.525922724	0.408704717	3.97416775	0.04620328	0.999830311
Sspo	1.333888522	1.221211028	4.641952331	0.03119949	0.999830311
Sytl4	0.681548408	0.475658157	5.983235248	0.014442486	0.999830311
Tacr1	-0.561922395	3.20321107	8.059301766	0.004527063	0.999830311
Th	-1.055313381	4.11335111	5.252397762	0.02191655	0.999830311
Tmco5	-0.875754764	-0.0584237	5.785250739	0.016161192	0.999830311
Tnn	0.78929072	0.035977058	7.351152959	0.006701976	0.999830311
Ush1g	-1.533398729	0.768563578	7.51051853	0.006133971	0.999830311
Zc2hc1c	0.504126973	1.183312694	5.498768471	0.019029871	0.999830311
Zfp953	0.629094648	0.736161227	7.095231696	0.00772893	0.999830311

P10VWT_1	P10VWT_2	P10VWT_3	P10VWT_4	P10VWT_5	P10VWT_6
0.900221253	0.827733762	0.881080883	0.647081127	0.920424551	0.495140325
1.050258129	1.504970477	0.734234069	1.058860026	1.380636827	0.919546318
0.975239691	1.053479334	0.95450429	0.941208912	0.690318414	0.636608989
1.050258129	0.902982286	0.95450429	0.705906684	0.287632672	0.424405993
1.800442506	2.407952762	2.936936275	1.882417825	2.818800189	2.122029964
1.200295004	1.580219	1.395044731	0.941208912	0.862898017	0.919546318
1.125276566	0.827733762	2.790089462	0.352953342	1.610742965	2.900107617
37.43420044	44.69762315	63.73151718	41.00141324	47.74702361	56.87040303
2.02549782	1.504970477	1.321621324	1.470638925	1.380636827	0.99028065
1.800442506	1.504970477	0.881080883	1.470638925	1.03547762	0.778077653
2.475608446	1.805964572	2.34954902	1.705941153	1.725796034	1.202483646
0.900221253	1.279224905	1.027927696	1.235336697	0.862898017	1.556155307
2.175534695	2.031710143	1.835585172	1.411813368	1.840849103	1.414686643
0.825202815	1.053479334	1.101351103	1.235336697	0.862898017	1.131749314
0.750184378	1.580219	1.395044731	0.705906684	0.977951086	0.778077653
2.475608446	3.386183572	2.34954902	2.294196724	1.553216431	2.051295632
0.600147502	2.784195382	1.982431986	2.941277851	1.03547762	0.848811986
1.500368755	1.655467524	1.909008579	0.764732241	0.632791879	2.617170289
2.175534695	1.128727857	2.202702207	1.823592268	1.725796034	1.414686643
3.600885013	2.031710143	2.863512869	3.882486763	3.106432861	2.687904621
2.100516257	2.407952762	3.377476717	2.470673395	1.093004155	1.909826968
2.475608446	2.106958667	1.615314951	1.529464482	2.128481775	1.414686643
6.37656721	7.901095002	8.884232233	11.3533325	5.004808499	10.75161848
2.925719073	1.655467524	3.891440565	3.058928965	2.818800189	1.556155307
1.950479382	1.881213096	1.835585172	1.529464482	1.265583758	1.626889639
1.200295004	1.429721953	0.660810662	0.411778899	0.862898017	0.919546318
1.650405631	2.031710143	1.688738358	1.705941153	2.070955241	2.051295632
1.050258129	0.902982286	0.807657476	0.941208912	0.575265345	0.848811986
1.35033188	1.730716048	1.762161765	1.529464482	1.553216431	1.34395231
5.476345957	5.11689962	4.47882782	4.117788991	3.566645137	2.758638953
1.35033188	1.881213096	1.395044731	2.17654561	1.03547762	1.414686643
3.525866575	4.289165858	3.230629903	2.058894496	2.18600831	1.768358303
1.800442506	1.429721953	1.17477451	1.470638925	1.553216431	1.34395231
1.35033188	1.429721953	1.027927696	1.17651114	1.265583758	1.34395231
1.275313442	8.503083193	2.643242648	0.647081127	0.805371483	1.485420975
9.602360034	5.417893716	17.91531128	3.176580079	6.730604533	15.20788141
0.975239691	1.429721953	0.881080883	1.058860026	1.265583758	1.556155307
1.725424069	1.354473429	1.101351103	1.294162254	1.265583758	1.131749314
1.050258129	1.504970477	0.587387255	0.823557798	0.862898017	0.848811986
1.875460944	1.730716048	1.321621324	1.470638925	1.610742965	0.778077653
1.35033188	1.128727857	0.95450429	1.470638925	1.553216431	0.99028065
9.752396909	10.61004186	14.46441116	9.235612452	8.11124136	16.76403671
2.625645322	1.881213096	1.027927696	2.000068939	1.323110293	2.617170289
9.902433785	14.97445624	17.0342304	24.70673395	10.06714353	9.266197509
1.050258129	1.504970477	1.027927696	1.17651114	1.265583758	1.626889639
2.175534695	1.95646162	1.688738358	1.470638925	2.761273654	2.122029964
6.076493459	10.53479334	4.625674634	6.235509044	6.788131067	3.819653935
1.35033188	1.655467524	4.258557599	0.882383355	1.898375637	3.890388267
0.525129064	2.633698334	1.615314951	2.058894496	0.460212276	1.061014982

3.825940326	2.182207191	5.727025737	6.176683487	4.774702361	3.678185271
9.002212532	1.354473429	4.038287379	0.470604456	1.150530689	1.202483646
6.076493459	6.019881906	2.643242648	3.411882307	3.394065534	3.748919603
5.476345957	4.063420287	7.268917282	7.706147969	6.327918792	6.436824224
93.54799189	107.0786494	208.1553585	115.533394	80.76725439	224.0863642
2.100516257	2.483201286	2.1292788	2.17654561	0.862898017	1.909826968
3.000737511	5.493142239	2.863512869	5.11782346	3.509118603	3.890388267
1.200295004	1.881213096	1.17477451	1.764766711	0.632791879	1.202483646
4.801180017	4.740657001	4.772521448	4.588393447	6.615551464	4.31479426
4.426087828	5.041651096	3.450900124	2.823626737	3.566645137	4.809934585
14.55357693	21.59632634	10.27927696	12.76514587	17.54559301	16.48109939
1.200295004	1.279224905	1.248197917	0.941208912	1.323110293	1.414686643
2.175534695	3.988171763	3.157206496	2.647150066	1.438163362	3.112310614
5.926456583	10.30904776	6.82837684	8.294403539	3.394065534	7.922245199
7.576862214	2.784195382	0.660810662	0.941208912	1.093004155	5.870949567
1.275313442	0.752485238	0.95450429	0.647081127	0.690318414	0.565874657
2.70066376	2.784195382	2.276125613	2.117720053	1.265583758	2.475701625
1.275313442	1.580219	1.321621324	1.058860026	1.150530689	0.919546318
3.825940326	1.580219	5.800449144	0.941208912	2.761273654	7.073433213
3.000737511	1.805964572	2.055855393	2.058894496	1.898375637	1.485420975
0.750184378	1.128727857	1.101351103	1.17651114	1.208057224	0.424405993
1.875460944	1.128727857	1.395044731	1.117685583	1.438163362	1.273217978
2.250553133	2.182207191	0.734234069	0.58825557	1.208057224	1.273217978
1.050258129	1.504970477	1.027927696	0.941208912	0.862898017	0.707343321
7.576862214	10.53479334	11.67432169	14.58873814	8.744033239	9.407666173
18.15446194	31.67962853	32.08602881	5.470776803	11.6778865	31.40604347
1.35033188	0.225745571	1.321621324	0.941208912	1.265583758	0.99028065
0.375092189	0.601988191	0.807657476	0.58825557	0.747844948	0.99028065
2.02549782	1.279224905	4.405404413	0.705906684	1.495689896	3.112310614
1.575387193	2.55844981	1.541891545	1.764766711	1.840849103	1.697623971
0.900221253	1.504970477	1.101351103	1.000034469	1.323110293	1.697623971

P10VDP24_1	P10VDP24_2	P10VDP24_3	P10VDP24_4
1.199913934	1.417322473	0.994715813	1.087346529
1.976328833	1.700786967	1.521330067	1.970815583
1.270497107	1.247243776	1.111741202	1.495101477
1.482246625	1.133857978	1.345791982	1.087346529
3.176242767	4.025195822	3.276710913	3.941631167
1.90574566	1.53070827	1.638355456	1.495101477
0.141166345	1.133857978	0.292563474	0.543673264
21.45728447	44.44723274	26.79881425	33.3679466
2.117495178	1.814172765	2.39902049	1.970815583
0.494082208	0.793700585	0.585126949	1.223264845
1.482246625	1.02047218	0.994715813	1.563060635
2.399827868	1.587401169	2.106457015	1.563060635
3.105659594	2.551180451	2.223482405	2.310611374
1.270497107	1.984251462	1.755380846	1.834897267
2.258661523	1.984251462	1.228766592	1.019387371
3.458575457	3.685038429	3.803325166	2.514488848
0.846998071	0.396850292	0.994715813	0.407754948
0.635248553	0.737007686	0.702152338	0.951428213
2.682160559	2.494487552	2.04794432	2.718366322
1.90574566	2.551180451	2.516045879	1.495101477
1.199913934	1.870865664	1.521330067	1.155305687
0.988164416	1.53070827	1.170253897	1.359183161
3.387992285	5.215746699	6.37788374	5.504691802
3.952657666	2.834644945	4.622502894	3.669794535
0.776414899	0.963779281	1.521330067	0.951428213
1.270497107	1.474015372	1.579842761	1.495101477
2.682160559	3.004723642	3.042660133	2.038774742
1.62341297	1.247243776	1.521330067	1.563060635
0.846998071	1.133857978	1.053228508	0.407754948
5.858403326	6.292911778	7.255574163	4.961018538
2.893910077	2.494487552	1.872406236	2.310611374
7.411233123	3.174802339	4.32993942	2.78632548
0.846998071	1.53070827	0.819177728	0.679591581
0.564665381	1.077165079	0.936203118	0.815509897
0.494082208	0.850393484	1.872406236	0.611632422
3.176242767	7.653541352	4.271426725	5.436732644
1.835162488	1.927558563	1.579842761	2.174693058
1.693996142	1.474015372	2.223482405	2.174693058
1.835162488	1.927558563	1.579842761	1.631019793
2.117495178	2.834644945	2.750096659	2.582448006
2.258661523	2.154330158	2.223482405	1.223264845
6.705401397	7.993698746	8.308802671	9.038568021
0.564665381	1.190550877	1.755380846	1.087346529
8.68173023	9.014170926	10.2397216	11.41713855
1.835162488	1.927558563	1.930918931	2.44652969
3.387992285	3.855117126	4.388452115	2.78632548
1.693996142	3.968502923	5.558706012	4.077549483
0.776414899	1.474015372	1.228766592	1.495101477
0.494082208	0.226771596	0.585126949	0.407754948

7.05831726	7.029919464	7.957726502	7.611425702
0.494082208	1.757479866	0.643639644	1.223264845
8.540563885	6.74645497	4.798040979	4.89305938
4.164407183	3.911810024	5.968294876	3.058162112
65.14826831	104.0314695	85.66258528	116.957711
0.917581244	1.644094068	0.643639644	1.019387371
4.234990356	6.689762071	6.845985299	4.89305938
1.62341297	1.814172765	2.106457015	2.718366322
7.834732159	7.086612363	8.367315366	5.91244675
9.316978783	5.952754385	3.920350556	4.213467799
26.39810655	26.41889089	19.25067661	18.55285015
1.835162488	1.927558563	1.989431625	1.359183161
1.764579315	1.474015372	1.579842761	1.223264845
3.740908148	3.741731328	7.314086858	4.077549483
0.776414899	0.623621888	1.930918931	1.563060635
1.693996142	1.02047218	0.760665033	1.698978951
1.199913934	1.02047218	1.638355456	1.019387371
2.046912005	1.644094068	1.579842761	1.631019793
0.28233269	2.097637259	0.994715813	1.902856425
1.341080279	1.644094068	1.228766592	1.155305687
1.129330762	1.360629574	1.579842761	1.698978951
1.058747589	0.793700585	0.877690423	1.087346529
0.917581244	3.11810944	0.585126949	9.242445495
0.917581244	2.040944361	1.638355456	1.834897267
5.999569671	5.782675688	7.665163027	8.834690547
4.940822082	16.78109808	7.021523384	13.04815835
0.635248553	0.51023609	0.468101559	0.611632422
1.199913934	1.077165079	1.462817372	1.019387371
0.141166345	1.587401169	0.526614254	0.679591581
2.823326904	2.154330158	3.159685523	2.242652216
2.117495178	1.587401169	1.989431625	2.1067339

GeneID	logFC	logCPM	LR	PValue	FDR	P10VWT_1
2410018L13Rik	0.569725479	1.368331647	4.157618842	0.041447633	0.999950496	3.208763614
4932411E22Rik	-0.584489418	1.886244206	4.214961994	0.040068964	0.999950496	3.059518795
9430065F17Rik	0.674140549	0.220405825	4.056751342	0.043995061	0.999950496	0.373112048
Akr1c18	-1.086824274	0.450216638	4.752258041	0.029259875	0.999950496	1.119336145
Ankfn1	-0.794999238	1.337453417	4.283619606	0.038481318	0.999950496	1.641693012
Atf3	1.026767858	0.561814485	6.108430848	0.013453852	0.999950496	1.492448193
Bves	0.72333052	0.652708874	4.494131865	0.034011379	0.999950496	0.895468916
Car12	-0.618329863	3.187336041	4.014046777	0.045122724	0.999950496	11.6410959
Ccdc125	-0.778216653	0.114336848	6.35031117	0.011736071	0.999950496	1.193958554
Ccdc33	-0.625819082	0.253872364	4.046787543	0.044255486	0.999950496	1.343203373
Ccl17	0.65318629	0.473255755	4.029994408	0.044698089	0.999950496	0.746224096
Cdc42ep5	0.517484528	1.144708651	4.532932748	0.033248592	0.999950496	2.01480506
Chrdl1	-0.579294139	4.327482335	8.472064888	0.003606418	0.999950496	29.92358626
Col3a1	-0.671763689	5.597464858	4.274630124	0.038685383	0.999950496	79.24899903
Cpz	-1.270908824	0.629546401	13.92444283	0.000190308	0.999950496	2.462539518
Cybrd1	-0.562704877	4.255167109	7.704134675	0.005509448	0.999950496	30.44594313
Dmgdh	0.673213975	0.429710774	4.920207515	0.026544329	0.999950496	1.193958554
Dmrt2	0.707757415	1.787678706	6.48293492	0.0108915	0.999950496	2.910273976
Dnah11	-0.671441508	1.614234652	4.611154507	0.031764641	0.999950496	4.551966988
Enpp1	-0.763783999	2.382504183	10.70924429	0.001066016	0.999950496	6.641394457
Fam124b	-0.792765411	0.186873444	5.434335823	0.019744598	0.999950496	1.343203373
Fau	0.727718998	0.569239239	6.869139885	0.008769685	0.999950496	1.044713735
Gbp9	-0.684664956	1.630312456	3.937820483	0.047211908	0.999950496	3.283386024
Gem	0.715813254	1.461190797	4.133536156	0.042041414	0.999950496	1.865560241
Gpr139	-0.837909327	0.373321548	3.949576245	0.046883172	0.999950496	0.447734458
Gprin2	-0.652382262	0.537745427	4.619945848	0.031602236	0.999950496	1.044713735
Hcrt	-2.848471734	1.039234119	11.29059645	0.000779007	0.999950496	1.567070602
Hgf	-0.558037521	1.577448753	3.885503021	0.04870467	0.999950496	3.358008434
Ifi44	-1.482104307	0.457670279	3.88595688	0.048691509	0.999950496	1.119336145
Ifit3	-1.069615045	1.39716801	4.38883107	0.036175107	0.999950496	1.865560241
Irf6	0.511516581	1.17634579	4.088578321	0.043173942	0.999950496	1.567070602
Isg15	-1.63340756	0.949065547	5.874939532	0.0153579	0.999950496	1.268580964
Itpr1p	0.664016697	1.846866079	4.280989638	0.038540902	0.999950496	4.253477349
Lama3	-0.705424073	2.507138622	7.280907788	0.006969131	0.999950496	9.103933975
Lgr5	-1.216975174	2.909316086	7.869996189	0.005026176	0.999950496	9.551668433
Lmo1	0.53731941	4.309506179	5.025220293	0.024980748	0.999950496	17.8347559
Lrriq1	-0.684613919	0.518181032	4.137777903	0.041936185	0.999950496	1.119336145
Ndnf	-0.749761705	4.079744347	6.782823964	0.009203916	0.999950496	20.52116265
Ngfr	-0.559622232	2.490528207	4.575237869	0.032437242	0.999950496	6.04441518
Npsr1	-0.764242944	1.011314198	4.803524705	0.028401574	0.999950496	0.895468916
Npy	-0.542887972	5.687831324	20.39473468	6.30E-06	0.090648577	56.41454168
Nxph2	0.811575913	2.550277869	8.676164277	0.003223988	0.999950496	3.805742891
Pde3a	-0.519372652	2.081456878	4.0276598	0.044759988	0.999950496	4.02961012
Pdlim3	-0.84269185	0.364487813	5.27306195	0.021657885	0.999950496	0.820846506
Plaur	0.715639709	0.515372154	5.10949819	0.023795202	0.999950496	0.970091325
Procr	-0.772270218	0.423875759	5.638071891	0.017574524	0.999950496	1.716315422
Ptch2	-0.596638528	1.3310543	4.15929674	0.041406593	0.999950496	2.611784337
Ptgs2	1.294763252	2.146588135	4.25862426	0.039051535	0.999950496	2.462539518
Rsg1	-0.765850199	0.123862497	5.645872938	0.017496503	0.999950496	1.044713735

Slc17a8	0.675206627	3.498275692	7.202822208	0.007278902	0.999950496	7.611485783
Sifn5	-0.612101932	3.480450754	4.179400266	0.040918178	0.999950496	15.29759397
Sp6	0.651640133	0.694490878	6.488371732	0.010858239	0.999950496	1.268580964
Stat5a	-0.595781701	1.59077568	6.150648903	0.013136389	0.999950496	4.02961012
Sypl2	0.509677159	1.943978912	3.943965755	0.047039761	0.999950496	4.328099759
Syt15	-0.536869419	1.532643159	5.196396669	0.02263376	0.999950496	4.253477349
Tacr1	-0.680489784	3.159452115	7.210685768	0.00724708	0.999950496	7.536863373
Th	-1.172384632	4.077428075	4.027208774	0.044771957	0.999950496	18.05862313
Thbs4	0.801379171	2.103129008	5.970080765	0.014550614	0.999950496	4.328099759
Tktl2	0.607309669	0.480938091	4.314552526	0.037787708	0.999950496	1.268580964
Tnfsf10	-0.658015965	1.578522245	4.036667645	0.044521653	0.999950496	3.805742891
Tnn	1.03194014	0.151517913	8.472932997	0.003604697	0.999950496	0.373112048
Ush1g	-1.173075378	0.828904162	4.857412336	0.027527594	0.999950496	2.01480506
Zfp831	-0.513799202	2.775137871	7.685720158	0.005565946	0.999950496	5.895170361

P10VWT_2	P10VWT_3	P10VWT_4	P10VWT_5	P10VWT_6	P10VGCG_1
2.395347905	1.387459964	2.165214015	1.487396305	1.688630346	3.524123542
3.443312614	5.111694603	4.798582412	3.661283213	4.643733451	2.610461883
1.272528575	1.022338921	0.702231572	0.972528353	0.63323638	1.56627713
0.823400842	2.774919927	0.351115786	1.601811406	2.884743508	0.717877018
2.769621016	3.797258848	2.80892629	2.574339759	3.799418278	1.1094463
0.673691598	1.022338921	0.877789466	0.800905703	0.773955575	0.978923206
1.272528575	1.022338921	1.228905252	0.858113253	1.54791115	2.479938789
13.39897735	6.645202984	7.724547297	16.93343486	6.2620042	7.048247084
1.197673953	0.876290503	1.228905252	1.258566104	1.125753564	0.391569282
1.497092441	1.387459964	0.994828061	1.086943454	1.196113162	1.239969394
1.571947063	1.387459964	0.702231572	0.972528353	0.773955575	1.370492489
1.721656307	1.60653259	1.228905252	1.830641606	2.251507128	2.349415695
14.22237819	27.74919927	22.17881383	22.88302008	21.03751973	16.90274069
54.3444556	51.99323654	55.47629422	56.97872	42.49719704	54.16708407
2.095929417	1.60653259	1.52150174	2.116679357	1.407191955	1.370492489
24.7768799	14.60484172	18.72617526	21.56724642	20.68572174	19.44794103
0.823400842	0.730242086	1.111866656	1.315773655	0.63323638	1.305230941
1.646801685	3.870283057	3.04300348	2.80316996	1.54791115	3.002031165
3.218748748	3.943307265	3.394119267	2.459924658	3.236541496	2.936769618
5.83866052	6.426130358	5.85192977	6.064000321	5.769487015	4.698831389
1.347383197	1.022338921	1.697059633	0.858113253	1.055393966	1.1094463
0.973110087	0.803266295	1.053347359	0.972528353	1.54791115	1.892584865
6.063224386	4.162379891	2.516329801	2.002264257	3.166181899	2.610461883
2.021074795	3.213065179	1.287424549	1.659018956	2.462585921	2.414677242
2.095929417	1.460484172	1.697059633	1.659018956	1.125753564	0.326307735
1.871365551	1.825605215	1.931136824	1.430188755	1.196113162	1.305230941
7.186043716	0.219072626	5.85192977	0.286037751	2.744024312	0.522092377
2.91933026	5.25774302	3.56967716	2.059471807	2.603305117	1.892584865
6.138079008	1.752581007	0.585192977	0.400452851	0.422157586	0.587353924
8.383717669	3.578186222	1.345943847	1.372981205	2.81438391	1.305230941
2.245638661	2.482823093	1.404463145	1.887849157	1.336832357	1.957846412
8.458572291	2.62887151	0.643712275	0.800905703	1.477551553	0.913661659
2.54505715	1.679556798	2.984484183	2.91758506	2.392226323	3.132554259
6.811770606	7.521493488	5.442294686	4.233358715	6.543442591	5.547231501
5.389532787	17.8179069	3.160042076	6.693283373	15.12731352	5.155662219
18.18967316	9.858268163	12.52312971	25.05690699	16.53450547	23.95098778
1.122819331	1.460484172	2.574849099	1.716226506	1.125753564	0.717877018
13.77325046	26.87290877	16.03428757	20.07985012	23.00758846	13.77018643
10.47964709	4.600525143	6.203045556	6.750490923	3.799418278	3.915692824
1.721656307	2.409798884	2.28225261	2.631547309	3.588339485	1.044184753
48.35608584	70.97953078	60.15783804	53.20302168	63.74579556	39.41797443
2.170784039	5.695888272	6.144526259	4.748226666	3.658699083	5.677754595
4.341568079	5.038670395	4.974140305	4.576604016	5.065891038	3.654646636
2.470202527	1.460484172	1.697059633	1.144151004	0.914674771	0.652615471
0.823400842	1.095363129	0.643712275	0.972528353	1.688630346	0.913661659
1.721656307	0.730242086	1.580021038	1.773434056	1.196113162	0.978923206
4.266713457	2.336774676	3.101522778	1.887849157	2.462585921	2.610461883
3.218748748	3.359113596	1.814098229	3.489660562	1.758989944	1.305230941
1.122819331	1.168387338	1.228905252	1.029735904	1.336832357	0.45683083

9.281973134	12.7062123	9.480126228	7.036528674	7.950634545	8.679785761
22.30667737	10.95363129	10.35791569	8.924377831	9.217107305	8.745047308
1.571947063	1.314435755	1.053347359	1.144151004	0.914674771	2.349415695
4.04214959	2.920968345	2.457810503	3.432453012	3.236541496	2.023107959
3.443312614	3.578186222	2.223733313	3.203622811	2.321866726	3.589385089
3.742731102	2.701895719	2.574849099	2.631547309	3.166181899	2.349415695
10.47964709	11.61084917	14.51278583	8.69554763	9.3578265	6.982985537
31.51379588	31.91157917	5.442294686	11.61313269	31.2396614	19.25215639
4.640986567	3.870283057	1.287424549	2.688754859	2.532945519	6.134585425
0.973110087	0.949314712	0.819270168	1.315773655	0.914674771	2.284154148
5.688951275	2.482823093	3.335599969	2.116679357	2.81438391	2.871508071
0.598836976	0.803266295	0.585192977	0.743698153	0.985034368	1.174707847
1.272528575	4.381452517	0.702231572	1.487396305	3.095822301	1.762061771
7.036334472	9.055001869	8.543817464	8.352302329	6.895240579	4.89461603

P10VGCG_2	P10VGCG_3	P10VGCG_4
3.888239686	2.266648977	2.470737529
1.543859875	4.417059546	2.400145028
1.715399861	1.220503295	0.776517509
0.972059921	0.63931125	0.635332507
0.628979949	3.022198636	1.905997522
4.059779672	1.452980114	1.129480013
2.858999769	1.162384091	0.988295012
4.116959667	8.078569432	7.976952593
0.914879926	0.63931125	0.705925008
0.571799954	0.523072841	0.917702511
2.23001982	0.988026477	1.835405021
3.316439732	2.441006591	1.976590023
11.72189905	15.34347	17.64812521
11.32163908	44.98426432	32.04899538
0.343079972	0.813668864	0.564740007
13.83755888	13.01870182	12.70665015
1.944119843	1.046145682	1.976590023
5.374919565	3.952105909	4.941475058
0.800519935	2.441006591	2.54133003
1.772579857	4.184582727	3.741402544
0.457439963	0.813668864	0.423555005
2.34437981	1.336741705	1.482442517
1.200779903	3.022198636	1.905997522
6.404159482	2.324768182	2.470737529
0.571799954	1.336741705	0.917702511
0.571799954	1.162384091	0.917702511
0.343079972	0.406834432	0.352962504
1.772579857	2.382887386	2.894292534
0.343079972	1.162384091	0.352962504
0.972059921	2.208529773	1.623627519
3.316439732	2.441006591	2.611922531
1.029239917	0.871788068	0.423555005
7.833659366	3.545271477	3.176662537
2.858999769	4.707655568	3.035477536
2.401559806	4.533297955	4.447327552
32.59259736	17.31952295	22.94256277
0.686159945	1.220503295	1.200072514
4.745939616	13.89048989	15.31857268
4.460039639	4.765774773	3.953180046
1.200779903	1.91793375	1.129480013
38.65367687	44.22871466	39.10824546
10.86419912	6.683708523	7.553397588
1.429499884	3.777748296	4.23555005
0.514619958	0.871788068	1.129480013
1.944119843	1.91793375	1.976590023
0.514619958	0.755549659	1.200072514
1.200779903	1.569218523	1.976590023
20.64197833	1.859814546	2.54133003
0.457439963	0.63931125	1.200072514

22.41455819	11.5076025	14.89501767
4.745939616	11.39136409	8.682877602
1.772579857	1.452980114	2.047182524
1.658219866	3.022198636	2.117775025
6.289799491	3.312794659	4.870882557
1.601039871	2.382887386	2.400145028
3.602339709	8.9503575	6.353325074
1.601039871	11.15888727	6.353325074
3.202079741	6.858066137	6.212140073
1.200779903	1.162384091	1.764812521
1.48667988	2.731602614	1.411850017
2.34437981	0.871788068	1.200072514
0.285899977	0.988026477	0.776517509
5.31773957	6.683708523	4.447327552

GeneID	logFC	logCPM	LR	PValue	FDR
4933408B17Rik	0.579091639	0.055006113	4.177739051	0.040958307	0.999997108
9430083A17Rik	0.511784765	1.596558445	9.815551584	0.001730424	0.999997108
Akr1c18	-1.306520236	0.218075601	9.291332147	0.002302407	0.999997108
Bves	0.732521579	0.770939191	7.865188531	0.005039557	0.999997108
Ccl17	0.657693847	0.577792674	5.970376851	0.014548171	0.999997108
Cdsn	0.766204185	0.122257474	7.331907227	0.006774114	0.999997108
Chat	-1.004878675	0.411526518	4.106280334	0.042724231	0.999997108
Chrna2	-0.781840639	0.324703269	4.937960158	0.026273025	0.999997108
Cpz	-0.874211602	0.588078007	11.0690786	0.000877793	0.999997108
Crabp1	-0.615887168	2.767550531	5.033426658	0.02486266	0.999997108
Cyp27a1	-0.520204545	1.13217301	4.375327001	0.036462833	0.999997108
Ddx60	-0.848814172	-0.065859197	4.267018651	0.038859053	0.999997108
Dmrt2	0.609282635	1.83983127	8.08326508	0.004467588	0.999997108
Dock2	-0.576500465	0.291119246	4.896960901	0.026904003	0.999997108
Fam221a	0.636753421	0.322481535	7.92717509	0.004869777	0.999997108
Fgf16	-0.536823144	0.472141141	6.112877953	0.013420043	0.999997108
Fosb	1.434050578	2.892021766	4.012353069	0.045168071	0.999997108
Frmd7	-1.053950365	3.619401436	4.94964099	0.026096087	0.999997108
Gbp3	-0.666946419	2.861058238	5.016479307	0.025107168	0.999997108
Gpnmb	-0.638373319	0.190695286	4.571925797	0.032500011	0.999997108
Hmga2-ps1	-0.595649193	0.377617527	5.423347727	0.019869228	0.999997108
Ifi44	-1.395168149	0.27854544	6.414527664	0.011319043	0.999997108
Isg15	-1.510403778	0.755149307	9.023310517	0.002665582	0.999997108
Lgr5	-1.054594756	2.780517629	10.42380186	0.001244015	0.999997108
Lrrc36	0.756823768	0.53066812	7.965104013	0.004768775	0.999997108
Mafa	-0.752019433	-0.186687922	5.08209059	0.024174205	0.999997108
Mdh1b	0.594036323	-0.082773357	4.697138863	0.030212873	0.999997108
Mmrn1	-0.538129271	0.373935057	4.08565078	0.043248794	0.999997108
Msx2	0.574294618	-0.049511746	4.565814677	0.032616158	0.999997108
Mybl2	0.57436258	0.818172394	7.510647209	0.006133533	0.999997108
Myh8	0.618988174	1.478142104	9.070499819	0.002597661	0.999997108
Myo1h	0.580207447	-0.076515013	4.283988923	0.038472958	0.999997108
Ndnf	-0.519147734	4.064452846	5.482124398	0.019211897	0.999997108
Ngfr	-0.640121005	2.364216324	7.446091057	0.006357437	0.999997108
Nppa	-0.713923751	0.931222648	4.507493911	0.033746651	0.999997108
Npsr1	-0.598819316	0.965220669	5.705296066	0.016913802	0.999997108
Ntrk1	-1.418805036	0.005712389	9.094583129	0.002563676	0.999997108
Nxph2	0.779916044	2.664626199	15.31221476	9.11E-05	0.991034909
Oasl2	-0.876637933	2.055484402	5.165194742	0.023043874	0.999997108
Omp	-1.183439856	1.019075338	4.530174278	0.033302226	0.999997108
Pdlim3	-0.734268072	0.282395684	6.852004689	0.008854187	0.999997108
Plaur	0.567339328	0.533250439	5.248496747	0.02196574	0.999997108
Ptch2	-0.531197132	1.267085526	6.418782657	0.011291954	0.999997108
Rtp4	-0.831170566	1.623862664	4.296373064	0.038193744	0.999997108
S100a9	1.340227201	-0.044727568	4.570201523	0.032532738	0.999997108
Shisa8	-0.593407597	2.634608296	4.767398538	0.02900362	0.999997108
Slc6a4	-1.112597706	1.180794923	4.783078366	0.028740699	0.999997108
Socs1	-0.506307264	0.99054595	4.774918448	0.028877214	0.999997108
Sp6	0.579487448	0.752565491	8.662943914	0.003247462	0.999997108

Sp7	-1.228274434	1.351471364	7.531766124	0.006062045	0.999997108
Spata20	0.519803	4.66E-05	4.56747633	0.032584534	0.999997108
Spp1	-0.736192874	2.804216922	4.365552611	0.036672587	0.999997108
Tacr1	-0.619582515	3.076895606	10.781435	0.001025232	0.999997108
Th	-1.11329817	3.915012525	6.354401152	0.011709046	0.999997108
Thbs4	0.757292611	2.208675033	5.612890708	0.017828828	0.999997108
Tktl2	0.50859598	0.517997152	4.950712812	0.026079913	0.999997108
Tnn	0.916596369	0.228018801	10.74692262	0.001044529	0.999997108
Ush1g	-1.34298255	0.598968186	8.757294781	0.003083661	0.999997108

P10VWT_1	P10VWT_2	P10VWT_3	P10VWT_4	P10VWT_5	P10VWT_6	P10VGCG_1
1.047840564	0.900455484	0.944284673	0.701582027	0.288105706	0.424752155	0.718483227
1.79629811	2.401214625	2.905491301	1.870885406	2.823435918	2.123760777	2.939249565
1.122686319	0.825417527	2.760216736	0.350791014	1.613391953	2.902473062	0.718483227
0.898149055	1.275645269	1.016921955	1.227768548	0.864317118	1.55742457	2.482032966
0.748457546	1.575797097	1.380108368	0.701582027	0.9795594	0.778712285	1.371649797
0.673611791	0.525265699	0.435823695	0.876977534	0.806695977	0.707920259	0.783799884
0.598766037	2.77640441	1.961206628	2.923258447	1.037180541	0.849504311	1.698233082
1.496915092	1.650835054	1.888569346	0.760047196	0.633832553	2.619304958	1.436966454
2.469909902	2.101062797	1.598020216	1.520094392	2.131982224	1.415840518	1.371649797
6.361889141	7.878985487	8.789111187	11.2837776	5.013039284	10.76038794	6.596982358
3.667441975	2.551290539	2.324393041	1.63702473	1.44052853	3.539601295	2.090133024
1.047840564	3.076556238	0.508460978	0.643116858	1.094801683	0.424752155	0.979749855
2.918984429	1.650835054	3.849775974	3.040188784	2.823435918	1.55742457	3.004566222
1.496915092	1.050531398	0.944284673	0.993907872	1.210043965	2.477720907	0.783799884
1.047840564	0.900455484	0.799010108	0.935442703	0.576211412	0.849504311	1.045066512
1.347223583	1.725873012	1.743294781	1.520094392	1.555770812	1.345048492	1.110383169
3.891979239	2.326176668	5.011972495	1.870885406	3.630131895	5.238609917	1.698233082
16.3163745	6.753416132	30.28974682	2.514002264	15.3848447	32.77670799	12.86738143
7.933649988	23.5619185	7.554277383	4.560283177	5.30114499	5.734154098	4.506849333
1.422069337	0.675341613	2.033843911	1.227768548	0.749074835	1.628216596	0.914433198
1.79629811	1.425721183	1.162196521	1.461629223	1.555770812	1.345048492	1.110383169
1.122686319	6.153112476	1.743294781	0.584651689	0.403347988	0.424752155	0.587849913
1.272377828	8.479289143	2.614942171	0.643116858	0.806695977	1.486632544	0.914433198
9.580256589	5.402732906	17.72349694	3.157119122	6.741673519	15.22028557	5.160015904
1.047840564	1.50075914	0.58109826	0.818512365	0.864317118	0.849504311	2.482032966
1.122686319	0.75037957	1.598020216	0.52618652	1.037180541	0.920296337	0.849116541
0.449074528	0.75037957	0.58109826	0.935442703	0.518590271	0.495544181	1.110383169
2.245372638	1.200607312	0.87164739	1.520094392	1.9591188	0.707920259	0.587849913
0.673611791	0.825417527	0.363186413	0.701582027	0.749074835	0.566336207	1.045066512
1.047840564	1.50075914	1.016921955	1.169303379	1.267665106	1.628216596	1.828866396
2.170526883	1.950986883	1.670657498	1.461629223	2.765814777	2.123760777	2.286082995
0.673611791	0.675341613	0.363186413	1.169303379	0.576211412	0.283168104	1.110383169
20.58258252	13.80698409	26.73051997	16.01945629	20.22502056	23.14899247	13.78181463
6.062506123	10.50531398	4.5761488	6.197307907	6.799294661	3.822769399	3.91899942
1.347223583	1.650835054	4.212962387	0.876977534	1.901497659	3.893561425	2.351399652
0.898149055	1.725873012	2.397030324	2.280141588	2.650572495	3.610393321	1.045066512
0.523920282	2.626328496	1.598020216	2.046280913	0.46096913	1.061880389	0.65316657
3.817133485	2.176100754	5.665708038	6.138842738	4.782554719	3.681185347	5.68254916
4.191362258	17.1086542	3.995050539	2.689397771	2.708193636	2.336136855	2.351399652
8.981490552	1.350683226	3.995050539	0.467721351	1.152422824	1.20346444	3.396466164
0.823303301	2.476252582	1.452745651	1.695489899	1.152422824	0.920296337	0.65316657
0.97299481	0.825417527	1.089559238	0.643116858	0.9795594	1.699008622	0.914433198
2.619601411	4.27716355	2.324393041	3.098653953	1.901497659	2.477720907	2.61266628
2.76929292	12.38126291	3.413952279	1.753955068	1.728634236	1.911384699	1.95949971
0.449074528	0.075037957	0.363186413	0.175395507	0.403347988	1.20346444	0.457216599
5.239202822	6.828454089	11.91251434	3.098653953	6.626431237	11.68068427	5.747865817
7.559421215	2.77640441	0.653735543	0.935442703	1.094801683	5.87573815	3.004566222
2.694447166	2.77640441	2.251755759	2.104746082	1.267665106	2.477720907	1.763549739
1.272377828	1.575797097	1.307471086	1.052373041	1.152422824	0.920296337	2.351399652

3.817133485	1.575797097	5.73834532	0.935442703	2.765814777	7.07920259	3.135199536
0.673611791	0.600303656	0.58109826	0.818512365	0.749074835	0.707920259	1.110383169
15.71760847	3.451746023	13.51053455	3.80023598	7.029779225	10.05246768	9.536231923
7.559421215	10.50531398	11.54932792	14.49936189	8.758413461	9.415339445	6.9888823
18.11267261	31.59097991	31.74249247	5.437260711	11.69709166	31.4316595	19.26841382
4.341053767	4.652353335	3.849775974	1.286233716	2.708193636	2.548512932	6.139765759
1.272377828	0.975493441	0.944284673	0.818512365	1.325286247	0.920296337	2.286082995
0.374228773	0.600303656	0.799010108	0.584651689	0.749074835	0.991088363	1.175699826
2.020835374	1.275645269	4.358236952	0.701582027	1.498149671	3.11484914	1.763549739

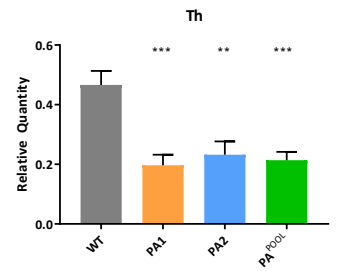
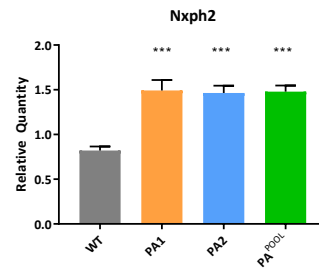
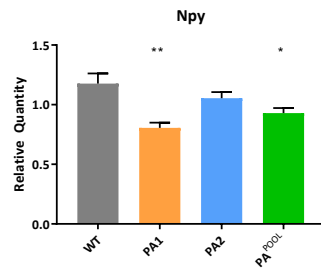
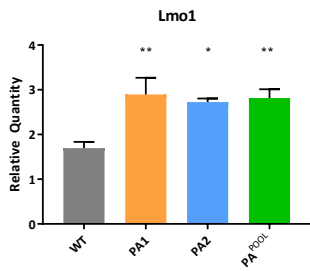
P10VGCG_2	P10VGCG_3	P10VGCG_4	P10VDP24_1	P10VDP24_2	P10VDP24_3	P10VDP24_4
1.149544883	0.642020109	0.91560423	1.485283841	1.130931713	1.336552702	1.08082769
3.218725672	2.684811363	3.310261445	3.182751088	4.014807581	3.254215275	3.918000376
0.97711315	0.642020109	0.633879851	0.141455604	1.130931713	0.290554935	0.540413845
2.873862207	1.167309288	0.986035324	2.404745266	1.583304398	2.091995534	1.553689804
2.241612522	0.992212895	1.831208459	2.263289662	1.979130498	1.220330728	1.013275959
1.839271813	0.817116502	1.549484081	1.343828237	1.074385127	0.639220858	1.283482882
0.172431732	1.98442579	0.211293284	0.848733623	0.3958261	0.98788678	0.405310384
0.402340709	1.575867539	0.493017662	0.636550218	0.735105613	0.697331845	0.945724229
0.344863465	0.817116502	0.563448757	0.990189227	1.526757812	1.162219741	1.351034613
1.66684008	8.754819662	6.127505228	3.394934493	5.202285879	6.334097589	5.471690181
1.092067639	1.98442579	1.549484081	1.131644831	2.374956597	1.685218625	2.026551919
0.172431732	0.642020109	0.633879851	0.636550218	0.622012442	0.755442832	0.540413845
5.402860949	3.96885158	4.930176621	3.960756909	2.827329282	4.590767977	3.647793454
0.919635906	0.992212895	0.845173135	1.273100435	1.130931713	0.697331845	0.607965576
1.034590395	1.108943824	1.479052986	1.626739445	1.244024884	1.510885663	1.553689804
1.379453859	1.400771146	1.056466419	0.848733623	1.130931713	1.045997767	0.405310384
56.21274477	5.369622726	3.662416918	2.19256186	5.767751736	1.452774676	2.837172686
1.724317324	7.704241303	8.522162444	3.748573503	11.76168981	5.985431667	14.45607035
5.345383705	6.303470157	5.634487566	6.294774373	5.993938078	6.275986602	5.40413845
0.229908977	0.700385573	1.126897513	0.990189227	1.017838542	0.697331845	0.945724229
0.517295197	1.575867539	0.563448757	0.848733623	1.526757812	0.813553819	0.675517306
0.344863465	1.167309288	0.352155473	0.636550218	0.735105613	1.104108754	0.270206923
1.034590395	0.875481966	0.422586567	0.495094614	0.848198785	1.859551586	0.607965576
2.414044254	4.552506224	4.437158959	3.182751088	7.633789062	4.242102055	5.40413845
0.804681418	1.050578359	1.479052986	1.838922851	1.922583912	1.56899665	1.621241535
0.287386221	0.291827322	0.422586567	0.495094614	0.848198785	0.348665922	1.148379421
0.747204174	0.583654644	0.77474204	1.485283841	1.074385127	0.871664806	1.013275959
1.092067639	0.933847431	1.479052986	0.848733623	0.961291956	0.929775793	1.013275959
0.517295197	0.817116502	1.197328608	1.202372633	1.187478299	1.162219741	0.675517306
1.149544883	1.634233004	2.535519405	1.838922851	1.922583912	1.917662573	2.431862303
3.391157404	2.159522183	2.676381594	3.394934493	3.845167824	4.358324029	2.769620956
1.034590395	0.817116502	0.986035324	1.060917029	1.017838542	1.045997767	0.540413845
4.770611264	13.949346	15.28354752	12.58954875	15.83304398	17.20085217	18.71182938
4.483225043	4.785968082	3.944141296	1.697467247	3.958260995	5.52054377	4.053103838
1.034590395	1.809329397	1.056466419	0.778005821	1.470211227	1.220330728	1.486138074
1.207022127	1.926060326	1.126897513	1.626739445	1.470211227	1.917662573	1.621241535
0.114954488	1.400771146	0.211293284	0.495094614	0.226186343	0.581109871	0.405310384
10.92067639	6.712028408	7.53612712	7.072780195	7.01177662	7.903094239	7.56579383
2.299089766	3.96885158	2.324226121	3.253478889	3.336248553	3.777214158	2.566965764
0.804681418	0.992212895	0.704310946	0.495094614	1.752944155	0.639220858	1.215931151
0.517295197	0.875481966	1.126897513	1.343828237	0.90474537	0.871664806	0.540413845
1.954226301	1.926060326	1.972070648	1.131644831	1.583304398	1.278441715	1.418586343
1.207022127	1.575867539	1.972070648	1.909650653	1.809490741	2.324439482	1.959000188
1.66684008	2.976638685	1.972070648	1.980378454	2.544596354	3.254215275	1.486138074
0.172431732	1.45913661	0.352155473	0.919461425	0.3958261	1.627107638	3.715345184
2.471521498	5.661450048	5.000607715	4.385123721	7.237962963	5.113766861	4.390862491
1.724317324	0.583654644	1.408621892	0.778005821	0.622012442	1.917662573	1.553689804
2.414044254	1.98442579	1.549484081	1.202372633	1.017838542	1.627107638	1.013275959
1.781794568	1.45913661	2.042501743	2.051106256	1.639850984	1.56899665	1.621241535

0.747204174	1.517502075	1.760777364	0.282911208	2.092223669	0.98788678	1.891448458
1.149544883	0.992212895	1.056466419	0.848733623	0.848198785	1.220330728	0.743069037
2.011703545	4.902699011	3.944141296	3.394934493	6.389764178	6.740874498	5.877000565
3.621066381	8.98828152	6.338798512	6.011863165	5.767751736	7.612539304	8.781724982
1.609362836	11.20616917	6.338798512	4.950946136	16.73778935	6.973318446	12.96993228
3.218725672	6.887124801	6.197936323	7.072780195	8.595081018	2.150106521	3.310034801
1.207022127	1.167309288	1.760777364	1.697467247	1.244024884	1.162219741	1.486138074
2.35656701	0.875481966	1.197328608	1.202372633	1.074385127	1.452774676	1.013275959
0.287386221	0.992212895	0.77474204	0.141455604	1.583304398	0.522998883	0.675517306

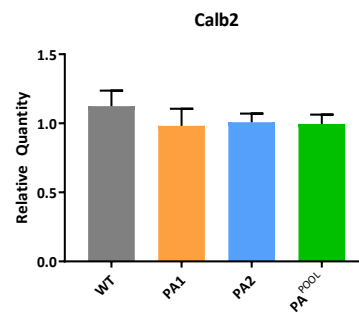
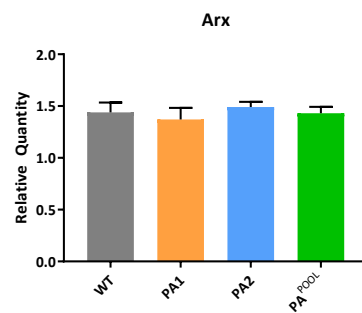
Appendix 5

A

Gene	RNAseq			qPCR			Validated?		
	PA1	PA2	PA ^{POOL}	PA1	PA2	PA ^{POOL}	PA1	PA2	PA ^{POOL}
<i>Lmo1</i>	↑	ns	ns	↑	↑	↑	✓	x	x
<i>Npy</i>	↓	ns	ns	↓	ns	↓	✓	✓	x
<i>Nxph2</i>	↑	↑	↑	↑	↑	↑	✓	✓	✓
<i>Th</i>	↓	↓	↓	↓	↓	↓	✓	✓	✓

**B**

Gene	RNAseq			qPCR			Validated?		
	PA1	PA2	PA ^{POOL}	PA1	PA2	PA ^{POOL}	PA1	PA2	PA ^{POOL}
<i>Arx</i>	ns			ns			✓	✓	✓
<i>Calb2</i>	ns			ns			✓	✓	✓



C

Gene	RNAseq			qPCR			Validated?		
	PA1	PA2	PA ^{POOL}	PA1	PA2	PA ^{POOL}	PA1	PA2	PA ^{POOL}
<i>Arc</i>	ns	↓	ns	ns			✓	x	✓
<i>Chrna2</i>	ns	↓	↓	ns			✓	x	x
<i>Gbp3</i>	ns	ns	↓	ns			✓	✓	x
<i>Pcp4l1</i>	ns	↓	ns	ns	ns	↓	✓	x	x
<i>Spp1</i>	ns	ns	↓	ns			✓	✓	x

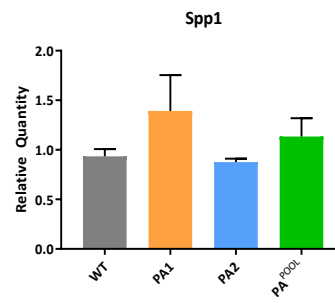
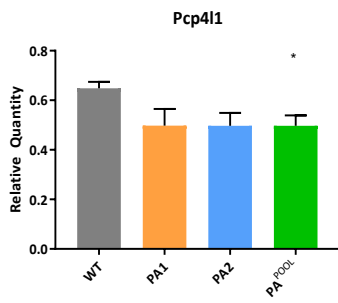
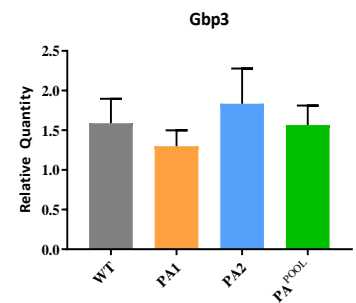
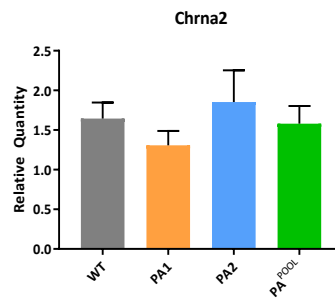
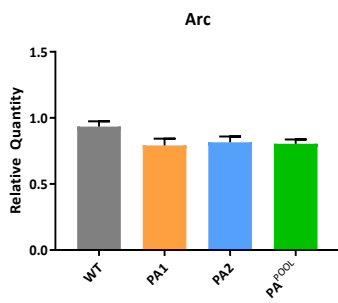


Figure 1: Biological validation of genes deregulated by disease in PA mutant mice by quantitative PCR (qPCR) analysis. Samples tested were RNA samples prepared from the cortex of vehicle-treated mice at postnatal day 10 across each genotype (WT; $n = 6$; PA1; $n = 4$; PA2; $n = 4$; PA^{pool}; $n = 4$ PA1 + 4 PA2 samples combined). Expression values were normalised to the reference gene, *β -Actin*. (A) Genes of mostly higher counts per million from our RNAseq data, where qPCR results agreed with RNAseq results. (B) Control genes that were non-significant in both RNAseq and qPCR analysis. (C) Genes where the breadth of signal was variable across the three genotype groups between the RNAseq and qPCR analysis. Summary tables show results of these genes in RNAseq and qPCR data, with final column showing whether the qPCR results agreed with the RNAseq data. Grayscale colours in significance tables represent significance of result (lightest grey $p < 0.05$, medium grey $p < 0.005$ and darkest grey $p < 0.0001$). Individual graphs show relative quantity for each gene for WT (grey), PA1 (orange), PA2 (blue) and PA^{pool} (green). * $p < 0.05$, ** $p < 0.005$, *** $p < 0.0001$ (one-tailed t-test of PA1, PA2 or PA^{pool} compared to WT).

Appendix 6

Autism and intellectual disability genes

<i>A2M</i>	<i>ADCY1</i>	<i>ALOXE3</i>	<i>ARID2</i>	<i>ATP6V0C</i>	<i>BMPER</i>
<i>A2ML1</i>	<i>ADD3</i>	<i>ALPL</i>	<i>ARID4A</i>	<i>ATP6V1B2</i>	<i>BOD1</i>
<i>AASS</i>	<i>ADNP</i>	<i>ALX1</i>	<i>ARL13B</i>	<i>ATP7A</i>	<i>BOLA3</i>
<i>ABAT</i>	<i>ADRA2B</i>	<i>ALX4</i>	<i>ARL14EP</i>	<i>ATP7B</i>	<i>BRAF</i>
<i>ABCA1</i>	<i>AFF3</i>	<i>AMACR</i>	<i>ARL2BP</i>	<i>ATP8A2</i>	<i>BRCC3</i>
<i>ABCA2</i>	<i>AFG3L2</i>	<i>AMMECR1</i>	<i>ARL6</i>	<i>ATR</i>	<i>BRD4</i>
<i>ABCA7</i>	<i>AGA</i>	<i>AMPD1</i>	<i>ARL6IP6</i>	<i>ATRIP</i>	<i>BRSK2</i>
<i>ABCB6</i>	<i>AGGF1</i>	<i>AMPD2</i>	<i>ARNT2</i>	<i>ATXN10</i>	<i>BRWD3</i>
<i>ABCB7</i>	<i>AGL</i>	<i>ANK3</i>	<i>ARSA</i>	<i>AUH</i>	<i>BSCL2</i>
<i>ABCC12</i>	<i>AGPAT2</i>	<i>ANKH</i>	<i>ARSF</i>	<i>AUTS2</i>	<i>BSN</i>
<i>ABCC8</i>	<i>AGTR2</i>	<i>ANKLE2</i>	<i>ARSH</i>	<i>AVPR2</i>	<i>BTK</i>
<i>ABCD3</i>	<i>AHCY</i>	<i>ANKS1A</i>	<i>ARV1</i>	<i>B3GALNT2</i>	<i>BTRC</i>
<i>ABCD4</i>	<i>AHDC1</i>	<i>ANKS3</i>	<i>ARVCF</i>	<i>B3GALT6</i>	<i>BUB1B</i>
<i>ABHD12</i>	<i>AHI1</i>	<i>ANO10</i>	<i>ARX</i>	<i>B3GAT3</i>	<i>C10orf2</i>
<i>ACADM</i>	<i>AHNAK</i>	<i>ANO3</i>	<i>ASAH1</i>	<i>B4GALNT1</i>	<i>C12orf4</i>
<i>ACADS</i>	<i>AHNAK2</i>	<i>ANTXR1</i>	<i>ASB1</i>	<i>B4GALT1</i>	<i>C12orf65</i>
<i>ACAT1</i>	<i>AHRR</i>	<i>AP1S1</i>	<i>ASCC3</i>	<i>B4GALT7</i>	<i>C2CD3</i>
<i>ACAT2</i>	<i>AIFM1</i>	<i>AP1S2</i>	<i>ASCL1</i>	<i>B4GAT1</i>	<i>C2orf71</i>
<i>ACBD6</i>	<i>AKAP13</i>	<i>AP3B1</i>	<i>ASH1L</i>	<i>B9D1</i>	<i>C5orf42</i>
<i>ACMSD</i>	<i>AKAP9</i>	<i>AP3D1</i>	<i>ASL</i>	<i>BAZ1B</i>	<i>C8orf37</i>
<i>ACO2</i>	<i>AKT2</i>	<i>AP4B1</i>	<i>ASMT</i>	<i>BBIP1</i>	<i>CA2</i>
<i>ACOT7</i>	<i>AKT3</i>	<i>AP4E1</i>	<i>ASNS</i>	<i>BBOX1</i>	<i>CA8</i>
<i>ACOX1</i>	<i>ALAD</i>	<i>AP4M1</i>	<i>ASPA</i>	<i>BBS1</i>	<i>CABIN1</i>
<i>ACSF3</i>	<i>ALAS2</i>	<i>APBA2</i>	<i>ASPH</i>	<i>BBS12</i>	<i>CABP2</i>
<i>ACSL4</i>	<i>ALDH18A1</i>	<i>APC2</i>	<i>ASPM</i>	<i>BBS2</i>	<i>CACHD1</i>
<i>ACTA1</i>	<i>ALDH3A2</i>	<i>APOL2</i>	<i>ASS1</i>	<i>BBS7</i>	<i>CACNA1D</i>
<i>ACTB</i>	<i>ALDH6A1</i>	<i>APOL4</i>	<i>ASTN2</i>	<i>BCKDK</i>	<i>CACNA1E</i>
<i>ACTG1</i>	<i>ALDH7A1</i>	<i>APTX</i>	<i>ASXL2</i>	<i>BCL10</i>	<i>CACNA1G</i>
<i>ACTN1</i>	<i>ALDOA</i>	<i>AQP2</i>	<i>ASXL3</i>	<i>BCL11A</i>	<i>CACNA1H</i>
<i>ACVRL1</i>	<i>ALDOB</i>	<i>ARFGEF2</i>	<i>ATG5</i>	<i>BCOR</i>	<i>CACNA2D1</i>
<i>ADAM9</i>	<i>ALG1</i>	<i>ARHGAP31</i>	<i>ATP10A</i>	<i>BCORL1</i>	<i>CACNA2D4</i>
<i>ADAMTS1</i>	<i>ALG11</i>	<i>ARHGAP4</i>	<i>ATP13A2</i>	<i>BCS1L</i>	<i>CACNG2</i>
<i>ADAMTS10</i>	<i>ALG13</i>	<i>ARHGDIA</i>	<i>ATP1A3</i>	<i>BDNF</i>	<i>CADM1</i>
<i>ADAMTS17</i>	<i>ALG2</i>	<i>ARHGEF15</i>	<i>ATP1B4</i>	<i>BIN1</i>	<i>CADPS2</i>
<i>ADAMTS2</i>	<i>ALG3</i>	<i>ARHGEF4</i>	<i>ATP2B3</i>	<i>BLNK</i>	<i>CALM1</i>
<i>ADAR</i>	<i>ALG6</i>	<i>ARHGEF9</i>	<i>ATP2B4</i>	<i>BMP1</i>	<i>CALM2</i>
<i>ADCK3</i>	<i>ALG8</i>	<i>ARID1A</i>	<i>ATP5A1</i>	<i>BMP2</i>	<i>CALM3</i>
<i>ADCK4</i>	<i>ALG9</i>	<i>ARID1B</i>	<i>ATP6V0A2</i>	<i>BMP3</i>	<i>CAMK2B</i>

<i>CAMK2G</i>	<i>CHAMP1</i>	<i>CLPB</i>	<i>COX10</i>	<i>DAG1</i>	<i>DLX3</i>
<i>CAMTA1</i>	<i>CHAT</i>	<i>CLPP</i>	<i>COX15</i>	<i>DAOA</i>	<i>DLX6</i>
<i>CANT1</i>	<i>CHD1</i>	<i>CLRN1</i>	<i>COX4I2</i>	<i>DARS</i>	<i>DMBX1</i>
<i>CAPN10</i>	<i>CHD1L</i>	<i>CLTC</i>	<i>COX7B</i>	<i>DARS2</i>	<i>DMXL1</i>
<i>CARD9</i>	<i>CHD2</i>	<i>CLTCL1</i>	<i>COX8A</i>	<i>DBH</i>	<i>DNA2</i>
<i>CARS2</i>	<i>CHD4</i>	<i>CMIP</i>	<i>CPQ</i>	<i>DBX2</i>	<i>DNAH10</i>
<i>CBL</i>	<i>CHD6</i>	<i>CNGA1</i>	<i>CPS1</i>	<i>DCHS1</i>	<i>DNAH11</i>
<i>CBS</i>	<i>CHD7</i>	<i>CNGA3</i>	<i>CPT1A</i>	<i>DCX</i>	<i>DNAJC12</i>
<i>CC2D2A</i>	<i>CHD8</i>	<i>CNKS2R2</i>	<i>CPT1B</i>	<i>DDB2</i>	<i>DNAJC19</i>
<i>CCAR2</i>	<i>CHI3L1</i>	<i>CNNM2</i>	<i>CPZ</i>	<i>DDC</i>	<i>DNAJC3</i>
<i>CCDC22</i>	<i>CHMP1A</i>	<i>CNOT3</i>	<i>CREB3L1</i>	<i>DDHD2</i>	<i>DNAJC5</i>
<i>CCDC88A</i>	<i>CHRNA1</i>	<i>CNTN2</i>	<i>CREBBP</i>	<i>DDOST</i>	<i>DNAJC6</i>
<i>CCM2</i>	<i>CHRNA2</i>	<i>CNTN3</i>	<i>CRIP1</i>	<i>DDR2</i>	<i>DNASE1L3</i>
<i>CCR1</i>	<i>CHRNA7</i>	<i>CNTN4</i>	<i>CRKL</i>	<i>DDX11</i>	<i>DNM1</i>
<i>CD96</i>	<i>CHRN2</i>	<i>CNTN6</i>	<i>CSNK2B</i>	<i>DDX24</i>	<i>DNM1L</i>
<i>CDC42BPB</i>	<i>CHRND</i>	<i>CNTNAP1</i>	<i>CSPP1</i>	<i>DDX3X</i>	<i>DNM2</i>
<i>CDC6</i>	<i>CHRNA1</i>	<i>CNTNAP3</i>	<i>CTBP1</i>	<i>DDX53</i>	<i>DNMT3A</i>
<i>CDH11</i>	<i>CHST14</i>	<i>COA3</i>	<i>CTC1</i>	<i>DDX59</i>	<i>DNMT3B</i>
<i>CDH15</i>	<i>CHST3</i>	<i>COASY</i>	<i>CTCF</i>	<i>DEAF1</i>	<i>DOCK6</i>
<i>CDH3</i>	<i>CIAO1</i>	<i>COCH</i>	<i>CTDP1</i>	<i>DENND5A</i>	<i>DOCK7</i>
<i>CDH8</i>	<i>CIB2</i>	<i>COG1</i>	<i>CTNNA1</i>	<i>DENR</i>	<i>DOLK</i>
<i>CDK5R1</i>	<i>CIC</i>	<i>COG2</i>	<i>CTNND2</i>	<i>DEPDC5</i>	<i>DPAGT1</i>
<i>CDK6</i>	<i>CIT</i>	<i>COG4</i>	<i>CTSA</i>	<i>DGCR2</i>	<i>DPH1</i>
<i>CDKL5</i>	<i>CKAP2L</i>	<i>COG6</i>	<i>CTSD</i>	<i>DGCR6</i>	<i>DPM1</i>
<i>CEACAM16</i>	<i>CLASP2</i>	<i>COG8</i>	<i>CTSF</i>	<i>DGKD</i>	<i>DPM2</i>
<i>CECR1</i>	<i>CLCN4</i>	<i>COL18A1</i>	<i>CTSH</i>	<i>DGUOK</i>	<i>DPM3</i>
<i>CELSR2</i>	<i>CLCN7</i>	<i>COL1A1</i>	<i>CUL3</i>	<i>DHCR24</i>	<i>DPP6</i>
<i>CELSR3</i>	<i>CLCNKA</i>	<i>COL25A1</i>	<i>CUL4B</i>	<i>DHCR7</i>	<i>DPYD</i>
<i>CENPE</i>	<i>CLCNKB</i>	<i>COL4A1</i>	<i>CUL5</i>	<i>DHFR</i>	<i>DRAM2</i>
<i>CENPJ</i>	<i>CLDN14</i>	<i>COL4A3BP</i>	<i>CUX2</i>	<i>DHTKD1</i>	<i>DRD2</i>
<i>CEP104</i>	<i>CLDN16</i>	<i>COL5A2</i>	<i>CWF19L1</i>	<i>DIAPH1</i>	<i>DRD3</i>
<i>CEP120</i>	<i>CLEC7A</i>	<i>COLEC10</i>	<i>CXCR4</i>	<i>DISC1</i>	<i>DRP2</i>
<i>CEP152</i>	<i>CLIC2</i>	<i>COLEC11</i>	<i>CYB5R3</i>	<i>DISP1</i>	<i>DSE</i>
<i>CEP164</i>	<i>CLIC5</i>	<i>COQ4</i>	<i>CYC1</i>	<i>DLAT</i>	<i>DTNB</i>
<i>CEP19</i>	<i>CLIP2</i>	<i>COQ5</i>	<i>CYFIP1</i>	<i>DLD</i>	<i>DTNBP1</i>
<i>CEP290</i>	<i>CLMP</i>	<i>COQ6</i>	<i>CYP27B1</i>	<i>DLG1</i>	<i>DUOX2</i>
<i>CEP83</i>	<i>CLN5</i>	<i>COQ7</i>	<i>CYP2C9</i>	<i>DLG3</i>	<i>DUOXA2</i>
<i>CEP89</i>	<i>CLN6</i>	<i>COQ9</i>	<i>CYP2U1</i>	<i>DLG4</i>	<i>DVL1</i>
<i>CERS3</i>	<i>CLN8</i>	<i>CORIN</i>	<i>D2HGDH</i>	<i>DLL1</i>	<i>DYM</i>

<i>DYNC1H1</i>	<i>EPG5</i>	<i>FASN</i>	<i>FRMD4A</i>	<i>GEMIN4</i>	<i>GRIN1</i>
<i>DYNC2LI1</i>	<i>EPHA3</i>	<i>FASTKD2</i>	<i>FRMPD4</i>	<i>GFAP</i>	<i>GRIN2A</i>
<i>DYRK1A</i>	<i>EPHA4</i>	<i>FAT4</i>	<i>FRY</i>	<i>GFM2</i>	<i>GRIN2B</i>
<i>EBF3</i>	<i>EPHA5</i>	<i>FBXL4</i>	<i>FTL</i>	<i>GFPT1</i>	<i>GRIP1</i>
<i>ECE1</i>	<i>EPHA7</i>	<i>FBXO18</i>	<i>FXVD2</i>	<i>GJA1</i>	<i>GRM1</i>
<i>ECHS1</i>	<i>ERAP1</i>	<i>FBXO28</i>	<i>G6PC3</i>	<i>GJB1</i>	<i>GRM5</i>
<i>EDA2R</i>	<i>ERC1</i>	<i>FBXO31</i>	<i>GAA</i>	<i>GJC2</i>	<i>GRM7</i>
<i>EDC3</i>	<i>ERCC1</i>	<i>FEZF1</i>	<i>GABBR2</i>	<i>GK</i>	<i>GRM8</i>
<i>EDN1</i>	<i>ERCC5</i>	<i>FEZF2</i>	<i>GABRA1</i>	<i>GLA</i>	<i>GRN</i>
<i>EED</i>	<i>ERCC8</i>	<i>FGF12</i>	<i>GABRA3</i>	<i>GLRB</i>	<i>GRXCRI</i>
<i>EEF1A2</i>	<i>ERF</i>	<i>FGF17</i>	<i>GABRA5</i>	<i>GLUL</i>	<i>GRXCR2</i>
<i>EEF1B2</i>	<i>ERLIN2</i>	<i>FGF23</i>	<i>GABRA6</i>	<i>GM2A</i>	<i>GSPT2</i>
<i>EFCAB5</i>	<i>ERMARD</i>	<i>FGF3</i>	<i>GABRG2</i>	<i>GMNN</i>	<i>GSS</i>
<i>EFHC1</i>	<i>ESCO2</i>	<i>FGF8</i>	<i>GABRG3</i>	<i>GMPPA</i>	<i>GTF2H5</i>
<i>EFHC2</i>	<i>ETFA</i>	<i>FGFR1</i>	<i>GABRQ</i>	<i>GMPPB</i>	<i>GTPBP3</i>
<i>EFNB1</i>	<i>ETFB</i>	<i>FGFR3</i>	<i>GABRR1</i>	<i>GNA11</i>	<i>GUCA1A</i>
<i>EFR3A</i>	<i>ETFDH</i>	<i>FGFRL1</i>	<i>GABRR3</i>	<i>GNAI3</i>	<i>GUCA1B</i>
<i>EFTUD2</i>	<i>ETHE1</i>	<i>FH</i>	<i>GAL</i>	<i>GNAL</i>	<i>GUCY1A3</i>
<i>EGF</i>	<i>EVC</i>	<i>FHL1</i>	<i>GALE</i>	<i>GNAO1</i>	<i>GUSB</i>
<i>EIF2AK3</i>	<i>EXOSC2</i>	<i>FIBP</i>	<i>GALNT9</i>	<i>GNAQ</i>	<i>GYG2</i>
<i>EIF2B1</i>	<i>EXOSC3</i>	<i>FIG4</i>	<i>GALNTL5</i>	<i>GNAS</i>	<i>GYS1</i>
<i>EIF2B2</i>	<i>EXT2</i>	<i>FKBP14</i>	<i>GAMT</i>	<i>GNE</i>	<i>GYS2</i>
<i>EIF2B3</i>	<i>EZR</i>	<i>FKRP</i>	<i>GAN</i>	<i>GNPTG</i>	<i>H3F3B</i>
<i>EIF2B4</i>	<i>FAAH2</i>	<i>FKTN</i>	<i>GAP43</i>	<i>GNRH1</i>	<i>HACE1</i>
<i>EIF2B5</i>	<i>FADD</i>	<i>FLI1</i>	<i>GARS</i>	<i>GNRHR</i>	<i>HADH</i>
<i>EIF4A3</i>	<i>FAM111A</i>	<i>FLNA</i>	<i>GAS1</i>	<i>GNS</i>	<i>HAP1</i>
<i>EIF4ENIF1</i>	<i>FAM120A</i>	<i>FLRT3</i>	<i>GATA1</i>	<i>GORAB</i>	<i>HAX1</i>
<i>ELAC2</i>	<i>FAM126A</i>	<i>FLVCR1</i>	<i>GATA6</i>	<i>GOSR2</i>	<i>HCFC1</i>
<i>ELMOD3</i>	<i>FAM134B</i>	<i>FLVCR2</i>	<i>GATM</i>	<i>GP1BB</i>	<i>HCN1</i>
<i>ELN</i>	<i>FAM177A1</i>	<i>FMN1</i>	<i>GBA</i>	<i>GPD2</i>	<i>HDAC8</i>
<i>ELP4</i>	<i>FAM20C</i>	<i>FMN2</i>	<i>GBE1</i>	<i>GPHN</i>	<i>HDX</i>
<i>EMC1</i>	<i>FAM58A</i>	<i>FOS</i>	<i>GCH1</i>	<i>GPI</i>	<i>HECW2</i>
<i>EML1</i>	<i>FANCC</i>	<i>FOXO1</i>	<i>GCM2</i>	<i>GPR37</i>	<i>HELLS</i>
<i>EMX2</i>	<i>FANCE</i>	<i>FOXG1</i>	<i>GCNT2</i>	<i>GPR88</i>	<i>HEPACAM</i>
<i>ENG</i>	<i>FANCF</i>	<i>FOXH1</i>	<i>GCSH</i>	<i>GPSM2</i>	<i>HERC2</i>
<i>ENPP1</i>	<i>FANCI</i>	<i>FOXRED1</i>	<i>GDF2</i>	<i>GRIA1</i>	<i>HES7</i>
<i>EP300</i>	<i>FAR1</i>	<i>FRAS1</i>	<i>GDF5</i>	<i>GRIA3</i>	<i>HESX1</i>
<i>EPC2</i>	<i>FARS2</i>	<i>FREM2</i>	<i>GDI1</i>	<i>GRID2</i>	<i>HGSNAT</i>
<i>EPCAM</i>	<i>FAS</i>	<i>FRG1</i>	<i>GDNF</i>	<i>GRIK2</i>	<i>HIBCH</i>

<i>HIC1</i>	<i>IFT140</i>	<i>KCNA1</i>	<i>KIF4A</i>	<i>LRP2</i>	<i>MDN1</i>
<i>HIRA</i>	<i>IFT172</i>	<i>KCNAB1</i>	<i>KIF5C</i>	<i>LRRC4</i>	<i>ME2</i>
<i>HIST1H1E</i>	<i>IFT43</i>	<i>KCNAB2</i>	<i>KISS1</i>	<i>LTBP1</i>	<i>MECP2</i>
<i>HIST3H3</i>	<i>IGF1</i>	<i>KCNC1</i>	<i>KIZ</i>	<i>LTBP4</i>	<i>MED12</i>
<i>HIVEP2</i>	<i>IGF1R</i>	<i>KCNC3</i>	<i>KLC2</i>	<i>LYRM4</i>	<i>MED13</i>
<i>HLCS</i>	<i>IKBKAP</i>	<i>KCND2</i>	<i>KLHL15</i>	<i>LYRM7</i>	<i>MED13L</i>
<i>HMBS</i>	<i>IL12A</i>	<i>KCND3</i>	<i>KLHL41</i>	<i>LZTFL1</i>	<i>MED17</i>
<i>HMGA2</i>	<i>IL17F</i>	<i>KCNH7</i>	<i>KLHL7</i>	<i>MAB21L2</i>	<i>MED23</i>
<i>HMGB1</i>	<i>IL17RA</i>	<i>KCNJ1</i>	<i>KLRC4</i>	<i>MACF1</i>	<i>MED25</i>
<i>HMGB3</i>	<i>IL17RC</i>	<i>KCNJ10</i>	<i>KMT2C</i>	<i>MAFB</i>	<i>MEF2C</i>
<i>HMGCCL</i>	<i>IL17RD</i>	<i>KCNJ13</i>	<i>KMT2E</i>	<i>MAG</i>	<i>MEFV</i>
<i>HMGCSS2</i>	<i>IL1RAPL1</i>	<i>KCNJ2</i>	<i>KPNA7</i>	<i>MAG11</i>	<i>MEGF10</i>
<i>HNMT</i>	<i>IL23R</i>	<i>KCNJ6</i>	<i>KRT25</i>	<i>MAGT1</i>	<i>MEIS2</i>
<i>HNRNPH2</i>	<i>IL27RA</i>	<i>KCNJ8</i>	<i>KRT83</i>	<i>MAK</i>	<i>MET</i>
<i>HNRNPK</i>	<i>IMPA1</i>	<i>KCNMA1</i>	<i>KSR2</i>	<i>MAN1B1</i>	<i>METTL23</i>
<i>HNRNPL</i>	<i>IMPAD1</i>	<i>KCNN3</i>	<i>L2HGDH</i>	<i>MAN2B1</i>	<i>MFAP5</i>
<i>HNRNPU</i>	<i>IMPDH2</i>	<i>KCNQ3</i>	<i>LAMA1</i>	<i>MAOA</i>	<i>MFF</i>
<i>HOXA1</i>	<i>INPP5E</i>	<i>KCNT1</i>	<i>LAMA2</i>	<i>MAP2K1</i>	<i>MFN2</i>
<i>HOXA2</i>	<i>INS</i>	<i>KCNV2</i>	<i>LAMB1</i>	<i>MAP2K2</i>	<i>MFSD2A</i>
<i>HOXB1</i>	<i>INSR</i>	<i>KCTD13</i>	<i>LAMC3</i>	<i>MAPK1</i>	<i>MFSD8</i>
<i>HPCA</i>	<i>INVS</i>	<i>KCTD3</i>	<i>LAMP2</i>	<i>MAPK10</i>	<i>MGAT2</i>
<i>HPRT1</i>	<i>IQGAP3</i>	<i>KDM1A</i>	<i>LARP7</i>	<i>MAPRE2</i>	<i>MGAT4C</i>
<i>HPS3</i>	<i>IQSEC2</i>	<i>KDM2B</i>	<i>LBR</i>	<i>MAPT</i>	<i>MGME1</i>
<i>HRAS</i>	<i>IRX5</i>	<i>KDM5A</i>	<i>LDHB</i>	<i>MARVELD2</i>	<i>MGP</i>
<i>HSD17B10</i>	<i>ISCA2</i>	<i>KDM5B</i>	<i>LEP</i>	<i>MASP1</i>	<i>MIB1</i>
<i>HSD17B4</i>	<i>ISCU</i>	<i>KDM5C</i>	<i>LFNG</i>	<i>MATN4</i>	<i>MID2</i>
<i>HSPD1</i>	<i>ISPD</i>	<i>KDM6A</i>	<i>LHX1</i>	<i>MBD1</i>	<i>MKKS</i>
<i>HSPG2</i>	<i>ITGA3</i>	<i>KDM6B</i>	<i>LIMK1</i>	<i>MBD4</i>	<i>MKRN3</i>
<i>HTR1A</i>	<i>ITGA7</i>	<i>KIAA0196</i>	<i>LIN7A</i>	<i>MBD5</i>	<i>MLC1</i>
<i>HTR2A</i>	<i>ITGA9</i>	<i>KIAA0556</i>	<i>LIN7B</i>	<i>MBOAT7</i>	<i>MLX</i>
<i>HTR3A</i>	<i>ITGB6</i>	<i>KIAA0586</i>	<i>LINGO1</i>	<i>MBTPS2</i>	<i>MLXIPL</i>
<i>HUWE1</i>	<i>ITK</i>	<i>KIAA1033</i>	<i>LINS</i>	<i>MC2R</i>	<i>MMAA</i>
<i>HYLS1</i>	<i>ITSN1</i>	<i>KIAA1210</i>	<i>LIPT1</i>	<i>MCCC1</i>	<i>MMAB</i>
<i>IARS</i>	<i>IVD</i>	<i>KIAA1279</i>	<i>LMAN2L</i>	<i>MCEE</i>	<i>MMADHC</i>
<i>IBA57</i>	<i>IYD</i>	<i>KIF14</i>	<i>LMBR1</i>	<i>MCM3AP</i>	<i>MMP13</i>
<i>IDH2</i>	<i>JRK</i>	<i>KIF17</i>	<i>LMBRD1</i>	<i>MCM4</i>	<i>MMP19</i>
<i>IDS</i>	<i>KANK1</i>	<i>KIF1A</i>	<i>LMNB2</i>	<i>MCOLN1</i>	<i>MNX1</i>
<i>IER3IP1</i>	<i>KAT6B</i>	<i>KIF22</i>	<i>LONP1</i>	<i>MCTP2</i>	<i>MOCS1</i>
<i>IFIH1</i>	<i>KATNB1</i>	<i>KIF2A</i>	<i>LRFN2</i>	<i>MDH2</i>	<i>MOGS</i>

<i>MORC2</i>	<i>NAV1</i>	<i>NKAIN2</i>	<i>OGDH</i>	<i>PDE10A</i>	<i>PIGS</i>
<i>MPC1</i>	<i>NAV2</i>	<i>NKX2-1</i>	<i>OMG</i>	<i>PDE4D</i>	<i>PIGT</i>
<i>MPDU1</i>	<i>NBN</i>	<i>NKX2-5</i>	<i>OPA1</i>	<i>PDE6D</i>	<i>PIGV</i>
<i>MPLKIP</i>	<i>NCS1</i>	<i>NLGN2</i>	<i>OPA3</i>	<i>PDE6G</i>	<i>PIK3API</i>
<i>MPP7</i>	<i>NDN</i>	<i>NLGN3</i>	<i>OPHN1</i>	<i>PDGFB</i>	<i>PIK3R2</i>
<i>MPV17</i>	<i>NDP</i>	<i>NLGN4Y</i>	<i>OPRL1</i>	<i>PDGFRB</i>	<i>PIK3R5</i>
<i>MRAP</i>	<i>NDUFA1</i>	<i>NLRP3</i>	<i>ORC1</i>	<i>PDHA1</i>	<i>PITRM1</i>
<i>MRPL10</i>	<i>NDUFA2</i>	<i>NME8</i>	<i>ORC4</i>	<i>PDHX</i>	<i>PLA2G6</i>
<i>MRPL3</i>	<i>NDUFA4</i>	<i>NMNAT1</i>	<i>ORC6</i>	<i>PDP1</i>	<i>PLAGL1</i>
<i>MRPS22</i>	<i>NDUFA9</i>	<i>NODAL</i>	<i>OSBPL2</i>	<i>PDSS1</i>	<i>PLAT</i>
<i>MSL3</i>	<i>NDUFAF1</i>	<i>NOL3</i>	<i>OTOGL</i>	<i>PDSS2</i>	<i>PLCB1</i>
<i>MSRB3</i>	<i>NDUFAF2</i>	<i>NONO</i>	<i>OTUD4</i>	<i>PECR</i>	<i>PLEKHG2</i>
<i>MSX2</i>	<i>NDUFAF3</i>	<i>NOP10</i>	<i>OXTR</i>	<i>PEPD</i>	<i>PLP1</i>
<i>MTFMT</i>	<i>NDUFAF4</i>	<i>NOS1AP</i>	<i>P4HB</i>	<i>PET100</i>	<i>PLXNB3</i>
<i>MTHFS</i>	<i>NDUFAF5</i>	<i>NPAP1</i>	<i>PABPC4L</i>	<i>PEX12</i>	<i>PLXND1</i>
<i>MTMR2</i>	<i>NDUFAF6</i>	<i>NPAS4</i>	<i>PAFAH1B1</i>	<i>PEX13</i>	<i>PMPCA</i>
<i>MTOR</i>	<i>NDUFS1</i>	<i>NPC2</i>	<i>PAFAH1B3</i>	<i>PEX14</i>	<i>PNKD</i>
<i>MTPAP</i>	<i>NDUFS2</i>	<i>NPEPPS</i>	<i>PAH</i>	<i>PEX16</i>	<i>PNKP</i>
<i>MTR</i>	<i>NDUFS4</i>	<i>NPHP1</i>	<i>PAM16</i>	<i>PEX19</i>	<i>PNP</i>
<i>MTRR</i>	<i>NDUFS6</i>	<i>NPHP3</i>	<i>PANK2</i>	<i>PEX2</i>	<i>PNPLA6</i>
<i>MTSSL</i>	<i>NDUFV1</i>	<i>NPHP4</i>	<i>PANX1</i>	<i>PEX26</i>	<i>PNPO</i>
<i>MVK</i>	<i>NDUFV2</i>	<i>NPRL2</i>	<i>PARK2</i>	<i>PEX5</i>	<i>PNPT1</i>
<i>MXRA5</i>	<i>NEDD4L</i>	<i>NR2F1</i>	<i>PARN</i>	<i>PEX6</i>	<i>POC1A</i>
<i>MXRA8</i>	<i>NELFA</i>	<i>NR4A2</i>	<i>PARS2</i>	<i>PFKFB1</i>	<i>POC1B</i>
<i>MYCN</i>	<i>NEU1</i>	<i>NRGN</i>	<i>PAX1</i>	<i>PGAP3</i>	<i>PODXL</i>
<i>MYEF2</i>	<i>NEUROD2</i>	<i>NRXN1</i>	<i>PAX2</i>	<i>PGK1</i>	<i>POGZ</i>
<i>MYO18B</i>	<i>NF1</i>	<i>NSD1</i>	<i>PAX5</i>	<i>PGM1</i>	<i>POLA1</i>
<i>MYO5A</i>	<i>NFASC</i>	<i>NSDHL</i>	<i>PAX8</i>	<i>PHC1</i>	<i>POLG</i>
<i>MYO7B</i>	<i>NFAT5</i>	<i>NSUN7</i>	<i>PBX1</i>	<i>PHF21A</i>	<i>POLR1C</i>
<i>MYOCD</i>	<i>NFIA</i>	<i>NTRK1</i>	<i>PCCA</i>	<i>PHF3</i>	<i>POMGNT1</i>
<i>MYOF</i>	<i>NFIB</i>	<i>NTRK2</i>	<i>PCCB</i>	<i>PHGDH</i>	<i>POMK</i>
<i>NAA15</i>	<i>NFIX</i>	<i>NUP107</i>	<i>PCDH11X</i>	<i>PHKA2</i>	<i>POMT1</i>
<i>NACC1</i>	<i>NGLY1</i>	<i>NUP62</i>	<i>PCDH19</i>	<i>PHKG2</i>	<i>POP1</i>
<i>NAGA</i>	<i>NHS</i>	<i>NXF5</i>	<i>PCDH7</i>	<i>PHYH</i>	<i>POR</i>
<i>NAGLU</i>	<i>NID1</i>	<i>NXPH3</i>	<i>PCDHB4</i>	<i>PIEZO2</i>	<i>POU3F2</i>
<i>NAGPA</i>	<i>NIN</i>	<i>OBSCN</i>	<i>PCLO</i>	<i>PIGA</i>	<i>POU4F3</i>
<i>NAGS</i>	<i>NIPA1</i>	<i>OCLN</i>	<i>PCM1</i>	<i>PIGG</i>	<i>PPARG</i>
<i>NALCN</i>	<i>NIPA2</i>	<i>OCRL</i>	<i>PCNT</i>	<i>PIGL</i>	<i>PPARGC1A</i>
<i>NAT8L</i>	<i>NIPBL</i>	<i>OFD1</i>	<i>PCSK1</i>	<i>PIGN</i>	<i>PPIB</i>

<i>PPM1B</i>	<i>PTPRK</i>	<i>RIMS1</i>	<i>SCN1B</i>	<i>SLC16A3</i>	<i>SMARCAL1</i>
<i>PPM1D</i>	<i>PTS</i>	<i>RIPK4</i>	<i>SCN3A</i>	<i>SLC17A3</i>	<i>SMARCE1</i>
<i>PPM1K</i>	<i>PUF60</i>	<i>RIPPLY2</i>	<i>SCN3B</i>	<i>SLC17A5</i>	<i>SMC1A</i>
<i>PPOX</i>	<i>PUS3</i>	<i>RIT1</i>	<i>SCN4B</i>	<i>SLC17A9</i>	<i>SMC3</i>
<i>PPP1CB</i>	<i>PYCR2</i>	<i>RMND1</i>	<i>SCO1</i>	<i>SLC18A2</i>	<i>SMCHD1</i>
<i>PPP1R15B</i>	<i>QDPR</i>	<i>RNASEH2C</i>	<i>SCO2</i>	<i>SLC1A3</i>	<i>SMO</i>
<i>PPP2R1A</i>	<i>QRICH1</i>	<i>RNASET2</i>	<i>SCP2</i>	<i>SLC1A4</i>	<i>SMOC1</i>
<i>PPP2R2C</i>	<i>RAB11B</i>	<i>RNF113A</i>	<i>SCRIB</i>	<i>SLC20A2</i>	<i>SMPD1</i>
<i>PPP2R5D</i>	<i>RAB11FIP5</i>	<i>RNF135</i>	<i>SCUBE2</i>	<i>SLC22A25</i>	<i>SMS</i>
<i>PRCD</i>	<i>RAB18</i>	<i>RNF216</i>	<i>SCYL1</i>	<i>SLC25A15</i>	<i>SNAP29</i>
<i>PREPL</i>	<i>RAB23</i>	<i>ROBO2</i>	<i>SDHAF1</i>	<i>SLC25A19</i>	<i>SNIP1</i>
<i>PRF1</i>	<i>RAB28</i>	<i>ROGDI</i>	<i>SEC23A</i>	<i>SLC25A3</i>	<i>SNRNP200</i>
<i>PRICKLE1</i>	<i>RAB39B</i>	<i>ROR2</i>	<i>SEC24C</i>	<i>SLC25A46</i>	<i>SNRNPB</i>
<i>PRIMA1</i>	<i>RAC1</i>	<i>RORA</i>	<i>SEMA3C</i>	<i>SLC26A1</i>	<i>SNRPN</i>
<i>PRKARIA</i>	<i>RAD50</i>	<i>ROS1</i>	<i>SEMA3D</i>	<i>SLC26A5</i>	<i>SNTG2</i>
<i>PRKCD</i>	<i>RAD51</i>	<i>RP2</i>	<i>SEMA4G</i>	<i>SLC2A1</i>	<i>SNX10</i>
<i>PRKDI</i>	<i>RALGDS</i>	<i>RPGRIP1L</i>	<i>SEMA5A</i>	<i>SLC2A10</i>	<i>SNX14</i>
<i>PRKDC</i>	<i>RAP1A</i>	<i>RPL10</i>	<i>SEMA6D</i>	<i>SLC2A3</i>	<i>SOBP</i>
<i>PRKRA</i>	<i>RARB</i>	<i>RPL11</i>	<i>SESN2</i>	<i>SLC33A1</i>	<i>SOGA3</i>
<i>PRMT9</i>	<i>RARS2</i>	<i>RPL15</i>	<i>SET</i>	<i>SLC35A1</i>	<i>SON</i>
<i>PRODH</i>	<i>RASA2</i>	<i>RPL26</i>	<i>SETBP1</i>	<i>SLC35A3</i>	<i>SOS1</i>
<i>PRODH2</i>	<i>RAX2</i>	<i>RPS28</i>	<i>SETD1A</i>	<i>SLC35C1</i>	<i>SOST</i>
<i>PROKR2</i>	<i>RBFOX1</i>	<i>RPS6KA3</i>	<i>SETD1B</i>	<i>SLC39A13</i>	<i>SOX10</i>
<i>PROP1</i>	<i>RBM10</i>	<i>RPS7</i>	<i>SETDB2</i>	<i>SLC39A5</i>	<i>SOX11</i>
<i>PROSC</i>	<i>RBPJ</i>	<i>RSPRY1</i>	<i>SGSH</i>	<i>SLC39A8</i>	<i>SOX2</i>
<i>PRPF31</i>	<i>RD3</i>	<i>RTEL1</i>	<i>SH2B1</i>	<i>SLC3A1</i>	<i>SOX3</i>
<i>PRPF8</i>	<i>RDH11</i>	<i>RTN4R</i>	<i>SH3PXD2B</i>	<i>SLC46A1</i>	<i>SOX5</i>
<i>PRSS12</i>	<i>RDX</i>	<i>RTTN</i>	<i>SHANK1</i>	<i>SLC5A5</i>	<i>SOX9</i>
<i>PRUNE</i>	<i>RECQL4</i>	<i>RUNX1T1</i>	<i>SHANK2</i>	<i>SLC5A7</i>	<i>SP7</i>
<i>PSAP</i>	<i>REEP1</i>	<i>SAG</i>	<i>SHANK3</i>	<i>SLC6A1</i>	<i>SPARC</i>
<i>PSPH</i>	<i>REEP6</i>	<i>SALL1</i>	<i>SHH</i>	<i>SLC6A13</i>	<i>SPAST</i>
<i>PTCHD1</i>	<i>RELN</i>	<i>SALL4</i>	<i>SHOX2</i>	<i>SLC6A8</i>	<i>SPATA7</i>
<i>PTDSS1</i>	<i>REPS2</i>	<i>SAR1B</i>	<i>SIM1</i>	<i>SLC9A1</i>	<i>SPECC1L</i>
<i>PTF1A</i>	<i>RERE</i>	<i>SARS2</i>	<i>SIPA1L1</i>	<i>SLC9A9</i>	<i>SPG11</i>
<i>PTH</i>	<i>REST</i>	<i>SATL1</i>	<i>SIX6</i>	<i>SLCO1C1</i>	<i>SPG20</i>
<i>PTH2R</i>	<i>REV3L</i>	<i>SC5D</i>	<i>SLC12A6</i>	<i>SLIT2</i>	<i>SPG7</i>
<i>PTPN11</i>	<i>RFT1</i>	<i>SCN10A</i>	<i>SLC13A5</i>	<i>SLX4</i>	<i>SPINK5</i>
<i>PTPN22</i>	<i>RFWD2</i>	<i>SCN11A</i>	<i>SLC16A1</i>	<i>SMARCA2</i>	<i>SPN</i>
<i>PTPN23</i>	<i>RILP</i>	<i>SCN1A</i>	<i>SLC16A2</i>	<i>SMARCA4</i>	<i>SPOCK1</i>

<i>SPP2</i>	<i>SYP</i>	<i>THRA</i>	<i>TPM2</i>	<i>TUBB</i>	<i>VPS13C</i>
<i>SPR</i>	<i>SYT1</i>	<i>THRB</i>	<i>TPM3</i>	<i>TUBB3</i>	<i>VPS33B</i>
<i>SPTBN2</i>	<i>SZT2</i>	<i>TINF2</i>	<i>TPP1</i>	<i>TUBB4A</i>	<i>VPS4A</i>
<i>SPTBN5</i>	<i>TAC3</i>	<i>TJP2</i>	<i>TPP2</i>	<i>TUBG1</i>	<i>VPS53</i>
<i>SRCAP</i>	<i>TAF2</i>	<i>TK2</i>	<i>TRAF3IP1</i>	<i>TUBGCP4</i>	<i>VRK1</i>
<i>SRD5A3</i>	<i>TAF6</i>	<i>TKT</i>	<i>TRAF3IP2</i>	<i>TUBGCP5</i>	<i>VSIG1</i>
<i>SRGAP3</i>	<i>TALDO1</i>	<i>TLK2</i>	<i>TRAF7</i>	<i>TUBGCP6</i>	<i>VSX2</i>
<i>SRPK2</i>	<i>TANC2</i>	<i>TLR4</i>	<i>TRAIP</i>	<i>TUFM</i>	<i>WAC</i>
<i>SRPX2</i>	<i>TANGO2</i>	<i>TM4SF20</i>	<i>TRAPPC11</i>	<i>TWIST1</i>	<i>WDFY3</i>
<i>SSTR5</i>	<i>TAOK2</i>	<i>TMEM107</i>	<i>TRAPPC9</i>	<i>TXN2</i>	<i>WDPCP</i>
<i>ST3GAL5</i>	<i>TAT</i>	<i>TMEM114</i>	<i>TREM2</i>	<i>TYMP</i>	<i>WDR13</i>
<i>ST7</i>	<i>TBC1D20</i>	<i>TMEM126A</i>	<i>TREX1</i>	<i>UBA1</i>	<i>WDR19</i>
<i>ST8SIA2</i>	<i>TBC1D23</i>	<i>TMEM126B</i>	<i>TRH</i>	<i>UBE2T</i>	<i>WDR26</i>
<i>STAG2</i>	<i>TBC1D24</i>	<i>TMEM135</i>	<i>TRHR</i>	<i>UBE3A</i>	<i>WDR34</i>
<i>STAT1</i>	<i>TBCK</i>	<i>TMEM216</i>	<i>TRIM8</i>	<i>UBE3B</i>	<i>WDR45</i>
<i>STAT2</i>	<i>TBR1</i>	<i>TMEM237</i>	<i>TRIP12</i>	<i>UBR3</i>	<i>WDR60</i>
<i>STIL</i>	<i>TBX1</i>	<i>TMEM240</i>	<i>TRIP4</i>	<i>UCP2</i>	<i>WDR62</i>
<i>STIM1</i>	<i>TBX19</i>	<i>TMEM38B</i>	<i>TRIT1</i>	<i>ULK4</i>	<i>WDR73</i>
<i>STOX1</i>	<i>TBX4</i>	<i>TMEM5</i>	<i>TRMT10A</i>	<i>UMPS</i>	<i>WFS1</i>
<i>STRA6</i>	<i>TCF12</i>	<i>TMEM67</i>	<i>TRMT5</i>	<i>UNC119</i>	<i>WHSC1</i>
<i>STRADA</i>	<i>TCF20</i>	<i>TMEM70</i>	<i>TRNT1</i>	<i>UNC13A</i>	<i>WNT1</i>
<i>STT3B</i>	<i>TCF3</i>	<i>TMEM92</i>	<i>TRPC5</i>	<i>UNC13B</i>	<i>WNT5A</i>
<i>STX16</i>	<i>TCF4</i>	<i>TMIE</i>	<i>TRPC6</i>	<i>UNC13D</i>	<i>WRAP53</i>
<i>STXBP1</i>	<i>TCN2</i>	<i>TMLHE</i>	<i>TRPM6</i>	<i>UQCRB</i>	<i>WVOX</i>
<i>STXBP2</i>	<i>TCTN1</i>	<i>TMPRSS6</i>	<i>TRPS1</i>	<i>UQCRQ</i>	<i>XK</i>
<i>STXBP5L</i>	<i>TDGF1</i>	<i>TNC</i>	<i>TSC1</i>	<i>UROC1</i>	<i>XPA</i>
<i>SUCLA2</i>	<i>TDP2</i>	<i>TNFRSF11A</i>	<i>TSC2</i>	<i>USB1</i>	<i>XPC</i>
<i>SUCO</i>	<i>TECPR2</i>	<i>TNFRSF11B</i>	<i>TSEN2</i>	<i>USP7</i>	<i>XPNPEP3</i>
<i>SUMF1</i>	<i>TECR</i>	<i>TNFRSF1A</i>	<i>TSEN34</i>	<i>USP9X</i>	<i>XPR1</i>
<i>SUPT16H</i>	<i>TECTA</i>	<i>TNFSF11</i>	<i>TSEN54</i>	<i>VAMP2</i>	<i>XRCC1</i>
<i>SURF1</i>	<i>TELO2</i>	<i>TNIK</i>	<i>TSHB</i>	<i>VARS2</i>	<i>XRCC4</i>
<i>SUV420H1</i>	<i>TENM1</i>	<i>TNNT1</i>	<i>TSPAN7</i>	<i>VAX1</i>	<i>XYLT2</i>
<i>SV2A</i>	<i>TEX15</i>	<i>TNS3</i>	<i>TTC19</i>	<i>VCP</i>	<i>YARS</i>
<i>SV2B</i>	<i>TFAP2B</i>	<i>TOE1</i>	<i>TTC21B</i>	<i>VCX3A</i>	<i>ZBTB18</i>
<i>SVIL</i>	<i>TFG</i>	<i>TONSL</i>	<i>TTL5</i>	<i>VDR</i>	<i>ZBTB20</i>
<i>SYN1</i>	<i>TGDS</i>	<i>TOP3B</i>	<i>TUB</i>	<i>VIPR2</i>	<i>ZBTB33</i>
<i>SYN2</i>	<i>TGFB1</i>	<i>TOR1AIP1</i>	<i>TUBA1A</i>	<i>VMA21</i>	<i>ZC3H14</i>
<i>SYNCRIP</i>	<i>TH</i>	<i>TP63</i>	<i>TUBA3E</i>	<i>VPS11</i>	<i>ZC4H2</i>
<i>SYNGAP1</i>	<i>THBS1</i>	<i>TPI1</i>	<i>TUBA8</i>	<i>VPS13A</i>	<i>ZCCHC12</i>

<i>ZCCHC8</i>	<i>ZFP57</i>	<i>ZIC2</i>	<i>ZNF365</i>	<i>ZNF41</i>	<i>ZNF71</i>
<i>ZDHHC15</i>	<i>ZFPM2</i>	<i>ZMYM2</i>	<i>ZNF385B</i>	<i>ZNF513</i>	
<i>ZEB1</i>	<i>ZFYVE26</i>	<i>ZNF277</i>	<i>ZNF407</i>	<i>ZNF526</i>	
<i>ZFHX4</i>	<i>ZIC1</i>	<i>ZNF292</i>	<i>ZNF408</i>	<i>ZNF592</i>	
<i>ZNF778</i>					
<i>ZNHIT3</i>					
<i>ZSCAN29</i>					
<i>ZSWIM6</i>					

Epilepsy gene list (in house)

<i>AAAS</i>	<i>ALPL</i>	<i>ATP6V0C</i>	<i>CALM2</i>	<i>CIT</i>
<i>AARS</i>	<i>AMACR</i>	<i>ATP7A</i>	<i>CAMTA1</i>	<i>CLCN1</i>
<i>AASS</i>	<i>AMER1</i>	<i>ATPAF2</i>	<i>CARD9</i>	<i>CLCN2</i>
<i>ABCA5</i>	<i>AMPD2</i>	<i>ATRX</i>	<i>CARS2</i>	<i>CLCN4</i>
<i>ABCC8</i>	<i>AMPH</i>	<i>ATXN10</i>	<i>CASK</i>	<i>CLCN6</i>
<i>ABHD12</i>	<i>AMT</i>	<i>ATXN2</i>	<i>CASQ2</i>	<i>CLDN16</i>
<i>ACADS</i>	<i>ANK3</i>	<i>AUH</i>	<i>CASR</i>	<i>CLIC2</i>
<i>ACADSB</i>	<i>ANKH</i>	<i>AUTS2</i>	<i>CAV3</i>	<i>CLN5</i>
<i>ACE</i>	<i>ANKRD11</i>	<i>AVPR2</i>	<i>CBL</i>	<i>CLN6</i>
<i>ACOT7</i>	<i>ANO10</i>	<i>B3GAT3</i>	<i>CCBE1</i>	<i>CLN8</i>
<i>ACSF3</i>	<i>ANOS1</i>	<i>B3GNT2</i>	<i>CCDC88A</i>	<i>CLP1</i>
<i>ACTB</i>	<i>AP1S2</i>	<i>BCAP31</i>	<i>CCDC88C</i>	<i>CLPP</i>
<i>ACVR1</i>	<i>AP4B1</i>	<i>BCKDHB</i>	<i>CCM2</i>	<i>CLSTN1</i>
<i>ACY1</i>	<i>AP4E1</i>	<i>BCKDK</i>	<i>CCNQ</i>	<i>CNNM2</i>
<i>ADAM22</i>	<i>AP4M1</i>	<i>BCS1L</i>	<i>CCS</i>	<i>CNTN2</i>
<i>ADGRG1</i>	<i>AP4S1</i>	<i>BDNF</i>	<i>CD46</i>	<i>CNTNAP1</i>
<i>ADGRV1</i>	<i>APOPT1</i>	<i>BMP4</i>	<i>CD59</i>	<i>CNTNAP2</i>
<i>ADK</i>	<i>ARFGEF2</i>	<i>BMP5</i>	<i>CD96</i>	<i>COG6</i>
<i>ADNP</i>	<i>ARG1</i>	<i>BOLA3</i>	<i>CDK5</i>	<i>COG7</i>
<i>ADRA2B</i>	<i>ARHGDI A</i>	<i>BRAF</i>	<i>CDKL5</i>	<i>COG8</i>
<i>AGL</i>	<i>ARHGGEF9</i>	<i>BRAT1</i>	<i>CELF4</i>	<i>COL18A1</i>
<i>AGPS</i>	<i>ARID1A</i>	<i>BRCA2</i>	<i>CELSR3</i>	<i>COL3A1</i>
<i>AGTR2</i>	<i>ARID1B</i>	<i>BRD2</i>	<i>CENPJ</i>	<i>COL4A1</i>
<i>AH11</i>	<i>ARNT2</i>	<i>BRWD3</i>	<i>CEP152</i>	<i>COL4A2</i>
<i>AIFM1</i>	<i>ARX</i>	<i>BSCL2</i>	<i>CEP164</i>	<i>COL6A2</i>
<i>AIMP1</i>	<i>ASAH1</i>	<i>BSN</i>	<i>CEP290</i>	<i>COL6A3</i>
<i>AKT3</i>	<i>ASL</i>	<i>BTD</i>	<i>CHD2</i>	<i>COQ2</i>
<i>ALDH18A1</i>	<i>ASNS</i>	<i>BUB1B</i>	<i>CHD3</i>	<i>COQ4</i>
<i>ALDH3A2</i>	<i>ASPM</i>	<i>C12orf57</i>	<i>CHD4</i>	<i>COQ6</i>
<i>ALDH4A1</i>	<i>ATIC</i>	<i>C3</i>	<i>CHD8</i>	<i>COQ8A</i>
<i>ALDH5A1</i>	<i>ATN1</i>	<i>C3orf58</i>	<i>CHKB</i>	<i>CORO1A</i>
<i>ALDH7A1</i>	<i>ATP13A2</i>	<i>CACNA1D</i>	<i>CHL1</i>	<i>COX15</i>
<i>ALG1</i>	<i>ATP1A2</i>	<i>CACNA1G</i>	<i>CHN1</i>	<i>COX6B1</i>
<i>ALG13</i>	<i>ATP1A3</i>	<i>CACNA1H</i>	<i>CHRFAM7A</i>	<i>CPA6</i>
<i>ALG2</i>	<i>ATP5F1A</i>	<i>CACNA2D2</i>	<i>CHRNA2</i>	<i>CPS1</i>
<i>ALG3</i>	<i>ATP6AP1</i>	<i>CACNB4</i>	<i>CHRNA4</i>	<i>CPT1A</i>
<i>ALG6</i>	<i>ATP6AP2</i>	<i>CACNG2</i>	<i>CHRNA7</i>	<i>CPT2</i>
<i>ALG9</i>	<i>ATP6V0A2</i>	<i>CAD</i>	<i>CHRN B2</i>	<i>CREBBP</i>

<i>CRYAB</i>	<i>DNM1L</i>	<i>FADD</i>	<i>GATA3</i>	<i>GRIA3</i>
<i>CSF1R</i>	<i>DNMT3A</i>	<i>FAM111A</i>	<i>GATA6</i>	<i>GRIK2</i>
<i>CSMD1</i>	<i>DOCK7</i>	<i>FAM126A</i>	<i>GATAD2B</i>	<i>GRIN1</i>
<i>CSNK1G1</i>	<i>DOCK8</i>	<i>FARS2</i>	<i>GBA</i>	<i>GRIN2A</i>
<i>CSPP1</i>	<i>DOLK</i>	<i>FASTKD2</i>	<i>GCH1</i>	<i>GRIN2B</i>
<i>CSTB</i>	<i>DPAGT1</i>	<i>FAT4</i>	<i>GCK</i>	<i>GRIN2D</i>
<i>CTCI</i>	<i>DPM1</i>	<i>FBP1</i>	<i>GCM2</i>	<i>GRINA</i>
<i>CTH</i>	<i>DPM2</i>	<i>FBXL4</i>	<i>GCSH</i>	<i>GRIP1</i>
<i>CTSA</i>	<i>DPYD</i>	<i>FCGR2B</i>	<i>GD1I</i>	<i>GRM1</i>
<i>CTSD</i>	<i>DPYS</i>	<i>FGD1</i>	<i>GFAP</i>	<i>GRPR</i>
<i>CTSF</i>	<i>DYNC1H1</i>	<i>FGF12</i>	<i>GFMI</i>	<i>GTPBP3</i>
<i>CUL4B</i>	<i>EARS2</i>	<i>FGF8</i>	<i>GFRA1</i>	<i>GUCY1A1</i>
<i>CUX1</i>	<i>EBP</i>	<i>FGFR2</i>	<i>GGT1</i>	<i>GUF1</i>
<i>CXCR4</i>	<i>ECM1</i>	<i>FGFR3</i>	<i>GIPC1</i>	<i>GYS1</i>
<i>CYB5R3</i>	<i>EFHC1</i>	<i>FLG</i>	<i>GIPC3</i>	<i>HADHA</i>
<i>CYP26C1</i>	<i>EFHC2</i>	<i>FLNA</i>	<i>GJA1</i>	<i>HADHB</i>
<i>CYP27A1</i>	<i>EGF</i>	<i>FLT4</i>	<i>GJC2</i>	<i>HAX1</i>
<i>CYP27B1</i>	<i>EHMT1</i>	<i>FMC1</i>	<i>GJD2</i>	<i>HCFC1</i>
<i>D2HGDH</i>	<i>EIF2B1</i>	<i>FMR1</i>	<i>GK</i>	<i>HCK</i>
<i>DAO</i>	<i>EIF2B4</i>	<i>FOLR1</i>	<i>GLB1</i>	<i>HCN1</i>
<i>DARS2</i>	<i>EIF2B5</i>	<i>FOXG1</i>	<i>GLDC</i>	<i>HCN2</i>
<i>DBT</i>	<i>EIF3E</i>	<i>FOXRED1</i>	<i>GLI2</i>	<i>HCN4</i>
<i>DCAF17</i>	<i>ELMO1</i>	<i>FRRS1L</i>	<i>GLI3</i>	<i>HDAC4</i>
<i>DCLK2</i>	<i>ELN</i>	<i>FSTL5</i>	<i>GLRA1</i>	<i>HEG1</i>
<i>DCX</i>	<i>ELOVL4</i>	<i>FTL</i>	<i>GLRB</i>	<i>HEPACAM</i>
<i>DEAF1</i>	<i>EMX2</i>	<i>FTO</i>	<i>GLUD1</i>	<i>HERC2</i>
<i>DEPDC5</i>	<i>ENG</i>	<i>FTSJ1</i>	<i>GLUL</i>	<i>HESX1</i>
<i>DGKD</i>	<i>EPHA5</i>	<i>GABBR2</i>	<i>GLYCTK</i>	<i>HEXA</i>
<i>DHCR24</i>	<i>EPM2A</i>	<i>GABRA1</i>	<i>GM2A</i>	<i>HFE</i>
<i>DHFR</i>	<i>ERBB4</i>	<i>GABRA6</i>	<i>GMEB2</i>	<i>HGSNAT</i>
<i>DHTKD1</i>	<i>ERCC6</i>	<i>GABRB1</i>	<i>GMPPB</i>	<i>HLCS</i>
<i>DIP2B</i>	<i>ERLIN2</i>	<i>GABRB3</i>	<i>GNAO1</i>	<i>HMGCS2</i>
<i>DKC1</i>	<i>ERMARD</i>	<i>GABRD</i>	<i>GNAQ</i>	<i>HNFB1B</i>
<i>DLD</i>	<i>ESCO2</i>	<i>GABRG2</i>	<i>GNB1</i>	<i>HOXA1</i>
<i>DLG2</i>	<i>ETFDH</i>	<i>GAD1</i>	<i>GNPAT</i>	<i>HRAS</i>
<i>DLG3</i>	<i>ETHE1</i>	<i>GAL</i>	<i>GPC3</i>	<i>HSD17B10</i>
<i>DMBX1</i>	<i>EXOC6B</i>	<i>GALC</i>	<i>GPHN</i>	<i>HSD17B4</i>
<i>DNAJC6</i>	<i>F2</i>	<i>GAS1</i>	<i>GPSM2</i>	<i>HSPD1</i>
<i>DNASE1</i>	<i>FA2H</i>	<i>GAS2L2</i>	<i>GPX4</i>	<i>HTR1A</i>

<i>HTR2A</i>	<i>KCNQ1</i>	<i>MAOA</i>	<i>MTMR11</i>	<i>NECAP1</i>
<i>HTT</i>	<i>KCNQ2</i>	<i>MAOB</i>	<i>MT-ND1</i>	<i>NEDD4</i>
<i>HUWE1</i>	<i>KCNQ3</i>	<i>MAP2K1</i>	<i>MT-ND4</i>	<i>NEDD4L</i>
<i>IDH2</i>	<i>KCNT1</i>	<i>MAPK10</i>	<i>MTO1</i>	<i>NELL1</i>
<i>IDS</i>	<i>KCNV1</i>	<i>MAPRE2</i>	<i>MTOR</i>	<i>NEU1</i>
<i>IER3IP1</i>	<i>KCTD7</i>	<i>MBD5</i>	<i>MTR</i>	<i>NEXMIF</i>
<i>IFIH1</i>	<i>KDM5C</i>	<i>MBTPS2</i>	<i>MYCN</i>	<i>NFIA</i>
<i>IFNAR2</i>	<i>KDM6A</i>	<i>MCCC1</i>	<i>MYH6</i>	<i>NGLY1</i>
<i>IFT140</i>	<i>KIF11</i>	<i>MCCC2</i>	<i>MYO5A</i>	<i>NHLRC1</i>
<i>IGSF8</i>	<i>KIF1A</i>	<i>MECP2</i>	<i>MYT1L</i>	<i>NID1</i>
<i>IL1B</i>	<i>KIF2A</i>	<i>MED12</i>	<i>NAA10</i>	<i>NIN</i>
<i>IL1RAPL1</i>	<i>KIF4A</i>	<i>MED17</i>	<i>NADK2</i>	<i>NIPA1</i>
<i>IL1RN</i>	<i>KIF5C</i>	<i>MEF2C</i>	<i>NAGA</i>	<i>NIPA2</i>
<i>IL27RA</i>	<i>KIF7</i>	<i>MEGF10</i>	<i>NALCN</i>	<i>NKAIN2</i>
<i>IL6</i>	<i>KLF13</i>	<i>MEN1</i>	<i>NANS</i>	<i>NLGN1</i>
<i>INO80</i>	<i>KMT2A</i>	<i>METTL23</i>	<i>NAPB</i>	<i>NLGN3</i>
<i>INPP4A</i>	<i>KMT2D</i>	<i>MFSD2A</i>	<i>NARS2</i>	<i>NNT</i>
<i>IQSEC2</i>	<i>KPNA7</i>	<i>MFSD8</i>	<i>NAT8L</i>	<i>NOD2</i>
<i>ITGB1BP1</i>	<i>KRAS</i>	<i>MGAT2</i>	<i>NCKAP5</i>	<i>NOL11</i>
<i>ITPR1</i>	<i>KRIT1</i>	<i>MGP</i>	<i>NDN</i>	<i>NOL3</i>
<i>JAM3</i>	<i>L1CAM</i>	<i>MID2</i>	<i>NDP</i>	<i>NONO</i>
<i>JRK</i>	<i>L2HGDH</i>	<i>MLC1</i>	<i>NDUFA1</i>	<i>NOTCH1</i>
<i>KANSL1</i>	<i>LAMA2</i>	<i>MLLT3</i>	<i>NDUFA2</i>	<i>NOTCH3</i>
<i>KARS</i>	<i>LAMB1</i>	<i>MMAA</i>	<i>NDUFA8</i>	<i>NPC1</i>
<i>KATNB1</i>	<i>LAMC3</i>	<i>MMACHC</i>	<i>NDUFAF1</i>	<i>NPC2</i>
<i>KCNA1</i>	<i>LARS</i>	<i>MMADHC</i>	<i>NDUFAF2</i>	<i>NPRL2</i>
<i>KCNAB1</i>	<i>LG1I</i>	<i>MOCS1</i>	<i>NDUFAF3</i>	<i>NPRL3</i>
<i>KCNAB2</i>	<i>LIAS</i>	<i>MOCS2</i>	<i>NDUFAF4</i>	<i>NPY</i>
<i>KCNC3</i>	<i>LMBRD1</i>	<i>MOGS</i>	<i>NDUFAF6</i>	<i>NRAS</i>
<i>KCND2</i>	<i>LMNB2</i>	<i>MPC1</i>	<i>NDUFB11</i>	<i>NRG2</i>
<i>KCND3</i>	<i>LRP1</i>	<i>MPDU1</i>	<i>NDUFB3</i>	<i>NRG3</i>
<i>KCNE1</i>	<i>LRP2</i>	<i>MPDZ</i>	<i>NDUFB9</i>	<i>NRXN1</i>
<i>KCNH2</i>	<i>LRPPRC</i>	<i>MPO</i>	<i>NDUFS1</i>	<i>NSD1</i>
<i>KCNH5</i>	<i>LRRK2</i>	<i>MRPS22</i>	<i>NDUFS2</i>	<i>NSDHL</i>
<i>KCNJ10</i>	<i>LYST</i>	<i>MSX2</i>	<i>NDUFS3</i>	<i>NSUN2</i>
<i>KCNJ11</i>	<i>MAGEL2</i>	<i>MT-ATP8</i>	<i>NDUFS4</i>	<i>NUBPL</i>
<i>KCNJ2</i>	<i>MAGI2</i>	<i>MT-CYB</i>	<i>NDUFS6</i>	<i>OCA2</i>
<i>KCNJ5</i>	<i>MAN1B1</i>	<i>MTFMT</i>	<i>NDUFS8</i>	<i>OCLN</i>
<i>KCNMA1</i>	<i>MANBA</i>	<i>MTHFR</i>	<i>NDUFV1</i>	<i>OCRL</i>

<i>OFD1</i>	<i>PHGDH</i>	<i>PRODH</i>	<i>RMND1</i>	<i>SLC12A5</i>
<i>OPA1</i>	<i>PHKG2</i>	<i>PROK2</i>	<i>RNASET2</i>	<i>SLC12A6</i>
<i>OPHN1</i>	<i>PHOX2B</i>	<i>PROS1</i>	<i>RNU4ATAC</i>	<i>SLC13A5</i>
<i>OPLAH</i>	<i>PHYKPL</i>	<i>PRPS1</i>	<i>RPGRIP1L</i>	<i>SLC16A1</i>
<i>OPRM1</i>	<i>PIGA</i>	<i>PRRC2B</i>	<i>RPIA</i>	<i>SLC17A5</i>
<i>OTC</i>	<i>PIGG</i>	<i>PRRT2</i>	<i>RPL10</i>	<i>SLC19A3</i>
<i>OTX2</i>	<i>PIGL</i>	<i>PSAP</i>	<i>RPS6KA3</i>	<i>SLC1A1</i>
<i>PAK3</i>	<i>PIGM</i>	<i>PSAT1</i>	<i>RRM2B</i>	<i>SLC1A2</i>
<i>PAQR8</i>	<i>PIGN</i>	<i>PSEN1</i>	<i>RTN4R</i>	<i>SLC1A3</i>
<i>PC</i>	<i>PIGO</i>	<i>PSEN2</i>	<i>RUBCN</i>	<i>SLC1A4</i>
<i>PCDH12</i>	<i>PIGV</i>	<i>PSMB8</i>	<i>RYR1</i>	<i>SLC20A2</i>
<i>PCDH15</i>	<i>PIGY</i>	<i>PSPH</i>	<i>RYR2</i>	<i>SLC25A1</i>
<i>PCDH19</i>	<i>PIK3CA</i>	<i>PTEN</i>	<i>SACS</i>	<i>SLC25A12</i>
<i>PCDHB4</i>	<i>PLA2G6</i>	<i>PTH</i>	<i>SASS6</i>	<i>SLC25A15</i>
<i>PCK1</i>	<i>PLP1</i>	<i>PTPN22</i>	<i>SATB2</i>	<i>SLC25A2</i>
<i>PCNT</i>	<i>PMP22</i>	<i>PTS</i>	<i>SCARB2</i>	<i>SLC25A20</i>
<i>PDCD6</i>	<i>PNKP</i>	<i>PUF60</i>	<i>SCN1A</i>	<i>SLC25A22</i>
<i>PDE10A</i>	<i>PNPO</i>	<i>PURA</i>	<i>SCN2A</i>	<i>SLC26A1</i>
<i>PDHA1</i>	<i>PNPT1</i>	<i>PUS3</i>	<i>SCN2B</i>	<i>SLC2A1</i>
<i>PDHX</i>	<i>POGZ</i>	<i>QARS</i>	<i>SCN3A</i>	<i>SLC30A3</i>
<i>PDP1</i>	<i>POLG</i>	<i>QDPR</i>	<i>SCN4A</i>	<i>SLC33A1</i>
<i>PDSS2</i>	<i>POLR3A</i>	<i>RAB18</i>	<i>SCN5A</i>	<i>SLC35A2</i>
<i>PDX1</i>	<i>POLR3B</i>	<i>RAB27A</i>	<i>SCN8A</i>	<i>SLC35A3</i>
<i>PEX1</i>	<i>POMC</i>	<i>RAB39B</i>	<i>SCN9A</i>	<i>SLC35C1</i>
<i>PEX10</i>	<i>POMGNT1</i>	<i>RAB3GAP1</i>	<i>SCO2</i>	<i>SLC39A8</i>
<i>PEX13</i>	<i>POMT1</i>	<i>RAI1</i>	<i>SDHD</i>	<i>SLC4A10</i>
<i>PEX14</i>	<i>POMT2</i>	<i>RANBP2</i>	<i>SEPSECS</i>	<i>SLC4A3</i>
<i>PEX16</i>	<i>PPOX</i>	<i>RANGAP1</i>	<i>SERAC1</i>	<i>SLC6A1</i>
<i>PEX2</i>	<i>PPP1R3C</i>	<i>RAPGEF6</i>	<i>SERPINI1</i>	<i>SLC6A19</i>
<i>PEX3</i>	<i>PPP2R1A</i>	<i>RAPSN</i>	<i>SETBP1</i>	<i>SLC6A20</i>
<i>PEX5</i>	<i>PPT1</i>	<i>RARS2</i>	<i>SETD2</i>	<i>SLC6A3</i>
<i>PEX6</i>	<i>PQBP1</i>	<i>RB1</i>	<i>SETD5</i>	<i>SLC6A8</i>
<i>PEX7</i>	<i>PRAG1</i>	<i>RBFOX1</i>	<i>SEZ6</i>	<i>SLC7A11</i>
<i>PGAP1</i>	<i>PRDM8</i>	<i>RBM10</i>	<i>SGCE</i>	<i>SLC7A6OS</i>
<i>PGAP2</i>	<i>PRF1</i>	<i>RBM8A</i>	<i>SHH</i>	<i>SLC9A1</i>
<i>PGK1</i>	<i>PRICKLE1</i>	<i>RBP4</i>	<i>SHROOM4</i>	<i>SLC9A6</i>
<i>PGM3</i>	<i>PRICKLE2</i>	<i>RBSN</i>	<i>SIK1</i>	<i>SLC9A9</i>
<i>PHF6</i>	<i>PRKDC</i>	<i>RELN</i>	<i>SIL1</i>	<i>SLCO1B7</i>
<i>PHF8</i>	<i>PRKN</i>	<i>RFT1</i>	<i>SIX3</i>	<i>SMAD4</i>

<i>SMARCA2</i>	<i>ST8SIA2</i>	<i>TBCE</i>	<i>TRMT44</i>	<i>VAR52</i>
<i>SMARCA4</i>	<i>STAMBP</i>	<i>TBL1XR1</i>	<i>TRMT9B</i>	<i>VLDLR</i>
<i>SMARCAL1</i>	<i>STAT1</i>	<i>TBP</i>	<i>TRPM1</i>	<i>VPS11</i>
<i>SMARCE1</i>	<i>STAT2</i>	<i>TBX1</i>	<i>TRPM6</i>	<i>VPS13A</i>
<i>SMC1A</i>	<i>STIL</i>	<i>TBX19</i>	<i>TSC1</i>	<i>VPS13B</i>
<i>SMG9</i>	<i>STRADA</i>	<i>TDP1</i>	<i>TSC2</i>	<i>WDR19</i>
<i>SMS</i>	<i>STT3A</i>	<i>TDP2</i>	<i>TSEN15</i>	<i>WDR45</i>
<i>SNIP1</i>	<i>STT3B</i>	<i>TECPR2</i>	<i>TSEN2</i>	<i>WDR62</i>
<i>SNRPN</i>	<i>STXBP1</i>	<i>TELO2</i>	<i>TSEN34</i>	<i>WFS1</i>
<i>SOBP</i>	<i>SUCLA2</i>	<i>TENM2</i>	<i>TSEN54</i>	<i>XK</i>
<i>SON</i>	<i>SUCO</i>	<i>THRB</i>	<i>TTN</i>	<i>XPNPEP3</i>
<i>SORL1</i>	<i>SUOX</i>	<i>TICAM1</i>	<i>TUBA1A</i>	<i>XPR1</i>
<i>SOX2</i>	<i>SV2A</i>	<i>TK2</i>	<i>TUBA8</i>	<i>YWHAE</i>
<i>SOX5</i>	<i>SYN1</i>	<i>TMEM67</i>	<i>TUBB</i>	<i>YWHAG</i>
<i>SPAST</i>	<i>SYN2</i>	<i>TMEM70</i>	<i>TUBB2A</i>	<i>ZBTB18</i>
<i>SPR</i>	<i>SYNGAP1</i>	<i>TMLHE</i>	<i>TUBB2B</i>	<i>ZC4H2</i>
<i>SPTAN1</i>	<i>SYNJ1</i>	<i>TNK2</i>	<i>TUBB3</i>	<i>ZDHHC15</i>
<i>SPTLC2</i>	<i>SYP</i>	<i>TOR1A</i>	<i>TUBGCP6</i>	<i>ZEB2</i>
<i>SQSTM1</i>	<i>SYT14</i>	<i>TPK1</i>	<i>TWNK</i>	<i>ZFP57</i>
<i>SRGAP2</i>	<i>SYT2</i>	<i>TPP1</i>	<i>TXN2</i>	<i>ZFYVE26</i>
<i>SRPX2</i>	<i>SZT2</i>	<i>TRAF3</i>	<i>UBE2A</i>	<i>ZMYND11</i>
<i>ST3GAL3</i>	<i>TANGO2</i>	<i>TRAPPC11</i>	<i>UBE3A</i>	
<i>ST3GAL5</i>	<i>TAP1</i>	<i>TRAPPC9</i>	<i>UCHL1</i>	
<i>ST5</i>	<i>TBC1D32</i>	<i>TREM2</i>	<i>UQCC2</i>	
<i>ST7</i>	<i>TBCD</i>	<i>TREX1</i>	<i>USP9X</i>	

Interneuron gene list (in house)

<i>9430021M05RIK</i>	<i>EDN3</i>	<i>KRT73</i>	<i>PVRL4</i>
<i>ACSBG1</i>	<i>EDNRB</i>	<i>LAMP5</i>	<i>RASL11A</i>
<i>ADAMTS18</i>	<i>EFCAB6</i>	<i>LHX6</i>	<i>RELN</i>
<i>AEBP1</i>	<i>EFEMP1</i>	<i>LRRC61</i>	<i>RGS12</i>
<i>AKR1C18</i>	<i>EGLN3</i>	<i>MAB21L1</i>	<i>RSPO2</i>
<i>ALOXE3</i>	<i>ETV1</i>	<i>MANIA</i>	<i>SCML4</i>
<i>ANO3</i>	<i>FAM107A</i>	<i>MEGF10</i>	<i>SEMA5B</i>
<i>ATP6AP1L</i>	<i>FIGN</i>	<i>MPPED1</i>	<i>SGPP2</i>
<i>BACE2</i>	<i>FOSB</i>	<i>MYBPC1</i>	<i>SLC18A3</i>
<i>BCAR3</i>	<i>FREM1</i>	<i>MYH8</i>	<i>SMAD3</i>
<i>BDNF</i>	<i>FRMD7</i>	<i>MYO5B</i>	<i>SNCA</i>
<i>CACNA2D3</i>	<i>FXYD6</i>	<i>NDST4</i>	<i>SNCG</i>
<i>CADPS2</i>	<i>GABRD</i>	<i>NELL1</i>	<i>SPP1</i>
<i>CALB1</i>	<i>GABRG1</i>	<i>NFIB</i>	<i>SST</i>
<i>CALCA</i>	<i>GFRA2</i>	<i>NOS1</i>	<i>ST6GALNAC5</i>
<i>CALN1</i>	<i>GLRA3</i>	<i>NPY</i>	<i>TAC1</i>
<i>CAR4</i>	<i>GPC3</i>	<i>NPY2R</i>	<i>TAC2</i>
<i>CARTPT</i>	<i>GPR151</i>	<i>NR2F2</i>	<i>TACR1</i>
<i>CBLN4</i>	<i>GPR88</i>	<i>NR4A2</i>	<i>TACR3</i>
<i>CCDC109B</i>	<i>GPX3</i>	<i>NRP1</i>	<i>TACSTD2</i>
<i>CD34</i>	<i>GRM3</i>	<i>NT5E</i>	<i>TH</i>
<i>CDCA7</i>	<i>GSTM6</i>	<i>NTF3</i>	<i>THSD7A</i>
<i>CHAT</i>	<i>HAS2</i>	<i>NTS</i>	<i>THSD7B</i>
<i>CHODL</i>	<i>HCRTR1</i>	<i>OLFM3</i>	<i>TIMP3</i>
<i>CHRNA2</i>	<i>HSPB3</i>	<i>PARM1</i>	<i>TLL1</i>
<i>CHRNB3</i>	<i>HTR2A</i>	<i>PBX3</i>	<i>TNFAIP8L3</i>
<i>CNTNAP5B</i>	<i>HTR7</i>	<i>PCDH15</i>	<i>TNNT1</i>
<i>COL14A1</i>	<i>IL1RAPL2</i>	<i>PCDH18</i>	<i>TPBG</i>
<i>COL25A1</i>	<i>IRS4</i>	<i>PCDH8</i>	<i>TPD52L1</i>
<i>COX6A2</i>	<i>ITIH5</i>	<i>PDE11A</i>	<i>TPM2</i>
<i>CPNE5</i>	<i>KCNS3</i>	<i>PDLIM3</i>	<i>TRPV6</i>
<i>CRH</i>	<i>KIT</i>	<i>PHLDA1</i>	<i>VIP</i>
<i>CRISPLD2</i>	<i>KLHL14</i>	<i>PLA2G4A</i>	
<i>CRYAB</i>	<i>KRT12</i>	<i>PPAPDC1A</i>	
<i>CXCL14</i>	<i>KRT18</i>	<i>PVALB</i>	

Arx target genes (Mattiske *et al.* 2016)

0610010B08RIK	4930578M01RIK	ADAMTSL3	ANKK1	ATG101
0610010F05RIK	4932411E22RIK	ADARB2	ANKRD22	ATG2B
0610012G03RIK	4932418E24RIK	ADCY9	ANKRD26	ATG4C
0610040B10RIK	4932438A13RIK	ADGRL3	ANKRD7	ATG5
1110001J03RIK	4933409G03RIK	ADORA3	ANO4	ATL2
1190005I06RIK	5031434O11RIK	AEBP1	ANXA10	ATP13A4
1600002K03RIK	5330426P16RIK	AEN	AOX4	ATP2B3
1700007G11RIK	5730408K05RIK	AFF2	AP1S3	ATP5E
1700007J10RIK	5830454E08RIK	AFF4	AP2A1	ATP5G1
1700008O03RIK	6330415B21RIK	AFFP	APLP2	ATP5G2
1700016K19RIK	6330418K02RIK	AGER	APOA1	ATP5H
1700020I14RIK	6330549D23RIK	AGO2	APOM	ATP5J
1700029I15RIK	8030462N17RIK	AGO3	AQP4	ATP5K
1700048O20RIK	9430020K01RIK	AHI1	ARFGEF3	ATP6V0E
1700067K01RIK	9430076C15RIK	AII18078	ARHGAP12	ATP7A
1700113A16RIK	9530082P21RIK	AI413582	ARHGAP32	ATP7B
1700123K08RIK	A330023F24RIK	AI506816	ARHGAP5	ATP8A2
2010320M18RIK	A630001G21RIK	AI597479	ARHGDIG	ATRNL1
2310002D06RIK	A630089N07RIK	AI606473	ARHGEF38	ATRX
2310057J18RIK	A730008H23RIK	AIMP1	ARID1A	AU040320
2610002M06RIK	AASDHPPT	AKAP6	ARID4B	AXIN2
2610005L07RIK	ABCA5	ALAD	ARID5A	B230119M05RIK
2610020H08RIK	ABCA8B	ALDH1B1	ARID5B	B3GNT7
2610318N02RIK	ABHD1	ALDH8A1	ARL5B	B4GALT1
2810405F15RIK	ABHD11	ALG10B	ARMCX2	BAHD1
2810428I15RIK	ABHD14A	ALG2	ARNTL	BARX1
3110021A11RIK	ABHD2	ALK	ARX	BATF
3110021N24RIK	ACBD4	ALKBH2	AS3MT	BAX
3300002I08RIK	ACE	ALKBH8	ASCC1	BBS12
4632427E13RIK	ACKR3	ALS2CR12	ASH1L	BC002163
4632428N05RIK	ACOT10	ALX1	ASIC5	BC003331
4921511H03RIK	ACTN2	AMD1	ASL	BC005537
4930404N11RIK	ACTR3	AMH	ASPDH	BC005561
4930444P10RIK	ACVR2B	AMPD2	ASPHD1	BC031181
4930447C04RIK	ACVRL1	ANAPC13	ASPM	BC094916
4930455C13RIK	ADAMTS12	ANK1	ASPRV1	BEX2
4930506C21RIK	ADAMTS6	ANK3	ATF7	BFSP2
4930565N06RIK	ADAMTS8	ANKFN1	ATF7IP	BHLHE22

<i>BHLHE40</i>	<i>CAPNS1</i>	<i>CDH13</i>	<i>CHRNA7</i>	<i>CPEB4</i>
<i>BICD1</i>	<i>CAR11</i>	<i>CDH2</i>	<i>CHRF18</i>	<i>CPNE2</i>
<i>BIRC6</i>	<i>CAR3</i>	<i>CDH3</i>	<i>CIB2</i>	<i>CPSF1</i>
<i>BIVM</i>	<i>CARF</i>	<i>CDH5</i>	<i>CISD3</i>	<i>CRABP1</i>
<i>BMPER</i>	<i>CARTPT</i>	<i>CDH6</i>	<i>CIT</i>	<i>CRABP2</i>
<i>BMPR2</i>	<i>CASC4</i>	<i>CDH8</i>	<i>CLCN5</i>	<i>CRB1</i>
<i>BOLA2</i>	<i>CASC5</i>	<i>CDK17</i>	<i>CLDN3</i>	<i>CREB3L1</i>
<i>BRD1</i>	<i>CASD1</i>	<i>CDK2AP2</i>	<i>CLDN6</i>	<i>CREB5</i>
<i>BRD2</i>	<i>CASQ1</i>	<i>CDK5RAP2</i>	<i>CLEC1B</i>	<i>CREBBP</i>
<i>BRICD5</i>	<i>CATSPERB</i>	<i>CDK6</i>	<i>CLEC9A</i>	<i>CRIP1</i>
<i>BRMS1</i>	<i>CAVI</i>	<i>CDKL5</i>	<i>CLOCK</i>	<i>CRIP3</i>
<i>BRS3</i>	<i>CBL</i>	<i>CDKN1A</i>	<i>CLUH</i>	<i>CRIPT</i>
<i>BRWD3</i>	<i>CBLC</i>	<i>CDKN2AIP</i>	<i>CMA1</i>	<i>CRTAC1</i>
<i>BTBD7</i>	<i>CBX3</i>	<i>CDKN2C</i>	<i>CNKSRR2</i>	<i>CRY2</i>
<i>BTBD8</i>	<i>CBY1</i>	<i>CDON</i>	<i>CNN2</i>	<i>CRYGE</i>
<i>BTD</i>	<i>CCDC101</i>	<i>CDX1</i>	<i>CNNM3</i>	<i>CRYM</i>
<i>BTG4</i>	<i>CCDC106</i>	<i>CEACAM9</i>	<i>CNOT6</i>	<i>CSF2RB2</i>
<i>BTN1A1</i>	<i>CCDC107</i>	<i>CELF2</i>	<i>CNTN1</i>	<i>CSMD1</i>
<i>C130021I20RIK</i>	<i>CCDC12</i>	<i>CELSR2</i>	<i>CNTN2</i>	<i>CSMD3</i>
<i>C130071C03RIK</i>	<i>CCDC124</i>	<i>CENPC1</i>	<i>CNTN5</i>	<i>CSN1S1</i>
<i>C1GALT1</i>	<i>CCDC171</i>	<i>CEP135</i>	<i>CNTNAP3</i>	<i>CSRNP3</i>
<i>C1QL3</i>	<i>CCDC23</i>	<i>CEP290</i>	<i>CNTNAP5A</i>	<i>CST13</i>
<i>C5AR2</i>	<i>CCDC24</i>	<i>CEP350</i>	<i>CNTNAP5B</i>	<i>CST7</i>
<i>C77370</i>	<i>CCDC28A</i>	<i>CEP85</i>	<i>COA3</i>	<i>CSTF2T</i>
<i>C78339</i>	<i>CCDC32</i>	<i>CEP85L</i>	<i>COL10A1</i>	<i>CTNNA2</i>
<i>C8B</i>	<i>CCDC38</i>	<i>CERS6</i>	<i>COL6A2</i>	<i>CTR9</i>
<i>CABP1</i>	<i>CCDC60</i>	<i>CFAP97</i>	<i>COL8A1</i>	<i>CUEDC2</i>
<i>CACFD1</i>	<i>CCDC88C</i>	<i>CFH</i>	<i>COLGALT2</i>	<i>CWC22</i>
<i>CACNA1B</i>	<i>CCHCR1</i>	<i>CGGBP1</i>	<i>COMTD1</i>	<i>CWH43</i>
<i>CACNA1E</i>	<i>CCKBR</i>	<i>CHCHD1</i>	<i>COTL1</i>	<i>CXCL10</i>
<i>CACNA2D1</i>	<i>CCL2</i>	<i>CHCHD6</i>	<i>COX17</i>	<i>CXCL11</i>
<i>CACNG4</i>	<i>CCNT1</i>	<i>CHD9</i>	<i>COX4I1</i>	<i>CXCL14</i>
<i>CADM3</i>	<i>CCR10</i>	<i>CHGA</i>	<i>COX6B2</i>	<i>CXCR2</i>
<i>CADPS2</i>	<i>CCRL2</i>	<i>CHKB</i>	<i>COX7A1</i>	<i>CXCR4</i>
<i>CALB1</i>	<i>CCT6A</i>	<i>CHMP2A</i>	<i>COX7A2L</i>	<i>CXCR5</i>
<i>CALB2</i>	<i>CD177</i>	<i>CHN1</i>	<i>COX7B2</i>	<i>CXX1A</i>
<i>CALCR</i>	<i>CD274</i>	<i>CHRM3</i>	<i>COX8B</i>	<i>CXX1B</i>
<i>CALNI</i>	<i>CD2AP</i>	<i>CHRM4</i>	<i>CPA2</i>	<i>CXXC4</i>
<i>CALU</i>	<i>CD84</i>	<i>CHRNA7</i>	<i>CPEB1</i>	<i>CXXC5</i>

<i>CYB5R4</i>	<i>DGKZ</i>	<i>DYNC2H1</i>	<i>EPHA3</i>	<i>FAM57B</i>
<i>CYBB</i>	<i>DHRS3</i>	<i>DYNLRB2</i>	<i>EPHB1</i>	<i>FAM83G</i>
<i>CYP1B1</i>	<i>DHX37</i>	<i>DYNLT1F</i>	<i>EPHX2</i>	<i>FAM92B</i>
<i>CYP26B1</i>	<i>DIP2B</i>	<i>DYRK2</i>	<i>EPPK1</i>	<i>FAP</i>
<i>CYP2B10</i>	<i>DISC1</i>	<i>E330009J07RIK</i>	<i>EPYC</i>	<i>FAT1</i>
<i>CYP2C55</i>	<i>DKKL1</i>	<i>EBF1</i>	<i>ERBB4</i>	<i>FAT3</i>
<i>CYP2C66</i>	<i>DLEU2</i>	<i>EBF3</i>	<i>ERICH5</i>	<i>FAU</i>
<i>CYP2R1</i>	<i>DLGAP2</i>	<i>EDA</i>	<i>ERMN</i>	<i>FBF1</i>
<i>CYP4X1</i>	<i>DLK2</i>	<i>EDA2R</i>	<i>ERN1</i>	<i>FBXL18</i>
<i>D030047H15RIK</i>	<i>DMP1</i>	<i>EDNRA</i>	<i>ESAM</i>	<i>FBXO15</i>
<i>D10JHU81E</i>	<i>DMRT3</i>	<i>EFCAB8</i>	<i>ESPN</i>	<i>FBXO40</i>
<i>D130040H23RIK</i>	<i>DMRTA2</i>	<i>EFNB3</i>	<i>ESRP1</i>	<i>FBXO48</i>
<i>D330041H03RIK</i>	<i>DMRTC1A</i>	<i>EFS</i>	<i>ESX1</i>	<i>FBXW4</i>
<i>D430020J02RIK</i>	<i>DMTF1</i>	<i>EGFL6</i>	<i>ESYT3</i>	<i>FCAMR</i>
<i>D630041G03RIK</i>	<i>DMXL2</i>	<i>EGFL8</i>	<i>ETS2</i>	<i>FCNA</i>
<i>D830031N03RIK</i>	<i>DNAH5</i>	<i>EGR1</i>	<i>ETV1</i>	<i>FER</i>
<i>D8ERTD738E</i>	<i>DNAJB14</i>	<i>EGR3</i>	<i>EVX2</i>	<i>FEV</i>
<i>D930028M14RIK</i>	<i>DNM2</i>	<i>EIF1</i>	<i>EXOC4</i>	<i>FGD4</i>
<i>DAND5</i>	<i>DNM3OS</i>	<i>EIF2AK3</i>	<i>EXOSC4</i>	<i>FGF13</i>
<i>DBNDD2</i>	<i>DOC2B</i>	<i>EIF2S1</i>	<i>F730043M19RIK</i>	<i>FGF20</i>
<i>DBNL</i>	<i>DOC2G</i>	<i>EIF2S3Y</i>	<i>FA2H</i>	<i>FGF4</i>
<i>DBPHT2</i>	<i>DOCK4</i>	<i>EIF3F</i>	<i>FABP3</i>	<i>FGFBP3</i>
<i>DBX1</i>	<i>DOK3</i>	<i>EIF4A2</i>	<i>FAM107B</i>	<i>FGFR1OP2</i>
<i>DCAF13</i>	<i>DOK6</i>	<i>EIF4EBP3</i>	<i>FAM124B</i>	<i>FGFR2</i>
<i>DCDC2B</i>	<i>DOPEY1</i>	<i>EIF5</i>	<i>FAM135B</i>	<i>FGR</i>
<i>DCT</i>	<i>DPM2</i>	<i>ELFN2</i>	<i>FAM159A</i>	<i>FHAD1</i>
<i>DCUN1D1</i>	<i>DPM3</i>	<i>ELK4</i>	<i>FAM160A1</i>	<i>FHOD1</i>
<i>DDI2</i>	<i>DPPA3</i>	<i>ELL3</i>	<i>FAM168B</i>	<i>FIBCD1</i>
<i>DDIT4</i>	<i>DPY19L4</i>	<i>EMC7</i>	<i>FAM171A2</i>	<i>FIGNL1</i>
<i>DDT</i>	<i>DPYD</i>	<i>EML6</i>	<i>FAM171B</i>	<i>FIS1</i>
<i>DDX3Y</i>	<i>DPYS</i>	<i>ENC1</i>	<i>FAM183B</i>	<i>FKBP11</i>
<i>DEFB2</i>	<i>DPYSL2</i>	<i>ENDOG</i>	<i>FAM204A</i>	<i>FKBP2</i>
<i>DEFB29</i>	<i>DPYSL3</i>	<i>ENO3</i>	<i>FAM212B</i>	<i>FKTN</i>
<i>DEFB50</i>	<i>DRAP1</i>	<i>ENPP4</i>	<i>FAM217B</i>	<i>FLRT1</i>
<i>DENND1C</i>	<i>DTNBP1</i>	<i>ENPP5</i>	<i>FAM219B</i>	<i>FLRT2</i>
<i>DEPTOR</i>	<i>DTX2</i>	<i>EOMES</i>	<i>FAM26F</i>	<i>FLYWCH2</i>
<i>DERL3</i>	<i>DUSP11</i>	<i>EPB4.1L1</i>	<i>FAM45A</i>	<i>FMNL1</i>
<i>DGKH</i>	<i>DUSP19</i>	<i>EPG5</i>	<i>FAM50A</i>	<i>FNDC3C1</i>
<i>DGKI</i>	<i>DUSP4</i>	<i>EPGN</i>	<i>FAM53B</i>	<i>FNIP1</i>

<i>FOS</i>	<i>GBX2</i>	<i>GM5617</i>	<i>GRID2</i>	<i>HIST1H1E</i>
<i>FOSB</i>	<i>GDAP10</i>	<i>GM5635</i>	<i>GRM1</i>	<i>HIST1H2AB</i>
<i>FOXA1</i>	<i>GDF1</i>	<i>GM5796</i>	<i>GSS</i>	<i>HIST1H2AC</i>
<i>FOXB2</i>	<i>GFI1B</i>	<i>GM6377</i>	<i>GSTK1</i>	<i>HIST1H2AD</i>
<i>FOXF1</i>	<i>GFOD1</i>	<i>GM6402</i>	<i>GTF2B</i>	<i>HIST1H2AE</i>
<i>FOXN4</i>	<i>GGCX</i>	<i>GM973</i>	<i>GUCY2C</i>	<i>HIST1H2AF</i>
<i>FOXO3</i>	<i>GGNBP1</i>	<i>GM9839</i>	<i>GVIN1</i>	<i>HIST1H2AG</i>
<i>FOXP1</i>	<i>GHDC</i>	<i>GM996</i>	<i>H2-DMA</i>	<i>HIST1H2AI</i>
<i>FREM2</i>	<i>GHRH</i>	<i>GMDS</i>	<i>H2-Q6</i>	<i>HIST1H2AN</i>
<i>FRMD6</i>	<i>GIMAP8</i>	<i>GNAI1</i>	<i>H2-Q8</i>	<i>HIST1H2AO</i>
<i>FRMD7</i>	<i>GJB2</i>	<i>GNAI3</i>	<i>H2-T24</i>	<i>HIST1H2BC</i>
<i>FRRS1L</i>	<i>GJD4</i>	<i>GNAO1</i>	<i>HAO1</i>	<i>HIST1H2BE</i>
<i>FRY</i>	<i>GK5</i>	<i>GNAS</i>	<i>HAP1</i>	<i>HIST1H2BF</i>
<i>FRYL</i>	<i>GLG1</i>	<i>GNB2</i>	<i>HAS3</i>	<i>HIST1H2BG</i>
<i>FTL1</i>	<i>GLIS3</i>	<i>GNG11</i>	<i>HAUS3</i>	<i>HIST1H2BJ</i>
<i>FUT7</i>	<i>GLRA3</i>	<i>GNG13</i>	<i>HAUS5</i>	<i>HIST1H2BL</i>
<i>FXYD6</i>	<i>GLRX3</i>	<i>GNG8</i>	<i>HBB-BH1</i>	<i>HIST1H2BN</i>
<i>FXYD7</i>	<i>GM10406</i>	<i>GNGT2</i>	<i>HBP1</i>	<i>HIST1H3B</i>
<i>FZD1</i>	<i>GM11974</i>	<i>GNL2</i>	<i>HC</i>	<i>HIST1H3C</i>
<i>G0S2</i>	<i>GM12060</i>	<i>GNMT</i>	<i>HCFC1</i>	<i>HIST1H3E</i>
<i>G6PD2</i>	<i>GM12070</i>	<i>GP1BB</i>	<i>HCRTR1</i>	<i>HIST1H3F</i>
<i>GAB3</i>	<i>GM12709</i>	<i>GPAM</i>	<i>HDAC4</i>	<i>HIST1H4A</i>
<i>GABARAP</i>	<i>GM14827</i>	<i>GPATCH2</i>	<i>HDGFL1</i>	<i>HIST1H4B</i>
<i>GABBR2</i>	<i>GM15421</i>	<i>GPD1</i>	<i>HDX</i>	<i>HIST1H4C</i>
<i>GABRB3</i>	<i>GM16386</i>	<i>GPNMB</i>	<i>HECTD2</i>	<i>HIST1H4D</i>
<i>GABRE</i>	<i>GM16576</i>	<i>GPR161</i>	<i>HECW1</i>	<i>HIST1H4F</i>
<i>GABRQ</i>	<i>GM16617</i>	<i>GPR165</i>	<i>HEG1</i>	<i>HIST1H4H</i>
<i>GAD2</i>	<i>GM1673</i>	<i>GPR21</i>	<i>HELZ</i>	<i>HIST1H4I</i>
<i>GADD45G</i>	<i>GM16982</i>	<i>GPR26</i>	<i>HEMGN</i>	<i>HIST1H4J</i>
<i>GALNT14</i>	<i>GM19557</i>	<i>GPR37</i>	<i>HEPACAM2</i>	<i>HIST1H4K</i>
<i>GALNTL6</i>	<i>GM19757</i>	<i>GPR50</i>	<i>HEPH</i>	<i>HIST1H4M</i>
<i>GAN</i>	<i>GM2694</i>	<i>GPR63</i>	<i>HERC1</i>	<i>HIST1H4N</i>
<i>GAPDHS</i>	<i>GM3414</i>	<i>GPRIN2</i>	<i>HERC2</i>	<i>HIST2H2BB</i>
<i>GAR1</i>	<i>GM3500</i>	<i>GPS2</i>	<i>HES6</i>	<i>HIST2H3B</i>
<i>GAREM</i>	<i>GM382</i>	<i>GPSM1</i>	<i>HHIPL1</i>	<i>HIST2H3C1</i>
<i>GATA3</i>	<i>GM4070</i>	<i>GRAMD1B</i>	<i>HIPK2</i>	<i>HIST2H4</i>
<i>GATAD2B</i>	<i>GM4861</i>	<i>GRCC10</i>	<i>HIST1H1A</i>	<i>HIST4H4</i>
<i>GATSL2</i>	<i>GM5176</i>	<i>GRIA1</i>	<i>HIST1H1B</i>	<i>HIVEP1</i>
<i>GBP6</i>	<i>GM5415</i>	<i>GRIA3</i>	<i>HIST1H1D</i>	<i>HIVEP3</i>

<i>HMBOX1</i>	<i>INPP5K</i>	<i>KCTD5</i>	<i>LCOR</i>	<i>LRRTM2</i>
<i>HMCN1</i>	<i>IPO4</i>	<i>KDM5D</i>	<i>LENEP</i>	<i>LSM3</i>
<i>HMGB3</i>	<i>IPW</i>	<i>KHDRBS2</i>	<i>LGALS4</i>	<i>LSM5</i>
<i>HMGN3</i>	<i>IQUB</i>	<i>KIDINS220</i>	<i>LGALS7</i>	<i>LSM7</i>
<i>HNFI1A</i>	<i>IRS1</i>	<i>KIF13B</i>	<i>LG11</i>	<i>LY6G5B</i>
<i>HNRNPF</i>	<i>IRX5</i>	<i>KIF26B</i>	<i>LHX5</i>	<i>LY75</i>
<i>HOOK1</i>	<i>ISG15</i>	<i>KIRREL3</i>	<i>LIMCH1</i>	<i>LYPD6</i>
<i>HPN</i>	<i>ITGA6</i>	<i>KITL</i>	<i>LIN7C</i>	<i>LYST</i>
<i>HPS5</i>	<i>ITGAV</i>	<i>KL</i>	<i>LINGO1</i>	<i>LZTS1</i>
<i>HR</i>	<i>ITGB1BP1</i>	<i>KLF10</i>	<i>LMBRD2</i>	<i>LZTS3</i>
<i>HS3ST1</i>	<i>ITGB3BP</i>	<i>KLF12</i>	<i>LMLN</i>	<i>MAF</i>
<i>HS3ST3A1</i>	<i>ITGB8</i>	<i>KLF13</i>	<i>LMNB2</i>	<i>MAFA</i>
<i>HSF2</i>	<i>ITM2C</i>	<i>KLF7</i>	<i>LMO1</i>	<i>MAGEL2</i>
<i>HSPA4L</i>	<i>IWS1</i>	<i>KLF9</i>	<i>LMO3</i>	<i>MAMDC2</i>
<i>HSPA5</i>	<i>IZUMO1</i>	<i>KLHDC9</i>	<i>LMO4</i>	<i>MAN1A2</i>
<i>HSPB1</i>	<i>JADE3</i>	<i>KLHL11</i>	<i>LNP</i>	<i>MANEA</i>
<i>HSPB3</i>	<i>JOSD2</i>	<i>KLHL15</i>	<i>LNPEP</i>	<i>MAP1B</i>
<i>HTATIP2</i>	<i>JPH4</i>	<i>KLHL22</i>	<i>LONRF3</i>	<i>MAP1LC3A</i>
<i>HTR7</i>	<i>KANK3</i>	<i>KLHL28</i>	<i>LPAR1</i>	<i>MAP3K13</i>
<i>HUWE1</i>	<i>KANSL3</i>	<i>KLHL3</i>	<i>LPAR4</i>	<i>MAP4</i>
<i>HYAL1</i>	<i>KAT6A</i>	<i>KLK1B11</i>	<i>LPP</i>	<i>MARK3</i>
<i>HY1</i>	<i>KBTBD8</i>	<i>KLRC1</i>	<i>LPPR2</i>	<i>MARK4</i>
<i>ID2</i>	<i>KCNA1</i>	<i>KLRG1</i>	<i>LRCH3</i>	<i>MASP1</i>
<i>IDO1</i>	<i>KCNA3</i>	<i>KRCC1</i>	<i>LRP1B</i>	<i>MBD3L2</i>
<i>IFNA15</i>	<i>KCNA5</i>	<i>KRT1</i>	<i>LRP2</i>	<i>MBIP</i>
<i>IFNA9</i>	<i>KCNAB1</i>	<i>KRT222</i>	<i>LRP6</i>	<i>MBOAT1</i>
<i>IFNB1</i>	<i>KCNAB3</i>	<i>KRT40</i>	<i>LRRC18</i>	<i>MC2R</i>
<i>IFT46</i>	<i>KCNB2</i>	<i>KRT78</i>	<i>LRRC23</i>	<i>MCM4</i>
<i>IGF1</i>	<i>KCNE3</i>	<i>KRT8</i>	<i>LRRC26</i>	<i>MDF1</i>
<i>IGFBP4</i>	<i>KCNH5</i>	<i>KRTAP6-2</i>	<i>LRRC3</i>	<i>MDK</i>
<i>IGFLR1</i>	<i>KCNH7</i>	<i>KSR2</i>	<i>LRRC46</i>	<i>MDM4</i>
<i>IGSF21</i>	<i>KCNJ14</i>	<i>L1CAM</i>	<i>LRRC49</i>	<i>MDN1</i>
<i>IGSF6</i>	<i>KCNJ3</i>	<i>LAMC2</i>	<i>LRRC7</i>	<i>ME3</i>
<i>IGSF9B</i>	<i>KCNMA1</i>	<i>LAMTOR3</i>	<i>LRRC8A</i>	<i>MED12L</i>
<i>IL17RD</i>	<i>KCNN3</i>	<i>LANCL3</i>	<i>LRRC8B</i>	<i>MED13L</i>
<i>IL18RAP</i>	<i>KCNQ3</i>	<i>LARS2</i>	<i>LRRC8D</i>	<i>MEF2A</i>
<i>IL1F5</i>	<i>KCNT1</i>	<i>LCAT</i>	<i>LRRC9</i>	<i>MEF2C</i>
<i>IL3RA</i>	<i>KCTD19</i>	<i>LCE1E</i>	<i>LRRD1</i>	<i>MEG3</i>
<i>IMP3</i>	<i>KCTD4</i>	<i>LCN12</i>	<i>LRRTM1</i>	<i>MEGF9</i>

<i>MEIG1</i>	<i>MRPL54</i>	<i>NAV3</i>	<i>NR2C2</i>	<i>OXR1</i>
<i>MEIS1</i>	<i>MRPS16</i>	<i>NBEA</i>	<i>NR2C2AP</i>	<i>P2RX1</i>
<i>MEIS2</i>	<i>MRPS22</i>	<i>NBEAL1</i>	<i>NR3C2</i>	<i>P2RX7</i>
<i>MEP1A</i>	<i>MRS2</i>	<i>NCAM2</i>	<i>NR4A1</i>	<i>P2RY10</i>
<i>MESDC2</i>	<i>MSX2</i>	<i>NDE1</i>	<i>NR4A2</i>	<i>PAD11</i>
<i>METTL15</i>	<i>MSX3</i>	<i>NDN</i>	<i>NRBP2</i>	<i>PAGR1A</i>
<i>METTL16</i>	<i>MT1</i>	<i>NDNL2</i>	<i>NRIP1</i>	<i>PALM2</i>
<i>MEX3D</i>	<i>MT2</i>	<i>NDRG1</i>	<i>NRL</i>	<i>PALMD</i>
<i>MGAT5</i>	<i>MT3</i>	<i>NDST1</i>	<i>NRP</i>	<i>PANK1</i>
<i>MIA</i>	<i>MTCH2</i>	<i>NDUFA13</i>	<i>NRP1</i>	<i>PARM1</i>
<i>MIB1</i>	<i>MTERF3</i>	<i>NDUFA2</i>	<i>NRSN2</i>	<i>PARP12</i>
<i>MID2</i>	<i>MTRF1L</i>	<i>NDUFA5</i>	<i>NRXN1</i>	<i>PARP8</i>
<i>MINOS1</i>	<i>MUC4</i>	<i>NDUFA8</i>	<i>NT5C1B</i>	<i>PATL1</i>
<i>MIOX</i>	<i>MUSK</i>	<i>NEDD8</i>	<i>NTNG1</i>	<i>PAX1</i>
<i>MIR1191</i>	<i>MVD</i>	<i>NEIL1</i>	<i>NTS</i>	<i>PBLD1</i>
<i>MIR124A-2</i>	<i>MX2</i>	<i>NENF</i>	<i>NTSR2</i>	<i>PCBD2</i>
<i>MIR16-1</i>	<i>MYCBP</i>	<i>NEO1</i>	<i>NUB1</i>	<i>PCDH11X</i>
<i>MIR186</i>	<i>MYCBP2</i>	<i>NFE2L3</i>	<i>NUDT16</i>	<i>PCDH17</i>
<i>MIR25</i>	<i>MYEOV2</i>	<i>NFIB</i>	<i>NUP98</i>	<i>PCDH19</i>
<i>MIR703</i>	<i>MYF5</i>	<i>NFIX</i>	<i>NWD1</i>	<i>PCDH9</i>
<i>MIRG</i>	<i>MYH8</i>	<i>NHLRC2</i>	<i>NXF1</i>	<i>PCDHA12</i>
<i>MLLT1</i>	<i>MYL6</i>	<i>NHLRC3</i>	<i>NXT2</i>	<i>PCDHA2</i>
<i>MLXIP</i>	<i>MYLPF</i>	<i>NHS</i>	<i>NYAP1</i>	<i>PCDHA3</i>
<i>MMP9</i>	<i>MYO16</i>	<i>NID2</i>	<i>NYAP2</i>	<i>PCDHA5</i>
<i>MNAT1</i>	<i>MYT1</i>	<i>NIPAL4</i>	<i>OAZ1</i>	<i>PCDHA6</i>
<i>MOB1A</i>	<i>MYT1L</i>	<i>NKAIN3</i>	<i>OCLN</i>	<i>PCDHA7</i>
<i>MOB1B</i>	<i>N28178</i>	<i>NLRP1A</i>	<i>ODAM</i>	<i>PCDHA9</i>
<i>MOSPD2</i>	<i>N4BP2</i>	<i>NMB</i>	<i>ODF3L1</i>	<i>PCDHAC1</i>
<i>MOXD1</i>	<i>NAA25</i>	<i>NME8</i>	<i>OLFM3</i>	<i>PCDHAC2</i>
<i>MPST</i>	<i>NAA35</i>	<i>NMS</i>	<i>OLFML3</i>	<i>PCDHB10</i>
<i>MPV17</i>	<i>NAALAD2</i>	<i>NOS1</i>	<i>OLFR856-PS1</i>	<i>PCDHB2</i>
<i>MPV17L2</i>	<i>NALCN</i>	<i>NOS1AP</i>	<i>OLIG3</i>	<i>PCDHB5</i>
<i>MRO</i>	<i>NANOS2</i>	<i>NOX4</i>	<i>ONECUT1</i>	<i>PCDHGA1</i>
<i>MRPL14</i>	<i>NANOS3</i>	<i>NPFF</i>	<i>OOSP1</i>	<i>PCDHGA10</i>
<i>MRPL23</i>	<i>NAP1L1</i>	<i>NPM2</i>	<i>OPRM1</i>	<i>PCDHGA11</i>
<i>MRPL27</i>	<i>NAP1L5</i>	<i>NPNT</i>	<i>ORMDL3</i>	<i>PCDHGA12</i>
<i>MRPL32</i>	<i>NAPEPLD</i>	<i>NPPC</i>	<i>OTP</i>	<i>PCDHGA2</i>
<i>MRPL33</i>	<i>NAT9</i>	<i>NPY</i>	<i>OTX1</i>	<i>PCDHGA3</i>
<i>MRPL52</i>	<i>NATD1</i>	<i>NPY6R</i>	<i>OVOL1</i>	<i>PCDHGA4</i>

<i>PCDHGA5</i>	<i>PFDN6</i>	<i>POLD4</i>	<i>PRL8A6</i>	<i>RAB43</i>
<i>PCDHGA6</i>	<i>PFN2</i>	<i>POLK</i>	<i>PRL8A9</i>	<i>RAB5A</i>
<i>PCDHGA7</i>	<i>PGF</i>	<i>POLL</i>	<i>PRMT6</i>	<i>RAD23B</i>
<i>PCDHGA8</i>	<i>PHF19</i>	<i>POLR2J</i>	<i>PROX1</i>	<i>RAD54L2</i>
<i>PCDHGA9</i>	<i>PHKG2</i>	<i>POLR2L</i>	<i>PRPF39</i>	<i>RALB</i>
<i>PCDHGB1</i>	<i>PHLDA1</i>	<i>POLR3E</i>	<i>PRPH</i>	<i>RALGPS1</i>
<i>PCDHGB2</i>	<i>PHOX2A</i>	<i>POMC</i>	<i>PRPSAP1</i>	<i>RAMP3</i>
<i>PCDHGB4</i>	<i>PHTF2</i>	<i>POP5</i>	<i>PRR19</i>	<i>RANBP10</i>
<i>PCDHGB5</i>	<i>PHYH</i>	<i>POR</i>	<i>PRR22</i>	<i>RANBP3</i>
<i>PCDHGB6</i>	<i>PIAS1</i>	<i>POSTN</i>	<i>PRRC2C</i>	<i>RANGRF</i>
<i>PCDHGC3</i>	<i>PIBF1</i>	<i>POT1A</i>	<i>PRSS12</i>	<i>RAPGEF3</i>
<i>PCDHGC4</i>	<i>PIGR</i>	<i>POU1F1</i>	<i>PRSS58</i>	<i>RAPGEF5</i>
<i>PCGF3</i>	<i>PIK3CA</i>	<i>POU3F4</i>	<i>PSD3</i>	<i>RASGEF1B</i>
<i>PCNXL4</i>	<i>PIK3R3</i>	<i>POU4F2</i>	<i>PSMA1</i>	<i>RASSF5</i>
<i>PCSK1N</i>	<i>PITPNB</i>	<i>POU4F3</i>	<i>PSMB3</i>	<i>RASSF8</i>
<i>PCTK2</i>	<i>PITX2</i>	<i>PPAP2A</i>	<i>PSMD7</i>	<i>RAVER1-FDX1L</i>
<i>PCYT1B</i>	<i>PKHD1L1</i>	<i>PPAP2B</i>	<i>PSMG3</i>	<i>RBBP5</i>
<i>PDAP1</i>	<i>PKMYT1</i>	<i>PPARG</i>	<i>PSMG4</i>	<i>RBCK1</i>
<i>PDCD5</i>	<i>PKP4</i>	<i>PPARGC1A</i>	<i>PTAR1</i>	<i>RBL1</i>
<i>PDCD6</i>	<i>PLA2G15</i>	<i>PPFIBP2</i>	<i>PTCH1</i>	<i>RBM26</i>
<i>PDE10A</i>	<i>PLA2G7</i>	<i>PPM1L</i>	<i>PTCRA</i>	<i>RBM38</i>
<i>PDE1A</i>	<i>PLAC1</i>	<i>PPP1R12A</i>	<i>PTEN</i>	<i>RBM42</i>
<i>PDE1C</i>	<i>PLAC9B</i>	<i>PPP1R12B</i>	<i>PTGER4</i>	<i>RBM47</i>
<i>PDE3A</i>	<i>PLAG1</i>	<i>PPP1R3A</i>	<i>PTGR1</i>	<i>RBMS2</i>
<i>PDE4DIP</i>	<i>PLCXD3</i>	<i>PPP2R1A</i>	<i>PTP4A1</i>	<i>RCL1</i>
<i>PDE6B</i>	<i>PLEC</i>	<i>PPP3CC</i>	<i>PTPN4</i>	<i>RCOR1</i>
<i>PDE8B</i>	<i>PLEKHF1</i>	<i>PQLC1</i>	<i>PTPRT</i>	<i>RDH11</i>
<i>PDE9A</i>	<i>PLEKHG5</i>	<i>PRC1</i>	<i>PXT1</i>	<i>RELN</i>
<i>PDGFRL</i>	<i>PLEKHG6</i>	<i>PRDM10</i>	<i>PXYLP1</i>	<i>REPS1</i>
<i>PDK3</i>	<i>PLGRKT</i>	<i>PRDM11</i>	<i>PYGO1</i>	<i>REST</i>
<i>PDLIM1</i>	<i>PLS3</i>	<i>PRDM8</i>	<i>PZP</i>	<i>REXO1</i>
<i>PDPR</i>	<i>PLSCR2</i>	<i>PRDX5</i>	<i>QK</i>	<i>RFFL</i>
<i>PDS5A</i>	<i>PLXNA2</i>	<i>PRG4</i>	<i>RAB11FIP4</i>	<i>RIMS1</i>
<i>PDS51</i>	<i>PLXNA4</i>	<i>PRKCB</i>	<i>RAB15</i>	<i>RIMS3</i>
<i>PDZD9</i>	<i>PLXND1</i>	<i>PRKCD</i>	<i>RAB21</i>	<i>RM11</i>
<i>PEG10</i>	<i>PMAIP1</i>	<i>PRKD3</i>	<i>RAB24</i>	<i>RMRP</i>
<i>PEG3</i>	<i>PNMAL1</i>	<i>PRKRIR</i>	<i>RAB2B</i>	<i>RN45S</i>
<i>PERP</i>	<i>PNMT</i>	<i>PRL</i>	<i>RAB39B</i>	<i>RNASEH2C</i>
<i>PET100</i>	<i>POC1B</i>	<i>PRL5A1</i>	<i>RAB3IP</i>	<i>RNF223</i>

<i>RNFT2</i>	<i>RPS21</i>	<i>SDC3</i>	<i>SIAH1B</i>	<i>SLC46A2</i>
<i>ROMO1</i>	<i>RPS24</i>	<i>SDC4</i>	<i>SIAH3</i>	<i>SLC46A3</i>
<i>RPE</i>	<i>RPS27L</i>	<i>SDK2</i>	<i>SIGLECE</i>	<i>SLC47A1</i>
<i>RPL12</i>	<i>RPS28</i>	<i>SDR39U1</i>	<i>SIGLECF</i>	<i>SLC48A1</i>
<i>RPL13</i>	<i>RPS5</i>	<i>SDR42E1</i>	<i>SIGMAR1</i>	<i>SLC4A4</i>
<i>RPL13A</i>	<i>RPS8</i>	<i>SEC22C</i>	<i>SIK1</i>	<i>SLC52A3</i>
<i>RPL18</i>	<i>RPS9</i>	<i>SELM</i>	<i>SIK2</i>	<i>SLC6A2</i>
<i>RPL18A</i>	<i>RPUSD4</i>	<i>SEMA3C</i>	<i>SIKE1</i>	<i>SLC6A20B</i>
<i>RPL21</i>	<i>RRAGA</i>	<i>SEMA3E</i>	<i>SIX2</i>	<i>SLC6A5</i>
<i>RPL23</i>	<i>RRAGB</i>	<i>SEMA3G</i>	<i>SIX6</i>	<i>SLC7A10</i>
<i>RPL28</i>	<i>RRP1B</i>	<i>SEMA6A</i>	<i>SKINT10</i>	<i>SLC7A5</i>
<i>RPL29</i>	<i>RSBN1</i>	<i>SEPSECS</i>	<i>SKINT11</i>	<i>SLC8A1</i>
<i>RPL31</i>	<i>RSG1</i>	<i>SEPW1</i>	<i>SKOR1</i>	<i>SLC9A7</i>
<i>RPL31-PS12</i>	<i>RSPH1</i>	<i>SERF2</i>	<i>SLA2</i>	<i>SLFN9</i>
<i>RPL35</i>	<i>RSPO3</i>	<i>SERP1</i>	<i>SLC10A5</i>	<i>SLIT1</i>
<i>RPL35A</i>	<i>RTN4R</i>	<i>SERP2</i>	<i>SLC10A7</i>	<i>SLIT2</i>
<i>RPL36</i>	<i>RTP1</i>	<i>SERPINA10</i>	<i>SLC12A5</i>	<i>SMAD1</i>
<i>RPL36AL</i>	<i>RTP2</i>	<i>SERPINB1B</i>	<i>SLC14A1</i>	<i>SMAD4</i>
<i>RPL37</i>	<i>RWDD1</i>	<i>SERPINB7</i>	<i>SLC16A10</i>	<i>SMARCD2</i>
<i>RPL37A</i>	<i>S100A1</i>	<i>SERPINB9C</i>	<i>SLC16A14</i>	<i>SMC6</i>
<i>RPL37RT</i>	<i>S100A10</i>	<i>SERPINI2</i>	<i>SLC16A4</i>	<i>SMIM11</i>
<i>RPL38</i>	<i>S100A16</i>	<i>SERTAD1</i>	<i>SLC1A1</i>	<i>SMIM4</i>
<i>RPL39</i>	<i>S100A6</i>	<i>SESN3</i>	<i>SLC22A23</i>	<i>SMU1</i>
<i>RPL41</i>	<i>S100PBP</i>	<i>SETD5</i>	<i>SLC25A10</i>	<i>SNAPC5</i>
<i>RPL8</i>	<i>S1PR5</i>	<i>SETD6</i>	<i>SLC26A1</i>	<i>SNAPIN</i>
<i>RPLP1</i>	<i>SAA1</i>	<i>SF1</i>	<i>SLC26A2</i>	<i>SNF8</i>
<i>RPLP2</i>	<i>SACS</i>	<i>SF3A2</i>	<i>SLC2A13</i>	<i>SNHG8</i>
<i>RPN1</i>	<i>SALL3</i>	<i>SFN</i>	<i>SLC2A2</i>	<i>SNORA28</i>
<i>RPP21</i>	<i>SAMD5</i>	<i>SFXN5</i>	<i>SLC2A3</i>	<i>SNORA31</i>
<i>RPPH1</i>	<i>SARS</i>	<i>SH2D7</i>	<i>SLC2A9</i>	<i>SNORA68</i>
<i>RPS12</i>	<i>SBF1</i>	<i>SH3BGRL3</i>	<i>SLC30A3</i>	<i>SNORD104</i>
<i>RPS14</i>	<i>SBK1</i>	<i>SH3TC2</i>	<i>SLC35B4</i>	<i>SNORD17</i>
<i>RPS15</i>	<i>SCAMP1</i>	<i>SHANK2</i>	<i>SLC35D1</i>	<i>SNORD2</i>
<i>RPS15A-PS6</i>	<i>SCARB2</i>	<i>SHC3</i>	<i>SLC35E1</i>	<i>SNORD64</i>
<i>RPS16</i>	<i>SCARNA9</i>	<i>SHFM1</i>	<i>SLC35F6</i>	<i>SNORD99</i>
<i>RPS18</i>	<i>SCFD2</i>	<i>SHOC2</i>	<i>SLC36A4</i>	<i>SNRNP70</i>
<i>RPS19</i>	<i>SCOC</i>	<i>SHOX2</i>	<i>SLC39A5</i>	<i>SNRPB</i>
<i>RPS19-PS3</i>	<i>SCTR</i>	<i>SHROOM3</i>	<i>SLC43A3</i>	<i>SNRPD2</i>
<i>RPS20</i>	<i>SCUBE2</i>	<i>SHROOM4</i>	<i>SLC44A1</i>	<i>SNRPG</i>

<i>SNRPN</i>	<i>SST</i>	<i>TCEB2</i>	<i>TMEM179B</i>	<i>TPPP3</i>
<i>SNTB2</i>	<i>ST6GAL2</i>	<i>TCERG1</i>	<i>TMEM191C</i>	<i>TRAPPC6A</i>
<i>SNURF</i>	<i>STAC3</i>	<i>TCF7</i>	<i>TMEM196</i>	<i>TRDMT1</i>
<i>SNX15</i>	<i>STAG3</i>	<i>TCL1</i>	<i>TMEM200A</i>	<i>TRIL</i>
<i>SNX2</i>	<i>STAM2</i>	<i>TCP11L2</i>	<i>TMEM222</i>	<i>TRIM21</i>
<i>SNX22</i>	<i>STAR10</i>	<i>TEDDM2</i>	<i>TMEM232</i>	<i>TRIM40</i>
<i>SNX29</i>	<i>STK11</i>	<i>TEKT1</i>	<i>TMEM245</i>	<i>TRIM43C</i>
<i>SNX30</i>	<i>STK33</i>	<i>TEKT4</i>	<i>TMEM246</i>	<i>TRIM44</i>
<i>SOCS2</i>	<i>STKLD1</i>	<i>TENM1</i>	<i>TMEM256</i>	<i>TRIM56</i>
<i>SOCS4</i>	<i>STMN1</i>	<i>TENM3</i>	<i>TMEM259</i>	<i>TRIP11</i>
<i>SOCS6</i>	<i>STMN4</i>	<i>TENM4</i>	<i>TMEM35</i>	<i>TRP53BP1</i>
<i>SOD1</i>	<i>STOX2</i>	<i>TFAP2A</i>	<i>TMEM42</i>	<i>TRP53INP2</i>
<i>SORCS3</i>	<i>STRA13</i>	<i>TFRC</i>	<i>TMEM47</i>	<i>TRPS1</i>
<i>SORL1</i>	<i>STRN</i>	<i>TGFB3</i>	<i>TMEM53</i>	<i>TSC22D3</i>
<i>SOX4</i>	<i>STX1B</i>	<i>TGFBI</i>	<i>TMEM65</i>	<i>TSPAN2</i>
<i>SOX8</i>	<i>STX8</i>	<i>TH</i>	<i>TMEM67</i>	<i>TSPAN3</i>
<i>SPA17</i>	<i>SUCNR1</i>	<i>THBS4</i>	<i>TMEM74</i>	<i>TSPAN32</i>
<i>SPAG16</i>	<i>SULT2B1</i>	<i>THEMIS</i>	<i>TMEM88</i>	<i>TSPAN4</i>
<i>SPAG9</i>	<i>SUPT4A</i>	<i>THNSL2</i>	<i>TMOD1</i>	<i>TSPAN7</i>
<i>SPATA16</i>	<i>SUSD4</i>	<i>THPO</i>	<i>TNFAIP8L2</i>	<i>TSPYL1</i>
<i>SPHKAP</i>	<i>SV2A</i>	<i>TIMM13</i>	<i>TNFRSF18</i>	<i>TSSC4</i>
<i>SPIC</i>	<i>SV2C</i>	<i>TIMM21</i>	<i>TNFRSF19</i>	<i>TST</i>
<i>SPOCK3</i>	<i>SVS4</i>	<i>TIMM8A1</i>	<i>TNFRSF4</i>	<i>TSTD1</i>
<i>SPPL2A</i>	<i>SYNDIG1L</i>	<i>TIMM8B</i>	<i>TNFSF18</i>	<i>TTBK2</i>
<i>SPRED2</i>	<i>SYNE2</i>	<i>TIPARP</i>	<i>TNKS</i>	<i>TTC28</i>
<i>SPRR2E</i>	<i>SYT14</i>	<i>TLE1</i>	<i>TNNI3</i>	<i>TTC3</i>
<i>SPRR2F</i>	<i>SYT15</i>	<i>TLE4</i>	<i>TNPO1</i>	<i>TTC32</i>
<i>SPRTN</i>	<i>SYTL5</i>	<i>TLE6</i>	<i>TNPO2</i>	<i>TTC37</i>
<i>SPRY2</i>	<i>TACR2</i>	<i>TLX2</i>	<i>TNR</i>	<i>TTC9B</i>
<i>SPTSSA</i>	<i>TAF10</i>	<i>TMC7</i>	<i>TNRC6B</i>	<i>TTK</i>
<i>SPTSSB</i>	<i>TAS2R102</i>	<i>TMCC2</i>	<i>TOB1</i>	<i>TTLA4</i>
<i>SPTY2D1</i>	<i>TAS2R113</i>	<i>TMCO4</i>	<i>TOMM6</i>	<i>TUBA1A</i>
<i>SREK1</i>	<i>TAS2R125</i>	<i>TMED9</i>	<i>TOMM7</i>	<i>TWIST1</i>
<i>SRPX</i>	<i>TAS2R129</i>	<i>TMEFF2</i>	<i>TOX</i>	<i>TXN1</i>
<i>SRRM3</i>	<i>TBCK</i>	<i>TMEM132D</i>	<i>TPBPA</i>	<i>UACA</i>
<i>SRSF1</i>	<i>TBL1X</i>	<i>TMEM136</i>	<i>TPBPB</i>	<i>UBA52</i>
<i>SRSF5</i>	<i>TBX15</i>	<i>TMEM150B</i>	<i>TPD52</i>	<i>UBALD2</i>
<i>SRSF7</i>	<i>TCEAL3</i>	<i>TMEM154</i>	<i>TPH1</i>	<i>UBE2I</i>
<i>SSH1</i>	<i>TCEAL8</i>	<i>TMEM178B</i>	<i>TPP2</i>	<i>UBQLN4</i>

<i>UBR4</i>	<i>UTP6</i>	<i>WFDC21</i>	<i>ZDBF2</i>	<i>ZFP551</i>
<i>UBR7</i>	<i>VAMP5</i>	<i>WFS1</i>	<i>ZDHHC2</i>	<i>ZFP579</i>
<i>UBXN1</i>	<i>VAMP8</i>	<i>WNK3</i>	<i>ZDHHC9</i>	<i>ZFP580</i>
<i>UBXN4</i>	<i>VARS</i>	<i>WRAP53</i>	<i>ZER1</i>	<i>ZFP618</i>
<i>UCN</i>	<i>VAT1</i>	<i>XKR4</i>	<i>ZFAND2B</i>	<i>ZFP619</i>
<i>UGCG</i>	<i>VCAN</i>	<i>XKR7</i>	<i>ZFAND5</i>	<i>ZFP64</i>
<i>UGT2A2</i>	<i>VGLL2</i>	<i>XPNPEP3</i>	<i>ZFAND6</i>	<i>ZFP644</i>
<i>UGT2B37</i>	<i>VKORC1</i>	<i>XPO4</i>	<i>ZFHX4</i>	<i>ZFP688</i>
<i>UHMK1</i>	<i>VNN1</i>	<i>XPO7</i>	<i>ZFP109</i>	<i>ZFP69</i>
<i>UNC13C</i>	<i>VPS13A</i>	<i>XRN1</i>	<i>ZFP169</i>	<i>ZFP81</i>
<i>UNC50</i>	<i>VPS13B</i>	<i>XYLT1</i>	<i>ZFP296</i>	<i>ZFPM2</i>
<i>UNC5D</i>	<i>VPS13C</i>	<i>YME1L1</i>	<i>ZFP35</i>	<i>ZGLP1</i>
<i>UNCX</i>	<i>VPS13D</i>	<i>YOD1</i>	<i>ZFP358</i>	<i>ZHX2</i>
<i>UPF3A</i>	<i>VPS4B</i>	<i>ZBED6</i>	<i>ZFP369</i>	<i>ZIC5</i>
<i>UPK1A</i>	<i>VSTM2B</i>	<i>ZBTB18</i>	<i>ZFP36L2</i>	<i>ZIM1</i>
<i>UPP2</i>	<i>VTI1B</i>	<i>ZBTB20</i>	<i>ZFP382</i>	<i>ZKSCAN16</i>
<i>UPRT</i>	<i>VWA2</i>	<i>ZBTB37</i>	<i>ZFP39</i>	<i>ZKSCAN2</i>
<i>UQCC2</i>	<i>WAC</i>	<i>ZBTB38</i>	<i>ZFP398</i>	<i>ZKSCAN7</i>
<i>USE1</i>	<i>WASF1</i>	<i>ZBTB41</i>	<i>ZFP408</i>	<i>ZPBP</i>
<i>USP3</i>	<i>WASF3</i>	<i>ZBTB7C</i>	<i>ZFP428</i>	<i>ZRANB1</i>
<i>USP34</i>	<i>WBSCR27</i>	<i>ZC3H11A</i>	<i>ZFP442</i>	<i>ZRSR2</i>
<i>USP47</i>	<i>WDFY2</i>	<i>ZC3H12B</i>	<i>ZFP458</i>	
<i>USP53</i>	<i>WDFY3</i>	<i>ZC3H12C</i>	<i>ZFP503</i>	
<i>USP8</i>	<i>WDR17</i>	<i>ZC3H12D</i>	<i>ZFP516</i>	
<i>UTP14B</i>	<i>WFDC1</i>	<i>ZC3HAV1L</i>	<i>ZFP536</i>	

Estrogen response element containing mouse genes (Bordeau *et al.* 2014)

0610006I08RIK	0610030E20RIK	1100001D10RIK	1110011F09RIK	1110027L01RIK
0610006K04RIK	0610030G03RIK	1100001F19RIK	1110012D08RIK	1110028E10RIK
0610006O14RIK	0610030H11RIK	1100001H23RIK	1110012E06RIK	1110028N05RIK
0610006O17RIK	0610033H09RIK	1100001I23RIK	1110012J17RIK	1110030J09RIK
0610007A03RIK	0610033M06RIK	1110001A07RIK	1110012M11RIK	1110030M18RIK
0610007H07RIK	0610034P02RIK	1110001E17RIK	1110013H04RIK	1110031C13RIK
0610007L01RIK	0610037B21RIK	1110001J12RIK	1110013O17RIK	1110031E24RIK
0610007P22RIK	0610037D15RIK	1110001M19RIK	1110014C03RIK	1110031K21RIK
0610008F14RIK	0610037H22RIK	1110001P11RIK	1110014F12RIK	1110032A10RIK
0610009B14RIK	0610038D11RIK	1110002H13RIK	1110014F24RIK	1110032N12RIK
0610009D10RIK	0610038F07RIK	1110002H14RIK	1110014H17RIK	1110033A15RIK
0610009H04RIK	0610038O04RIK	1110002O23RIK	1110014P06RIK	1110033G01RIK
0610009J22RIK	0610039C21RIK	1110003E01RIK	1110015E18RIK	1110033K02RIK
0610009K11RIK	0610039G24RIK	1110003N12RIK	1110015K06RIK	1110033O10RIK
0610009M14RIK	0610039J01RIK	1110003P16RIK	1110015M06RIK	1110034A24RIK
0610009O03RIK	0610039K22RIK	1110003P22RIK	1110017L09RIK	1110034C04RIK
0610009O20RIK	0610039P13RIK	1110004B15RIK	1110017N23RIK	1110035G07RIK
0610010E03RIK	0610040D20RIK	1110004D19RIK	1110017P05RIK	1110035H23RIK
0610010I12RIK	0610040F04RIK	1110004E09RIK	1110018D06RIK	1110036B12RIK
0610010I20RIK	0610040H15RIK	1110005F07RIK	1110018E21RIK	1110036C17RIK
0610010O12RIK	0610041D19RIK	1110005L13RIK	1110018H23RIK	1110036H21RIK
0610011B16RIK	0610041L09RIK	1110005N04RIK	1110018J12RIK	1110037D04RIK
0610011C19RIK	0610042E07RIK	1110006G06RIK	1110018J18RIK	1110038F21RIK
0610011D08RIK	0610043A03RIK	1110006I15RIK	1110018J23RIK	1110038G02RIK
0610011H20RIK	0610043B10RIK	1110007A10RIK	1110018N15RIK	1110038G14RIK
0610011L13RIK	0710001E19RIK	1110007A14RIK	1110018O08RIK	1110038I05RIK
0610011L14RIK	0710001F19RIK	1110007C09RIK	1110018O12RIK	1110038O14RIK
0610011N22RIK	0710001P18RIK	1110007C24RIK	1110019J04RIK	1110039B18RIK
0610012A05RIK	0710007C18RIK	1110007F12RIK	1110019O13RIK	1110049G11RIK
0610012F07RIK	0710008A13RIK	1110007F23RIK	1110020B03RIK	1110051N18RIK
0610012J09RIK	0710008C12RIK	1110007H17RIK	1110020E07RIK	1110053F04RIK
0610012P18RIK	0710008D09RIK	1110008B24RIK	1110021E09RIK	1110054M18RIK
0610013E23RIK	0910001B06RIK	1110008E08RIK	1110021H13RIK	1110054N06RIK
0610013I17RIK	1010001D01RIK	1110008F13RIK	1110025F24RIK	1110054O05RIK
0610016J10RIK	1010001J12RIK	1110008I14RIK	1110025G12RIK	1110055B05RIK
0610016O18RIK	1010001M12RIK	1110008J03RIK	1110025H10RIK	1110055J05RIK
0610025O11RIK	1010001N08RIK	1110008L20RIK	1110025I09RIK	1110058B13RIK
0610027O18RIK	1010001P06RIK	1110008P14RIK	1110025J15RIK	1110059G10RIK

1110059H15RIK	1200011I18RIK	1300017C10RIK	1600002O04RIK	1700008P20RIK
1110061N23RIK	1200013B07RIK	1300017K07RIK	1600010M23RIK	1700009B20RIK
1110063B05RIK	1200013B22RIK	1300018G05RIK	1600012P17RIK	1700009P17RIK
1110063G11RIK	1200013P24RIK	1300018J18RIK	1600013K19RIK	1700010D01RIK
1110064A23RIK	1200014D22RIK	1300019H02RIK	1600013L13RIK	1700010H22RIK
1110064N10RIK	1200014F01RIK	1500001M20RIK	1600013P15RIK	1700010L19RIK
1110064P04RIK	1200014H14RIK	1500002I10RIK	1600014C23RIK	1700010O16RIK
1110065L07RIK	1200014J11RIK	1500003O22RIK	1600014E20RIK	1700010P07RIK
1110067B02RIK	1200014K04RIK	1500004C10RIK	1600015I10RIK	1700011F03RIK
1110067D22RIK	1200015A19RIK	1500005N04RIK	1600016B17RIK	1700011I11RIK
1110068E08RIK	1200016B10RIK	1500006O09RIK	1600016N20RIK	1700012A03RIK
1110069M14RIK	1200016D23RIK	1500009C09RIK	1600017L04RIK	1700012B07RIK
1190003K14RIK	1200016G03RIK	1500009M05RIK	1600017N11RIK	1700012B15RIK
1190005L05RIK	1200017K05RIK	1500010G04RIK	1600020E01RIK	1700012P16RIK
1190005L06RIK	1210002B07RIK	1500010J02RIK	1600022D10RIK	1700013B14RIK
1190005P08RIK	1210002E11RIK	1500010M16RIK	1600025M17RIK	1700013B16RIK
1190005P17RIK	1300002F13RIK	1500011H22RIK	1600025P05RIK	1700013E18RIK
1190006A08RIK	1300002K09RIK	1500012D09RIK	1600029N02RIK	1700013G24RIK
1190006E07RIK	1300003D03RIK	1500012F11RIK	1620401A02RIK	1700013J11RIK
1190006F07RIK	1300003K24RIK	1500015A01RIK	1700001A24RIK	1700013L23RIK
1190007F08RIK	1300003O07RIK	1500015O20RIK	1700001C02RIK	1700013O04RIK
1200002H13RIK	1300003P13RIK	1500019G21RIK	1700001E04RIK	1700014D04RIK
1200003G01RIK	1300004C08RIK	1500019J17RIK	1700001F22RIK	1700014N06RIK
1200003M09RIK	1300004G08RIK	1500019M23RIK	1700003M02RIK	1700014P03RIK
1200003O06RIK	1300006C06RIK	1500031H04RIK	1700006C06RIK	1700016C15RIK
1200004M23RIK	1300006E06RIK	1500031J01RIK	1700006C19RIK	1700016M24RIK
1200006P13RIK	1300006L01RIK	1500031K13RIK	1700006E09RIK	1700017B05RIK
1200007B05RIK	1300006N24RIK	1500032A09RIK	1700007B13RIK	1700017F11RIK
1200007D18RIK	1300006O23RIK	1500032B08RIK	1700007D07RIK	1700017G19RIK
1200008A18RIK	1300007F04RIK	1500032D16RIK	1700007H16RIK	1700017G21RIK
1200009A02RIK	1300007K12RIK	1500032H18RIK	1700007H20RIK	1700018A14RIK
1200009C21RIK	1300010C19RIK	1500032L24RIK	1700007I06RIK	1700018B08RIK
1200009I24RIK	1300011C24RIK	1500032M01RIK	1700007N03RIK	1700018F16RIK
1200009K13RIK	1300011L04RIK	1500034J20RIK	1700007N18RIK	1700018H16RIK
1200010B10RIK	1300011P19RIK	1500035H01RIK	1700008A05RIK	1700018L24RIK
1200010C09RIK	1300012G16RIK	1500041J02RIK	1700008C22RIK	1700019B03RIK
1200011C15RIK	1300013F15RIK	1500041N16RIK	1700008E09RIK	1700019D03RIK
1200011D03RIK	1300013J15RIK	1520402A15RIK	1700008H23RIK	1700019D05RIK
1200011I03RIK	1300015D01RIK	1600002H07RIK	1700008O03RIK	1700019E19RIK

1700019F09RIK	1700028J19RIK	1700084J12RIK	1810015A11RIK	1810046J19RIK
1700019L13RIK	1700028K03RIK	1700086N05RIK	1810015C04RIK	1810046K07RIK
1700019N12RIK	1700028N11RIK	1700092K14RIK	1810015E19RIK	1810047H21RIK
1700019N19RIK	1700028P14RIK	1700095G12RIK	1810015P03RIK	1810049H13RIK
1700019P01RIK	1700029F22RIK	1700095J03RIK	1810018L02RIK	1810054G18RIK
1700020A23RIK	1700029G01RIK	1700096C12RIK	1810018L08RIK	1810054O13RIK
1700020C07RIK	1700029I08RIK	1700102P08RIK	1810018M05RIK	1810055E12RIK
1700020F09RIK	1700029J11RIK	1700104B16RIK	1810019C21RIK	1810057P16RIK
1700020G18RIK	1700029M07RIK	1700105P06RIK	1810020M02RIK	1810058I14RIK
1700020H17RIK	1700030B21RIK	1700109H08RIK	1810021J13RIK	1810058N15RIK
1700020L11RIK	1700030F18RIK	1700110C19RIK	1810022C01RIK	1810059G22RIK
1700020L13RIK	1700030G11RIK	1700111I05RIK	1810022F11RIK	1810059J10RIK
1700020O03RIK	1700030K09RIK	1700112C13RIK	1810022O10RIK	1810061H24RIK
1700021A07RIK	1700034J04RIK	1700112N14RIK	1810024J13RIK	1810061M12RIK
1700021B12RIK	1700034J06RIK	1700112P19RIK	1810024K12RIK	1810062G17RIK
1700021F07RIK	1700034K16RIK	1700113I22RIK	1810027I20RIK	1810062O14RIK
1700021I09RIK	1700036D21RIK	1700120K04RIK	1810028F09RIK	1810063B07RIK
1700021K02RIK	1700043E15RIK	1700121K02RIK	1810029B16RIK	1810073J13RIK
1700021K07RIK	1700045I19RIK	1700122O11RIK	1810029C22RIK	1810073N04RIK
1700021O15RIK	1700048E23RIK	1700123D08RIK	1810029F08RIK	1810073P09RIK
1700021P10RIK	1700051A21RIK	1700123O20RIK	1810030J14RIK	1810074D23RIK
1700021P22RIK	1700051I12RIK	1700124B08RIK	1810030M08RIK	1810074K20RIK
1700022A21RIK	1700054A03RIK	1700126L06RIK	1810030N24RIK	2010000G05RIK
1700022P22RIK	1700054O13RIK	1700127B04RIK	1810031L05RIK	2010001C14RIK
1700023A16RIK	1700054O19RIK	1700127D06RIK	1810033B17RIK	2010001K21RIK
1700023E05RIK	1700058F15RIK	1810008A18RIK	1810033K10RIK	2010001O09RIK
1700023F20RIK	1700058M13RIK	1810009A15RIK	1810033M07RIK	2010002E04RIK
1700023H08RIK	1700060E18RIK	1810009J06RIK	1810034B16RIK	2010002I23RIK
1700023M09RIK	1700060H10RIK	1810009K13RIK	1810034K20RIK	2010002L15RIK
1700024B07RIK	1700061A03RIK	1810010E01RIK	1810035I07RIK	2010003I19RIK
1700024G10RIK	1700061I17RIK	1810010L20RIK	1810036J22RIK	2010003J03RIK
1700024G13RIK	1700061J05RIK	1810011E08RIK	1810037K07RIK	2010003K11RIK
1700025B11RIK	1700063H04RIK	1810011O10RIK	1810037O03RIK	2010004A03RIK
1700025E21RIK	1700064K09RIK	1810011O16RIK	1810038L18RIK	2010005B09RIK
1700025J14RIK	1700067P10RIK	1810012H11RIK	1810038N03RIK	2010005I16RIK
1700026A16RIK	1700069L16RIK	1810013P09RIK	1810038N08RIK	2010005J08RIK
1700026N20RIK	1700072E05RIK	1810014F10RIK	1810041F13RIK	2010008K16RIK
1700027D21RIK	1700081D17RIK	1810014J18RIK	1810041L15RIK	2010009K05RIK
1700027J07RIK	1700081O22RIK	1810014L12RIK	1810046I24RIK	2010011I20RIK

2010012C16RIK	2210401N16RIK	2310003L22RIK	2310024K08RIK	2310046M08RIK
2010012D11RIK	2210402A09RIK	2310003P10RIK	2310026E23RIK	2310046N15RIK
2010012F05RIK	2210402C18RIK	2310004L02RIK	2310028H24RIK	2310047B19RIK
2010013M14RIK	2210403B10RIK	2310004N24RIK	2310030G06RIK	2310047D01
2010015A21RIK	2210403N08RIK	2310005D12RIK	2310030N02RIK	2310047D07RIK
2010015J01RIK	2210404D11RIK	2310005E10RIK	2310031A18RIK	2310047E01RIK
2010015L04RIK	2210404E10RIK	2310005E17RIK	2310032D16RIK	2310047H23RIK
2010100O12RIK	2210404G23RIK	2310005K03RIK	2310032K21RIK	2310047M15RIK
2010109A12RIK	2210407C18RIK	2310005N03RIK	2310034J19RIK	2310047N01RIK
2010109K11RIK	2210407P13RIK	2310005O14RIK	2310034K10RIK	2310047O13RIK
2010110O04RIK	2210409B11RIK	2310007A19RIK	2310034L21RIK	2310050C09RIK
2010111I01RIK	2210409H23RIK	2310007D09RIK	2310035K24RIK	2310051B21RIK
2010200P20RIK	2210412D01RIK	2310007F21RIK	2310036D04RIK	2310051D06RIK
2010203J19RIK	2210413I17RIK	2310008H09RIK	2310036D22RIK	2310051M13RIK
2010208K18RIK	2210414K06RIK	2310008J16RIK	2310037B18RIK	2310051N18RIK
2010301N04RIK	2210415F13RIK	2310009E07RIK	2310037I18RIK	2310056K19RIK
2010305A19RIK	2210415M20RIK	2310009M18RIK	2310037I24RIK	2310057D15RIK
2010305C02RIK	2210417D09RIK	2310010I16RIK	2310039D24RIK	2310057H16RIK
2010306G19RIK	2210418J09RIK	2310011D08RIK	2310039E09RIK	2310057J18RIK
2010308M01RIK	2210421G13RIK	2310011J03RIK	2310039L15RIK	2310057M21RIK
2010315L10RIK	2300001E01RIK	2310012I10RIK	2310040A13RIK	2310058A11RIK
2010316F05RIK	2300002L21RIK	2310012M03RIK	2310040C09RIK	2310061B02RIK
2010317E24RIK	2300002M23RIK	2310012P17RIK	2310040G17RIK	2310061C15RIK
2010320B01RIK	2300003P22RIK	2310014L03RIK	2310040I01RIK	2310061F22RIK
2200001G21RIK	2300005B03RIK	2310014L17RIK	2310040M23RIK	2310061I09RIK
2200002K21RIK	2300006M17RIK	2310015C21RIK	2310041H06RIK	2310061K06RIK
2200008D09RIK	2300006N05RIK	2310015G09RIK	2310042D10RIK	2310061O04RIK
2210003I03RIK	2300007F24RIK	2310015I10RIK	2310042D19RIK	2310066I10RIK
2210008F15RIK	2300008B03RIK	2310015K15RIK	2310042E05RIK	2310066K23RIK
2210010C17RIK	2300009A05RIK	2310015N21RIK	2310042M24RIK	2310067B10RIK
2210010N10RIK	2310001H12RIK	2310016C19RIK	2310043I08RIK	2310067E08RIK
2210013M04RIK	2310001H13RIK	2310016K04RIK	2310043L02RIK	2310067L16RIK
2210018M03RIK	2310001H17RIK	2310020D23RIK	2310044F10RIK	2310068O22RIK
2210018M11RIK	2310001L23RIK	2310020H20RIK	2310044H10RIK	2310069I04RIK
2210021A15RIK	2310001O04RIK	2310020P08RIK	2310044P18RIK	2310075E07RIK
2210021G21RIK	2310002A08RIK	2310021G01RIK	2310045A20RIK	2310075G12RIK
2210021J22RIK	2310002J15RIK	2310021J05RIK	2310045I24RIK	2310075M15RIK
2210023K21RIK	2310003C23RIK	2310024D23RIK	2310045O21RIK	2310076N22RIK
2210401K11RIK	2310003F16RIK	2310024J23RIK	2310046K01RIK	2310076O14RIK

2310079F23RIK	2410015N17RIK	2510009N07RIK	2610020J05RIK	2610205J15RIK
2310079H06RIK	2410017E24RIK	2510010F15RIK	2610020P18RIK	2610207I05RIK
2400002F02RIK	2410018E23RIK	2510012J08RIK	2610022G08RIK	2610207I16RIK
2400003B06RIK	2410018G23RIK	2510019J09RIK	2610022K04RIK	2610207P08RIK
2400003L07RIK	2410018I08RIK	2510026C23RIK	2610023M21RIK	2610209L21RIK
2400004H09RIK	2410018M14RIK	2510027D20RIK	2610024I03RIK	2610300B10RIK
2400006A19RIK	2410021P16RIK	2510027J23RIK	2610024N24RIK	2610301B20RIK
2400008B06RIK	2410025L10RIK	2510027N19RIK	2610025M23RIK	2610301D06RIK
2400009B11RIK	2410027J01RIK	2510038A11RIK	2610027L16RIK	2610301K12RIK
2400010D15RIK	2410039E07RIK	2510039O18RIK	2610028F08RIK	2610304F08RIK
2400010G15RIK	2410043F08RIK	2510040D07RIK	2610028H14RIK	2610307C23RIK
2410001C21RIK	2410043G19RIK	2510048O06RIK	2610028I09RIK	2610315E15RIK
2410001H17RIK	2410050E11RIK	2510049I19RIK	2610029G23RIK	2610318I18RIK
2410002F23RIK	2410075D05RIK	2600002E23RIK	2610029I01RIK	2610507B11RIK
2410002I01RIK	2410077I05RIK	2600005C20RIK	2610030J16RIK	2610507L03RIK
2410002L19RIK	2410081M15RIK	2600005O03RIK	2610030N08RIK	2610507N02RIK
2410003C07RIK	2410089B13RIK	2600009E05RIK	2610033C09RIK	2610510D14RIK
2410003H12RIK	2410089E03RIK	2600010N21RIK	2610034B18RIK	2610510H01RIK
2410003M15RIK	2410090P21RIK	2600011L02RIK	2610034E13RIK	2610510J17RIK
2410004A20RIK	2410095B20RIK	2600013E07RIK	2610034H20RIK	2610510L01RIK
2410004B18RIK	2410104C19RIK	2600013G09RIK	2610034N03RIK	2610511E03RIK
2410004D18RIK	2410112O06RIK	2600016J21RIK	2610036L13RIK	2610511M17RIK
2410004H02RIK	2410116I05RIK	2600017A12RIK	2610037M15RIK	2610524H06RIK
2410004I17RIK	2410124H12RIK	2600017H08RIK	2610039C10RIK	2610528B01RIK
2410004K13RIK	2410133M08RIK	2610001E06RIK	2610039E05RIK	2610528C06RIK
2410004N11RIK	2410141K03RIK	2610002K22RIK	2610040C18RIK	2610528H13RIK
2410005C22RIK	2410153K17RIK	2610003J06RIK	2610041P16RIK	2610528J11RIK
2410005K20RIK	2410166I05RIK	2610005H11RIK	2610042J10RIK	2610528J18RIK
2410005O16RIK	2500002A22RIK	2610010O19RIK	2610042L04RIK	2610529I12RIK
2410008A19RIK	2500002E12RIK	2610011N19RIK	2610043O12RIK	2700002I20RIK
2410008J05RIK	2500002G23RIK	2610014H22RIK	2610100E10RIK	2700002L06RIK
2410008M22RIK	2500002K03RIK	2610016F04RIK	2610100K07RIK	2700008G24RIK
2410011D02RIK	2500003O20RIK	2610016K11RIK	2610101J03RIK	2700018N07RIK
2410012A13RIK	2510002A14RIK	2610018I03RIK	2610101N07RIK	2700019D07RIK
2410012H22RIK	2510002D24RIK	2610019A05RIK	2610108D09RIK	2700023B17RIK
2410012M04RIK	2510004M07RIK	2610019I03RIK	2610200G18RIK	2700027J02RIK
2410015B03RIK	2510006C20RIK	2610019M19RIK	2610202E01RIK	2700029C06RIK
2410015C20RIK	2510006D16RIK	2610019P18RIK	2610204L23RIK	2700029E10RIK
2410015K21RIK	2510008M08RIK	2610020C11RIK	2610205E22RIK	2700029M09RIK

2700033G17RIK	2810013J18RIK	2810433K01RIK	2900083I11RIK	3110052D19RIK
2700033I16RIK	2810014D17RIK	2810439M11RIK	2900083L08RIK	3110054G10RIK
2700038C24RIK	2810014I23RIK	2810441C07RIK	2900084M21RIK	3110056H04RIK
2700038N03RIK	2810017C20RIK	2810441O16RIK	2900090M10RIK	3110057M17RIK
2700038P16RIK	2810019K23RIK	2810449C13RIK	2900092E17RIK	3110065C23RIK
2700048G21RIK	2810022L02RIK	2810449K13RIK	3000003F02RIK	3110079O15RIK
2700049A03RIK	2810027J07	2810451D06RIK	3000004C01RIK	3200001I04RIK
2700050F09RIK	2810028A01RIK	2810452K22RIK	3010015K02RIK	3200002I06RIK
2700055K07RIK	2810029C07RIK	2810457I06RIK	3010020C06	3200002M13RIK
2700059D02RIK	2810031J10RIK	2810459M11RIK	3010027C24RIK	3222401G21RIK
2700060E02RIK	2810032G03RIK	2810460C24RIK	3010027G13RIK	3222401L13RIK
2700061N24RIK	2810036M19RIK	2810465F10RIK	3010033P07RIK	3222401M22RIK
2700062C07RIK	2810037C14RIK	2810474O19RIK	3100001N19RIK	3230401I01RIK
2700063A19RIK	2810037F07RIK	2810477H02RIK	3100002H09RIK	3230401M21RIK
2700063P19RIK	2810039F03RIK	2810484M10RIK	3100002P13RIK	3230401N03RIK
2700067D09RIK	2810043G13RIK	2810489O06RIK	3100004P22RIK	3230401O13RIK
2700068H02RIK	2810047M21RIK	2900002H16RIK	3110001A13RIK	3230402J05RIK
2700069E09RIK	2810048G17RIK	2900005C20RIK	3110001E11RIK	3300001M08RIK
2700071E21RIK	2810052M02RIK	2900006B13RIK	3110001I17RIK	3300002C04RIK
2700082D03RIK	2810055F11RIK	2900006N09RIK	3110001M13RIK	3300002N10RIK
2700083B01RIK	2810403B08RIK	2900008M13RIK	3110002K08RIK	3322402E17RIK
2700083B06RIK	2810403L02RIK	2900010D03RIK	3110005G23RIK	3632410F03RIK
2700084L22RIK	2810406K24RIK	2900010J23RIK	3110006E14RIK	3632410G24RIK
2700085A14RIK	2810407E01RIK	2900024D24RIK	3110007G05RIK	3632451O06RIK
2700085E05RIK	2810410C14RIK	2900029I10RIK	3110010F15RIK	3830408D24RIK
2700086I23RIK	2810411G20RIK	2900040K06RIK	3110018I06RIK	3830408P06RIK
2700087H15RIK	2810418J22RIK	2900045N06RIK	3110023B02RIK	3830421G21RIK
2700091H24RIK	2810422O20RIK	2900052E22RIK	3110027H23RIK	3830613O22RIK
2700094F01RIK	2810423G08RIK	2900052L18RIK	3110030K17RIK	3930402F13RIK
2700094L05RIK	2810425K19RIK	2900052N01RIK	3110031B13RIK	3930402F23RIK
2700097O09RIK	2810427I04RIK	2900053E13RIK	3110037I16RIK	3930402I10RIK
2810003C17RIK	2810428J06RIK	2900054P12RIK	3110038K10RIK	4021401A16RIK
2810003H13RIK	2810429I04RIK	2900055D03RIK	3110038L01RIK	425O18-1
2810003K23RIK	2810429K17RIK	2900057C04RIK	3110041O18RIK	4430402O11RIK
2810008P14RIK	2810430B18RIK	2900057D21RIK	3110041P15RIK	4432405B04RIK
2810011G06RIK	2810431B21RIK	2900069M18RIK	3110043J09RIK	4432409B16
2810011K15RIK	2810432D09RIK	2900073H19RIK	3110043O21RIK	4432409D24RIK
2810011L19RIK	2810432L12RIK	2900075A18RIK	3110048E14RIK	4432411E13RIK
2810013E07RIK	2810432O22RIK	2900076A07RIK	3110049J23RIK	4432412D04RIK

4432412E01RIK	4732481H14RIK	4833444A01RIK	4922502J04RIK	4930455C21RIK
4432416J03RIK	4732486J07RIK	4921501M07	4930400E23RIK	4930463O16RIK
4432417N03RIK	4732490B19RIK	4921501M20RIK	4930400K19RIK	4930466G16RIK
4631409J12	4732493F09RIK	4921503C21RIK	4930401A09RIK	4930467B06RIK
4631412G21RIK	4732496G21RIK	4921504K03RIK	4930401F20	4930467B22RIK
4631422C05RIK	4732497O03RIK	4921507I02RIK	4930402E16RIK	4930468A15RIK
4631426H08RIK	4733401H18RIK	4921508E09RIK	4930402F06RIK	4930469P12RIK
4631427C17RIK	4733401K02RIK	4921508O11RIK	4930402H05RIK	4930470G03RIK
4631428G15	4733401L19RIK	4921509B22RIK	4930404K22RIK	4930470H14RIK
4632408A20RIK	4733401N12RIK	4921509E05RIK	4930412C18RIK	4930470P17RIK
4632411J06RIK	4733401O11RIK	4921510J17RIK	4930414C09RIK	4930471A21RIK
4632412N22RIK	4733401P19RIK	4921511I05RIK	4930415K13	4930471D02RIK
4632413C14RIK	4831440E17RIK	4921513D09RIK	4930415K17RIK	4930471O16RIK
4632413E21RIK	4831440I19RIK	4921513E08RIK	4930415M08RIK	4930474F22RIK
4632415K11RIK	4832406C22	4921513I03RIK	4930418P06RIK	4930479F15RIK
4632415N18RIK	4832412O06RIK	4921513O20RIK	4930425K24RIK	4930479M11RIK
4632416I05RIK	4832426G23RIK	4921517A06RIK	4930425N13RIK	4930481A15RIK
4632417N05RIK	4832428G11	4921517B04RIK	4930429B21RIK	4930481F22RIK
4632419I22RIK	4833403I15RIK	4921517D21RIK	4930429J24RIK	4930483I10
4632427C23RIK	4833406P10RIK	4921517J23RIK	4930430E16RIK	4930485G23RIK
4632428M11RIK	4833408P15RIK	4921517O11RIK	4930431L18RIK	4930488P06RIK
4632432J16RIK	4833411B01RIK	4921520P21RIK	4930432K21RIK	4930500E24RIK
4632435A09RIK	4833412C19RIK	4921521K07RIK	4930432N10RIK	4930500J03RIK
4633401M22RIK	4833413E03RIK	4921522D01RIK	4930435C18RIK	4930503E15RIK
4633402C03RIK	4833413G11RIK	4921522K05RIK	4930438C08RIK	4930503L19RIK
4731413G05RIK	4833414G05RIK	4921524J06RIK	4930438O05RIK	4930504H06RIK
4732406D01RIK	4833414I07RIK	4921524P20RIK	4930441O14RIK	4930505A04RIK
4732415M23RIK	4833419K08RIK	4921525D22	4930442L21RIK	4930505I07RIK
4732416F18	4833420N02RIK	4921528H16RIK	4930444G20RIK	4930506C02RIK
4732427B05	4833422F24RIK	4921528I01RIK	4930445E18RIK	4930506D01RIK
4732429I09RIK	4833424K13RIK	4921530G04RIK	4930447F04RIK	4930506F14RIK
4732437J24RIK	4833424O15RIK	4921532D18RIK	4930447P04RIK	4930509E16RIK
4732440A06	4833425H18RIK	4921533L14RIK	4930449E01RIK	4930510E17RIK
4732452J19RIK	4833426H19RIK	4921535I01RIK	4930451C15RIK	4930511H01RIK
4732459H24RIK	4833427P12RIK	4921536I21RIK	4930451E13RIK	4930511H11RIK
4732461B14RIK	4833431A01RIK	4921536K21RIK	4930451G09RIK	4930511J24RIK
4732462I11RIK	4833435D08RIK	4921538N17RIK	4930451I11RIK	4930511N13RIK
4732465I17RIK	4833436C18RIK	4921539K22RIK	4930453N24RIK	4930511O11RIK
4732474A20RIK	4833438B11RIK	4922501H04RIK	4930455B06RIK	4930512M02RIK

4930513F16RIK	4930555F03RIK	4931417G12RIK	4933406B17RIK	4933427G17RIK
4930513O06RIK	4930555I21RIK	4931417M11RIK	4933406J08RIK	4933428C20RIK
4930515G01RIK	4930556L07RIK	4931426N11RIK	4933407A11RIK	4933428G20RIK
4930517G15RIK	4930557A04RIK	4931428L18RIK	4933407H18RIK	4933429D11RIK
4930519G04RIK	4930560D03RIK	4931429L15RIK	4933407K12RIK	4933430F08RIK
4930519L02RIK	4930562A09RIK	4931431L11RIK	4933407L21RIK	4933430L12RIK
4930519N13RIK	4930562N12RIK	4932408B21	4933408F15	4933432B09RIK
4930521A18RIK	4930563C04RIK	4932409F11RIK	4933409E02RIK	4933432I09RIK
4930523C07RIK	4930563D23RIK	4932414K18	4933409N07RIK	4933432K11RIK
4930523M17RIK	4930564N15RIK	4932414N04RIK	4933411B09RIK	4933433B15RIK
4930524E20RIK	4930565D16RIK	4932415O19	4933411C14RIK	4933433C09RIK
4930525N13RIK	4930568D16RIK	4932416A11RIK	4933411G06RIK	4933433D23RIK
4930526B11RIK	4930569K13RIK	4932416A15	4933411J24RIK	4933434G05RIK
4930527G07RIK	4930571C24RIK	4932417H02RIK	4933413B09RIK	4933434I20RIK
4930527J03RIK	4930572G02RIK	4932418K24	4933413G11RIK	4933434M16RIK
4930527L09RIK	4930572I07RIK	4932420K09	4933413G19RIK	4933435A13RIK
4930528H02RIK	4930572L20RIK	4932422M17RIK	4933414E04RIK	4933435E02RIK
4930528H21RIK	4930572O07RIK	4932432N04RIK	4933415A04RIK	4933435E20RIK
4930529C04RIK	4930573H18RIK	4932434G09RIK	4933415I03RIK	4933436I01RIK
4930529M08RIK	4930578F03RIK	4932437H03	4933415L06RIK	4933436O18RIK
4930529M09RIK	4930578I06RIK	4932438A13RIK	4933416E05RIK	4933439B08RIK
4930532L20RIK	4930579A11RIK	4932438H23RIK	4933417L02RIK	4933439F10RIK
4930533G20RIK	4930579F01RIK	4932438M10	4933417L10RIK	4933439J11RIK
4930534P07RIK	4930579G24RIK	4932443D16RIK	4933417N20RIK	4933440J22RIK
4930535B06RIK	4930579J09RIK	4932703P14	4933417O08RIK	4933440M02RIK
4930535F04RIK	4930580F03RIK	4933400E14RIK	4933421G18RIK	5031401C21RIK
4930538D17RIK	4930581F22RIK	4933402G07RIK	4933421L13RIK	5031407H10
4930539A06RIK	4930583C14RIK	4933402J24RIK	4933424B01RIK	5031409G22RIK
4930544L10RIK	4930583K01RIK	4933402K10RIK	4933424G06RIK	5031425F14RIK
4930545L08RIK	4930588G17RIK	4933402P03RIK	4933424M23RIK	5031434M05RIK
4930546K05RIK	4930588N13RIK	4933403C17RIK	4933425F06RIK	5031439G07RIK
4930547K05RIK	4930590A17RIK	4933403G14RIK	4933425K02RIK	5033402L14RIK
4930550B20RIK	4930592A21RIK	4933403M22RIK	4933425L03RIK	5033406L14RIK
4930550C14RIK	4931405B09RIK	4933404A18RIK	4933425L06RIK	5033413A03RIK
4930550G17RIK	4931406C07RIK	4933404G15RIK	4933425O20RIK	5033415K03RIK
4930550L24RIK	4931406O17RIK	4933405H16RIK	4933426E21RIK	5033430I15RIK
4930552P12RIK	4931412F17	4933405K01RIK	4933426G20RIK	5133400C09RIK
4930553M18RIK	4931413A09RIK	4933405L10RIK	4933426L22RIK	5133401N09RIK
4930554C01RIK	4931417E11RIK	4933405P08RIK	4933427E13RIK	5230400G24RIK

5230400J09RIK	5730409F23RIK	5730599O09RIK	6030470M02RIK	6430550D23RIK
5330410G16RIK	5730409G15RIK	5830400A04RIK	6230400G14RIK	6430571L13RIK
5330415H22RIK	5730414C17RIK	5830400N10RIK	6230418K12RIK	6430573B13RIK
5330421F07RIK	5730415P04RIK	5830403F22RIK	6230420N16RIK	6430573F11RIK
5330426D11RIK	5730419I09RIK	5830405N20RIK	6230421J19RIK	6430584G11RIK
5330426L24RIK	5730419O14RIK	5830406C15RIK	6230425C21RIK	6430598A04RIK
5330427D05RIK	5730420B22RIK	5830406J20RIK	6230429P13RIK	6430598J10RIK
5330435L01RIK	5730422A13RIK	5830408F06RIK	6330404A12RIK	6430601A21RIK
5330439J01RIK	5730427C23RIK	5830411E10RIK	6330404M18RIK	6430703N11
5330440G10RIK	5730427N09RIK	5830411N06RIK	6330406P08RIK	6430704M03RIK
5430400H23RIK	5730442K12RIK	5830415F09RIK	6330408J11RIK	6430706C13RIK
5430401O09RIK	5730445F03RIK	5830417C01RIK	6330408P19RIK	6530401L14RIK
5430402E10RIK	5730448P06RIK	5830426C09RIK	6330410L21RIK	6530403F17RIK
5430405K24RIK	5730453I16RIK	5830426I05RIK	6330410P18RIK	6530406P05RIK
5430408M01RIK	5730455O13RIK	5830427H10RIK	6330415L08RIK	6530409C15RIK
5430411C10RIK	5730463C12RIK	5830433M19RIK	6330415N05RIK	6530415H11RIK
5430411K18RIK	5730469M10RIK	5830443C21RIK	6330416C07RIK	6530416A09RIK
5430416O09RIK	5730470L24RIK	5830443L24RIK	6330416L11RIK	6530418L21RIK
5430420C16RIK	5730476P14RIK	5830457J20RIK	6330417G02RIK	6530420C11RIK
5430425C04RIK	5730478M09RIK	5830457O10RIK	6330500A18RIK	6620401K05RIK
5430425K04RIK	5730485C17RIK	5830458K16RIK	6330516O20RIK	6720407G21RIK
5430428G01RIK	5730493B19RIK	5830462I21RIK	6330530A05RIK	6720456B07RIK
5430429M05RIK	5730494G16RIK	5830467P10RIK	6330544B05RIK	6720460F02RIK
5430431G03RIK	5730502D15RIK	5830480G12RIK	6330548O06RIK	6720460I06RIK
5430437K10RIK	5730505K17RIK	5830482F20RIK	6330551K01RIK	6720461J16RIK
5430438H03RIK	5730507A09RIK	5832424M12	6330563C09RIK	6720465F12RIK
5530400B01RIK	5730509E04RIK	5930402B05RIK	6330576B01RIK	6720469N11RIK
5530401A14RIK	5730510P18RIK	5930405J04RIK	6330577E15RIK	6720474K14RIK
5530601I19RIK	5730519E19RIK	5930416I19RIK	6330580J24RIK	6720480F16RIK
5630401D06RIK	5730522G15RIK	5930422O12RIK	6330591G05RIK	6720481I12
5630401M14RIK	5730525G14RIK	5930431H10	6430407N22	6720484B16
5730402C15RIK	5730537D05RIK	5930434B04RIK	6430511D02RIK	6820401C03
5730403J10RIK	5730544D12RIK	6030430C21	6430513E09RIK	6820428L09
5730405M13RIK	5730551F12RIK	6030430O11	6430517J16RIK	6820429M01
5730406I15RIK	5730552M22RIK	6030432N09RIK	6430526J12RIK	7420700F21
5730407K14RIK	5730576P14RIK	6030435N04	6430526N21RIK	7420700M05RIK
5730408I11RIK	5730583K22RIK	6030449J21	6430527G18RIK	7530419J18RIK
5730408I21RIK	5730589K01RIK	6030465J18RIK	6430529J03RIK	8030423J24RIK
5730409E15RIK	5730592L21RIK	6030466N05RIK	6430549H08RIK	8030425L21

8030448M07	9130011B11RIK	9330166I04	9530004P13RIK	9930035G10RIK
8030460J03RIK	9130011E15RIK	9330170P05RIK	9530006B08RIK	9930038B18RIK
8030475D13RIK	9130011J15RIK	9330175N02	9530006G20RIK	9930039A11RIK
8430401C09RIK	9130012B15RIK	9330182L06RIK	9530018I07RIK	9930111I18RIK
8430401K06RIK	9130012G04RIK	9330186A19RIK	9530019H02RIK	A030002D08RIK
8430404F20RIK	9130017A15RIK	9330196J05RIK	9530020I12RIK	A030004J04RIK
8430406N16RIK	9130017C17RIK	9330199A09RIK	9530021D13RIK	A030005L19RIK
8430408H12RIK	9130017N09RIK	9430010P06RIK	9530023G02	A030009A06
8430410J10RIK	9130019O22RIK	9430020K01	9530029I04RIK	A030009H04RIK
8430415E04RIK	9130020G10RIK	9430022A14	9530033F24RIK	A030014E15RIK
8430417G17RIK	9130022A11RIK	9430023L20RIK	9530034F03RIK	A130006I12RIK
8430417G19RIK	9130023G24RIK	9430024C03RIK	9530043P15RIK	A130010J15RIK
8430419L09RIK	9130023N17RIK	9430024E24RIK	9530044G19	A130010L24
8430427K15	9130206I24RIK	9430025F20RIK	9530051K01RIK	A130012E19RIK
8430430L24RIK	9130208G10	9430027B09RIK	9530056K15RIK	A130038L21RIK
8430437G08RIK	9130222L19RIK	9430029K10RIK	9530074E10RIK	A130039I20RIK
8430437G11RIK	9130402C12RIK	9430031J16RIK	9530077C24RIK	A130042E20
9030012M21	9130403P13RIK	9430034D17RIK	9530091C08RIK	A130077B15RIK
9030022E12RIK	9130404D14RIK	9430038B09RIK	9530098N22RIK	A130092J06RIK
9030227G01RIK	9130411I17RIK	9430059D04RIK	9630005C02	A230016E22
9030406N13RIK	9130413I22RIK	9430060M22RIK	9630008F14	A230025G20
9030409C19RIK	9130417I07RIK	9430065N20RIK	9630016P15RIK	A230025O18
9030409G11RIK	9230101F08RIK	9430066I12RIK	9630020G10RIK	A230034F01RIK
9030420J04RIK	9230102I19RIK	9430069J07	9630036J22	A230048G03RIK
9030421L11RIK	9230102N17RIK	9430070G18	9630036L12RIK	A230051G13
9030425C21RIK	9230106D23	9430073N08RIK	9630039I18RIK	A230053A07RIK
9030425E11RIK	9230106L14RIK	9430075G12RIK	9630050M13RIK	A230058J24
9030612E09RIK	9230110F15RIK	9430077A04RIK	9630054P07RIK	A230062G08RIK
9030612I22RIK	9230111C08RIK	9430077C05RIK	9630059J11	A230067G21
9030616F16	9230116L04RIK	9430078C22RIK	9630060C05RIK	A230072I16RIK
9030623N16RIK	9330104G04RIK	9430078K24RIK	9830006J20RIK	A230084G12RIK
9030624C24RIK	9330128H10RIK	9430088F20	9830131G07	A230084J22
9030625A04RIK	9330132E09RIK	9430092A03RIK	9830160G03RIK	A230085M13RIK
9030625G08RIK	9330132O05RIK	9430095K15RIK	9830160H19RIK	A230102L03RIK
9130006A14RIK	9330140I15RIK	9430096L06RIK	9830169C18RIK	A230106M20
9130008F23RIK	9330151F09RIK	9430097D07RIK	9930014A18RIK	A230108P17
9130009C22RIK	9330155M09RIK	9430098E02RIK	9930016O13	A330015D16RIK
9130009D18RIK	9330158F14RIK	9530002B09RIK	9930022D16RIK	A330021E22RIK
9130010J17RIK	9330166G04RIK	9530003A05	9930033G19RIK	A330041G23RIK

A330041N06	A630031M04RIK	A930013K19	AATK	ACR
A330042I05RIK	A630056B21RIK	A930014C21RIK	AB030188	ACRBP
A330051M14RIK	A630065K24RIK	A930017N06RIK	AB030198	ACRVI
A330070M20RIK	A630076O07	A930019C19RIK	AB041544	ACTA1
A330097D03RIK	A630077B13RIK	A930019D11RIK	AB041545	ACTG
A330103J02RIK	A630086P08RIK	A930021C24RIK	AB041549	ACTG2
A330104H05RIK	A630091E08RIK	A930025D01RIK	AB041550	ACTL
A330106H01RIK	A730011E05RIK	A930026L03RIK	AB041568	ACTL6
A430025D11RIK	A730011F23RIK	A930027H06RIK	AB041661	ACTL7A
A430081P20RIK	A730016F12RIK	A930027K05RIK	AB041662	ACTL7B
A430103C15RIK	A730017C20RIK	A930031E15RIK	AB041803	ACTN1
A430105I19	A730018C14RIK	A930031F18RIK	ABCA1	ACTN4
A430106B11RIK	A730032D07RIK	A930031L14RIK	ABCA6	ACT
A430107J06RIK	A730039N16RIK	A930033C23RIK	ABCA7	ACVR1B
A430107P09RIK	A730055F12RIK	A930038C07RIK	ABCB11	ACVRIP1
A430109M18RIK	A730055L17RIK	A930040J07	ABCB1A	ACY1
A430109M19RIK	A730060M23RIK	AA238765	ABCB6	ADA
A430110D14RIK	A730063M14RIK	AA407306	ABCB9	ADAM12
A530016O06RIK	A730069N07RIK	AA407588	ABCC10	ADAM19
A530023P05	A730096F01	AA407995	ABCC3	ADAM23
A530024P18	A730098A19RIK	AA409164	ABCD3	ADAM25
A530027J04RIK	A830007P12RIK	AA409446	ABCG1	ADAM28
A530037C04RIK	A830014L09RIK	AA410078	ABO	ADAM33
A530053G22RIK	A830021K08RIK	AA536972	ABP1	ADAM5
A530057A03	A830039B04RIK	AA589507	ABTB1	ADAM7
A530057M15RIK	A830048P05	AA589632	ACAA1	ADAMTS-12
A530081C03RIK	A830053O21RIK	AA591047	ACADS	ADAMTS16
A530081L18RIK	A830059A17RIK	AA617276	ACAS2L	ADAMTS19
A530088H08RIK	A830073O21RIK	AA673488	ACAT1	ADAMTS4
A530089G06	A830084F09RIK	AA691260	ACATE3	ADAMTS8
A530094D01	A830094I09RIK	AA959601	ACCN2	ADAMTS9
A530095G11	A830096D10RIK	AA959742	ACF	ADAT1
A630014C11RIK	A830097C19	AA960365	ACINUS	ADCY2
A630014H24	A930001N09RIK	AA968343	ACO2	ADCY3
A630018G05RIK	A930009E05RIK	AA986709	ACOX1	ADCY4
A630023P12RIK	A930010E21RIK	AAMP	ACOX2	ADCY6
A630024J02RIK	A930011L17	AANAT	ACOX3	ADCY7
A630026L20	A930011O12RIK	AASS	ACP2	ADCY8
A630029F06	A930012L18RIK	AATF	ACP5	ADCY9

<i>ADD2</i>	<i>AI267078</i>	<i>AI481105</i>	<i>AI845279</i>	<i>AL033311</i>
<i>ADH5</i>	<i>AI314111</i>	<i>AI481402</i>	<i>AI850305</i>	<i>ALAS1</i>
<i>ADH7</i>	<i>AI314783</i>	<i>AI481750</i>	<i>AI851877</i>	<i>ALCAM</i>
<i>ADN</i>	<i>AI315068</i>	<i>AI504353</i>	<i>AI853319</i>	<i>ALDH1A3</i>
<i>ADORA2B</i>	<i>AI315208</i>	<i>AI504701</i>	<i>AI853514</i>	<i>ALDH1B1</i>
<i>ADORA3</i>	<i>AI323585</i>	<i>AI504961</i>	<i>AI854251</i>	<i>ALDH2</i>
<i>ADPRTL2</i>	<i>AI326867</i>	<i>AI505034</i>	<i>AI874665</i>	<i>ALDH3A1</i>
<i>ADPRTL3</i>	<i>AI326906</i>	<i>AI552599</i>	<i>AI876593</i>	<i>ALDH7A1</i>
<i>ADRA1B</i>	<i>AI326939</i>	<i>AI573938</i>	<i>AI894218</i>	<i>ALDH9A1</i>
<i>ADRA2C</i>	<i>AI413471</i>	<i>AI591529</i>	<i>AI931714</i>	<i>ALG12</i>
<i>ADRM1</i>	<i>AI414849</i>	<i>AI593353</i>	<i>AI956815</i>	<i>ALKBH</i>
<i>ADSS1</i>	<i>AI415282</i>	<i>AI607300</i>	<i>AI987662</i>	<i>ALOX12B</i>
<i>AEBP1</i>	<i>AI415330</i>	<i>AI643885</i>	<i>AIBZIP</i>	<i>ALOX12E</i>
<i>AF006998</i>	<i>AI426038</i>	<i>AI646725</i>	<i>AICDA</i>	<i>ALOX15</i>
<i>AF229032</i>	<i>AI426465</i>	<i>AI647528</i>	<i>AIF1</i>	<i>ALOXE3</i>
<i>AF261233</i>	<i>AI426782</i>	<i>AI647760</i>	<i>AIG1</i>	<i>ALX3</i>
<i>AFG3L1</i>	<i>AI427833</i>	<i>AI648866</i>	<i>AIPL1</i>	<i>AMBP</i>
<i>AFM</i>	<i>AI428238</i>	<i>AI649009</i>	<i>AIRE</i>	<i>AMY2</i>
<i>AGA</i>	<i>AI428804</i>	<i>AI649385</i>	<i>AJ237586</i>	<i>ANAPC5</i>
<i>AGPAT1</i>	<i>AI428889</i>	<i>AI661311</i>	<i>AJ430384</i>	<i>ANGPTL4</i>
<i>AGPAT3</i>	<i>AI429152</i>	<i>AI661438</i>	<i>AK3L</i>	<i>ANGRP</i>
<i>AGPT4</i>	<i>AI429612</i>	<i>AI661919</i>	<i>AK4</i>	<i>ANK</i>
<i>AGRP</i>	<i>AI429613</i>	<i>AI664004</i>	<i>AK5</i>	<i>ANK1</i>
<i>AGT</i>	<i>AI447493</i>	<i>AI666698</i>	<i>AKAP10</i>	<i>ANK3</i>
<i>AHCY</i>	<i>AI447729</i>	<i>AI666765</i>	<i>AKAP12</i>	<i>ANKHZN</i>
<i>AHCYL1</i>	<i>AI447804</i>	<i>AI785303</i>	<i>AKAP2</i>	<i>ANKRD2</i>
<i>AI047808</i>	<i>AI447928</i>	<i>AI787289</i>	<i>AKAP8</i>	<i>ANKRD5</i>
<i>AI060904</i>	<i>AI447930</i>	<i>AI788959</i>	<i>AKP5</i>	<i>ANP32B</i>
<i>AI115348</i>	<i>AI448302</i>	<i>AI790298</i>	<i>AKR1A4</i>	<i>ANXA1</i>
<i>AI118089</i>	<i>AI448583</i>	<i>AI790326</i>	<i>AKR1B7</i>	<i>ANXA13</i>
<i>AI118201</i>	<i>AI451006</i>	<i>AI790744</i>	<i>AKR1C18</i>	<i>ANXA3</i>
<i>AI173001</i>	<i>AI451340</i>	<i>AI834978</i>	<i>AL022610</i>	<i>ANXA5</i>
<i>AI181996</i>	<i>AI461653</i>	<i>AI836109</i>	<i>AL022641</i>	<i>ANXA6</i>
<i>AI194308</i>	<i>AI461933</i>	<i>AI837757</i>	<i>AL023001</i>	<i>ANXA7</i>
<i>AI195023</i>	<i>AI462012</i>	<i>AI840044</i>	<i>AL024016</i>	<i>ANXA9</i>
<i>AI195350</i>	<i>AI463271</i>	<i>AI840675</i>	<i>AL024077</i>	<i>AOAH</i>
<i>AI255964</i>	<i>AI467246</i>	<i>AI841135</i>	<i>AL024210</i>	<i>AOC3</i>
<i>AI256840</i>	<i>AI480570</i>	<i>AI841487</i>	<i>AL024221</i>	<i>AP1G1</i>
<i>AI266900</i>	<i>AI480612</i>	<i>AI842396</i>	<i>AL024279</i>	<i>AP1G2</i>

<i>AP1M2</i>	<i>ARHV</i>	<i>ATP5L</i>	<i>AW121933</i>	<i>B230210E21RIK</i>
<i>AP2A2</i>	<i>ARL2</i>	<i>ATP6V0D1</i>	<i>AW124591</i>	<i>B230214N19RIK</i>
<i>AP2M1</i>	<i>ARL6IP</i>	<i>ATP6V1D</i>	<i>AW125391</i>	<i>B230219I23</i>
<i>AP3D</i>	<i>ARL6IP4</i>	<i>ATP6V1E2</i>	<i>AW125441</i>	<i>B230312A22RIK</i>
<i>AP4M1</i>	<i>ARPC1A</i>	<i>ATP6V1G1</i>	<i>AW125446</i>	<i>B230331L10RIK</i>
<i>APBA2BP</i>	<i>ARPC2</i>	<i>ATP6V1G2</i>	<i>AW209491</i>	<i>B230339H12RIK</i>
<i>APBA3</i>	<i>ART1</i>	<i>ATP7A</i>	<i>AW212394</i>	<i>B230340J04RIK</i>
<i>APBB1IP</i>	<i>ART5</i>	<i>ATP7B</i>	<i>AW259676</i>	<i>B230354B21RIK</i>
<i>APBB2</i>	<i>ARTS1</i>	<i>ATP8A1</i>	<i>AW319638</i>	<i>B230358H09RIK</i>
<i>APCS</i>	<i>ARVCF</i>	<i>ATP9B</i>	<i>AW413091</i>	<i>B230363K08RIK</i>
<i>APLP1</i>	<i>ASAH3</i>	<i>ATRX</i>	<i>AW413625</i>	<i>B230365D05RIK</i>
<i>APOA1</i>	<i>ASB1</i>	<i>AU016405</i>	<i>AW455481</i>	<i>B230365F16RIK</i>
<i>APOA4</i>	<i>ASB14</i>	<i>AU018638</i>	<i>AW456442</i>	<i>B230369F24RIK</i>
<i>APOB48R</i>	<i>ASB16</i>	<i>AU019489</i>	<i>AW489850</i>	<i>B230398H18RIK</i>
<i>APOC3</i>	<i>ASB-18</i>	<i>AU023234</i>	<i>AW489976</i>	<i>B3GALT4</i>
<i>APOH</i>	<i>ASB3</i>	<i>AU040320</i>	<i>AW491445</i>	<i>B3GALT6</i>
<i>APPBP1</i>	<i>ASB6</i>	<i>AU040575</i>	<i>AW492152</i>	<i>B3GNT1</i>
<i>APRT</i>	<i>ASB8</i>	<i>AU040576</i>	<i>AW494535</i>	<i>B3GNT5</i>
<i>APS</i>	<i>ASCL3</i>	<i>AU040950</i>	<i>AW536104</i>	<i>B3GNT7</i>
<i>AQP2</i>	<i>ASC</i>	<i>AU041707</i>	<i>AW545847</i>	<i>B430006D22RIK</i>
<i>AQP3</i>	<i>ASH2L</i>	<i>AU042952</i>	<i>AW549877</i>	<i>B430108F07RIK</i>
<i>AQP4</i>	<i>ASL</i>	<i>AU044684</i>	<i>AW553050</i>	<i>B430201G11RIK</i>
<i>AQP5</i>	<i>ASML3A</i>	<i>AU045678</i>	<i>AW558560</i>	<i>B430306N03RIK</i>
<i>ARBP</i>	<i>ASS1</i>	<i>AUP1</i>	<i>AW743042</i>	<i>B4GALT3</i>
<i>ARCNI</i>	<i>ASTN2</i>	<i>AV046776</i>	<i>AW822216</i>	<i>B4GALT5</i>
<i>ARD1</i>	<i>ATE1</i>	<i>AVP</i>	<i>AW822253</i>	<i>B4GALT6</i>
<i>ARF3</i>	<i>ATF3</i>	<i>AW011752</i>	<i>AW990386</i>	<i>B4GALT7</i>
<i>ARFGAP1</i>	<i>ATF4</i>	<i>AW045245</i>	<i>AXCAM</i>	<i>B630009I04RIK</i>
<i>ARG2</i>	<i>ATF5</i>	<i>AW046014</i>	<i>AXUD1</i>	<i>B830017A01RIK</i>
<i>ARHB</i>	<i>ATOH1</i>	<i>AW047143</i>	<i>AZII</i>	<i>B830026H24RIK</i>
<i>ARHD</i>	<i>ATOX1</i>	<i>AW048023</i>	<i>B130005I07RIK</i>	<i>B930001P07RIK</i>
<i>ARHE</i>	<i>ATP10A</i>	<i>AW048498</i>	<i>B130009M24RIK</i>	<i>B930011H20RIK</i>
<i>ARHGAP4</i>	<i>ATP1A1</i>	<i>AW049390</i>	<i>B130016L12RIK</i>	<i>B930025P03RIK</i>
<i>ARHGDIG</i>	<i>ATP1B1</i>	<i>AW049604</i>	<i>B130016O10RIK</i>	<i>B930037P14RIK</i>
<i>ARHGEF1</i>	<i>ATP2A3</i>	<i>AW049765</i>	<i>B130039D23RIK</i>	<i>B930041F14RIK</i>
<i>ARHGEF11</i>	<i>ATP4B</i>	<i>AW061076</i>	<i>B130055L10RIK</i>	<i>B930044J06</i>
<i>ARHGEF7</i>	<i>ATP5A1</i>	<i>AW109744</i>	<i>B230106I24RIK</i>	<i>B930062P21RIK</i>
<i>ARHJ</i>	<i>ATP5J2</i>	<i>AW111961</i>	<i>B230207H15RIK</i>	<i>B930067F20RIK</i>
<i>ARHN</i>	<i>ATP5K</i>	<i>AW121052</i>	<i>B230208J24RIK</i>	<i>B930096L08RIK</i>

<i>BAAT</i>	<i>BC024092</i>	<i>BHLHB2</i>	<i>C030001A19RIK</i>	<i>C1QG</i>
<i>BACE2</i>	<i>BC024131</i>	<i>BHLHB4</i>	<i>C030002O17RIK</i>	<i>C1QR1</i>
<i>BACH</i>	<i>BC025519</i>	<i>BICC1</i>	<i>C030005H24RIK</i>	<i>C1QRF</i>
<i>BAD</i>	<i>BC025586</i>	<i>BICD2</i>	<i>C030006K11RIK</i>	<i>C1SB</i>
<i>BAG3</i>	<i>BC025890</i>	<i>BID3</i>	<i>C030014M07RIK</i>	<i>C2</i>
<i>BAI1</i>	<i>BC026401</i>	<i>BIKLK</i>	<i>C030017C09RIK</i>	<i>C230001H08RIK</i>
<i>BARD1</i>	<i>BC027342</i>	<i>BIN3</i>	<i>C030018L16RIK</i>	<i>C230008H04RIK</i>
<i>BARX1</i>	<i>BC028953</i>	<i>BING4</i>	<i>C030022K24RIK</i>	<i>C230009H10RIK</i>
<i>BASPI</i>	<i>BC030314</i>	<i>BIRC1A</i>	<i>C030025P15RIK</i>	<i>C230030N03</i>
<i>BAT1A</i>	<i>BC030934</i>	<i>BIRC2</i>	<i>C030033M19RIK</i>	<i>C230055H22RIK</i>
<i>BAT8</i>	<i>BC031365</i>	<i>BLK</i>	<i>C030039E19RIK</i>	<i>C230075L19RIK</i>
<i>BATF</i>	<i>BC031407</i>	<i>BLM</i>	<i>C030044C12RIK</i>	<i>C230078B22</i>
<i>BB026216</i>	<i>BC031748</i>	<i>BLU</i>	<i>C030044P22RIK</i>	<i>C230078M14</i>
<i>BBP</i>	<i>BC034099</i>	<i>BM88</i>	<i>C030048B08RIK</i>	<i>C230088J01RIK</i>
<i>BC002292</i>	<i>BC034204</i>	<i>BMF</i>	<i>C030048H19RIK</i>	<i>C230094F14RIK</i>
<i>BC003236</i>	<i>BC034653</i>	<i>BMP2</i>	<i>C030048H21RIK</i>	<i>C230097P10</i>
<i>BC003251</i>	<i>BC038058</i>	<i>BMP8A</i>	<i>C030048J01RIK</i>	<i>C330001H22RIK</i>
<i>BC003266</i>	<i>BCAS3</i>	<i>BMP8B</i>	<i>C130010K08RIK</i>	<i>C330001K17RIK</i>
<i>BC003332</i>	<i>BCAT2</i>	<i>BMPR1B</i>	<i>C130023C01RIK</i>	<i>C330006K01RIK</i>
<i>BC003494</i>	<i>BCDO1</i>	<i>BOK</i>	<i>C130031G21RIK</i>	<i>C330008I15RIK</i>
<i>BC003945</i>	<i>BCKDHA</i>	<i>BRAL1</i>	<i>C130031J23</i>	<i>C330013D05RIK</i>
<i>BC005471</i>	<i>BCKDHB</i>	<i>BRAP</i>	<i>C130032F08</i>	<i>C330016E03RIK</i>
<i>BC005494</i>	<i>BCL11B</i>	<i>BRD8</i>	<i>C130035G06RIK</i>	<i>C330019F22RIK</i>
<i>BC005662</i>	<i>BCL2</i>	<i>BRF1</i>	<i>C130036J11</i>	<i>C330021B20RIK</i>
<i>BC006705</i>	<i>BCL2L10</i>	<i>BRF2</i>	<i>C130039O16</i>	<i>C330023M02RIK</i>
<i>BC006909</i>	<i>BCL2L13</i>	<i>BRP16</i>	<i>C130044A18RIK</i>	<i>C330026P08RIK</i>
<i>BC007145</i>	<i>BCL2L2</i>	<i>BRP17</i>	<i>C130052G03RIK</i>	<i>C4</i>
<i>BC010245</i>	<i>BCL6</i>	<i>BRP44L</i>	<i>C130064B19RIK</i>	<i>C430003P19RIK</i>
<i>BC013712</i>	<i>BCL7A</i>	<i>BRS3</i>	<i>C130070B15RIK</i>	<i>C430014N20RIK</i>
<i>BC016493</i>	<i>BCRP1</i>	<i>BSG</i>	<i>C130070J12RIK</i>	<i>C430041M20</i>
<i>BC017545</i>	<i>BCS1L</i>	<i>BSND</i>	<i>C130073D16RIK</i>	<i>C430046P22RIK</i>
<i>BC017634</i>	<i>BDH</i>	<i>BST1</i>	<i>C130074G19RIK</i>	<i>C4BP</i>
<i>BC019776</i>	<i>BDNF</i>	<i>BTBD2</i>	<i>C130076O07RIK</i>	<i>C4ST2</i>
<i>BC019977</i>	<i>BEAN</i>	<i>BTG1</i>	<i>C130078N17RIK</i>	<i>C4ST</i>
<i>BC020175</i>	<i>BET1</i>	<i>BTG2</i>	<i>C130080N23RIK</i>	<i>C530002L11RIK</i>
<i>BC021367</i>	<i>BEX2</i>	<i>BTK</i>	<i>C130099A20RIK</i>	<i>C530008M07</i>
<i>BC021530</i>	<i>BFZB</i>	<i>BVES</i>	<i>C1GALT1</i>	<i>C530008M17RIK</i>
<i>BC021611</i>	<i>BGLAP1</i>	<i>BZRP</i>	<i>C1QA</i>	<i>C530024P05RIK</i>
<i>BC023845</i>	<i>BGLAP2</i>	<i>BZW2</i>	<i>C1QB</i>	<i>C530025M09RIK</i>

<i>C530043A13RIK</i>	<i>CABP1</i>	<i>CASP1</i>	<i>CD22</i>	<i>CEACAM13</i>
<i>C530046K05RIK</i>	<i>CABP7</i>	<i>CASP2</i>	<i>CD24A</i>	<i>CEBPB</i>
<i>C6</i>	<i>CACNA1A</i>	<i>CASP3</i>	<i>CD2AP</i>	<i>CEBPD</i>
<i>C630004H02RIK</i>	<i>CACNA1C</i>	<i>CASP4</i>	<i>CD2BP2</i>	<i>CECR2</i>
<i>C630005D06RIK</i>	<i>CACNA1D</i>	<i>CASP6</i>	<i>CD37</i>	<i>CEL</i>
<i>C630007C17RIK</i>	<i>CACNA1F</i>	<i>CASP7</i>	<i>CD3D</i>	<i>CELSR1</i>
<i>C630016B22RIK</i>	<i>CACNA2D2</i>	<i>CASP9</i>	<i>CD4</i>	<i>CEP2</i>
<i>C630016O21RIK</i>	<i>CACNB2</i>	<i>CASQ2</i>	<i>CD47</i>	<i>CETN2</i>
<i>C630024K23RIK</i>	<i>CACNG1</i>	<i>CATNA1</i>	<i>CD59A</i>	<i>CFH</i>
<i>C630025L14</i>	<i>CACNG4</i>	<i>CATNAL1</i>	<i>CD68</i>	<i>CFLAR</i>
<i>C630028L02RIK</i>	<i>CACNG5</i>	<i>CATNBIP1</i>	<i>CD7</i>	<i>CFTR</i>
<i>C630029C19RIK</i>	<i>CACYBP</i>	<i>CATNS</i>	<i>CD79A</i>	<i>CGBP</i>
<i>C630035N08RIK</i>	<i>CALM3</i>	<i>CAV</i>	<i>CD81</i>	<i>CHAF1A</i>
<i>C630036E02RIK</i>	<i>CALP</i>	<i>CAV3</i>	<i>CD83</i>	<i>CHEK1</i>
<i>C630041L24RIK</i>	<i>CALR3</i>	<i>CBFA2T3H</i>	<i>CD97</i>	<i>CHGA</i>
<i>C630046B20RIK</i>	<i>CAMK2B</i>	<i>CBL</i>	<i>CDC25A</i>	<i>CHI3L3</i>
<i>C730007L20RIK</i>	<i>CAMK2D</i>	<i>CBLN1</i>	<i>CDC2A</i>	<i>CHIA</i>
<i>C730015A02RIK</i>	<i>CAMK2G</i>	<i>CBX1</i>	<i>CDC2L2</i>	<i>CHK</i>
<i>C730024G19RIK</i>	<i>CAMKK1</i>	<i>CCC9</i>	<i>CDC42</i>	<i>CHKL</i>
<i>C730025P13RIK</i>	<i>CANX</i>	<i>CCK</i>	<i>CDC42EP1</i>	<i>CHL12</i>
<i>C730026E21RIK</i>	<i>CAP1</i>	<i>CCKAR</i>	<i>CDC42EP4</i>	<i>CHM</i>
<i>C730027J19RIK</i>	<i>CAPN12</i>	<i>CCKBR</i>	<i>CDH1</i>	<i>CHML</i>
<i>C730034F03RIK</i>	<i>CAPN8</i>	<i>CCL1</i>	<i>CDH2</i>	<i>CHORDC1</i>
<i>C730036H08</i>	<i>CAPN9</i>	<i>CCL25</i>	<i>CDH22</i>	<i>CHRAC1</i>
<i>C730042F17RIK</i>	<i>CAPNS1</i>	<i>CCL6</i>	<i>CDH23</i>	<i>CHRM1</i>
<i>C77020</i>	<i>CAPPA1</i>	<i>CCL7</i>	<i>CDH3</i>	<i>CHRM3</i>
<i>C78541</i>	<i>CAPZB</i>	<i>CCNB2</i>	<i>CDH4</i>	<i>CHRNA3</i>
<i>C78606</i>	<i>CAR11</i>	<i>CCND3</i>	<i>CDK2</i>	<i>CHRNA4</i>
<i>C79672</i>	<i>CAR13</i>	<i>CCNH</i>	<i>CDK3</i>	<i>CHRN4</i>
<i>C80633</i>	<i>CAR14</i>	<i>CCR8</i>	<i>CDK4</i>	<i>CHRND</i>
<i>C820010P03RIK</i>	<i>CAR3</i>	<i>CCR9</i>	<i>CDK5</i>	<i>CHRNE</i>
<i>C86045</i>	<i>CAR4</i>	<i>CCRL1</i>	<i>CDKN1A</i>	<i>CHST2</i>
<i>C87750</i>	<i>CAR6</i>	<i>CCRN4L</i>	<i>CDKN1B</i>	<i>CHST3</i>
<i>C8A</i>	<i>CAR7</i>	<i>CCT6A</i>	<i>CDKN2C</i>	<i>CHST4</i>
<i>C920006C10RIK</i>	<i>CAR9</i>	<i>CD14</i>	<i>CDON</i>	<i>CHST5</i>
<i>C920008G01RIK</i>	<i>CARD14</i>	<i>CD1D1</i>	<i>CDR2</i>	<i>CHST8</i>
<i>CAB140</i>	<i>CARKL</i>	<i>CD2</i>	<i>CDX1</i>	<i>CHX10</i>
<i>CABLES</i>	<i>CASK</i>	<i>CD209C</i>	<i>CEACAM10</i>	<i>CIAO1</i>
<i>CABLES2</i>	<i>CASKIN2</i>	<i>CD209E</i>	<i>CEACAM12</i>	<i>CIB1</i>

<i>CIDEB</i>	<i>CML2</i>	<i>COX5A</i>	<i>CRYAB</i>	<i>CXCL16</i>
<i>CIP1</i>	<i>CNBP</i>	<i>COX6A1</i>	<i>CRYBA4</i>	<i>CXCL2</i>
<i>CIPP</i>	<i>CNIH</i>	<i>COX6C</i>	<i>CRYBB2</i>	<i>CXCL9</i>
<i>CIRBP</i>	<i>CNK</i>	<i>COX7A2L</i>	<i>CRYGD</i>	<i>CXCR3</i>
<i>CISH</i>	<i>CNN2</i>	<i>COX7C</i>	<i>CRYL1</i>	<i>CYB5</i>
<i>CITED1</i>	<i>CNNM1</i>	<i>CPA5</i>	<i>CRYZ</i>	<i>CYBA</i>
<i>CITED2</i>	<i>CNNM3</i>	<i>CPD</i>	<i>CRYZL1</i>	<i>CYLN2</i>
<i>CITED4</i>	<i>CNNM4</i>	<i>CPEB</i>	<i>CSAD</i>	<i>CYP11A</i>
<i>CKLF</i>	<i>CNOT7</i>	<i>CPNE1</i>	<i>CSDA</i>	<i>CYP19</i>
<i>CKN1</i>	<i>CNP1</i>	<i>CPNE3</i>	<i>CSEIL</i>	<i>CYP1A1</i>
<i>CKT2</i>	<i>CNR2</i>	<i>CPNE4</i>	<i>CSF2</i>	<i>CYP1B1</i>
<i>CLASP1</i>	<i>CNTN1</i>	<i>CPNE5</i>	<i>CSF2RA</i>	<i>CYP24</i>
<i>CLCN1</i>	<i>CNTN2</i>	<i>CPO</i>	<i>CSF3</i>	<i>CYP2B13</i>
<i>CLCN3</i>	<i>COG1</i>	<i>CPR2</i>	<i>CSH1</i>	<i>CYP2B9</i>
<i>CLCNK1</i>	<i>COG2</i>	<i>CPSF2</i>	<i>CSK</i>	<i>CYP2D10</i>
<i>CLCNK1L</i>	<i>COG4</i>	<i>CPSF4</i>	<i>CSMD1</i>	<i>CYP2D9</i>
<i>CLDN10</i>	<i>COL11A2</i>	<i>CPT1B</i>	<i>CSNG</i>	<i>CYP2E1</i>
<i>CLDN2</i>	<i>COL16A1</i>	<i>CPT1C</i>	<i>CSNK</i>	<i>CYP2F2</i>
<i>CLDN3</i>	<i>COL18A1</i>	<i>CPXM1</i>	<i>CSNK1D</i>	<i>CYP39A1</i>
<i>CLDN4</i>	<i>COL23A1</i>	<i>CRABP1</i>	<i>CSNK1E</i>	<i>CYP3A25</i>
<i>CLDN6</i>	<i>COL4A2</i>	<i>CRADD</i>	<i>CSNK2A1</i>	<i>CYP40</i>
<i>CLDN7</i>	<i>COL4A3BP</i>	<i>CRAD-L</i>	<i>CSNK2A2</i>	<i>CYP4A10</i>
<i>CLDN9</i>	<i>COL4A5</i>	<i>CRCP</i>	<i>CSRP1</i>	<i>CYP4B1</i>
<i>CLECSF13</i>	<i>COL5A1</i>	<i>CRELD1</i>	<i>CSRP3</i>	<i>CYP4F14</i>
<i>CLECSF6</i>	<i>COL6A1</i>	<i>CREM</i>	<i>CST6</i>	<i>CYP8B1</i>
<i>CLIC1</i>	<i>COL6A2</i>	<i>CRF2-12</i>	<i>CST8</i>	<i>CYPF13</i>
<i>CLK</i>	<i>COL6A3</i>	<i>CRHR1</i>	<i>CTNS</i>	<i>CYS1</i>
<i>CLK4</i>	<i>COL7A1</i>	<i>CRIM1</i>	<i>CTSB</i>	<i>CYSLTR1</i>
<i>CLN3</i>	<i>COMP</i>	<i>CRIPT</i>	<i>CTSD</i>	<i>CYSLTR2</i>
<i>CLN5</i>	<i>COMT</i>	<i>CRK</i>	<i>CTSH</i>	<i>D030010E02</i>
<i>CLN8</i>	<i>COP1</i>	<i>CRLF3</i>	<i>CTSZ</i>	<i>D030011O10RIK</i>
<i>CLNK</i>	<i>COPE</i>	<i>CRMP5</i>	<i>CTTN</i>	<i>D030014N22RIK</i>
<i>CLP1</i>	<i>COPS3</i>	<i>CRNKL1</i>	<i>CUTL1</i>	<i>D030020D09RIK</i>
<i>CLSTN1</i>	<i>COPZ2</i>	<i>CRRY</i>	<i>CX39</i>	<i>D030020G18RIK</i>
<i>CLSTN2</i>	<i>COQ6</i>	<i>CRSP3</i>	<i>CX3CL1</i>	<i>D030024H03RIK</i>
<i>CLSTN3</i>	<i>CORO6</i>	<i>CRTR1</i>	<i>CX3CR1</i>	<i>D030026A21RIK</i>
<i>CLTA</i>	<i>CORS</i>	<i>CRY1</i>	<i>CXCL11</i>	<i>D030059C06RIK</i>
<i>CMAS</i>	<i>CORT</i>	<i>CRY2</i>	<i>CXCL12</i>	<i>D030060M11RIK</i>
<i>CMKOR1</i>	<i>COX4A</i>	<i>CRYAA</i>	<i>CXCL13</i>	<i>D030068E18RIK</i>

D030070L09RIK	D17H6S56E-2	D430024F16RIK	D830007E07	DDB2
D030073L15RIK	D17H6S56E-3	D430024K22RIK	D830007G01RIK	DDC8
D0HXS9928E	D17WSU92E	D430038H04RIK	D830019J24RIK	DDEF1
D10UCLA1	D17WSU94E	D430042O09RIK	D830019K17RIK	DDT
D11ERTD175E	D19397	D430043L16	D830044D21RIK	DDX1
D11ERTD497E	D19ERTD703E	D430044G18RIK	D830044I16RIK	DDX19
D11ERTD498E	D19WSU55E	D4BWG0593E	D8ERTD531E	DDX24
D11ERTD736E	D1BWG0212E	D4ERTD174E	D8ERTD633E	DDX25
D11ERTD759E	D1BWG1363E	D4ERTD22E	D8ERTD812E	DDX5
D11ERTD99E	D1ERTD251E	D4ERTD421E	D930001I21RIK	DDX50
D11LGP1E	D1ERTD8E	D4ERTD89E	D930001I22RIK	DEB1
D11LGP2E	D230005F13RIK	D530039E11RIK	D930020E02	DEF6
D12ERTD482E	D230014K01RIK	D5ERTD33E	D930035B09RIK	DEF8
D12ERTD647E	D230016K05	D5ERTD593E	D930036B08RIK	DEFB2
D12ERTD748E	D230018M15RIK	D5ERTD689E	D930036F22RIK	DEFB4
D130006K24RIK	D230019K24RIK	D5WSU45E	D930040F23RIK	DEFB5
D130017D06RIK	D230022C05RIK	D630024B06RIK	D930047P17	DEF3CR3
D130023A07RIK	D230039K05RIK	D630032B01RIK	D9WSU149E	DEF3CR6
D130026O08RIK	D2BWG1335E	D630032F02	D9WSU18E	DEF3CR-RS1
D130029J02	D2ERTD391E	D630039A03RIK	DAAM2	DEP1
D130040H23RIK	D2ERTD435E	D630042P16RIK	DAB2	DERMO1
D130043K22	D2WSU81E	D630045D17RIK	DAD1	DES
D130067I03RIK	D330001F17RIK	D630049P08RIK	DAP3	DFFA
D130071N24RIK	D330008N11RIK	D6ERTD263E	DAPK2	DFFB
D130075J17RIK	D330010C22	D6H12S2489E	DAZAP1	DFY
D130086K05RIK	D330012D11RIK	D6WSU116E	DBCCR1	DGAT1
D13BWG1146E	D330012D13	D6WSU157E	DBHL1	DGAT2L1
D13WSU177E	D330012F22RIK	D730001G18RIK	DBIL5	DGCR8
D13WSU50E	D330015H01RIK	D730005E14RIK	DBNL	DGUOK
D14ERTD484E	D330023I21RIK	D730039F16RIK	DBX1	DHCR24
D15ERTD417E	D330028D13RIK	D730040F13RIK	DCL1	DHCR7
D15ERTD747E	D3ERTD250E	D730042P09RIK	DCT	DHFR
D15ERTD785E	D3ERTD330E	D730043B02RIK	DCTN3	DHODH
D15ERTD806E	D3JFR1	D7BWG0575E	DCTN4	DIAP3
D15WSU59E	D3UCLA1	D7ERTD458E	DCTN5	DIDO1
D15WSU75E	D430004I08RIK	D7ERTD671E	DCX	DIRAS1
D16ERTD36E	D430005B17	D7ERTD743E	DDA3	DISP2
D16ERTD454E	D430019H16RIK	D7ERTD753E	DDAH2	DJI
D16IUM22E	D430020F16	D7WSU128E	DDB1	DKFZP761A132

<i>DKFZP761L0424</i>	<i>DPEP1</i>	<i>E030011D16RIK</i>	<i>E330017M15</i>	<i>EGFR</i>
<i>DKK3</i>	<i>DPF3</i>	<i>E030011K20</i>	<i>E330017O07RIK</i>	<i>EGFR-RS</i>
<i>DLGH1</i>	<i>DPM1</i>	<i>E030011O05RIK</i>	<i>E330036I19RIK</i>	<i>EGLN2</i>
<i>DLGH3</i>	<i>DPM2</i>	<i>E030019A03RIK</i>	<i>E330036L07RIK</i>	<i>EGR1</i>
<i>DLL3</i>	<i>DPP7</i>	<i>E030022H21</i>	<i>E330039K12RIK</i>	<i>EHD2</i>
<i>DLX2</i>	<i>DPT</i>	<i>E030029A11RIK</i>	<i>E430004N23</i>	<i>EHD3</i>
<i>DLX4</i>	<i>DPYSL4</i>	<i>E130013P03</i>	<i>E430012M05RIK</i>	<i>EIF2A</i>
<i>DM15</i>	<i>DRCTNNB1A</i>	<i>E130016E03RIK</i>	<i>E430016J11RIK</i>	<i>EIF2AK1</i>
<i>DM9</i>	<i>DRD2</i>	<i>E130103I17RIK</i>	<i>E430019B13RIK</i>	<i>EIF2AK4</i>
<i>DMBX1</i>	<i>DRD4</i>	<i>E130104F11</i>	<i>E430021K24RIK</i>	<i>EIF2B</i>
<i>DMRT3</i>	<i>DRD5</i>	<i>E130107N23RIK</i>	<i>E430029F06</i>	<i>EIF2C1</i>
<i>DMTAP1</i>	<i>DRG11</i>	<i>E130115E03RIK</i>	<i>E530005C20RIK</i>	<i>EIF2C2</i>
<i>DNAJA1</i>	<i>DRI2</i>	<i>E130115J16RIK</i>	<i>EAR4</i>	<i>EIF2S2</i>
<i>DNAJA3</i>	<i>DRPLA</i>	<i>E130201N16RIK</i>	<i>EAR5</i>	<i>EIF2S3X</i>
<i>DNAJA4</i>	<i>DSC2</i>	<i>E130203B14RIK</i>	<i>EBAG9</i>	<i>EIF2S3Y</i>
<i>DNAJB11</i>	<i>DSC3</i>	<i>E130206H14RIK</i>	<i>EBF4</i>	<i>EIF3S2</i>
<i>DNAJB12</i>	<i>DSCR2</i>	<i>E130207K11</i>	<i>EBNA1BP2</i>	<i>EIF3S3</i>
<i>DNAJB3</i>	<i>DSCR3</i>	<i>E130301F19</i>	<i>EBP</i>	<i>EIF3S7</i>
<i>DNAJB5</i>	<i>DSCR5</i>	<i>E130306D19</i>	<i>ECE2</i>	<i>EIF3S8</i>
<i>DNAJB6</i>	<i>DSG2</i>	<i>E130306M17RIK</i>	<i>ECELI</i>	<i>EIF4A2</i>
<i>DNAJC3</i>	<i>DTNB</i>	<i>E130307D12</i>	<i>ECM1</i>	<i>EIF4EBP1</i>
<i>DNAJC4</i>	<i>DTR</i>	<i>E130307M08RIK</i>	<i>EDA</i>	<i>ELA2</i>
<i>DNAJC5</i>	<i>DTX1</i>	<i>E130308H01</i>	<i>EDARADD</i>	<i>ELA3B</i>
<i>DNASE1</i>	<i>DTX2</i>	<i>E130309D02RIK</i>	<i>EDEM</i>	<i>ELAC2</i>
<i>DNASE1L3</i>	<i>DULLARD</i>	<i>E130314M08RIK</i>	<i>EDF1</i>	<i>ELAVL3</i>
<i>DNCL2A</i>	<i>DUSP12</i>	<i>E130315B21RIK</i>	<i>EDG2</i>	<i>ELF1</i>
<i>DNCL2B</i>	<i>DUSP15</i>	<i>E130319N12RIK</i>	<i>EDG5</i>	<i>ELF3</i>
<i>DNCLIC1</i>	<i>DUSP19</i>	<i>E230011G24RIK</i>	<i>EDN3</i>	<i>ELF5</i>
<i>DNMT3A</i>	<i>DUSP2</i>	<i>E230012L24</i>	<i>EDR1</i>	<i>ELK1</i>
<i>DNMT3L</i>	<i>DUSP3</i>	<i>E230015B07RIK</i>	<i>EEF1A2</i>	<i>ELL</i>
<i>DOC2G</i>	<i>DUSP7</i>	<i>E230015K02RIK</i>	<i>EEF1B2</i>	<i>ELMO2</i>
<i>DOCK1</i>	<i>DUTP</i>	<i>E230025K04RIK</i>	<i>EEFSEC</i>	<i>ELN</i>
<i>DOCK2</i>	<i>DVL3</i>	<i>E2F5</i>	<i>EEG1</i>	<i>ELOVL2</i>
<i>DOCK3</i>	<i>DXHXS1008E</i>	<i>E330005F07RIK</i>	<i>EFNA1</i>	<i>ELOVL3</i>
<i>DOKL</i>	<i>DXIMX38E</i>	<i>E330009J07RIK</i>	<i>EFNA2</i>	<i>ELOVL4</i>
<i>DOM3Z</i>	<i>DXIMX40E</i>	<i>E330009O14RIK</i>	<i>EFNB1</i>	<i>ELP4</i>
<i>DP1</i>	<i>DXIMX41E</i>	<i>E330010H22RIK</i>	<i>EFNB3</i>	<i>EMCN</i>
<i>DP1L1</i>	<i>E030002B02RIK</i>	<i>E330016A19RIK</i>	<i>EGF</i>	<i>EMX1</i>
<i>DPAGT1</i>	<i>E030002L01RIK</i>	<i>E330017A01</i>	<i>EGFL6</i>	<i>ENAH</i>

<i>ENDOG</i>	<i>ESR2</i>	<i>FABP7</i>	<i>FGF8</i>	<i>FPR-RS4</i>
<i>ENO1</i>	<i>ESRRB</i>	<i>FABP9</i>	<i>FGF9</i>	<i>FRABIN</i>
<i>ENO2</i>	<i>EST478828</i>	<i>FADD</i>	<i>FGLS</i>	<i>FRG1</i>
<i>ENPEP</i>	<i>ETFA</i>	<i>FADS2</i>	<i>FHL3</i>	<i>FRZB</i>
<i>ENPP5</i>	<i>ETS1</i>	<i>FADS3</i>	<i>FIBP</i>	<i>FSHR</i>
<i>ENTPD1</i>	<i>ETSRP71</i>	<i>FAF1</i>	<i>FIGLA</i>	<i>FSP27</i>
<i>ENTPD3</i>	<i>ETV3</i>	<i>FANCG</i>	<i>FIGN</i>	<i>FS</i>
<i>ENTPD5</i>	<i>ETV4</i>	<i>FARP2</i>	<i>FIGNL1</i>	<i>FTH</i>
<i>ENTPD6</i>	<i>ETV5</i>	<i>FASN</i>	<i>FIN15</i>	<i>FTHFD</i>
<i>EPAS1</i>	<i>EVC</i>	<i>FATH</i>	<i>FIZ1</i>	<i>FTHL17</i>
<i>EPB4</i>	<i>EVII</i>	<i>FAU</i>	<i>FKBP4</i>	<i>FTS</i>
<i>EPB7</i>	<i>EVI2</i>	<i>FBLN2</i>	<i>FKBP5</i>	<i>FTSJ</i>
<i>EPHA2</i>	<i>EVI5</i>	<i>FBP2</i>	<i>FKH3</i>	<i>FUT1</i>
<i>EPHA3</i>	<i>EVL</i>	<i>FBXL10</i>	<i>FKRP</i>	<i>FUT9</i>
<i>EPHA4</i>	<i>EVPL</i>	<i>FBXL12</i>	<i>FKSG27</i>	<i>FXR1H</i>
<i>EPHA6</i>	<i>EVX2</i>	<i>FBXL3A</i>	<i>FLIZ1</i>	<i>FXYD1</i>
<i>EPHB1</i>	<i>EXO70</i>	<i>FBXL6</i>	<i>FLT1</i>	<i>FXYD3</i>
<i>EPHB3</i>	<i>EXPI</i>	<i>FBXO13</i>	<i>FLT3</i>	<i>FXYD7</i>
<i>EPHB4</i>	<i>EXT2</i>	<i>FBXO24</i>	<i>FMIP</i>	<i>FZD2</i>
<i>EPN1</i>	<i>EXTL1</i>	<i>FBXO34</i>	<i>FMN2</i>	<i>FZD6</i>
<i>EPO</i>	<i>EXTL2</i>	<i>FBXW5</i>	<i>FMNL</i>	<i>FZD7</i>
<i>EPOR</i>	<i>EYA3</i>	<i>FBXW7</i>	<i>FMOD</i>	<i>FZD8</i>
<i>EPS15-RS</i>	<i>EZH1</i>	<i>FCAMR</i>	<i>FN3K</i>	<i>FZD9</i>
<i>EPS8</i>	<i>F10</i>	<i>FCER1G</i>	<i>FNBP1</i>	<i>G1RZFP</i>
<i>ERAL1</i>	<i>F13B</i>	<i>FCGR3</i>	<i>FNTB</i>	<i>G22P1</i>
<i>ERCC1</i>	<i>F2RL2</i>	<i>FCNA</i>	<i>FOLH1</i>	<i>G2AN</i>
<i>ERCC2</i>	<i>F2RL3</i>	<i>FCNB</i>	<i>FOSB</i>	<i>G3BP</i>
<i>ERCC3</i>	<i>F3</i>	<i>FDPS</i>	<i>FOSL2</i>	<i>G430029E23RIK</i>
<i>ERCC4</i>	<i>F630021I08RIK</i>	<i>FDX1</i>	<i>FOXA1</i>	<i>G430055L02RIK</i>
<i>ERH</i>	<i>F630111L10RIK</i>	<i>FEM1A</i>	<i>FOXB2</i>	<i>G430127E12RIK</i>
<i>ERMELIN</i>	<i>F7</i>	<i>FEM1B</i>	<i>FOXC1</i>	<i>G431004K08RIK</i>
<i>ERN1</i>	<i>F730001G15RIK</i>	<i>FES</i>	<i>FOXD2</i>	<i>G630009D10RIK</i>
<i>ERN2</i>	<i>F730001J03</i>	<i>FGF10</i>	<i>FOXI1</i>	<i>G630024C07RIK</i>
<i>ERO1L</i>	<i>F730007C19RIK</i>	<i>FGF11</i>	<i>FOXJ1</i>	<i>G630049C14RIK</i>
<i>ERP29</i>	<i>F730011J02</i>	<i>FGF15</i>	<i>FOXJ2</i>	<i>G630080D20RIK</i>
<i>ESAM</i>	<i>F730040C21</i>	<i>FGF17</i>	<i>FOXK1</i>	<i>G6PDX</i>
<i>ESDN</i>	<i>F730108M23RIK</i>	<i>FGF2</i>	<i>FOXL1</i>	<i>G6PT1</i>
<i>ESM1</i>	<i>FABP1</i>	<i>FGF21</i>	<i>FOXN1</i>	<i>GAB1</i>
<i>ESPN</i>	<i>FABP5</i>	<i>FGF3</i>	<i>FPR-RS3</i>	<i>GAB2</i>

<i>GABBR1</i>	<i>GDAP2</i>	<i>GNA13</i>	<i>GPR97</i>	<i>GTLF3B</i>
<i>GABRA6</i>	<i>GDAP3</i>	<i>GNA15</i>	<i>GPRC5B</i>	<i>GTPBP3</i>
<i>GABT3</i>	<i>GDF10</i>	<i>GNAI2</i>	<i>GPS1</i>	<i>GTRGEO22</i>
<i>GABT4</i>	<i>GDF3</i>	<i>GNAI3</i>	<i>GPSN2</i>	<i>GUCA1A</i>
<i>GAD2</i>	<i>GDI1</i>	<i>GNAQ</i>	<i>GPX1</i>	<i>GUCA1B</i>
<i>GADD45A</i>	<i>GDI3</i>	<i>GNA-RS1</i>	<i>GPX2</i>	<i>GUCA2</i>
<i>GADD45B</i>	<i>GEMIN4</i>	<i>GNAT2</i>	<i>GPX5</i>	<i>GUCA2B</i>
<i>GALE</i>	<i>GEMIN5</i>	<i>GNB1</i>	<i>GRAP</i>	<i>GUCY1A3</i>
<i>GALGT1</i>	<i>GEMIN7</i>	<i>GNB2-RS1</i>	<i>GRCC2F</i>	<i>GUCY2E</i>
<i>GALNT1</i>	<i>GFAP</i>	<i>GNB3</i>	<i>GRCC3F</i>	<i>GYK</i>
<i>GALNT6</i>	<i>GFI1B</i>	<i>GNB4</i>	<i>GRCC9</i>	<i>GYP A</i>
<i>GALNT9</i>	<i>GFM</i>	<i>GNB5</i>	<i>GRHL1</i>	<i>GYS1</i>
<i>GALR2</i>	<i>GFPT2</i>	<i>GNG4</i>	<i>GRHPR</i>	<i>GZMA</i>
<i>GALR3</i>	<i>GFRA1</i>	<i>GNG7</i>	<i>GRIA1</i>	<i>GZMD</i>
<i>GAP43</i>	<i>GGA3</i>	<i>GNG8</i>	<i>GRIA4</i>	<i>GZME</i>
<i>GAPD</i>	<i>GGCX</i>	<i>GNGT2</i>	<i>GRID2IP</i>	<i>GZMG</i>
<i>GAPDS</i>	<i>GGT1</i>	<i>GNT-IVA</i>	<i>GRIFIN</i>	<i>GZMK</i>
<i>GAS41</i>	<i>GGTLA1</i>	<i>GOLGA3</i>	<i>GRIK3</i>	<i>H2AFX</i>
<i>GAS5</i>	<i>GIT2</i>	<i>GOLPH3</i>	<i>GRIK5</i>	<i>H2-BF</i>
<i>GAS6</i>	<i>GJA3</i>	<i>GOSR1</i>	<i>GRIN1</i>	<i>H2-D1</i>
<i>GAS7</i>	<i>GJA4</i>	<i>GPC4</i>	<i>GRIN2A</i>	<i>H2-DMA</i>
<i>GAS8</i>	<i>GJA5</i>	<i>GPCR12</i>	<i>GRIN2B</i>	<i>H2-DMB1</i>
<i>GATA2</i>	<i>GJB3</i>	<i>GPLD1</i>	<i>GRINL1A</i>	<i>H2-DMB2</i>
<i>GATA6</i>	<i>GJB4</i>	<i>GPR1</i>	<i>GRM8</i>	<i>H2-EB1</i>
<i>GATS</i>	<i>GJB5</i>	<i>GPR14</i>	<i>GRN</i>	<i>H2-KE4</i>
<i>GBA2</i>	<i>GLA</i>	<i>GPR3</i>	<i>GRPEL1</i>	<i>H2-KE6</i>
<i>GBI</i>	<i>GLCC11</i>	<i>GPR33</i>	<i>GRPEL2</i>	<i>H2-OB</i>
<i>GBIF</i>	<i>GLI6</i>	<i>GPR37</i>	<i>GSBS</i>	<i>HAAO</i>
<i>GBL</i>	<i>GLIPR1</i>	<i>GPR37L1</i>	<i>GSC</i>	<i>HAGH</i>
<i>GBP2</i>	<i>GLIPR2</i>	<i>GPR4</i>	<i>GSDM</i>	<i>HALAPX</i>
<i>GCAT</i>	<i>GLRA1</i>	<i>GPR44</i>	<i>GSH2</i>	<i>HAO3</i>
<i>GCGR</i>	<i>GLRP1</i>	<i>GPR49</i>	<i>GSN</i>	<i>HARS</i>
<i>GCK</i>	<i>GLTP</i>	<i>GPR54</i>	<i>GSPT1</i>	<i>HARSL</i>
<i>GCL</i>	<i>GLUD</i>	<i>GPR56</i>	<i>GSR</i>	<i>HBA-A1</i>
<i>GCM1</i>	<i>GMEB1</i>	<i>GPR73L1</i>	<i>GSTT1</i>	<i>HBA-X</i>
<i>GCN5L2</i>	<i>GMFB</i>	<i>GPR81</i>	<i>GT(ROSA)26ASSO R</i>	<i>HBB</i>
<i>GCNT1</i>	<i>GMFG</i>	<i>GPR86</i>	<i>GTF2E2</i>	<i>HCAPG</i>
<i>GCS1</i>	<i>GMPR</i>	<i>GPR87</i>	<i>GTLF3A</i>	<i>HCK</i>
<i>GDA</i>	<i>GNA11</i>	<i>GPR90</i>		<i>HCN1</i>

<i>HCNGP</i>	<i>HMGB2L1</i>	<i>HSD17B12</i>	<i>IDB1</i>	<i>IL17B</i>
<i>HCRT</i>	<i>HMGCL</i>	<i>HSD17B9</i>	<i>IDH3A</i>	<i>IL17BR</i>
<i>HCRTR1</i>	<i>HMGCR</i>	<i>HSD3B1</i>	<i>IDH3G</i>	<i>IL17D</i>
<i>HCST</i>	<i>HMGCS2</i>	<i>HSD3B2</i>	<i>IFI202A</i>	<i>IL17RL</i>
<i>HDAC10</i>	<i>HMGNI</i>	<i>HSD3B6</i>	<i>IFI203</i>	<i>IL18BP</i>
<i>HDAC2</i>	<i>HMGN3</i>	<i>HSF1</i>	<i>IFIT2</i>	<i>IL1F9</i>
<i>HDAC7A</i>	<i>HNFB4G</i>	<i>HSF2BP</i>	<i>IFITM3L</i>	<i>IL1RAP</i>
<i>HDGF</i>	<i>HNRPA1</i>	<i>HSP70-4</i>	<i>IFLD1</i>	<i>IL1RAPL2</i>
<i>HEBP1</i>	<i>HNRPAB</i>	<i>HSP86-1</i>	<i>IFLD2</i>	<i>IL1RL1</i>
<i>HEBP2</i>	<i>HNRPDL</i>	<i>HSPA1B</i>	<i>IFNA2</i>	<i>IL2</i>
<i>HELB</i>	<i>HNRPH2</i>	<i>HSPA1L</i>	<i>IFNA4</i>	<i>IL21</i>
<i>HELLS</i>	<i>HNRPL</i>	<i>HSPA2</i>	<i>IFNA5</i>	<i>IL2RB</i>
<i>HERC1</i>	<i>HNRPU</i>	<i>HSPA8</i>	<i>IFNA6</i>	<i>IL3RA</i>
<i>HERC3</i>	<i>HOXA9</i>	<i>HSPB2</i>	<i>IFNAB</i>	<i>IL4I1</i>
<i>HERPUD1</i>	<i>HOXB1</i>	<i>HSPB7</i>	<i>IFNAR1</i>	<i>IL5</i>
<i>HES3</i>	<i>HOXB5</i>	<i>HSPD1</i>	<i>IFNG</i>	<i>IL6ST</i>
<i>HES5</i>	<i>HOXB6</i>	<i>HSPE1</i>	<i>IFNGR2</i>	<i>IL7R</i>
<i>HEXA</i>	<i>HOXB9</i>	<i>HSPG2</i>	<i>IFRD1</i>	<i>ILF2</i>
<i>HEXB</i>	<i>HOXC12</i>	<i>HTR1A</i>	<i>IFRD2</i>	<i>ILF3</i>
<i>HEY2</i>	<i>HOXC13</i>	<i>HTR1D</i>	<i>IGBP1</i>	<i>ILK</i>
<i>HEYL</i>	<i>HOXD13</i>	<i>HTR2A</i>	<i>IGF1</i>	<i>IMAP38</i>
<i>HGF</i>	<i>HOXD4</i>	<i>HTR3A</i>	<i>IGFBP3</i>	<i>IMMT</i>
<i>HGFAC</i>	<i>HP</i>	<i>HTR3B</i>	<i>IGFBP4</i>	<i>IMP4A</i>
<i>HGS</i>	<i>HP1BP3</i>	<i>HTR5B</i>	<i>IGSF11</i>	<i>IMPA1</i>
<i>HHIP</i>	<i>HPS3</i>	<i>HTR6</i>	<i>IGTP</i>	<i>IMPA2</i>
<i>HIC1</i>	<i>HPVC2</i>	<i>HURP</i>	<i>IHH</i>	<i>INAC</i>
<i>HIF1A</i>	<i>HR</i>	<i>HYAL3</i>	<i>II</i>	<i>INCENP</i>
<i>HIP1R</i>	<i>HRAS1</i>	<i>IANI</i>	<i>IK</i>	<i>INGAPRP</i>
<i>HIPK1</i>	<i>HRASRS</i>	<i>IAP</i>	<i>IKAPPABNS</i>	<i>INHA</i>
<i>HIPK2</i>	<i>HRC</i>	<i>ICAM1</i>	<i>IKBKB</i>	<i>INSL5</i>
<i>HIST1H1A</i>	<i>HRH1</i>	<i>ICAM2</i>	<i>IKBKE</i>	<i>INSM2</i>
<i>HIST1H3F</i>	<i>HRH2</i>	<i>ICAM4</i>	<i>IKBKG</i>	<i>INSRR</i>
<i>HIST2H2AA1</i>	<i>HRH3</i>	<i>ICAM5</i>	<i>IL10</i>	<i>IQGAP1</i>
<i>HIST2H4</i>	<i>HRMP1</i>	<i>ICMT</i>	<i>IL11</i>	<i>IRAK1</i>
<i>HLCS</i>	<i>HRSP12</i>	<i>ICOS</i>	<i>IL12A</i>	<i>IRAK3</i>
<i>HLXB9</i>	<i>HS1BP1</i>	<i>ICOSL</i>	<i>IL12B</i>	<i>IRAK4</i>
<i>HMBS</i>	<i>HSD11B1</i>	<i>ICRFP703B1614Q</i>	<i>IL15</i>	<i>IRF4</i>
<i>HMGA1</i>	<i>HSD11B2</i>	5	<i>IL15RA</i>	<i>IRF6</i>
<i>HMGA2</i>	<i>HSD17B1</i>	<i>ICT1</i>	<i>IL16</i>	<i>IRS1</i>

<i>IRS4</i>	<i>KCNH2</i>	<i>KLB</i>	<i>LARS2</i>	<i>LITAF</i>
<i>IRX3</i>	<i>KCNIP2</i>	<i>KLC2</i>	<i>LASS1</i>	<i>LLGLH</i>
<i>IRX6</i>	<i>KCNJ11</i>	<i>KLF16</i>	<i>LATS1</i>	<i>LMNA</i>
<i>ISG15</i>	<i>KCNJ14</i>	<i>KLK16</i>	<i>LBCL1</i>	<i>LMNB1</i>
<i>ISP1</i>	<i>KCNJ2</i>	<i>KLK21</i>	<i>LBX2H</i>	<i>LMO6</i>
<i>ISP2</i>	<i>KCNJ4</i>	<i>KLK26</i>	<i>LCN2</i>	<i>LNXI</i>
<i>ITCH</i>	<i>KCNJ5</i>	<i>KLK7</i>	<i>LCN5</i>	<i>LOBEL</i>
<i>ITGA4</i>	<i>KCNK1</i>	<i>KLK8</i>	<i>LCTL</i>	<i>LOXL4</i>
<i>ITGA6</i>	<i>KCNK2</i>	<i>KLK9</i>	<i>LDB1</i>	<i>LPD</i>
<i>ITGA9</i>	<i>KCNK3</i>	<i>KLRA13</i>	<i>LDH2</i>	<i>LPIN1</i>
<i>ITGAM</i>	<i>KCNK4</i>	<i>KLRA2</i>	<i>LDH3</i>	<i>LPL</i>
<i>ITGB1</i>	<i>KCNK5</i>	<i>KLRA4</i>	<i>LECT1</i>	<i>LRAT</i>
<i>ITGB2</i>	<i>KCNK7</i>	<i>KLRB1C</i>	<i>LECT2</i>	<i>LRBA</i>
<i>ITGB2L</i>	<i>KCNMA1</i>	<i>KLRC3</i>	<i>LENEP</i>	<i>LRDD</i>
<i>ITIH1</i>	<i>KCNMA3</i>	<i>KNS2</i>	<i>LEP</i>	<i>LRP4</i>
<i>ITIH2</i>	<i>KCNMB1</i>	<i>KPNA2</i>	<i>LEPR</i>	<i>LRPAP1</i>
<i>ITIH4</i>	<i>KCNMB4</i>	<i>KPNA6</i>	<i>LEPRE1</i>	<i>LRPB7</i>
<i>ITM2B</i>	<i>KCNN2</i>	<i>KREMEN2</i>	<i>LGALS1</i>	<i>LRRC2</i>
<i>ITM2C</i>	<i>KCNQ2</i>	<i>KRT1-10</i>	<i>LGALS3</i>	<i>LRRC3</i>
<i>ITPA</i>	<i>KCNS2</i>	<i>KRT1-12</i>	<i>LGI2</i>	<i>LRRC6</i>
<i>ITPR3</i>	<i>KDT1</i>	<i>KRT1-17</i>	<i>LGI3</i>	<i>LRRN1</i>
<i>ITPR5</i>	<i>KEAP1</i>	<i>KRT2-1</i>	<i>LGI4</i>	<i>LRRN2</i>
<i>ITSN</i>	<i>KEL</i>	<i>KRT2-17</i>	<i>LGMN</i>	<i>LSM4</i>
<i>JAG1</i>	<i>KHDRBS2</i>	<i>KRTAP12-1</i>	<i>LGS</i>	<i>LSP1</i>
<i>JAG2</i>	<i>KHDRBS3</i>	<i>KSR</i>	<i>LGTN</i>	<i>LTA</i>
<i>JAK3</i>	<i>KIF12</i>	<i>KY</i>	<i>LHB</i>	<i>LTB</i>
<i>JMJ</i>	<i>KIF17</i>	<i>KYNU</i>	<i>LHCGR</i>	<i>LTB4R1</i>
<i>JUB</i>	<i>KIF1A</i>	<i>L259</i>	<i>LHX3</i>	<i>LTB4R2</i>
<i>KAI1</i>	<i>KIF1C</i>	<i>LAD1</i>	<i>LHX8</i>	<i>LTF</i>
<i>KAISO</i>	<i>KIF20A</i>	<i>LAMA1</i>	<i>LHX9</i>	<i>LU</i>
<i>KARS</i>	<i>KIF21A</i>	<i>LAMB1-1</i>	<i>LIF</i>	<i>LUC7L</i>
<i>KCNA1</i>	<i>KIF24</i>	<i>LAMC2</i>	<i>LIFR</i>	<i>LUM</i>
<i>KCNA2</i>	<i>KIF2B</i>	<i>LAMP1</i>	<i>LIG3</i>	<i>LY108</i>
<i>KCNA7</i>	<i>KIF2C</i>	<i>LAMP3</i>	<i>LIMK1</i>	<i>LY64</i>
<i>KCNAB1</i>	<i>KIF3B</i>	<i>LAMR1</i>	<i>LIMK2</i>	<i>LY6A</i>
<i>KCNAB2</i>	<i>KIF5C</i>	<i>LANCL1</i>	<i>LIMS1</i>	<i>LY6F</i>
<i>KCNE1</i>	<i>KIFC3</i>	<i>LAO1</i>	<i>LIN7B</i>	<i>LY6G5C</i>
<i>KCNE2</i>	<i>KIT</i>	<i>LAPTM5</i>	<i>LIPC</i>	<i>LY6G6C</i>
<i>KCNE4</i>	<i>KL</i>	<i>LARGE</i>	<i>LIPH</i>	<i>LY6G6D</i>

<i>LY6I</i>	<i>MAP4K1</i>	<i>MDM2</i>	<i>MGC27784</i>	<i>MGC36672</i>
<i>LYL1</i>	<i>MAP4K2</i>	<i>MEAI</i>	<i>MGC27795</i>	<i>MGC37079</i>
<i>LYNX1</i>	<i>MAP4K4</i>	<i>MEF2D</i>	<i>MGC27915</i>	<i>MGC37309</i>
<i>LYPLA1</i>	<i>MAPA</i>	<i>MEG3</i>	<i>MGC27931</i>	<i>MGC37389</i>
<i>LZTR1</i>	<i>MAPBP1P</i>	<i>MELL1</i>	<i>MGC27952</i>	<i>MGC37548</i>
<i>M32486</i>	<i>MAPK11</i>	<i>MEN1</i>	<i>MGC28116</i>	<i>MGC37568</i>
<i>M6PR</i>	<i>MAPK13</i>	<i>MEOX1</i>	<i>MGC28149</i>	<i>MGC37569</i>
<i>MAD</i>	<i>MAPK14</i>	<i>MEPIA</i>	<i>MGC28394</i>	<i>MGC37588</i>
<i>MAD1L1</i>	<i>MAPK8IP2</i>	<i>MESP1</i>	<i>MGC28622</i>	<i>MGC37805</i>
<i>MAD2L1</i>	<i>MAPK9</i>	<i>METAP2</i>	<i>MGC28646</i>	<i>MGC37820</i>
<i>MAD4</i>	<i>MARCO</i>	<i>METTL1</i>	<i>MGC28663</i>	<i>MGC37938</i>
<i>MADCAM1</i>	<i>MASS1</i>	<i>MFAP2</i>	<i>MGC28751</i>	<i>MGC37950</i>
<i>MADH2</i>	<i>MAT1A</i>	<i>MFAP5</i>	<i>MGC28864</i>	<i>MGC38046</i>
<i>MADH6</i>	<i>MATA2</i>	<i>MFI2</i>	<i>MGC28888</i>	<i>MGC38133</i>
<i>MADH7</i>	<i>MATN2</i>	<i>MFN2</i>	<i>MGC28924</i>	<i>MGC38417</i>
<i>MADH9</i>	<i>MATN4</i>	<i>MFNG</i>	<i>MGC28931</i>	<i>MGC38710</i>
<i>MAFF</i>	<i>MATR3</i>	<i>MGA</i>	<i>MGC28972</i>	<i>MGC38715</i>
<i>MAFG</i>	<i>MAZ</i>	<i>MGAT3</i>	<i>MGC28978</i>	<i>MGC38922</i>
<i>MAGEA4</i>	<i>MB</i>	<i>MGAT5</i>	<i>MGC29251</i>	<i>MGC38960</i>
<i>MAGED1</i>	<i>MBD1</i>	<i>MGC11742</i>	<i>MGC29260</i>	<i>MGC40669</i>
<i>MAID</i>	<i>MBD3L2</i>	<i>MGC18745</i>	<i>MGC29331</i>	<i>MGC40768</i>
<i>MAN2A2</i>	<i>MBL1</i>	<i>MGC18752</i>	<i>MGC29978</i>	<i>MGC40815</i>
<i>MAN2B1</i>	<i>MBNL</i>	<i>MGC19022</i>	<i>MGC30456</i>	<i>MGC40840</i>
<i>MANBA</i>	<i>MBP</i>	<i>MGC19067</i>	<i>MGC30495</i>	<i>MGC40841</i>
<i>MAOB</i>	<i>MBTD1</i>	<i>MGC19382</i>	<i>MGC30595</i>	<i>MGC41750</i>
<i>MAP17</i>	<i>MC3R</i>	<i>MGC25352</i>	<i>MGC30806</i>	<i>MGC47001</i>
<i>MAP1LC3</i>	<i>MC7</i>	<i>MGC25529</i>	<i>MGC30809</i>	<i>MGC47262</i>
<i>MAP2K1</i>	<i>MCF2L</i>	<i>MGC25558</i>	<i>MGC30955</i>	<i>MGC47306</i>
<i>MAP2K3</i>	<i>MCM3AP</i>	<i>MGC25719</i>	<i>MGC31216</i>	<i>MGC49785</i>
<i>MAP2K4</i>	<i>MCMD</i>	<i>MGC25852</i>	<i>MGC31423</i>	<i>MGC6696</i>
<i>MAP2K5</i>	<i>MCMD2</i>	<i>MGC25863</i>	<i>MGC31450</i>	<i>MGC6835</i>
<i>MAP2K6</i>	<i>MCMD4</i>	<i>MGC25878</i>	<i>MGC32391</i>	<i>MGC6998</i>
<i>MAP2K7</i>	<i>MCMD7</i>	<i>MGC25910</i>	<i>MGC32441</i>	<i>MGC7221</i>
<i>MAP3K11</i>	<i>MCOLN3</i>	<i>MGC25951</i>	<i>MGC36238</i>	<i>MGC7793</i>
<i>MAP3K14</i>	<i>MCPT5</i>	<i>MGC25977</i>	<i>MGC36320</i>	<i>MGLAP</i>
<i>MAP3K2</i>	<i>MCPT7</i>	<i>MGC27560</i>	<i>MGC36325</i>	<i>MGLL</i>
<i>MAP3K5</i>	<i>MCPT8</i>	<i>MGC27631</i>	<i>MGC36374</i>	<i>MGMT</i>
<i>MAP3K6</i>	<i>MDFI</i>	<i>MGC27648</i>	<i>MGC36471</i>	<i>MIA</i>
<i>MAP3K7</i>	<i>MDK</i>	<i>MGC27770</i>	<i>MGC36491</i>	<i>MICAL-3</i>

<i>MIDN</i>	<i>MOR123-2</i>	<i>MOR184-1</i>	<i>MOR231-3</i>	<i>MOR283-6</i>
<i>MIP</i>	<i>MOR126-2</i>	<i>MOR184-4</i>	<i>MOR231-6</i>	<i>MOR31-6</i>
<i>MIST1</i>	<i>MOR127-1</i>	<i>MOR184-5</i>	<i>MOR231-8</i>	<i>MOR32-1</i>
<i>MIZI</i>	<i>MOR127-3</i>	<i>MOR184-7</i>	<i>MOR234-1</i>	<i>MOR32-3</i>
<i>MIZF</i>	<i>MOR127-4</i>	<i>MOR185-1</i>	<i>MOR234-3</i>	<i>MOR34-6</i>
<i>MKNK1</i>	<i>MOR128-2</i>	<i>MOR185-4</i>	<i>MOR238-1</i>	<i>MOR35-1</i>
<i>MKRNI</i>	<i>MOR130-1</i>	<i>MOR185-7</i>	<i>MOR239-1</i>	<i>MOR36-1</i>
<i>MLLT10</i>	<i>MOR13-4</i>	<i>MOR186-1</i>	<i>MOR245-21</i>	<i>MOR5-1</i>
<i>MLLT3</i>	<i>MOR135-2</i>	<i>MOR186-2</i>	<i>MOR246-2</i>	<i>MOR8-3</i>
<i>MLP</i>	<i>MOR136-11</i>	<i>MOR194-1</i>	<i>MOR246-3</i>	<i>MORF</i>
<i>MMD2</i>	<i>MOR139-2</i>	<i>MOR202-36</i>	<i>MOR246-4</i>	<i>MPA2</i>
<i>MME</i>	<i>MOR14-1</i>	<i>MOR202-37</i>	<i>MOR248-7</i>	<i>MPDU1</i>
<i>MMIG1</i>	<i>MOR14-10</i>	<i>MOR202-7</i>	<i>MOR25-1</i>	<i>MPEG1</i>
<i>MMP14</i>	<i>MOR142-1</i>	<i>MOR203-1</i>	<i>MOR253-4</i>	<i>MPG</i>
<i>MMP15</i>	<i>MOR144-1</i>	<i>MOR204-11</i>	<i>MOR254-2</i>	<i>MPI1</i>
<i>MMP2</i>	<i>MOR147-1</i>	<i>MOR204-13</i>	<i>MOR255-1</i>	<i>MPP1</i>
<i>MMP20</i>	<i>MOR149-3</i>	<i>MOR204-15</i>	<i>MOR255-2</i>	<i>MPP4</i>
<i>MMP23</i>	<i>MOR154-1</i>	<i>MOR204-20</i>	<i>MOR255-3</i>	<i>MPP6</i>
<i>MMP7</i>	<i>MOR158-1</i>	<i>MOR204-7</i>	<i>MOR256-22</i>	<i>MPST</i>
<i>MNT</i>	<i>MOR160-4</i>	<i>MOR208-1</i>	<i>MOR256-48</i>	<i>MPV17L</i>
<i>MOAP1</i>	<i>MOR160-5</i>	<i>MOR208-2</i>	<i>MOR256-7</i>	<i>MPZ</i>
<i>MOBP</i>	<i>MOR161-2</i>	<i>MOR209-1</i>	<i>MOR257-2</i>	<i>MRC2</i>
<i>MOD1</i>	<i>MOR162-1</i>	<i>MOR2-1</i>	<i>MOR257-4</i>	<i>MRGA3</i>
<i>MONA</i>	<i>MOR164-3</i>	<i>MOR21-1</i>	<i>MOR258-1</i>	<i>MRPL1</i>
<i>MOR103-10</i>	<i>MOR165-4</i>	<i>MOR216-1</i>	<i>MOR258-3</i>	<i>MRPL15</i>
<i>MOR103-2</i>	<i>MOR167-2</i>	<i>MOR217-1</i>	<i>MOR258-4P</i>	<i>MRPL17</i>
<i>MOR103-3</i>	<i>MOR167-3</i>	<i>MOR218-8</i>	<i>MOR260-1</i>	<i>MRPL2</i>
<i>MOR103-7</i>	<i>MOR170-3</i>	<i>MOR218-9</i>	<i>MOR261-2</i>	<i>MRPL3</i>
<i>MOR105-1</i>	<i>MOR170-6</i>	<i>MOR223-4</i>	<i>MOR261-3</i>	<i>MRPL30</i>
<i>MOR107-1</i>	<i>MOR171-10</i>	<i>MOR224-10</i>	<i>MOR264-17</i>	<i>MRPL33</i>
<i>MOR108-1</i>	<i>MOR171-21</i>	<i>MOR224-2</i>	<i>MOR266-2</i>	<i>MRPL36</i>
<i>MOR108-4</i>	<i>MOR171-6</i>	<i>MOR224-9</i>	<i>MOR267-3</i>	<i>MRPL37</i>
<i>MOR110-4</i>	<i>MOR172-6</i>	<i>MOR225-3</i>	<i>MOR267-7</i>	<i>MRPL39</i>
<i>MOR112-1</i>	<i>MOR174-5</i>	<i>MOR227-1</i>	<i>MOR268-5</i>	<i>MRPL4</i>
<i>MOR112-2</i>	<i>MOR175-2</i>	<i>MOR227-4</i>	<i>MOR272-1</i>	<i>MRPL43</i>
<i>MOR117-1</i>	<i>MOR177-14</i>	<i>MOR228-3</i>	<i>MOR273-2</i>	<i>MRPL52</i>
<i>MOR120-1</i>	<i>MOR18-1</i>	<i>MOR229-1</i>	<i>MOR274-2</i>	<i>MRPL53</i>
<i>MOR120-2</i>	<i>MOR182-5</i>	<i>MOR231-10</i>	<i>MOR275-1</i>	<i>MRPL54</i>
<i>MOR123-1</i>	<i>MOR18-3</i>	<i>MOR231-18</i>	<i>MOR283-3</i>	<i>MRPS10</i>

<i>MRPS12</i>	<i>MUC1</i>	<i>NAPA</i>	<i>NEUROD6</i>	<i>NPFF</i>
<i>MRPS18A</i>	<i>MUC4</i>	<i>NAPB</i>	<i>NEUROG3</i>	<i>NPHP1</i>
<i>MRPS21</i>	<i>MUC5B</i>	<i>NARS</i>	<i>NFE2L1</i>	<i>NPHP4</i>
<i>MRPS23</i>	<i>MUG2</i>	<i>NAT1</i>	<i>NFE2L2</i>	<i>NPHS1</i>
<i>MRPS25</i>	<i>MUSK</i>	<i>NAT2</i>	<i>NFE2L3</i>	<i>NPM3</i>
<i>MRPS6</i>	<i>MVK</i>	<i>NAT6</i>	<i>NFKBIA</i>	<i>NPPC</i>
<i>MRPS7</i>	<i>MVP</i>	<i>NAV1</i>	<i>NFKBIL1</i>	<i>NPRI</i>
<i>MRS3</i>	<i>MX1</i>	<i>NCDN</i>	<i>NFS1</i>	<i>NPR3</i>
<i>MS4A10</i>	<i>MYB</i>	<i>NCF2</i>	<i>NFX1</i>	<i>NPTX1</i>
<i>MS4A3</i>	<i>MYBL1</i>	<i>NCL</i>	<i>NFYA</i>	<i>NPTX2</i>
<i>MS4A8A</i>	<i>MYD116</i>	<i>NCOA3</i>	<i>NGB</i>	<i>NPY6R</i>
<i>MSCP</i>	<i>MYD88</i>	<i>NCOA6IP</i>	<i>NGP</i>	<i>NQO1</i>
<i>MSGN1</i>	<i>MYEF2</i>	<i>ND1</i>	<i>NHLH1</i>	<i>NQO2</i>
<i>MSH3</i>	<i>MYH2</i>	<i>NDR1</i>	<i>NIBAN</i>	<i>NR0B2</i>
<i>MSH4</i>	<i>MYH4</i>	<i>NDR2</i>	<i>NIF3L1</i>	<i>NR1D1</i>
<i>MSH5</i>	<i>MYL9</i>	<i>NDR3</i>	<i>NINJ2</i>	<i>NR1H3</i>
<i>MSI1H</i>	<i>MYLA</i>	<i>NDST2</i>	<i>NIPA1</i>	<i>NR4A1</i>
<i>MSL3L1</i>	<i>MYLC2PL</i>	<i>NDUFA6</i>	<i>NISCH</i>	<i>NR4A3</i>
<i>MSMB</i>	<i>MYLN</i>	<i>NDUFB5</i>	<i>NKTR</i>	<i>NR6A1</i>
<i>MSR2</i>	<i>MYLPF</i>	<i>NDUFS1</i>	<i>NKX2-2</i>	<i>NRAP</i>
<i>MST1</i>	<i>MYO15</i>	<i>NDUFS3</i>	<i>NKX2-4</i>	<i>NRARP</i>
<i>MST1R</i>	<i>MYO1A</i>	<i>NDUFV2</i>	<i>NKX2-5</i>	<i>NRAS</i>
<i>MSX3</i>	<i>MYO1B</i>	<i>NEDD4L</i>	<i>NKX6-1</i>	<i>NRBP</i>
<i>MT1</i>	<i>MYO1C</i>	<i>NEDD7</i>	<i>NME3</i>	<i>NRIP1</i>
<i>MT1A</i>	<i>MYO3A</i>	<i>NEF3</i>	<i>NMRK</i>	<i>NRN1</i>
<i>MTA1</i>	<i>MYO5B</i>	<i>NEIL1</i>	<i>NMU</i>	<i>NRTN</i>
<i>MTAP6</i>	<i>MYO7B</i>	<i>NEK1</i>	<i>NMYC1</i>	<i>NSAP1L</i>
<i>MTCP1</i>	<i>MYO9B</i>	<i>NEK3</i>	<i>NOA36</i>	<i>NSCCN1</i>
<i>MTE1</i>	<i>MYOG</i>	<i>NEK4</i>	<i>NOC4</i>	<i>NSD1</i>
<i>MTF1</i>	<i>MYOM2</i>	<i>NEK7</i>	<i>NODAL</i>	<i>NSDHL</i>
<i>MTF2</i>	<i>MYOZ1</i>	<i>NEK8</i>	<i>NOG</i>	<i>NSG1</i>
<i>MTMR1</i>	<i>MYRIP</i>	<i>NELF</i>	<i>NOLC1</i>	<i>NSSR</i>
<i>MTMR2</i>	<i>N6AMT1</i>	<i>NETO1</i>	<i>NOPE</i>	<i>NT5C</i>
<i>MTMR4</i>	<i>NAALAD2</i>	<i>NETO2</i>	<i>NOS1</i>	<i>NT5M</i>
<i>MTNR1A</i>	<i>NAGA</i>	<i>NEU1</i>	<i>NOS3</i>	<i>NTAN1</i>
<i>MTO1</i>	<i>NAGLU</i>	<i>NEU2</i>	<i>NOTCH4</i>	<i>NTRK3</i>
<i>MTR3</i>	<i>NAGS</i>	<i>NEUD4</i>	<i>NP15</i>	<i>NTT4</i>
<i>MTSSK</i>	<i>NANS</i>	<i>NEURL</i>	<i>NP220</i>	<i>NUBP1</i>
<i>MTX1</i>	<i>NAP1L3</i>	<i>NEUROD2</i>	<i>NPDC1</i>	<i>NUCB</i>

<i>NUCB2</i>	<i>OLFR73</i>	<i>P4HA2</i>	<i>PCDHB1</i>	<i>PEPF</i>
<i>NUDC</i>	<i>OLIG2</i>	<i>PACE4</i>	<i>PCDHB2</i>	<i>PER1</i>
<i>NUDT1</i>	<i>OMT2A</i>	<i>PADI1</i>	<i>PCG</i>	<i>PER2</i>
<i>NUDT2</i>	<i>ONECUT1</i>	<i>PADI3</i>	<i>PCK1</i>	<i>PERP</i>
<i>NUDT7</i>	<i>ONECUT3</i>	<i>PADI4</i>	<i>PCM1</i>	<i>PEX1</i>
<i>NUFIP1</i>	<i>OPN3</i>	<i>PAFAH1B1</i>	<i>PCMT1</i>	<i>PEX13</i>
<i>NULP1</i>	<i>OPN4</i>	<i>PAFAH1B3</i>	<i>PCNXL3</i>	<i>PEX14</i>
<i>NUMBL</i>	<i>ORA16</i>	<i>PAICS</i>	<i>PCSK4</i>	<i>PEX16</i>
<i>NUP153</i>	<i>ORC5L</i>	<i>PALD</i>	<i>PCSK7</i>	<i>PEX5</i>
<i>NUP155</i>	<i>ORF11</i>	<i>PALM2</i>	<i>PCTK1</i>	<i>PEX6</i>
<i>NUP62</i>	<i>ORF19</i>	<i>PANK1</i>	<i>PCTK2</i>	<i>PFKFB1</i>
<i>NXPH3</i>	<i>ORF5</i>	<i>PANK2</i>	<i>PCX</i>	<i>PFKFB2</i>
<i>NYREN18</i>	<i>ORF6</i>	<i>PANK3</i>	<i>PDCD6IP</i>	<i>PFPL</i>
<i>OAS1B</i>	<i>ORNT2</i>	<i>PAP</i>	<i>PDCD7</i>	<i>PGAM1</i>
<i>OAS1C</i>	<i>ORS16</i>	<i>PAPK</i>	<i>PDCD8</i>	<i>PGAM2</i>
<i>OAS1E</i>	<i>OSBP2</i>	<i>PAPLN</i>	<i>PDCL</i>	<i>PGBD5</i>
<i>OASL2</i>	<i>OSBPL1A</i>	<i>PAPOLA</i>	<i>PDE10A</i>	<i>PGBPLL</i>
<i>OAZ1</i>	<i>OSBPL3</i>	<i>PAPPA</i>	<i>PDE1B</i>	<i>PGCP</i>
<i>OAZ2</i>	<i>OSBPL5</i>	<i>PAPSS1</i>	<i>PDE3B</i>	<i>PGGTB1</i>
<i>OC90</i>	<i>OSF2</i>	<i>PARD3</i>	<i>PDE4D</i>	<i>PGK2</i>
<i>OCIL</i>	<i>OSR1</i>	<i>PARD6A</i>	<i>PDE6B</i>	<i>PGLS</i>
<i>ODF1</i>	<i>OSR2</i>	<i>PARG</i>	<i>PDE7A</i>	<i>PGM3</i>
<i>OFD1</i>	<i>OTG1</i>	<i>PARK2</i>	<i>PDE8A</i>	<i>PHAX</i>
<i>OG2X</i>	<i>OTOA</i>	<i>PARVA</i>	<i>PDGFA</i>	<i>PHB</i>
<i>OGG1</i>	<i>OTOF</i>	<i>PARVG</i>	<i>PDGFC</i>	<i>PHC3</i>
<i>OGN</i>	<i>OTT</i>	<i>PAX3</i>	<i>PDGFD</i>	<i>PHEX</i>
<i>OIT3</i>	<i>OVCA2</i>	<i>PAX6</i>	<i>PDGFRB</i>	<i>PHF2</i>
<i>OLFM3</i>	<i>OVCOV1</i>	<i>PAX7</i>	<i>PDHA1</i>	<i>PHF5A</i>
<i>OLFR15</i>	<i>OVOL1</i>	<i>PAX8</i>	<i>PDK4</i>	<i>PHKA1</i>
<i>OLFR19</i>	<i>OXCT</i>	<i>PAX9</i>	<i>PDLIM1</i>	<i>PHOSPHO1</i>
<i>OLFR23</i>	<i>OXT</i>	<i>PBP</i>	<i>PDLIM3</i>	<i>PHOX2A</i>
<i>OLFR30</i>	<i>OXTR</i>	<i>PBX4</i>	<i>PDPK1</i>	<i>PHXR1</i>
<i>OLFR33</i>	<i>P</i>	<i>PCBP1</i>	<i>PDZK3</i>	<i>PIGA</i>
<i>OLFR37E</i>	<i>P2RX2</i>	<i>PCBP3</i>	<i>PEA15</i>	<i>PIGB</i>
<i>OLFR47</i>	<i>P2RX5</i>	<i>PCBP4</i>	<i>PECI</i>	<i>PIGH</i>
<i>OLFR51</i>	<i>P2RXL1</i>	<i>PCDH12</i>	<i>PELO</i>	<i>PIGM</i>
<i>OLFR62</i>	<i>P2RY12</i>	<i>PCDH13</i>	<i>PEM</i>	<i>PIK3C2G</i>
<i>OLFR70</i>	<i>P2RY4</i>	<i>PCDH8</i>	<i>PEMT</i>	<i>PIK3CA</i>
<i>OLFR71</i>	<i>P42POP</i>	<i>PCDHA@</i>	<i>PEP4</i>	<i>PIK3CD</i>

<i>PIK3R2</i>	<i>PLN</i>	<i>PPIB</i>	<i>PRKR</i>	<i>PTBP1</i>
<i>PIM2</i>	<i>PLOD1</i>	<i>PPICAP</i>	<i>PRKRA</i>	<i>PTBP2</i>
<i>PIN1</i>	<i>PLSCR1</i>	<i>PPL</i>	<i>PRKRIR</i>	<i>PTCH</i>
<i>PIP5K1A</i>	<i>PLVAP</i>	<i>PPN</i>	<i>PRLPC1</i>	<i>PTDSR</i>
<i>PIP5K1B</i>	<i>PLXNB3</i>	<i>PPOX</i>	<i>PRLPI</i>	<i>PTDSS2</i>
<i>PIP5K1C</i>	<i>PLXNC1</i>	<i>PPP1CA</i>	<i>PRM3</i>	<i>PTE1</i>
<i>PIP5K2C</i>	<i>PM5</i>	<i>PPP1R12A</i>	<i>PRND</i>	<i>PTE2A</i>
<i>PIT1</i>	<i>PML</i>	<i>PPP1R14A</i>	<i>PRNPIP1</i>	<i>PTF1A</i>
<i>PITPNB</i>	<i>PMM1</i>	<i>PPP1R14B</i>	<i>PROCR</i>	<i>PTGDS</i>
<i>PITX1</i>	<i>PMS2</i>	<i>PPP1R14C</i>	<i>PRODH2</i>	<i>PTGER1</i>
<i>PITX2</i>	<i>PMSCL1</i>	<i>PPP1R16B</i>	<i>PROK2</i>	<i>PTGES2</i>
<i>PIWIL2</i>	<i>PMSCL2</i>	<i>PPP1R1A</i>	<i>PROSC</i>	<i>PTGIS</i>
<i>PKD1</i>	<i>PNLIPRP1</i>	<i>PPP1R2</i>	<i>PRPS2</i>	<i>PTGS2</i>
<i>PKD1L1</i>	<i>PODXL</i>	<i>PPP1R3A</i>	<i>PRPSAP2</i>	<i>PTHR2</i>
<i>PKD2</i>	<i>POLA1</i>	<i>PPP2CB</i>	<i>PRRG2</i>	<i>PTK6</i>
<i>PKM2</i>	<i>POLA2</i>	<i>PPP2R1A</i>	<i>PRRX2</i>	<i>PTK9L</i>
<i>PKNOX2</i>	<i>POLB</i>	<i>PPP4R1</i>	<i>PRSS11</i>	<i>PTOV1</i>
<i>PKP1</i>	<i>POLD2</i>	<i>PPP5C</i>	<i>PRSS8</i>	<i>PTPN13</i>
<i>PKP3</i>	<i>POLE</i>	<i>PPY</i>	<i>PS1D</i>	<i>PTPN14</i>
<i>PL6</i>	<i>POLE2</i>	<i>PRAMEL1</i>	<i>PSA</i>	<i>PTPN18</i>
<i>PLA2G10</i>	<i>POLH</i>	<i>PRAMEL3</i>	<i>PSAP</i>	<i>PTPRB</i>
<i>PLA2G1BR</i>	<i>POLI</i>	<i>PRCAD</i>	<i>PSAT</i>	<i>PTPRC</i>
<i>PLA2G2A</i>	<i>POLM</i>	<i>PRCC</i>	<i>PSCD2</i>	<i>PTPRCAP</i>
<i>PLA2G2E</i>	<i>POLR2C</i>	<i>PRDC</i>	<i>PSEN2</i>	<i>PTRF</i>
<i>PLA2G4A</i>	<i>POLR2E</i>	<i>PRDX1</i>	<i>PSE</i>	<i>PTTG1</i>
<i>PLA2G5</i>	<i>POLR2I</i>	<i>PRDX5</i>	<i>PSG16</i>	<i>PTX3</i>
<i>PLA2G7</i>	<i>POLYDOM</i>	<i>PREI3</i>	<i>PSG19</i>	<i>PUM1</i>
<i>PLAGL1</i>	<i>POR</i>	<i>PRG4</i>	<i>PSG30</i>	<i>PUMAG</i>
<i>PLAUR</i>	<i>POU2F3</i>	<i>PRIMI</i>	<i>PSMB2</i>	<i>PURA</i>
<i>PLCE1</i>	<i>POU3F1</i>	<i>PRKAB1</i>	<i>PSMB5</i>	<i>PURB</i>
<i>PLCG1</i>	<i>POU3F2</i>	<i>PRKAB2</i>	<i>PSMB7</i>	<i>PURG</i>
<i>PLD2</i>	<i>POU5F1</i>	<i>PRKARIA</i>	<i>PSMB8</i>	<i>PVA</i>
<i>PLDN</i>	<i>PPAP2A</i>	<i>PRKAR2A</i>	<i>PSMC4</i>	<i>PVRL2</i>
<i>PLEC1</i>	<i>PPAP2C</i>	<i>PRKAR2B</i>	<i>PSMD5</i>	<i>PVRL3</i>
<i>PLEK2</i>	<i>PPARA</i>	<i>PRKCABP</i>	<i>PSMD9</i>	<i>PWDMP</i>
<i>PLEKHB1</i>	<i>PPARBP</i>	<i>PRKCB</i>	<i>PSO</i>	<i>PXMP2</i>
<i>PLFR</i>	<i>PPEF2</i>	<i>PRKCD</i>	<i>PSP</i>	<i>PXMP3</i>
<i>PLG</i>	<i>PPFIBP1</i>	<i>PRKCQ</i>	<i>PSTPIP1</i>	<i>PXMP4</i>
<i>PLIN</i>	<i>PPGB</i>	<i>PRKDC</i>	<i>PSX2</i>	<i>PXN</i>

<i>PYCS</i>	<i>RARB</i>	<i>RFNG</i>	<i>RP2H</i>	<i>RPS6KA4</i>
<i>PYGB</i>	<i>RARG</i>	<i>RFX4</i>	<i>RP9H</i>	<i>RPS6KB2</i>
<i>QDPR</i>	<i>RASGRF2</i>	<i>RGA</i>	<i>RPA1</i>	<i>RRAS</i>
<i>R74613</i>	<i>RASGRP1</i>	<i>RGL2</i>	<i>RPE</i>	<i>RRH</i>
<i>R74720</i>	<i>RASSF1</i>	<i>RGPR</i>	<i>RPGR</i>	<i>RRM2</i>
<i>R74726</i>	<i>RASSF5</i>	<i>RGS11</i>	<i>RPH3A</i>	<i>RTN2</i>
<i>R74862</i>	<i>RB1</i>	<i>RGS12</i>	<i>RPIA</i>	<i>RTN3</i>
<i>R75183</i>	<i>RB1CC1</i>	<i>RGS13</i>	<i>RPL10</i>	<i>RTN4</i>
<i>RAB11A</i>	<i>RBBP9</i>	<i>RGS19IP3-</i>	<i>RPL10A</i>	<i>RTN4IP1</i>
<i>RAB12</i>	<i>RBL1</i>	<i>RGS20</i>	<i>RPL12</i>	<i>RTN4R</i>
<i>RAB14</i>	<i>RBL2</i>	<i>RGS3</i>	<i>RPL17</i>	<i>RTTN</i>
<i>RAB17</i>	<i>RBM6</i>	<i>RGS4</i>	<i>RPL22</i>	<i>RUFY1</i>
<i>RAB18</i>	<i>RBMX</i>	<i>RGS9BP</i>	<i>RPL27</i>	<i>RUVBL2</i>
<i>RAB19</i>	<i>RBP1</i>	<i>RHAG</i>	<i>RPL27A</i>	<i>RXR8</i>
<i>RAB20</i>	<i>RBP2</i>	<i>RHBDL</i>	<i>RPL3</i>	<i>S100A3</i>
<i>RAB21</i>	<i>RBP7</i>	<i>RHBG</i>	<i>RPL30</i>	<i>S100A4</i>
<i>RAB27B</i>	<i>RBPSUHL</i>	<i>RHCED</i>	<i>RPL32</i>	<i>S100A5</i>
<i>RAB33A</i>	<i>RCE1</i>	<i>RHOK</i>	<i>RPL35</i>	<i>S100A6</i>
<i>RAB34</i>	<i>RCOR</i>	<i>RHPN1</i>	<i>RPL41</i>	<i>S100A8</i>
<i>RAB37</i>	<i>RCVRN</i>	<i>RIB1</i>	<i>RPL44</i>	<i>S100B</i>
<i>RAB3B</i>	<i>RDBP</i>	<i>RIL</i>	<i>RPL7A</i>	<i>S3-12</i>
<i>RAB3D</i>	<i>RDH-S2</i>	<i>RING1</i>	<i>RPLP2</i>	<i>SAA1</i>
<i>RAB40C</i>	<i>RDS</i>	<i>RIPK2</i>	<i>RPO1-1</i>	<i>SAA2</i>
<i>RAB5C</i>	<i>REC8</i>	<i>RIS2</i>	<i>RPS14</i>	<i>SACM2L</i>
<i>RAB5EF</i>	<i>RECC1</i>	<i>RIT1</i>	<i>RPS15</i>	<i>SALPR</i>
<i>RAB5EP</i>	<i>RECK</i>	<i>RNASEP2</i>	<i>RPS16</i>	<i>SAMSN1</i>
<i>RAB9</i>	<i>RECQL5</i>	<i>RNF10</i>	<i>RPS17</i>	<i>SANG</i>
<i>RAC2</i>	<i>REG2</i>	<i>RNF11</i>	<i>RPS18</i>	<i>SAP18</i>
<i>RAD17</i>	<i>REG3A</i>	<i>RNF14</i>	<i>RPS19</i>	<i>SARA</i>
<i>RAD50</i>	<i>REL</i>	<i>RNF25</i>	<i>RPS2</i>	<i>SARS1</i>
<i>RAD54L</i>	<i>RELA</i>	<i>RNF5</i>	<i>RPS24</i>	<i>SART3</i>
<i>RAE1</i>	<i>REM</i>	<i>ROCK1</i>	<i>RPS25</i>	<i>SAT</i>
<i>RAI12</i>	<i>REM2</i>	<i>ROCK2</i>	<i>RPS26</i>	<i>SATB1</i>
<i>RAI2</i>	<i>REN2</i>	<i>ROG</i>	<i>RPS27L</i>	<i>SBK</i>
<i>RALBP1</i>	<i>REPS1</i>	<i>ROPN1</i>	<i>RPS3</i>	<i>SCA2</i>
<i>RAP1A</i>	<i>RESP18</i>	<i>ROR1</i>	<i>RPS4X</i>	<i>SCAMP2</i>
<i>RAP1GA1</i>	<i>RETN</i>	<i>ROR2</i>	<i>RPS5</i>	<i>SCAMP5</i>
<i>RAPSN</i>	<i>RFC3</i>	<i>RORA</i>	<i>RPS6</i>	<i>SCD3</i>
<i>RARA</i>	<i>RFC5</i>	<i>RORC</i>	<i>RPS6KA1</i>	<i>SCGB1A1</i>

<i>SCGB3A1</i>	<i>SERF2</i>	<i>SIAT6</i>	<i>SLC24A3</i>	<i>SLC8A1</i>
<i>SCGF</i>	<i>SERPINA6</i>	<i>SIAT7B</i>	<i>SLC24A4</i>	<i>SLC8A2</i>
<i>SCN11A</i>	<i>SERPINB5</i>	<i>SIAT7D</i>	<i>SLC25A1</i>	<i>SLC9A3R1</i>
<i>SCN1B</i>	<i>SERPINB7</i>	<i>SIAT7E</i>	<i>SLC25A12</i>	<i>SLFN1</i>
<i>SCN3A</i>	<i>SERPINE1</i>	<i>SIAT7F</i>	<i>SLC25A13</i>	<i>SLITL2</i>
<i>SCNN1B</i>	<i>SERPINE2</i>	<i>SIAT8F</i>	<i>SLC25A17</i>	<i>SLPI</i>
<i>SCOTIN</i>	<i>SERPINF2</i>	<i>SIAT9</i>	<i>SLC25A18</i>	<i>SLU7</i>
<i>SCRG1</i>	<i>SET</i>	<i>SIGIRR</i>	<i>SLC25A19</i>	<i>SMAF1</i>
<i>SCRT1</i>	<i>SET7</i>	<i>SIL</i>	<i>SLC26A8</i>	<i>SMARCA5</i>
<i>SCT</i>	<i>SFPI1</i>	<i>SIL1</i>	<i>SLC27A1</i>	<i>SMARCB1</i>
<i>SCUBE1</i>	<i>SFPQ</i>	<i>SILG41</i>	<i>SLC27A5</i>	<i>SMARCD3</i>
<i>SDBCAG84</i>	<i>SFRP4</i>	<i>SIM2</i>	<i>SLC28A3</i>	<i>SMC1L1</i>
<i>SDC1</i>	<i>SFRS14</i>	<i>SIN</i>	<i>SLC29A1</i>	<i>SMOC1</i>
<i>SDC3</i>	<i>SFRS2</i>	<i>SIN3B</i>	<i>SLC29A2</i>	<i>SMOX</i>
<i>SDC4</i>	<i>SFRS4</i>	<i>SIPA1</i>	<i>SLC29A3</i>	<i>SMPX</i>
<i>SDCBP</i>	<i>SFTPBP</i>	<i>SIRT6</i>	<i>SLC29A4</i>	<i>SMTN</i>
<i>SDF2</i>	<i>SFTPC</i>	<i>SIRT7</i>	<i>SLC2A8</i>	<i>SN</i>
<i>SDF2L1</i>	<i>SFTPD</i>	<i>SITPEC</i>	<i>SLC30A1</i>	<i>SNAI2</i>
<i>SDF4</i>	<i>SFXN3</i>	<i>SIVA</i>	<i>SLC30A3</i>	<i>SNCAIP</i>
<i>SDHA</i>	<i>SGK</i>	<i>SKIV2L</i>	<i>SLC30A4</i>	<i>SNRK</i>
<i>SEC22L3</i>	<i>SGPL1</i>	<i>SKZ1</i>	<i>SLC31A1</i>	<i>SNRPA</i>
<i>SEC23B</i>	<i>SGT</i>	<i>SLAM</i>	<i>SLC34A1</i>	<i>SNRPB2</i>
<i>SEC61G</i>	<i>SGY1</i>	<i>SLC10A2</i>	<i>SLC34A2</i>	<i>SNRPE</i>
<i>SEC63</i>	<i>SH2D3C</i>	<i>SLC11A1</i>	<i>SLC38A3</i>	<i>SNTA1</i>
<i>SECTM1</i>	<i>SH3BGRL3</i>	<i>SLC11A2</i>	<i>SLC39A3</i>	<i>SNTB2</i>
<i>SELIH</i>	<i>SH3BP1</i>	<i>SLC12A3</i>	<i>SLC3A2</i>	<i>SNX17</i>
<i>SELEL</i>	<i>SH3BP5</i>	<i>SLC12A4</i>	<i>SLC4A10</i>	<i>SNX4</i>
<i>SELENBP1</i>	<i>SH3GL1</i>	<i>SLC12A7</i>	<i>SLC4A2</i>	<i>SNX9</i>
<i>SELENBP2</i>	<i>SH3GL2</i>	<i>SLC13A1</i>	<i>SLC4A4</i>	<i>SOAT1</i>
<i>SEMA3C</i>	<i>SH3KBP1</i>	<i>SLC14A1</i>	<i>SLC5A2</i>	<i>SOCS1</i>
<i>SEMA4A</i>	<i>SHANK3</i>	<i>SLC16A1</i>	<i>SLC5A4B</i>	<i>SOCS3</i>
<i>SEMA4B</i>	<i>SHFDG1</i>	<i>SLC16A8</i>	<i>SLC5A5</i>	<i>SOCS4</i>
<i>SEMA4G</i>	<i>SHH</i>	<i>SLC17A1</i>	<i>SLC5A7</i>	<i>SOCS5</i>
<i>SEMA6B</i>	<i>SHRM</i>	<i>SLC1A1</i>	<i>SLC6A2</i>	<i>SOCS7</i>
<i>SEMA6D</i>	<i>SHYC</i>	<i>SLC21A13</i>	<i>SLC6A4</i>	<i>SOD1</i>
<i>SEMA7A</i>	<i>SI</i>	<i>SLC22A2</i>	<i>SLC7A10</i>	<i>SOLH</i>
<i>SEPM</i>	<i>SIAH1B</i>	<i>SLC22A4</i>	<i>SLC7A12</i>	<i>SORL1</i>
<i>SEPWI</i>	<i>SIAT4A</i>	<i>SLC22A6</i>	<i>SLC7A2</i>	<i>SOS1</i>
<i>SERF1</i>	<i>SIAT4C</i>	<i>SLC23A2</i>	<i>SLC7A9</i>	<i>SOX1</i>

<i>SOX10</i>	<i>SREBF1</i>	<i>STK23</i>	<i>SYNPO2</i>	<i>TCF12</i>
<i>SOX13</i>	<i>SRFCP</i>	<i>STK31</i>	<i>SYT12</i>	<i>TCF15</i>
<i>SOX15</i>	<i>SRP54</i>	<i>STK33</i>	<i>SYT13</i>	<i>TCF21</i>
<i>SOX18</i>	<i>SRP9</i>	<i>STK39</i>	<i>SYT3</i>	<i>TCF3</i>
<i>SOX5</i>	<i>SSB4</i>	<i>STK4</i>	<i>SYT7</i>	<i>TCF7</i>
<i>SOX6</i>	<i>SSBP3</i>	<i>STMN3</i>	<i>SYT8</i>	<i>TCFAP2A</i>
<i>SOX7</i>	<i>SSFA2</i>	<i>STMN4</i>	<i>SYTL1</i>	<i>TCFAP2C</i>
<i>SOX9</i>	<i>SSH3BP1</i>	<i>STRA13</i>	<i>SYTL2</i>	<i>TCFE3</i>
<i>SP1</i>	<i>SSPN</i>	<i>STRA6</i>	<i>T</i>	<i>TCFL1</i>
<i>SP100</i>	<i>SSRI</i>	<i>STRA8</i>	<i>T2</i>	<i>TCIRG1</i>
<i>SP4</i>	<i>SSR4</i>	<i>STRAP</i>	<i>TAC1</i>	<i>TCL1</i>
<i>SPAG1</i>	<i>SSRP1</i>	<i>STRM</i>	<i>TAC2</i>	<i>TCL1B1</i>
<i>SPAG4</i>	<i>SST</i>	<i>STRN4</i>	<i>TACSTD1</i>	<i>TCL1B3</i>
<i>SPEER2</i>	<i>SSTR1</i>	<i>STUB1</i>	<i>TACTILE</i>	<i>TCL1B5</i>
<i>SPHK1</i>	<i>SSTR3</i>	<i>STX18</i>	<i>TAF1C</i>	<i>TCN2</i>
<i>SPHK2</i>	<i>ST7</i>	<i>STX1A</i>	<i>TAF6</i>	<i>TCRB-V13</i>
<i>SP110</i>	<i>ST7L</i>	<i>STX5A</i>	<i>TAF9</i>	<i>TCTE3</i>
<i>SP112</i>	<i>STAC</i>	<i>STX8</i>	<i>TAGLN</i>	<i>TCTEX3</i>
<i>SP113</i>	<i>STARD3</i>	<i>STXBP1</i>	<i>TAP2</i>	<i>TDGF1</i>
<i>SP114</i>	<i>STARD4</i>	<i>SUDD</i>	<i>TAR1</i>	<i>TDH</i>
<i>SP11-4</i>	<i>STARD5</i>	<i>SULT1A1</i>	<i>TARBP2</i>	<i>TDRD1</i>
<i>SPIN</i>	<i>STARD6</i>	<i>SULT1A2</i>	<i>TARDBP</i>	<i>TEAD2</i>
<i>SPINT2</i>	<i>STAT2</i>	<i>SULT1B1</i>	<i>TAS1R2</i>	<i>TEAD4</i>
<i>SPN</i>	<i>STAT3</i>	<i>SULT1C1</i>	<i>TBC1D1</i>	<i>TEMT</i>
<i>SPNA2</i>	<i>STAT5A</i>	<i>SULT2B1</i>	<i>TBCE</i>	<i>TENR</i>
<i>SPNB2</i>	<i>STAT5B</i>	<i>SUPT5H</i>	<i>TBK1</i>	<i>TEP1</i>
<i>SPNB4</i>	<i>STATIP1</i>	<i>SUPT6H</i>	<i>TBL2</i>	<i>TERF2IP</i>
<i>SPNR</i>	<i>STC2</i>	<i>SURF1</i>	<i>TBN</i>	<i>TESC</i>
<i>SPO11</i>	<i>STEAP</i>	<i>SURF2</i>	<i>TBPL1</i>	<i>TESK1</i>
<i>SPOCK2</i>	<i>STELLA</i>	<i>SURF4</i>	<i>TBR1</i>	<i>TESP2</i>
<i>SPRR2B</i>	<i>STFA2</i>	<i>SURF5</i>	<i>TBRG1</i>	<i>TEX15</i>
<i>SPRR2F</i>	<i>STH2</i>	<i>SURF6</i>	<i>TBX4</i>	<i>TEX16</i>
<i>SPRY1</i>	<i>STIP1</i>	<i>SV2A</i>	<i>TBX6</i>	<i>TEX292</i>
<i>SPRY4</i>	<i>STK10</i>	<i>SVIL</i>	<i>TC10</i>	<i>TFAP2D</i>
<i>SPS2</i>	<i>STK12</i>	<i>SWAM2</i>	<i>TCAM1</i>	<i>TFDP1</i>
<i>SQLE</i>	<i>STK13</i>	<i>SYCP3</i>	<i>TCEA2</i>	<i>TFE3</i>
<i>SQRDL</i>	<i>STK19</i>	<i>SYK</i>	<i>TCEA3</i>	<i>TFIP11</i>
<i>SQSTM1</i>	<i>STK22A</i>	<i>SYN1</i>	<i>TCEB1L</i>	<i>TGFB2</i>
<i>SRC</i>	<i>STK22C</i>	<i>SYNC</i>	<i>TCF1</i>	<i>TGFB3</i>

<i>TGFB1</i>	<i>TM4SF11</i>	<i>TNFSF14</i>	<i>TREM3</i>	<i>TTC3</i>
<i>TGFBR2</i>	<i>TM4SF2</i>	<i>TNFSF4</i>	<i>TREML1</i>	<i>TTGN1</i>
<i>TGM1</i>	<i>TM4SF3</i>	<i>TNFSF5</i>	<i>TREX1</i>	<i>TTK</i>
<i>TGM2</i>	<i>TM6SF1</i>	<i>TNK1</i>	<i>TREX2</i>	<i>TTN</i>
<i>TGTP</i>	<i>TM9SF2</i>	<i>TNKS</i>	<i>TRFR2</i>	<i>TPPA</i>
<i>TGUT</i>	<i>TMC1</i>	<i>TNNI1</i>	<i>TRIF</i>	<i>TUBA4</i>
<i>THBS2</i>	<i>TMEFF2</i>	<i>TNNI2</i>	<i>TRIM11</i>	<i>TUBA6</i>
<i>THBS3</i>	<i>TMEM5</i>	<i>TNNT2</i>	<i>TRIM2</i>	<i>TUBB2</i>
<i>THEA</i>	<i>TMEM7</i>	<i>TNNT3</i>	<i>TRIM26</i>	<i>TUBB4</i>
<i>THEG</i>	<i>TMEM8</i>	<i>TNP1</i>	<i>TRIM27</i>	<i>TUBGCP5</i>
<i>THOP1</i>	<i>TMOD1</i>	<i>TNP2</i>	<i>TRIM30</i>	<i>TUFT1</i>
<i>THRSP</i>	<i>TMOD3</i>	<i>TNXB</i>	<i>TRIM41</i>	<i>TXNDC1</i>
<i>THY1</i>	<i>TMOD4</i>	<i>TOMM40</i>	<i>TRIM6</i>	<i>TXNL2</i>
<i>TIAM2</i>	<i>TMPO</i>	<i>TOP1</i>	<i>TRNT1</i>	<i>TXNRD1</i>
<i>TIEG</i>	<i>TMPRSS2</i>	<i>TOP2A</i>	<i>TRP53</i>	<i>TXNRD2</i>
<i>TIF2</i>	<i>TMPRSS4</i>	<i>TOP3A</i>	<i>TRP53BP1</i>	<i>TYKI</i>
<i>TIFP39</i>	<i>TMPRSS5</i>	<i>TPARL</i>	<i>TRP63</i>	<i>U2AF1</i>
<i>TIGD4</i>	<i>TMPRSS6</i>	<i>TPBG</i>	<i>TRPC2</i>	<i>U2AF2</i>
<i>TIMD2</i>	<i>TMSB10</i>	<i>TPBPA</i>	<i>TRPC3</i>	<i>U2AF26</i>
<i>TIMELESS</i>	<i>TMSB4X</i>	<i>TPC1</i>	<i>TRPC4</i>	<i>U3-55K</i>
<i>TIMM17B</i>	<i>TNA</i>	<i>TPD52</i>	<i>TRPC4AP</i>	<i>UBA52</i>
<i>TIMM23</i>	<i>TNCC</i>	<i>TPI</i>	<i>TRPM1</i>	<i>UBAP1</i>
<i>TIMM8B</i>	<i>TNCS</i>	<i>TPK1</i>	<i>TRPM2</i>	<i>UBCE7IP3</i>
<i>TIMM9</i>	<i>TNF</i>	<i>TPM2</i>	<i>TRPM5</i>	<i>UBCE7IP4</i>
<i>TIMP3</i>	<i>TNFAIP1</i>	<i>TPM3</i>	<i>TRPM6</i>	<i>UBD</i>
<i>TIRAP</i>	<i>TNFAIP3</i>	<i>TPRA40</i>	<i>TRPM7</i>	<i>UBE2D2</i>
<i>TISP78</i>	<i>TNFRSF12A</i>	<i>TPT1</i>	<i>TRPV2</i>	<i>UBE2E1</i>
<i>TJP3</i>	<i>TNFRSF13B</i>	<i>TPT1H</i>	<i>TRPV3</i>	<i>UBE2G2</i>
<i>TK1</i>	<i>TNFRSF13C</i>	<i>TPTF</i>	<i>TRPV4</i>	<i>UBE2R2</i>
<i>TLE3</i>	<i>TNFRSF17</i>	<i>TRAF2</i>	<i>TSBP</i>	<i>UBE2V2</i>
<i>TLMP</i>	<i>TNFRSF19</i>	<i>TRAF3</i>	<i>TSG101</i>	<i>UBE4A</i>
<i>TLR1</i>	<i>TNFRSF21</i>	<i>TRAF4</i>	<i>TSHB</i>	<i>UBE4B</i>
<i>TLR2</i>	<i>TNFRSF22</i>	<i>TRAF5</i>	<i>TSLP</i>	<i>UBL1</i>
<i>TLR4</i>	<i>TNFRSF23</i>	<i>TRAP1A</i>	<i>TSNAXIP1</i>	<i>UBL3</i>
<i>TLR5</i>	<i>TNFRSF25</i>	<i>TRB-2</i>	<i>TSSC4</i>	<i>UBL4</i>
<i>TLR8</i>	<i>TNFRSF4</i>	<i>TREM1</i>	<i>TST</i>	<i>UBL5</i>
<i>TLR9</i>	<i>TNFRSF6</i>	<i>TREM2A</i>	<i>TSTAP35B</i>	<i>UBP1</i>
<i>TLX1</i>	<i>TNFRSF7</i>	<i>TREM2B</i>	<i>TSX</i>	<i>UBTF</i>
<i>TLX3</i>	<i>TNFRSF9</i>	<i>TREM2C</i>	<i>TTBK1</i>	<i>UCP2</i>

<i>UCP3</i>	<i>VIRC3</i>	<i>VPREB3</i>	<i>WWP4</i>	<i>ZFP30</i>
<i>UGALT2</i>	<i>VIRC30</i>	<i>VPS11</i>	<i>X61497</i>	<i>ZFP316</i>
<i>UGCG</i>	<i>VIRC4</i>	<i>VPS26</i>	<i>X83328</i>	<i>ZFP354A</i>
<i>UGT2B5</i>	<i>VIRE11</i>	<i>VPS28</i>	<i>XIN</i>	<i>ZFP358</i>
<i>ULK1</i>	<i>VIRE8</i>	<i>VPS29</i>	<i>XLR</i>	<i>ZFP36</i>
<i>UMPK</i>	<i>VIRF4</i>	<i>VPS45</i>	<i>XLR4</i>	<i>ZFP364</i>
<i>UNC119H</i>	<i>VIRG1</i>	<i>VRP</i>	<i>XLR5</i>	<i>ZFP369</i>
<i>UNC13H1</i>	<i>VIRG6</i>	<i>WAP</i>	<i>XPC</i>	<i>ZFP36L1</i>
<i>UNC13H3</i>	<i>VIRH14</i>	<i>WASBP</i>	<i>XPNPEP1</i>	<i>ZFP37</i>
<i>UNC5H1</i>	<i>VIRH16</i>	<i>WASL</i>	<i>XPNPEP2</i>	<i>ZFP371</i>
<i>UNC93B</i>	<i>VIRH17</i>	<i>WAVE2</i>	<i>XPOT</i>	<i>ZFP46</i>
<i>UNG</i>	<i>VIRH5</i>	<i>WBP1</i>	<i>XRCC2</i>	<i>ZFP51</i>
<i>UPK1A</i>	<i>VIRH8</i>	<i>WBP11</i>	<i>XTRP3S1</i>	<i>ZFP52</i>
<i>UPK3</i>	<i>VIRJ2</i>	<i>WBP5</i>	<i>YAF2</i>	<i>ZFP64</i>
<i>UROD</i>	<i>V2R16</i>	<i>WBSCR14</i>	<i>YKT6</i>	<i>ZFP68</i>
<i>USF1</i>	<i>V3R1</i>	<i>WBSCR5</i>	<i>YME1L1</i>	<i>ZFP92</i>
<i>USH1C</i>	<i>VAMP2</i>	<i>WDR10</i>	<i>YWHAH</i>	<i>ZFP93</i>
<i>USH2A</i>	<i>VAPA</i>	<i>WDR13</i>	<i>YY1</i>	<i>ZFP96</i>
<i>USP14</i>	<i>VAPB</i>	<i>WDR4</i>	<i>ZAN</i>	<i>ZIPRO1</i>
<i>USP2</i>	<i>VASP</i>	<i>WDR6</i>	<i>ZAP3</i>	<i>ZMPSTE24</i>
<i>USP21</i>	<i>VAT1</i>	<i>WDR8</i>	<i>ZAP70</i>	<i>ZNFN1A4</i>
<i>USP4</i>	<i>VAV1</i>	<i>WDT3</i>	<i>ZDHHC3</i>	<i>ZP1</i>
<i>USP5</i>	<i>VAV2</i>	<i>WEE1</i>	<i>ZDHHC7</i>	<i>ZP2</i>
<i>UTRN</i>	<i>VAX1</i>	<i>WFS1</i>	<i>ZEC</i>	<i>ZP3</i>
<i>UXS1</i>	<i>VAX2</i>	<i>WIZ</i>	<i>ZFA</i>	<i>ZPBP</i>
<i>UXT</i>	<i>VCAM1</i>	<i>WNT10B</i>	<i>ZFP105</i>	<i>ZYX</i>
<i>VIRA5</i>	<i>VCP</i>	<i>WNT16</i>	<i>ZFP109</i>	
<i>VIRA8</i>	<i>VDAC1</i>	<i>WNT2B</i>	<i>ZFP133</i>	
<i>VIRB4</i>	<i>VDP</i>	<i>WNT4</i>	<i>ZFP142</i>	
<i>VIRB9</i>	<i>VDU1</i>	<i>WNT7A</i>	<i>ZFP143</i>	
<i>VIRC10</i>	<i>VEGFA</i>	<i>WNT7B</i>	<i>ZFP162</i>	
<i>VIRC11</i>	<i>VEGFB</i>	<i>WNT8B</i>	<i>ZFP185</i>	
<i>VIRC14</i>	<i>VIG1</i>	<i>WNT9B</i>	<i>ZFP216</i>	
<i>VIRC16</i>	<i>VIL</i>	<i>WSB1</i>	<i>ZFP219</i>	
<i>VIRC23</i>	<i>VIP</i>	<i>WT1</i>	<i>ZFP265</i>	
<i>VIRC24</i>	<i>VMD2</i>	<i>WTAP</i>	<i>ZFP288</i>	
<i>VIRC25</i>	<i>VMD2L1</i>	<i>WWOX</i>	<i>ZFP289</i>	
<i>VIRC27</i>	<i>VNN1</i>	<i>WWP1</i>	<i>ZFP296</i>	
<i>VIRC28</i>	<i>VNN3</i>	<i>WWP2</i>	<i>ZFP297B</i>	

Appendix 7

Supplementary Table 3: WT and PA overlapping E2 genes

Overlapping genes - WT + PA1		Overlapping genes - WT + PA2		Overlapping genes - WT + PA ^{POOL}	
WT	PA1	WT	PA2	WT	PA ^{POOL}
<i>Pitx2</i>	2210408F21Rik	<i>Pitx2</i>	1700001L05Rik	<i>Pitx2</i>	<i>Aldh1a3</i>
<i>Pou4f1</i>	A230057D06Rik	<i>Pou4f1</i>	1700010I14Rik	<i>Pou4f1</i>	<i>Aldh3a1</i>
<i>Lmx1a</i>	A830009L08Rik	<i>Lmx1a</i>	1700019D03Rik	<i>Lmx1a</i>	<i>Atp8b3</i>
<i>Plekhhg4</i>	<i>Acr</i>	<i>Plekhhg4</i>	2310002F09Rik	<i>Plekhhg4</i>	AW822252
<i>Dsc1</i>	<i>Adam33</i>	<i>Dsc1</i>	3632454L22Rik	<i>Dsc1</i>	<i>Barhl1</i>
<i>Crybb3</i>	<i>Adamts14</i>	<i>Crybb3</i>	4930594C11Rik	<i>Crybb3</i>	<i>CSar1</i>
<i>Edn3</i>	<i>Amy1</i>	<i>Edn3</i>	A330074K22Rik	<i>Edn3</i>	<i>Calca</i>
<i>Apoc1</i>	<i>Ap1g2</i>	<i>Apoc1</i>	<i>Abi3bp</i>	<i>Apoc1</i>	<i>Cbln3</i>
<i>Nlrp3</i>	<i>Arc</i>	<i>Nlrp3</i>	<i>Acad10</i>	<i>Nlrp3</i>	<i>Cbln4</i>
<i>Ptpn18</i>	<i>Arhgap28</i>	<i>Ptpn18</i>	<i>Acta2</i>	<i>Ptpn18</i>	<i>Chrna6</i>
<i>Cldn1</i>	<i>Bdnf</i>	<i>Cldn1</i>	<i>Adcy4</i>	<i>Cldn1</i>	<i>Col17a1</i>
<i>Uba52</i>	<i>C5ar1</i>	<i>Uba52</i>	<i>Adgrg2</i>	<i>Uba52</i>	<i>Col1a1</i>
<i>Recql4</i>	C920006O11Rik	<i>Recql4</i>	<i>Agt</i>	<i>Recql4</i>	<i>Cpz</i>
<i>Ebi3</i>	<i>Cacna1h</i>	<i>Ebi3</i>	<i>Akr1c14</i>	<i>Ebi3</i>	<i>Dbh</i>
<i>Bmp3</i>	<i>Cckbr</i>	<i>Bmp3</i>	<i>Aldh1a3</i>	<i>Bmp3</i>	<i>Dhrs7c</i>
<i>Gpr151</i>	<i>Cdk3-ps</i>	<i>Gpr151</i>	<i>Arc</i>	<i>Gpr151</i>	<i>Dock2</i>
<i>Cdk3-ps</i>	<i>Col16a1</i>	<i>Cdk3-ps</i>	<i>Arhgap6</i>	<i>Cdk3-ps</i>	<i>Dpy19l2</i>
<i>Cd163</i>	<i>Col1a1</i>	<i>Cd163</i>	<i>Arhgef33</i>	<i>Cd163</i>	<i>Ebf3</i>
<i>Mirg</i>	<i>Col1a2</i>	<i>Mirg</i>	<i>Arsj</i>	<i>Mirg</i>	<i>En2</i>
<i>Pparg</i>	<i>Col6a5</i>	<i>Pparg</i>	<i>Atp6v1c2</i>	<i>Pparg</i>	<i>Eps8l2</i>
<i>Fmod</i>	<i>Colq</i>	<i>Fmod</i>	AW551984	<i>Fmod</i>	<i>Fat2</i>
<i>Slc22a6</i>	<i>Cox6a2</i>	<i>Slc22a6</i>	B330016D10Rik	<i>Slc22a6</i>	<i>Fosb</i>
<i>Syt15</i>	<i>Cpz</i>	<i>Syt15</i>	<i>Barhl2</i>	<i>Syt15</i>	<i>Foxl2os</i>
<i>Cryba4</i>	<i>Dbh</i>	<i>Cryba4</i>	BC048546	<i>Cryba4</i>	<i>Galr1</i>
<i>Pgm5</i>	<i>Dcdc2b</i>	<i>Pgm5</i>	<i>Best1</i>	<i>Pgm5</i>	<i>Gata3</i>
<i>Slc13a4</i>	<i>Dnah9</i>	<i>Slc13a4</i>	<i>C1ql2</i>	<i>Slc13a4</i>	<i>Gbgt1</i>
<i>Six3</i>	<i>Dusp5</i>	<i>Six3</i>	<i>C2</i>	<i>Six3</i>	<i>Gmnc</i>
<i>Rxfp2</i>	<i>Efna1</i>	<i>Rxfp2</i>	<i>Calca</i>	<i>Rxfp2</i>	<i>Hsbp1l1</i>
<i>Lat2</i>	<i>Egr2</i>	<i>Lat2</i>	<i>Calcr</i>	<i>Lat2</i>	<i>Hspb2</i>
<i>Pcdhb6</i>	<i>Egr3</i>	<i>Pcdhb6</i>	<i>Car13</i>	<i>Pcdhb6</i>	<i>Ido1</i>
<i>Ttn</i>	<i>Egr4</i>	<i>Ttn</i>	<i>Cbln3</i>	<i>Ttn</i>	<i>Lhx1</i>
<i>Ush1g</i>	<i>Eln</i>	<i>Ush1g</i>	<i>Cbln4</i>	<i>Ush1g</i>	<i>Lhx1os</i>
4930426D05F	<i>Eps8l1</i>	4930426D05F	<i>Ccdc180</i>	4930426D05F	<i>Lhx5</i>
<i>Henmt1</i>	<i>Epx</i>	<i>Henmt1</i>	<i>Ccdc36</i>	<i>Henmt1</i>	<i>Mab21l1</i>
<i>Myoc</i>	<i>Exoc3l</i>	<i>Myoc</i>	<i>Ccl12</i>	<i>Myoc</i>	<i>Mybpc3</i>
<i>Rsg1</i>	<i>Fam129c</i>	<i>Rsg1</i>	<i>Chodl</i>	<i>Rsg1</i>	<i>Myh2</i>
<i>Arhgef39</i>	<i>Fanca</i>	<i>Arhgef39</i>	<i>Chrm5</i>	<i>Arhgef39</i>	<i>Myo3b</i>
<i>Tusc5</i>	<i>Fat2</i>	<i>Tusc5</i>	<i>Chrna6</i>	<i>Tusc5</i>	<i>Nlrp3</i>
<i>Slc6a20a</i>	<i>Fbln5</i>	<i>Slc6a20a</i>	<i>Clrn1</i>	<i>Slc6a20a</i>	<i>Nr4a2</i>
<i>Pin1rt1</i>	<i>Fhod1</i>	<i>Pin1rt1</i>	<i>Cmb1</i>	<i>Pin1rt1</i>	<i>Olfr1344</i>
<i>Dnase1l1</i>	<i>Flna</i>	<i>Dnase1l1</i>	<i>Cngb1</i>	<i>Dnase1l1</i>	<i>Pex11g</i>
<i>Dsc3</i>	<i>Fos</i>	<i>Dsc3</i>	<i>Col6a6</i>	<i>Dsc3</i>	<i>Phex</i>
<i>Lect1</i>	<i>Fosb</i>	<i>Lect1</i>	<i>Colq</i>	<i>Lect1</i>	<i>Ppp1r17</i>
C230091D08F	<i>Foxl2os</i>	C230091D08F	<i>Cox7a1</i>	C230091D08F	<i>Rmi2</i>
<i>Aox3</i>	<i>Ggnbp1</i>	<i>Aox3</i>	<i>Crb1</i>	<i>Aox3</i>	<i>Rps13</i>
<i>Gngt2</i>	<i>Gipr</i>	<i>Gngt2</i>	<i>Crhr2</i>	<i>Gngt2</i>	<i>Serpinb1b</i>
<i>C4a</i>	<i>Gm11549</i>	<i>C4a</i>	<i>Ctxn2</i>	<i>C4a</i>	<i>Shox2</i>
<i>Scara5</i>	<i>Gm14420</i>	<i>Scara5</i>	<i>Dcn</i>	<i>Scara5</i>	<i>Siglec1</i>
<i>Msx1</i>	<i>Gm15446</i>	<i>Msx1</i>	<i>Des</i>	<i>Msx1</i>	<i>Siglece</i>
4930481A15F	<i>Gm20219</i>	4930481A15F	<i>Diap3</i>	4930481A15F	<i>Spp1</i>
<i>Ccdc33</i>	<i>Gm2115</i>	<i>Ccdc33</i>	<i>Dnaaf3</i>	<i>Ccdc33</i>	<i>T2</i>
<i>Ybx2</i>	<i>Gm38413</i>	<i>Ybx2</i>	<i>Dock2</i>	<i>Ybx2</i>	<i>Twist1</i>
<i>Aldh1a2</i>	<i>Gpr139</i>	<i>Aldh1a2</i>	<i>Drd5</i>	<i>Aldh1a2</i>	<i>Uncx</i>
<i>Gm20219</i>	<i>Gpr3</i>	<i>Gm20219</i>	<i>Dsc3</i>	<i>Gm20219</i>	<i>Upp2</i>
<i>Cpz</i>	<i>Gsap</i>	<i>Cpz</i>	<i>Ebf2</i>	<i>Cpz</i>	<i>Zfp114</i>
<i>Pabpc5</i>	<i>H19</i>	<i>Pabpc5</i>	<i>Ebf3</i>	<i>Pabpc5</i>	
	<i>H2-M5</i>		<i>Edar</i>		
	<i>Hcrt</i>		<i>Egfl6</i>		
	<i>Hspa1b</i>		<i>Egr1</i>		
	<i>Iffit3b</i>		<i>Egr2</i>		
	<i>Il18bp</i>		<i>Eps8l2</i>		
	<i>Inhba</i>		<i>Exoc3l4</i>		
	<i>Itgbl1</i>		<i>F13a1</i>		
	<i>Iyd</i>		<i>Fam221a</i>		
	<i>Kif20b</i>		<i>Fam228a</i>		
	<i>Leng8</i>		<i>Fat2</i>		
	<i>Mab21l1</i>		<i>Fos</i>		
	<i>Mbd6</i>		<i>Foxr2</i>		
	<i>Med12</i>		<i>Gabraq</i>		
	<i>Mfsd2b</i>		<i>Galr1</i>		
	<i>Mvp</i>		<i>Gata3</i>		
	<i>Myh11</i>		<i>Gatsl3</i>		
	<i>Neat1</i>		<i>Gimap1</i>		

Overlapping genes in each group are highlighted

Nlrp3

Nox4
Npas4
Npy2r
Nr3c2
Nt5e
Ovgp1
P3h3
Pabpc4l
Parp3
Pdgrl
Pisd-ps1
Pisd-ps2
Plekha4
Plscr4
Pmch
Procr
Prox1
Psd4
Ptch2
Ptgs2
Rad9b
Rbp4
Reck
S100a4
Scarf2
Serpib1a
Sgk2
Siglec1
Slc17a8
Slc2a9
Slc9a2
Sowahb
Spaca6
Spp1
Ssc5d
Styk1
Susc5
Sypl2
Tbxa2r
Tcap
Thbs3
Thbs4
Tmc4
Tnxb
Traip
Trim68
Tspan18
Unc13d
Wnt10a
Wnt10b
Zan
Zfp456
Zfp69
Zkscan2

Gm10638
Gm14634
Gm5148
Gm5741
Gm694
Gmnc
Gpr101
Hap1
Hpcal1
Hspb2
Hspb3
Ifit3
Igfbp6
Inhba
Irs4
Itgal
Itgb3
Jph2
Lars2
Lhx1
Lhx1os
Lhx5
Lppos
Lrrn4
Ltbp2
Mab21l1
Magel2
Map3k15
Map3k6
Meig1
Mir6236
Mxd3
Myh2
Myo3b
Myoc
Myzap
Neil2
Neurl2
Nhej1
Nkx2-1
Nod2
Npas4
Nppa
Npy2r
Nr2f2
Nrtn
Nupr1
Olfm4
Optc
Ovgp1
Ovol2
Oxt
Pappa2
Pdzd3
Pex11g
Pla2g3
Plk5
Plp2
Popdc3
Ppp1r17
Prlr
Prr15
Ptafr
Rad54l
Rhoh
Rn45s
Rtl1

Rxfp2

Samd11
Serpib1b
Sim1
Slc35d3
Slc47a1
Snord22
Stpg1
Susc3
Tacr3

Tal1
Tbx15
Tmem140
Trhr
Trim34a
Ttc32
Wnt9b
Zan
Zc2hc1c
Zfp599
Zfp953

Appendix 8

GeneID	logFC	logCPM	PValue	P10VDP24_1	P10VDP24_2
1700001L05Rik	-0.549307505	2.660856812	0.000859115	7.154181856	8.479808966
1700010I14Rik	-0.571938331	0.688133884	0.01784733	1.983337544	1.695961793
1700019D03Rik	-0.517201126	1.930462873	0.001333566	4.391675991	4.239904483
2310002F09Rik	-0.736804454	0.402394742	0.028815468	2.195837995	1.639429733
3632454L22Rik	-0.582488424	0.969988783	0.013696485	1.629170126	2.091686212
4930594C11Rik	0.840589064	0.483544537	0.002410886	0.920835288	0.961045016
A330074K22Rik	-0.698796869	1.148481724	0.025362551	2.408338446	3.109263288
Abi3bp	0.619292845	4.539483008	0.047830099	14.30836371	14.01995082
Acad10	0.509319601	0.947677941	0.048266045	1.983337544	1.413301494
Acta2	-0.644476103	3.027348345	2.87E-05	10.76668953	10.79762342
Adcy4	-0.506918624	2.159981449	0.00369895	5.241677795	4.861757141
Adgrg2	-0.512675545	2.498275354	0.008100158	7.650016242	4.692160961
Agt	-0.851770933	5.802526808	0.00302737	95.12936864	82.42374315
Akr1c14	0.587391514	0.953038247	0.033913869	1.062502256	1.695961793
Aldh1a3	1.232775852	2.770964656	5.56E-09	4.462509474	3.278859467
Arc	0.795810351	5.432898654	5.37E-06	21.53337905	44.32113486
Arhgap6	-0.539956197	3.169433608	0.000216181	9.1375194	11.64560431
Arhgef33	-0.83115306	0.760976838	0.002787027	1.700003609	1.582897674
Arsj	-0.728127665	0.664229303	0.010701483	2.054171028	1.695961793
Atp6v1c2	-0.564812394	1.425933274	0.010014596	3.61250767	2.54394269
AW551984	-0.521050177	6.323952466	0.00061255	74.87099229	92.65604597
B330016D10Rik	-0.806756957	1.320261613	0.000324941	3.470840702	3.731115945
Barhl2	-0.526840604	0.883494109	0.025655224	2.195837995	1.469833554
BC048546	-0.598660592	3.037014903	0.000202402	11.19169043	10.23230282
Best1	-0.696510936	0.768786747	0.024068527	2.266671479	1.469833554
C1ql2	-0.896486173	2.55314801	5.50E-05	8.00418366	9.214725743
C2	-0.825074841	0.697092565	0.004087788	2.054171028	2.035154152
Calca	-0.759765168	1.666031595	0.004524027	3.541674186	2.939667108
Calcr	-0.961979029	2.128444014	0.00346846	4.250009023	8.027552488
Car13	-0.522402284	0.795087221	0.042424594	1.91250406	1.582897674
Cbln3	-1.379505424	1.154088077	0.005243862	1.770837093	1.752493853
Cbln4	-0.615818384	4.393837061	0.007635041	19.83337544	23.06508039
Ccdc180	0.564508695	0.419900477	0.039850967	0.991668772	0.791448837
Ccdc36	-0.62074907	0.201906001	0.03920111	0.779168321	1.187173255
Ccl12	-1.087574982	0.387352079	0.001078468	2.125004512	1.526365614
Chodl	-0.608026959	1.922042899	0.021348597	3.470840702	4.409500662
Chrm5	-0.588433106	1.030076817	0.048865113	1.700003609	2.939667108
Chrna6	-0.623380073	0.810345714	0.031100526	1.91250406	2.204750331
Clrn1	-0.986186656	0.657538298	0.000941506	2.054171028	1.074109136
Cmb1	-0.51632138	3.349774382	5.41E-06	10.76668953	12.60664933
Cngb1	-0.783294764	0.910377019	0.000922595	2.833339349	2.204750331
Col6a6	-0.701383213	0.264266538	0.0181173	1.13333574	1.300237375
Colq	1.166550494	1.309075148	1.28E-05	1.204169223	1.865557973
Cox7a1	-0.612802848	0.327789773	0.025680217	1.416669674	1.300237375
Crb1	-0.746358644	0.320065684	0.033289232	1.700003609	0.904512956
Crhr2	-0.559319101	1.387679743	0.004817913	2.833339349	2.770070929
Ctxn2	-0.639245301	3.079211745	0.000256724	11.12085694	9.553918102
Dcn	-0.590803258	4.911261766	2.25E-05	27.69589213	35.50213354
Des	-0.510558407	0.935272044	0.022759757	1.770837093	2.43087857

Diap3	0.531886419	1.770088088	0.001576148	2.904172833	2.826602989
Dnaaf3	-0.505199738	1.258109255	0.012953568	2.904172833	2.317814451
Dock2	0.869947243	0.518838913	0.042597151	1.275002707	1.130641196
Drd5	-0.525878699	2.023702233	0.00103474	4.604176442	4.409500662
Dsc3	-1.698558181	0.686757234	0.000223312	1.558336642	1.413301494
Ebf2	-0.546404738	1.973014418	0.017130966	5.383344763	3.222327407
Ebf3	-1.046697432	2.936468318	7.05E-06	9.987521205	6.727315113
Edar	0.575064425	0.700672298	0.036688968	1.13333574	1.243705315
Egfl6	-0.574574231	2.461171062	0.004375609	5.52501173	8.197148667
Egr1	0.583569124	6.716375583	7.62E-05	78.12933254	107.3543815
Egr2	0.507039653	2.075545777	0.046574087	3.754174637	3.674583885
Eps8l2	-0.768386981	0.519216865	0.008738003	1.345836191	2.204750331
Exoc3l4	-1.010427447	0.276221055	0.000274261	1.275002707	1.469833554
F13a1	-0.543167544	2.627029301	0.00027507	7.154181856	6.388122755
Fam221a	-0.597715223	0.430492014	0.025670824	1.629170126	1.243705315
Fam228a	-0.523418326	1.260148294	0.021729284	2.691672381	2.60047475
Fat2	-2.109760698	1.560372716	0.00172836	1.275002707	2.148218271
Fos	0.748196804	3.989772994	0.004775958	8.712518498	17.92066295
Foxr2	-0.763097493	0.295111557	0.020410778	1.13333574	1.639429733
Gabrq	-0.78364339	3.582694775	0.000607423	10.41252211	17.52493853
Galr1	-1.162476107	0.313516424	8.03E-05	1.770837093	1.413301494
Gata3	-1.506613043	0.569032866	0.016371184	2.125004512	1.695961793
Gatsl3	-0.70137311	1.671835727	0.023377931	5.170844312	4.013776244
Gimap1	-0.635233482	0.720801311	0.01970221	1.629170126	1.922090032
Gm10638	-0.852853638	0.637356845	0.000549851	1.983337544	2.035154152
Gm14634	0.56476181	0.478066587	0.046441724	1.204169223	1.130641196
Gm5148	-0.908688177	1.020648391	4.92E-05	2.620838898	2.374346511
Gm5741	1.429372892	0.837061647	0.007161992	0.850001805	0.847980897
Gm694	-0.583473456	1.009063991	0.018080516	3.116673284	2.148218271
Gmnc	0.543328893	0.89780242	0.022550812	1.416669674	1.526365614
Gpr101	-0.951275984	3.445337264	1.77E-05	10.48335559	15.0375279
Hap1	-0.555217443	8.331017058	7.41E-06	336.6007146	402.90399
Hpcal1	-0.745957857	5.273685971	1.12E-11	45.82926397	45.28217988
Hspb2	-0.849722798	-0.090504847	0.034810484	1.13333574	1.300237375
Hspb3	0.546816808	1.886553055	0.014774251	3.683341153	2.43087857
Ifit3	-0.761526682	1.167095966	0.009739468	3.400007219	2.317814451
Igfbp6	-0.593038149	1.661429398	0.002953991	3.258340251	3.222327407
Inhba	0.640387239	1.632606656	0.004135228	1.275002707	2.60047475
Irs4	-0.950640859	4.15176908	0.004235182	14.73336461	32.11020995
Itgal	0.618338999	1.382972308	0.030650726	1.204169223	2.317814451
Itgb3	0.510084927	3.59440939	0.000921226	8.145850628	10.1192387
Jph2	-0.585561001	0.908579209	0.011115651	2.47917193	1.809025913
Lars2	-1.381902691	8.022417582	0.010659213	1031.052189	189.7781247
Lhx1	-1.329399586	0.701683655	0.000126513	1.629170126	1.865557973
Lhx1os	-1.105021105	-0.093650864	0.007687635	1.204169223	1.130641196
Lhx5	-1.079821303	0.861267896	0.000186777	1.841670577	1.978622092
Lppos	-0.640686073	1.915404911	0.002803928	5.666678698	4.013776244
Lrrn4	-0.663228127	0.181797258	0.036284918	1.345836191	0.904512956
Ltbp2	-0.730504335	0.531037207	0.022816693	0.850001805	1.752493853
Mab21l1	-1.088427769	1.52475113	0.008873557	3.825008121	1.469833554

Magel2	-0.544449928	4.190142226	4.20E-06	17.14170306	22.38669567
Map3k15	-0.525457931	1.797921025	0.00665973	3.470840702	3.618051826
Map3k6	-0.592279469	0.969037419	0.010920734	1.91250406	1.809025913
Meig1	-0.718685131	0.881639444	0.001974246	2.125004512	2.60047475
Mir6236	-1.60565234	3.109078172	0.011313831	37.25841244	6.953443352
Mxd3	0.541522451	1.709036838	0.006395974	2.408338446	2.60047475
Myh2	0.748552127	0.111796155	0.019195139	0.991668772	0.282660299
Myo3b	0.654563127	1.947198763	0.030464264	2.762505865	3.222327407
Myoc	-0.560624468	4.633742219	0.001921645	36.19591018	26.45700397
Myzap	-0.6118644	0.58600323	0.01700407	1.558336642	1.469833554
Neil2	0.545197699	0.582578782	0.031089758	0.920835288	1.243705315
Neurl2	-0.551910458	1.636129641	0.0145674	3.754174637	3.957244184
Nhej1	-0.509870458	0.74452257	0.043822089	1.91250406	1.469833554
Nkx2-1	-0.53649901	1.548311462	0.006105182	2.762505865	3.109263288
Nod2	0.582757232	0.347834207	0.039667372	0.991668772	0.734916777
Npas4	0.656331832	4.280686133	0.000146658	12.89169404	16.56389351
Nppa	0.709438979	0.82606896	0.028002682	0.779168321	1.469833554
Npy2r	-0.600519259	3.74784331	0.000342937	16.57503519	15.15059202
Nr2f2	-0.982605987	5.295544397	2.29E-16	42.28758978	49.97434084
Nrtn	-0.663598452	0.382545385	0.028990401	1.91250406	1.187173255
Nupr1	-0.511514896	2.366949083	0.005275089	7.508349274	5.540141858
Olfm4	-0.966636044	0.4887757	0.000442045	2.125004512	1.526365614
Optc	-1.007264125	0.744057509	5.69E-05	1.983337544	1.695961793
Ovgp1	-0.557637272	2.419598884	0.013924717	8.57085153	6.727315113
Ovol2	0.500896073	1.544067859	0.044761248	2.125004512	2.317814451
Oxt	-1.639510519	2.125680412	0.005305517	7.862516693	10.1192387
Pappa2	0.705780221	2.525549017	0.001611913	4.17917554	3.900712125
Pdzd3	-0.568235987	0.27143488	0.042616204	1.062502256	1.469833554
Pex11g	0.95731891	0.370746507	0.001046017	1.275002707	0.678384717
Pla2g3	-0.660991552	3.833960394	9.37E-05	19.19587409	13.34156611
Plk5	-0.750674265	1.777138632	0.000213676	3.825008121	3.448455646
Plp2	0.502276716	0.81375429	0.043301738	1.345836191	1.469833554
Popdc3	-0.898611909	0.955414205	0.000555148	2.054171028	2.148218271
Ppp1r17	-0.886806475	0.816385772	0.00369195	1.983337544	1.922090032
Prlr	-0.754911938	2.215536284	0.000126486	4.250009023	6.670783053
Prr15	-0.635388033	0.163471275	0.035463452	1.558336642	0.904512956
Ptafr	0.716442103	0.228950685	0.032973218	0.495834386	1.017577076
Rad54l	0.547830202	0.628356178	0.043653579	0.850001805	1.130641196
Rhoh	-0.639289976	0.367541151	0.02734038	1.983337544	1.356769435
Rn45s	-1.921240752	11.52914222	0.002048231	13815.15016	2256.251038
Rtl1	-0.697110488	0.628865117	0.013664534	1.487503158	2.035154152
Rxfp2	0.790696298	1.474896967	0.009960121	2.266671479	3.278859467
Samd11	-0.614468378	1.720608327	0.001040268	3.61250767	3.391923587
Serp1b1b	-0.960536454	0.653870227	0.010611567	1.275002707	1.300237375
Sim1	-1.829660546	0.075187105	3.07E-07	1.558336642	1.639429733
Slc35d3	0.653330751	2.654289655	0.012187972	3.683341153	4.126840364
Slc47a1	-0.597631308	1.456896324	0.022563926	2.266671479	2.883135049
Snord22	-0.757731199	0.18233395	0.039092995	1.700003609	1.017577076
Stpg1	-0.877421689	0.934117682	0.02234336	4.037508572	1.413301494
Susd3	-0.5364457	0.938315698	0.021091606	2.47917193	2.261282391

Tacr3	-0.687975349	2.671502996	0.00142822	5.808345665	5.766270097
Tal1	-0.610358651	2.363857239	0.002447418	6.233346567	5.483609798
Tbx15	-0.608360846	0.827812141	0.018753528	1.629170126	2.148218271
Tmem140	-0.646798546	0.765574011	0.009902117	2.195837995	2.204750331
Trhr	-0.59270469	3.017885633	0.00051864	7.295848823	9.327789863
Trim34a	-0.506103054	0.912992197	0.037050871	1.770837093	1.922090032
Ttc32	-0.649185273	1.127953054	0.002757828	2.47917193	2.770070929
Wnt9b	-0.867764859	0.921635301	0.021396757	1.700003609	1.243705315
Zan	-0.76634195	0.828515348	0.001404795	1.91250406	1.922090032
Zc2hc1c	-0.66473974	1.161650432	0.003681833	2.833339349	2.148218271
Zfp599	0.529158817	2.349606859	0.00679351	3.400007219	3.278859467
Zfp953	-0.533881312	0.818050571	0.022950094	2.125004512	1.582897674

P10VDP24_3	P10VDP24_4	P10E2DP24_1	P10E2DP24_2	P10E2DP24_3
5.9440069	7.92877395	4.514040982	5.821495552	4.349446577
1.515139014	1.965251663	1.057978355	1.133388515	1.175526102
4.312318732	4.472641715	2.891807504	3.142577245	3.35024939
0.932393239	1.287578676	0.634787013	1.287941494	1.116749797
2.680630563	2.371855455	1.340105917	1.236423834	1.763289153
0.757569507	1.016509481	0.987446465	1.906153411	1.880841763
2.97200345	1.829717065	2.609679943	0.824282556	1.234302407
33.68270577	10.84276779	23.27552381	28.74685414	40.02666377
1.165491549	1.423113273	1.97489293	1.648565112	1.939618068
9.149108661	8.403145041	7.546912267	4.997212996	6.289064645
4.953339084	5.353616599	3.667658298	2.678918307	4.349446577
6.992949295	6.776729872	3.808722079	5.769977892	4.408222882
55.71049605	53.46839869	59.52891545	31.42577245	19.51373329
1.748237324	1.219811377	1.904361039	1.390976813	2.762486339
2.97200345	5.353616599	7.970103609	9.685320033	7.758472272
26.68975647	33.27374367	56.00232094	58.73013212	47.55003082
10.19805105	10.97830239	7.758507938	5.615424913	7.582143357
2.855454295	1.897484364	1.410637807	1.339459154	0.822868271
1.923061056	1.626415169	0.846382684	0.618211917	1.234302407
2.622355986	3.523899533	1.97489293	1.751600432	1.880841763
122.2017889	87.28428075	55.64966148	65.06680426	59.30529184
2.389257676	2.507390053	1.551701588	1.648565112	1.939618068
2.272708521	2.236320858	1.410637807	1.442494473	1.234302407
10.02322732	7.454402859	7.687976048	5.357836614	6.23028834
2.214433943	1.897484364	1.340105917	0.669729577	0.881644576
5.769183168	6.912264469	5.642551228	4.12141278	2.644933729
2.447532253	1.084276779	1.410637807	0.978835535	0.764091966
5.186437394	3.659434131	2.327552381	1.442494473	1.998394373
6.701576407	3.388364936	3.314998846	2.16374171	1.645736543
1.981335633	2.168553559	0.775850794	1.597047452	1.116749797
7.167773027	1.355345974	1.057978355	1.442494473	0.705315661
35.37266852	22.83757967	12.62520837	17.25841602	11.69648471
1.048942394	1.084276779	1.410637807	1.030353195	1.704512848
1.689962746	1.287578676	0.634787013	0.875800216	0.705315661
1.165491549	1.694182468	1.410637807	0.618211917	0.705315661
6.701576407	3.049528442	2.11595671	2.627400647	3.35024939
3.263376338	1.219811377	1.763297259	1.597047452	1.351855017
1.748237324	2.033018962	2.11595671	0.875800216	0.764091966
1.923061056	2.778459247	0.916914575	1.081870855	0.999197187
11.8880138	12.13034647	8.675422513	8.603449178	8.052353797
1.864786479	2.033018962	1.269574026	1.236423834	1.116749797
1.340315281	1.558647871	0.916914575	0.618211917	0.528986746
1.515139014	1.152044078	3.667658298	2.00918873	3.996788746
1.340315281	1.423113273	0.987446465	0.721247237	0.705315661
1.282040704	1.829717065	0.846382684	1.442494473	0.470210441
2.73890514	3.591666832	1.97489293	2.266777029	1.763289153
12.12111211	7.725472054	7.405848487	5.821495552	5.289867458
43.47283478	37.33978159	27.43690535	26.27400647	21.57090397
2.214433943	1.965251663	1.199042136	1.597047452	1.528183932

2.505806831	2.507390053	4.09084964	3.966859801	3.702907221
2.73890514	2.710691949	1.904361039	1.545529793	2.115946983
0.699294929	0.609905688	1.057978355	0.927317876	1.293078712
4.545417042	5.082547404	3.667658298	3.245612564	3.11514417
4.836789929	1.219811377	1.057978355	0.618211917	0.705315661
4.079220422	5.489151196	2.04542482	3.245612564	3.761683526
8.508088309	15.51871141	4.937232324	4.842660017	4.290670272
1.515139014	0.880974883	1.833829149	1.236423834	1.704512848
6.526752675	5.421383897	5.007764215	4.12141278	3.056367865
59.84799105	90.94371488	128.2975085	135.4914451	131.8940286
1.923061056	4.20157252	3.738190188	6.542742788	4.819657017
1.223766127	1.829717065	0.916914575	1.184906174	1.175526102
1.573413591	1.490880572	0.846382684	0.669729577	0.646539356
7.517420492	7.657704755	4.796168544	4.12141278	5.113538543
1.515139014	1.558647871	0.916914575	1.287941494	0.764091966
2.505806831	2.913993845	2.11595671	1.184906174	1.822065458
13.28660366	1.423113273	0.564255123	1.081870855	1.645736543
7.867067957	12.46918296	15.30542021	29.67417202	16.75124695
1.981335633	0.745440286	0.634787013	1.133388515	0.646539356
18.06511901	13.89229624	9.028081965	6.23363683	6.935604001
1.864786479	1.152044078	0.493723232	0.618211917	0.646539356
2.156159366	2.168553559	0.916914575	0.10303532	0.058776305
2.272708521	3.794968728	3.385530737	2.781953627	1.234302407
1.631688169	2.236320858	1.481169697	0.978835535	0.705315661
1.689962746	1.694182468	0.987446465	1.184906174	1.057973492
0.757569507	1.016509481	0.916914575	1.648565112	1.998394373
2.330983098	2.64292465	1.340105917	1.184906174	1.057973492
1.107216972	0.813207585	1.481169697	0.618211917	1.822065458
2.156159366	1.694182468	1.199042136	1.390976813	1.880841763
1.048942394	1.694182468	1.622233478	2.369812349	2.292275899
18.82268852	12.33364837	7.476380377	4.688107037	7.640919662
422.9568832	369.7383818	254.4790604	242.1330008	215.2976055
58.21630288	43.77767497	30.89296797	24.831512	29.21182363
0.699294929	1.084276779	1.340105917	0.309105959	0.352657831
2.389257676	3.18506304	3.879253969	5.563907253	4.290670272
3.67129838	1.287578676	1.410637807	1.545529793	1.645736543
4.079220422	4.066037923	1.97489293	2.215259369	2.351052204
2.389257676	2.981761144	3.526594517	3.245612564	4.173117661
28.03007176	18.09386876	12.62520837	7.160954705	7.288261831
1.515139014	2.778459247	2.962339395	2.215259369	4.231893966
10.13977648	11.04606969	10.79137922	17.30993368	13.57732648
2.156159366	2.033018962	1.128510246	1.648565112	1.234302407
108.7986361	173.3487501	180.3500436	143.4766824	131.7176997
2.797179718	2.304088156	0.916914575	0.824282556	0.23510522
1.048942394	1.084276779	1.269574026	0.463658938	0.11755261
3.379925492	1.965251663	1.269574026	1.287941494	0.646539356
4.661966196	3.456132235	3.667658298	2.421330008	2.292275899
1.573413591	1.152044078	0.916914575	0.566694257	1.175526102
2.564081408	1.355345974	1.199042136	1.081870855	0.940420881
5.9440069	3.794968728	1.763297259	2.215259369	0.646539356

23.60120387	22.83757967	13.8947824	14.73405069	14.34141844
4.254044154	4.540409014	2.327552381	3.451683203	2.821262644
2.73890514	2.371855455	1.269574026	1.648565112	1.351855017
1.981335633	1.829717065	1.128510246	1.236423834	1.351855017
2.564081408	4.879245508	6.559465802	3.863824481	3.35024939
2.505806831	2.710691949	4.302445311	4.018377461	2.644933729
0.990667817	0.609905688	1.269574026	1.030353195	1.234302407
2.097884788	3.523899533	5.219359886	2.524365328	7.111932916
28.90419042	26.2259446	27.7895648	14.27039175	20.68925939
1.689962746	1.965251663	1.340105917	0.927317876	1.293078712
1.048942394	1.219811377	1.763297259	1.442494473	1.410631322
3.321650915	3.18506304	2.327552381	2.575882988	3.291473085
2.214433943	1.694182468	1.551701588	1.133388515	0.940420881
3.962671267	3.388364936	2.398084272	2.16374171	1.998394373
0.815844084	1.152044078	1.622233478	1.030353195	1.234302407
11.3635426	19.17814554	21.9354179	30.24086627	20.7480357
1.223766127	1.490880572	1.269574026	2.678918307	1.293078712
16.54998	15.9253152	13.68318673	12.415756	8.640116848
57.16736048	58.48317879	28.07169236	27.51043031	21.62968027
1.689962746	1.016509481	1.269574026	0.566694257	1.057973492
5.302986548	5.353616599	5.007764215	3.503200863	3.58535461
1.631688169	1.558647871	0.916914575	1.133388515	0.881644576
2.389257676	2.236320858	1.128510246	0.978835535	0.764091966
4.778515351	4.879245508	5.148827995	4.739624697	3.056367865
1.515139014	3.320597637	3.173935066	2.421330008	3.879236136
5.9440069	1.761949767	2.11595671	0.360623618	1.410631322
5.9440069	3.049528442	5.924678789	8.809519817	7.758472272
1.456864436	1.152044078	0.705318903	0.772764896	0.881644576
0.641020352	0.609905688	1.763297259	1.390976813	1.234302407
20.45437669	16.33191899	13.75371862	11.07629685	10.75606383
4.079220422	5.2858493	2.891807504	2.472847668	2.586157424
1.223766127	1.355345974	1.692765368	2.00918873	1.410631322
3.088552605	2.168553559	1.199042136	1.803118091	1.116749797
3.20510176	1.355345974	0.916914575	1.236423834	0.822868271
6.818125562	4.879245508	2.962339395	3.091059585	3.644130916
1.223766127	1.219811377	0.493723232	0.669729577	1.057973492
1.048942394	0.54213839	1.763297259	0.721247237	1.528183932
1.689962746	0.880974883	1.551701588	1.390976813	1.763289153
1.165491549	1.219811377	1.199042136	0.772764896	0.646539356
944.3395277	1688.761084	1313.162735	1158.529132	1302.776802
2.039610211	1.423113273	1.269574026	0.824282556	0.705315661
1.107216972	1.084276779	3.456062627	2.988024266	3.526578305
4.195769577	4.20157252	2.04542482	2.988024266	2.292275899
1.631688169	3.523899533	0.987446465	1.390976813	0.528986746
1.515139014	1.084276779	0.775850794	0.206070639	0.11755261
4.545417042	6.84449717	7.053189035	4.482036398	10.52095861
4.370593309	3.049528442	2.327552381	1.390976813	1.939618068
0.757569507	1.694182468	0.564255123	0.412141278	1.293078712
2.797179718	1.084276779	1.481169697	1.339459154	1.469407627
1.923061056	1.829717065	1.481169697	1.081870855	1.645736543

10.83907141	8.403145041	4.796168544	5.151765975	3.996788746
7.167773027	5.353616599	5.007764215	2.936506606	3.23269678
2.156159366	2.033018962	1.340105917	1.236423834	1.880841763
1.923061056	1.355345974	1.340105917	1.184906174	0.940420881
11.8880138	9.758491015	6.559465802	5.203283635	6.34784095
2.389257676	2.168553559	1.199042136	1.133388515	1.998394373
2.447532253	2.371855455	1.692765368	1.390976813	2.057170678
3.962671267	2.236320858	1.057978355	1.184906174	0.764091966
2.330983098	2.168553559	0.916914575	1.030353195	1.586960237
3.146827183	2.236320858	1.763297259	1.339459154	1.469407627
5.361261126	4.20157252	5.99521068	4.945695336	7.111932916
1.981335633	2.10078626	1.622233478	1.133388515	1.351855017

P10E2DP24_4

5.404507218
1.418683145
2.702253609
0.472894382
1.553795825
1.688908506
1.824021186
19.92912037
2.97247897
6.350295981
3.715598712
4.120936754
48.50545228
2.702253609
12.16014124
56.40954409
8.106760827
0.945788763
1.756464846
2.702253609
82.82407312
1.756464846
1.553795825
6.552965002
2.026690207
3.715598712
1.216014124
3.377817011
4.458718455
1.756464846
1.418683145
24.45539516
1.688908506
1.013345103
0.337781701
3.512929692
1.418683145
1.486239485
0.878232423
7.836535466
1.553795825
1.283570464
3.445373352
1.216014124
0.540450722
2.026690207
7.633866446
20.40201475
1.553795825

3.783155053
1.959133867
3.580486032
2.90492263
0.405338041
3.242704331
5.607176239
2.499584588
5.201838197
108.225257
3.985824073
0.540450722
0.743119742
5.742288919
0.878232423
2.432028248
0.878232423
17.15931042
0.810676083
12.7681483
1.013345103
1.824021186
1.959133867
1.688908506
0.810676083
1.418683145
1.756464846
5.94495794
1.553795825
1.891577526
9.660556652
331.0936235
30.46790944
0.405338041
3.10759165
1.688908506
3.175147991
3.580486032
21.14513449
2.634697269
14.38950047
1.553795825
121.128518
1.486239485
0.270225361
1.148457784
3.10759165
0.472894382
0.743119742
2.432028248

16.07840897
2.296915568
1.553795825
1.486239485
3.175147991
3.985824073
1.283570464
3.445373352
17.22686676
0.810676083
1.959133867
1.418683145
1.553795825
2.634697269
1.688908506
21.48291619
2.90492263
7.566310105
28.10343753
0.810676083
4.593831135
0.472894382
1.283570464
3.985824073
3.648042372
4.391162115
5.336950878
1.148457784
1.824021186
8.241873508
1.891577526
2.567140929
0.878232423
1.621352165
3.783155053
0.878232423
1.283570464
2.094246547
1.080901444
1163.995742
1.621352165
3.512929692
2.634697269
1.013345103
0.608007062
8.174317167
2.769809949
0.743119742
0.743119742
1.688908506

5.201838197
4.864056496
0.743119742
1.486239485
7.431197425
1.486239485
1.283570464
2.026690207
1.351126805
2.026690207
5.472063558
1.283570464

GeneID	logFC	logCPM	LR	PValue	FDR
2210408F21Rik	-0.759162358	1.251211064	6.493864233	0.010824743	0.999653626
A230057D06Rik	0.555101373	3.91578165	3.842465461	0.049969992	0.999653626
A830009L08Rik	-0.731944179	3.081118602	6.612625905	0.010125824	0.999653626
Acr	1.037587941	1.622797584	6.013162452	0.014199557	0.999653626
Adam33	0.836408024	1.137070443	4.324690243	0.03756325	0.999653626
Adamts14	0.76962167	0.586742654	4.053797317	0.044072102	0.999653626
Amy1	0.553694355	4.556351508	4.707940521	0.030023599	0.999653626
Ap1g2	0.856297264	3.778797342	6.993636794	0.008179998	0.999653626
Arc	-0.774576505	5.539478364	5.006457181	0.025252936	0.999653626
Arhgap28	0.609261921	1.800554488	3.913556359	0.047898137	0.999653626
Bdnf	-0.899492726	4.599640648	4.517356392	0.033552638	0.999653626
C5ar1	-0.62675033	0.178717324	3.902033536	0.048227699	0.999653626
C920006O11Rik	0.559633876	2.11059746	3.877875189	0.048926441	0.999653626
Cacna1h	0.501852579	6.939577112	6.84962669	0.00886598	0.999653626
Cckbr	-0.510537023	4.97296319	5.30456556	0.021269603	0.999653626
Cdk3-ps	0.810724991	0.794706566	6.918613864	0.008530307	0.999653626
Col16a1	0.661219232	4.804803438	5.970745655	0.014545129	0.999653626
Col1a1	1.540626123	5.699305577	6.354883146	0.011705865	0.999653626
Col1a2	1.000509612	6.425939194	4.337970749	0.03727132	0.999653626
Col6a5	0.77958306	2.269000509	9.64110415	0.001902708	0.999653626
Colq	-0.679869376	1.162029433	5.82025	0.015842693	0.999653626
Cox6a2	-0.587363472	2.931830524	4.991069653	0.025478455	0.999653626
Cpz	1.15484745	0.457326883	6.935147745	0.008451808	0.999653626
Dbh	-0.778118363	0.638984858	6.476673381	0.010929936	0.999653626
Dcdc2b	0.81347127	1.341862146	5.925346689	0.014924602	0.999653626
Dnah9	0.542181405	3.279520589	5.259981308	0.021821253	0.999653626
Dusp5	-0.949066417	1.65754125	8.061700668	0.004521073	0.999653626
Efna1	0.597445364	1.992440197	5.454365749	0.019519489	0.999653626
Egr2	-0.95577968	2.323781921	5.287099968	0.021483968	0.999653626
Egr3	-0.503452287	6.333761214	3.898890784	0.048317999	0.999653626
Egr4	-0.676765863	4.586887556	4.003619295	0.04540267	0.999653626
Eln	0.524253847	6.171277639	7.510992652	0.006132357	0.999653626
Eps8l1	1.049504998	2.687805992	8.249603999	0.004076089	0.999653626
Epx	0.746256739	0.769960717	4.089327171	0.043154818	0.999653626
Exoc3l	0.521242146	1.54861144	3.926232598	0.047538329	0.999653626
Fam129c	0.793130797	1.264273805	5.573239117	0.018236994	0.999653626
Fanca	0.560715757	1.655094244	4.168924445	0.041171928	0.999653626
Fat2	-2.163391836	1.557570217	5.617399892	0.017783012	0.999653626
Fbln5	0.652932515	3.497344082	4.115064045	0.042502916	0.999653626
Fhod1	0.515588942	2.631281248	4.085847844	0.043243751	0.999653626
Flna	0.602402583	8.347645551	4.346756473	0.037079501	0.999653626
Fos	-1.966085887	4.741566263	8.355720634	0.00384475	0.999653626
Fosb	-2.649958106	3.313165948	9.443622029	0.002118846	0.999653626
Foxl2os	0.948509972	0.487133768	7.69960929	0.005523278	0.999653626
Ggnbp1	0.599276992	1.841457763	4.245364643	0.039357617	0.999653626
Gipr	0.66580427	2.420428231	5.077996891	0.024231349	0.999653626
Gm11549	-0.673495311	3.954163291	4.939141981	0.026255067	0.999653626
Gm14420	0.519165745	2.743985417	6.925118505	0.008499336	0.999653626
Gm15446	0.555511497	1.95039307	5.007950056	0.025231167	0.999653626

Gm20219	0.671093929	0.871451874	4.026478044	0.044791356	0.999653626
Gm2115	0.532924828	2.299878677	4.808938961	0.028312473	0.999653626
Gm38413	0.697335382	1.797752118	5.425296758	0.019847062	0.999653626
Gpr139	0.957985069	0.3871237	3.97380912	0.04621312	0.999653626
Gpr3	-0.767662745	2.365167089	4.828426394	0.02799417	0.999653626
Gsap	0.542411201	3.299187408	5.942721621	0.014778181	0.999653626
H19	0.845585875	3.602456815	4.854353987	0.027576439	0.999653626
H2-M5	0.714857007	1.280508136	3.963448521	0.046498353	0.999653626
Hcrt	2.470962514	0.561586301	58.03014508	2.58E-14	3.69E-10
Hspa1b	0.785413988	0.37512913	4.702300451	0.030122273	0.999653626
Ifit3b	0.827880798	0.115659743	4.071432763	0.043614266	0.999653626
Il18bp	0.653485735	2.84729028	3.929749473	0.047439011	0.999653626
Inhba	-0.896404249	1.75697806	5.647548431	0.017479793	0.999653626
Itgbl1	0.819722011	1.900606517	7.010329459	0.008104077	0.999653626
Iyd	0.68856293	0.922230463	5.262586751	0.021788611	0.999653626
Kif20b	0.640476073	1.719353099	4.117577286	0.042439814	0.999653626
Leng8	0.563860987	8.097117936	5.352405015	0.020693708	0.999653626
Mab21l1	-1.023393437	1.737385452	7.5867821	0.005879781	0.999653626
Mbd6	0.521607723	5.706722635	3.865887281	0.049277132	0.999653626
Med12	0.52390389	5.844013941	4.8154693	0.02820539	0.999653626
Mfsd2b	0.85121248	0.91014852	5.227493118	0.022232554	0.999653626
Mvp	0.522835214	2.539313509	4.506756244	0.033761209	0.999653626
Myh11	0.673175889	1.953005733	6.948980188	0.008386703	0.999653626
Neat1	0.536084871	4.25445683	5.39809624	0.020158729	0.999653626
Nlrp3	0.98343933	0.837486468	5.965131063	0.014591516	0.999653626
Nox4	0.742560764	0.41876705	4.456600876	0.034766615	0.999653626
Npas4	-1.051955805	4.90900969	4.039438556	0.044448607	0.999653626
Npy2r	0.542532447	3.723825768	8.470099753	0.003610316	0.999653626
Nr3c2	0.541137389	4.725291674	6.872081397	0.008755262	0.999653626
Nt5e	0.513565843	2.999846341	4.608934891	0.031805782	0.999653626
Ovgp1	0.772626957	2.841867095	6.348235648	0.01174981	0.999653626
P3h3	0.530616649	5.088759879	5.487155296	0.019156688	0.999653626
Pabpc4l	0.776582445	0.245345344	4.581809457	0.032313076	0.999653626
Parp3	0.595308254	1.991607527	4.577579375	0.032392944	0.999653626
Pdgfrl	0.587796562	1.500301881	4.736739688	0.029524974	0.999653626
Pisd-ps1	0.798962305	7.991185456	9.586162483	0.001960493	0.999653626
Pisd-ps2	0.649741903	4.818221331	6.819578951	0.009016382	0.999653626
Plekha4	0.749728474	1.142912177	3.865573888	0.049286336	0.999653626
Plscr4	0.654969842	1.906280726	7.177871393	0.007380822	0.999653626
Pmch	1.664355273	2.763694178	11.1894817	0.000822623	0.999653626
Procr	1.044416091	0.524335015	10.69958633	0.001071595	0.999653626
Prox1	0.611709851	4.033802576	4.948154692	0.026118532	0.999653626
Psd4	0.519554307	1.441286582	4.32281241	0.037604722	0.999653626
Ptch2	0.660880189	1.319549442	4.475791601	0.034378274	0.999653626
Ptgs2	-1.820204728	2.148191997	5.669289227	0.01726445	0.999653626
Rad9b	0.507601256	1.962003239	5.352047474	0.020697951	0.999653626
Rbp4	-0.514938228	2.613112251	4.376571767	0.036436212	0.999653626
Reck	0.534352597	3.752343588	4.748285941	0.029327493	0.999653626
S100a4	0.556240528	2.4510559	4.5516354	0.03288732	0.999653626
Scarf2	0.630198689	2.909973262	5.988962517	0.014395667	0.999653626

Serpinb1a	0.902416035	0.765036277	4.941658283	0.026216873	0.999653626
Sgk2	-0.975747782	0.231753845	5.032175326	0.024880629	0.999653626
Siglec1	1.186676245	0.33010555	9.806439362	0.001739019	0.999653626
Slc17a8	-0.791277768	3.530067994	7.951773928	0.004804027	0.999653626
Slc2a9	0.549806852	1.340202041	4.716502883	0.029874441	0.999653626
Slc9a2	0.769307499	2.584793202	7.782463303	0.005275581	0.999653626
Sowahb	-0.896552949	1.904390482	7.287037527	0.006945391	0.999653626
Spaca6	0.577753548	3.343848033	5.444553328	0.019629434	0.999653626
Spp1	1.326876452	3.176984413	5.930533097	0.014880739	0.999653626
Ssc5d	0.685446162	1.969938591	4.327324511	0.037505154	0.999653626
Styk1	0.663099102	1.512869545	4.981755762	0.025615973	0.999653626
Susd5	-0.562771788	3.521261858	6.212056426	0.012688315	0.999653626
Sypl2	-0.629678258	1.952012576	5.495142851	0.01906937	0.999653626
Tbxa2r	0.501138824	1.280391664	4.20210566	0.040373818	0.999653626
Tcap	-0.733411791	1.125609971	5.957080005	0.014658298	0.999653626
Thbs3	0.658815486	4.664721446	5.877942365	0.015331729	0.999653626
Thbs4	-0.688177908	2.226860505	6.022715353	0.014122901	0.999653626
Tmc4	0.693735655	2.348737178	4.244527921	0.039377016	0.999653626
Tnxb	0.758237408	1.787081262	4.388582302	0.036180386	0.999653626
Traip	0.519505122	4.240608831	7.940969838	0.004832793	0.999653626
Trim68	0.532847689	2.702668612	5.70880699	0.016880007	0.999653626
Tspan18	0.519315543	4.086700933	4.210003456	0.040186255	0.999653626
Unc13d	0.705475979	0.016883508	4.003185479	0.045414356	0.999653626
Wnt10a	-0.867485153	0.435822321	5.586126361	0.018103288	0.999653626
Wnt10b	0.939770383	0.369623528	4.151538942	0.041596702	0.999653626
Zan	0.591957772	1.026495554	4.044898217	0.04430505	0.999653626
Zfp456	0.787272514	0.344390315	5.312419882	0.021173926	0.999653626
Zfp69	0.842840359	0.955455495	4.004963673	0.045366475	0.999653626
Zkscan2	0.555746738	4.657923513	5.070458717	0.024336943	0.999653626

P10VGCG_1	P10VGCG_2	P10VGCG_3	P10VGCG_4	P10E2GCG_1	P10E2GCG_2
2.345823628	2.424230407	3.528213934	3.045333253	1.337990494	1.491964563
17.13754484	8.427086652	10.87865963	12.11051131	20.00295789	14.74749588
7.884573862	16.0460965	7.526856393	10.12750361	6.355454847	4.361127185
2.997441303	1.500714061	1.528892705	1.770542589	5.084363878	2.754396117
2.085176558	1.269834975	1.822910533	0.779038739	4.013971482	1.664114321
1.694205954	0.577197716	0.823249918	0.99150385	2.073885266	1.549347816
27.23761879	13.56414632	19.22876594	15.8640616	35.45674809	23.46975025
13.29300056	7.388130763	8.467713442	9.631751685	25.15422129	11.13235097
32.18991312	104.4727866	63.97827934	33.35702238	33.78425998	37.29911408
3.32325014	1.731593148	1.764106967	3.895193696	5.017464353	4.303743933
16.68141247	72.3228738	18.58192672	17.8470693	16.39038355	16.92805947
1.238073582	1.154395432	1.293678443	1.203968961	0.869693821	0.975515291
4.105191349	2.943708351	3.410606803	3.116154957	4.883665304	4.074210923
114.4892254	76.82501598	98.5547759	116.2184156	169.9247928	118.6111828
26.65116289	53.04447009	37.63428197	29.60347209	23.14723555	21.97778568
1.824529489	0.865796574	0.940857049	1.062325554	2.475282414	1.951030583
34.34025145	13.39098701	19.6403909	18.90939485	44.4212844	25.47816408
40.59578112	5.137059671	31.22469332	29.24936357	60.61096938	41.83239103
86.20901834	16.91189308	69.79983233	56.09078923	99.54649276	70.92570001
4.235514884	2.943708351	2.587356885	4.107658807	6.221655798	5.853091748
1.824529489	2.424230407	3.175392541	2.97451155	1.471789544	1.205048301
7.363279722	13.56414632	8.585320573	6.444775025	5.418861501	6.541690778
1.368397116	0.34631863	0.823249918	0.566573629	3.010478612	1.319814806
1.824529489	2.308790864	1.646499836	1.416434071	0.869693821	0.975515291
2.345823628	1.038955889	1.528892705	2.124651107	4.348469106	1.89364733
10.42588279	4.963900357	6.350785082	9.560929982	11.77431635	10.09945243
2.020014791	6.291455103	3.763428197	3.824371993	2.341483365	2.12318034
3.518735442	2.53966995	3.175392541	3.045333253	5.218162927	4.188977428
2.671632466	13.10238815	5.115910205	4.745054139	2.876679562	2.983929127
52.6507081	150.5331643	78.5615636	95.96340834	59.54057699	69.89280147
11.92460344	52.17867352	26.8144259	26.62896054	15.05239306	18.24787427
72.00375303	40.2306808	68.44735032	55.38257219	100.8175837	69.26158569
6.581338513	1.44299429	3.528213934	4.95751925	10.36942633	9.009170632
1.759367721	0.981236117	0.940857049	1.062325554	2.140784791	1.836264078
3.06260307	2.308790864	1.646499836	2.195472811	4.080871007	2.869162622
2.801956	1.038955889	1.234874877	1.628899182	3.010478612	2.926545874
2.671632466	2.135631549	1.764106967	3.257798364	3.612574334	3.213462136
1.954853024	0.230879086	0.999660615	15.72241819	1.271090969	1.032898544
10.62136809	3.751785153	12.58396303	7.790387393	18.39736929	10.44375194
6.711662047	3.001428123	5.762749426	4.532589028	8.563139162	6.082624758
345.3573675	171.7740402	194.9926234	322.4512163	481.8103769	297.8764634
9.252970978	126.0022614	19.6403909	14.30598412	12.04191445	11.53403374
1.694205954	56.44993661	5.409928033	3.682728586	2.609081464	2.926545874
1.172911814	0.634917487	0.646839221	1.062325554	1.940086216	1.262431554
3.58389721	1.847032691	2.704964016	2.903689846	5.351961977	2.926545874
4.887132559	3.347746752	2.352142623	5.665736285	7.225148668	5.049726214
11.72911814	22.62615046	19.40517664	21.8130847	9.232134409	7.804122331
6.38585321	4.271263098	5.939160123	5.028340953	7.626545817	7.05814005
3.06260307	2.308790864	3.763428197	2.97451155	5.218162927	3.672528156

1.498720651	0.981236117	1.646499836	1.133147257	2.675980988	1.319814806
4.170353117	4.675301499	3.351803238	3.470263475	5.619560075	4.418510438
2.736794233	2.885988579	2.469749754	2.124651107	5.619560075	3.385611894
0.325808837	0.577197716	1.352482008	0.920682146	0.735894772	2.869162622
4.235514884	11.89027295	4.704285246	4.390945621	3.344976235	4.016827671
10.36072102	5.425658529	7.762070655	8.14449591	13.71440256	10.90281796
15.37817712	2.943708351	7.468052827	8.640247835	19.60156074	17.32974224
2.801956	1.385274518	0.999660615	1.841364293	2.876679562	2.467479855
0.52129414	0.34631863	0.411624959	0.354108518	2.542181939	2.065797088
1.107750047	1.09667566	0.705642787	0.495751925	1.471789544	1.377198058
0.781941209	0.34631863	1.117267746	0.495751925	1.070392395	0.803365534
8.014897397	3.98266424	4.527874549	5.524092878	11.84121587	6.59907403
2.476147163	6.580053961	2.822571147	5.028340953	1.806287167	3.156078884
2.997441303	2.481950178	1.411285574	3.611906882	5.820258649	3.442995146
1.107750047	1.731593148	0.823249918	1.770542589	1.940086216	2.12318034
3.32325014	1.154395432	2.293339057	3.186976661	4.616067205	4.24636068
277.393644	148.5129723	215.9854963	241.7144743	425.3471781	238.7717134
6.841985582	2.077911777	2.881374713	5.524092878	1.873186692	2.008413835
55.0616935	26.72425425	42.04454938	47.37971969	78.74074058	46.36566797
60.53528196	27.30145196	45.86678115	54.46189004	77.46964961	57.32586918
1.824529489	0.808076802	0.999660615	1.416434071	3.211177186	1.549347816
5.669073768	3.463186295	4.821892377	4.745054139	7.091349619	4.877576457
3.453573675	2.135631549	3.410606803	2.549581328	4.749866254	3.270845389
21.11241265	11.54395432	14.70089139	14.58927094	27.8971018	15.95254418
1.629044186	0.692637259	1.176071311	0.99150385	1.538689068	1.262431554
0.716779442	0.865796574	1.176071311	0.849860443	2.006985741	1.549347816
19.67885377	106.6084181	19.22876594	15.72241819	21.74234553	19.9119886
11.66395637	8.138487794	11.99592738	10.83572065	14.11579971	12.73908204
17.46335368	16.73873376	22.05133709	29.60347209	25.02042224	29.4376085
5.603912001	4.386702641	8.056088483	7.9320308	8.763837737	10.78805146
8.471029769	4.098103783	3.822231762	4.461767325	10.36942633	6.312157768
35.70864856	19.97104097	25.16792606	30.17004572	51.31193545	30.35574054
0.716779442	0.461758173	0.646839221	1.345612368	1.739387642	1.434581311
3.714220745	2.251071092	3.410606803	2.903689846	3.612574334	3.328228641
2.606470698	1.789312919	1.470089139	2.832868143	3.278076711	3.270845389
205.2595675	128.7150906	196.0510876	212.6067541	415.9143451	221.3845879
25.217604	15.00714061	23.28621197	24.00855751	41.94600199	23.87143301
2.997441303	0.750357031	1.293678443	1.203968961	2.943579087	2.524863107
3.518735442	2.943708351	2.646160451	2.124651107	5.619560075	4.361127185
4.105191349	4.617581727	3.410606803	0.566573629	7.492746767	8.72225437
0.977426512	0.519477944	0.764446352	1.203968961	2.207684315	1.836264078
13.8142947	6.291455103	12.2899452	19.12185996	17.92907262	21.28918665
2.345823628	1.673873376	2.116928361	2.407937921	3.41187576	2.811779369
2.606470698	1.212115203	1.58769627	1.9830077	3.344976235	2.524863107
1.303235349	20.83683754	1.881714098	2.549581328	1.940086216	0.975515291
3.909706047	3.059147894	3.05778541	2.407937921	4.415368631	4.820193205
5.929720838	10.27411934	6.056767254	5.878201396	4.749866254	4.074210923
13.29300056	7.388130763	11.58430242	11.40229427	18.1297712	12.39478253
5.538750233	4.271263098	3.05778541	4.461767325	5.820258649	4.303743933
5.669073768	3.98266424	7.409249262	6.16148821	11.17222063	8.607487865

1.629044186	0.519477944	1.05846418	1.203968961	2.341483365	2.983929127
1.238073582	0.692637259	2.410946188	1.203968961	0.602095722	0.573832524
0.781941209	0.404038401	1.05846418	0.495751925	1.873186692	1.090281796
8.666515071	22.62615046	11.64310598	14.94337945	8.696938212	8.894404128
1.954853024	2.077911777	2.116928361	1.628899182	3.144277661	2.295330097
6.060044373	3.059147894	3.704624631	4.603410732	8.630038687	6.36954102
2.345823628	7.041812134	3.822231762	5.594914582	2.542181939	2.12318034
9.904588653	6.17601556	7.232838565	8.92353465	14.38339781	8.148421846
9.513618048	2.020192006	4.939499508	3.9660154	9.031435835	8.205805098
4.626485489	1.44299429	3.116588975	2.478759625	5.485761026	3.557761651
2.541308931	2.597389721	1.528892705	1.770542589	3.679473859	3.844677913
11.07750047	13.56414632	12.23114164	17.35131737	9.365933459	6.943373545
3.58389721	6.349174875	3.351803238	4.886697546	2.943579087	2.467479855
2.150338326	1.731593148	2.234535492	1.487255775	2.341483365	2.58224636
2.280661861	2.53966995	3.292999672	2.124651107	1.404890019	1.090281796
25.93438345	15.98837673	15.75935557	20.67993744	40.94250912	21.05965364
6.12520614	3.232307209	6.938820737	6.232309914	2.809780038	3.557761651
5.538750233	2.712829265	2.822571147	4.178480511	8.696938212	3.615144903
3.32325014	1.44299429	1.940517664	3.257798364	3.813272908	2.869162622
16.48592717	15.98837673	13.87764147	15.36830967	26.89360893	17.38712549
6.516176745	3.809504925	4.586678115	6.019844803	8.228641539	6.254774515
19.74401554	8.253927337	14.11285574	13.38530197	19.53466121	20.94488714
0.977426512	0.634917487	0.705642787	0.354108518	1.204191445	1.262431554
1.889691256	1.327554747	2.234535492	0.849860443	0.735894772	1.262431554
1.238073582	0.230879086	0.823249918	0.920682146	1.13729192	0.918132039
1.824529489	1.558433833	1.234874877	1.487255775	3.278076711	1.606731068
0.977426512	0.519477944	0.823249918	1.062325554	1.204191445	2.008413835
1.368397116	0.750357031	1.764106967	1.345612368	3.077378136	1.032898544
23.00210391	12.35203112	24.16826545	21.8839064	32.64696806	23.35498374

P10E2GCG_3	P10E2GCG_4
2.57252079	1.23411323
10.87474697	25.77118804
8.302226185	6.025376358
1.637058684	6.606135525
1.520125921	3.557149898
2.338655263	0.943733646
18.65077572	33.90181638
9.822352106	24.17410033
42.68045855	23.01258199
3.157184605	3.774934586
19.11850678	14.80935876
0.643130197	0.653354063
3.391050132	7.767653859
108.1043395	178.4382541
33.15043836	24.90004929
1.637058684	2.177846876
29.46705632	37.0959918
27.36226658	179.2367979
59.46031007	228.3109475
4.326512237	7.40467938
1.870924211	1.960062189
7.308297698	4.646073336
1.169327632	1.451897918
0.876995724	1.524492814
2.923319079	3.194175419
12.33640651	11.25220886
2.163256119	1.597087709
3.157184605	6.097971254
4.092646711	3.266770315
64.66381803	72.37711119
20.28783441	19.96359637
77.00022454	92.48589735
8.243759803	6.460945733
0.993928487	3.048985627
2.747919934	3.557149898
2.046323355	3.629744794
2.806386316	4.863858024
0.584663816	1.306708126
12.6872048	13.13967615
6.782100263	7.186894692
242.4600844	548.5996282
13.38880138	6.315755942
3.33258375	1.814872397
1.286260395	2.323036668
3.33258375	5.154237608
5.203507961	8.27581813
19.9955025	10.30847522
8.945356382	7.332084484
3.624915658	5.372022295

1.578592303	2.903795835
7.77602875	4.863858024
2.397121645	5.299427399
1.403193158	1.161518334
4.326512237	3.121580523
9.120755527	12.4137272
11.7517427	13.13967615
1.929390592	4.283098857
2.338655263	2.250441772
2.163256119	0.871138751
1.929390592	1.088923438
4.677310527	11.61518334
2.747919934	1.306708126
3.741848421	5.517212087
2.689453553	1.960062189
3.449516513	3.121580523
229.5390141	412.5567933
1.929390592	2.686011148
40.28333691	80.43514464
51.68428132	84.06488943
1.403193158	2.976390731
5.963570921	9.001767089
5.086575198	5.372022295
19.17697316	26.86011148
2.2217225	3.920124378
0.760062961	1.814872397
17.24758257	18.87467293
17.18911618	18.07612907
39.46480757	30.85283075
7.132898553	10.38107011
7.01596579	11.97815782
30.4609848	48.27560576
1.227794013	0.943733646
6.314369211	5.299427399
2.630987171	3.847529482
212.2329651	442.6110802
24.67281303	46.89630274
1.987856974	3.048985627
3.507982895	4.283098857
17.65684724	6.533540629
1.578592303	1.451897918
22.56802329	16.76942095
3.624915658	2.323036668
1.987856974	3.847529482
2.923319079	1.669682605
3.917247566	4.573478441
5.963570921	4.93645292
11.51787717	21.27030449
7.951427895	7.40467938
5.846638158	10.38107011

0.935462105	1.960062189
1.169327632	0.435569375
2.163256119	1.161518334
9.646952961	6.17056615
2.455588026	3.629744794
5.145041579	9.582526256
3.098718224	2.323036668
9.880818487	15.75309241
5.145041579	28.96536346
4.151113092	5.589806983
1.987856974	3.920124378
12.62873842	7.695058963
2.747919934	3.629744794
2.981785461	2.903795835
2.338655263	1.306708126
20.11243526	41.66947024
4.560377763	2.976390731
4.618844145	7.767653859
3.215650987	6.969110005
17.77378	26.56973189
7.132898553	8.63879261
14.38272987	24.6822646
1.11086125	0.798543855
0.643130197	0.798543855
2.689453553	1.379303022
2.046323355	2.323036668
1.052394868	1.524492814
1.578592303	3.774934586
22.56802329	41.16130596

Appendix 9

A

Gene	RNAseq			qPCR			Validated?		
	PA1	PA2	PA ^{POOL}	PA1	PA2	PA ^{POOL}	PA1	PA2	PA ^{POOL}
<i>Egr1</i>	ns	↑	ns	ns			✓	x	✓
<i>Nkx2-1</i>	ns	↓	ns	ns			✓	x	✓
<i>Inhba</i>	↓	↑	ns	ns	↑	ns	x	✓	✓
<i>Lhx1</i>	ns	↓	↓	ns			✓	x	x
<i>Ncald</i>	ns			ns	↑	↑	✓	x	x
<i>Spp1</i>	↑	ns	↑	ns			x	✓	x
<i>Npy2r</i>	↑	↓	ns	ns	↑	ns	x	x	✓
<i>Fos</i>	↓	↑	ns	↑	ns	↑	x	x	x
<i>Nt5e</i>	↑	ns	ns	ns	↑	↑	x	x	x

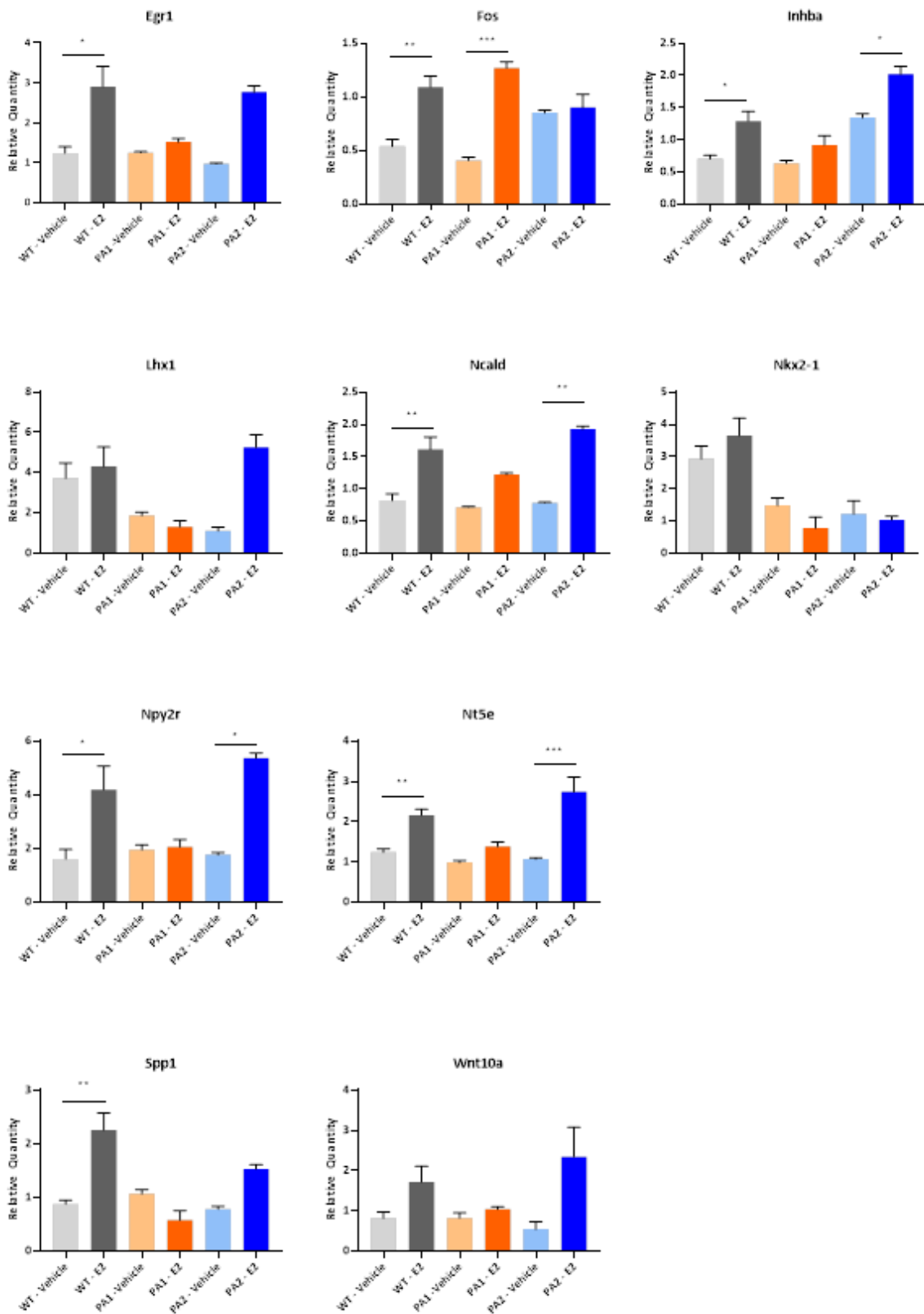
B

Figure 2: Biological validation of genes deregulated by estradiol in PA mutant mice by quantitative PCR (qPCR) analysis. Samples tested were pooled RNA samples prepared from the cortex of vehicle and estradiol treated mice at postnatal day 10 across each genotype. WT pooled samples contained RNA from $n = 6$ cortex samples for each treatment group. PA1 and PA2 pooled samples contained RNA from $n = 4$ cortex samples for each treatment group. Expression values were normalised to the reference gene, *B-Actin*. (A) Summary table shows results of these genes in RNAseq and qPCR data, with final column showing whether the qPCR results agreed with the RNAseq data. Grayscale colours in significance tables represent significance of result (lightest grey $p < 0.05$, medium grey $p < 0.005$ and darkest grey $p < 0.0001$). (B) Individual graphs of relative quantity for each genes for WT (vehicle = light grey; estradiol = dark grey), PA1 (vehicle = light orange; estradiol = dark orange), and PA2 (vehicle = light blue; estradiol = dark blue). Significance indicated by * $p < 0.05$, ** $p < 0.005$ and *** $p < 0.0001$, one-tailed t-test of vehicle treated WT, PA1 and PA2 mice compared to estradiol treated WT, PA1 and PA2.

Appendix 10

Final Cluster ID	Transcriptomic type		Present Markers	Sparse Markers
f01	Vip	Mybpc1	Crispld2, Cxcl14, Tpm2, Itih5, Cox6a2	Tmem182
f02	Vip	Parm1	Cxcl14, Car4, Tac2	Dmp1, Syt10
f03	Vip	Sncg	Reln, Npy2r, Tnfaip8l3, Cadps2, 2310042E22Rik, EglN3, Tpd52l1, Megf10	Casq2, Edn3
f04	Vip	Chat	Aebp1, Slc18a3, Pvrl4, Nrp1, Sema5b, Pcdh15, Phlda1	
f05	Vip	Gpc3	Bcar3, Mab21l1, Pbx3, Nrp1, Crh	
f06	Ndnf	Car4	Lamp5, Tnfaip8l3, Atp6ap1l, Gabrd, Npy, Pde11a, Has2, Krt12, 2310042E22Rik, Ndst4, Tnnt1, Reln, Mpped1	
f07	Ndnf	Cxcl14	Pde1a, Pcdh18, 4921511H03Rik, Rgs12, Cd34, EglN3, Thsd7b, Reln, Krt12, 2310042E22Rik, Ndst4	Scrg1
f08	Igtp		Lhx6, Cdca7, Myo5b, Pdlim3, Efcab6, Tnnt1, Cryab, Nfib, Kit, Lamp5	
f09	Smad3		Cd34, Sln, Npy, Col14a1, Rasl11a	
f10	Sncg		FrmD7, Edn3, Tnfaip8l3, Frem1, Scml4, St6galnac5, Pbx3, Fam107a, Krt73, Cyb5r2	Krt73, Cyb5r2
f11	Sst	Cbln4	Kcns3, Rasl11a, Timp3, Adamts18, Ano3, Rasl11a, Tnni3k, Bdnf	Nmbr, Bdnf
f12	Sst	Th	Gabrg1, Spp1, Nr4a2, Hspb3, Nts, Myh8	
f13	Sst	Myh8	Chrna2, Glra3, Kit, Ppapdc1a, Nr2f2, Gfra2, Myh1, Myh4, Myh13, Grm3, Il1rapl2, Tnni3k, Cartpt	
f14	Sst	Cdk6	Chrna2, Tmem90a, Nr2f2, Myh4, Myh13, Myh1, C1qtnf7, 4930503E14Rik, Gm5622, Gm8267, Efemp1, Grm3, Cartpt	Gm5800, BC061237
f15	Sst	Tacstd2	Crh, Pla2g4a, Sgpp2, Trpv6, Klhl14, ChrnB3, Grm3, Ano3, Fam5c, Htr2a, Irs4	
f16	Sst	Chodl	Tacr1, Nos1, Bace2, Ccdc109b, Dnase1l3, Gpr126, Gpr151, Gstm6, Hcrtr1, Htr7, Krt18, Insl6, Ndst4, Sit1, 9430021M05Rik, Gabrg1, Cdca7, Ndst4, Gpr88, Man1a	Stac
f17	Pvalb	Gpx3	Th, Calca, Nell1, Fxyd6, Tac1	
f18	Pvalb	Tpbg	Tacr3, Ednrb, Thsd7a, Fosb, Il1rapl2, Tll1, Col25a1, Calb1, Kit, Etv1, Bdnf, Aloxe3	

f19	Pvalb	Cpne5	Nt5e, Cntnap5b, Thsd7a, Snca, Cacna2d3, Kit, Pcdh8, Olfm3, Pdlim3, Nfib, Krt12, Cdca7	1300014I06Rik, Gm4980
f20	Pvalb	Tacr3	Thsd7a, Gm1051, Caln1, Calb1, Il1rapl2, Col25a1, Tac1, Tpbg	Ndst4
f21	Pvalb	Rspo2	Gpx3, Akr1c18, Ntf3, Lrrc61, Tac1	
f22	Pvalb	Wt1	Tusc5, Fign, Il1rapl2	
f23	Pvalb	Obox3	Acsbg1, Tac1, Il1rapl2	Ier5
f24	L4	Ctxn3	Rspo1, Inhba, Sparcl1, Pde1a, Lmo3, Rorb, Whrn	
f25	L4	Scnn1a	Rspo1, Endou, Tmem215, Rorb, Whrn	Shisa3, Barx2, Bglap2, Mbnl3
f26	L5a	Hsd11b1	Pde1a, Endou, Plb1, Aldh1l1, Etv1, Deptor, Rorb, Whrn, Cpne7	Shisa3, Barx2, Bglap2, Crym
f27	L4	Arf5	Scnn1a, Endou, Rspo1, Whrn	Lemd2, Shisa3, Barx2, Bglap2, Mbnl3
f28	L2/3	Ptgs2	Stard8, Inhba, Wfs1, Otof, Enpp2, Palmd, Rgs8, Dgkb	Car12
f29	L2	Ngb	Adamts2, Fst, Matn2, Cdh13, Dgkb, Otof	
f30	L5a	Tcerg1l	Pacsin2, Myl4, Deptor, Tmem91, Whrn, Il1rapl2, Hsd11b1	Pcsk5, Arhgap25, Cpne2, Crym
f31	L5a	Pde1c	Nnat, Syt17, Myl4, D430036J16Rik, Deptor, Arhgap25, Cpne2, Il1rapl2	Crym
f32	L5a	Batf3	Foxo1, Deptor, Myl4, Aldoc, Arhgap25, Il1rapl2	Pde1c, Crym
f33	L5	Ucma	Hhatl, Itga7, Myl4, Arhgap25, Man1a	
f34	L6a	Car12	Penk, Anxa11, Cd7, Cited1, Lipg, Nnat, Ptchd2, Sorcs3, Inhba, C1ql3, Pter, Acvr1c	
f35	L6a	Syt17	Fst, Prss22, Traip, Ptprk, Il1rapl2	
f36	L6b	Serpinb11	Ctgf, Tnmd, Nxph4, Col24a1, Trh, Fam46a, Ngf, Moxd1, Ndrgr1, Tmem40, Cplx3, Cidea, Inpp4b, Lman1l, Igsf3	Htr1d, Clic5
f37	L6b	Rgs12	Ctgf, Nxph4, Cidea, Ly6g6e, Sla, Cplx3, Clic5, Lman1l, Gpr126, Arhgap25	Mup5, Mup2, Mup19, Pappa2, Mapk13, Defb1, Gm2083, Tceal7, Foxp2, Trh, Tnmd
f38	L6a	Mgp	Foxp2, Ly6d, Rprm, Ifitm2, Ctxn3, Crym	
f39	L6a	Sla	Foxp2, Gabra5, Rprm, Plekhh1, Slc6a11, Crym	Mndal, Ptpru
f40	L5b	Chrna6	Chrn3, Scml2, Ngf, Klk8, Plac9, Ddit4l, Fam84b	

f41	L5b	Tph2	Qrfpr, Samd3, Stac, Ddit4l, 2310042E22Rik, Kcns3, Mc4r, Coro6, Sema3c, Kctd8, Crym, Fam84b, Ptgfr, Depdc7	Anxa1, Man1a, Pvalb
f42	L5b	Cdh13	Qrfpr, Col6a1, Syt17, 2310042E22Rik, Crym, Man1a, Fam84b, Ctxn3	4921511H03Rik, Igfbp2
f43	Astro	Aqp4	F3, Rorb, Acsbg1, Slc39a12, Ntsr2, Plcd4, Gja1, Gjb6, Cbs, Chrdl1, Prodh, Mlc1, Acsl6, Slc4a4, Gabrg1, Cxcl14, Slco1c1, Vcam1, Ednrb, Scrg1, Bcan	Gfap
f44	OPC	Pdgfra	Cspg4, Pcdh15, Gria3, Cacng4, E130309F12Rik, Vcan, Ednrb, Scrg1, Bcan, Gpr17	F3, 1110015O18Rik
f45	Oligo	9630013A20Rik	Brca1, Rnf122, Mbp, Zcchc12, Enpp6, Kif19a, Enpp6, Dct, Tmeff2, Gpr17, 1700040N02Rik, 1810041L15Rik, St18, Vcan, Bcan, 9530059O14Rik, Cldn11, 1700047M11Rik	
f46	Oligo	Opalin	Mbp, Mog, Aspa, Mobp, Gpr37, Ppp1r14a, Gjb1, Tmeff2, St18, Cldn11, 1700047M11Rik, Kctd13, Cntn2, Eml1, A530088E08Rik	
f47	Micro	Ctss	Cx3cr1, C1qb, Cd53, Csf1r, Itgam, Abi3, C1qa, Aif1, Trem2, P2ry13, Tmem119, C1qc, Cd14, Fcgr3, Gpr34, Inpp5d, Nckap1l, Mpeg1, Siglech, Susd3, Hk2, Ly86, Sparc, Fli1	1700110I01Rik, 1810011H11Rik
f48	Endo	Xdh	Tbc1d4, Al467606, Exosc7, Eltd1, Fas, Hmgcs2, Nostrin, Paqr5, Slc16a4, Id1, Ptprb, Cd93, Sparc, Fli1, Ly6a, Ly6c1, Ly6c2, Flt1, Pglyrp1, Slco1a4, Ifitm3, Abcb1a, Ahnak	Edn3, Tgfbr3
f49	SMC	Myl9	Bgn, Nupr1, Casq2, Mylk, Gprc5c, Slc38a11, Slc6a20a, Pcolce, Vtn, Cnn2, Nid1, Gpr30, Higd1b, Ifitm1, P2ry14, Serping1, Sparc, Fli1, Cald1, Abcb1a, Flt1, Ly6a, Ly6c1, Ly6c2, Pglyrp1, Slco1a4, Ahnak	Plac9, 0610007N19Rik, Ace2, Vtn, Edn3, Sncg